

Ena Ray Banerjee

# Perspectives in Translational Research in Life Sciences and Biomedicine

Translational Outcomes Research in Life  
Sciences and Translational Medicine, Volume 1

---

# Perspectives in Translational Research in Life Sciences and Biomedicine

---

Ena Ray Banerjee

# Perspectives in Translational Research in Life Sciences and Biomedicine

Translational Outcomes Research  
in Life Sciences and Translational  
Medicine, Volume 1

 Springer

Ena Ray Banerjee  
Department of Zoology  
University of Calcutta  
Kolkata  
India

ISBN 978-981-10-0988-4      ISBN 978-981-10-0989-1 (eBook)  
DOI 10.1007/978-981-10-0989-1

Library of Congress Control Number: 2016937522

© Springer Science+Business Media Singapore 2016

This work is subject to copyright. All rights are reserved by the Publisher, whether the whole or part of the material is concerned, specifically the rights of translation, reprinting, reuse of illustrations, recitation, broadcasting, reproduction on microfilms or in any other physical way, and transmission or information storage and retrieval, electronic adaptation, computer software, or by similar or dissimilar methodology now known or hereafter developed.

The use of general descriptive names, registered names, trademarks, service marks, etc. in this publication does not imply, even in the absence of a specific statement, that such names are exempt from the relevant protective laws and regulations and therefore free for general use.

The publisher, the authors and the editors are safe to assume that the advice and information in this book are believed to be true and accurate at the date of publication. Neither the publisher nor the authors or the editors give a warranty, express or implied, with respect to the material contained herein or for any errors or omissions that may have been made.

Printed on acid-free paper

This Springer imprint is published by Springer Nature  
The registered company is Springer Science+Business Media Singapore Pte Ltd.

*To my children  
Urbi, Adit and Arit*

---

## Preface

To the student of biosciences, this being the century of biology, opportunity seems infinite. The student of life sciences therefore, be it zoology, botany, physiology, microbiology, immunology, biochemistry, biotechnology and other much specialized branches, has the scope to leverage their individual specialized training in a multidisciplinary platform, and produce innovative, path-breaking, and life-changing work that can contribute to the assessment of environment, food production, biomedicine, information technology, and even functional ecology. The understanding of complex systems happening in tandem may be tapped in from the life sciences perspective and translated into nuances of real life. Innovation is the key to finding affordable solution to the pressing national needs in agriculture, health, and energy. One must also stay competitive in the international market. Such translational studies may also bridge the gap between an academic institute and a corporate house by permitting say a university, small business, or nonprofit institution to elect to pursue ownership of an invention in preference to the government. This may also make a marriage between academic thinking simply to generate knowledge and industrial compulsion to generate revenue. Translational research harnesses technology coming out of great academic minds and turns them into brilliant applications by the discipline of commerce. One must also not forget the exigencies imposed by natural disasters, unforeseen exigencies that puts the wind in the sails of scientific drive and expedites remarkable bench-to-bedside turnarounds of life-saving technologies. Powerful technology has been used by nations to tap in nature's potential to unforeseen heights, but irresponsibly used that mother earth is vastly devastated as a result. So to echo the age-old wisdom that with great power comes great responsibility, the onus is now on the scientist technocrat entrepreneurs to develop economically viable rapid turnaround customized technology which are biodegradable at the product level and eco-friendly at the process level. Green technology is thus the *mantra* of the day. Scientists working at the micro or macro level are thus guided by the twin principles of efficiency and nature-friendly work philosophy. Products to improve or replace the old

order and process to maximally tap the potential of a system and an inter-disciplinary approach is what should drive any happening organization, be it in the public or the private sector and a marriage of the two if possible, or at least some cross talk, to best utilize available resources to their full potency.

Kolkata, India  
August 2015

Dr. Ena Ray Banerjee

---

# Contents

<b>Translational Research in Life Sciences . . . . .</b>	<b>1</b>
<b>Part I Preclinical Disease Models as a Platform for Drug Discovery</b>	
<b>Idiopathic Lung Fibrosis Model for Drug Discovery . . . . .</b>	<b>13</b>
<b>Aseptic Peritonitis Model for Drug Discovery (As Therapy). . . . .</b>	<b>33</b>
<b>Aseptic Peritonitis Model for Drug Discovery (for Prophylaxis) . . . . .</b>	<b>51</b>
<b>Dissecting Key Cellular Players Regulating Pathophysiology of Acute and Chronic Allergic Asthma . . . . .</b>	<b>77</b>
<b>Dissecting Asthma Pathogenesis Through Study of Patterns of Cellular Traffic Indicative of Molecular Switches Operative in Inflammation. . . . .</b>	<b>89</b>
<b><i>Drosophila</i> Stem Cell Niches—Studies in Developmental Biology . . . . .</b>	<b>119</b>
<b>Part II Novel Antibodies as a Replacement for Antibiotics</b>	
<b>Camelid Antibody-Based Therapeutics for Animal and Human Health . . . . .</b>	<b>131</b>
<b>Development of a Novel Format of Stable Single Chain Antibodies Against <i>Staphylococcus aureus</i> and Allergen-Specific IgE in Allergic Asthma . . . . .</b>	<b>153</b>
<b>Development of a Novel Format of Stable Single-Chain Antibodies Against Alkaline Phosphatase as Therapeutic Molecules. . . . .</b>	<b>169</b>
<b>Development of a Novel Format of Stable Single-Chain Antibodies Against Alpha Amylase as Therapeutic Molecules . . . . .</b>	<b>183</b>
<b>Figures of Quantifiable Data in Support of Achieved Goals. . . . .</b>	<b>187</b>



---

<b>Part III Functional Food and Nutraceuticals</b>	
<b>Subchapter-A</b> . . . . .	197
<b>Subchapter-B</b> . . . . .	205
<b>Subchapter-C: Translational Outcome Research with Date Extracts as Functional Food in Diseases Involving Oxi-Flammatory Pathways</b> . . . . .	233
<b>Part IV Bio-Green-Technology as a Multi-disciplinary Interface Amongst the Life Sciences</b>	
<b>Nanomedicine: Nanoparticles and Its Relevance in Drug Discovery vis-a-vis Biomedicine</b> . . . . .	265

---

## About the Author



**Dr. Ena Ray Banerjee** is Associate Professor of Zoology in University of Calcutta, India and heads the Immunobiology and Regenerative Research Unit of the department. Her interests are manifold but centered around translational outcomes research in life sciences by exploring biodiversity through bioprospecting and converting them into bioresources currency. Alumnus of the premier educational institutions Lady Brabourne College and Gokhale Memorial Girls' school, Dr. Ray Banerjee has trained in Immunobiology during her Ph.D. and worked extensively in immune modulation in inflammation in general and cytokine-mediated inflammation in particular in Indian Institute of Chemical Biology, under Center for Scientific and Industrial Research. She has taught under- and postgraduate zoology with special emphasis on endocrinology and immunology under University of Calcutta, India. She then pursued her postdoctoral studies as visiting scientist and subsequently faculty of University of Washington School of Medicine, Seattle, USA in Pathobiology, Hematology, and Allergy and Infectious Diseases departments. Her work on target identification and validation in asthma and other related lung diseases helped her transition from a completely academic pursuit to a more applied one. She began with immunological studies defining key molecules in inflammation and eventually super-specialized into lung inflammation particularly allergy and made a natural transition onto regenerative medicine of the lung, having worked with some renowned names in the field. Her work validated several key targets in hematopoiesis and inflammation and also pioneered in tissue engineering of lung lineage specific cells of the non-ciliated variety from human embryonic stem cells and identified stem cell niches in mouse lung. She returned to India and worked in a leadership role in a drug discovery company where her team led drug discovery efforts in inflammation, specially pertaining to the lung using rigorous structure-activity correlation studies to reject or recommend pharmacological molecules working in tandem with Chemistry and Pharmacology departments.

Her experience of working in India, in the US, in academia, and industry prepared her for a unique role—translational research in life sciences. With this aim she returned to the renowned University of Calcutta to leverage her unique training in academia and industry, fundamental and applied research, she began her activities developing technology-intensive processes or products with a core knowledge of zoology. Whether developing animal models of diseases for screening novel drug entities, or models to understand fundamental life processes such as developmental biology, or looking for bioresources from local biodiversity, her group works on drug discovery efforts using novel drugs (small molecules), herbal extracts (functional food), probiotics (nutraceuticals), novel antibody-mediated (camelid antibody), and cells (tissue engineering of stem cells of embryonic origin, adult tissue origin, and umbilical cord-derived) in inflammatory disease models (tissue specific inflammation in the lung and systemic inflammation) and degenerative disease models. She has published widely in premier scientific journals and her publications are widely cited in “methods” volumes as well as “drug discovery” web sites and portals. She is also respected as an academician and educationist *par excellence* and has spearheaded the rejuvenation of a world-class heritage museum because she believes that to do bioprospecting and molecular drug discovery, knowing and respecting your biodiversity is the key. Through her efforts, this archived faunal repository is positioned to become a center of excellence for technology-based capacity building and an important educational interpretive center.

---

## Abstract

Translational research in life sciences has become increasingly interesting and important in current scenario. Basically, translational research in life sciences tries to translate the existing basic research outcomes of life sciences into practices (treatment options) and products (drugs, devices, etc.), which could enhance the quality of health of human beings. It has gained impetus during last two decades due to larger investments of global economy to the researches oriented to human health benefits. The final aim of the translational research in life science is to incorporate scientific discoveries into improved patient care and population health. In this review article, issues regarding nutrition research (functional food, nutraceuticals, edible vaccine, medical foods, etc.), pharmaceutical research (novel drugs, biosimilars, interchangeable, etc.), nanomedicine (nanoparticle-based functional molecules), research on preclinical animal model of diseases, medical genetics, tissue engineering, and regenerative medicine have been dealt briefly with the focus on the recent developments in these areas and their implications.

---

## Keywords

Translational research • Regenerative medicine • Functional food • Stem cells • Nanomedicine • Animal model • Nutraceuticals • Tissue engineering • Antibody engineering • Probiotics • Nanoantibody

---

## 1.1 Introduction

The need to strengthen the bridge between basic and clinical research gave rise to a new area called translational research. Translational research tries to make use of basic research to the

benefit of human beings (patients) or engages directly in the research, which could translate into actual therapy or, at the very least, improve their condition or delay or arrest the disease progression, when cure is not possible. In other words, translational research is the

transformation of research from bench top to bedside and finally bedside to practices.

The concept of translational research is as easy to define as difficult to achieve. The main idea behind it is to facilitate the transition from the research laboratories to the clinical applications or to the benefits of human beings. Although the basic research gives many new discoveries and innovations, which have potential to resolve the health problems, converting them to the deliverable products is not an easy task. It has gained impetus during last two decades due to larger investments of global economy to research, oriented to health benefits. The final aim of the translational research in life science is to incorporate scientific discoveries into improved patient care and population health. Translational researches in life sciences including nutrition research (functional food, nutraceutical molecules, edible vaccine, medical foods, etc.), pharmaceutical research (novel drugs, biosimilars, interchangeable, etc.), nanomedicine (nanoparticle-based functional molecules), and research on preclinical animal model of diseases, medical genetics, stem cells, and tissue engineering are making significant advances during past decades. Here, we discuss and describe the different areas of translational research in life sciences briefly.

## 1.2 Nutraceuticals and Functional Food

Functional food and nutraceuticals improve health and reduce healthcare cost. Long ago, Hippocrates stated, “Let food be thy medicine and medicine be thy food.” This concept has received huge interest to the food scientists as well as to the general public largely due to greater public awareness toward healthy food. The term “nutraceutical” is coined from the combination of “nutrition” and “pharmaceutical” by Stephen DeFelice, MD, the founder and the chairman of the Foundation for Innovation in Medicine (FIM), Cranford, NJ in 1989 [1]. Nutraceuticals are foods or part of foods having medicinal properties or health benefits including prevention, delay, arrest, or treatment of diseases.

It includes nutrients, fortified foods, food supplements, processed food, herbal products, and others, which are especially packaged like drugs in the form of pills, powder, or syrup. Functional food is the food that gives health benefits beyond its basic nutrition it contains. When the functional food proves its therapeutic potential to prevent, treat, or delay certain disease progression or disorder, it is called nutraceutical. With the new approaches and techniques of functional genomics that throw light on the effects of nutrients on gene expression (aka nutrigenomics), protein synthesis, and metabolism, it has become evident that nutrients play crucial role in gene expression and metabolism [2]. Nutraceuticals can be classified on the basis of source of food, mechanism of action, and their chemical nature as follows [3]. On the basis of source of food, nutraceuticals can be classified into the following: (1) plant-based nutraceuticals—quercetin, fisetin, curcumin, capsaicin, allium, lycopene, ascorbic acid, pectin, resveratrol, etc.; (2) animal-based nutraceuticals—docosahexanoic acid (DHA), eicosapentanoic acid (EPA), creatine, Zn, conjugated linoleic acid (CLA), etc.; and (3) microbial-based nutraceuticals—*Saccharomyces boulardii*, *Bifidobacterium bifidum*, *B. longum*, *Lactobacillus acidophilus*, *Streptococcus salvarius* (*sub. Thermophiles*), etc. On the basis of their effects, they can be classified into the following: (1) anticarcinogenic—limonene, curcumin, capsaicin, genistein, *Lactobacillus acidophilus*, sphingolipid, etc.; (2) positive effect on blood lipid profile: resveratrol, pectin, saponin, monounsaturated fatty acid (MUFA),  $\omega$ -3 poly unsaturated fatty acid,  $\beta$ -sitosterol, etc.; (3) antioxidant—ascorbic acid, tocopherol,  $\beta$ -carotene, glutathione, lycopene, etc.; (4) anti-inflammatory—linolenic acid, curcumin, capsaicin, quercetin, EPA, DHA,  $\gamma$ -linolenic acid (GLA), etc.; and (5) osteogenic or bone protective—soya protein, casein phosphopeptides, inulin, CLA, genistein, etc. On the basis of chemical nature, they can be classified into the following: (1) isoprenoids (terpenoides)—carotenoids, saponins, tocotrienol, tocopherol, etc.; (2) phenolic compounds—coumarin, tannis, anthocyanins, fisetin, curcumin, isoflavones,

flavones, etc.; (3) proteins or amino acids—amino acids, indole, folate, capsaicinoides, allyl-s-compounds, choline, etc.; (4) carbohydrates and derivatives—oligosaccharides, ascorbic acid, non-starch polysaccharides, etc.; (5) fatty acid and structural lipids—CLA, MUFA,  $\omega$ -3 PUFA, EPA, DHA, sphingolipids, lecithin, etc.; (6) Minerals—calcium (Ca), selenium (Se), zinc (Zn), copper (Cu), iron (Fe), potassium (K), etc.; and (7) live microbes—*Lactobacillus*, *Bifidobacterium*, *Saccharomyces boulardii*, *Streptococcus salvarius*, etc. Although none of these classifications is complete and exhaustive, each one of these provides certain important aspects. Some marine environments offer unique and diverse nutraceuticals with an array of health benefits such as use of  $\omega$ -3 PUFA obtained from discarded fishmeal for brain health, use of glucosamine obtained from hydrolyzed chitosan from crab and shrimps for joint health, and use of chitin, chitosan, and partially hydrolyzed chitosan for fat- and cholesterol-absorbing agents in functional foods and nutraceuticals. Nutraceuticals research is one of import part of several researches going on in our laboratory. Our laboratory involved in finding out the therapeutic effects of several foods or herbal extracts. We have found the therapeutic effects of fisetin in preclinical model of mice of acute allergic asthma [4].

---

### 1.3 Probiotics, Prebiotics, and Synbiotics

Probiotics are live microorganism, which provides health benefits to the host, when administered in adequate numbers. Beneficial gut microbiota comes under probiotics. Fermented dairy products (e.g., yogurt and fermented cheese) and pickles are common form of probiotics used in daily foods since ancient times. Our laboratory has also involved in finding out the therapeutic effects of probiotics; for example, we have found anti-inflammatory and proregenerative effect of probiotics [5]. Prebiotics are food component, which encourage the growth of probiotics in the host when consumed. Some

prebiotics have also been found to help in the absorption of calcium and magnesium [6]. These prebiotic components are found naturally in onion, garlic, leek, artichoke, honey, fortified foods, beverages, and dietary supplements and are also found as synthetic food components, e.g., inulin, fructo-oligosaccharides, polydextrose, arabinogalactan, polyols, lactitol, and lactulose. Synbiotics are the combinations of probiotics and prebiotics, which give enhanced health benefits to the host organisms when consumed in certain determined dose. Synbiotics are also considered under the category of nutraceutical factors as mentioned above.

Some other related terms are also being used for special purpose, such as medical food. The term “medical food” is defined by the FDA as a food which is formulated to be consumed or administered enterally under the supervision of a physician and which is intended for the specific dietary management of a disease or condition for which distinctive nutritional requirements, based on recognized scientific principles, are established by medical evaluation [7]. Phenylfree-1<sup>®</sup>, a phenylalanine-free food product for babies with phenylketonuria, and Ketonox<sup>®</sup>-1, a branched chain amino acid-free food formula for babies with maple syrup urine disease, are examples of medical food. Other examples are Banatrol Plus (banana flakes) for diarrhea, Deplin (1-methylfolate) for depression, Axona (caprylic triglyceride) for Alzheimer’s disease, and Limbrel (flavocoxid) for osteoarthritis. Medical foods strictly follow FDA criteria for their approval, while nutraceuticals, functional foods, and dietary supplements are market terms and FDA does not define them.

---

### 1.4 Genetically Modified Food

Genetically modified foods (GM foods) or genetically engineered foods are derived from organisms by introducing exogenous gene into their genome through genetic engineering to introduce new traits such as enhanced shelf life, better nutrient profile, resistance to pesticides and herbicides, etc. The Flavr-Savr delayed ripening tomato was the first GM food commercialized by

Calgene in 1994, since then number of GM foods are in market for consumption such as soybean, corn, canola, cotton seed oil, papaya, zucchini, potato, pineapple, apple, and sugar beet. The FDA recently approved the first altered animal, i.e., GM salmon (faster growth) for human consumption in the USA on Nov 19, 2015. However, these GM foods in theory have advantages in some aspects over that of the naturally available option, but their effects on ecosystem health and human health must be evaluated carefully before their release for cultivation or for animal and human use.

---

### 1.5 Biosimilars and Interchangeables

According to FDA, biosimilar is biological product that is approved based on the fact that it is highly similar to an FDA-approved biological product (reference product) and has no clinically meaningful differences in terms of safety and effectiveness from the reference product. Only minor differences in clinically inactive components are allowable in biosimilar products.

An interchangeable biological product is a biosimilar to an FDA-approved reference product and meets additional standards for interchangeability. It can be substituted for the reference product by a pharmacist without the intervention of the healthcare provider, who prescribed the reference product [7]. Zarxio is the only FDA-approved biosimilar till now, and around 45 other biosimilars are approved by different agencies worldwide to date. Basically, biosimilars provide cheaper options for the reference products (medicines) by introducing competitions in the pharmaceutical market.

---

### 1.6 Stem Cells and Tissue Engineering

Stem cell research is considered as the poster child of translational research in life sciences and has captured the imagination of scientists as

wells as non-scientist for their extraordinary potential in cell therapy. Stem cells and tissue engineering offer a great hope for the treatment of majority of diseases and injuries, where there is a lack of adequate treatment options. The increasing knowledge of stem cell biology and the response of stem cells to different environments (cellular influences, soluble factors, physical factors, scaffold, etc.) are progressively bringing significant shift in its translation to the patients. Stem cells can replace the diseased and damaged cells or tissues in degenerative diseases, where the degeneration of cells or tissues is the primary culprit.

There are mainly two types of stem cells participating in the entire life of an individual. One is originated from inner cell mass of an embryo and is called embryonic stem cell (ESC), and another is originated from other tissues of the organism and is called adult stem cell or somatic stem cell or tissue stem cell, responsible for maintaining the tissues or the organs. Former is pluripotent in nature, i.e., possesses the capacity to give rise any cells or tissues upon receiving appropriate cues or signals, and the later is somewhat restricted in plasticity but may give rise to one or more than one type of specific cells or tissues (unipotent/oligopotent/multipotent).

In spite of having greater plasticity of ESCs, they are far behind in the use of clinical trial for number of diseases with respect to adult stem cells, especially mesenchymal stem cells, due to having ethical hurdles, teratoma formation, and other concerns. The success of making precise three-dimensional retina in dish by coaxing the mouse and human ESCs is a great achievement in stem cell research and tissue engineering so far [8, 9]. Recently, human adipose tissue-derived mesenchymal stem cells have been demonstrated to show neuroprotective and antiapoptotic effects over retinal tissue under in vitro condition [10, 11].

Three adult stem cells, viz. bone marrow stem cells, peripheral blood stem cells, and umbilical chord blood stem cells, have been used in transplant to treat various blood disorders. Mesenchymal stem cells have been utilized in number of clinical trials mainly for three aspects,

i.e., plasticity (replacing of dead and damaged cells or tissues), repairing of damaged tissues, and immunomodulatory effects to reduce the chance of rejection in organ transplants. Skin stem cells are used in therapy since long time to repair the burnt or damaged skin. Wake Forest Institute for Regenerative Medicine at North Carolina, an international leader in regenerative medicine, is intensely involved in engineering more than 30 different tissues and organs either using organ-specific cells or pluripotent stem cells.

The invention of mechanism to reprogram somatic cells into ESCs like pluripotent stem cells (aka induced pluripotent stem cells, iPSCs) has brought great shift in stem cell research because of high potential of resulting iPSCs for proliferation, self-renewal, and differentiation, and more importantly, they furnish an invaluable tool for deriving patient-specific pluripotent stem cells without any ethical quandary [12, 13]. Since the first clinically relevant success in tissue engineering of bioengineered skin substitute from skin stem cells for severely burned patients, there is a significant advance in making wide variety of miniature organs or organoids. Stem cell researchers have coaxed stem cells into various miniature three-dimensional organoids such as functional liver bud from human iPSCs [14, 15] and adipose stromal vascular fractions [16], optic cup from hESCs [9], intestine (crypt-villus unit) from intestinal stem cells [17], mini-stomach from human ESCs and iPSCs [18], neural tube from hESCs [19], pituitary from mouse ESCs [20], renal organoid from hESCs [21], mini-lung from human ESCs and iPSCs [22], and cerebral organoid from ESCs and iPSCs [23]. The team of Dr. Doris A Taylor at Texas Heart Institute, University of Minnesota, USA, made beating heart by seeding laboratory grown heart sooth muscle cells on decellularized mouse heart scaffold. Scientists are also trying hard to make soft tissues and organ by using 3D bioprinter such as 3D printing of layered brain-like structure [24]. These 3D organoids or multilayered microstructure of cells with scaffolds are examples of great achievements in regenerative medicine, and they offer more accurate in vitro 3D model at least for studying

pathology of diseases or injuries and effectiveness of new potential drugs.

Clinical studies in patients have shown promising results that stem cells taken from a limbal region from healthy eye can be used to repair the severely damaged cornea in the accompanied eye with efficacy and safety [25]. Scottish Blood National Transfusion Service made type O blood group and determined to make blood transfusion till the end of 2016, which would fulfill the huge demand of blood to some extent. Although there are significant advances in regenerative medicine, there is a still long but promising way to go, unveiling the code of regeneration to be available for the personalized issues.

---

## 1.7 Nanomedicine

Nanomedicine is the combination of nanotechnology, biology, and medicine for the improvement of human health using molecular knowledge of human biology. Nanomedicine is one of the fast-growing areas especially in pharmaceutical research and development for delivering drugs/therapeutic genetic materials/photosensitizers and for imaging (diagnostic) purpose. It offers very high hope to large number of patients for better, effective, and economic health care and has capability to provide promising solutions to many illness including cancers their diagnosis.

Nanoparticle-based methods have very high potential for medical applications ranging from diagnosing diseases to developing novel treatment options. The cutoff size for nanoparticles is usually considered 100 nm, but it may go up to 300 nm [26]. There are various different types of nanoparticles used in the drug delivery such as polymeric nanoparticle (dendrimer) either made of synthetic polymers (polylactide–polyglycolide copolymer, polyacrylate, polycaprolactone, etc.) or made of natural polymers (alginate, collagen, albumin, gelatin, chitosan, etc.), peptide-based nanoparticle, inorganic nanoparticles made of silica (mesoporous silica nanoparticle—MSN) or carbon (mesoporous carbon nanoparticle—MCN),



magnetic compounds ( $\text{Fe}_3\text{O}_4$ ,  $\text{Mn}_2\text{O}_3$ ), gold, silver, lanthanides, quantum dots, etc. Our laboratory is involved in the regenerative medicine research using various nanoparticles including MCNs, which have been investigated as a drug carrier agent for controlled drug delivery [4]. Drug delivery systems, lipid- or polymer-based nanoparticles, are designed to improve pharmacokinetics and pharmacodynamics of the loaded drugs.

Nanodiagnostic is the part of nanomedicine, where nanoparticles are designed to have properties used for the in vivo imaging (molecular diagnostics), which helps in developing personalized medicine or precision medicine. The nanoparticles, equipped with superparamagnetic materials such as iron oxide, fluorescent materials such as quantum dots, radionuclides-labeled compounds, and micro-/nanobubbles, enhance the contrast in imaging via magnetic resonance imaging, optical imaging, positron emission tomography, and ultrasound imaging, respectively. The integration of therapeutics and diagnostic features in the same nanoparticle helps in image-guided therapies and is termed as nanotheranostics. Nanotheranostics have huge potential in medicine and biomedical research because of having concurrent capacity of therapy and imaging. The importance of nanotheranostics is significantly enhanced when they are localized to a specific site in diseases to mitigate the undesired side effects such as in cancer. This localization or specificity to tumor also facilitates the photothermal or hyperthermia and photodynamic therapy. The chance of clearing of these nanomaterials by kidney is greatly reduced due to their nanometric size, thereby extending their retention time in the blood, which in turn increases the efficacy of drugs loaded. Nanomaterials have high surface-area-to-volume ratio, which increases their drug-loading capacity. Although the nanomedicine is one of the intensive areas of research, still there are only 247 products or applications related to nanomedicine, which are under clinical study or on the verge of clinical study probably due to safety issues associated with nanoparticle-based products [26].

## 1.8 Antibody Engineering

Antibody is very specific in its affinity toward antigen and is very useful in biotechnology and biomedical applications due to its manipulations in the laboratory. The field of recombinant antibody technology has made a significant progress mainly because of the interest in their human therapeutic use. The antibody engineering includes methods of expression of antibody fragments in bacterial system and screening of combinatorial libraries and making structure–function database for making antibodies with desired properties for specific applications. The high affinity and specificity of antibody have been exploited in plethora of applications in biomedical field and in biotechnology such as antibody-based assay, in vivo toxin neutralization, passive immunization, delivery of radionuclide for imaging purpose, cancer therapy, immunosuppression, neurodegenerative diseases, and others.

Serendipitous discovery of these HCAs from camelid was made 23 year ago, and it offered tremendous opportunities for various diagnostic and therapeutic applications [27]. Traditional antibody is a relatively large macromolecule (150 kDa), which poses various challenges in formulation, manufacturing, stability, and process development. Members of camelid family (camel—*Camelus bactrianus*, dromedary—*Camelus dromedarius*, alpaca—*Vicugna pacos*, llama—*Lama glama*, guanaco—*Lama guanicoe*, and Vigogna/vicuna—*Lama vicugna*) and sharks produce antibody with no associated light chain and are called heavy chain antibodies (HCAs) or immunoglobulin (IgG) new antigen receptor (IgNAR), respectively. Variable domain of camelid HCAs is termed as VHH and that of shark HCAs is called VNAR, and more generally, they are called as single-domain antibodies (sdAbs) or nanobodies (nAbs) due to their small size (ca 15 kDa and 2 nm diameter and 4 nm long). Our laboratory is involved in research on camelid HCAs specific for different molecules. This VHH is gaining huge importance in translational research because of high thermal and

chemical stability, physicochemical stability, refolding capacity, solubility, facile genetic manipulation, and capability to bind epitope inaccessible to conventional antibodies due to very small sizes. Additionally, this nAb can easily be expressed and purified in bacteria, yeast, mammalian cells, and in plants. In this way, it could also facilitate the production of food of therapeutic values.

Conventional antibodies have problems of poor penetration into tissues (e.g., solid tumors) and poor or non-binding to regions on the surface of some molecules (e.g., glycoproteins of HIV envelop), which can be fully accessed by nAbs; thus, these nAbs offer a better therapeutic potential against different diseases. These nAbs are more amenable to faster engineering and cheaper production and show better tissue penetration and lower immunogenicity, thus paved the way for novel and highly valuable application in diagnostics, proteins, cell research, and agricultural research. These nAbs could be used in cancer therapy by conjugating toxic substance to it and targeting to tumors. This could be very effective due to their rapid tissue penetration and would show lesser side effects on other tissues due to fast blood clearance (very short serum half life of 2 h). Nanoscale size of nAbs make them efficient for crossing the blood–brain barrier (BBB) and which could be used as immune therapy against neurodegenerative diseases or brain disorders. Several potential targets such as cell surface proteins, cytokines, other secreted proteins, and intracellular proteins could be used for immune therapy by using nAbs. Due to high cost of immunization of Camelidae family animals, transgenic mice could give more economic tools to produce nAbs for therapeutic applications [28, 29].

Because of high recurrence of resistance against antibiotics in the pathogens, several alternatives have been reconsidered. Passive immunization, i.e., administration of pathogen-specific antibodies (isolated from immunized convalescent individuals) to the patients before or after exposure to the pathogens, is reconsidered as an alternative to antibiotics and gaining importance again in biomedical

applications. Passive immunization, formerly known as serum therapy, is the oldest antimicrobial therapy. Antibiotics either kill the microorganism or interfere with their replications, while antibody use more potent and versatile mechanism to control them, which include encouraging phagocytosis at the infection sites, activation of complement factors and inflammatory response, attraction of phagocytes, initiation of antibody-dependent cellular toxicity by monocytes, and neutrophils and natural killer (NK) cells. In addition, antibody promotes agglutination of pathogens by reducing the number of infectious units in the blood, restricts the mobility of pathogens, and inhibits microbial metabolism and growth, when it binds to the bacterial transport protein [30]. Existence of pathogens with multiple serotypes poses significant challenge to serum therapy. In addition, serum therapy has number of drawbacks, which include occurrence of serum sickness, risk of disease transmission, variations among different lots of serum preparations, lack of broad spectrum antiserum, and requirement of antiserum of same species in order to avoid anti-isotype immune reactions, pharmacokinetics, and economics. Antibodies are still the best options for neutralizing certain toxins (snake venom) and viral infections, e.g., hepatitis B, varicella, Ebola, rabies, and others, against which antibiotics obviously are not a treatment option. The use of egg yolk antibodies (IgY), nanobodies or single-domain antibodies, economical transgenic animals, antibody engineering, and molecular farming of antibody (antibody engineering) in various expression systems has huge potential to overcome the above hurdles. In particular, the expression of antibodies in food crops is going to be reality in the next few decades [31–33].

---

## 1.9 Animal Models

Animal models provide invaluable tools for biomedical as well as for translational research. They help greatly to make decision for potential therapy from preclinical studies to patients, i.e., from bench to bedside. Animal models have

played a vital role in almost every major field of biomedical advance during last century for both human as well as animal health care. Antibiotics, blood transfusion, dialysis, organ transplant, bypass surgery, vaccination, chemotherapy, drug development, and virtually every protocol of present-day treatment of diseases and sufferings came through the studies in animal models. A variety of animals such as non-human primates, mice, rats, pigs, fish, dogs, cats, birds, guinea pigs, sheep, insects, and others provide useful models for studying human diseases. They are very important for understanding the mechanism of diseases and for helping in guiding subsequent drug discovery. An animal model for human disease has limitation that it represents a particular aspect of that disease and does not represent the whole complexities of that disease in it. So for the same human disease, different animal models are produced, which represent different aspects of the disease. However, choosing an animal model closer to human makes it more suitable for the pathophysiological similarity to the human diseases. Only mice and rats constitute around 95 % of all the animal models used worldwide for research purpose. For making more identical disease models, immune-deficient models are humanized; for example, humanized mouse models of disease are the immune-deficient mice in which human cells or tissues are engrafted for doing functional studies. They are very important for clinical translation such as human tumor xenograft model for cancer study as they imitate human immune system [34]. An animal model for particular disease can be transgenic or knockout model in which gene or set of genes are completely knocked out to generate the symptoms of that particular disease. Some animal models are very relevant for particular disease due to their low cost, high fecundity, and short life span and for the particular aspects. For example, zebra fish (*Danio rerio*) is well suited for the study of macular degeneration studies as it has cone-dominated retina. Zebra fish is also very suitable for in vivo screening of potential drugs for their anticarcinogenic effects. For efficient translation of any in vivo outcomes to the human,

their robustness, relevance, and reproducibility to the in vivo study must be taken care of.

Translational research is one of the priority areas in industrialized countries especially in UK, USA, Sweden, and whole Europe, which resulted significant increase in the percentage of translational research globally. Private pharmaceutical companies are also making huge investment in these areas because the results obtained in these areas could readily be put to the commercial process and have potential to give them huge benefits in the long run.

In India, there is still a lag for translational research probably due to lack of strong political will and healthy and organized research environment. Indian Council for Medical Research (ICMR) is encouraging translational and clinical researches by giving them priorities in funding. It has also mapped 69 major life science research institutions and 39 central universities throughout India and made clusters of Regional Centre for Biotechnology (RCB) and Translational Health Sciences and Technology Institute (THISTI) for nurturing translational researches. Still, we need to go long to increase more funding to foment the translational research for providing better health care.

---

## 1.10 Conclusions

The rise of translational research in life sciences is going to affect the quality of health sector in a very dramatic way in coming two to three decades. The penetrance of all advance therapies to people of all economic strata has to be worked out, or there is a danger of limitation of these therapies to the upper strata of human population. To be successful therapies, they must be very cost effective, so that general public may get benefits from these advances. There is a dire need to make giant investment toward understanding the mechanism of stem cell biology and the mechanism of their specification to various kinds of determined cells or tissues. This would bring huge shift in the potential of regenerative medicine toward better health. In near future, the stem cell research outcomes could change the notions of scientist as well

as of public toward translational research, and the regenerative medicine will be the leader of the twenty-first-century health care.

## References

1. El Sohaimy S. Functional foods and nutraceuticals-modern approach to food science. *World Appl Sci J.* 2012;20(5):691–708.
2. Elliott R, Pico C, Dommels Y, Wybranska I, Hesketh J, Keijer J. Nutrigenomic approaches for benefit-risk analysis of foods and food components: defining markers of health. *Br J Nutr.* 2007;98(6):1095–100.
3. Wildman R, Wildman R, Wallace TC. *Handbook of nutraceuticals and functional foods.* 2nd ed. Boca Raton: CRC Press; 2006. 560 p.
4. Mitra S, Paul P, Mukherjee K, Biswas S, Jain M, Sinha A, Jana NR, Banerjee ER. Mesoporous nano-carbon particle loaded fisetin has a positive therapeutic effect in a murine preclinical model of ovalbumin induced acute allergic asthma. *J Nanomed Biotherapeutic Discov.* 2015;5:132.
5. Das R, Trafadar B, Das P, Kar S, Mitra S, Hore G, Biswas S, Banerjee ER. Anti-inflammatory and regenerative potential of probiotics to combat inflammatory bowel disease (IBD). *Biotechnol Biomaterials.* 2015;5(2).
6. Adolfsson O, Meydani SN, Russell RM. Yogurt and gut function. *Am J Clin Nutr Rev.* 2004;80(2):245–56.
7. Food and Drug Administration Compliance program guidance manual. Program 7321.002. Medical food program-import and domestic. Revised Sept 2008. Available at <http://www.fda.gov/downloads/Food/GuidanceComplianceRegulatoryInformation/ComplianceEnforcement/ucm073339.pdf>. Accessed 10 Sept 2015.
8. Eiraku M, Takata N, Ishibashi H, Kawada M, Sakakura E, Okuda S, Sekiguchi K, Adachi T, Sasai Y. Self-organizing optic-cup morphogenesis in three-dimensional culture. *Nature.* 2011;472(7341):51–6.
9. Nakano T, Ando S, Takata N, Kawada M, Muguruma K, Sekiguchi K, Saito K, Yonemura S, Eiraku M, Sasai Y. Self-formation of optic cups and storable stratified neural retina from human ESCs. *Cell Stem Cell.* 2012;10(6):771–85.
10. Singh AK, Srivastava GK, García-Gutiérrez MT, Pastor JC. Adipose derived mesenchymal stem cells partially rescue mitomycin C treated ARPE19 cells from death in co-culture condition. *Histol Histopathol.* 2013;28(12):1577–83.
11. Rodriguez-Crespo D, Di Lauro S, Singh AK, Garcia-Gutierrez MT, Garrosa M, Pastor JC, Fernandez-Bueno I, Srivastava GK. Triple-layered mixed co-culture model of RPE cells with neuroretina for evaluating the neuroprotective effects of adipose-MSCs. *Cell Tissue Res.* 2014;358(3):705–16.
12. Takahashi K, Yamanaka S. Induction of pluripotent stem cells from mouse embryonic and adult fibroblast cultures by defined factors. *Cell.* 2006;126:663–76.
13. Takahashi K, Tanabe K, Ohnuki M, Narita M, Ichisaka T, Tomoda K, Yamanaka S. Induction of pluripotent stem cells from adult human fibroblasts by defined factors. *Cell.* 2007;131:861–72.
14. Takebe T, Sekine K, Enomura M, Koike H, Kimura M, Ogaeri T, Zhang RR, Ueno Y, Zheng YW, Koike N, Aoyama S, Adachi Y, Taniguchi H. Vascularized and functional human liver from an iPSC-derived organ bud transplant. *Nature.* 2013;499(7459):481–4.
15. Takebe T, Zhang RR, Koike H, Kimura M, Yoshizawa E, Enomura M, Koike N, Sekine K, Taniguchi H. Generation of a vascularized and functional human liver from an iPSC-derived organ bud transplant. *Nat Protoc.* 2014;9(2):396–409.
16. Nunes SS, Majjub JG, Krishnan L, Ramakrishnan VM, Clayton LR, Williams SK, Hoying JB, Boyd NL. Generation of a functional liver tissue mimic using adipose stromal vascular fraction cell-derived vasculatures. *Sci Rep.* 2013;3:2141.
17. Sato T, Vries RG, Snippert HJ, van de Wetering M, Barker N, Stange DE, van Es JH, Abo A, Kujala P, Peters PJ, Clevers H. Single Lgr5 stem cells build crypt-villus structures in vitro without a mesenchymal niche. *Nature.* 2009;459(7244):262–5.
18. McCracken KW, Catá EM, Crawford CM, Sinagoga KL, Schumacher M, Rockich BE, Tsai YH, Mayhew CN, Spence JR, Zavros Y, Wells JM. Modelling human development and disease in pluripotent stem-cell-derived gastric organoids. *Nature.* 2014;516(7531):400–4.
19. Meinhardt A, Eberle D, Tazaki A, Ranga A, Niesche M, Wilsch-Bräuninger M, Stec A, Schackert G, Lutolf M, Tanaka EM. 3D reconstitution of the patterned neural tube from embryonic stem cells. *Stem Cell Reports.* 2014;3(6):987–99.
20. Suga H, Kadoshima T, Minaguchi M, Ohgushi M, Soen M, Nakano T, Takata N, Wataya T, Muguruma K, Miyoshi H, Yonemura S, Oiso Y, Sasai Y. Self-formation of functional adenohypophysis in three-dimensional culture. *Nature.* 2011;480(7375):57–62.
21. Freedman BS, Brooks CR, Lam AQ, Fu H, Morizane R, Agrawal V, Saad AF, Li MK, Hughes MR, Werff RV, Peters DT, Lu J, Bacceti A, Siedlecki AM, Valerius MT, Musunuru K, McNagny KM, Steinman TI, Zhou J, Lerou PH, Bonventre JV. Modelling kidney disease with CRISPR-mutant kidney organoids derived from human pluripotent epiblast spheroids. *Nat Commun.* 2015;23(6):8715.
22. Dye BR, Hill DR, Ferguson MA, Tsai YH, Nagy MS, Dyal R, Wells JM, Mayhew CN, Nattiv R, Klein OD, White ES, Deutsch GH, Spence JR. In vitro generation of human pluripotent stem cell derived lung organoids. *Elife.* 2015;24:4.

23. Lancaster MA, Renner M, Martin CA, Wenzel D, Bicknell LS, Hurles ME, Homfray T, Penninger JM, Jackson AP, Knoblich JA. Cerebral organoids model human brain development and microcephaly. *Nature*. 2013;501(7467):373–9.
24. Lozano R, Stevens L, Thompson BC, Gilmore KJ, Gorkin R, Stewart EM, Panhuis M, Romero-Ortega M, Wallace GG. 3D printing of layered brain-like structures using peptide modified gellan gum substrates. *Biomaterials*. 2015;67:264–73.
25. Pellegrini G, Traverso CE, Franzini AT, Zingirian M, Cancedda R, De Luca M. Long-term restoration of damaged corneal surfaces with autologous cultivated corneal epithelium. *Lancet*. 1997;349(9057):990–3.
26. Etheridge ML, Campbell SA, Erdman AG, Haynes CL, Wolf SM, McCullough J. The big picture on nanomedicine: the state of investigational and approved nanomedicine products. *Nanomedicine*. 2013;9(1):1–14.
27. Hamers-Casterman C, Atarhouch T, Muyldermans S, Robinson G, Hamers C, Songa EB, Bendahman N, Hamers R. Naturally occurring antibodies devoid of light chains. *Nature*. 1993;363(6428):446–8.
28. Zou X, Smith JA, Nguyen VK, Ren L, Luyten K, Muyldermans S, Bruggemann M. Expression of a dromedary heavy chain-only antibody and B cell development in the mouse. *J Immunol*. 2005;175(6):3769–79.
29. Janssens R, Dekker S, Hendriks RW, Panayotou G, van Remoortere A, San JK, Grosveld F, Drabek D. Generation of heavy-chain-only antibodies in mice. *Proc Nat Acad Sci USA*. 2006;103(41):15130–5.
30. Oral HB, Ozakin C, Akdis CA. Back to the future: antibody-based strategies for the treatment of infectious diseases. *Mol Biotechnol*. 2002;21:225–39.
31. Chan HT, Daniell H. Plant-made oral vaccines against human infectious diseases-Are we there yet? *Plant Biotechnol J Rev*. 2015; 13(8):1056–70. Epub 7 Sep 2015.
32. Rybicki EP. Plant-based vaccines against viruses. *Virology*. 2014;3(11):205.
33. Tokuhara D, Álvarez B, Mejima M, Hiroiwa T, Takahashi Y, Kurokawa S, Kuroda M, Oyama M, Kozuka-Hata H, Nochi T, Sagara H, Aladin F, Marcotte H, Frenken LG, Iturriza-Gómara M, Kiyono H, Hammarström L, Yuki Y. Rice-based oral antibody fragment prophylaxis and therapy against rotavirus infection. *J Clin Invest*. 2013;123(9):3829–38.
34. Ito R, Takahashi T, Katano I, Ito M. Current advances in humanized mouse models. *Cell Mol Immunol*. 2012;9(3):208–14.

---

**Part I**

**Preclinical Disease Models as a Platform  
for Drug Discovery**

## 2.1 Summary of the Original Research

Idiopathic pulmonary fibrosis (IPF) is a devastating disease of unknown etiology, for which there is no curative pharmacological therapy. Bleomycin, an antineoplastic agent that causes lung fibrosis in human patients has been used extensively in rodent models to mimic IPF. The conventional therapy has been steroids and immunosuppressive agents. But only a minority of patients responds to such a therapy. IPF is a progressive, ultimately fatal disorder for which substantive medical therapy is desperately needed. Fisetin is a flavonol which inhibits the activity of several proinflammatory cytokines. The polyphenol curcumin is used to treat inflammatory diseases, abdominal disorders, and a variety of other ailments. The aim of this study was to evaluate the beneficial effect of fisetin, curcumin, and mesoporous carbon nanoparticle (MCN)-loaded fisetin as an anti-inflammatory agent against bleomycin-induced changes in mice with IPF. In our study, flavonoids showed their antifibrotic action. The inflammatory cell count was greatly increased for bleo-treated individuals,

---

Therapeutic use of fisetin, curcumin, and mesoporous carbon nanoparticle-loaded fisetin in bleomycin-induced idiopathic pulmonary fibrosis.

The original research work included in this chapter has been communicated to OMICS Biological Systems (20-5-2015).

and effectiveness of fisetin was increased after the addition of MCN particles with it; curcumin also showed anti-inflammatory effects. In another experiment, bleomycin effectively inhibits the cellular recruitment to the spleen and treatment with fisetin, and curcumin increases the cellular recruitment in spleen. Colony count was also increased in MCN + fisetin-treated groups, and it was statistically significant. We also observed the increased level of cytokines with fisetin treatment, with curcumin treatment, and with MCN + fisetin treatment as compared to the bleo-treated sample. In conclusion, the present research suggests that fisetin and curcumin and MCN-loaded fisetin may be a promising therapeutic agent for bleomycin-induced changes in mice with IPF. This will open up new perspectives for a potential role of these drugs as a molecular target in idiopathic pulmonary fibrosis.

---

## 2.2 Introduction

Idiopathic pulmonary fibrosis (IPF) is a chronic, progressive, and lethal lung disorder of unknown etiology [1–3]. IPF primarily occurs between 60 and 70 years of age and is slightly more predominant in males [2, 4]. Data from around the world demonstrate that IPF favors no particular race or ethnic group. IPF is considered a complex disease where both genetic and environmental factors are believed to contribute to disease susceptibility [3]. The disease appears to be driven by abnormal and/or dysfunctional alveolar epithelial cells

(AECs) that promote fibroblast recruitment, proliferation, and differentiation, resulting in scarring of the lung, architectural distortion, and irreversible loss of function [5]. Exercise-induced breathlessness and chronic dry cough are the prominent symptoms. The onset of symptoms is slow, but symptoms become progressively worse over time. The initial presentation of breathlessness is commonly attributed to aging, cardiac disease, or emphysema which results in typical delays of diagnosis. At the cellular level, IPF is characterized by alveolar epithelial injury, initiation of inflammatory cascades, exaggerated profibrotic cytokine expression, increased extracellular matrix (ECM) deposition, and the development of fibrotic lesions known as fibroblast “foci” [6]. Injured epithelium could release growth factors, cytokines, and matrix metalloproteinase, which caused the activation or proliferation of mesenchymal cell, deposition of extracellular matrix, and the accumulation of fibroblasts [7]. The disease progresses toward chronic restrictive respiratory failure and death [8, 9]. IPF is associated with a median survival of only 3–5 years following diagnosis [10]. In their study, Japanese physicians were the first to describe acute, unexpected deterioration in patients with IPF. This phenomenon has been called the “acute exacerbation” or, more euphemistically, the “terminal complication” of IPF [3].

IPF belongs to a family of lung disorders known as the interstitial lung diseases (ILDs) or, more accurately, the diffuse parenchymal lung diseases (DPLDs). Within this broad category of diffuse lung diseases, IPF belongs to the subgroup known as idiopathic interstitial pneumonia (IIP). During IPF, airway remodeling occurs which can be defined as changes in the composition, content, and organization of the cellular and molecular constituents of the airway wall [3, 14].

The pathogenesis of the disease remains poorly understood, although current paradigms focus on the importance of alveolar epithelial cell injury as a critical initiating event with subsequent dysregulated wound healing and fibrosis, resulting in distortion of the lung architecture. The activation of cell-signaling pathways

through tyrosine kinases such as vascular endothelial growth factor (VEGF), fibroblast growth factor (FGF), and platelet-derived growth factor (PDGF) has been implicated in the pathogenesis of the disease [11–13]. IPF not only destroys the normal lung parenchyma but also affects the pulmonary vasculature with aberrant microvascular and macrovascular remodeling [14]. Previous studies showed that IPF develops from chronic epithelial cell injury and aberrant activation of progressive fibrosis [15]. Therefore, the therapeutic strategy against IPF has shifted from corticosteroids and/or immunosuppressants to antifibrotic agents [16, 17].

Current medical therapy for IPF is poorly effective. However, IPF is a progressive, ultimately fatal disorder for which substantive medical therapy is desperately needed. The only care options endorsed by guidelines published in 2011 were pulmonary rehabilitation, long-term oxygen therapy, lung transplantation, and enrollment in a clinical trial [8].

Animal models play an important role in the investigation of diseases, and many models are established to examine pulmonary pathobiology. Chronic diseases such as IPF are more difficult to model, since the etiology and natural history of the disease are unclear, and no single trigger is known that is able to induce IPF in animals. Different models of pulmonary fibrosis have been developed over the years. Common methods include radiation damage, instillation of bleomycin, silica or asbestos, and transgenic mice or gene transfer employing fibrogenic cytokines. So far, the standard agent for induction of experimental pulmonary fibrosis in animals is bleomycin [18].

Bleomycin (bleo) is a glycopeptide-derived antibiotic, isolated from the soil fungus *Streptomyces verticillus*. It is a chemotherapeutic agent with side effects especially on skin. The most serious complication of bleomycin is pulmonary fibrosis and impaired lung function. It has been suggested that bleomycin induces sensitivity to oxygen toxicity and some studies support the role of the proinflammatory cytokines IL-18 and IL-1 $\beta$  in the mechanism of bleomycin-induced lung injury [19]. Animal models are often used to



investigate pulmonary fibrosis, and they play an important role in understanding the pathogenesis of this disease. Bleomycin model is the most widely used animal model of pulmonary fibrosis. It is widely used as an inducer in the animal models [18, 20]. Lung fibrosis induced by bleomycin delivered to animals via different routes has different pattern of foci distributions. Using the bleomycin-induced pulmonary fibrosis model, it has been previously reported that pulmonary inflammation and fibrosis are mediated by the secretion of the proinflammatory and profibrotic cytokine IL-1 $\beta$  through Nlrp3 inflammasome activation and IL-1R1/MyD88 signaling [21–23]. Fibrosis associated with bleomycin treatment has also been linked to toxic reactive oxygen and nitrogen species produced by infiltrating inflammatory cells [24]. Thus, agents that depress oxidative stress are also of potential clinical value and could have additional protective effects against bleomycin-induced pulmonary fibrosis.

Plant polyphenols are a class of molecules characterized by the presence of multiple phenol groups in their structural moiety. Over the past several years, polyphenols have been studied for their potential to modulate the production and activity of inflammatory molecules [25]. Fisetin (3, 7, 3', 4'-tetrahydroxyflavone) is a flavonol, a structurally distinct chemical substance that belongs to the flavonoid group of polyphenols found in many plants fruits and vegetables, such as strawberries, apples, persimmons, onions, and cucumbers. Fisetin inhibits the activity of several proinflammatory cytokines, including tumor necrosis factor alpha, interleukin-6, and nuclear factor kappa B [26, 27]. In addition, fisetin is a potent natural anticancer agent.

The polyphenol curcumin is the active ingredient in the herbal remedy and dietary spice turmeric. Chemically, curcumin exhibits keto-enol tautomerism having a predominant keto form in acidic and neutral solutions and stable enol form in alkaline medium [28]. This vibrant yellow spice, derived from the rhizome of the plant *Curcuma longa*, has a long history of use in traditional medicines of China and India, where it is used to treat inflammatory diseases, abdominal

disorders, and a variety of other ailments [29]. Curcumin has been shown to exhibit antioxidant, anti-inflammatory, antiviral, antibacterial, antifungal, and anticancer activities and thus has a potential against various malignant diseases, diabetes, allergies, arthritis, Alzheimer's disease, and other chronic illnesses [30, 31]. Extensive scientific research over the past decade has shown the ability of this compound to modulate multiple cellular targets and hence possesses preventive and therapeutic value against a wide variety of diseases [28]. Curcumin has been shown to suppress TNF expression in in vitro, in vivo, and human studies. It can suppress TNF expression induced by numerous stimuli and by numerous cell types. Recent work has suggested that curcumin acts as a cancer chemopreventive and chemotherapeutic agent [32–35]. Curcumin inhibits activation of nuclear factor  $\kappa$ B through blockade of I $\kappa$ B kinase and inhibits activation of cyclooxygenase 2 (COX2). It also alters activator protein 1 (AP1) complexes and inhibits Akt. In addition to the effects on transcription and cell signaling, curcumin possesses chemical features that may further modulate its chemopreventive activity [36–38].

In light of the promising properties and broad spectrum of activities of fisetin and curcumin, the aim of our study was to evaluate the beneficial effect of fisetin, curcumin, and mesoporous carbon nanoparticle (MCN)-loaded fisetin as an anti-inflammatory agent against bleomycin-induced changes in mice with idiopathic pulmonary fibrosis.

---

## 2.3 Materials and Methods

**Mice** Balb/C mice from National Institute of Nutrition (NIN), Hyderabad, were used. The following numbers of animals used in each group were as follows: (a) control [3], (b) bleomycin-treated [4], (c) bleomycin + fisetin-treated [4], (d) bleomycin + curcumin-treated [4], and (e) bleomycin + fisetin + mesoporous carbon nanoparticle-treated [4]. Total 19 animals were maintained under pathogen-free condition and given food and water routinely. All experiments were

performed according to rules laid down by the Institutional and Departmental Animal Ethics Committee, and the animals housed under specific pathogen-free conditions at the animal house of the department of Zoology, University of Calcutta.

**Treatment of mice** Treatment was performed with adult Balb/C mice. 16 mice were anaesthetized using propofol received a single dose of bleomycin (naprobleo, miracalus) both intratracheally and intranasally, bleomycin 0.075 U/ml bleomycin dissolved in 1 ml of 0.09 % sterile saline water, from here 16 mice received a single dose of bleomycin at day 0.20  $\mu$ l was administered intranasally and 40  $\mu$ l from intratracheally. Mice were administered with 40  $\mu$ l of fisetin, 40  $\mu$ l of curcumin, and 40  $\mu$ l of mesoporous carbon nanoparticle (MCN)-conjugated fisetin intratracheally at day 7, 14, and 21, and at the 28th day, they were killed, and organs such as lung, bone marrow, liver, bronchoalveolar lavage, and peripheral blood were collected. Weight and other parameter of mice were taken on a regular basis according to rodent health monitoring program (RHMP).

Mice developed marked interstitial and alveolar fibrosis, collagen content was detected by hydroxyproline estimation, blood smear preparation and cytospin sample staining with hematoxylin were used to quantify the differential cell count of blood, clonogenic potential was detected by colony-forming unit (CFU) assay, cytokine analysis of BALF and peripheral blood was used to study the cytokine profile, and weight of mice was taken in a regular basis to observe the development of fibrosis.

**Colony-forming unit (CFU)-c assay** For quantification of committed progenitors of all lineages, colony-forming units in culture (CFU-c) were performed using standard protocol. Briefly, after dissection, the tissues (spleen, lung) were immediately kept in Iscove's modified Dulbecco's media (IMDM) (purchased from Himedia, India) maintaining aseptic conditions. For bone marrow samples, the bone was taken into the biosafety cabinet (Vision Scientific,

Korea) and flushed with PBS until the bone turns white. The cell suspension was then kept in IMDM. The tissues were minced, and the cell suspension was collected with the help of a nylon mesh. Spleen and lung samples were centrifuged at 5000 rpm for 5 min. Bone marrow was centrifuged at 5000 rpm for 10 min. Cell count was taken. Number of cells per well taken was  $1 \times 10^4$ . For bone marrow,  $-4 \times 10^4$  cells were taken per well. CFU-c media were prepared using IMDM, supplemented with 30 % FBS (Himedia, India), 10 % BSA (Biosera), 1 % penicillin-streptomycin (Himedia, India), and 5 ng/ml murine SCF (Biovision). Lastly, 1.5 % methylcellulose (in powdered form purchased from Himedia, India) was added into the concoction. 1 ml CFU-c assay media and 500  $\mu$ l cell suspension were plated in each 24-well cell culture plate. The 24-well plate (NEST Biotech Co. Ltd.) was kept in CO<sub>2</sub> incubator (Thermo Scientific) at 5 % CO<sub>2</sub> and 37 °C for 14 days. All colony types were counted using Fluid Cell Imaging Station (Life Technologies, India.) and pooled to get total CFU-c.

**Total count/differential count** White blood cells (WBCs) are a heterogeneous group of nucleated cells. They play an important role in phagocytosis and immunity. Differential white blood cell count is an examination and enumeration of the distribution of leukocytes in a stained blood smear. The different kinds of white cells are counted and reported as percentages of the total WBCs examined. Increases in any of the normal leukocyte types, or the presence of immature leukocytes or erythrocytes in peripheral blood, are important diagnostically in a wide variety of inflammatory disorders. Differential count was taken using the following protocol. Blood was collected in 1X RBC lysis buffer. It was kept at room temperature for 5 min, then flushed with 1X PBS [137 mM NaCl (Merck), 2.7 mM KCl (Himedia), 10 mM Na<sub>2</sub>HPO<sub>4</sub> (Qualigens), 2 mM KH<sub>2</sub>PO<sub>4</sub> (Himedia)], and centrifuged (Cold Centrifuge Vision VS-15000CFN) at 4000 rpm for 5 min at 4 °C. The supernatant was discarded. The pellet is dissolved in 1X PBS and stored at 4 °C.  $10^5$

cells, dissolved in PBS, were diluted in cold 1 % BSA–PBS. Quickly, 100  $\mu$ l of each sample was added to appropriate wells of the cytospin (Centurion Scientific), and the slides and filters were placed in the correct slots of the cytospin. The slides were centrifuged at 2000 rpm for 3 min. The slides were removed and air-dried. They were then fixed with methanol (SRL) and air-dried before staining. The fixed slides were placed in 100 % ethanol in a Coplin jar for 5 min, followed by 10 min in 90 % ethanol. They were then stained with hematoxylin for 5 min, rinsed in 70 % ethanol, counterstained with eosin for 2 min, and again rinsed in 70 % ethanol. Then, they were placed in 100 % ethanol for 1 min and then observed under the microscope (Debro DX-200).

**Collagen content estimation by hydroxyproline assay** Collagen is the major structural protein of the cellular matrix of the lung. The most common method for evaluating tissue fibrosis/collagen deposition is hydroxyproline quantification. 4-hydroxyproline is a major component of collagen, comprising around 13.5 % of its amino acid composition. The basis of hydroxyproline quantification is that total collagen can be assessed by acid hydralization of proteins followed by measurement of hydroxyproline content.

The hydroxyproline content of mouse lung was determined by standard methods. The pulmonary vasculature was perfused with PBS until free of blood. Lung tissue was excised, trimmed free of surrounding conducting airways, and homogenized in 1.8 ml of 0.5 mol/L glacial acetic acid. This mixture was dried in a speed vacuum and weighed. The dried sample was redissolved sample in 2 ml of 6 N HCl and hydrolyzed at high temperature overnight. 7  $\mu$ l samples were transferred to eppendorf tubes, dried, and resuspended in citrate–acetate buffer (5 % citric acid, 1.2 % glacial acetic acid, 7.24 % sodium acetate, and 3.4 % NaOH dissolved in distilled water and adjusted to pH 6.0). Freshly prepared chloramine-T solution [0.282 g

chloramine-T (Merck), 2 ml n-propanol, 2 ml distilled H<sub>2</sub>O to 20 ml with citrate–acetate buffer], 150  $\mu$ l, was added and the sample allowed to stand at room temperature for 20 min. 150  $\mu$ l freshly prepared Ehrlich's solution [4.5 g 4-dimethylaminobenzaldehyde (Merck) dissolved in 18.6 ml n-propanol, 7.8 ml of 70 % perchloric acid] was added and the sample heated to 65 °C for 15 min. Optical density was measured at 550 nm. A standard curve of samples with known quantity of hydroxyproline (Sigma) was generated for each assay. Absorbance of unknown samples was compared to the standard curve, and hydroxyproline content per lung was calculated.

**Cytokine analysis of BALF and peripheral blood** The BD CBA Mouse Th1/Th2 Cytokine Kit (Catalog NO 551287) was used to measure interleukin-2, (IL-2), interleukin-4 (IL-4), interleukin-5 (IL-5), interferon- $\gamma$  (IFN- $\gamma$ ), and tumor necrosis factor (TNF) protein levels in both BALF and peripheral blood samples. This uses bead array technology to simultaneously detect multiple cytokines in the samples. 5 bead populations with distinct fluorescent intensities are coated with capture antibodies, specific for the above-mentioned proteins. The beads are mixed to form the bead array and resolved in a red channel of a flow cytometer. After addition of the sample to the sample assay tubes containing the capture beads, the mouse Th1/Th2 PE detection reagents were added to each tubes. The tubes were incubated for 1 h at room temperature, in the dark, and then washed with 1 ml of wash buffer, centrifuge at 200 g for 5 min. The supernatant was carefully discarded and 300  $\mu$ l of wash buffer added to resuspend the bead pellet.

**Statistical method** Results are given as means  $\pm$  SD. The differences were assessed by 1-tail Student's *t*-test, one-way at  $\alpha = 5$  % using GraphPad Prism 6. A *P* value of <0.05 was considered to indicate a significant difference. ★ denotes significance in samples compared to

control, ★ denotes significance in samples treated with only bleo, ☆ denotes significance in samples treated with fisetin, curcumin, and MCN-treated fisetin compared to bleo.

## 2.4 Result

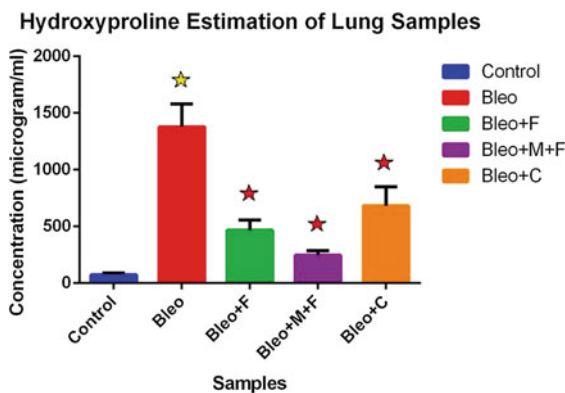
Figure 2.1 shows comparison between control and treated sample with respect to their hydroxyproline concentration. We found that there is 19-fold increase in collagen concentration for bleo-treated group, sixfold increase for bleo + fisetin-treated group, threefold increase for bleo + fisetin + MCN-treated group, and ninefold increase for bleo + curcumin-treated group. Here, we observed that bleomycin is highly effective in causing fibrosis in mice as compared to control groups, and the plant flavonoids also showed their antifibrotic action.

The average weights of different groups of mice were significantly different at the 0th day. During the treatment mainly from the day 7 (Fig. 2.2), we observed that the weight of bleo-treated groups were significantly reduced. Weight reduced by 45, 42, and 19 % on 7th, 14th, and 21st day, respectively, as compared to control groups. When we challenged the bleo-treated group with flavonoids (curcumin and fisetin), the weight of the mice was significantly increased to 39, 37, and 5 % at day 7, 14,

and 21, respectively, for the curcumin-treated group; 55, 33, and 9 % at the respective days for fisetin-treated groups; and 46, 33, and 14 % at the respective days for MCN-loaded fisetin groups. Significant weight loss indicates development of fibrosis after treating with bleomycin.

We found that total cell count in peripheral circulating blood increases by 1.7-fold in the bleo-treated group as compared to control. We also found that the count decreases by 1.43-fold with fisetin, 1.40-fold with MCN + fisetin, and 1.5-fold with curcumin when compared to only bleo. This indicates 1.3-fold increase with fisetin, 1.2-fold increase with MCN + fisetin, and onefold increase as compared to control-treated groups (Fig. 2.3). These findings indicate that after the development of fibrosis during bleomycin treatment, the total cell count was greatly increased which was decreased significantly after challenging with the plant flavonoids.

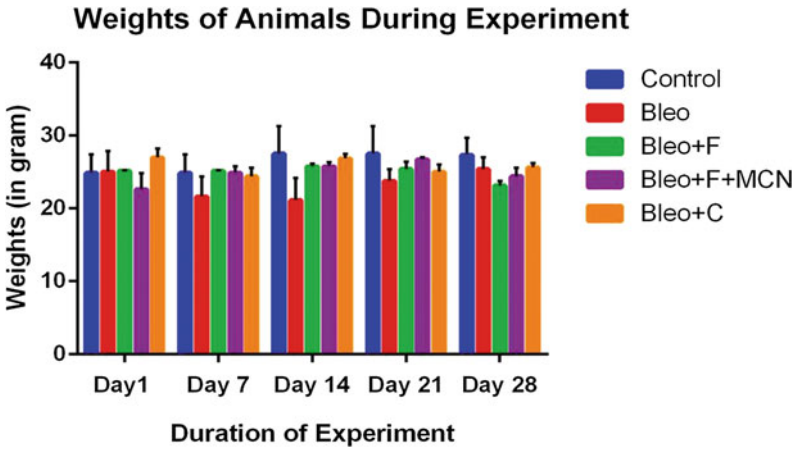
The polymorphonuclear (PMN) cell count was increased by 5.6 % and the mononuclear (MN) cell count by 2 % for bleo-treated as compared to placebo groups. Both PMN and MN cell counts decreased after treatment with fisetin, curcumin, and MCN-loaded fisetin. PMN cell count decreased 5 % by fisetin treatment and 4 % by both curcumin and MCN-loaded fisetin treatment, and the MN cell count decreased by 3 % for fisetin and 5 % by both curcumin and MCN-loaded fisetin as compared to only



Concentration(μg/ml) of hydroxyproline in lung samples	
Control	73.33 ± 17.64
Bleo	1377.50 ± 202.34
Bleo+F	465.00 ± 91.70
Bleo+MCN+F	245.00 ± 42.72
Bleo+C	682.50 ± 168.79

**Fig. 2.1** Graphical representation of hydroxyproline estimation of lung sample of different groups using GraphPad Prism software

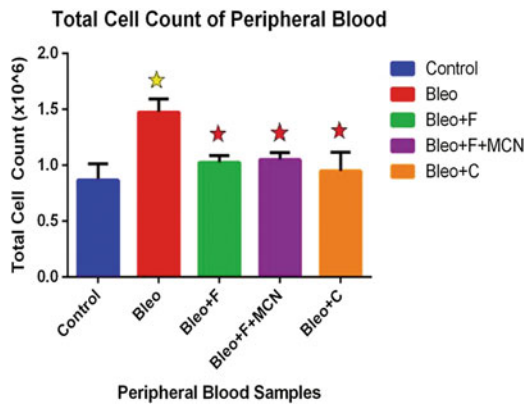
**Weight of mice**



	Control	Bleo	Bleo+F	Bleo+MCN+F	Bleo+C
1 day	24.83±2.59	25.00±2.89	25.13±0.13	22.63±2.19	27.00±1.22
7 days	24.83±2.59	21.63±2.72	25.13±0.13	24.88±0.92	24.38±1.20
14 days	27.50±3.82	21.13±3.03	25.75±0.43	25.75±0.63	26.88±0.63
21 days	27.50±3.82	23.75±1.61	25.38±1.07	26.75±0.25	25.00±1.02
28 days	27.33±2.33	25.38±1.69	23.13±0.63	24.38±1.20	25.63±0.63

**Fig. 2.2** Represents the weight of mice for each group

**Results of blood cell count**



Total cell count of peripheral blood using hemocytometer	
	TC (x 10 <sup>6</sup> )
Control	0.87 ± 0.15
Bleo	1.48 ± 0.12
Bleo+F	1.03 ± 0.06
Bleo+MCN+F	1.05 ± 0.06
Bleo+C	0.95 ± 0.17

**Fig. 2.3** Total cell count of peripheral blood of all groups using hemocytometer

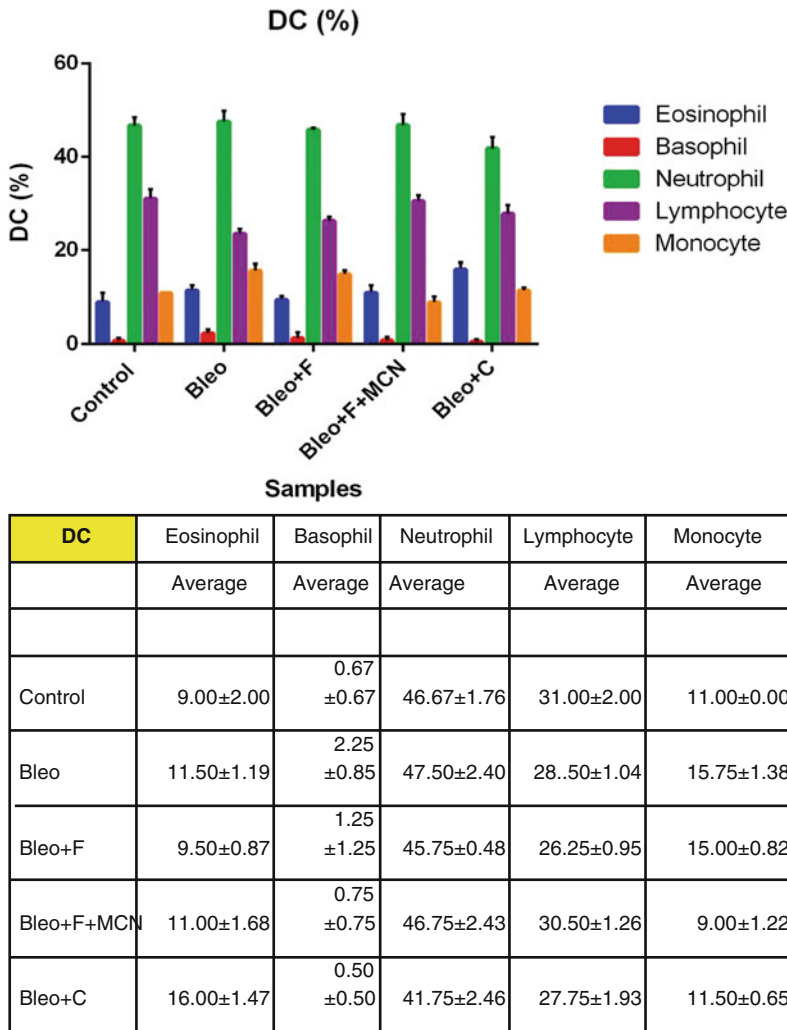


**Fig. 2.4** Differential count of peripheral blood of both control and treated individuals using cytospin

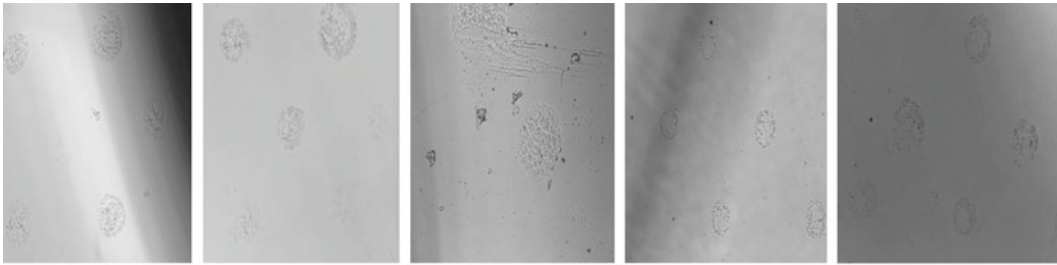
bleo-treated samples. Here, we found that the inflammatory cell count was greatly increased for bleo-treated individuals and the effectiveness of fisetin was increased after addition of MCN with it; curcumin also showed anti-inflammatory effects (Fig. 2.4).

The clonogenic potential in spleen decreases by 1.94-fold in the bleo treated as compared to control. The count decreases by 1.94-fold with fisetin, 1.07-fold with MCN + fisetin, and 1.4-fold with curcumin as compared to control. 1.80-fold increase with MCN + fisetin, and 1.38

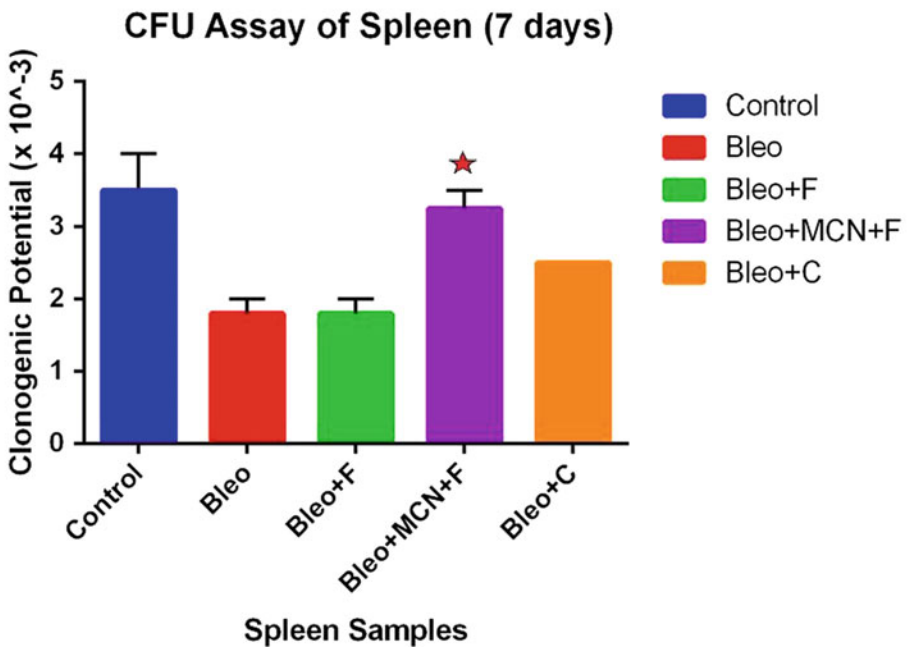
fold increase with curcumin as compared to only bleo. Bleomycin effectively inhibits the cellular recruitment to the spleen and treatment with fisetin, and curcumin increases the cellular recruitment in spleen. Colony count was also increased in MCN + F-treated groups, and it shows a statistical significance as compared to both bleo and bleo + fisetin (Fig. 2.5a).

The clonogenic potential in lung decreases by twofold significantly ( $p < 0.05$ ) than the untreated control groups after challenge with bleomycin, whereas the total number of lung progenitor cells

**(a)**  
**Colony forming unit assay:**



Control spleen    Bleo spleen    Bleo+F spleen    Bleo+MCN+F spleen    Bleo+C spleen



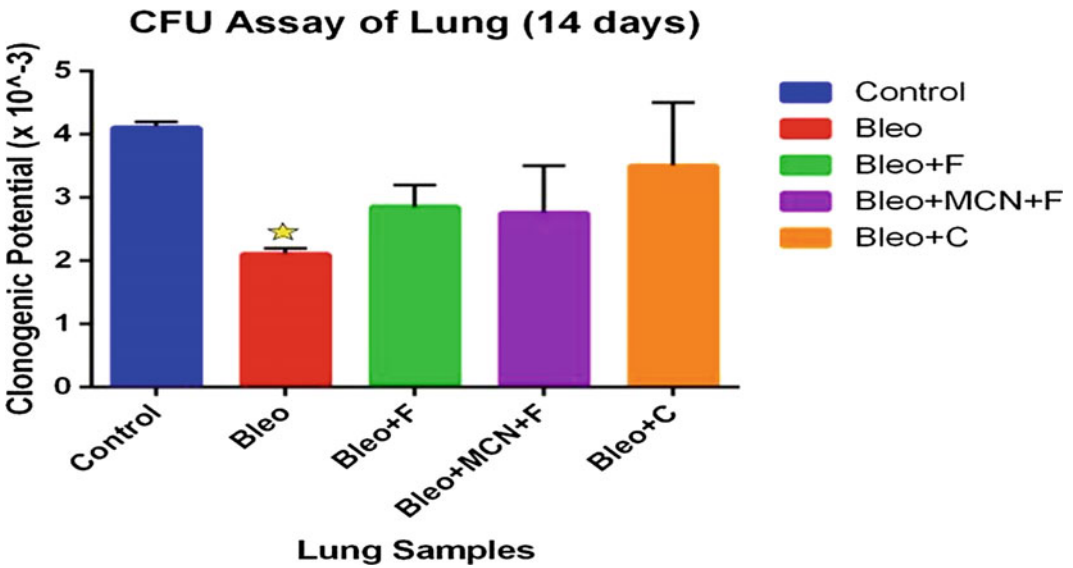
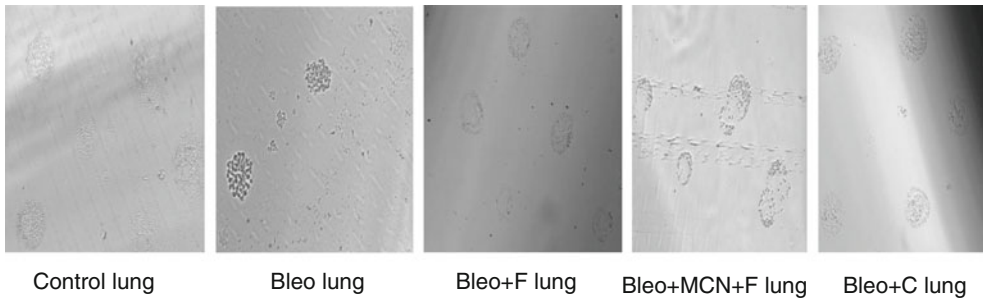
Clonogenic potential of spleen sample (1x10 <sup>3</sup> )					
	Control	Bleo	Bleo+F	Bleo+MCN+F	Bleo+C
7 days	3.50± 0.50	1.80± 0.20	1.80± 0.20	3.25±0.25	2.50± 0.00
14 days	3.75±0.75	2.75± 0.25	2.20 +0.00	3.90± 0.90	2.65± 0.15

**Fig. 2.5** **a** Clonogenic potential of spleen samples. **b** Clonogenic potential of lung sample. **c** Clonogenic potential of bone marrow sample. **d** Clonogenic potential of peripheral blood sample

increases by 1.35-fold with fisetin, 1.30-fold with MCN-loaded fisetin, and 1.66-fold with curcumin as compared to the bleo-treated groups. This

denotes that bleomycin effectively decreases the clonogenic potential of the lung cells, and fisetin, MCN-loaded fisetin, and curcumin also show its

(b)



Clonogenic potential of Lung sample (1x10 <sup>3</sup> )					
	Control	Bleo	Bleo+F	Bleo+MCN+F	Bleo+C
7 days	3.05 ± 0.45	1.35 ± 0.15	2.40 ± 0.40	2.20 ± 0.20	2.60 ± 0.40
14 days	4.10 ± 0.10	2.10 ± 0.10	2.85 ± 0.35	2.75 ± 0.75	3.50 ± 1.00

**Fig. 2.5** (continued)

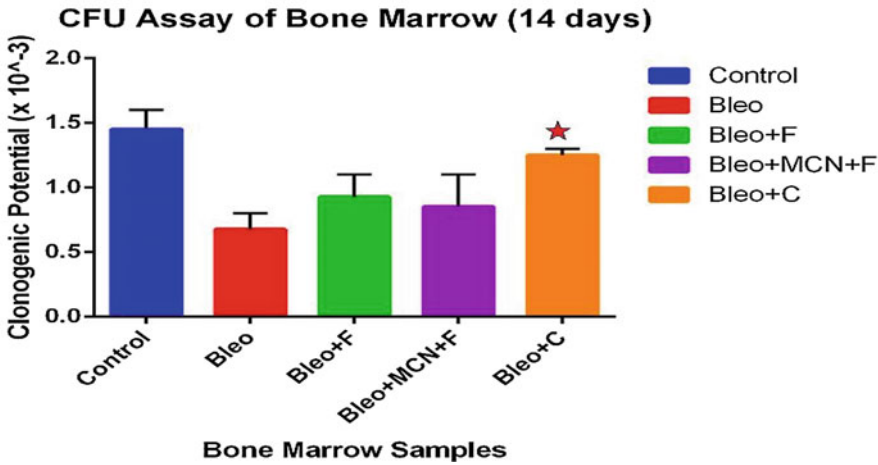
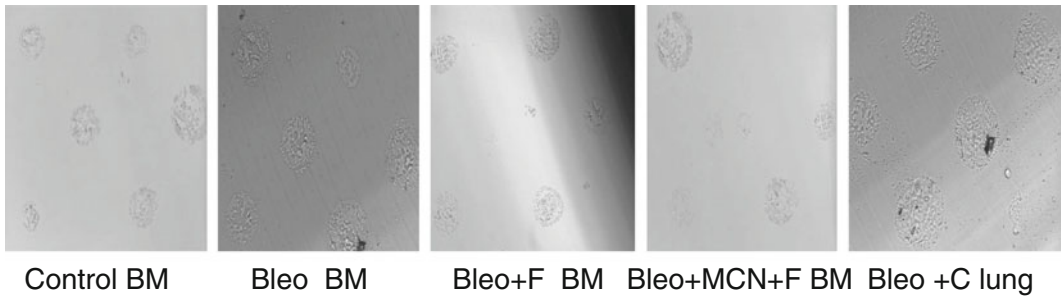
regenerative effect on it; among them, curcumin showed the best results (Fig. 2.5b).

The clonogenic potential of bone marrow (aspirated from the femur), the site of poiesis, decreases by twofold than the untreated control groups after bleomycin challenge, whereas in fisetin-treated groups, total cell number in bone

marrow increases by 1.36-fold, in MCN + fisetin-treated groups, total cell number increases by fourfold, and in curcumin-treated group by 1.83-fold when compared to only bleo. This indicates a 126.43-fold decrease with fisetin and a 2.82-fold decrease with MCN + fisetin, as compared to only Ova. This shows that the



(c)



Clonogenic potential of Bone marrow sample (1x10 <sup>3</sup> )					
	Control	Bleo	Bleo+F	Bleo+MCN+F	Bleo+C
7 days	0.87 ± 0.01	0.69 ± 0.15	0.94 ± 0.06	0.75 ± 0.05	0.82 ± 0.07
14 days	1.45 ± 0.15	0.68 ± 0.10	0.93 ± 0.18	2.75 ± 0.25	1.25 ± 1.00

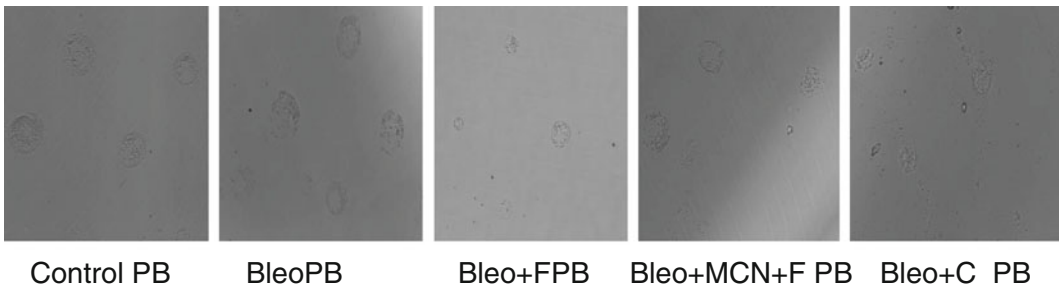
**Fig. 2.5** (continued)

synthesis of cells in the bone marrow, which decreases after challenge with bleomycin, is increased due to the treatment (Fig. 2.5c).

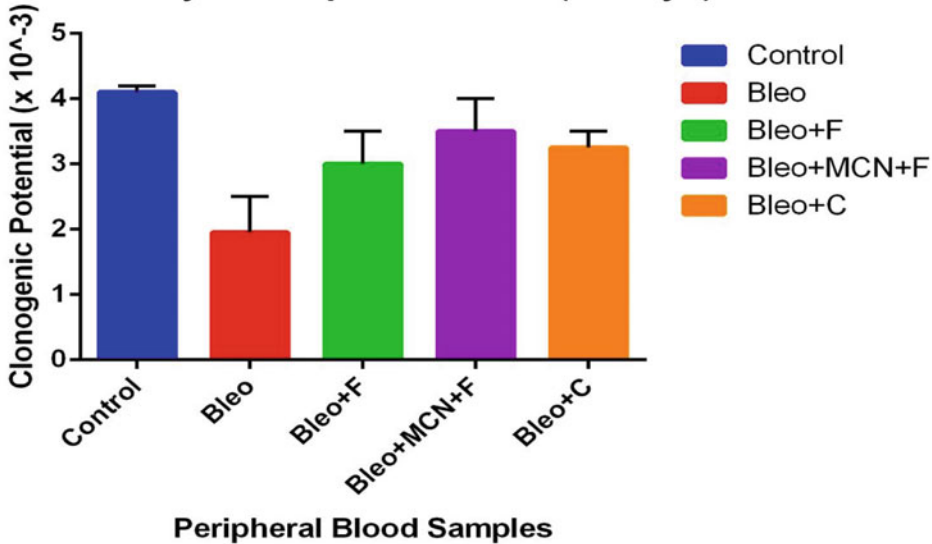
Clonogenic potential of peripheral blood was also decreased (2 fold) for bleo-treated groups, treatment with the plant flavonoids trying to show its regenerative affect against bleomycin, among

the 3 groups here MCN-loaded fisetin showed the best affect, it increases the clonogenic potential by twofold as compared to bleo-treated groups, fisetin and curcumin also showed its regenerative affect by increasing the clonogenic potential to 1.9-fold and 1.7-fold, respectively, compared to bleo-treated groups (Fig. 2.5d).

(d)



**CFU Assay of Peripheral Blood (14 days)**



Clonogenic potential of Peripheral blood sample (1x10 <sup>3</sup> )					
	Control	Bleo	Bleo+F	Bleo+MCN+F	Bleo+C
7 days	2.35 ± 0.15	2.20 ± 0.20	2.65 ± 0.15	2.50 ± 0.30	2.90 ± 0.30
14 days	4.10 ± 0.10	1.95 ± 0.55	3.00 ± 0.50	3.50 ± 0.50	3.25 ± 0.25

**Fig. 2.5** (continued)

Figure 2.6a demonstrated that, after challenging with bleomycin, there was an decrease in the levels of IL-4 (1.06-fold), IL-5 (1.16-fold), IFN-γ (1.01-fold), and TNF-α (1.08-fold) as compared to control except IL-2 (1.06-fold increase), and there was an increase in the level of cytokines with fisetin treatment (1.03-fold for

IL-2, 1.04-fold for IL-4, 1.11-fold for IL-5, 1.11-fold for IFN-γ, and 1.03-fold for TNF-α), with curcumin treatment (1.03-fold for IL-2, 1.06-fold for IL-4, 1.14-fold for IL-5, 1.29-fold for IFN-γ, and onefold for TNF-α), and with MCN + F treatment (1.03-fold for IL-2, 1.01-fold for IL-4, 1.04-fold for IL-5, 1.15-fold

for IFN- $\gamma$ , and 1.15-fold for TNF- $\alpha$ ) as compared to the bleo-treated samples.

After challenging with bleomycin, there was an decrease in the levels of IL-2 (1.36-fold), IL-4 (1.39-fold), IL-5 (1.04-fold), IFN- $\gamma$  (1.67-fold), and TNF- $\alpha$  (1.41-fold) as compared to control, and there is an increase in the level of cytokines with curcumin treatment (1.31-fold for IL-2, 1.30-fold for IL-4, 1.45-fold for IL-5,

1.35-fold for IFN- $\gamma$ , and 1.17-fold for TNF- $\alpha$ ), with fisetin treatment (1.29-fold for IL-2, 1.35-fold for IL-4, 1.29-fold for IL-5, 1.46-fold for IFN- $\gamma$ , and 1.42-fold for TNF- $\alpha$ ), and with MCN + fisetin treatment (1.38-fold for IL-2, 1.41-fold for IL-4, 1.45-fold for IL-5, 1.81-fold for IFN- $\gamma$ , and 1.44-fold for TNF- $\alpha$ ) as compared to the bleo-treated sample (Fig. 2.6b).

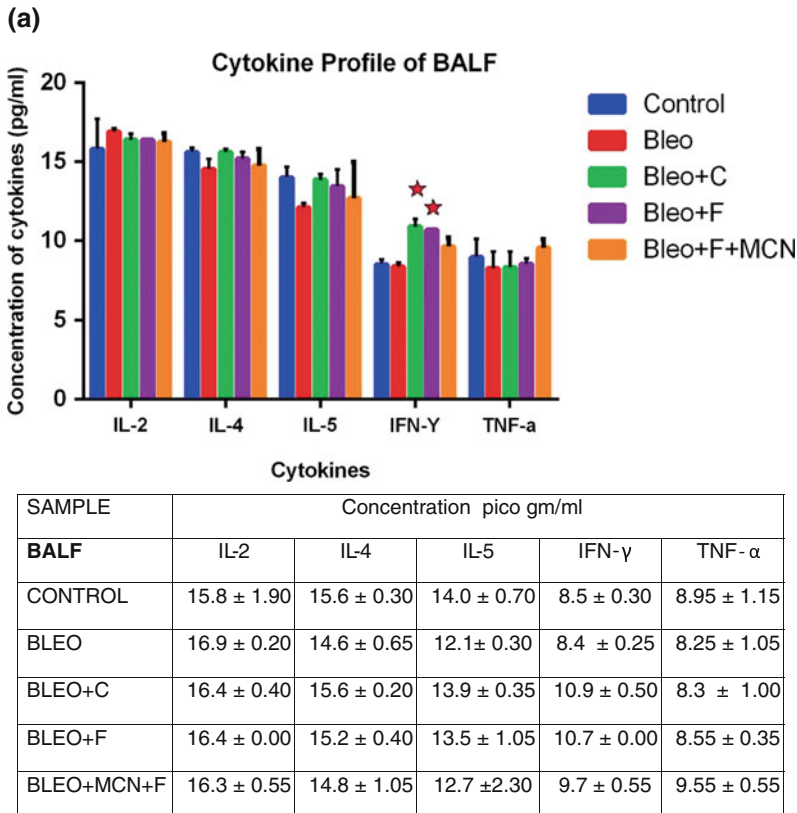
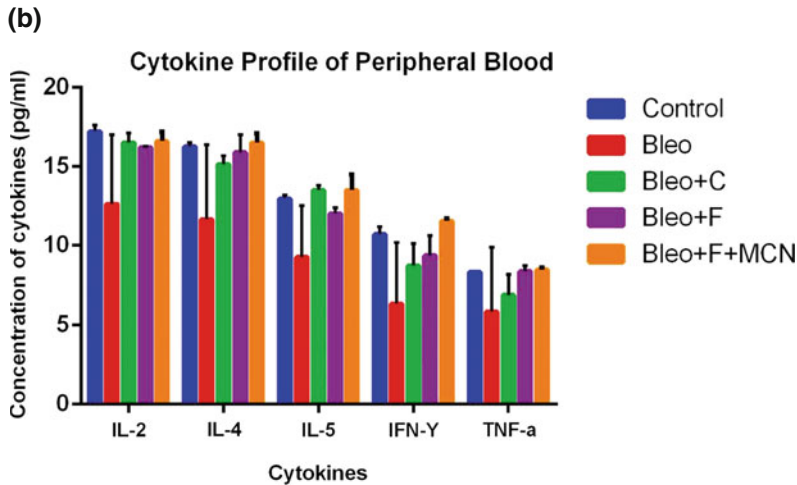


**Fig. 2.6** a Cytokine profile of BALF. b Cytokine profile of peripheral blood sample



SAMPLE	Concentration pico gm/ml				
	IL-2	IL-4	IL-5	IFN- $\gamma$	TNF- $\alpha$
<b>Peripheral blood</b>					
CONTROL	17.2 $\pm$ 0.40	16.3 $\pm$ 0.25	13.0 $\pm$ 0.25	10.7 $\pm$ 0.50	8.3 $\pm$ 0.00
BLEO	12.6 $\pm$ 4.40	11.7 $\pm$ 4.75	92.5 $\pm$ 3.25	6.4 $\pm$ 3.85	5.85 $\pm$ 4.05
BLEO+C	16.5 $\pm$ 0.60	15.2 $\pm$ 0.55	13.5 $\pm$ 0.30	8.7 $\pm$ 1.40	6.9 $\pm$ 1.30
BLEO+F	16.2 $\pm$ 0.10	15.9 $\pm$ 1.10	12.0 $\pm$ 0.40	93.50 $\pm$ 1.25	8.35 $\pm$ 0.35
BLEO+MCN+F	16.6 $\pm$ 0.60	16.5 $\pm$ 0.60	13.5 $\pm$ 1.00	11.6 $\pm$ 0.15	8.45 $\pm$ 0.15

**Fig. 2.6** (continued)

## 2.5 Discussion

For the first time, our study presents evidence that fisetin, curcumin, and mesoporous carbon nanoparticle (MCN)-loaded fisetin could be a promising therapeutic option against idiopathic pulmonary fibrosis (IPF).

Bleomycin-induced pulmonary fibrosis is a well-established disease model for IPF and widely used in the investigation of the efficacy and mechanism of therapeutic candidates [39]. IPF is a progressive interstitial pneumonia of unknown etiology, while its pathogenesis is not fully understood [40]. The risk of developing IPF is likely due to both host and environmental factors, and their elucidation may lead to

improved prevention and treatment strategies [41]. Elevated levels of TNF- $\alpha$ , a cytokine with inflammatory and fibrogenic properties, have been detected in the lungs in patients with IPF. IPF remains a major cause of morbidity and mortality around the world, and there is still a large unmet medical need. There is no definitive approach to the treatment of IPF because evidence for effective medical therapy is still lacking. A better understanding of the basic biology of IPF is crucial to enable the development of novel therapeutic agents for this disease. Animal models supported the concept not only of abnormal vascular remodeling as a pathogenic mechanism in pulmonary fibrosis (PF), with reports of newly formed vascular networks within the fibrotic lung, but also of increased

capillary irregularity and dilatation [42]. Progressive fibrosis with loss of normal lung tissue leads to restricted ventilation, impaired gas exchange, respiratory symptoms and exercise limitation, poor quality of life, and ultimately death [41]. Bleomycin is a chemotherapeutic drug used clinically for a variety of human malignancies, including lymphoma. It has been reported that administration of a high dose of bleomycin often leads to lethal lung injury and pulmonary fibrosis in human patients, as well as in rodent [19]. Therefore, it has been widely used in making pulmonary fibrosis animal models [43]. The bleomycin model has the advantage that it is quite easy to perform, widely accessible, and reproducible, and therefore fulfills important criteria expected from a good animal model [44]. Bleomycin inhibits the incorporation of thymidine, causing DNA fragmentation resulting in apoptosis with the release of chemical mediators for the recruitment of immune cells. On the other hand, the epidermal atrophy could be related to the effect of bleomycin, which has been shown to cause cessation of the epidermal cell cycle, with induction of epidermal cell apoptosis [45, 46]. The bleomycin model has contributed tremendously to elucidate the roles of cytokines, growth factors, and signaling pathways involved in pulmonary fibrosis. For instance, it has helped to determine transforming growth factor (TGF)  $\beta$  as one of the key factors in the development of pulmonary fibrosis [47].

Unfortunately, no pharmacologic therapy exists at this time that has been proven to improve survival. Due to the heterogeneity of IPF's clinical course, lack of complete understanding of the pathogenesis, and infrequency of the disease itself, there is a lack of large-scale randomized controlled trials. During the last decade, several clinical trials for IPF have been conducted worldwide to determine an effective treatment regimen for IPF, but the results have been disappointing. Clinical trial failures may arise for many reasons, including disease heterogeneity, lack of readily measurable clinical end points other than overall survival, and, perhaps most of all, a lack of understanding of the underlying molecular mechanisms of the

progression of IPF [48]. Some clinical trials are presently assessing the utility of novel agents in the treatment of IPF. Most medications are not recommended due to their side effects and lack of proven benefit [49].

Fisetin has recently received attention for its beneficial effects against several diseases. In the past years, fisetin was a subject of research because of its antiproliferative [50–52], apoptotic [52, 53], and antioxidant [54] activities. Several studies indicate that fisetin is a promising novel antioxidant. Fisetin has been reported to inhibit human low-density lipoprotein (LDL) oxidation in vitro [55]. It induced quinone oxidoreductase activity in murine hepatoma 1c1c7 cells in a time- and dose-dependent manner, and the induction of activity was associated with increase in mRNA expression. It was found that fisetin prevented LDL from oxidation, in part, through reducing CD36 gene expression in macrophages, a possible effect in ameliorating atherosclerosis [56]. Curcumin is the active ingredient in the traditional herbal remedy and dietary spice turmeric. Research has revealed that curcumin has a surprisingly wide range of beneficial properties, including anti-inflammatory, antioxidant, chemopreventive, and chemotherapeutic activity. These activities have been demonstrated both in cultured cells and in animal models and have paved the way for ongoing human clinical trials [35]. Previous report showed that curcumin inhibits the production of proinflammatory monocyte/macrophage-derived cytokines in PMA- or LPS-stimulated peripheral blood monocytes and alveolar macrophages [57]. Clinical trials of curcumin in humans have been promising. Phase I studies demonstrated virtually no toxicity in humans consuming up to 8 g curcumin per day for 3 months or a single dose of up to 12 g [58, 59]. Based on the encouraging preclinical and phase I clinical data, several additional human trials have been initiated and are currently enrolling patients. This includes trials testing the activity of curcumin in patients with colon cancer, pancreatic cancer, multiple myeloma, and myelodysplasia [32]. Nanoparticles have promising applications in medicine [60]. Recently, targeted and triggered drug delivery systems accompanied by nanoparticle technology

have emerged as prominent solutions to the bioavailability of therapeutic agents. The factors affecting the immune response are complex, including particle composition, size, surface chemistry, plasma protein binding, and exposure route. Investigation of the relationship between properties of nanoparticles and systemic immune response is crucial for their application in medicine and other areas.

In our study, we found that bleomycin is highly effective in causing fibrosis in mice as compared to control groups and the plant flavonoids also showed their antifibrotic action (Fig. 2.1). The average weights of different groups of mice were significantly different at the 0th day, and the weight of bleo-treated groups was significantly reduced mainly from the day 7 (Fig. 2.2). We demonstrated that total cell count in peripheral circulating blood increases by 1.7-fold in the bleo-treated group as compared to control. The count decreases by 1.43-fold with fisetin, 1.40-fold with MCN + fisetin, and 1.5-fold with curcumin as compared to only bleo. This indicates 1.3-fold increase with fisetin, 1.2-fold increase with MCN + fisetin, and onefold increase as compared to control-treated groups (Fig. 2.3). These indicates that after the development of fibrosis during bleomycin treatment, the total cell count was greatly increased which was decreased significantly after challenging with the plant flavonoids. In this study, the inflammatory cell count was greatly increased for bleo-treated individuals and the effectiveness of fisein was increased after addition of MCN particles with it; curcumin also showed anti-inflammatory effects (Fig. 2.4). In another experiment, bleomycin effectively inhibits the cellular recruitment to the spleen and treatment with fisetin, and curcumin increases the cellular recruitment in spleen. Colony count was also increased in MCN + fisetin-treated groups, and it was statistically significant (Fig. 2.5a). Figure 2.5b demonstrated that bleomycin effectively decreases the clonogenic potential of the lung cells, and fisetin, MCN-loaded fisetin, and curcumin also showed its regenerative effect on it; among them, curcumin showed the best results. We also observed the increased level of cytokines with fisetin treatment, with curcumin treatment,

and with MCN + fisetin treatment as compared to the bleo-treated sample (Fig. 2.6a). In other experimental assays, fisetin, curcumin, and MCN + fisetin showed promising results in bleomycin-induced idiopathic pulmonary fibrosis in mice.

It is important to emphasize that probably no single agent is going to work in this disease and that a combination, including agents fisetin and curcumin, will be necessary. Improvement of our knowledge about the biopathological principles of the disease will increase the opportunities of finding new agents.

In conclusion, idiopathic pulmonary fibrosis is a challenging, terminal disease characterized by progressive dyspnea and cough and the present research suggests that fisetin and curcumin may be a promising therapeutic agent for bleomycin-induced changes in mice with IPF. Additionally, the administration of mesoporous carbon nanoparticle-loaded fisetin enhanced the beneficial effects. This may open up new perspectives for a potential role of these drugs as a molecular target in idiopathic pulmonary fibrosis.

---

## References

1. Cottin V, Crestani B, Valeyre D, Wallaert B, Cad-ranel J, Dalphin JC, Delaval P, Israel-Biet D, Kessler R, Reynaud-Gaubert M, Aguilaniu B, Bouquillon B, Carré P, Danel C, Faivre JB, Ferretti G, Just N, Kouzan S, Lebagry F, Marchand-Adam S, Philippe B, Prévot G, Stach B, Thivolet-Béjui F, Cordier JF. French national reference centre; network of competence centres for rare lung diseases. Diagnosis and management of idiopathic pulmonary fibrosis: French practical guidelines. *Eur Respir Rev.* 2014;23(132):193–214.
2. Raghu G, Freudenberger TD, Yang S, Curtis JR, Spada C, Hayes J, Sillery JK, Pope CE 2nd, Pellegrini CA. High prevalence of abnormal acid gastro-oesophageal reflux in idiopathic pulmonary fibrosis. *Eur Respir J.* 2006;27:136–42.
3. Kondoh Y, Taniguchi H, Kawabata Y, Yokoi T, Suzuki K, Takagi K. Acute exacerbation in idiopathic pulmonary fibrosis. analysis of clinical and pathologic findings in three cases. *Chest.* 1993;103(6):1808–12.
4. Gribbin J, Hubbard RB, Le Jeune I, Smith CJ, West J, Tata LJ. Incidence and mortality of idiopathic pulmonary fibrosis and sarcoidosis in the UK. *Thorax.* 2006;61:980–5.

5. King TE Jr, Pardo A, Selman M. Idiopathic pulmonary fibrosis. *Lancet*. 2011;378:1949–61.
6. Selman M, King TE, Pardo A. Idiopathic pulmonary fibrosis: prevailing and evolving hypotheses about its pathogenesis and implications for therapy. *Ann Intern Med*. 2001;134(2):136–51.
7. Yan Z, Kui Z, Ping Z. Reviews and prospectives of signaling pathway analysis in idiopathic pulmonary fibrosis. *Autoimmun Rev*. 2014;13(10):1020–5.
8. Raghu G, Collard HR, Egan JJ, Martinez FJ, Behr J, Brown KK, Colby TV, Cordier JF, Flaherty KR, Lasky JA, Lynch DA, Ryu JH, Swigris JJ, Wells AU, Ancochea J, Bourros D, Carvalho C, Costabel U, Ebina M, Hansell DM, Johkoh T, Kim DS, King TE Jr, Kondoh Y, Myers J, Müller NL, Nicholson AG, Richeldi L, Selman M, Duden RF, Griss BS, Protzko SL, Schönemann HJ. ATS/ERS/JRS/ALAT Committee on idiopathic pulmonary fibrosis. An official ATS/ERS/JRS/ALAT statement: idiopathic pulmonary fibrosis: evidence-based guidelines for diagnosis and management. *Am J Respir Crit Care Med*. 2011;183:788–824.
9. Cottin V, Cordier JF. Velcro crackles: the key for early diagnosis of idiopathic pulmonary fibrosis? *Eur Respir J*. 2012;40:519–21.
10. Collard HR, King TE Jr, Bartelson BB, Vourlekis JS, Schwarz MI, Brown KK. Changes in clinical and physiologic variables predict survival in idiopathic pulmonary fibrosis. *Am J Respir Crit Care Med*. 2003;168:538–42.
11. Chaudhary NI, Roth GJ, Hilberg F, et al. Inhibition of PDGF, VEGF and FGF signalling attenuates fibrosis. *Eur Respir J*. 2007;29:976–85.
12. Coward WR, Saini G, Jenkins G. The pathogenesis of idiopathic pulmonary fibrosis. *Ther Adv Respir Dis*. 2010;4:367–88.
13. Wollin L, Maillet I, Quesniaux V, Holweg A, Ryffel B. Anti-fibrotic and anti-inflammatory activity of the tyrosine kinase inhibitor nintedanib in experimental models of lung fibrosis. *J Pharmacol Exp Ther*. 2014;349:209–20.
14. Barratt S, Millar A. Vascular remodelling in the pathogenesis of idiopathic pulmonary fibrosis. *QJM*. 2014;107(7):515–9.
15. Selman M, Pardo A. Role of epithelial cells in idiopathic pulmonary fibrosis: from innocent targets to serial killers. *Proc Am Thorac Soc*. 2006;3:364–72.
16. King TE Jr, Behr J, Brown KK, du Bois RM, Lancaster L, de Andrade JA, Stähler G, Leconte I, Roux S, Raghu G. BUILD-1: a randomized placebo-controlled trial of bosentan in idiopathic pulmonary fibrosis. *Am J Respir Crit Care Med*. 2008;177:75–81.
17. Taniguchi H, Ebina M, Kondoh Y, Ogura T, Azuma A, Suga M, Taguchi Y, Takahashi H, Nakata K, Sato A, Takeuchi M, Raghu G, Kudoh S, Nukiwa T. Pirfenidone clinical study group in Japan. Pirfenidone in idiopathic pulmonary fibrosis. *Eur Respir J*. 2010;35(4):821–9.
18. Moeller A, Ask K, Warburton D, Gauldie J, Kolb M. The bleomycin animal model: a useful tool to investigate treatment options for idiopathic pulmonary fibrosis? *Int J Biochem Cell Biol*. 2008;40:362–82.
19. Hoshino T, Okamoto M, Sakazaki Y, Kato S, Young HA, Aizawa H. Role of proinflammatory cytokine IL-18 and IL-1 $\beta$  in Bleomycin-induced lung injury in humans and mice. *Am J Respir Cell Mol Biol*. 2009;41(6):661–70.
20. Manali ED, Moschos C, Triantafyllidou C, Kotanidou A, Psallidas I, Karabela SP, Roussos C, Papiris S, Armaganidis A, Stathopoulos GT, Maniatis NA. Static and dynamic mechanics of the murine lung after intratracheal bleomycin. *BMC Pulm. Med*. 2011;11:33.
21. Gasse P, Mary C, Guenon I, Noulain N, Charron S, Schnyder-Candrian S, et al. IL-1R1/MyD88 signaling and the inflammasome are essential in pulmonary inflammation and fibrosis in mice. *J Clin Invest*. 2007;117:3786e99.
22. François A, Gombault A, Villeret B, Alsaleh G, Fanny M, Gasse P, Adam SM, Crestani B, Sibilia J, Schneider P, Bahram S, Quesniaux V, Ryffel B, Wachsmann D, Gottenberg JE, Couillin I. Cell activating factor is central to bleomycin- and IL-17-mediated experimental pulmonary fibrosis. *J Autoimmun*. 2015;56:1–11.
23. Chen LJ, Ye H, Zhang Q, Li FZ, Song LJ, Yang J, Mu Q, Rao SS, Cai PC, Xiang F, Zhang JC, Su Y, Xin JB, Ma WL. Bleomycin induced epithelial-mesenchymal transition (EMT) in pleural mesothelial cells. *Toxicol Appl Pharmacol*. 2015;283(2):75–82.
24. Yamazaki C, Hoshino J, Sekiguchi T, Hori Y, Miyauchi S, Mizuno S, Horie K. Production of superoxide and nitric oxide by alveolar macrophages in the bleomycin-induced interstitial pneumonia mice model. *Jpn J Pharmacol*. 1998;78(1):69–73.
25. Quideau S, Deffieux D, Douat-Casassus C, Pouységou L. Plant polyphenols: chemical properties, biological activities, and synthesis. *Angew Chem Int Ed Engl*. 2011;50(3):586–621.
26. Sahu BD, Kalvala AK, Koneru M, Mahesh Kumar J, Kuncha M, Rachamalla SS, Sistla R. Ameliorative effect of fisetin on cisplatin-induced nephrotoxicity in rats via modulation of NF- $\kappa$ B activation and antioxidant defence. *PLoS ONE*. 2014;9(9):e105070.
27. Gupta SC, Tyagi AK, Deshmukh-Taskar P, Hinojosa M, Prasad S, Aggarwal BB. Downregulation of tumor necrosis factor and other proinflammatory biomarkers by polyphenols. *Arch Biochem Biophys*. 2014;1(559):91–9.
28. Anand P, Kunnumakkara AB, Newman RA, Aggarwal BB. Bioavailability of curcumin: problems and promises. *Mol Pharm*. 2007;4(6):807–18.
29. Ammon H, Wahl MA. Pharmacology of Curcuma longa. *Planta Med*. 1991;57:1–7.
30. Aggarwal BB, Surh Y-J, Shishodia S, editors. The molecular targets and therapeutic uses of curcumin in health and disease. Heidelberg: Springer; 2007.

31. Manolova Y, Deneva V, Antonov L, Drakalska E, Momekova D, Lambov N. The effect of the water on the curcumin tautomerism: a quantitative approach. *Spectrochim Acta A Mol Biomol Spectrosc.* 2014;11(132):815–20.
32. Jiao Y, Wilkinson J 4th, Di X, Wang W, Hatcher H, Kock ND, D'Agostino R Jr, Knovich MA, Torti FM, Torti SV. Curcumin, cancer chemopreventive and chemotherapeutic agent, is a biologically active iron chelator. *Blood.* 2009;113(2):462–9.
33. Chuang SE, Kuo ML, Hsu CH, Chen CR, Lin JK, Lai GM, Hsieh CY, Cheng AL. Curcumin containing diet inhibits diethylnitrosamine induced murine hepatocarcinogenesis. *Carcinogenesis.* 2000;21:331–5.
34. Goel A, Kunnumakkara AB, Aggarwal BB. Curcumin as “Curecumin”: from kitchen to clinic. *Biochem Pharmacol.* 2008;75:787–809.
35. Hatcher H, Planalp R, Cho J, Torti FM, Torti SV. Curcumin: from ancient medicine to current clinical trials. *Cell Mol Life Sci.* 2008;65:1631–52.
36. Jobin C, Bradham CA, Russo MP, Juma B, Narula AS, Brenner DA, Sartor RB. Curcumin blocks cytokinemediated NF kappa B activation and proinflammatory gene expression by inhibiting inhibitory factor I kappa B kinase activity. *J Immunol.* 1999;163:3474–83.
37. Deeb D, Jiang H, Gao X, Al-Holou S, Danyluk AL, Dulchavsky SA, Gautam SC. Curcumin [1,7-bis(4-hydroxy-3-methoxyphenyl)-1-6-heptadine3,5-dione: C<sub>21</sub>H<sub>20</sub>O<sub>6</sub>] sensitizes human prostate cancer cells to tumor necrosis factorrelated apoptosis inducing ligand/Apo2L induced apoptosis by suppressing nuclear factor kappa B via inhibition of the prosurvival Akt signaling pathway. *J Pharmacol Exp Ther.* 2007;321:616–25.
38. Woo JH, Kim YH, Choi YJ, Kim DG, Lee KS, Bae JH, Min DS, Chang JS, Jeong YJ, Lee YH, Park JW, Kwon TK. Molecular mechanisms of curcumin induced cytotoxicity: induction of apoptosis through generation of reactive oxygen species, down-regulation of BclXL and IAP, the release of cytochrome c and inhibition of Akt. *Carcinogenesis.* 2003;24:1199–208.
39. Song JS, Kang CM, Kang HH, Yoon HK, Kim YK, Kim KH, Moon HS, Park SH. Inhibitory effect of CXC chemokine receptor 4 antagonist AMD3100 on bleomycin induced murine pulmonary fibrosis. *Exp Mol Med.* 2010;42:465–72.
40. Raghu G. Idiopathic pulmonary fibrosis: guidelines for diagnosis and clinical management have advanced from consensus-based in 2000 to evidence-based in 2011. *Eur Respir J.* 2011;37:743–6.
41. Ley B, Collard HR. Epidemiology of idiopathic pulmonary fibrosis. *Clin Epidemiol.* 2013;25(5):483–92.
42. Peao MN, Aguas AP, de Sa CM, Grande NR. Neof ormation of blood vessels in association with rat lung fibrosis induced by bleomycin. *Anat Rec.* 1994;238:57–67.
43. Lee R, Reese C, Bonner M, Tourkina E, Hajdu Z, Riemer EC, Silver RM, Visconti RP, Hoffman S. Bleomycin delivery by osmotic minipump: similarity to human scleroderma interstitial lung disease. *Am J Physiol Lung Cell Mol Physiol.* 2014;306:L736–48.
44. Mouratis MA, Aidinis V. Modeling pulmonary fibrosiswith bleomycin. *Curr Opin Pulm Med.* 2011;17:355–61.
45. Juniantito V, Izawa T, Yuasa T, Ichikawa C, Tanaka M, Kuwamura M, Yamate J. Immunophenotypical analysis of myofibroblasts and mesenchymal cells in the bleomycin-induced rat scleroderma, with particular reference to their origin. *Exp Toxicol Pathol.* 2013;65:567–77.
46. Kandeel S, Balaha M. The possible protective effect of simvastatin and pioglitazone separately and in combination on bleomycin-induced changes in mice thin skin. *Tissue Cell.* 2015.
47. Zhao J, Shi W, Wang YL, Chen H, Bringas P Jr, Datto MB, Frederick JP, Wang XF, Warburton D. Smad3 deficiency attenuates bleomycin induced pulmonary fibrosis in mice. *Am J Physiol Lung Cell Mol Physiol.* 2002;282(3):L585–93.
48. Camelo A, Dunmore R, Sleeman MA, Clarke DL. The epithelium in idiopathic pulmonary fibrosis: breaking the barrier. *Front Pharmacol.* 2014;10(4):173.
49. Kekevan A, Gershwin ME, Chang C. Diagnosis and classification of idiopathic pulmonary fibrosis. *Autoimmun Rev.* 2014;13(4–5):508–12.
50. Khan N, Asim M, Afaq F, Abu Zaid M, Mukhtar H. A novel dietary flavonoid fisetin inhibits androgen receptor signaling and tumor growth in athymic nude mice. *Cancer Res.* 2008;68:8555–63.
51. Haddad AQ, Venkateswaran V, Viswanathan L, Teahan SJ, Fleshner NE, Klotz LH. Novel antiproliferative flavonoids induce cell cycle arrest in human prostate cancer cell lines. *Prostate Cancer Prostatic Dis.* 2006;9:68–76.
52. Suh Y, Afaq F, Johnson JJ, Mukhtar H. A plant flavonoid fisetin induces apoptosis in colon cancer cells by inhibition of COX2 and Wnt/EGFR/NF-kappa B-signaling pathways. *Carcinogenesis.* 2009;30:300–7.
53. Sung B, Pandey MK, Aggarwal BB. Fisetin, an inhibitor of cyclin-dependent kinase 6, down-regulates nuclear factor kappa B-regulated cell proliferation, antiapoptotic and metastatic gene products through the suppression of TAK-1 and receptor-interacting protein-regulated I kappa B alpha kinase activation. *Mol Pharmacol.* 2007;71:1703–14.
54. Hou DX, Fukuda M, Johnson JA, Miyamori K, Ushikai M, Fujii M. Fisetin induces transcription of NADPH: quinone oxidoreductase gene through an antioxidant responsive element-involved activation. *Int J Oncol.* 2001;18:1175–9.
55. Myara I, Pico I, Védie B, Moatti N. A method to screen for the antioxidant effect of compounds on low-density lipoprotein (LDL): illustration with flavonoids. *J Pharmacol Toxicol Methods.* 1993;30:69–73.
56. Lian TW, Wang L, Lo YH, Huang IJ, Wu MJ. Fisetin, morin and myricetin attenuate CD36 expression and



- oxLDL uptake in U937-derived macrophages. *Biochim Biophys Acta*. 2008;1781:601–9.
57. Abe Y, Hashimoto S, Horie T. Curcumin inhibition of inflammatory cytokine production by human peripheral blood monocytes and alveolar macrophages. *Pharmacol Res*. 1999;39:41–7.
58. Hsu CH, Chuang SE, Hergenahn M, Kuo ML, Lin JK, Hsieh CY, Cheng AL. Preclinical and early phase clinical studies of curcumin as chemopreventive agent for endemic cancers in Taiwan. *Gan To Kagaku Ryoho*. 2002;29(Suppl 1):194–200.
59. Lao CD, Ruffin MT 4th, Normolle D, Heath DD, Murray SI, Bailey JM, Boggs ME, Crowell J, Rock CL, Brenner DE. Dose escalation of a curcuminoid formulation. *BMC Complement Altern Med*. 2006;6:10.
60. Jiao Q, Li L, Mu Q, Zhang Q. Immunomodulation of nanoparticles in nanomedicine applications. *Biomed Res Int*. 2014;2014:426028.

---

### Abstract

Peritonitis is defined as an inflammation of the serosal membrane that lines the abdominal cavity and the organs contained therein. The peritoneum, which is an otherwise sterile environment, reacts to various pathologic stimuli with a fairly uniform inflammatory response. Depending on the underlying pathology, the resultant peritonitis may be infectious or sterile (i.e., chemical or mechanical). The pathophysiology of peritonitis is complicated and is involved in various processes, of which, the most important one is the inflammatory reaction. During the pathological process of the peritonitis, NF- $\kappa$ B plays an activating role in the inflammatory reaction, which might be a potential therapeutic target in the future clinical work. The aim of the study was to test the anti-inflammatory and proregenerative actions of fisetin, a flavonol found in many plants, in a mouse model of thioglycollate-induced peritonitis as well as the actions of fisetin administered with a nanoparticle such as mesoporous carbon nanoparticle (MCN). BALB/c mice were used in this study. We found cell recruitment in the blood increases with the administration of TG after 24, 48, and 96 h, showing that it has induced inflammation. Cell recruitment is successfully inhibited by fisetin after 24 h ( $p < 0.05$ ), and with MCN + fisetin after 48 h ( $p < 0.05$ ). In the peritoneal fluid, total cell recruitment has increased after 24 h ( $p < 0.05$ ), which is successfully inhibited with fisetin treatment after 96 h. TG treatment has significantly reduced cell proliferation in the blood, PF and BM, within 24 h, till 96 h. Interestingly, cell proliferation has increased with fisetin treatment after 24 h, and with MCN + fisetin after 24 h (in PF) and after 48 h (in PB and BM). The clonogenic potential of the tissues decreases significantly within 24 h, with administration of TG. Both fisetin treatment and MCN + fisetin treatment have restored the

---



Therapeutic use of fisetin and fisetin loaded on mesoporous carbon nanoparticle (MCN) in thioglycollate-induced peritonitis.

clonogenic potential of the tissues after 24 h. There was a decrease in Th2 cytokines with TG treatment, in blood after 48 h and fisetin and MCN + fisetin has increased the cytokine content. In conclusion, we found that fisetin had a promising therapeutic effect on the peritonitis.

#### Abbreviations

TG	Thioglycollate
F	Only fisetin
MF	Fisetin loaded on MCN
TG24, TG48, TG72, TG96	Treatment with only TG; kill after 24, 48, 72, 96 h, respectively
TG24F, TG48F, TG72F, TG96F	Treatment with TG, followed by fisetin; kill after 24, 48, 72, 96 h, respectively
TG24MF, TG48MF, TG72MF, TG96MF	Treatment with TG, followed by MF; kill after 24, 48, 72, 96 h, respectively
PB	Peripheral blood sample
PF	Peritoneal fluid sample
BM	Bone marrow sample
TC	Total cell count
DC	Differential cell count
PMN Cells	Polymorphonuclear cells
MN Cells	Mononuclear cells
NO	Nitric oxide
MTS	[3-(4, 5-dimethyl thiazol-2-yl)-5-(3-carboxy methoxy phenyl)-2-(4-sulfohenyl)-2H-tetrazolium, inner salt]
PMS	Phenazine methosulfate
CFU-c	Colony-forming units in culture
MPK	Milligram per kilogram of body weight

#### Symbols

-  Denotes significance in samples compared to control
-  Denotes significance in samples compared to samples treated with only TG

### 3.1 Introduction

Peritonitis is the inflammation of the peritoneum, which is the thin tissue that lines the inner wall of the abdomen, and covers most of the abdominal organs. Infected peritonitis is caused by perforation of part of the *gastrointestinal (GI)* tract, by disruption of the peritoneum or by systemic infections. Local intra-abdominal focus of inflammation caused by the microorganisms can

promote the synthesis and secretion of massive inflammatory cytokines, which would destroy the endothelial junctions and provide access for bacteria into the systemic circulation leading to lethal bacteremia [1, 2]. A more severe inflammatory response process usually indicates a much higher mortality. The oxidative stress induced by the direct effect of bacteria and indirect effect of inflammation also contributes to the severity of peritonitis [3]. The

microorganisms and their components can immediately activate the transcription factors—nuclear factor- $\kappa$ B (NF- $\kappa$ B). NF- $\kappa$ B can initiate gene expression of cytokines, adhesion molecules, chemokines, and cytotoxic enzymes, which are considered to be directly responsible for the organ injury and death [4–8]. Non-infected peritonitis may be caused by leakage of sterile body fluids into the peritoneum, or by sterile abdominal surgery, which may inadvertently leave behind foreign bodies. In normal conditions, the peritoneum appears grayish and glistening; it becomes dull 2–4 h after the onset of peritonitis, initially with scarce serous or slightly turbid fluid. Later on, the exudate becomes creamy and evidently suppurative. Although high-class antibiotics and advanced intensive care have proven to be effective on the treatment, the morbidity and mortality remain kept at a high level [9, 10].

Inflammation is part of the complex biological response of vascular tissues to harmful stimuli, such as pathogens, damaged cells, or irritants [11, 12]. It is a protective mechanism by the organism to eliminate injurious stimuli and to initiate the healing process. Inflammation is a mechanism of innate immunity [13, 14]. Acute inflammation is the initial response of the body to harmful stimuli and is achieved by the increased movement of plasma and leukocytes from the blood into the injured tissues. Prolonged inflammation, known as chronic inflammation, leads to a progressive shift in the type of cells present at the site of inflammation and is characterized by simultaneous destruction and healing of the tissue from the inflammatory process. The process of acute inflammation is initiated by cells already present in all tissues, mainly resident macrophages, dendritic cells, histiocytes, Kupffer cells, and mastocytes. At the onset of an infection, these cells are activated and release inflammatory mediators, which are responsible for the clinical signs of inflammation [15]. Inflammation leads to increased production of reactive species such as reactive oxygen species (ROS), nitric oxide synthase (NOS), and their product peroxynitrite ( $\text{ONO}_2^-$ ) by activated

macrophages. This increase in oxidative stress leads to decrease in effectiveness of oxidant defenses, that is, reduction in antioxidants.

Due to the various side effects and other complications of modern medicine, the use of traditional medicines and natural products is gaining popularity. Phytochemicals from fruits are being exploited as possible sources of therapeutic agents. Different biological activities of these chemicals, including their antioxidant properties and their anti-inflammatory properties, have been tested in vitro, as well as in vivo [16–18]. Nanomaterials, either as nanodrugs or as nanovehicles, have the advantages of being small devices that are less invasive than normal medicines, that can be targeted to reach a particular site, and that can possibly be implanted inside the body; also biochemical reaction times are much shorter. These devices are faster and more sensitive than typical drug delivery [19–21].

The aim of our study was to test the anti-inflammatory and proregenerative actions of fisetin, a flavonol found in many plants, including strawberries and apples, in a mouse model of thioglycollate-induced peritonitis. It protects against oxidative stress-induced cell death, by upregulating expression of heme oxygenase 1 (HO-1). We also aimed to test whether the anti-inflammatory and proregenerative actions of fisetin were enhanced when it was administered with a nanovehicle such as mesoporous carbon nanoparticle (MCN).

---

## 3.2 Materials and Methods

**Reagents and Materials** Sodium thioglycollate, fetal bovine serum (FBS), RBC lysis buffer, Iscove's modified Dulbecco's media (IMDM), powdered methyl cellulose, and penicillin–streptomycin were bought from Himedia, India. EDTA, methanol, sulfanilamide, and NED were bought from Sisco Research Laboratory (SRL), India. DMEM from Gibco, murine stem cell factor (SCF) from Biovision, and bovine serum albumin (BSA) from Biosera were used.

Ortho-phosphoric acid and  $\text{NaNO}_2$  were purchased from Merck, India. 1X phosphate buffered saline (PBS) was prepared using 137 mM NaCl (Merck, India), 2.7 mM KCl (Himedia, India), 10 mM  $\text{Na}_2\text{HPO}_4$  (Qualigens, India), and 2 mM  $\text{KH}_2\text{PO}_4$  (Himedia, India).

The 24-well plates and 96-well plates were obtained from Nest Biotech Co. Ltd., China. Dispovan syringes were used to obtain blood and peritoneal fluid. Smears for cell counting were prepared using cytospin (Centurion Scientific C2 series) after centrifuging the sample in a cold centrifuge (Vision VS-15000CFN). Smears were observed under a light microscope (Debro DX-200). Absorbance readings were taken in a multiplate reader (Thermo Fisher Multiskan EX). Plates were incubated in a  $\text{CO}_2$  incubator (Thermo Fisher), and colonies in CFU assay were observed using Fluid Cell Imaging Station (Life Technologies, India). All cell culture work was done inside the biosafety cabinet.

**Animals** BALB/c mice were used in this study. All experiments were performed according to the rules laid down by the institutional and departmental animal ethics committee and the animals housed under specific pathogen-free conditions at the animal housing vivarium of the Department of Zoology, University of Calcutta. All data are presented as mean  $\pm$  SEM, and only p values of less than 0.05 have been considered.

**Induction of Peritonitis** 39 BALB/c mice (6–8 week old, weighing 25 gm) were divided into 13 groups ( $n = 3$ ): control, TG24, TG24F, TG24MF, TG48, TG48F, TG48MF, TG72, TG72F, TG72MF, TG96, TG96F, and TG96MF. 400  $\mu\text{l}$  of 3 % thioglycollate (TG) was injected intraperitoneally (200  $\mu\text{l}$  near each hind leg).

**Treatment with Fisetin and Fisetin loaded onto MCN** 1 h after treatment with TG, mice from four groups (TG24F, TG48F, TG72F, and TG96F) were given 40  $\mu\text{l}$  of 2  $\mu\text{M}/\text{kg}$  (0.57 MPK) fisetin orally. 1 h after treatment with TG, mice from the other four groups (TG24MF, TG48MF, TG72MF, and TG96MF) were given 40  $\mu\text{l}$  of a 1:1

mixture of 2  $\mu\text{M}/\text{kg}$  (0.57 MPK) fisetin and 5.1 mg/ml MCN. Mice were killed after 24, 48, 72, and 96 h, and tissues were collected.

**Peripheral Blood (PB)** Blood was collected, with EDTA to prevent clotting, in DMEM. For cell counting, blood was collected in RBC lysis buffer, kept at room temperature for 5 min, then flushed with 1X PBS, and centrifuged at 4000 rpm for 5 min at 4 °C. The supernatant was discarded, and the pellet was dissolved in 1X PBS and stored at 4 °C.

**Peritoneal Fluid (PF)** 2 ml of 1X PBS was slowly injected into the peritoneal cavity, and the cavity was massaged well to wash the cavity extensively. A 5-ml syringe was inserted into the side of the mouse, and the plunger slowly pulled out to retrieve the maximal amount of peritoneal fluid. The PF was collected in DMEM medium.

**Bone Marrow (BM)** The bone of the hind leg of the mouse was taken into the biosafety cabinet and flushed with DMEM till the bone turned white.

**Total and Differential Cell Count (TC/DC)** Differential white blood cell count is an examination and enumeration of the distribution of leukocytes in a stained blood smear. Increases in any of the normal leukocyte types or the presence of immature leukocytes or erythrocytes in peripheral blood are important diagnostically in a wide variety of inflammatory disorders.

The normal ranges of the leukocytes are follows:

- Neutrophils: 50–70 %,
- Lymphocytes: 20–40 %,
- Eosinophils: 0–6 %,
- Monocytes: 2–6 %,
- Basophils: 0–1 %.

The smear is stained with hematoxylin and counterstained with eosin.

Quickly, 100  $\mu\text{l}$  of each sample was added to appropriate wells of the cytospin, and the slides and filters were placed in the correct slots of the cytospin. The slides were centrifuged at 2000 rpm for 3 min. The slides were removed and air-dried. They were then fixed with methanol, and air-dried before staining. The fixed

slides were placed in 100 % ethanol in a Coplin jar for 5 min, followed by 10 min in 90 % ethanol. They were then stained with hematoxylin for 5 min, rinsed in 70 % ethanol, counterstained with eosin for 2 min, and again rinsed in 70 % ethanol. Then, they were placed in 100 % ethanol for 1 min, and then observed under the microscope.

The total cell count (TC) was plotted against each sample. The differential cell count (DC) was also plotted against each sample.

**Determination of Nitric Oxide Content (NO Assay)** Activation of immune system is associated with increase in macrophage NO production. Transient nature of NO makes it unsuitable for detection, but it is oxidized to nitrite ( $\text{NO}_2^-$ ) and nitrate ( $\text{NO}_3^-$ ) by nitrate reductase. The concentrations of these anions are used as quantitative measure of NO production using the Griess reaction. In this reaction, acidified  $\text{NO}_2^-$  produces a nitrosating agent, which reacts with sulfanilic acid to produce diazonium ion. This ion couples with NED (*N*-1-naphthyl ethylene diamine dihydrochloride) to form a colored product that is measured spectrophotometrically at 540 nm.

The reaction was standardized using different concentrations of  $\text{NaNO}_2$  (100, 50, 25, 12.5, 6.25, 3.13, 1.56, and 0  $\mu\text{M}$ ), using the method in Promega User Guide (Product G2930). 50  $\mu\text{l}$  of cells from each sample (PB, PF and BM) from all the groups (Control, TG24, TG24F, TG24MF, TG48, TG48F, TG48MF, TG72, TG72F, TG72MF, TG96, TG96F, and TG96MF) were plated in the wells of a 96-well plate. The cells were incubated for 24 h, in a  $\text{CO}_2$  incubator at 5 %  $\text{CO}_2$ , 37 °C. Sulfanilamide solution was prepared by dissolving 1 % sulfanilamide in 5 % ortho-phosphoric acid. 0.1 % NED solution was prepared in distilled water. 50  $\mu\text{l}$  of sulfanilamide solution was added to each well and incubated at room temperature for 5 min, in dark. 50  $\mu\text{l}$  of NED solution was then added and incubated at room temperature for 5 min, in dark. Absorbance was measured in a plate reader at 540 nm. Using the standard curve prepared, the absorbance values of the samples were plotted to get the concentrations of NO produced (in  $\mu\text{M}$ ). The concentrations of NO were plotted against each sample.

**Cell Proliferation Assay (MTS Assay)** The MTS assay is a colorimetric method for determining the number of viable cells in culture. It uses solutions of a novel tetrazolium compound MTS [3-(4, 5-dimethyl thiazol-2-yl)-5-(3-carboxy methoxy phenyl)-2-(4-sulfophenyl)-2H-tetrazolium, inner salt] and an electron-coupling reagent PMS (Phenazine Methosulfate). MTS is bioreduced by cells into a formazan product that is soluble in tissue culture medium. Absorbance of formazan is measured at 490 nm. The conversion of MTS to aqueous soluble formazan is accomplished by dehydrogenase enzymes found in metabolically active cells. Quantity of formazan product, as measured by the absorbance at 490 nm, is directly proportional to the number of living cells in culture. The assay was standardized using various numbers of cells ( $0.5 \times 10^5$ ,  $1.0 \times 10^5$ ,  $0.5 \times 10^6$ ,  $1.0 \times 10^6$ ,  $0.5 \times 10^7$  and  $1.0 \times 10^7$  cells per well), using the Promega CellTiter 96<sup>®</sup> Aqueous Non-Radioactive Cell Proliferation Assay Kit. 100  $\mu\text{l}$  of cells (PB, PF, and BM) from all the samples were added to the wells of a 96-well plate and incubated for 1 h in a  $\text{CO}_2$  incubator at 5 %  $\text{CO}_2$ , 37 °C. 20  $\mu\text{l}$  of MTS/PMS solution was added to each well and incubated in a  $\text{CO}_2$  incubator for 1–4 h. Absorbance was measured immediately in a plate reader at 490 nm.

Using the standard curve, the absorbance values of the samples were plotted to get the number of cells in each well. Numbers of cells were plotted against each sample.

**Determination of Clonogenic Potential of Cells (CFU-c Assay)** Colony-forming units in culture (CFU-c) assay measures the clonogenic potential of cells. The assay is based on the ability of cells to proliferate and differentiate into colonies in a semisolid medium, in response to cytokine stimulation. The colonies formed can be enumerated and characterized according to their unique morphology.

Number of cells per well taken was  $1 \times 10^6$ . For PF,  $10^5$  cells were taken per well. CFU-c media was prepared using IMDM, supplemented with 30 % FBS, 10 % BSA, 1 % penicillin–streptomycin and 5 ng/ml murine SCF. Lastly,

1.5 % methylcellulose was added into the concoction. 1 ml CFU-c assay media and 500  $\mu$ l cell suspension was plated in each 24-well cell culture plate. The plates were kept in CO<sub>2</sub> incubator at 5 % CO<sub>2</sub> and 37 °C. All colony types were counted after 7 days using Fluid Cell Imaging Station and pooled to get total CFU-c. A graph of clonogenic potential versus samples was plotted for each tissue sample.

**Cytokine analysis of BAL fluid** The BD CBA Mouse Th1/Th2 Cytokine Kit (Catalog No. 551287) was used to measure interleukin-2 (IL-2), interleukin-4 (IL-4), interleukin-5 (IL-5), interferon- $\gamma$  (IFN-  $\gamma$ ), and tumor necrosis factor (TNF) protein levels in BAL fluid samples. Bead array technology was used to simultaneously detect multiple cytokines in samples. Five bead populations with distinct fluorescent intensities are coated with capture antibodies, specific for the above-mentioned proteins. The beads are mixed to form the bead array and resolved in a red channel of a flow cytometer. After addition of the samples to the sample assay tubes containing the capture beads, the mouse Th1/Th2 PE detection reagent was added to each tube. The tubes were incubated for 1 h at room temperature, in the dark, and then washed with 1 ml of wash buffer (centrifuge at 200 g for 5 min). The supernatant is carefully discarded and 300  $\mu$ l of wash buffer added to resuspend the bead pellet.

### 3.3 Results

- TC of PB:** The TC of blood has increased 1.94-fold ( $p < 0.05$ ) after 24 h, 1.57-fold after 48 h, and 1.94-fold ( $p < 0.05$ ) after 96 h, on treatment with TG, as compared to untreated control groups. With fisetin treatment, the TC has decreased 1.06-fold ( $p < 0.05$ ) after 24 h, but has increased 1.24-fold after 48 h, 2.21-fold after 72 h and 1.04-fold after 96 h, compared to only TG. With MCN + fisetin treatment, the TC has decreased 1.11-fold ( $p < 0.05$ ) after 48 h, but has increased 1.29-fold after 24 h, 1.89-fold after 72 h, and 1.62-fold after 96 h.

**Table 3.1** Total cell count of blood samples, taken by hemocytometry

Treatment	Avg. cell count ( $\times 10^6/\text{ml}$ )	Fold change	
		wrt control	wrt TG
Control	0.53 $\pm$ 0.03		
TG24	1.03 $\pm$ 0.03	<b>+1.94*</b>	
TG24F	0.97 $\pm$ 0.03		<b>-1.06*</b>
TG24MF	1.33 $\pm$ 0.09		+1.29
TG48	0.83 $\pm$ 0.09	<b>+1.57</b>	
TG48F	1.03 $\pm$ 0.09		+1.24
TG48MF	0.75 $\pm$ 0.05		<b>-1.11*</b>
TG72	0.53 $\pm$ 0.03	1.00	
TG72F	1.17 $\pm$ 0.09		+2.21
TG72MF	1.00 $\pm$ 0.06		+1.89
TG96	1.03 $\pm$ 0.03	<b>+1.94*</b>	
TG96F	1.07 $\pm$ 0.03		+1.04
TG96MF	1.67 $\pm$ 0.09		+1.62

There is a 1.06-fold decrease ( $p < 0.05$ ) with fisetin treatment, and a 1.11-fold decrease ( $p < 0.05$ ) with MCN + fisetin treatment

Bold represents significant (statistically or not)

\* denotes statistically significant change

This shows that cell recruitment increases in response to the inflammatory stimulus, as TG induces a systemic inflammation. Fisetin and MCN + fisetin both successfully inhibit cell recruitment, but while it takes 24 h for fisetin alone to take effect, it takes MCN-fisetin longer (Table 3.1; Fig. 3.1).

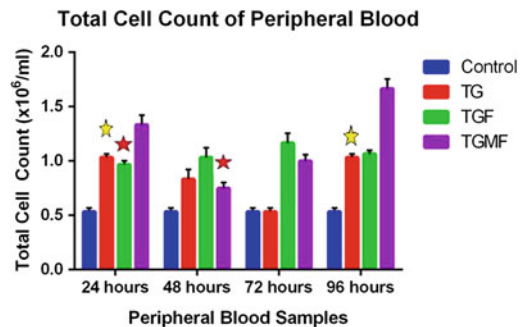


**Fig. 3.1** Effect of fisetin and MCN + fisetin on total cell count of peripheral blood

2. **TC of PF:** The TC of blood has increased 1.53-fold ( $p < 0.05$ ) after 24 h, but has decreased 1.21-fold after 48 h, 1.75-fold after 72 h, and 1.15-fold after 96 h, on treatment with TG, as compared to untreated control groups. With fisetin treatment, the TC has decreased 1.05-fold after 96 h, but has increased 1.07-fold after 24 h, 1.65-fold after 48 h, and 3.11-fold after 72 h, compared to only TG. With MCN + fisetin treatment, the TC has increased 1.02-fold after 24 h, 1.27-fold after 48 h, 2.40-fold after 72 h, and 1.69-fold after 96 h. This shows that cell recruitment increases after 24 h in response to the inflammatory stimulus, as TG induces a systemic inflammation. Fisetin successfully inhibit cell recruitment, but it takes 96 h for fisetin alone to take effect. MCN + fisetin has not been very successful in inhibiting cell recruitment (Table 3.2; Fig. 3.2).
- a. **DC (PMN Cells) of PB**—The count of polymorphonuclear (PMN) cells in the blood—eosinophils, basophils, and neutrophils, has increased 1.03-fold after 48 h, 1.28-fold

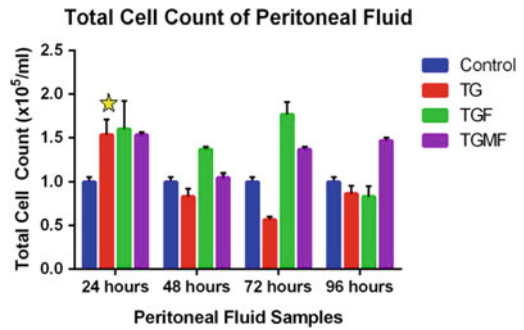


**Fig. 3.2** Effect of fisetin and MCN + fisetin on total cell count of peritoneal fluid

( $p < 0.05$ ) after 72 h, and 1.14-fold after 96 h, but has decreased 1.24-fold after 24 h. This indicates an influx of inflammatory cells in the blood in response to TG administration. Cell recruitment is successfully inhibited after 72 h, where there is a 1.09-fold decrease ( $p < 0.05$ ) with fisetin, and a 1.04-fold decrease with MCN + fisetin, as compared to only TG (Table 3.3; Fig. 3.3).

- b. **DC (MN Cells) of PB:** The count of mononuclear (MN) cells in the blood—

**Table 3.2** Total cell count of peritoneal fluid samples, taken by hemocytometry

Treatment	Avg. cell count (x10 <sup>5</sup> /ml)	Fold change	
		wrt control	wrt TG
Control	1.00 ± 0.06		
TG24	1.53 ± 0.18	<b>+1.53*</b>	
TG24F	1.60 ± 0.32		+1.07
TG24MF	1.53 ± 0.03		+1.02
TG48	0.83 ± 0.09	-1.21	
TG48F	1.37 ± 0.03		+1.65
TG48MF	1.05 ± 0.05		+1.27
TG72	0.57 ± 0.03	-1.75	
TG72F	1.77 ± 0.15		+3.11
TG72MF	1.37 ± 0.03		+2.40
TG96	0.87 ± 0.09	-1.15	
TG96F	0.83 ± 0.12		<b>-1.05</b>
TG96MF	1.47 ± 0.03		+1.69

There is a 1.05-fold decrease with fisetin treatment

**Table 3.3** Differential count of PMN cells in peripheral blood, seen after HE staining, under light microscope

Treatment	Polymorphonuclear cells			
	Avg. cell count (x10 <sup>5</sup> /ml)	% of TC	Fold change	
			wrt control	wrt TG
Control	4.97 ± 0.37	49.15		
TG24	3.97 ± 0.19	39.56	-1.24	
TG24F	5.80 ± 0.51	54.08		+1.37
TG24MF	5.55 ± 0.28	55.95		+1.41
TG48	5.00 ± 0.12	50.70	<b>+1.03</b>	
TG48F	6.05 ± 0.05	60.50		+1.19
TG48MF	5.77 ± 0.02	57.70		+1.10
TG72	6.23 ± 0.10	63.00	<b>+1.28*</b>	
TG72F	5.80 ± 0.03	58.00		<b>-1.09*</b>
TG72MF	6.10 ± 0.20	61.00		<b>-1.04</b>
TG96	5.62 ± 0.03	56.20	<b>+1.14</b>	
TG96F	5.78 ± 0.27	57.80		+1.03
TG96MF	5.67 ± 0.13	56.70		+1.01

There is a 1.09-fold decrease ( $p < 0.05$ ) with fisetin, and a 1.04-fold decrease with MCN + fisetin, after 72 h



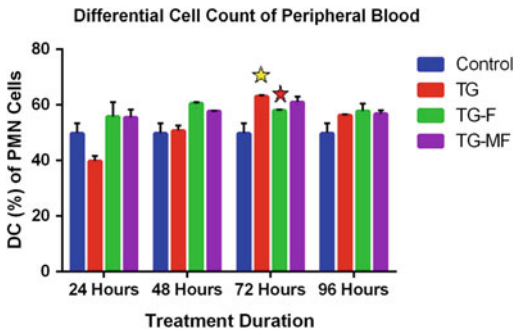


**Fig. 3.3** Effect of fisetin and MCN + fisetin on differential count of PMN cells of peripheral blood

lymphocytes and monocytes, has increased 1.20-fold after 24 h, 1.22-fold after 48 h, and 1.58-fold ( $p < 0.05$ ) after 96 h, but has decreased 1.33-fold after 72 h. This indicates an influx of inflammatory cells in the blood in response to TG administration. With fisetin treatment, the DC decreased 1.48-fold ( $p < 0.05$ ) after 24 h, 1.29-fold ( $p < 0.05$ ) after 48 h, and 1.05-fold ( $p < 0.05$ ) after 96 h, but has increased 1.14-fold after 72 h. With MCN + fisetin, the DC has decreased 1.37-fold ( $p < 0.05$ ) after 24 h, 1.20-fold after 48 h, and 1.02-fold ( $p < 0.05$ ) after 96 h, but has increased 1.05-fold after 72 h. This indicates a successful inhibition of cell recruitment (Table 3.4; Fig. 3.4).

- NO Estimation of PB:** The NO concentration of peripheral blood shows a 3.85-fold decrease after 24 h, a 1.28-fold decrease after 48 h, a 1.85-fold decrease after 72 h, and a 1.92-fold decrease after 96 h, with TG, as compared to control. Administration of fisetin alone shows a 1.54-fold increase after 24 h, a 1.16-fold increase after 48 h, and a 1.42-fold increase after 72 h, but a 2.38-fold decrease after 96 h. With MCN + fisetin, the NO concentration decreases 1.16-fold after 24 h and 1.04-fold after 48 h, but increases 1.94-fold after 72 h and 1.29-fold after 96 h (Table 3.5; Fig. 3.5).
- NO Estimation of PF:** The NO concentration of peritoneal fluid shows a 15.46-fold increase after 24 h, a 3.09-fold increase after

**Table 3.4** Differential count of MN cells in peripheral blood, seen after HE staining, under light microscope

Treatment	Mononuclear cells			
	Avg. cell count ( $\times 10^5/ml$ )	% of TC	Fold change	
			wrt control	wrt TG
Control	5.03 $\pm$ 0.37	50.30		
TG24	6.03 $\pm$ 0.19	60.30	<b>+1.20</b>	
TG24F	4.20 $\pm$ 0.51	44.30		<b>-1.48*</b>
TG24MF	4.45 $\pm$ 0.28	44.50		<b>-1.37*</b>
TG48	5.00 $\pm$ 0.12	49.30	<b>+1.22</b>	
TG48F	3.95 $\pm$ 0.05	39.50		<b>-1.29*</b>
TG48MF	4.23 $\pm$ 0.02	42.30		<b>-1.20</b>
TG72	3.77 $\pm$ 0.10	37.00	-1.33	
TG72F	4.20 $\pm$ 0.03	42.00		+1.14
TG72MF	3.90 $\pm$ 0.20	39.00		+1.05
TG96	4.38 $\pm$ 0.03	63.80	<b>+1.58*</b>	
TG96F	4.22 $\pm$ 0.27	42.20		<b>-1.05*</b>
TG96MF	4.33 $\pm$ 0.13	43.30		<b>-1.02*</b>

There is a decrease in DC with fisetin and MCN + fisetin treatment, after 24 h ( $p < 0.05$ ), 48 h ( $p < 0.05$ ), and 96 h ( $p < 0.05$ )

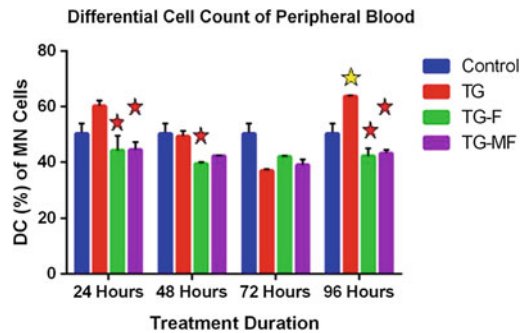


**Fig. 3.4** Effect of fisetin and MCN + fisetin on differential count of MN cells of peripheral blood

48 h, and a 33.41-fold increase after 72 h, but a 1.32-fold decrease after 96 h, with TG, as compared to control. Administration of fisetin alone shows a 1.55-fold increase after 24 h, and a 5.46-fold increase after 48 h, but there is a 1.09-fold decrease after 72 h and a 1.41-fold decrease after 96 h. With MCN + fisetin, the NO concentration decreases

**Table 3.5** Concentration and fold changes in nitric oxide produced in peripheral blood, assayed by Griess reagent, at 540 nm

Treatment	Concentration of NO (µM)	Fold change	
		wrt control	wrt TG
Control	45.45 ± 9.60		
TG24	11.80 ± 6.81	-3.85	
TG24F	18.13 ± 6.97		+1.54
TG24MF	10.17 ± 5.90		-1.16
TG48	35.39 ± 0.49	-1.28	
TG48F	40.95 ± 22.18		+1.16
TG48MF	34.10 ± 15.76		-1.04
TG72	24.65 ± 4.24	-1.85	
TG72F	35.05 ± 9.09		+1.42
TG72MF	47.79 ± 6.04		+1.94
TG96	23.78 ± 8.89	-1.92	
TG96F	9.89 ± 1.84		-2.38
TG96MF	30.65 ± 8.90		+1.29

There is a 2.38-fold decrease with fisetin after 96 h. With MCN + fisetin, there is a 1.16-fold decrease after 24 h and a 1.04-fold decrease after 48 h

**Table 3.6** Concentration and fold changes in nitric oxide produced in peritoneal fluid, assayed by Griess reagent, at 540 nm

Treatment	Concentration of NO (µM)	Fold change	
		wrt control	wrt TG
Control	0.78 ± 0.95		
TG24	12.08 ± 9.11	+15.46	
TG24F	18.72 ± 8.54		+1.55
TG24MF	12.95 ± 7.15		+1.07
TG48	2.42 ± 0.96	+3.09	
TG48F	13.20 ± 9.32		+5.46
TG48MF	6.59 ± 4.75		+2.73
TG72	26.09 ± 12.63	+33.41	
TG72F	23.97 ± 3.87		-1.09
TG72MF	23.54 ± 4.35		-1.11
TG96	0.59 ± 0.38	-1.32	
TG96F	0.42 ± 0.34		-1.41
TG96MF	1.23 ± 0.44		+2.08

With fisetin, there is a 1.09-fold decrease after 72 h and a 1.41-fold decrease after 96 h. With MCN + fisetin, there is a 1.11-fold decrease 72 h

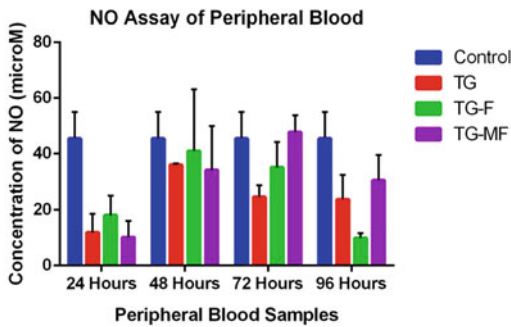


**Fig. 3.5** Effect of fisetin and MCN + fisetin on the production of nitric oxide in the blood

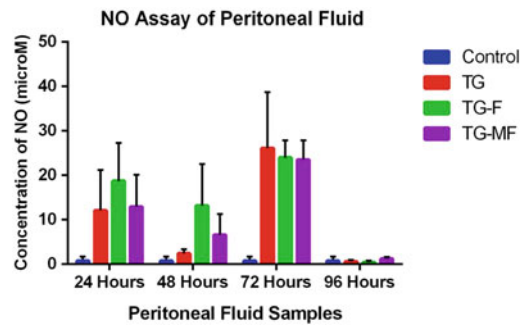


**Fig. 3.6** Effect of fisetin and MCN + fisetin on the production of nitric oxide in the peritoneal fluid

1.11-fold after 72 h, but increases 1.07-fold after 24 h, 2.73-fold after 48 h, and 2.08-fold after 96 h (Table 3.6; Fig. 3.6).

- NO Estimation of BM:** The NO concentration of bone marrow shows a 3.15-fold increase after 24 h and a 6.13-fold ( $p < 0.05$ ) increase after 72 h, but a 2.29-fold decrease after 48 h and a 1.82-fold decrease after 96 h, with TG, as compared to control.

Administration of fisetin alone shows a 1.55-fold increase after 24 h, but there is a 1.22-fold decrease after 48 h, a 2.39-fold decrease after 72 h, and a 1.29-fold decrease after 96 h. With MCN + fisetin, the NO concentration decreases 1.50-fold after 24 h and 1.07-fold after 96 h, but increases 1.15-fold after 48 h and 1.08-fold after 72 h (Table 3.7; Fig. 3.7).

**Table 3.7** Concentration and fold changes in nitric oxide produced in bone marrow, assayed by Griess reagent, at 540 nm

Treatment	Concentration of NO ( $\mu\text{M}$ )	Fold change	
		wrt control	wrt TG
Control	5.56 $\pm$ 2.77		
TG24	17.50 $\pm$ 6.50	<b>+3.15</b>	
TG24F	27.13 $\pm$ 5.10		+1.55
TG24MF	11.65 $\pm$ 5.63		<b>-1.50</b>
TG48	2.43 $\pm$ 1.40	-2.29	
TG48F	1.99 $\pm$ 0.45		<b>-1.22</b>
TG48MF	2.80 $\pm$ 0.25		+1.15
TG72	34.07 $\pm$ 7.80	<b>+6.13*</b>	
TG72F	14.28 $\pm$ 2.68		<b>-2.39</b>
TG72MF	36.94 $\pm$ 9.87		+1.08
TG96	3.05 $\pm$ 1.32	-1.82	
TG96F	2.37 $\pm$ 1.84		<b>-1.29</b>
TG96MF	2.86 $\pm$ 1.59		<b>-1.07</b>

With fisetin, there is a 1.22-fold decrease after 48 h, a 2.39-fold decrease after 72 h, and a 1.29-fold decrease after 96 h. With MCN + fisetin, there is a 1.50-fold decrease 24 h and a 1.07-fold decrease after 96 h

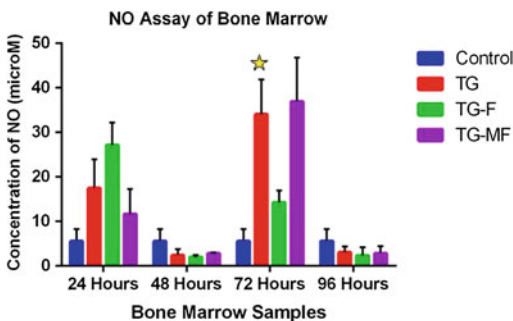


**Fig. 3.7** Effect of fisetin and MCN + fisetin on the production of nitric oxide in the bone marrow

## 6. Cell Proliferation (MTS) Assay of PB:

The MTS assay gives an idea about the proliferative potential of the cells. The cell number in the blood decreases with TG treatment, as compared to untreated control. There is a 1.33-fold decrease after 24 h, a 1.08-fold decrease after 48 h, a 1.71-fold decrease after 72 h, and a 2.04-fold decrease ( $p < 0.05$ ) after 96 h, with TG. With fisetin

treatment, there is a 1.21-fold increase after 24 h and a 1.30-fold increase after 72 h, but a 1.06-fold decrease after 48 h and a 1.96-fold decrease after 96 h. With MCN + fisetin treatment, there is a 1.08-fold increase after 48 h and a 1.92-fold increase ( $p < 0.05$ ) after 96 h, but a 1.14-fold decrease after 24 h and a 1.60-fold decrease after 72 h (Table 3.8; Fig. 3.8).

**Table 3.8** No. of cells and fold changes in cell number in peripheral blood, assayed by MTS reagent, at 490 nm

Treatment	Concentration of cells ( $\times 10^6/\text{ml}$ )	Fold change	
		wrt control	wrt TG
Control	94.91 $\pm$ 13.30		
TG24	71.62 $\pm$ 24.35	<b>-1.33</b>	
TG24F	86.49 $\pm$ 19.95		<b>+1.21</b>
TG24MF	62.94 $\pm$ 15.58		-1.14
TG48	88.05 $\pm$ 3.54	<b>-1.08</b>	
TG48F	83.18 $\pm$ 5.69		-1.06
TG48MF	94.69 $\pm$ 3.41		<b>+1.08</b>
TG72	55.46 $\pm$ 17.35	<b>-1.71</b>	
TG72F	72.28 $\pm$ 17.84		<b>+1.30</b>
TG72MF	34.73 $\pm$ 19.80		-1.60
TG96	46.50 $\pm$ 10.66	<b>-2.04*</b>	
TG96F	23.77 $\pm$ 11.47		-1.96
TG96MF	89.23 $\pm$ 5.78		<b>+1.92*</b>

With fisetin, there is a 1.21-fold increase in cell number after 24 h and a 1.30-fold increase after 72 h. With MCN + fisetin, there is a 1.08-fold increase after 48 h and a 1.92-fold increase ( $p < 0.05$ ) after 96 h

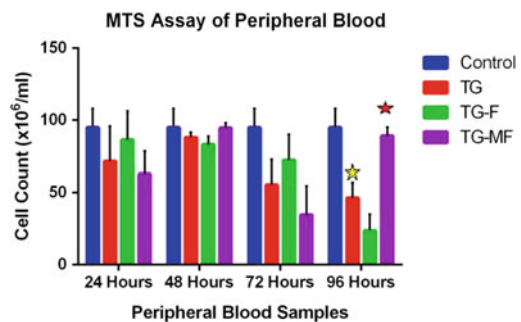


**Fig. 3.8** Effect of fisetin and MCN + fisetin on proliferation of cells in the peripheral blood

**7. Cell Proliferation (MTS) Assay of PF:** The cell number in the peritoneal fluid decreases after 24 and 72 h with TG treatment, as compared to untreated control. There is a 1.07-fold decrease after 24 h and a 2.38-fold decrease after 72 h, but a 16.46-fold increase after 48 h, with TG. With fisetin treatment, there is a 4.04-fold increase after 24 h, a 1.01-fold increase after 48 h, and a 1.21-fold increase after 72 h. With MCN + fisetin treatment, there is a 2.16-fold increase after 24 h and a 19.82-fold increase after 72 h, but a 1.65-fold decrease after 48 h (Table 3.9; Fig. 3.9).

**Table 3.9** No. of cells and fold changes in cell number in peritoneal fluid, assayed by MTS reagent, at 490 nm

Treatment	Concentration of cells ( $\times 10^6/ml$ )	Fold change	
		wrt control	wrt TG
Control	3.09 $\pm$ 13.46		
TG24	2.90 $\pm$ 9.02	-1.07	
TG24F	11.71 $\pm$ 17.43		+4.04
TG24MF	6.26 $\pm$ 16.74		+2.16
TG48	50.86 $\pm$ 13.61	+16.46	
TG48F	51.36 $\pm$ 19.20		+1.01
TG48MF	30.79 $\pm$ 11.33		-1.65
TG72	1.30 $\pm$ 4.91	-2.38	
TG72F	1.57 $\pm$ 6.73		+1.21
TG72MF	25.76 $\pm$ 18.49		+19.82

With fisetin, there is a 4.04-fold increase in cell number after 24 h, a 1.01-fold increase after 48 h, and a 1.21-fold increase after 72 h. With MCN + fisetin, there is a 2.16-fold increase after 24 h and a 19.82-fold increase after 72 h

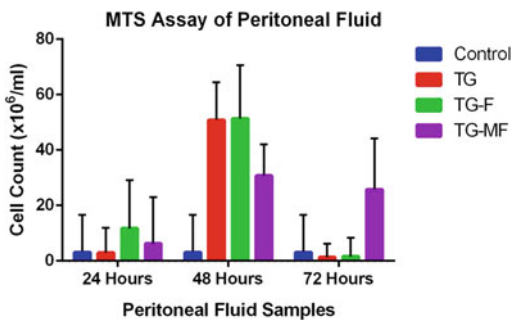


**Fig. 3.9** Effect of fisetin and MCN + fisetin on proliferation of cells in the peritoneal fluid

**8. Cell Proliferation (MTS) Assay of BM:** The cell number in the bone marrow decreases with TG treatment after 24, 48, and 96 h, as compared to untreated control. There is a 28.94-fold decrease after 24 h, a 1.23-fold decrease after 48 h, and a 1.64-fold decrease after 96 h, with TG, but a 1.31-fold increase after 72 h. With fisetin treatment, there is a 10.81-fold increase after 24 h and a 1.59-fold increase after 48 h, but a 1.24-fold decrease after 72 h and a 3.27-fold decrease after 96 h. With MCN + fisetin treatment, there is a 1.68-fold increase after 48 h, but a 1.27-fold decrease after 24 h, a 1.44-fold decrease after 72 h and a 6.77-fold decrease after 96 h (Table 3.10; Fig. 3.10).

**Table 3.10** No. of cells and fold changes in cell number in bone marrow, assayed by MTS reagent, at 490 nm

Treatment	Concentration of cells ( $\times 10^6/ml$ )	Fold change	
		wrt control	wrt TG
Control	47.75 $\pm$ 27.60		
TG24	1.64 $\pm$ 1.85	-28.94	
TG24F	17.73 $\pm$ 36.51		+10.81
TG24MF	1.29 $\pm$ 3.09		-1.27
TG48	38.72 $\pm$ 17.84	-1.23	
TG48F	61.60 $\pm$ 10.89		+1.59
TG48MF	65.17 $\pm$ 25.85		+1.68
TG72	62.64 $\pm$ 5.17	+1.31	
TG72F	50.47 $\pm$ 20.93		-1.24
TG72MF	43.42 $\pm$ 27.40		-1.44
TG96	29.05 $\pm$ 24.60	-1.64	
TG96F	8.89 $\pm$ 27.06		-3.27
TG96MF	4.29 $\pm$ 11.61		-6.77

With fisetin, there is a 10.81-fold increase in cell number after 24 h and a 1.59-fold increase after 48 h. With MCN + fisetin, there is a 1.68-fold increase after 48 h

**9. CFU-c Assay of PB:** CFU-c assay gives the clonogenic potential of cells, which is the ability of cells to form colonies on a semi-solid matrix. The clonogenic potential of cells in the peripheral blood decreases with TG treatment, as compared to control. There

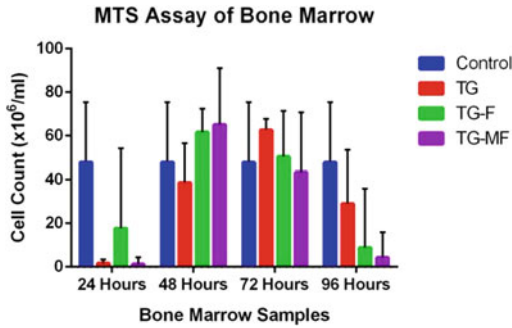


**Fig. 3.10** Effect of fisetin and MCN + fisetin on proliferation of cells in the bone marrow

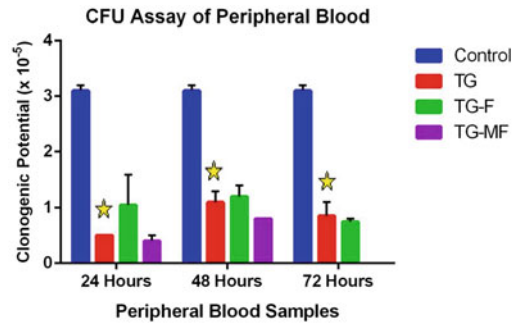


**Fig. 3.11** Effect of fisetin and MCN + fisetin on the clonogenic potential of cells in the peripheral blood

is a 6.20-fold decrease ( $p < 0.05$ ) after 24 h, a 2.82-fold decrease ( $p < 0.05$ ) after 48 h, and a 3.65-fold decrease ( $p < 0.05$ ) after 72 h, with TG. It increases 2.10-fold after 24 h and 1.05-fold after 48 h, with fisetin treatment, but decreases 1.13-fold after 72 h. With MCN + fisetin, the clonogenic potential has decreased 1.25-fold after 24 h and 1.38-fold after 48 h (Table 3.11; Figs. 3.11, 3.12).

10. **CFU-c Assay of PF:** There is a 3.20-fold decrease in clonogenic potential of cells in the peritoneal fluid after 24 h, with TG as compared to control. However, there is a

1.56-fold increase after 48 h, and a 1.69-fold increase after 72 h, with TG. It increases 3.20-fold after 24 h, but decreases 1.47-fold after 48 h and 1.29-fold after 72 h, with fisetin treatment. With MCN + fisetin, the clonogenic potential has increased 6.80-fold after 24 h, but has decreased by 1.56-fold after 48 h (Table 3.12; Figs. 3.13, 3.14).

11. **CFU-c Assay of BM:** The clonogenic potential of cells in the bone marrow decreases with TG treatment, as compared to control. There is a 4.59-fold decrease ( $p < 0.05$ ) after 24 h, a 2.52-fold decrease ( $p < 0.05$ ) after 48 h, and a 3.39-fold decrease ( $p < 0.05$ ) after 72 h, with TG. It increases by 1.53-fold after 24 h with fisetin, but decreases by 1.11-fold after 48 h and 1.05-fold after 72 h. With MCN + fisetin, the clonogenic potential has increased by 1.88-fold after 24 h, but has decreased by 1.24-fold after 48 h (Table 3.13; Figs. 3.15 and 3.16).

12. **Cytokine levels in peripheral blood after 48 h of treatment:** 48 h after challenge with TG, there is an increase in the levels of IL-4 (1.03-fold) and IFN- $\gamma$  (1.13-fold), and a decrease in the levels of IL-2 (1.06-fold,  $p < 0.05$ ), IL-5 (1.05-fold), and TNF- $\alpha$  (1.05-fold) compared to control. Compared to TG-treated groups, there is an increase in the levels of the cytokines with fisetin treatment (1.13-fold for IL-2, 1.12-fold ( $p < 0.05$ ) for IL-4, 1.11-fold for IL-5, 1.03-fold for IFN- $\gamma$ , and 1.02-fold for

**Table 3.11** The change in clonogenic potential of cells in the peripheral blood, assessed by CFU-c assay using methylcellulose

Treatment	Clonogenic Potential ( $\times 10^{-5}$ )	Fold change	
		wrt control	wrt TG
Control	3.10 $\pm$ 0.10		
TG24	0.50 $\pm$ 0.00	-6.20*	
TG24F	1.05 $\pm$ 0.55		+2.10
TG24MF	0.40 $\pm$ 0.10		-1.25
TG48	1.10 $\pm$ 0.20	-2.82*	
TG48F	1.15 $\pm$ 0.20		+1.05
TG48MF	0.80 $\pm$ 0.00		-1.38
TG72	0.85 $\pm$ 0.25	-3.65*	
TG72F	0.75 $\pm$ 0.05		-1.13

There is a 2.10-fold increase in clonogenic potential after 24 h and a 1.05-fold increase after 48 h, with fisetin treatment

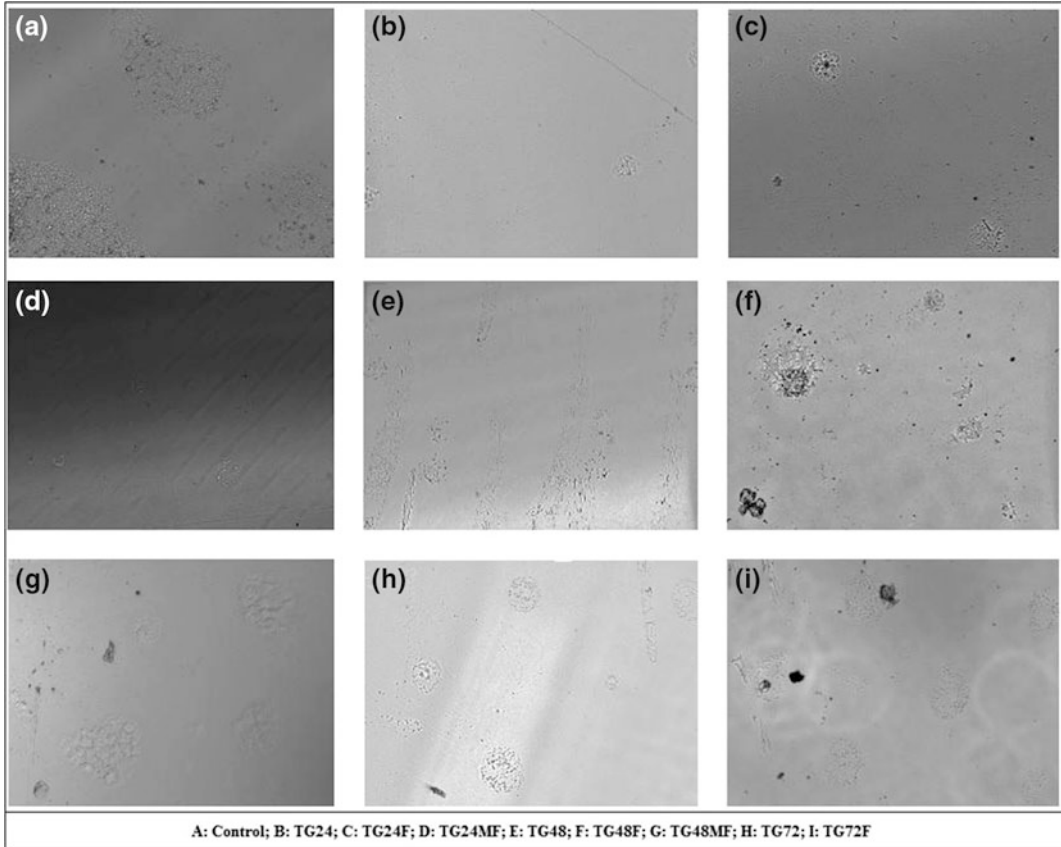


**Fig. 3.12** Effect of fisetin and MCN + fisetin on the clonogenic potential of cells in the peripheral blood, as seen under Fluid Cell Imaging Station

**Table 3.12** The change in clonogenic potential of cells in the peritoneal fluid, assessed by CFU-c assay using methylcellulose

Treatment	Clonogenic Potential ( $\times 10^{-4}$ )	Fold change	
		wrt control	wrt TG
Control	$0.80 \pm 0.20$		
TG24	$0.25 \pm 0.05$	<b>-3.20</b>	
TG24F	$0.80 \pm 0.40$		<b>+3.20</b>
TG24MF	$1.70 \pm 0.60$		<b>+6.80</b>
TG48	$1.25 \pm 0.25$	+1.56	
TG48F	$0.85 \pm 0.05$		-1.47
TG48MF	$0.80 \pm 0.40$		-1.56
TG72	$1.35 \pm 0.15$	+1.69	
TG72F	$1.05 \pm 0.05$		-1.29

There is a 3.20-fold increase in clonogenic potential after 24 h with fisetin treatment, and a 6.80-fold increase after 24 h with MCN + fisetin treatment

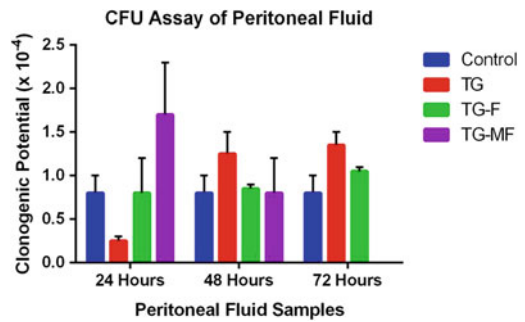


**Fig. 3.13** Effect of fisetin and MCN + fisetin on the clonogenic potential of cells in the peritoneal fluid

TNF- $\alpha$ ), and with MCN + F treatment (1.12-fold for IL-2, 1.27-fold for IL-4, 1.14-fold for IL-5, 1.07-fold for IFN- $\gamma$ , and 1.03-fold for TNF- $\alpha$ ) (Table 3.14; Fig. 3.17).

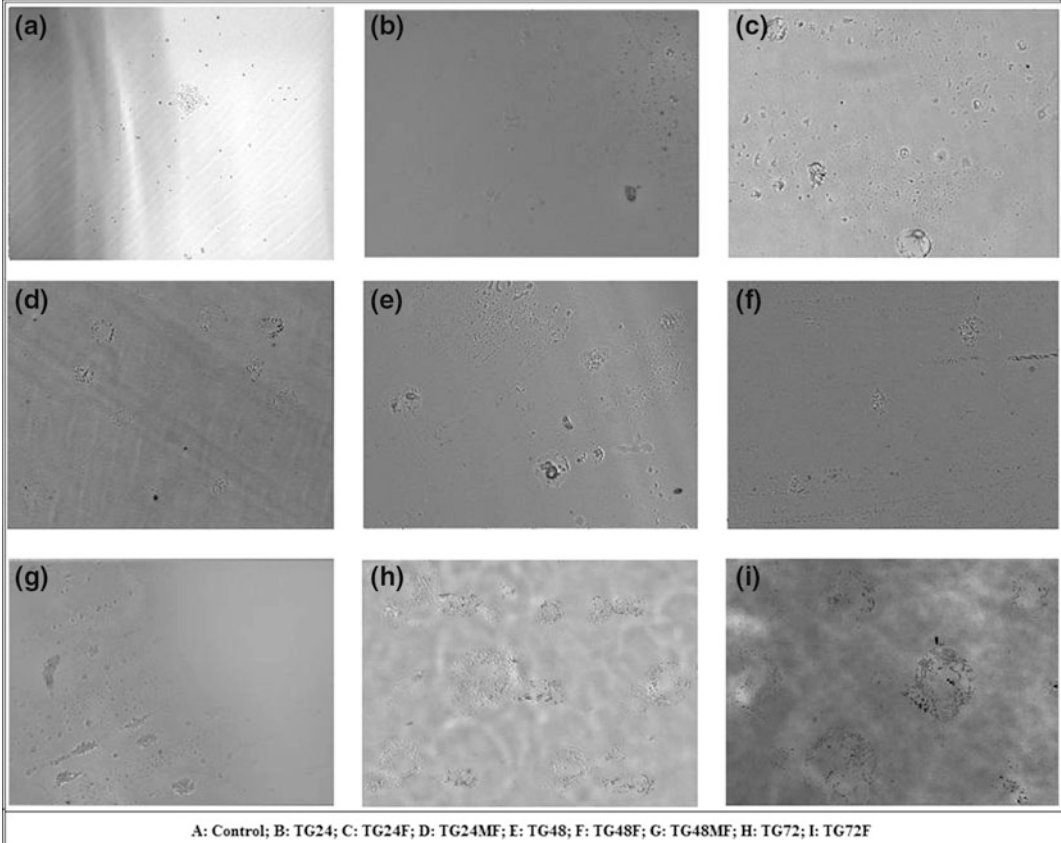


**Fig. 3.14** Effect of fisetin and MCN + fisetin on the clonogenic potential of cells in the peritoneal fluid, as seen under Flويد Cell Imaging Station

**Table 3.13** The change in clonogenic potential of cells in the bone marrow, assessed by CFU-c assay using methylcellulose

Treatment	Clonogenic potential ( $\times 10^{-5}$ )	Fold change	
		wrt control	wrt TG
Control	$3.90 \pm 0.10$		
TG24	$0.85 \pm 0.25$	-4.59*	
TG24F	$1.30 \pm 0.10$		+1.53
TG24MF	$1.60 \pm 0.40$		+1.88
TG48	$1.55 \pm 0.15$	-2.52*	
TG48F	$1.40 \pm 0.00$		-1.11
TG48MF	$1.25 \pm 0.05$		-1.24
TG72	$1.15 \pm 0.25$	-3.39*	
TG72F	$1.10 \pm 0.20$		-1.05

There is a 1.53-fold increase in clonogenic potential after 24 h with fisetin treatment, and a 1.88-fold increase after 24 h with MCN + fisetin treatment

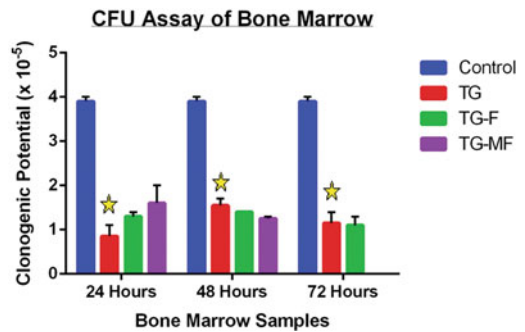


**Fig. 3.15** Effect of fisetin and MCN + fisetin on the clonogenic potential of cells in the bone marrow

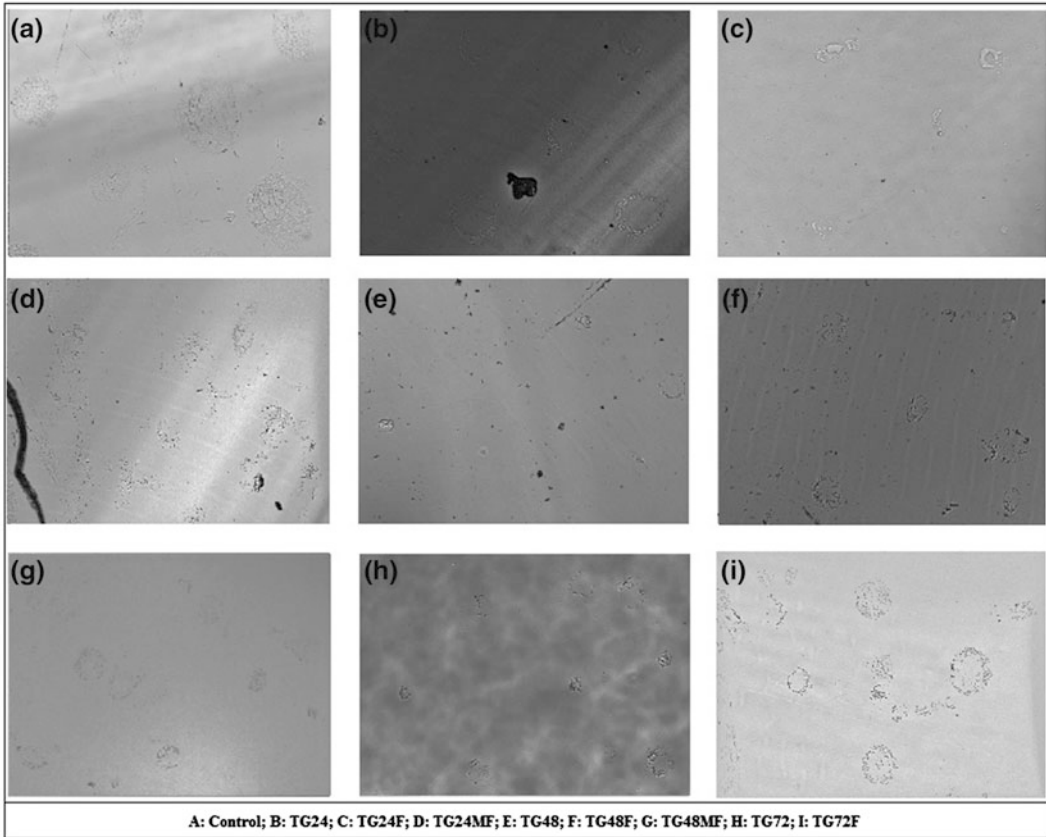


**Fig. 3.16** Effect of fisetin and MCN + fisetin on the clonogenic potential of cells in the peritoneal fluid, as seen under Floid Cell Imaging Station

**Table 3.14** Concentration (in pg/ml) of cytokines IL-2, IL-4, IL-5, IFN- $\gamma$ , and TNF- $\alpha$ , in peripheral blood, after 48 h of treatment, assayed using BD CBA Mouse Th1/Th2 Cytokine Kit

	Concentration of cytokines in peripheral blood (in pg/ml)				
	IL-2	IL-4	IL-5	IFN- $\gamma$	TNF- $\alpha$
Control	19.05 $\pm$ 0.15	15.25 $\pm$ 0.05	14.60 $\pm$ 0.20	10.75 $\pm$ 0.45	10.80 $\pm$ 1.10
TG	18.05 $\pm$ 0.15*	15.65 $\pm$ 0.35	13.85 $\pm$ 0.55	12.10 $\pm$ 0.30	10.30 $\pm$ 0.30
TG + fisetin	20.40 $\pm$ 0.70	17.50 $\pm$ 0.20*	15.30 $\pm$ 0.30	12.45 $\pm$ 1.65	10.55 $\pm$ 1.05
TG + (MCN + F)	20.25 $\pm$ 1.15	19.85 $\pm$ 0.95	15.85 $\pm$ 1.75	12.90 $\pm$ 1.60	10.60 $\pm$ 1.40

Cytokine analysis shows an increase in the levels of the cytokines with both, fisetin and MCN + fisetin, compared to TG



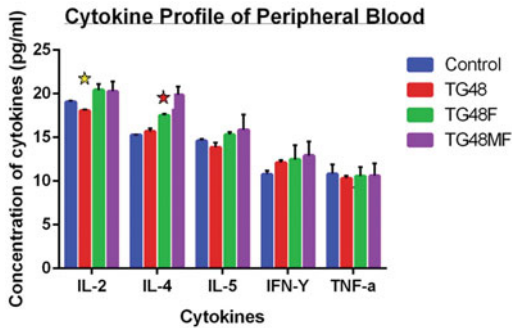


**Fig. 3.17** Effect of fisetin and MCN + fisetin on the cytokine profile of peripheral blood

### 3.4 Discussion

The pathophysiology of peritonitis is complicated and is involved in various processes, of which, the most important one is the inflammatory reaction [22]. During the pathological process of the peritonitis, NF- $\kappa$ B plays an activating role in the inflammatory reaction, which might be a potential therapeutic target in the future clinical work [7].

Our study was designed to investigate the potential therapeutic effects of fisetin and fisetin loaded on MCN on the thioglycollate-induced peritonitis in rodent models. The thioglycollate-induced peritonitis in mice is used as a model to study for potential anti-inflammatory action of investigated test compounds [23]. In this present study, we have induced peritonitis in 6–8-week-old BALB/c mice using thioglycollate and then assessed the anti-inflammatory effects of plant flavonoid, fisetin, when administered therapeutically. We have also assessed the anti-inflammatory effects of fisetin, when administered with a nanovehicle, MCN. We found that fisetin had a positive therapeutic effect on the peritonitis.

Acute peritonitis differs from other infections because of the broad variety of causes, severity of the infection [24]. Acute peritonitis is one of the most headachy postoperative complications, which is an important cause of death in surgical practice and intensive care units [9]. The most serious consequence of acute peritonitis is sepsis,

often leading to an unacceptably high morbidity and mortality [25]. So the research of acute peritonitis is always the hotspot of surgery and critical care medicine. The animal model is one of the most important methods in the scientific research. It cannot only provide convenience in deriving a better understanding of the pathophysiology of disease, but also provide important and indispensable tools to explore the therapy of disease. It is the bridge between the fundamental research and clinical application.

The process of peritonitis is mediated by the activation of inducible transcription factors, such as NF- $\kappa$ B, which play a pivotal role in the immune and inflammatory responses. Previous investigators have found that acute peritonitis and sepsis were associated with the activation of the transcription factor NF- $\kappa$ B in various organs and tissues [10, 26, 27] which can regulate the synthesis of TNF- $\alpha$ , IL-6, inducible nitric oxide synthase, cyclooxygenase-2, and many other molecules involved in the inflammatory reaction [18, 28].

In this study, we found cell recruitment in the blood increases with the administration of TG after 24 h ( $p < 0.05$ ), 48 and 96 h ( $p < 0.05$ ), showing that it has induced inflammation, and the body is synthesizing more immune cells to counter the infection. Cell recruitment is successfully inhibited by fisetin after 24 h ( $p < 0.05$ ), and with MCN + fisetin after 48 h ( $p < 0.05$ ). In the peritoneal fluid, total cell recruitment has increased after 24 h ( $p < 0.05$ ), which is successfully inhibited with fisetin treatment after 96 h. There is no noticeable change in TC with MCN + fisetin treatment in the PF.

Nitric acid is produced by macrophages as a defense against oxidative stress. In case of inflammation, NO content is expected to increase. Our assays have shown that the NO content of the tissues has increased with TG challenge, mainly after 24 and 72 h. Fisetin treatment has reduced NO content, especially after 96 h, and with MCN + fisetin after 24 h.

We found that TG treatment has significantly reduced cell proliferation in the blood, PF, and BM, within 24, till 96 h. Interestingly, cell

proliferation has increased with fisetin treatment after 24 h, and with MCN + fisetin after 24 h (in PF) and after 48 h (in PB and BM). In another assay, the clonogenic potential of the tissues decreases significantly within 24 h, with administration of TG. Both fisetin treatment and MCN + fisetin treatment have restored the clonogenic potential of the tissues after 24 h. Our study demonstrated that there was a decrease in Th2 cytokines (IL-2, IL-5, and TNF- $\alpha$ ) with TG treatment, in blood after 48 h, and fisetin and MCN + fisetin have increased the cytokine content.

In conclusion, we demonstrated that fisetin and fisetin loaded on MCN may have anti-inflammatory effects on thioglycollate-induced peritonitis. To our knowledge, this is the first study to date to assess new therapeutic approaches using phytochemicals such as fisetin against peritonitis. Further studies required to verify the clinical use of fisetin in the treatment of peritonitis. The future research could focus on the combination of fisetin therapy and traditional antibiotics, which might be more efficient than using antibiotics alone.

### Contribution of authors

SM performed all experiments and analyzed data; SB gave valuable input to the manuscript; AS and NRJ have prepared the MCN; and ERB initiated the project with her idea, designed the experiments, analyzed all data, and wrote the manuscript.

**Acknowledgements** The authors wish to acknowledge UGC for providing fellowship and contingency grant to SM, ICMR for providing a Research Associateship to SB and to WB DBT, and SERB for funding the project of which ERB is the PI, and provide funds for infrastructure development and necessary funds to undertake expenses related to the project. The authors also acknowledge Sattar Sekh and Manisha Murmu for technical help and Priyanka Dutta for her support for all purchase and accounts-related activities critical for the smooth running of the project.

## References

1. Anel RL, Kumar A. Experimental and emerging therapies for sepsis and septic shock. *Expert Opin Investig Drugs*. 2001;10:1471–85.
2. Dellinger RP. Inflammation and coagulation: implications for the septic patient. *Clin Infect Dis*. 2003;36:1259–65.
3. Ritter C, Andrades ME, Reinke A, Menna-Barreto S, Moreira JCF, Dal-Pizzol F. Treatment with N-acetylcysteine plus deferoxamine protects rats against oxidative stress and improves survival in sepsis. *Crit Care Med*. 2004;32:342–9.
4. Baeuerle PA. I kappa B-NF-kappa B structures: at the interface of inflammation control. *Cell*. 1998;95:729–31.
5. Zingarelli B, Sheehan M, Wong HR. Nuclear factor-kappa B as a therapeutic target in critical care medicine. *Crit Care Med*. 2003;31:S105–11.
6. Woltmann A, Hamann L, Ulmer AJ, Gerdes J, Bruch HP, Rietschel ET. Molecular mechanisms of sepsis. *Langenbecks Arch Surg*. 1998;383:2–10.
7. Hayden MS, Ghosh S. Signaling to NF-kappa B. *Genes Dev*. 2004;18:2195–224.
8. Liu SF, Malik AB. NF-kappa B activation as a pathological mechanism of septic shock and inflammation. *Am J Physiol Lung Cell Mol Physiol*. 2006;290:L622–45.
9. Billing AG, Frohlich D, Konecny G, Schildberg FW, Machleidt W, Fritz H, et al. Local serum application—restoration of sufficient host-defense in human peritonitis. *Eur J Clin Invest*. 1994;24:28–35.
10. Feng X, Liu J, Yu M, Zhu S, Xu J. Protective roles of hydroxyethyl starch 130/0.4 in intestinal inflammatory response and survival in rats challenged with polymicrobial sepsis. *Clin Chim Acta*. 2007;376:60–7.
11. Ferrero-Miliani L, Nielsen OH, Andersen PS, Girardin SE. Chronic inflammation: importance of NOD2 and NALP3 in interleukin-1beta generation. *Clin Exp Immunol*. 2007;147(2):227–35.
12. Porth C. *Essentials of pathophysiology: concepts of altered health states*. Hagerstown, MD: Lippincott Williams & Wilkins; (2007). p. 270. ISBN 0-7817-7087-4.
13. Abbas AB, Lichtman AH. Ch. 2 Innate immunity. In Saunders (Elsevier). *Basic immunology. Functions and disorders of the immune system (3rd ed.)*; (2009). ISBN 978-1-4160-4688-2.
14. Crunkhon P, Meacock S. Mediators of the inflammation induced in the rat paw by carrageenan. *Br J Pharmacol*. 1971;42:392–402.

15. Cotran RS; Kumar V, Collins SL. Robbins "pathologic basis of disease." Philadelphia: W.B Saunders Company; 1998. ISBN 0-7216-7335-X.
16. Khan N, Syed DN, Ahmad N, Mukhtar H. Fisetin: a dietary antioxidant for health promotion. *Antioxid Redox Signal*. 2013;19(2):151–62.
17. Khan N, Adhami VM, Mukhtar H. Apoptosis by dietary agents for prevention and treatment of prostate cancer. *Endocr Relat Cancer*. 2010;17:R39–52.
18. Khan N, Afaq F, Mukhtar H. Cancer chemoprevention through dietary antioxidants: progress and promise. *Antioxid Redox Signal*. 2008;10:475–510.
19. Boisseau P, Loubaton B. Nanomedicine, nanotechnology in medicine. *CR Phys*. 2011;12(7):620.
20. Kaur G, Narang RK, Rath G, Goyal AK. Advances in pulmonary delivery of nanoparticles. *Artif Cells Blood Substit Immobil Biotechnol*. 2012;40:75–96.
21. Mohamud R, Xiang SD, Selomulya C, Rolland JM, O'Hehir RE, Hardy CL, Plebanski M. The effects of engineered nanoparticles on pulmonary immune homeostasis. *Drug Metab Rev*. 2014;46(2):176–90.
22. Remick DG. Pathophysiology of sepsis. *Am J Pathol*. 2007;170:1435–44.
23. Fakhruddin N, Waltenberger B, Cabaravdic M, Atanasov AG, Malainer C, Schachner D, Heiss EH, Liu R, Noha SM, Grzywacz AM, Mihaly-Bison J, Awad EM, Schuster D, Breuss JM, Rollinger JM, Bochkov V, Stuppner H, Dirsch VM. Identification of plumericin as a potent new inhibitor of the NF- $\kappa$ B pathway with anti-inflammatory activity in vitro and in vivo. *Br J Pharmacol*. 2014;171(7):1676–86.
24. Ghiselli R, Giacometti A, Cirioni O, Mocchegiani F, Orlando F, Silvestri C, et al. Efficacy of the bovine antimicrobial peptide indolicidin combined with piperacillin/tazobactam in experimental rat models of polymicrobial peritonitis. *Crit Care Med*. 2008;36:240–5.
25. Davies MG, Hagen PO. Systemic inflammatory response syndrome. *Br J Surg*. 1997;84:920–35.
26. Tian J, Lin X, Guan R, Xu JG. The effects of hydroxyethyl starch on lung capillary permeability in endotoxic rats and possible mechanisms. *Anesth Analg*. 2004;98:768–74.
27. Perkins ND. The Rel/NF-kappa B family: friend and foe. *Trends Biochem Sci*. 2000;25:434–40.
28. Sha WC. Regulation of immune responses by NF-kappa B/Rel transcription factors. *J Exp Med*. 1998;187:143–6.

---

## Abbreviations

ASA	Ascorbic acid
BM	Bone marrow
CFU-c	Colony-forming units in culture
DC	Differential cell count
F	Fisetin
Ins	Intestine
LPS	Lipopolysachharide
MN Cells	Mononuclear cells
MTS	[3-(4, 5-dimethyl thiazol-2-yl)-5-(3-carboxy methoxy phenyl)-2-(4-sulfophenyl)-2H-tetrazolium, inner salt]
MTT	3-(4, 5-dimethyl thiazol-2-yl)-2, 5-diphenyl tetrazolium bromide
MPK	Milligram per kilogram of body weight
NO	Nitric oxide
PB	Peripheral blood
PF	Peritoneal fluid
PMA	Phorbol 12-myristate 13-acetate
PMN Cells	Polymorphonuclear cells
PMS	Phenazine methosulfate
PP	Peyer's patch
Spl	Spleen
TC	Total cell count
TG	Thioglycollate

---

Prophylactic use of fisetin in thioglycollate-induced peritonitis in mice.

The original research work included in this chapter has been communicated to *BMC Immunology* (under revision 8-6-2015).

TG3F, TG9F, TG24F	Treatment with fisetin for 4 days, followed by treatment with 3 % TG 1 h after last fisetin treatment; Kill 3, 9, and 24 h after TG treatment, respectively
TG3, TG9, TG72, TG24	Treatment with only TG; kill after 3, 9, 24 h, respectively

---

### Symbols

- ★ Denotes significance in samples compared to control
- ★ Denotes significance in samples compared to samples treated with only TG

---

## 4.1 Summary of the Original Research

Infectious or non-infectious peritonitis leads to systemic inflammation due to violation of the peritoneum which is often fatal. Fisetin, a flavonol compound, exhibits a broad spectrum of biological activities including antioxidant, anti-inflammatory, anticancer, and neuroprotective effects was used in a murine model of thioglycollate-induced aseptic peritonitis to investigate in, and on RAW macrophage cells. In this study, peritonitis was induced in C57BL/6J mice using thioglycollate, and anti-inflammatory effects of fisetin, was assessed prophylactically. In in vitro study, cells treated with inflammatory agents such as LPS and PMA lose their viability and proliferative capacity. Fisetin has been shown to prevent the loss of viability when given prophylactically. In in vivo model, total cell recruitment was found to increase with TG, showing that it has induced inflammation and interestingly cell recruitment was successfully inhibited by fisetin. The differential count of peripheral blood, treated only with TG, shows an increase in the polymorphonuclear (PMN) cell count, as compared to control. On treatment with fisetin, PMN number decreases. Concentration of nitric oxide (NO) in intestine has increased by 1.90-fold after 3 h ( $p < 0.05$ ) and 1.24-fold after 24 h ( $p < 0.05$ ), after treatment with TG as compared to control. NO concentration has decreased by 1.28-fold after 3 h ( $p < 0.05$ ) and

2.15-fold after 24 h ( $p < 0.05$ ) with fisetin treatment, compared to only TG. Concentration of ascorbic acid in peritoneal fluid has increased by 1.06-fold after 3 h, 1.02-fold after 9 h, and 1.05-fold after 24 h, on treatment with only TG, as compared to control. The ASA concentration increases significantly ( $p < 0.05$ ) after treatment with fisetin, compared to only TG, after 3 h (1.38-fold), 9 h (1.44-fold), and 24 h (2.19-fold). In conclusion, we found that fisetin had a positive prophylactic effect against peritonitis in mice.

---

## 4.2 Introduction

Peritonitis is the inflammation of the peritoneum, which is the thin tissue that lines the inner wall of the abdomen, and covers most of the abdominal organs. Infected peritonitis is caused by perforation of part of the GI tract, by disruption of the peritoneum or by systemic infections. Non-infected peritonitis may be caused by leakage of sterile body fluids into the peritoneum, or by sterile abdominal surgery, which may inadvertently leave behind foreign bodies. Primary or spontaneous bacterial peritonitis (SBP) typically occurs when a bacterial infection spreads to the peritoneum across the gut wall or mesenteric lymphatics. Peritonitis is a common postoperative complication that can develop into lethal sepsis in case of delayed diagnosis or inappropriate treatment [1, 2]. The pathophysiology of peritonitis is complicated and is involved in

various processes, of which the most important one is the inflammatory reaction [3]. Inflammation leads to increased production of reactive species such as reactive oxygen species (ROS), nitric oxide synthase (NOS), and their product peroxynitrite by activated macrophages. This increase in oxidative stress leads to decrease in effectiveness of oxidant defenses, that is, reduction in antioxidants. Local intra-abdominal focus of inflammation caused by the microorganisms can promote the synthesis and secretion of massive inflammatory cytokines, which would destroy the endothelial junctions and provide access for bacteria into the systemic circulation leading to lethal bacteremia [4–6]. During the pathological process of the peritonitis, NF- $\kappa$ B plays an activating role in the inflammatory reaction [6]. Acute peritonitis is one of the most headachy postoperative complications, which is an important cause of death in surgical practice and intensive care units (ICUs) [7]. Acute peritonitis differs from other infections because of the broad variety of causes, severity of the infection, polymicrobial pathogenesis, and complex pathological process [8].

Perforation of part of the gastrointestinal tract is the most common cause of peritonitis. Disruption of the peritoneum, even in the absence of perforation of a hollow viscous, may also cause infection simply by letting microorganisms into the peritoneal cavity. Examples include trauma, surgical wound, continuous ambulatory peritoneal dialysis, and intraperitoneal chemotherapy. Again, in most of the cases, mixed bacteria are isolated; the most common agents include cutaneous species such as *Staphylococcus aureus*, and coagulase-negative staphylococci, but many others are possible, including fungi such as *Candida* [9]. Women can experience localized peritonitis from an infected fallopian tube or a ruptured ovarian cyst. Patients may present with an acute onset of symptoms, limited and mild disease, or systemic and severe disease with septic shock. It has been proven that delayed diagnosis of peritonitis was an important factor for its high mortality [10].

Peritoneal infections are classified as primary (i.e., from hematogenous dissemination, usually

in the setting of an immunocompromised state), secondary (i.e., related to a pathologic process in a visceral organ, such as perforation or trauma), or tertiary (i.e., persistent or recurrent infection after adequate initial therapy). Primary peritonitis is most often SBP seen mostly in patients with chronic liver disease. Secondary peritonitis is by far the most common form of peritonitis encountered in clinical practice. Tertiary peritonitis (TP) often develops in the absence of the original visceral organ pathology [9, 11–17]. Infections of the peritoneum are further divided into generalized (peritonitis) and localized (intra-abdominal abscess). The diagnosis of peritonitis is usually clinical. Diagnostic peritoneal lavage may be helpful in patients who do not have conclusive signs on physical examination or who cannot provide an adequate history [11]. An optimal treatment strategy against peritonitis has not yet established. In many cases, the surgical and antimicrobial treatment fails in this disease.

The animal model is one of the most important methods in the scientific research. Thioglycollate broth is a multipurpose, enriched differential medium used primarily to determine the oxygen requirements of microorganisms. Sodium thioglycollate in the medium consumes oxygen and permits the growth of obligate anaerobes. The thioglycollate-induced peritonitis in mice is used as a model to study for potential anti-inflammatory action of investigated test compounds [18].

Flavonoids, the most common group of polyphenolic compounds in the human diet, are abundant in fruits and vegetables. Fisetin is a bioactive polyphenolic flavonoid, commonly found in many fruits and vegetables such as strawberries, apples, persimmons, onions, and cucumbers. It has been shown to possess both direct intrinsic antioxidant as well as indirect antioxidant effects [19, 20]. Fisetin exerts multiple beneficial pharmacological activities such as anti-inflammatory, anticancer and in rheumatoid arthritis [21–25]. Recently, there has been an increasing interest in fisetin because of its antiproliferative and apoptotic activities [26, 27]. It was also considered to possess neuroprotective

effects against the aging process, cerebral damage, and neurodegenerative disorders [28]. In addition, several studies show that fisetin protects against several types of cancer, including prostate, cervical, colorectal, breast, bladder, and lung cancer [29, 30]. The aim of this study was to investigate the prophylactic effect of fisetin in thioglycollate-induced peritonitis in mice.

### 4.3 Materials and Methods

**Reagents:** LPS (cell wall lipopolysaccharide from *Escherichia coli* 0111:B4) was bought from Sigma Aldrich, USA. PMA (phorbol 12-myristate 13-acetate) was obtained from Calbiochem, USA. MTT was obtained from Spectrochem Pvt. Ltd., Mumbai, India. Sodium thioglycollate, fetal bovine serum (FBS), and RBC lysis buffer were bought from Himedia, India. Dimethyl sulfoxide (DMSO), EDTA, methanol, L-ascorbic acid (L-ASA), dinitrophenyl hydrazine (DNPH), thiourea, sulfanilamide, and NED were bought from Sisco Research Laboratory (SRL), India. Dulbecco's modified Eagle medium (DMEM) from Gibco was used. potassium dichromate, orthophosphoric acid, and  $\text{NaNO}_2$  were purchased from Merck, India. Sulfuric acid was bought from Finar Chemicals Limited, India, and 6 %  $\text{H}_2\text{O}_2$  was bought from B.D. Pharmaceutical Works Pvt. Ltd., India. 1X phosphate-buffered saline (PBS) was prepared using 137 mM NaCl (Merck, India), 2.7 mM KCl (Himedia, India), 10 mM  $\text{Na}_2\text{HPO}_4$  (Qualigens, India), and 2 mM  $\text{KH}_2\text{PO}_4$  (Himedia, India).

96-well plates were obtained from Nest Biotech Co. Ltd., China. Dispovan syringes were used to obtain blood and peritoneal fluid.

Cells were incubated in a  $\text{CO}_2$  incubator (Thermo Fisher), and cells were observed using Fluid Cell Imaging Station (Life Technologies, India).

Smears for cell counting were prepared using cytospin (Centurion Scientific C2 series) after centrifuging the sample in a cold centrifuge (Vision VS-15000CFN). Smears were observed under a light microscope (Debro DX-200).

Absorbance readings were taken in a multiplate reader (Thermo Fisher Multiskan EX). Plates were incubated in a  $\text{CO}_2$  incubator (Thermo Fisher).

All cell culture work was done inside the biosafety cabinet (Vision Scientific, Korea).

**In vitro cell proliferation studies:** RAW macrophages were cultured, treated with inflammatory agents (LPS and PMA) and the effect of fisetin on cell viability was assessed using MTT test. Viable, proliferating cells produce NAD(P)H-dependent oxidoreductases, which can reduce the tetrazolium dye MTT [3-(4,5-dimethylthiazol-2-yl)-2,5-diphenyl tetrazolium bromide], to its insoluble formazan (purple). These insoluble crystals are dissolved in DMSO, and absorbance is measured at 570 nm.  $5 \times 10^4$  RAW 264.7 cells were seeded into the wells of a 96-well plate and after 24 h, were treated with various concentrations of fisetin (10, 20, 30, 40, and 50  $\mu\text{M}$ ), followed by 1  $\mu\text{g}/\text{ml}$  LPS (bacterial cell wall lipopolysaccharide) for one group and 50 ng/ml PMA (phorbol 12-myristate 13-acetate) for another, and incubated for 24 h. Then, the cells were incubated with 5 mg/ml MTT working solution for 3 h at 37 °C followed by treatment with 100  $\mu\text{l}$  DMSO to dissolve the formazan crystals. Absorbance was measured in a microplate reader (Shimadzu) at 570 nm. Cell viability for cells without treatment (control) was taken to be 100 %, and the cell viability of the experimental groups calculated accordingly.

**In vitro assay for cellular uptake of fisetin:** RAW 264.7 cells have been treated with different concentrations of fisetin (10, 25 and 50  $\mu\text{M}$ ), followed by 1  $\mu\text{g}/\text{ml}$  LPS, and observed under the microscope (Fluid Cell Imaging Station). The change in uptake of fisetin by the cells was noted.

**Animals:** C57BL/6J mice were used. All experiments were performed according to rules laid down by the institutional and departmental animal ethics committee and the animals housed under specific pathogen-free conditions at the animal housing vivarium of the Department of Zoology, University of Calcutta.

**Treatment:** 5–6-week-old male C57 mice were divided into seven groups: Control ( $n = 3$ ),

TG3 ( $n = 3$ ), TG3F ( $n = 2$ ), TG9 ( $n = 3$ ), TG9F ( $n = 2$ ), TG24 ( $n = 3$ ) and TG24F ( $n = 2$ ). Three groups (TG3, TG9, and TG24) were treated with 3 % thioglycollate (Himedia, India) intraperitoneally (i.p). Three groups (TG3F, TG9F, and TG24F) were treated with 3 MPK fisetin (i.p) for four consecutive days. After 1 h of 4th day's treatment, they were intraperitoneally treated with 3 % thioglycollate. One group remained as placebo-treated control.

The mice were killed 3, 9, and 24 h after the final treatments, and the following tissues were collected: peripheral blood (PB), serum, peritoneal fluid (PF), bone marrow (BM), spleen (Spl), Peyer's patch (PP), intestine (Ins), liver, and kidney.

The following estimations and assays were done with the collected tissues: total cell count (TC), differential cell count (DC), nitric oxide (NO) estimation, catalase estimation, and ascorbic acid estimation.

**Total and Differential Cell Count (TC/DC):** Differential white blood cell count is an examination and enumeration of the distribution of leukocytes in a stained blood smear. Increases in any of the normal leukocyte types or the presence of immature leukocytes or erythrocytes in peripheral blood are important diagnostically in a wide variety of inflammatory disorders.

The normal range of the leukocytes is as follows:

- Neutrophils: 50–70 %,
- Lymphocytes: 20–40 %,
- Eosinophils: 0–6 %,
- Monocytes: 2–6 %, and
- Basophils: 0–1 %.

The smear is stained with hematoxylin, and counterstained with eosin.

Total cell counts of PB, PF, BM, and Spl samples were taken, using hemocytometry. Differential counts of PB and PF were taken. Quickly, 100  $\mu$ l of each sample was added to appropriate wells of the cytospin, and the slides and filters were placed in the correct slots of the cytospin. The slides were centrifuged at 2000 rpm for 3 min. The slides were removed and air-dried. They were then fixed with methanol and air-dried before staining. The fixed slides were placed in

100 % ethanol in a Coplin jar for 5 min, followed by 10 min in 90 % ethanol. They were then stained with hematoxylin for 5 min, rinsed in 70 % ethanol, counterstained with eosin for 2 min, and again rinsed in 70 % ethanol. Then, they were placed in 100 % ethanol for 1 min and then observed under the microscope.

The total cell count (TC) and the differential cell count (DC) were plotted against each sample using GraphPad Prism 6.

**NO Estimation:** Activation of immune system is associated with increase in macrophage NO production. Transient nature of NO makes it unsuitable for detection, but it is oxidized to nitrite ( $\text{NO}_2^-$ ) and nitrate ( $\text{NO}_3^-$ ) by nitrate reductase. The concentrations of these anions are used as quantitative measure of NO production using the Griess reaction. In this reaction, acidified  $\text{NO}_2^-$  produces a nitrosating agent, which reacts with sulfanilic acid to produce diazonium ion. This ion couples with NED (N-1-naphthyl ethylene diamine dihydrochloride) to form a colored product that is measured spectrophotometrically at 540 nm.

The reaction was standardized using different concentrations of  $\text{NaNO}_2$ , using the method in Promega User Guide (Product G2930). 50  $\mu$ l of cells from each sample (PF, BM, Serum, Ins, and PP & Spl) from all the groups (control, TG3, TG3F, TG9, TG9F, TG24, and TG24F) were plated in the wells of a 96-well plate. The cells were incubated for 24 h, in a  $\text{CO}_2$  incubator at 5 %  $\text{CO}_2$ , 37 °C. Sulfanilamide solution was prepared by dissolving 1 % sulfanilamide in 5 % ortho-phosphoric acid. 0.1 % NED solution was prepared in distilled water. 50  $\mu$ l of sulfanilamide solution was added to each well and incubated at room temperature for 5 min, in dark. 50  $\mu$ l of NED solution was then added and incubated at room temperature for 5 min, in dark. Absorbance was measured in a plate reader at 540 nm. Using the standard curve prepared, the absorbance values of the samples were plotted to get the concentrations of NO produced (in  $\mu\text{M}$ ). The concentrations of NO were plotted against each sample.

**Catalase Estimation:** Catalase is an antioxidant enzyme, present in the peroxisomes of all aerobic organisms, that protects against harmful



ROS, produced during metabolism. Catalase concentration was measured in this study. 0.5 ml of culture medium supernatant (lung sample) was added to the reaction mixture containing 1 ml of 0.01 M phosphate buffer (pH 7.0), 0.5 ml of 0.2 M H<sub>2</sub>O<sub>2</sub>, and 0.4 ml of H<sub>2</sub>O. The reaction was stopped by adding 2 ml of acid reagent (dichromate/acetic acid), made by mixing 5 % potassium dichromate with glacial acetic acid, in the ratio of 1:3 by volume. The tubes were heated for 10 min, and absorbance was measured at 610 nm using a spectrophotometer (Shimadzu). The concentration of catalase produced was determined from a standard curve.

**Ascorbic Acid Estimation:** L-ascorbic acid (vitamin C) is an antioxidant, free-radical scavenger, which is present in normal conditions to protect against ROS. Inflammation leads to a decrease in the concentration of ascorbic acid, which can be measured colorimetrically. The reaction mixture for quantification of ASA comprised 0.1 ml of the sample, 2.9 ml distilled water, 1 ml of 2 % DNPH, and 1–2 drops of thiourea. After incubation for 3 h at 37 °C, the osazone crystals formed were dissolved with 7 ml of 80 % sulfuric acid. Absorbance was read after 30 min at 540 nm using a spectrophotometer. The concentration of ASA was determined from a standard curve.

**Statistics:** All data are presented as mean  $\pm$  SEM, and only *p* values of less than 0.05 have been considered as significant. Graphs are plotted using GraphPad Prism 6.

## 4.4 Results

### 4.4.1 In Vitro Cell Proliferation Assay

(a) **With 1  $\mu$ g/ml LPS treatment**—We found that administration of LPS has led to a 1.82-fold decrease ( $p < 0.05$ ) in cell viability, as compared to untreated control. Administration of fisetin has led to an increase ( $p < 0.05$ ), compared to LPS-treated cells, with the maximum

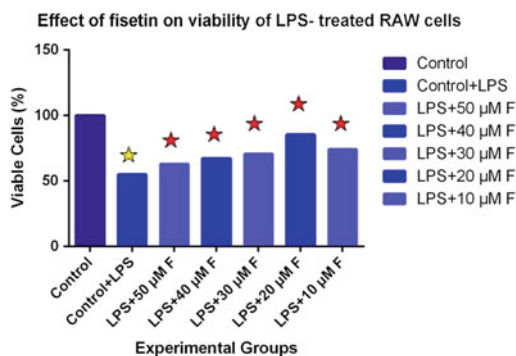


**Fig. 4.1** Effect of different concentrations of fisetin on LPS-treated RAW 264.7 macrophages (\*— $p < 0.05$  vs. control. \*— $p < 0.05$  vs. LPS-treated). The absorbance of control, at 570 nm, is assumed to be for 100 % viability. The viabilities of the other samples are calculated with respect to control and plotted. Since the viability plotted in the graph is calculated from the average absorbance, it is a single value, and hence, error bars could not be plotted

increase with 20  $\mu$ M fisetin (1.56-fold). This shows that fisetin is capable of restoring the cell's proliferative capacity, which had been reduced with LPS treatment.

The absorbance of control, at 570 nm, is assumed to be for 100 % viability. The viabilities of the other samples are calculated with respect to control and plotted (Fig. 4.1 and Table 4.1).

(b) **With 50 ng/ml PMA treatment**—Here, we demonstrated that administration of PMA has led to a 2.39-fold decrease ( $p < 0.05$ ) in cell viability, as compared to untreated control. Administration of fisetin has led to an increase ( $p < 0.05$ ), compared to LPS-treated cells, with the maximum increase with 10  $\mu$ M fisetin (2.23-fold). This shows that fisetin is capable of restoring the cell's proliferative capacity, which had been reduced with PMA treatment. The absorbance of control, at 570 nm, is assumed to be for 100 % viability. The viabilities of the other samples are calculated with respect to control and plotted (Fig. 4.2 and Table 4.2).

**Table 4.1** Cell proliferation assay using MTT, on LPS- and fisetin-treated RAW 264.7 macrophages

	Percentage viability (%)	Fold change	
		wrt control	wrt LPS
Control	100.00		
LPS (1 µg/ml)	54.95	(-) <b>1.82*</b>	
LPS (1 µg/ml) + 50 µM fisetin	62.95		(+) <b>1.15*</b>
LPS (1 µg/ml) + 40 µM fisetin	67.34		(+) <b>1.23*</b>
LPS (1 µg/ml) + 30 µM fisetin	70.72		(+) <b>1.29*</b>
LPS (1 µg/ml) + 20 µM fisetin	85.48		(+) <b>1.56*</b>
LPS (1 µg/ml) + 10 µM fisetin	74.27		(+) <b>1.35*</b>

Fisetin leads to an increase ( $p < 0.05$ ) in cell viability, with maximum increase with 20 µM fisetin

Bold value denotes biological significance in terms of trend

\* statistically significant with p value less than 1-5 % of significance

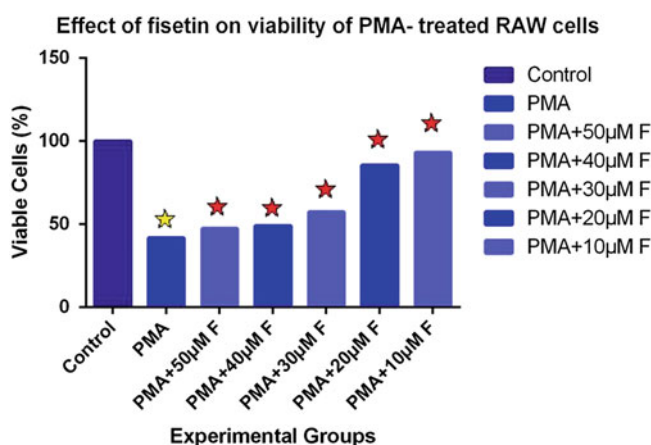


**Fig. 4.2** Effect of different concentrations of fisetin on PMA-treated RAW 264.7 macrophages (\*— $p < 0.05$  vs. control. \*— $p < 0.05$  vs. LPS-treated). The absorbance of control, at 570 nm, is assumed to be for 100 % viability.

The viabilities of the other samples are calculated with respect to control and plotted. Since the viability plotted in the graph is calculated from the average absorbance, it is a single value, and hence, error bars could not be plotted

**Table 4.2** Cell proliferation assay using MTT, on PMA- and fisetin-treated RAW 264.7 macrophages

	Percentage viability (%)	Fold change	
		wrt control	wrt LPS
Control	100.00		
PMA (50 ng/ml)	41.76	(-) <b>2.39*</b>	
PMA (50 ng/ml) + 50 µM fisetin	47.54		(+) <b>1.14*</b>
PMA (50 ng/ml) + 40 µM fisetin	49.07		(+) <b>1.18*</b>
PMA (50 ng/ml) + 30 µM fisetin	57.45		(+) <b>1.38*</b>
PMA (50 ng/ml) + 20 µM fisetin	85.59		(+) <b>2.05*</b>
PMA (50 ng/ml) + 10 µM fisetin	93.16		(+) <b>2.23*</b>

Fisetin leads to an increase ( $p < 0.05$ ) in cell viability, with maximum increase with 10 µM fisetin

Bold value denotes biological significance in terms of trend

\* statistically significant with p value less than 1-5 % of significance

#### 4.4.2 *In Vitro* Cellular Uptake of Fisetin

The uptake of various concentrations of fisetin is assessed by fluorescent microscopy. We found that maximum uptake occurs with 50  $\mu$ M fisetin, and the uptake reduces with lower concentrations of fisetin (Fig. 4.3).

#### 4.4.3 Total Cell Count (TC)

- (a) **Peritoneal Fluid**—The total cell count of peritoneal fluid has increased on treatment with only TG, as compared to control. There is a 1.61-fold increase ( $p < 0.05$ ) after 3 h, a 2.03-fold increase ( $p < 0.05$ ) after 9 h, and a 3.35-fold increase ( $p < 0.05$ ) after 24 h of treatment with TG, as compared to control. The cell count has decreased after treatment with fisetin, compared to only TG, after 3 h (1.08-fold), 9 h (1.19-fold), and after 24 h (1.96-fold,  $p < 0.05$ ). The increase in TC with administration of fisetin indicates cell recruitment has occurred in response to the inflammation caused by TG. Large numbers of activated cells are recruited to the PF. Fisetin is successful in inhibiting cell recruitment, as shown by the decrease in TC (Fig. 4.4 and Table 4.3).
- (b) **Bone Marrow**—The total cell count of bone marrow, the site of hematopoiesis, has increased on treatment with only TG, as compared to control, 3 h (1.09-fold), 9 h (1.48-fold) and 24 h (1.72-fold) after treatment. This shows that inflammatory cells are being synthesized in response to the inflammation caused by TG. The cell count has decreased after treatment with fisetin, compared to only TG, after 3 h (1.15-fold), 9 h (1.68-fold), and 24 h (1.80-fold). The decrease in TC with fisetin is indicative of the reduction in inflammation, since synthesis of the cells is reduced (Fig. 4.5 and Table 4.4).
- (c) **Peripheral Blood**—The total cell count of peripheral blood has increased on treatment with only TG, as compared to control, 3 h (1.46-fold), 9 h (1.99-fold), and 24 h

(1.71-fold) after treatment. This increase indicates systemic inflammation caused by TG, which leads to greater number of cells in the blood for supply to tissues. The cell count has decreased after treatment with fisetin, compared to only TG, after 3 h (1.20-fold), 9 h (1.66-fold), and 24 h (1.54-fold). Fisetin effectively inhibits cell recruitment (Fig. 4.6 and Table 4.5).

- (d) **Spleen**—The total cell count of spleen has increased on treatment with only TG, as compared to control. There is a 1.18-fold increase ( $p < 0.05$ ) after 3 h, a 1.23-fold increase ( $p < 0.05$ ) after 9 h, and a 2.01-fold increase ( $p < 0.05$ ) after 24 h of treatment. The cell count has decreased in all the samples after treatment with fisetin, compared to only TG. There is a 1.27-fold decrease ( $p < 0.05$ ) after 3 h, a 1.41-fold decrease ( $p < 0.05$ ) after 9 h, and a 1.62-fold decrease ( $p < 0.05$ ) after 24 h. This indicates that cell recruitment, which had increased as a response to the inflammation caused by TG, is successfully inhibited by fisetin (Fig. 4.7 and Table 4.6).

#### 4.4.4 Differential Cell Count (DC)

- (a) **Peritoneal Fluid**—The differential count of peritoneal fluid, treated only with TG, shows an increase in the PMN cell count, as compared to control, 3 h (2.01-fold), 9 h (3.07-fold), and 24 h (2.23-fold) after treatment. On treatment with fisetin, the PMN cell count decreases, compared to only TG, after 3 h (1.34-fold), 9 h (2.26-fold), and 24 h (1.64-fold). The differential count of peritoneal fluid, treated only with TG, shows an increase in the mononuclear (MN) cell count, as compared to control, 3 h (1.38-fold), 9 h (2.02-fold), and 24 h (3.14-fold) after treatment. On treatment with fisetin, the MN cell count decreases, compared to only TG, after 3 h (1.07-fold), 9 h (1.60-fold), and 24 h (2.14-fold) (Fig. 4.8 and Table 4.7).
- (b) **Peripheral Blood**—The differential count of peripheral blood, treated only with TG, shows an increase in the PMN cell count, as compared to control, 3 h (1.81-fold), 9 h

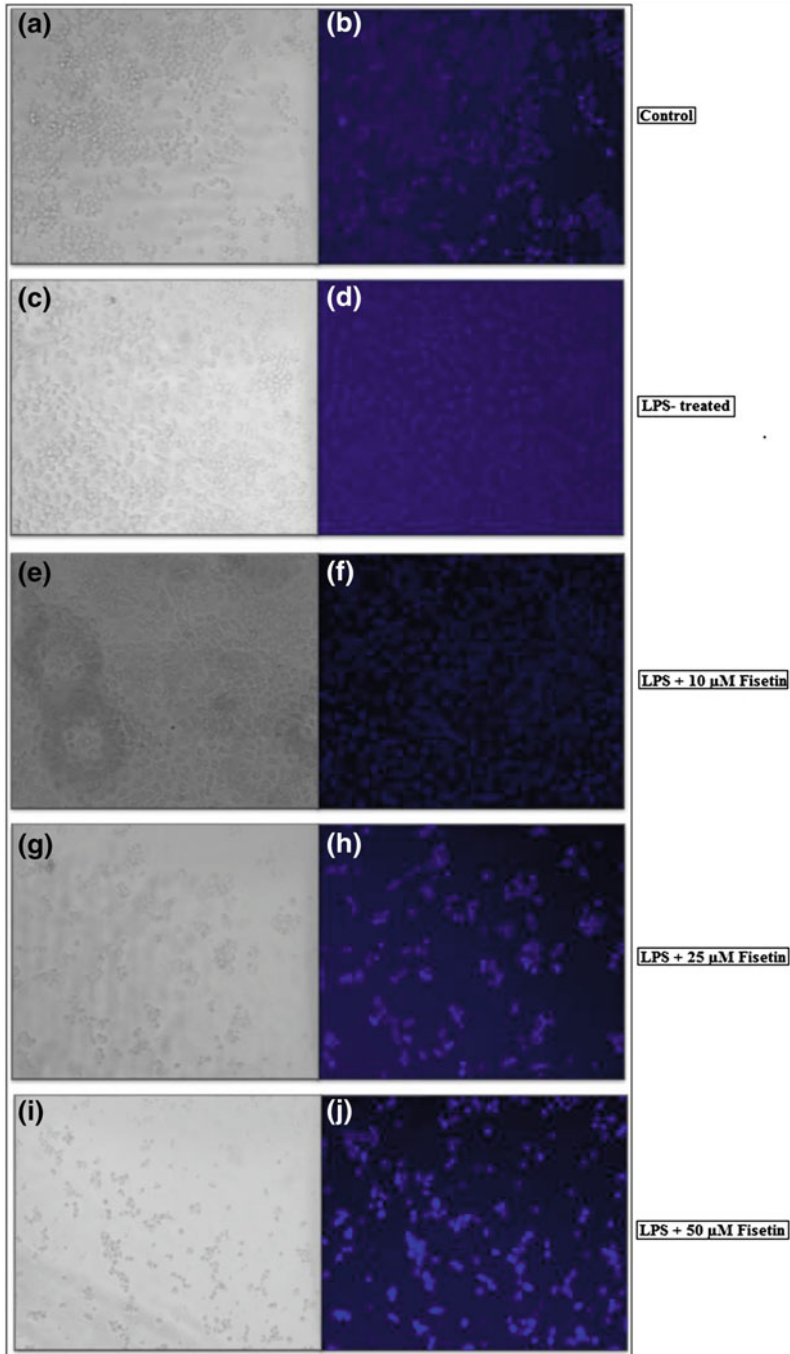


**Fig. 4.3** Effect of fisetin on LPS-treated RAW 264.7 cells, as seen under phase contrast and *blue light* of Fluid Cell Imaging Station (a, c, e, g, i—phase contrast images. b, d, f, h, j—fluorescent images)

(2.90-fold), and 24 h (3.26-fold) after treatment. On treatment with fisetin, the PMN cell count decreases, compared to only TG, after 3 h (1.43-fold), 9 h (1.45-fold), and

24 h (2.37-fold). The differential count of PB, treated only with TG, shows an increase in the MN cell count, as compared to control, 3 h (1.50-fold), 9 h (1.63-fold), and 24 h

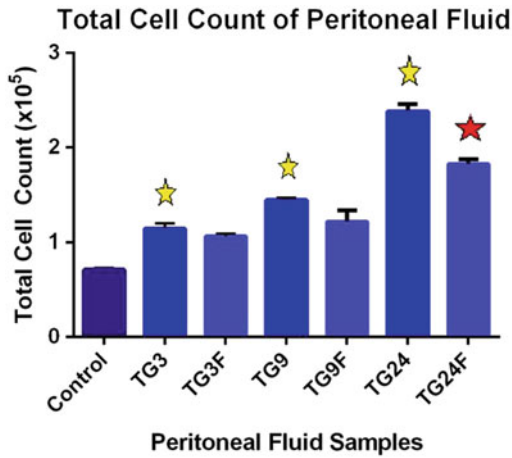


**Fig. 4.4** Effect of fisetin on the total cell count of peritoneal fluid (\*— $p < 0.05$  vs. control. \*— $p < 0.05$  vs. TG)

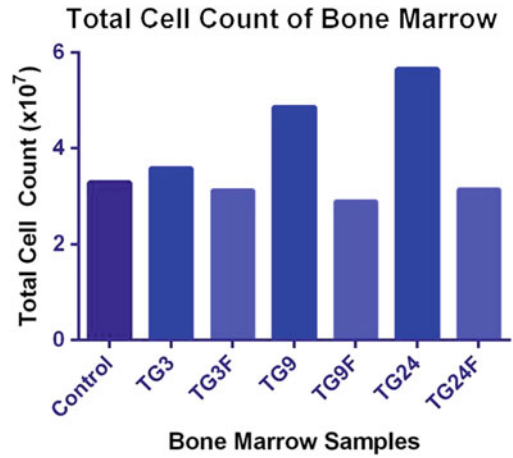


**Fig. 4.5** Effect of fisetin on the total cell count of bone marrow

**Table 4.3** Total cell count of peritoneal fluid, taken by hemocytometry

PF	Cell count (×10 <sup>5</sup> )	Fold change	
		wrt control	wrt TG
Control	0.71 ± 0.02		
TG3	1.14 ± 0.06	<b>+1.61*</b>	
TG3F	1.06 ± 0.03		<b>-1.08</b>
TG9	1.44 ± 0.03	<b>+2.03*</b>	
TG9F	1.21 ± 0.12		<b>-1.19</b>
TG24	2.38 ± 0.08	<b>+3.35*</b>	
TG24F	1.82 ± 0.05		<b>-1.31*</b>

There is a 1.08-fold decrease after 3 h, a 1.19-fold decrease after 9 h, and a 1.31-fold decrease ( $p < 0.05$ ) after 24 h of fisetin treatment

Bold value denotes biological significance in terms of trend  
\* statistically significant with p value less than 1-5 % of significance

(1.96-fold) after treatment. On treatment with fisetin, the MN cell count decreases, compared to only TG, after 3 h (1.22-fold), 9 h (1.46-fold), and 24 h (1.72-fold) (Fig. 4.9 and Table 4.8).

#### 4.4.5 NO Estimation

(a) **Peritoneal Fluid**—The concentration of nitric oxide (NO) in peritoneal fluid has increased by 1.49-fold after 3 h ( $p < 0.05$ ),

**Table 4.4** Total cell count of bone marrow, taken by hemocytometry

BM	Cell count (×10 <sup>7</sup> )	Fold change	
		wrt control	wrt TG
Control	3.29 ± 0.049		
TG3	3.58 ± 0.101	<b>+1.09</b>	
TG3F	3.12 ± 0.335		<b>-1.15</b>
TG9	4.86 ± 0.139	<b>+1.48</b>	
TG9F	2.89 ± 0.037		<b>-1.68</b>
TG24	5.66 ± 0.333	<b>+1.72</b>	
TG24F	3.14 ± 0.049		<b>-1.80</b>

There is a 1.15-fold decrease after 3 h, a 1.68-fold decrease after 9 h, and a 1.80-fold decrease after 24 h of fisetin treatment

Bold value denotes biological significance in terms of trend

1.52-fold after 9 h ( $p < 0.05$ ), and 1.51-fold after 24 h ( $p < 0.05$ ), after treatment with TG as compared to control. The NO concentration has decreased 1.29-fold after 3 h, 1.18-fold after 9 h and 1.23-fold after 24 h ( $p < 0.05$ ) with fisetin, as compared to TG. The increase in NO concentration in peritoneal fluid on administration of TG indicates inflammation, which is reduced by the administration of fisetin. The level of

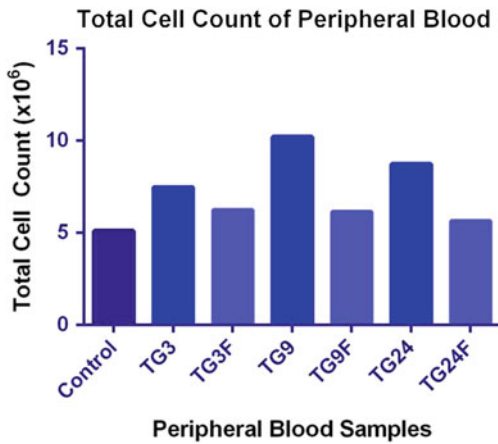


**Fig. 4.6** Effect of fisetin on the total cell count of peritoneal fluid

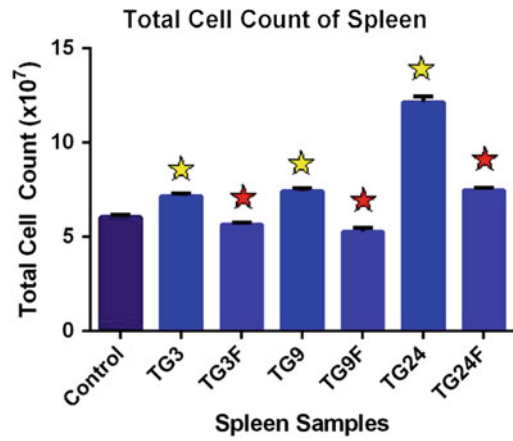


**Fig. 4.7** Effect of fisetin on the total cell count of spleen (\*— $p < 0.05$  vs. control. \*— $p < 0.05$  vs. TG)

**Table 4.5** Total cell count of peripheral blood, taken by hemocytometry

PB	Cell count (×10 <sup>6</sup> )	Fold change	
		wrt control	wrt TG
Control	5.12 ± 0.226		
TG3	7.48 ± 0.126	<b>+1.46</b>	
TG3F	6.24 ± 0.14		<b>-1.20</b>
TG9	10.22 ± 0.128	<b>+1.99</b>	
TG9F	6.16 ± 0.332		<b>-1.66</b>
TG24	8.74 ± 0.243	<b>+1.71</b>	
TG24F	5.66 ± 0.244		<b>-1.54</b>

There is a 1.20-fold decrease after 3 h, a 1.66-fold decrease after 9 h, and a 1.54-fold decrease after 24 h of fisetin treatment

Bold value denotes biological significance in terms of trend

inflammation does not undergo much variation over time (Fig. 4.10 and Table 4.9).

- (b) **Bone Marrow**—The concentration of nitric oxide (NO) in bone marrow has decreased 1.12-fold after 3 h and 1.09-fold after 9 h, but has increased 1.48-fold after 24 h ( $p < 0.05$ ), after treatment with TG as compared to control. With fisetin treatment, the NO concentration has decreased 1.18-fold after 3 h, 1.01-fold after 9 h and 1.69-fold after 24 h ( $p < 0.05$ ), compared to only TG. The increase in NO concentration in bone

**Table 4.6** Total cell count of spleen, taken by hemocytometry

Spl	Cell count (×10 <sup>7</sup> )	Fold change	
		wrt control	wrt TG
Control	6.04 ± 0.13		
TG3	7.15 ± 0.16	<b>+1.18*</b>	
TG3F	5.65 ± 0.11		<b>-1.27*</b>
TG9	7.42 ± 0.16	<b>+1.23*</b>	
TG9F	5.27 ± 0.21		<b>-1.41*</b>
TG24	12.13 ± 0.31	<b>+2.01*</b>	
TG24F	7.47 ± 0.13		<b>-1.62*</b>

There is a 1.27-fold decrease ( $p < 0.05$ ) after 3 h, a 1.41-fold decrease ( $p < 0.05$ ) after 9 h, and a 1.62-fold decrease ( $p < 0.05$ ) after 24 h of fisetin treatment

Bold value denotes biological significance in terms of trend \* statistically significant with p value less than 1-5 % of significance

marrow on administration of TG after 24 h indicates inflammation, which is reduced by the administration of fisetin. There is not much change after 3 and 9 h (Fig. 4.11 and Table 4.10).

- (c) **Serum**—The concentration of nitric oxide (NO) in serum has decreased by 1.13-fold after 3 h ( $p < 0.05$ ) and 1.12-fold after 9 h, but has increased by 1.11-fold after 24 h ( $p < 0.05$ ), after treatment with TG as compared to control. The NO concentration has

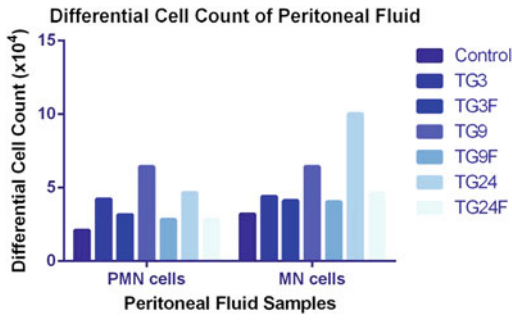


**Fig. 4.8** Effect of fisetin on the differential count of cells in peritoneal fluid

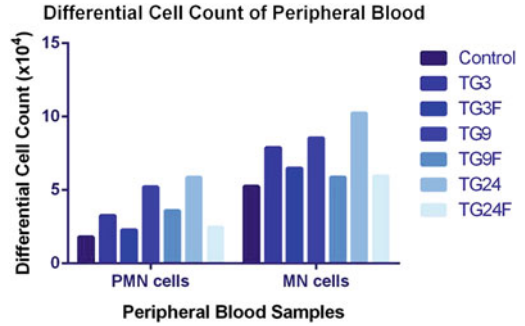


**Fig. 4.9** Effect of fisetin on the differential count of cells in peripheral blood

**Table 4.7** Differential cell count of peritoneal fluid, seen after HE staining, under light microscope

PF	Polymorphonuclear cells			Mononuclear cells		
	Cell count ( $\times 10^4$ )	Fold change		Cell count ( $\times 10^4$ )	Fold change	
		wrt control	wrt TG		wrt control	wrt TG
Control	2.10			3.20		
TG3	4.22	<b>+2.01</b>		4.40	<b>+1.38</b>	
TG3+F	3.16		<b>-1.34</b>	4.12		<b>-1.07</b>
TG9	6.44	<b>+3.07</b>		6.45	<b>+2.02</b>	
TG9+F	2.85		<b>-2.26</b>	4.04		<b>-1.60</b>
TG24	4.68	<b>+2.23</b>		10.04	<b>+3.14</b>	
TG24+F	2.85		<b>-1.64</b>	4.66		<b>-2.14</b>

There is a 1.34-fold decrease in PMN cells, a 1.07-fold decrease in MN cells after 3 h; a 2.26-fold decrease in PMN cells; a 1.60-fold decrease on MN cells after 9 h, and a 1.64-fold decrease in PMN cells and a 2.14-fold decrease in MN cells after 24 h, of treatment with fisetin

Bold value denotes biological significance in terms of trend

**Table 4.8** Differential cell count of peripheral blood, seen after HE staining, under light microscope

PB	Polymorphonuclear cells			Mononuclear cells		
	Cell count ( $\times 10^4$ )	Fold change		Cell count ( $\times 10^4$ )	Fold change	
		wrt control	wrt TG		wrt control	wrt TG
Control	1.80			5.24		
TG3	3.26	<b>+1.81</b>		7.88	<b>+1.50</b>	
TG3+F	2.28		<b>-1.43</b>	6.48		<b>-1.22</b>
TG9	5.22	<b>+2.90</b>		8.56	<b>+1.63</b>	
TG9+F	3.60		<b>-1.45</b>	5.88		<b>-1.46</b>
TG24	5.87	<b>+3.26</b>		10.26	<b>+1.96</b>	
TG24+F	2.48		<b>-2.37</b>	5.98		<b>-1.72</b>

There is a 1.43-fold decrease in PMN cells and a 1.22-fold decrease in MN cells after 3 h, a 1.45-fold decrease in PMN cells and a 1.46-fold decrease on MN cells after 9 h, and a 2.37-fold decrease in PMN cells and a 1.72-fold decrease in MN cells after 24 h, of treatment with fisetin

Bold value denotes biological significance in terms of trend

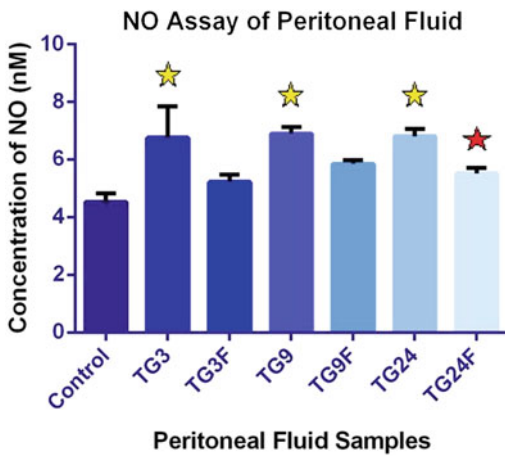


**Fig. 4.10** Effect of fisetin on the production of nitric oxide in the peritoneal fluid (\*— $p < 0.05$  vs. control. \*— $p < 0.05$  vs. TG)

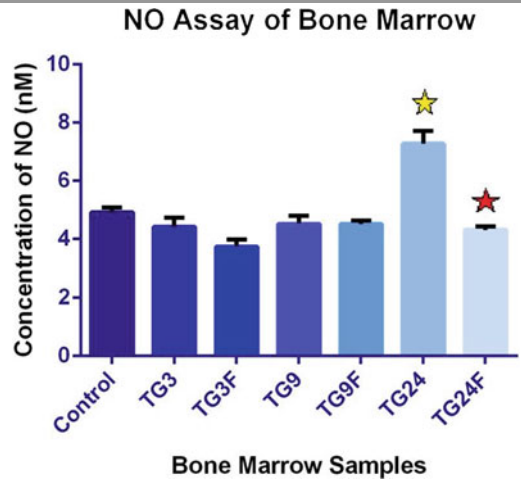


**Fig. 4.11** Effect of fisetin on the production of nitric oxide in the bone marrow (\*— $p < 0.05$  vs. control. \*— $p < 0.05$  vs. TG)

**Table 4.9** Concentration of NO produced in peritoneal fluid

PF	NO concentration (nM)	Fold change	
		wrt control	wrt TG
Control	4.52 ± 0.17		
TG3	6.75 ± 0.63	<b>+1.49*</b>	
TG3F	5.23 ± 0.25		<b>-1.29</b>
TG9	6.89 ± 0.24	<b>+1.52*</b>	
TG9F	5.85 ± 0.13		<b>-1.18</b>
TG24	6.81 ± 0.26	<b>+1.51*</b>	
TG24F	5.53 ± 0.14		<b>-1.23*</b>

There is a 1.29-fold decrease after 3 h, a 1.18-fold decrease after 9 h, and a 1.23-fold decrease ( $p < 0.05$ ) after 24 h of fisetin treatment

Bold value denotes biological significance in terms of trend

\* statistically significant with p value less than 1-5 % of significance

decreased 1.23-fold after 3 h ( $p < 0.05$ ) and 1.26-fold after 9 h ( $p < 0.05$ ), but has remained almost same after 24 h, with fisetin treatment. The increase in NO concentration in serum on administration of TG after 24 h indicates inflammation, which is reduced slightly by the administration of fisetin. The NO concentration decreases after 3 h

**Table 4.10** Concentration of NO produced in bone marrow

BM	NO concentration (nM)	Fold change	
		wrt control	wrt TG
Control	4.92 ± 0.16		
TG3	4.41 ± 0.32	-1.12	
TG3F	3.74 ± 0.24		-1.18
TG9	4.52 ± 0.28	-1.09	
TG9F	4.51 ± 0.09		-1.01
TG24	7.28 ± 0.25	<b>+1.48*</b>	
TG24F	4.32 ± 0.09		<b>-1.69*</b>

There is a 1.18-fold decrease after 3 h, a 1.01-fold decrease after 9 h, and a 1.69-fold decrease ( $p < 0.05$ ) after 24 h of fisetin treatment

Bold value denotes biological significance in terms of trend \* statistically significant with p value less than 1-5 % of significance

and 9 h, which is further reduced by fisetin (Fig. 4.12 and Table 4.11).

- (d) **Peyer's Patch**—The concentration of nitric oxide (NO) in Peyer's patch has increased by 3.81-fold after 3 h ( $p < 0.05$ ), 1.40-fold after 9 h ( $p < 0.05$ ), and 2.38-fold after 24 h ( $p < 0.05$ ), after treatment with TG as compared to control. The NO concentration has decreased 1.52-fold after 3 h ( $p < 0.05$ ) and



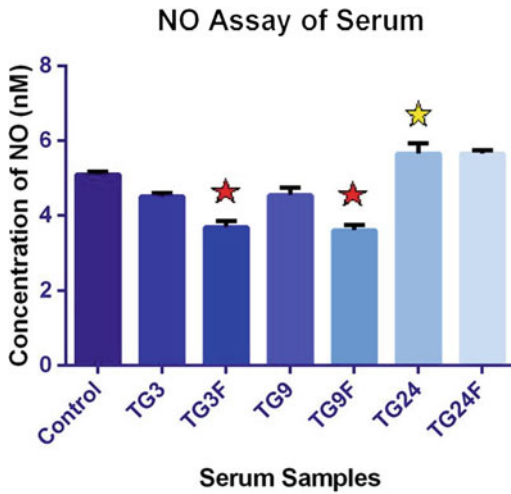


**Fig. 4.12** Effect of fisetin on the production of nitric oxide in the serum (\* $p < 0.05$  vs. control. \* $p < 0.05$  vs. TG)

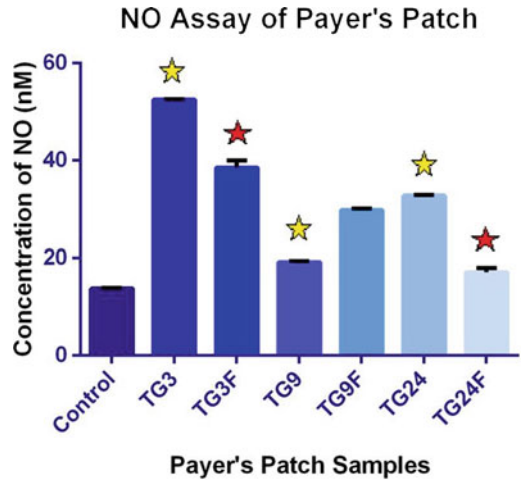


**Fig. 4.13** Effect of fisetin on the production of nitric oxide in the Peyer's patch (\* $p < 0.05$  vs. control. \* $p < 0.05$  vs. TG)

**Table 4.11** Concentration of NO produced in serum

Ser	NO concentration (nM)	Fold change	
		wrt control	wrt TG
Control	5.10 ± 0.07		
TG3	4.51 ± 0.09	-1.13	
TG3F	3.68 ± 0.18		<b>-1.23*</b>
TG9	4.55 ± 0.21	-1.12	
TG9F	3.60 ± 0.10		<b>-1.26*</b>
TG24	5.66 ± 0.16	<b>+1.11*</b>	
TG24F	5.66 ± 0.06		1.00

There is a 1.23-fold decrease ( $p < 0.05$ ) after 3 h and a 1.26-fold decrease ( $p < 0.05$ ) after 9 h of fisetin treatment. Bold value denotes biological significance in terms of trend. \* statistically significant with p value less than 1-5 % of significance.

1.91-fold after 24 h ( $p < 0.05$ ) with fisetin, compared to only TG, but has increased 1.55-fold after 9 h. The increase in NO concentration in Peyer's patch on administration of TG indicates inflammation, which is reduced by the administration of fisetin after 3 and 24 h (Fig. 4.13 and Table 4.12).

- (e) **Intestine**—The concentration of nitric oxide (NO) in the intestine has increased 2.69-fold after 3 h ( $p < 0.05$ ), 1.17-fold after 9 h

**Table 4.12** Concentration of NO produced in Peyer's patch

PP	NO concentration (nM)	Fold change	
		wrt control	wrt TG
Control	13.76 ± 0.14		
TG3	52.48 ± 0.11	<b>+3.81*</b>	
TG3F	34.48 ± 1.54		<b>-1.52*</b>
TG9	19.23 ± 0.13	<b>+1.40*</b>	
TG9F	29.75 ± 0.33		+1.55
TG24	32.75 ± 0.12	<b>+2.38*</b>	
TG24F	17.13 ± 0.87		<b>-1.91*</b>

There is a 1.52-fold decrease ( $p < 0.05$ ) after 3 h and a 1.91-fold decrease ( $p < 0.05$ ) after 24 h of fisetin treatment. Bold value denotes biological significance in terms of trend. \* statistically significant with p value less than 1-5 % of significance.

( $p < 0.05$ ) and 1.98-fold after 24 h ( $p < 0.05$ ), after treatment with TG as compared to control. The NO concentration has decreased by 1.96-fold after 3 h ( $p < 0.05$ ), 1.63-fold after 9 h ( $p < 0.05$ ), and 3.44-fold after 24 h ( $p < 0.05$ ), with fisetin as compared to TG. The increase in NO concentration in intestine on administration of TG indicates inflammation, which is reduced by the administration of fisetin (Fig. 4.14 and Table 4.13).

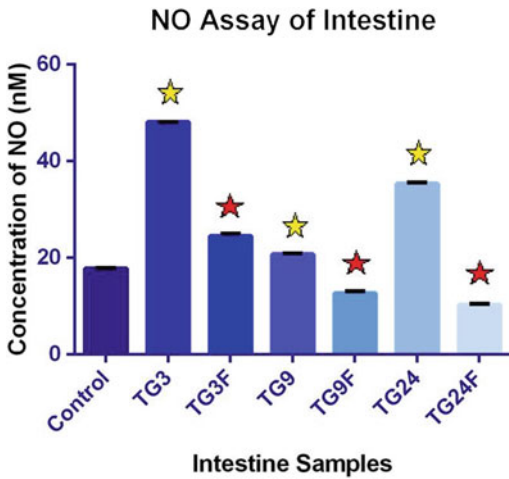


**Fig. 4.14** Effect of fisetin on the production of nitric oxide in the intestine (\*— $p < 0.05$  vs. control. \*— $p < 0.05$  vs. TG)

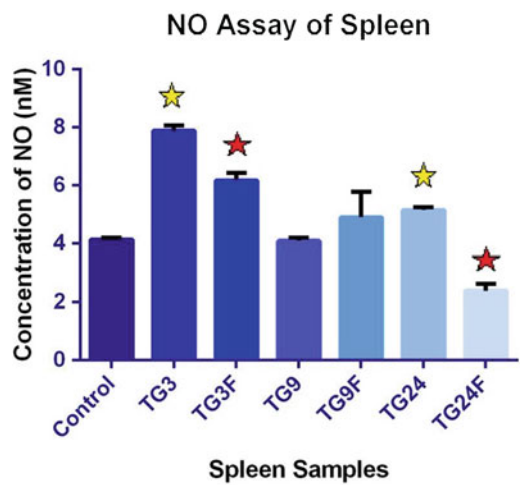


**Fig. 4.15** Effect of fisetin on the production of nitric oxide in the spleen (\*— $p < 0.05$  vs. control. \*— $p < 0.05$  vs. TG)

**Table 4.13** Concentration of NO produced in intestine

Ins	NO concentration (nM)	Fold change	
		wrt control	wrt TG
Control	17.84 ± 0.10		
TG3	48.06 ± 0.08	<b>+2.69*</b>	
TG3F	24.48 ± 0.48		<b>-1.96*</b>
TG9	20.79 ± 0.12	<b>+1.17*</b>	
TG9F	12.73 ± 0.32		<b>-1.63*</b>
TG24	35.36 ± 0.23	<b>+1.98*</b>	
TG24F	10.28 ± 0.23		<b>-3.44*</b>

There is a 1.96-fold decrease ( $p < 0.05$ ) after 3 h, a 1.63-fold decrease ( $p < 0.05$ ) after 9 h, and a 3.44-fold decrease ( $p < 0.05$ ) after 24 h of fisetin treatment

Bold value denotes biological significance in terms of trend  
\* statistically significant with  $p$  value less than 1-5 % of significance

(f) **Spleen**—The concentration of nitric oxide (NO) in the intestine has increased by 1.90-fold after 3 h ( $p < 0.05$ ) and 1.24-fold after 24 h ( $p < 0.05$ ), after treatment with TG as compared to control, but has decreased slightly (1.01-fold) after 9 h. The NO concentration has decreased by 1.28-fold after 3 h ( $p < 0.05$ ) and 2.15-fold after 24 h ( $p < 0.05$ ) with fisetin treatment, compared to only TG, but has increased

**Table 4.14** Concentration of NO produced in spleen

Spl	NO concentration (nM)	Fold change	
		wrt control	wrt TG
Control	4.14 ± 0.06		
TG3	7.88 ± 0.19	<b>+1.90*</b>	
TG3F	6.17 ± 0.27		<b>-1.28*</b>
TG9	4.09 ± 0.10	-1.01	
TG9F	4.91 ± 0.88		+1.20
TG24	5.15 ± 0.09	<b>+1.24*</b>	
TG24F	2.40 ± 0.24		<b>-2.15*</b>

There is a 1.28-fold decrease ( $p < 0.05$ ) after 3 h and a 2.15-fold decrease ( $p < 0.05$ ) after 24 h of fisetin treatment  
Bold value denotes biological significance in terms of trend  
\* statistically significant with  $p$  value less than 1-5 % of significance

1.20-fold after 9 h. The increase in NO concentration in spleen on administration of TG indicates inflammation, which is reduced by the administration of fisetin (Fig. 4.15 and Table 4.14).

#### 4.4.6 Catalase Estimation

(a) **Peritoneal Fluid**—The concentration of catalase in peritoneal fluid has decreased on treatment with only TG, as compared to

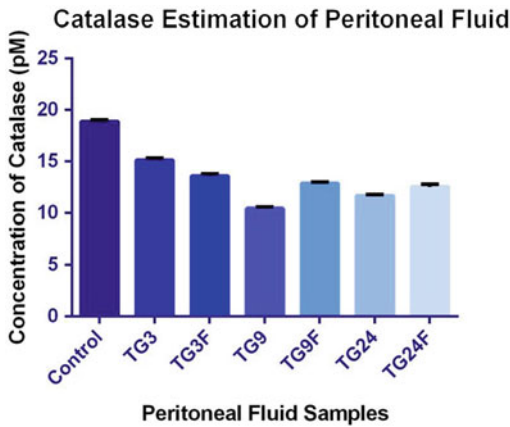


**Fig. 4.16** Effect of fisetin on the production of catalase in the peritoneal fluid

**Table 4.15** Concentration of catalase produced in peritoneal fluid

PF	Catalase concentration (pM)	Fold change	
		wrt control	wrt TG
Control	18.89 ± 0.16		
TG3	15.14 ± 0.17	-1.25	
TG3F	13.58 ± 0.23		<b>-1.12</b>
TG9	10.45 ± 0.14	-1.81	
TG9F	12.88 ± 0.12		+1.23
TG24	11.69 ± 0.12	-1.62	
TG24F	12.53 ± 0.28		+1.07

There is a 1.12-fold decrease after 3 h of fisetin treatment. Bold value denotes biological significance in terms of trend.

control, 3 h (1.25-fold), 9 h (1.81-fold), and 24 h (1.62-fold) after treatment. The catalase concentration has increased after treatment with fisetin, compared to only TG, after 9 h (1.23-fold) and 24 h (1.07-fold), but has decreased after 3 h (1.12-fold) (Fig. 4.16 and Table 4.15).

- (b) **Bone Marrow**—The concentration of catalase in bone marrow has decreased after 9 h (1.16-fold) and 24 h (1.15-fold), on treatment with only TG, as compared to control, but has increased 3 h (1.04-fold) after treatment. The catalase concentration has

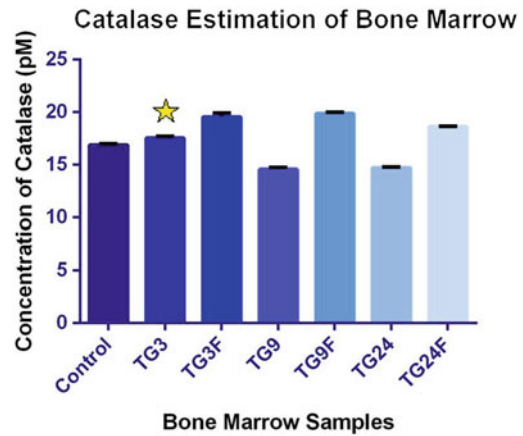


**Fig. 4.17** Effect of fisetin on the production of catalase in the bone marrow (\*— $p < 0.05$  vs. control. \*— $p < 0.05$  vs. TG)

**Table 4.16** Concentration of catalase produced in bone marrow

BM	Catalase concentration (pM)	Fold change	
		wrt control	wrt TG
Control	16.89 ± 0.12		
TG3	17.55 ± 0.18	<b>+1.04*</b>	
TG3F	19.56 ± 0.34		+1.12
TG9	14.58 ± 0.16	-1.16	
TG9F	19.89 ± 0.16		+1.36
TG24	14.71 ± 0.07	-1.15	
TG24F	18.61 ± 0.07		+1.27

There is a 1.04-fold increase ( $p < 0.05$ ) after 3 h of TG treatment.

Bold value denotes biological significance in terms of trend. \* statistically significant with p value less than 1-5 % of significance.

increased after treatment with fisetin, compared to only TG, after 3 h (1.12-fold), 9 h (1.36-fold), and 24 h (1.27-fold) (Fig. 4.17 and Table 4.16).

- (c) **Serum**—The concentration of catalase in serum has decreased on treatment with only TG, as compared to control, 3 h (1.41-fold), 9 h (1.95-fold), and 24 h (1.34-fold) after treatment. The catalase concentration has increased after treatment with fisetin,

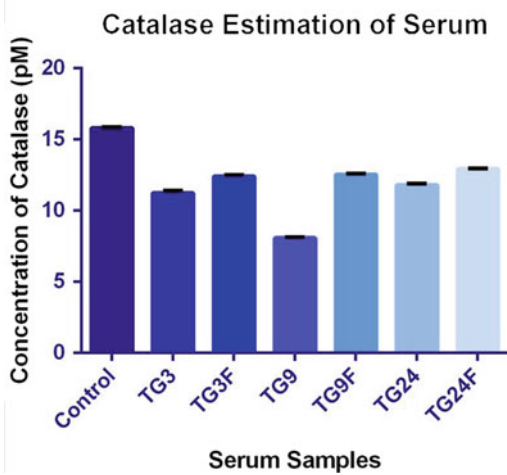


**Fig. 4.18** Effect of fisetin on the production of catalase in the bone marrow

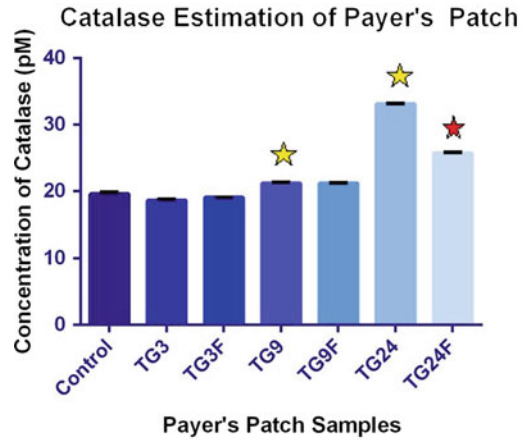


**Fig. 4.19** Effect of fisetin on the production of catalase in the Peyer's patch (\*— $p < 0.05$  vs. control. \*— $p < 0.05$  vs. TG)

**Table 4.17** Concentration of catalase produced in serum

Ser	Catalase concentration (pM)	Fold change	
		wrt control	wrt TG
Control	15.81 ± 0.07		
TG3	11.22 ± 0.18	-1.41	
TG3F	12.41 ± 0.10		+1.11
TG9	8.09 ± 0.04	-1.95	
TG9F	12.53 ± 0.08		+1.55
TG24	11.82 ± 0.08	-1.34	
TG24F	12.92 ± 0.06		+1.09

compared to only TG, after 3 h (1.11-fold), 9 h (1.55-fold), and 24 h (1.09-fold) (Fig. 4.18 and Table 4.17).

- (d) **Peyer's Patch**—The concentration of catalase in Peyer's patch has decreased on treatment with only TG, as compared to control, 3 h (1.05-fold) after treatment, but has increased significantly ( $p < 0.05$ ) after 9 h (1.08-fold) and 24 h (1.69-fold). The catalase concentration has increased after treatment with fisetin, compared to only TG, after 3 h (1.02-fold), but has remained almost unchanged after 9 h, and has decreased by 1.29-fold after 24 h ( $p < 0.05$ ) (Fig. 4.19 and Table 4.18).

**Table 4.18** Concentration of catalase produced in Peyer's patch

PP	Catalase concentration (pM)	Fold change	
		wrt control	wrt TG
Control	19.59 ± 0.25		
TG3	18.61 ± 0.19	-1.05	
TG3F	19.04 ± 0.04		+1.02
TG9	21.22 ± 0.10	<b>+1.08*</b>	
TG9F	21.20 ± 0.10		1.00
TG24	33.15 ± 0.08	<b>+1.69*</b>	
TG24F	25.70 ± 0.18		<b>-1.29*</b>

There is a 1.29-fold decrease ( $p < 0.05$ ) after 9 h of fisetin treatment

Bold value denotes biological significance in terms of trend

\* statistically significant with p value less than 1-5 % of significance

- (e) **Intestine**—The concentration of catalase in intestine has decreased on treatment with only TG, as compared to control, 1.17-fold after 3 h, 1.91-fold after 9 h, and 1.96-fold after 24 h after treatment. The catalase concentration has increased after treatment with fisetin, compared to only TG, after 3 h (1.09-fold), 9 h (1.09-fold), and 24 h (1.16-fold) (Fig. 4.20 and Table 4.19).

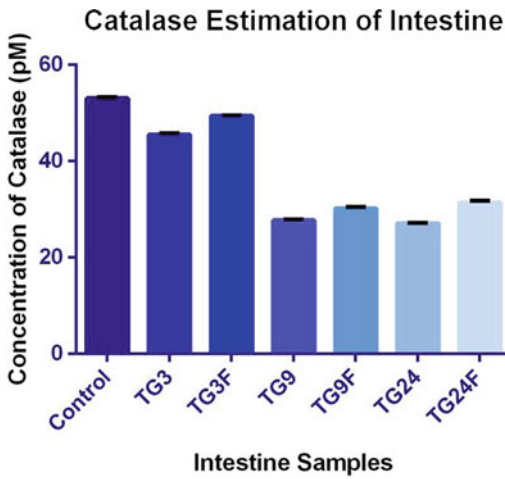


**Fig. 4.20** Effect of fisetin on the production of catalase in the intestine

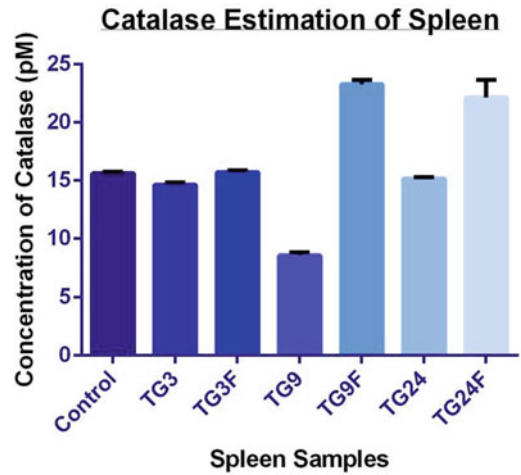


**Fig. 4.21** Effect of fisetin on the production of catalase in the spleen

**Table 4.19** Concentration of catalase produced in intestine

Ins	Catalase concentration (pM)	Fold change	
		wrt control	wrt TG
Control	53.09 ± 0.16		
TG3	45.55 ± 0.25	-1.17	
TG3F	49.44 ± 0.04		+1.09
TG9	27.79 ± 0.13	-1.91	
TG9F	30.17 ± 0.39		+1.09
TG24	27.10 ± 0.11	-1.96	
TG24F	31.44 ± 0.34		+1.16

**Table 4.20** Concentration of catalase produced in spleen

Spl	Catalase concentration (pM)	Fold change	
		wrt control	wrt TG
Control	15.62 ± 0.13		
TG3	14.64 ± 0.19	-1.07	
TG3F	15.71 ± 0.15		+1.07
TG9	8.61 ± 0.27	-1.81	
TG9F	23.29 ± 0.39		+2.71
TG24	15.18 ± 0.12	-1.03	
TG24F	22.17 ± 1.49		+1.46

(f) **Spleen**—The concentration of catalase in spleen has decreased on treatment by 1.07-fold after 3 h, 1.81-fold after 9 h, and 1.03-fold after 24 h, with only TG, as compared to control. The catalase concentration has increased after treatment with fisetin, compared to only TG, after 3 h (1.07-fold), 9 h (2.71-fold), and 24 h (1.46-fold) (Fig. 4.21 and Table 4.20).

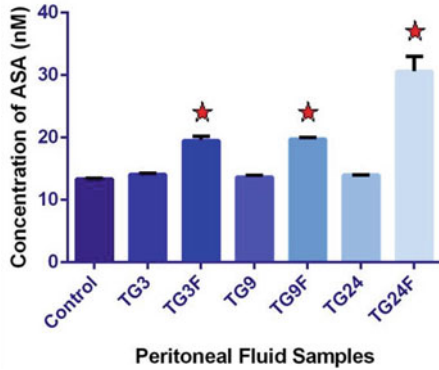
#### 4.4.7 Ascorbic Acid Estimation

(a) **Peritoneal fluid**—The concentration of ascorbic acid in peritoneal fluid has increased

by 1.06-fold after 3 h, 1.02-fold after 9 h, and 1.05-fold after 24 h, on treatment with only TG, as compared to control. The ASA concentration has increased significantly ( $p < 0.05$ ) after treatment with fisetin, compared to only TG, after 3 h (1.38-fold), 9 h (1.44-fold), and 24 h (2.19-fold) (Fig. 4.22 and Table 4.21).

(b) **Bone marrow**—The concentration of ascorbic acid in bone marrow has decreased by 1.11-fold after 3 h ( $p < 0.05$ ) and 1.02-fold after 9 h, on treatment with only TG, as compared to control. It has increased

**Ascorbic Acid Estimation of Peritoneal Fluid**



**Ascorbic Acid Estimation of Bone Marrow**

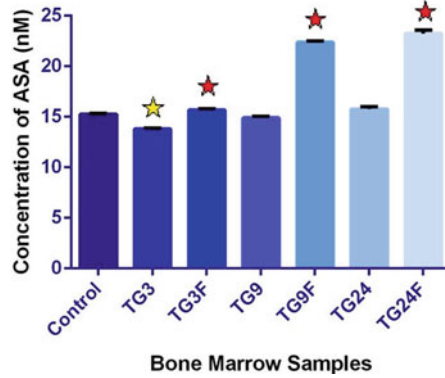


**Fig. 4.22** Effect of fisetin on the production of ascorbic acid in the peritoneal fluid (\*— $p < 0.05$  vs. control. \*— $p < 0.05$  vs. TG)

**Fig. 4.23** Effect of fisetin on the production of ascorbic acid in the bone marrow (\*— $p < 0.05$  vs. control. \*— $p < 0.05$  vs. TG)

**Table 4.21** Concentration of ASA produced in peritoneal fluid

PF	ASA concentration (nM)	Fold change	
		wrt control	wrt TG
Control	13.36 ± 0.12		
TG3	14.09 ± 0.16	+1.06	
TG3F	19.48 ± 0.73		<b>+1.38*</b>
TG9	13.68 ± 0.25	+1.02	
TG9F	19.70 ± 0.30		<b>+1.44*</b>
TG24	13.98 ± 0.06	+1.05	
TG24F	30.63 ± 2.37		<b>+2.19*</b>

There is a 1.38-fold increase ( $p < 0.05$ ) after 3 h, a 1.44-fold increase ( $p < 0.05$ ) after 9 h, and a 2.19-fold increase ( $p < 0.05$ ) after 24 h of fisetin treatment  
 Bold value denotes biological significance in terms of trend

\* statistically significant with p value less than 1-5 % of significance

**Table 4.22** Concentration of ASA produced in bone marrow

BM	ASA concentration (nM)	Fold change	
		wrt control	wrt TG
Control	15.27 ± 0.07		
TG3	13.79 ± 0.09	<b>-1.11*</b>	
TG3F	15.65 ± 0.15		<b>+1.14*</b>
TG9	14.91 ± 0.16	<b>-1.02</b>	
TG9F	22.37 ± 0.13		<b>+1.50*</b>
TG24	15.77 ± 0.22	+1.03	
TG24F	23.23 ± 0.37		<b>+1.47*</b>

There is a 1.14-fold increase ( $p < 0.05$ ) after 3 h, a 1.50-fold increase ( $p < 0.05$ ) after 9 h, and a 1.47-fold increase ( $p < 0.05$ ) after 24 h of fisetin treatment  
 Bold value denotes biological significance in terms of trend

\* statistically significant with p value less than 1-5 % of significance

slightly after 24 h (1.03-fold). The ASA concentration has increased significantly ( $p < 0.05$ ) after treatment with fisetin, compared to only TG, after 3 h (1.14-fold), 9 h (1.50-fold), and 24 h (1.47-fold) (Fig. 4.23 and Table 4.22).

(c) **Serum**—After treatment with only TG, as compared to control, the concentration of ascorbic acid in serum has decreased by 1.01-fold, 3 h after treatment, but has increased after 9 h (1.07-fold) and 24 h (1.03-fold). The ASA concentration has

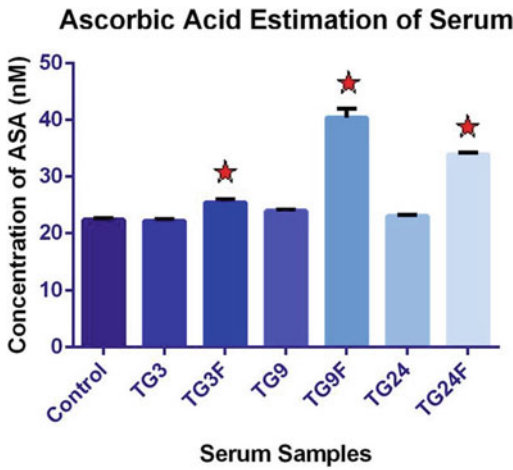


**Fig. 4.24** Effect of fisetin on the production of ascorbic acid in the serum (\*— $p < 0.05$  vs. control. \*— $p < 0.05$  vs. TG)

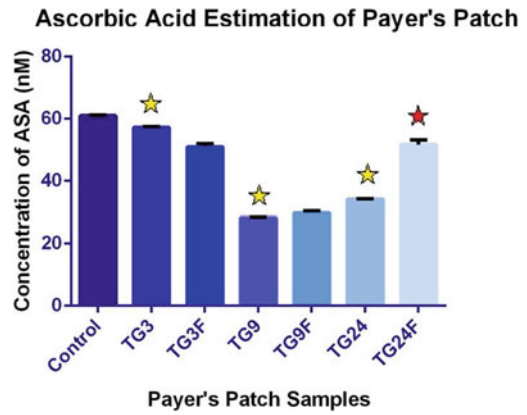


**Fig. 4.25** Effect of fisetin on the production of ascorbic acid in the Peyer's patch (\*— $p < 0.05$  vs. control. \*— $p < 0.05$  vs. TG)

**Table 4.23** Concentration of ASA produced in serum

Ser	ASA concentration (nM)	Fold change	
		wrt control	wrt TG
Control	22.42 ± 0.22		
TG3	22.18 ± 0.31	<b>-1.01</b>	
TG3F	25.45 ± 0.55		<b>+1.15*</b>
TG9	23.97 ± 0.22	+1.07	
TG9F	40.39 ± 1.61		<b>+1.69*</b>
TG24	23.05 ± 0.17	+1.03	
TG24F	33.91 ± 0.35		<b>+1.47*</b>

There is a 1.15-fold increase ( $p < 0.05$ ) after 3 h, a 1.69-fold increase ( $p < 0.05$ ) after 9 h, and a 1.47-fold increase ( $p < 0.05$ ) after 24 h of fisetin treatment  
 Bold value denotes biological significance in terms of trend  
 \* statistically significant with p value less than 1-5 % of significance

increased significantly ( $p < 0.05$ ) after treatment with fisetin, compared to only TG, after 3 h (1.15-fold), 9 h (1.69-fold), and 24 h (1.47-fold) (Fig. 4.24 and Table 4.23).

- (d) **Peyer's patch**—The concentration of ascorbic acid in Peyer's patch has decreased significantly ( $p < 0.05$ ) on treatment with only TG, as compared to control, 3 h (1.07-fold), 9 h (2.16-fold), and 24 h

**Table 4.24** Concentration of ASA produced in Peyer's patch

PP	ASA concentration (nM)	Fold change	
		wrt control	wrt TG
Control	61.06 ± 0.12		
TG3	57.21 ± 0.22	<b>-1.07*</b>	
TG3F	50.99 ± 1.01		-1.12
TG9	28.27 ± 0.17	<b>-2.16*</b>	
TG9F	29.80 ± 0.60		<b>+1.05</b>
TG24	34.14 ± 0.08	<b>-1.79*</b>	
TG24F	51.73 ± 1.47		<b>+1.52*</b>

There is a 1.05-fold increase ( $p < 0.05$ ) after 9 h and a 1.52-fold increase ( $p < 0.05$ ) after 24 h of fisetin treatment  
 Bold value denotes biological significance in terms of trend  
 \* statistically significant with p value less than 1-5 % of significance

(1.79-fold) after treatment. The ASA concentration has increased 1.05-fold after 9 h and 1.52-fold after 24 h ( $p < 0.05$ ) after treatment with fisetin, compared to only TG, but has decreased 1.12-fold after 3 h (Fig. 4.25 and Table 4.24).

- (e) **Intestine**—The concentration of ascorbic acid in intestine has decreased significantly ( $p < 0.05$ ) on treatment with only TG, as compared to control, 3 h (1.36-fold), 9 h

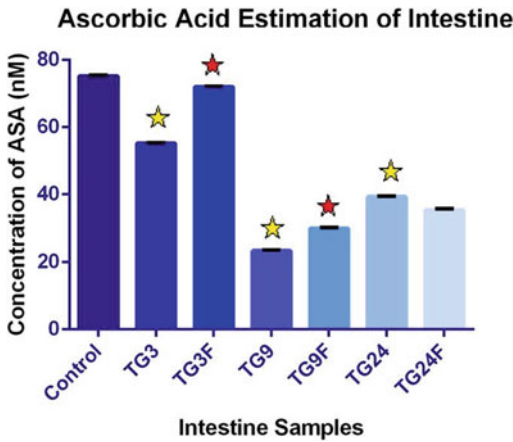


**Fig. 4.26** Effect of fisetin on the production of ascorbic acid in the intestine (\*— $p < 0.05$  vs. control. \*— $p < 0.05$  vs. TG)

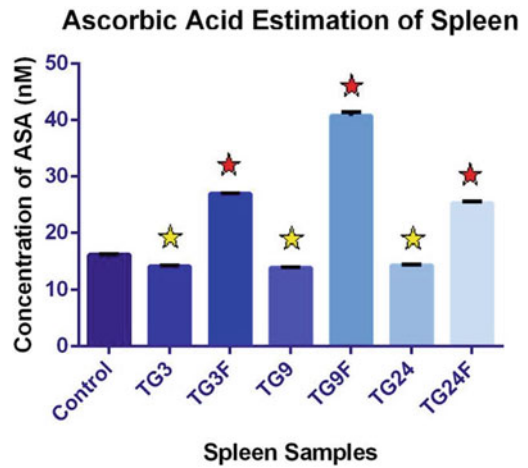


**Fig. 4.27** Effect of fisetin on the production of ascorbic acid in the spleen (\*— $p < 0.05$  vs. control. \*— $p < 0.05$  vs. TG)

**Table 4.25** Concentration of ASA produced in intestine

Ins	ASA concentration (nM)	Fold change	
		wrt control	wrt TG
Control	75.25 ± 0.20		
TG3	55.22 ± 0.13	<b>-1.36</b>	
TG3F	72.01 ± 0.19		<b>+1.30*</b>
TG9	23.46 ± 0.12	<b>-3.21</b>	
TG9F	29.85 ± 0.25		<b>+1.27*</b>
TG24	39.32 ± 0.18	<b>-1.91</b>	
TG24F	35.38 ± 0.43		-1.11

There is a 1.30-fold increase ( $p < 0.05$ ) after 3 h and a 1.27-fold increase ( $p < 0.05$ ) after 9 h of fisetin treatment. Bold value denotes biological significance in terms of trend.

\* statistically significant with p value less than 1-5 % of significance.

(3.21-fold), and 24 h (1.91-fold) after treatment. The ASA concentration has increased significantly ( $p < 0.05$ ) after treatment with fisetin, compared to only TG, after 3 h (1.30-fold) and 9 h (1.27-fold), but has decreased after 24 h (1.11-fold) (Fig. 4.26 and Table 4.25).

(f) **Spleen**—The concentration of ascorbic acid in spleen has decreased significantly

**Table 4.26** Concentration of ASA produced in spleen

Spl	ASA concentration (nM)	Fold change	
		wrt control	wrt TG
Control	16.24 ± 0.09		
TG3	14.19 ± 0.11	<b>-1.44*</b>	
TG3F	26.95 ± 0.05		<b>+1.90*</b>
TG9	13.93 ± 0.06	<b>-1.17*</b>	
TG9F	40.74 ± 0.66		<b>+2.92*</b>
TG24	14.35 ± 0.13	<b>-1.13*</b>	
TG24F	25.28 ± 0.32		<b>+1.76*</b>

There is a 1.90-fold increase ( $p < 0.05$ ) after 3 h, a 2.92-fold increase ( $p < 0.05$ ) after 9 h, and a 1.76-fold increase ( $p < 0.05$ ) after 24 h of fisetin treatment.

Bold value denotes biological significance in terms of trend.

\* statistically significant with p value less than 1-5 % of significance.

( $p < 0.05$ ) on treatment with only TG, as compared to control, 3 h (1.44-fold), 9 h (1.17-fold), and 24 h (1.13-fold) after treatment. The ASA concentration has increased significantly ( $p < 0.05$ ) after treatment with fisetin, compared to only TG, after 3 h (1.90-fold), 9 h (2.92-fold), and 24 h (1.76-fold) (Fig. 4.27 and Table 4.26).



## 4.5 Discussion

In this present study, we have induced peritonitis in C57BL/6 J mice using thioglycollate and then assessed the anti-inflammatory effects of plant flavonoid, fisetin, when administered prophylactically, by *in vitro* and *in vivo* assays. We have also induced inflammation on RAW macrophages and seen the effect of fisetin on them. We have used fisetin which is traditionally used to treat different inflammation-related diseases. We found that fisetin had a positive prophylactic effect on the peritonitis. This is the first evidence showed that fisetin may have prophylactic effect against the thioglycollate-induced peritonitis in mice.

Intraperitoneal infection known as peritonitis is a major killer in the practice of clinical surgery and it is also one of the most frequent diagnoses in a surgical ICU leading to severe sepsis [31]. Intra-abdominal sepsis, although it affects all age groups, takes a greater toll on the elderly population than it does on younger populations. In approximately 80 % of the patients with a secondary peritonitis, the initial surgical intervention may sanitize the abdominal cavity from the infectious lesion. The remaining patients develop a persisting peritonitis with a considerable number of subsequent surgical interventions, infectious complications, a high rate of severe sepsis, and septic shock as well as a mortality double as high ranging between 30 and 63 % [32–34]. Hospital-acquired infections especially the TP have the highest mortality. High mortality is the consequence of the large number of difficult clinical courses and high rates of severe sepsis and septic shock. Several authors defined TP as a diffuse, therapy-resistant peritonitis with fungi or low-grade pathogenic bacteria in the absence of a well-defined infective focus after apparently adequate therapy [35–38]. Primary peritonitis is also known as SBP and has a low incidence on surgical ICUs as it is managed purely without any surgical intervention and mostly by physician. Secondary peritonitis is the most common entity in critical surgical patients and is defined as an infection of the peritoneal cavity resulting from hollow viscous perforation, ischemic

necrosis, or other injuries of the gastrointestinal tract [39]. There is significant difference between the microbial flora in tertiary and secondary peritonitis and TP comprises of mostly opportunistic and nosocomial facultative pathogenic bacteria and fungi (e.g., enterococci, *Enterobacter*, and *Candida*). The development of multidrug resistance has also been observed in microbes causing TP due to use of broad spectrum antibiotic therapy [15]. Due to the character of disease, medical treatment for secondary and TP differs considerably.

Peritonitis remains as a serious complication influencing patients' mortality [40]. In the process of peritonitis, bacteria are the main source of local and systemic infections. Bacterial pathogens and their products trigger the inflammatory response by transcriptional activation of inflammatory genes, leading to the release of large number of inflammatory mediators, including cytokines, chemokines, adhesion molecules, reactive oxygen, which can easily cause sepsis when they are uncontrolled and excessive [41]. Previous investigators found that acute peritonitis was associated with the activation of the transcription factor NF- $\kappa$ B in various organs and tissues, which can regulate the synthesis of TNF- $\alpha$ , IL-6 and many other molecules involved in the inflammatory reaction [42–45]. The spectrum of peritonitis in India continues to differ from Western countries.

Flavonoids are polyphenol compounds, widely distributed in plant foods, which may exert beneficial effects in various diseases. Many of the biological actions of flavonoids have been attributed to their antioxidant properties [46]. The highest levels of fisetin, a flavonoid compound (160  $\mu$ g/g) are found in strawberries with 5–10-fold lower levels in apples and persimmons and smaller amounts in kiwi fruit, peaches, grapes, tomatoes, onions, and cucumbers [47, 48]. Emerging data from *in vitro* and *in vivo* studies indicate that fisetin possesses antiproliferative properties against several cancers [49, 50].

In our study, cells treated with inflammatory agents such as LPS and PMA lose their viability and their proliferative capacity. Fisetin has been shown to prevent the loss of viability when given

prophylactically. Cellular uptake studies have shown that cells take up the fisetin, so it can act from within the cell. We also found that total cell recruitment increases with the administration of TG, showing that it has induced inflammation, and the body is synthesizing more immune cells to counter the infection. Cell recruitment was successfully inhibited by fisetin. Nitric acid is produced by macrophages as a defense against oxidative stress. Catalase is produced by cells to break down harmful ROS. Ascorbic acid, an antioxidant, is normally present in the body to protect against ROS. In case of inflammation, both NO and catalase content are expected to increase, but ascorbic acid content is expected to decrease. Our assays have shown this to be the case, except with catalase. The NO content of the tissues has increased with TG challenge and has decreased with fisetin. The ASA concentration has decreased with TG and has increased significantly with fisetin treatment. Plant-derived natural products contributed significantly to drug discovery in the past and still provide an effective source for new drug development. Although fisetin is not particularly abundant in many fruits and vegetables, the incorporation of significant quantities of fisetin-rich foods into the diet of diseased patients might provide an alternative approach.

In conclusion, peritonitis continues to be an important problem in the healthcare system. Fisetin, has recently received some attention for its beneficial effects against several diseases. Our research study showed that the use of fisetin could effectively reduce the severity of acute peritonitis in our rodent model. Further studies need to be done to verify the effect of flavonoid compound, explore the mechanisms, and promote the clinical use. An accurate biomarker for the early identification of peritonitis would be of great diagnostic value. An early finding of the correct diagnosis of peritonitis and the subsequent effective initiation of an appropriate treatment may help to lower the complication rate and to improve the prognosis.

## References

1. Angus DC, Wax RS. Epidemiology of sepsis: an update. *Crit Care Med*. 2001;29:S109–16.
2. Hardaway RM. A review of septic shock. *Am Surg*. 2000;66:22–9.
3. Remick DG. Pathophysiology of sepsis. *Am J Pathol*. 2007;170:1435–44.
4. Anel RL, Kumar A. Experimental and emerging therapies for sepsis and septic shock. *Expert Opin Investig Drugs*. 2001;10:1471–85.
5. Dellinger RP. Inflammation and coagulation: implications for the septic patient. *Clin Infect Dis*. 2003;36:1259–65.
6. Zhang J, Wu Q, Song S, Wan Y, Zhang R, Tai M, Liu C. Effect of hydrogen-rich water on acute peritonitis of rat models. *Int Immunopharmacol*. 2014;21(1):94–101.
7. Billing AG, Frohlich D, Konecny G, Schildberg FW, Machleidt W, Fritz H, et al. Local serum application—restoration of sufficient host-defense in human peritonitis. *Eur J Clin Invest*. 1994;24:28–35.
8. Ghiselli R, Giacometti A, Cirioni O, Mocchegiani F, Orlando F, Silvestri C, et al. Efficacy of the bovine antimicrobial peptide indolicidin combined with piperacillin/tazobactam in experimental rat models of polymicrobial peritonitis. *Crit Care Med*. 2008;36:240–5.
9. Lippi G, Danese E, Cervellin G, Montagnana M. Laboratory diagnostics of spontaneous bacterial peritonitis. *Clin Chim Acta*. 2014;20(430):164–70.
10. Yang SK, Xiao L, Zhang H, Xu XX, Song PA, Liu FY, Sun L. Significance of serum procalcitonin as biomarker for detection of bacterial peritonitis: a systematic review and meta-analysis. *BMC Infect Dis*. 2014;22(14):452.
11. Cai ZH, Fan CL, Zheng JF, Zhang X, Zhao WM, Li B, Li L, Dong PL, Ding HG. Measurement of serum procalcitonin levels for the early diagnosis of spontaneous bacterial peritonitis in patients with decompensated liver cirrhosis. *BMC Infect Dis*. 2015;15(1):55.
12. Lutz P, Nischalke HD, Strassburg CP, Spengler U. Spontaneous bacterial peritonitis: the clinical challenge of a leaky gut and a cirrhotic liver. *World J Hepatol*. 2015;7(3):304–14.
13. Doklešić SK, Bajec DD, Djukić RV, Bumbaširević V, Detanac AD, Detanac SD, Bracanović M, Karamković RA. Secondary peritonitis—evaluation of 204 cases and literature review. *J Med Life*. 2014;7(2):132–8.
14. Alessiani M, Gianola M, Rossi S, Perfetti V, Serra P, Zelaschi D, Magnani E, Cobianchi L. Peritonitis secondary to spontaneous perforation of a primary gastrointestinal stromal tumour of the small intestine:

- a case report and a literature review. *Int J Surg Case Rep.* 2015;6C:58–62.
15. Mishra SP, Tiwary SK, Mishra M, Gupta SK. An introduction of tertiary peritonitis. *J Emerg Trauma Shock.* 2014;7(2):121–3.
  16. Panhofer P, Izay B, Riedl M, Ferenc V, Ploder M, Jakesz R, Götzinger P. Age, microbiology and prognostic scores help to differentiate between secondary and tertiary peritonitis. *Langenbecks Arch Surg.* 2009;394(2):265–71.
  17. Weiss G, Meyer F, Lippert H. Infectiological diagnostic problems in tertiary peritonitis. *Langenbecks Arch Surg.* 2006;391(5):473–82.
  18. Fakhruddin N, Waltenberger B, Cabaravdic M, Atanasov AG, Malainer C, Schachner D, Heiss EH, Liu R, Noha SM, Grzywacz AM, Mihaly-Bison J, Awad EM, Schuster D, Breuss JM, Rollinger JM, Bochkov V, Stuppner H, Dirsch VM. Identification of plumericin as a potent new inhibitor of the NF- $\kappa$ B pathway with anti-inflammatory activity in vitro and in vivo. *Br J Pharmacol.* 2014;171(7):1676–86.
  19. Gelderblom M, Leypoldt F, Lewerenz J, Birkenmayer G, Orozco D, et al. The flavonoid fisetin attenuates post ischemic immune cell infiltration, activation and infarct size after transient cerebral middle artery occlusion in mice. *J Cereb Blood Flow Metab.* 2012;32:835–43.
  20. Sahu BD, Kalvala AK, Koneru M, Mahesh Kumar J, Kuncha M, Rachamalla SS, Sistla R. Ameliorative effect of fisetin on cisplatin-induced nephrotoxicity in rats via modulation of NF- $\kappa$ B activation and antioxidant defence. *PLoS ONE.* 2014;9(9):e105070.
  21. Khan N, Asim M, Afaq F, Abu Zaid M, Mukhtar H. A novel dietary flavonoid fisetin inhibits androgen receptor signaling and tumor growth in athymic nude mice. *Cancer Res.* 2008;68:8555–63.
  22. Murtaza I, Adhami VM, Hafeez BB, Saleem M, Mukhtar H. Fisetin, a natural flavonoid, targets chemoresistant human pancreatic cancer AsPC-1 cells through DR3-mediated inhibition of NF- $\kappa$ B. *Int J Cancer.* 2009;125:2465–73.
  23. Syed DN, Afaq F, Maddodi N, Johnson JJ, Sarfaraz S, Ahmad A, Setaluri V, Mukhtar H. Inhibition of human melanoma cell growth by the dietary flavonoid fisetin is associated with disruption of Wnt/ $\beta$ -catenin signaling and decreased Mitf levels. *J Invest Dermatol.* 2011;131:1291–9.
  24. Chen YC, Shen SC, Lee WR, Lin HY, Ko CH, Shih CM, Yang LL. Wogonin and fisetin induction of apoptosis through activation of caspase 3 cascade and alternative expression of p21 protein in hepatocellular carcinoma cells SK-HEP-1. *Arch Toxicol.* 2002;76:351–9.
  25. Leotoing L, Wauquier F, Guicheux J, Miot-Noirault E, Wittrant Y, et al. The polyphenol fisetin protects bone by repressing NF- $\kappa$ B and MKP-1-dependent signaling pathways in osteoclasts. *PLoS ONE.* 2013;8:e68388.
  26. Khan N, Afaq F, Syed DN, Mukhtar H. Fisetin, a novel dietary flavonoid, causes apoptosis and cell cycle arrest in human prostate cancer LNCaP cells. *Carcinogenesis.* 2008;29:1049–56.
  27. Sung B, Pandey MK, Aggarwal BB. Fisetin, an inhibitor of cyclin-dependent kinase 6, down-regulates nuclear factor kappa B-regulated cell proliferation, anti apoptotic and metastatic gene products through the suppression of TAK-1 and receptor-interacting protein-regulated IkappaB alpha kinase activation. *Mol Pharmacol.* 2007;71:1703–14.
  28. Chen PY, Ho YR, Wu MJ, Huang SP, Chen PK, Tai MH, Ho CT, Yen JH. Cytoprotective effects of fisetin against hypoxia-induced cell death in PC12 cells. *Food Funct.* 2015;6(1):287–96.
  29. Ravichandran N, Suresh G, Ramesh B, Manikandan R, Choi YW, Vijaiyan Siva G. Fisetin modulates mitochondrial enzymes and apoptotic signals in benzo (a)pyrene-induced lung cancer. *Mol Cell Biochem.* 2014;390:225–34.
  30. Yang PM, Tseng HH, Peng CW, Chen WS, Chiu SJ. Dietary flavonoid fisetin targets caspase-3-deficient human breast cancer MCF-7 cells by induction of caspase-7-associated apoptosis and inhibition of autophagy. *Int J Oncol.* 2012;40:469–78.
  31. Weiss G, Steffanie W, Lippert H. Peritonitis: main reason of severe sepsis in surgical intensive care. *Zentralbl Chir.* 2007;132:130–7.
  32. Buijk SE, Bruining HA. Future directions in the management of tertiary peritonitis. *Intensive Care Med.* 2002;28:1024–9.
  33. Marshall JC, Innes M. Intensive care unit management of intra abdominal infection. *Crit Care Med.* 2003;31:2228–37.
  34. Nathens AB, Rotstein O, Marshall JC. Tertiary peritonitis: clinical features of a complex nosocomial infection. *World J Surg.* 1998;22:158–63.
  35. Malangoni MA. Evaluation and management of tertiary peritonitis. *Am Surg.* 2000;66(2):157–61.
  36. Chromik AM, Meiser A, Hölling J, Sülberg D, Daigeler A, Meurer K, Vogelsang H, Seelig MH, Uhl W. Identification of patients at risk for development of tertiary peritonitis on a surgical intensive care unit. *J Gastrointest Surg.* 2009;13(7):1358–67.
  37. Evans HL, Raymond DP, Pelletier SJ, Crabtree TD, Pruett TL, Sawyer RG. Tertiary peritonitis (recurrent diffuse or localized disease) is not an independent predictor of mortality in surgical patients with intraabdominal infection. *Surg Infect.* 2001;2:255–63.
  38. Panhofer P, Riedl M, Izay B, Ferenc V, Ploder M, Jakesz R, Götzinger P. Clinical outcome and microbial flora in patients with secondary and tertiary peritonitis. *Eur Surg.* 2007;39:259–64.
  39. Calandra T, Cohen J. The international sepsis forum consensus conference on definitions of infection in the intensive care unit. *Crit Care Med.* 2005;33:1538–48.
  40. Davenport A. Peritonitis remains the major clinical complication of peritoneal dialysis: the London, UK, peritonitis audit 2002–2003. *Perit Dial Int.* 2009;29:297–302.
  41. Cohen J. The immunopathogenesis of sepsis. *Nature.* 2002;420:885–91.

42. Tian J, Lin X, Guan R, Xu JG. The effects of hydroxyethyl starch on lung capillary permeability in endotoxic rats and possible mechanisms. *Anesth Analg*. 2004;98:768–74.
43. Feng X, Liu J, Yu M, Zhu S, Xu J. Protective roles of hydroxyethyl starch 130/0.4 in intestinal inflammatory response and survival in rats challenged with polymicrobial sepsis. *Clin Chim Acta*. 2007;376:60–7.
44. Perkins ND. The Rel/NF-kappa B family: friend and foe. *Trends Biochem Sci*. 2000;25:434–40.
45. Sha WC. Regulation of immune responses by NF-kappa B/Rel transcription factors. *J Exp Med*. 1998;187:143–6.
46. Fiorani M, Accorsi A. Dietary flavonoids as intracellular substrates for an erythrocyte trans-plasma membrane oxidoreductase activity. *Br J Nutr*. 2005;94(3):338–45.
47. Arai Y, Watanabe S, Kimira M, Shimoi K, Mochizuki R, et al. Dietary intakes of flavonols, flavones and isoflavones by Japanese women and the inverse correlation between quercetin intake and plasma LDL cholesterol concentration. *J Nutr*. 2000;130:2243–50.
48. Maher P, Dargusch R, Ehren JL, Okada S, Sharma K, Schubert D. Fisetin lowers methylglyoxal dependent protein glycation and limits the complications of diabetes. *PLoS ONE*. 2011;6(6):e21226.
49. Syed DN, Suh Y, Afaq F, Mukhtar H. Dietary agents for chemoprevention of prostate cancer. *Cancer Lett*. 2008;265:167–76.
50. Khan N, Syed DN, Ahmad N, Mukhtar H. Fisetin: a dietary antioxidant for health promotion. *Antioxid Redox Signal*. 2013;19(2):151–62.

---

## 5.1 Aims and Significance of the Project

The Global Initiative in Asthma (2009) defines asthma as “a chronic inflammatory disorder of the airways in which many cells and cellular elements play a role. The chronic inflammation is associated with airway hyper-responsiveness that leads to recurrent episodes of wheezing, breathlessness, chest tightness, and coughing, particularly at night or in the early morning. These episodes are usually associated with widespread, but variable, airflow obstruction within the lung that is often reversible either spontaneously or with treatment.” Over a past few decades, different researchers throughout the globe have involved themselves on the understanding of the pathophysiological basis of asthma at the cellular and molecular levels though the fundamental causes of the disease and the reasons for increased prevalence rates remain unclear.

Asthma, an inflammatory disease in lungs, includes accumulation of inflammatory cells in the lungs and airway epithelial desquamation, goblet cell hyperplasia, hypersecretion of mucus, and thickening of submucosa resulting in bronchoconstriction, airway hyper-responsiveness, and bronchospasm. At the cellular and molecular levels, the development of asthma in an experimental animal model can be summarized as,

when an animal is challenged by an allergen then it stimulates the T cells, especially the TH2 cells, to make IL-4 and IL-5 cytokines in one hand and on the other hand stimulate mast cells to release histamine and leukotrienes responsible for bronchospasm. Mast cells also produce tryptase which stimulate the neutrophils to promote inflammatory responses. Primed mast cells and produced IL-4 and IL-5 activate the eosinophils resulting in eosinophil recruitment in the site of inflammation elevating the level of IgG, potent biomarker for inflammation, in the serum. Allergen treatment causes elevated level of reactive oxygen species (ROS) and reactive nitrogen species (RNS) in the site of inflammation altering the expression of cell adhesion molecules, such as selectin and VCAM, which promote the transendothelial migration (TEM) of leukocytes, critical event for inflammatory responses, immune surveillance, leukocyte homing, and mobilization of hematopoietic progenitor cells. Activation of NADPH oxidase found on the membrane of neutrophils, eosinophils, monocytes, and macrophages, and this enzyme catalyzes the production of superoxide from oxygen and then dismutates it into hydrogen peroxide by the help of superoxide dismutase (SOD), another important enzyme in this pathway. Once formed, the oxidizing potential of hydrogen peroxide may be amplified by eosinophil- and neutrophil-derived peroxidases, eosinophil peroxidase (EPO), and myeloperoxidase (MPO), and these ultimately prime and activate

---

Proposal for the translational research project and its relevance.

different cell types to develop asthma phenotype. Similarly, higher level of RNS also promotes nitration of different proteins following post-translational modification, thus altering their activities. So this can be truly concluded that increased ROS and RNS play crucial role during asthmatic exacerbations [1].

An important feature of inflammation is infiltration of inflamed tissues by immune cells such as neutrophils, eosinophils, and macrophages. As recent evidences indicate that oxidative stress and mitochondrial dysfunction also have important roles in the activation of inflammatory pathways, and during the past decade, apart from the classical concepts, it became clear that metabolic dysfunction is a key feature of inflammation as metabolic, inflammatory, and innate immune processes are also coordinately regulated, and only for this reason, it is essential to explore the question of causality between the state of inflammation and the components that make up the cluster of metabolic pathologies and therefore to develop effective mechanistic models and, ultimately, therapeutic strategies for asthma, most studied inflammatory disorder. A closely linked configuration and coordinated regulation of metabolic and immune responses are likely to be linked to organize and redistribute its energy resources during the mounting of an immune or inflammatory response. But unfortunately there is little or no works have been done to correlate the inflammatory responses with the metabolic alternations ( ) from the energetic parameters as our group have been hypothesized that if one can control the energy utilization by the various immune cell types by controlling its metabolic pathways then only we can take over the ROS and RNS burden to arrest the Inflammatory cell recruitment at the inflammatory tissues as well as it will be possible to stop the tissue degeneration, main concern for asthma. So in this proposal, the main concern is the identification of key regulatory molecule in this pathway on the one hand, while on the other hand development or characterization of specific chemical or nanoparticle or mesenchymal stem cells which will be able to

fine-tune this molecule from therapeutic point of view. So our group has planned to dissect out this disease at the cellular and molecular level aiming at the following points:

1. Fine-tuning of an immunological preclinical model for acute and chronic allergic asthma as from the data of various experiments we know that mice do not spontaneously develop asthma; for this reason to investigate the processes underlying the asthma, an artificial asthmatic-like reaction has to be induced in the airways of the experimental animals. Mouse models of the allergic response to inhaled allergens have been widely used to elucidate the mechanisms underlying the immunologic and inflammatory responses in asthma, and for the identification and investigation of novel targets for controlling allergic inflammation and for this purpose, different gene knockout animal models have been developed in recent past [2].
2. Identification and characterization of specific cellular trafficking and molecular switches in key hematopoietic tissues concentrating on the leukocyte homing in lungs due to alternations in ROS and RNS generation pathways [1, 2].
3. After the identification of the key players in this pathway, our next target is to find out the direct correlation among these various ways, so that identification of the central regulator will be possible which will be later on a subject of drug designing to treat asthma pathophysiology .

---

## 5.2 Plan of Work, Methods, and Techniques to Be Used

### 5.2.1 Animals Used in These Experiments

From the data of various experiments, we know that mice do not spontaneously develop asthma; for this reason, to investigate the processes

underlying the asthma, an artificial asthmatic-like reaction has to be induced in the airways of the experimental animals. The most commonly used strain of mouse for antigen challenge models is BALB/c as they develop a good T helper cell 2 (Th2)-biased immunological response. However, C57BL/6 strain has been used successfully in allergen challenge studies. So in this experimental purpose inbred BALB/c, C57BL/6 and swiss albino strain of mice, collected from the available animal facility of us, will be selected as wild type from which different knockout model, both single and double knockout model, will be generated.

### 5.2.2 Allergen Sensitization and Challenge

For acute asthma model, mice will be sensitized and later challenged with OVA. Mice will be immunized with OVA (100 µg) complexed with aluminum sulfate in a 0.2 ml volume, administered by i.p. injection on day 0. On day 8 (250 µg of OVA) and on days 15, 18, and 21 (125 µg of OVA), mice will be anesthetized briefly with inhalation of isoflurane in a standard anesthesia chamber and given OVA by intratracheal (i.t.) administration. Mice will be anesthetized and placed in a supine position on the board and extending the animal's tongue with lined forceps 50 µg/l of OVA (in the required concentration) will be placed at the back of its tongue. The control group will receive normal saline with aluminum sulfate by i.p. route on day 0 and 0.05 ml of 0.9 % saline by i.t. route on days 8, 15, 18, and 21.

For chronic model, mice (8- to 12-week-old) will be sensitized with 50 µg OVA (grade V; Sigma-Aldrich, St. Louis, MO) in 0.5 mg aluminum hydroxide by s.c. injections on days 0, 7, 14, and 21 and then challenged with OVA (20 µg per mouse) intranasally on days 23, 25, and 28 [3] followed by additional intranasal challenges with OVA twice a week for 8 weeks.

Control mice will be administered PBS instead of OVA for sensitization and challenges.

### 5.2.3 Bronchoalveolar Lavage Fluid and Lung Tissue Collection

Mice will be killed 24 h after the last allergen challenge, and bronchoalveolar lavage fluid (BALF) will be pooled after three washes with saline (0.5 ml each). Total and differential cell counts will be done, and BALF supernatants will be stored at  $-70^{\circ}\text{C}$  for further evaluation. Right lungs are snap-frozen, and left lungs are perfused with 4 % paraformaldehyde to preserve pulmonary structure, fixed in 4 % paraformaldehyde, and paraffin-embedded for histological analysis.

### 5.2.4 Assessments of Cell Viability, Cell Number and Cell Shape and Size

Specific cell counter cum image analyzer will be used to count and assess the cell number, viability, and their shape, collected from the BALF, bone marrow, and spleen.

### 5.2.5 Flow Chamber Studies

Rolling of bone marrow cells collected from the femurs of control and treated mice on endothelial adhesion molecules under conditions of flow will be evaluated in an in vitro parallel plate flow chamber [4, 5]. Interaction of bone marrow cells ( $2 \times 10^5$ ) with recombinant mouse (rm) VCAM-1, rmGal-3-, ICAM-1-, Selectin (10 mg/ml in PBS, 200 µl per coverslip), or PBS (control)-coated glass coverslips at a flow rate of 1 ml/min (wall shear stress,  $1.0\text{--}2.0$  dynes/cm<sup>2</sup>) will be evaluated and recorded to manually determine the number of interacting cells. Results will be expressed as the number of rolling cells per minute.

### 5.3 Determination of ROS and RNS Levels

To detect the ROS and RNS, the following methods will be applied:

1. Assessment of myeloperoxidase (MPO): Myeloperoxidase, found in circulating neutrophils, monocytes, and lung tissue macrophages, is a member of heme peroxidase superfamily stored within the azurophilic granules of leukocytes. This has ability to use chloride as a cosubstrate with hydrogen peroxide to generate chlorinating oxidants such as hypochlorous acid which causes tissue damage and initiation of propagation of acute and chronic inflammatory diseases, so MPO-derived chlorinated compounds are specific biomarkers for disease progression.
2. Thiol detection method: Thiols are extremely efficient antioxidants which are able to protect cellular lipids, proteins, and nucleic acids against peroxidative damage due to their strong reductive capacity and their ability to react with free radicals, so the detection and measurement of free thiols (i.e., free cysteine, glutathione, and cysteine residues on proteins) are important to study the ROS and RNS production.
3. Glucose assay: Glucose ( $C_6H_{12}O_6$ ) is a ubiquitous fuel molecule in biological system. It is oxidized through a series of enzyme-catalyzed reactions to form carbon dioxide and water, yielding the universal energy molecule ATP. Due to its importance in metabolism, glucose level is a key diagnostic parameter for many metabolic disorders.
4. Nitrate and nitrite estimation: In response to inflammatory stimuli, endothelial cells and macrophages produce nitric oxide (NO) which leads to the peroxynitrite, destruction of iron sulfur clusters, thiol nitrosation, and nitration of protein tyrosine residues at its elevated level. So, the amount of NO produced in different biological systems can vary over several orders of magnitude and its subsequent chemical reactivity is diverse. In

the system, the produced NO is converted into nitrate and nitrite, and the relative proportion of these two molecules is variable.

5. Flow cytometric study to detect ROS production: The fluorescent intensity of the compounds oxidized by ROS can be measured by dihydrorhodamine 123 and 2,7 dichlorofluorescein diacetate compounds that can diffuse into the cells and then deacetylated and loose their fluorescence [6]. When oxidized by ROS, they become highly fluorescent. It can be quantified which reflect the rate and quantity of the ROS produced in the concerned sample tissue or cell.
6. Electron spin resonance spectroscopy: Hydroxyl radical formation after allergen treatment in both in vivo and in vitro models will be assessed by electron spin resonance (ESR) spectroscopy [7].
7. Immune cytochemical methods to detect nitrotyrosine: The immunohistochemical method to detect the nitrotyrosine is a good method to detect peroxynitrite and other RNSs [8] as the peroxynitrite is the reaction product of superoxide and nitric oxide and it plays a crucial role in the inflammatory responses in asthma.

---

### 5.4 Cytochrome c Reduction or Nitroblue Tetrazolium (NBT) Reduction Method (Used for Leukocyte NADPH Oxidase Activity)

Cytochrome c reduction and NBT reduction both can accurately predict whether ROS has been produced by leukocytes or by others. The two most commonly used reagents to detect superoxide anion radicals are NBT and ferricytochrome c (Cyt). Superoxide formed by electron transfer from a donor to molecular oxygen can be quenched by NBT and Cyt, and these reagents get reduced to diformazan and ferricytochrome c, respectively. Detection of superoxide is confirmed when the addition of the enzyme superoxide dismutase (SOD) causes a decrease in the



production of diformazan from NBT or no production of ferricytochrome c from cytochrome c. Hence, it is concluded that cytochrome c reduction only measures extracellularly released superoxide, whereas NBT may be reduced by extracellular superoxide, or other molecules as well.

#### 5.4.1 Biochemical Assessments of ROS- and RNS-Regulating Enzymes

Different enzymes, such as SOD and catalase regulating the reactive oxygen and nitrogen species, will be biochemically evaluated along with the quantitative measurements of ascorbic acid as a potent antioxidant by following conventional methodologies. SOD, an essential antioxidant that catalyzes superoxide radicals to hydrogen peroxide, is present in three forms in the mammalian system as (i) the copper–zinc superoxide dismutase (Cu, ZnSOD) located in the cytosol, (ii) the manganese superoxide dismutase (MnSOD), primarily a mitochondrial enzyme, and (iii) extracellular superoxide dismutase (EC-SOD) usually found on the outside of the plasma membrane. Both intracellular and extracellular SOD activities are decreased in asthmatic lungs, which may be related to oxidant inactivation and/or nitration of various SOD isoforms. Loss of SOD activity undoubtedly potentiates extracellular matrix damage and tissue injury through increased formation of reactive oxygen and nitrogen species.

#### 5.4.2 NO Estimation

Nitric oxide (NO), a relatively stable free radical, is increased in exhaled air of asthmatic individuals, threefold higher than normal NO concentrations in the lower airway and in the exhaled breath, as compared to healthy individuals, and this excessive NO production is increasingly implicated in the pathogenesis of inflammation in

asthma [1, 9], and due to this reason, exhaled NO levels are inversely correlated with airflow parameters in asthmatic patients [1, 10–12].

---

### 5.5 Immunoblots

After extraction and quantification of proteins from the lung, spleen, and lymph nodes, 10 % (w/v) homogenate will be prepared for Western blot. Equal amounts of proteins (50 µg) determined by Folin's method will be loaded on SDS-PAGE (10 %) for electrophoresis. Thereafter, proteins will be transferred electrophoretically to nitrocellulose membrane (NC) (Sigma-Aldrich, St. Louis, USA) overnight at 4 °C. NC will then be blocked for 60 min with Tris-buffered saline (TBS) (Tris 50 mM, pH 7.6) and then incubated with primary antiserum for 1 h. Then, membranes will be washed for 10 min each (3 washes) in TBS-Tween 20. Then, NC membrane will be incubated with secondary conjugated with serum immunoglobulin (anti-rabbit IgG HRP, Santa Cruz, USA) (1:500) for 30 min and then again washed in TBS for 10 min (3 times). Signals will be detected using an ECL kit (Bio-Rad, Hercules, CA, USA). Blot for each protein will be repeated three times. The densitometric analysis of the blots will be performed by scanning and quantifying the bands for density value by using computer-assisted image analysis (ImageJ 1, 38x, NIH, USA), and then, only the densitometric data will be presented as the mean of the integrated density value ± SEM. A prestained multicolor broad-range marker will be also run along with sample proteins to clarify the position of band obtained.

#### 5.5.1 Assessment of GLUTs

To correlate the inflammatory pathways with the metabolic alternations, targeting the glucose transporters (GLUTs) helps in the transportation of main energy fuel glucose inside a cell, which is very essential. As reported that GLUT1 plays a crucial role in mouse lung, so after allergen treatment this

has been aimed to find out any kind of alternations in GLUT1 protein expression. On the other hand, from the work of several researchers, this has been established that expression of GLUT4 and 8 is insulin dependent, so these two also have been targeted after allergen treatment.

### 5.5.2 Assessment of IRS1

It has now been established that IRS-1 is phosphorylated at serine residues by various kinases that interfere with the ability of this protein to engage in insulin receptor signaling and result in alterations in insulin action [13–15]. In addition, suppressor of cytokine signaling (SOCS) proteins seems to inhibit insulin action at the level of insulin receptor substrates, although through a different mechanism 55–57 [16–18] via the IRS-modifying enzymes, mounting evidence indicates that activation of JNK, IKK, and conventional protein kinase C (PKC) is central to mediating insulin resistance in response to various stresses leading to insulin resistance. They have all been reported to be able to inhibit insulin action by serine phosphorylation of IRS-1 [19, 20], although the activity of IKK in this regard has not yet been well established under physiological conditions. IRS-1 serine phosphorylation disrupts insulin receptor signaling through several distinct mechanisms and blocks insulin action 60, 61. These kinases also exert powerful effects on gene expression, including promoting further inflammatory gene expression through the activation of activator protein-1 (AP-1) complexes and NF- $\kappa$ B [21]. However, this aspect has not yet been thoroughly explored in metabolic homeostasis.

### 5.5.3 Expressional Profiling of MUC5AC

Hyperproduction of goblet cells and mucin in the airway epithelium is an important feature of airway inflammatory diseases such as asthma. MUC5AC expression involves the Notch signaling pathways depending on the epidermal growth factor (EGF)-stimulated generation of the

Notch intracellular domain (NICD) in a RBP-J $\kappa$ -dependent manner ( ). It is now established that ERK activation is necessary for the regulation of EGF receptor (EGFR)-mediated MUC5AC expression by Notch signaling. So expressional profiling of this protein molecule is important biomarker to investigate both acute and chronic forms of asthma pathophysiology in an experimental model system.

### 5.5.4 Expressional Profiling of NOS2 Protein

Nitric oxide synthases (NOS) are enzymes responsible for the synthesis of endogenous NO. These enzymes, present in three isoforms as NOS1 (neuronal), NOS2 (inducible), and NOS3 (endothelial), convert L-arginine to NO and L-citrulline in a reaction that requires oxygen and NADPH. Airway epithelia are a major cellular source of NOS2 in the healthy lung [9] as they produce high levels of NO in asthma due to increased NOS2 protein and activity. At the transcriptional level, murine NOS2 protein is regulated by a combination of the interferon- $\gamma$  (IFN- $\gamma$ ) activation of Janus kinase (JAK)/signal transducer and activator of transcription 1 (STAT1) pathway with the interleukin-1 $\beta$  (IL-1 $\beta$ ) and/or tumor necrosis factor alpha (TNF- $\alpha$ ) and/or endotoxin-mediated activation of nuclear factor  $\kappa$ B (NF- $\kappa$ B) [22, 23].

### 5.5.5 Expressional Profiling of Cell Adhesion Molecules

Our previous studies [2, 24–26] have shown the involvement of various families of adhesion molecules, viz. a4b1, b2, and VCAM-1, and selectin facilitates leukocyte transmigration, adherence to parenchymal cells, and Th2 response, in the pathophysiology of various inflammatory disease models such as allergic asthma. Assessment of these key cell adhesion molecules in response to high ROS and RNS levels in allergen-treated animal model in relation to metabolic alternations is a key goal to investigate in this project.

### 5.5.6 Expressional Profiling of Cyclooxygenase 2 (COX-2) and Lipoygenase (LOX)

As the experimental data suggest that two enzymes, cyclooxygenase 2 (COX-2) and lipoygenase (LOX), are involved in inflammation [27], so the expressional profiling of these two molecules is a key feature in this pathway.

### 5.5.7 Expressional Profiling of Proinflammatory Molecules

TNF- $\alpha$  is a proinflammatory cytokine that activates various signal transduction cascades improving the insulin sensitivity and glucose homeostasis, advocating the fact that metabolic, inflammatory, and innate immune processes are coordinately regulated and it is also proved that ligands of all three PPAR family members suppress the production of proinflammatory cytokines, mostly through the suppression of NF- $\kappa$ B [28]. So our aim is to correlate the expression of TNF- $\alpha$  along with the metabolic alternations in case of inflammatory responses in asthma as this field has still remained untouched by researchers.

TGF- $\beta$  is another important mediator involved in tissue remodeling in the asthmatic lung where TGF- $\beta$  is believed to play an important role in most of the cellular biological processes leading to airway remodeling involving itself in epithelial changes, subepithelial fibrosis, airway smooth muscle remodeling, and microvascular changes as in the lungs, almost all structural immune cells, as well as inflammatory cells recruited to the airways during an exacerbation of asthma, are able to express and secrete TGF- $\beta$ 1. In individuals without asthma, airway epithelium seems to be the major site of TGF- $\beta$ 1 expression [29]. However, other structural cells in the airways, such as fibroblasts [30], endothelial cells [31], vascular smooth muscle cells [32], and ASM cells [33], are also potential sources of this cytokine. Here, we have aimed to find out the

molecular switch which correlates the expression of these cytokines with the metabolic alternations at the genomic levels. By using specific inhibitors or monoclonal antibodies (GC1008) against the TGF- $\beta$  [<http://clinicaltrials.gov/ct/show/NCT00125385>, at ClinicalTrials.gov; accessed February 20, 2010] or its signaling molecules [34] in recent years have explore the window to study this.

### 5.5.8 Use of Two-Dimensional Electrophoresis System to Assess the Novel Proteins

Two-dimensional electrophoresis is a useful tool to analyze the protein pattern of various and complex biological materials to connect the genome to the proteome and to provide valuable information on various protein expressions by which we can get a picture of some novel protein molecule involved in this pathway, except the traditional ones.

### 5.5.9 Fluorescin-Activated Cell Sorter (FACS) Analysis

Cells from hemolyzed peripheral blood (PB), bone marrow (BM), bronchoalveolar lavage (BAL), lung parenchyma (LP), spleen, mesenteric lymph nodes (MLN), cervical lymph nodes (CLN), axillary lymph nodes (LNX), and inguinal lymph nodes (LNI) will be analyzed on a FACSCalibur (BD Immunocytometry Systems, San Jose, CA) by using the CELLQuest program. Staining will be performed by using antibodies conjugated to fluorescin isothiocyanate (FITC), phycoerythrin (PE), allophycocyanin (APC), peridinin-chlorophyll-protein (Per CP-Cy5.5), and Cy-chrome (PE-Cy5 and PE-Cy7). The following antibodies will be used for cell surface staining: CD45, CD3, CD4, CD45RC, CD8, B220, IgM, CD19, CD21, CD23, GR-1, Mac1 (M1/70), F4/80 (Cl: A3-1 (F4/80), anti- $\alpha$ 4 integrin, antiselectin, and anti-VCAM-1(M/K-2). Irrelevant isotype-matched antibodies will be used as controls.

### 5.5.10 Measurement of Lung Cytokines by Cytometric Bead Array

Lung tissue of control and OVA-exposed mice will be homogenized in lysis buffer (PBS containing 1 % Triton X-100, 1 mM PMSF, and protease inhibitor mixture). After measuring the protein concentration of the lysates, Th1 (IL-2 and IFN- $\gamma$ ) and Th2 (IL-4 and IL-5) cytokine levels and that of IL-13 in the lung lysate supernatants will be analyzed using mouse Th1/Th2 cytokine and IL-13 cytometric bead array (CBA) kits (catalogue Nos 551287 and 558349; BD Biosciences, San Jose, CA) expressing the level of each cytokine as picograms of cytokine per milligram of protein.

### 5.5.11 Quantitative Assessments of Specific Protein Molecules

ELISA for TNF- $\alpha$ , MIP-2, and IFN- $\gamma$  in BAL and serum (previously frozen at  $-80^{\circ}\text{C}$ ) will be measured along with the quantitative assessments of OVA-specific IgE and IgG1 (in serum previously frozen at  $-70^{\circ}\text{C}$ ).

### 5.5.12 Histological Assessments

1. Hematoxylin and eosin staining for lung tissues:  
Paraffin-embedded lung tissue sections will be stained by hematoxylin and eosin to detect detailed cellular architectures.
2. Masson's trichrome staining for collagen fibers:  
This will be used to detect the deposition of collagen fibers in airways which is the important biomarker for airway remodeling.
3. Alcian blue/PAS for acid and neutral mucopolysaccharides:
4. Toluidine blue stain for mast cells:
5. Wright's stain for differential blood cell counting:

### 5.5.13 Immunohistochemical Techniques

Immunohistochemical methods will be applied for the localization of GLUT1, GLUT4, GLUT8, MMP9, MMP12, TNF- $\alpha$ , TGF- $\beta$ 1, NOS2, nitrotyrosine, MUC5AC, VCAM1, selectin, and MIP-2.

### 5.5.14 Collection of Airway Smooth Muscle Cells and Its Culture

Collection and treatment of airway smooth muscle cells will be done by method proposed by Willems et al. [35].

Here after collecting ASM those will be treated by TNF- $\alpha$ , TGF- $\beta$ 1 and allergen to detect the different ROS and RNS biomarkers along with the measurement of GLUT1, GLUT4, GLUT8, NOS2 as well as the screening of different cytokines to correlate them in a *in vitro* system.

### 5.5.15 Collection of Alveolar Macrophages and Their Treatment

Collection and treatment of macrophage cells from the lung will be done by method proposed by Willems et al. [35]. Such cells will be similarly treated and assessed as mentioned above.

### 5.5.16 Use of Specific Inhibitors

Specific inhibitor molecules will be used in this purpose to investigate our goal of which few inhibitors are listed below:

1. NEM: NADPH oxidase inhibitor,
2. S1: MMP12 inhibitor,
3. TIMP1: endogenous inhibitor of MMP9,
4. Dideoxy glucose: specific inhibitor for glucose metabolism,
5. Mercaptoethylguanidine (MEG): inhibitor of iNOS.

**5.5.17 Use of RNAi Techniques**

Specific siRNAs will be used for this purpose to correlate the metabolic alternations with the inflammatory responses in asthma. Here, some siRNAs are enlisted which will be extensively used for this purpose: GLUT1, GLUT4, GLUT8, MMP9, MMP12, and NOS2.

**5.5.18 Use of Anti-inflammatory Substances as Nanobodies**

Recently, targeted and triggered drug delivery systems accompanied by nanobody technology have emerged as prominent solutions to the bioavailability of therapeutic agents. So we have planned to use hydrophobic agents such as curcumin and fisetin, anti-inflammatory substances, as nanobodies in both in vivo and in vitro models to prevent the OVA-induced acute and chronic asthma, to find out their correlation with the metabolomics.

**5.5.19 Timeline of the Work**

Expected time period of this work is about 3 years. The detail timeline is described below:

Time period	Expected work to be done
1st six months	Standardization of all protocols
Next six months	Immunization of the animal by ovalbumin and assessment of ROS and RNS levels along with the flow cytometric study of different cytokines
Next six months	Immunoblot studies to detect above-mentioned proteins along with the histological methods
Next six months	Assessment of mentioned proteins in in vitro model system
Next six months	Use of specific inhibitors and siRNAs to confirm the available data which we will get throughout this time span

(continued)

Time period	Expected work to be done
Last six months	Use of specific anti-inflammatory molecules along with the use of positive and negative controls to reach the climax of this long story

**5.5.20 Hypothesis and Expected Outcome**

Alternations in metabolic pathways should alter the immune inflammatory mechanisms which can be correlated with the insulin responsiveness in the effector tissues, for example. In the high glucose availability, it will prime the specific T lymphocytes especially the Th2 interacting with specific costimulatory molecules, to release Th2-specific cytokines which stimulate the mast cells to release their contents which stimulate the B lymphocytes to release higher amounts of IgE in the serum as well as recruited eosinophils at the site of inflammation. Due to impairment in glucose metabolism, it elicits the ROS and RNS levels in the system which ultimately modulates the immune inflammatory responses. So targeting this metabolic pathway may be a key regulator of this mechanistic phenomenon. We are hypothesizing that by fine-tuning, the expression of specific GLUTs will be able to arrest the inflammatory responses against a specific allergen challenge and this model can be mimicked by using definite nanobodies or mesenchymal stem cells. We do not know anything related to this as this field of research has been remained untouched by workers till date.

**References**

1. Guo FH, Comhair SA, Zheng S, Dweik RA, Eissa NT, Thomassen MJ, Calhoun W, Erzurum SC. Molecular mechanisms of increased nitric oxide (NO) in asthma: evidence for transcriptional and post-translational regulation of NO synthesis. *J Immunol.* 2000;164:5970–80.
2. Ray Banerjee E. Triple selectin knockout (ELP<sup>-/-</sup>) mice fail to develop OVA-induced acute asthma phenotype. *J. Inflamm.* 2011;8:19.

3. Song DJ, Cho JY, Lee SY, Miller M, Rosenthal P, Soroosh P, Croft M, Zhang M, Varki A, Broide DH. Anti-Siglec-F antibody reduces allergen-induced eosinophilic inflammation and airway remodeling. *J Immunol.* 2009;183:5333–41.
4. Rao SP, Wang Z, Zuberi RI, Sikora L, Bahaie NS, Zuraw BL, Liu F-T, Sriramarao P. Galectin-3 functions as an adhesion molecule to support eosinophil rolling and adhesion under conditions of flow. *J Immunol.* 2007;179:7800–7.
5. Han JL, Ding RY, Zhao L, Ren Z, Jiang XJ. Rosiglitazone attenuates allergic inflammation and inhibits expression of galectin-3 in a mouse model of allergic rhinitis. *J Int Med Res.* 2008;36:830–6.
6. Imrich A, Kobzik L. Flow cytometric analysis of macrophage oxidative metabolism using DCFH. *Methods Mol Biol.* 1998;91:97–108.
7. Shi T, Schins RP, Knaapen AM, Kuhlbusch T, Pitz M, Heinrich J, Borm PJ. Hydroxyl radical generation by electron paramagnetic resonance as a new method to monitor ambient particulate matter composition. *J Environ Monit.* 2003;5:550–6.
8. Liliaua, et al. *Methods Enzymol.* 1999;301:373–81.
9. Dweik RA, Comhair SA, Gaston B, Thunnissen FB, Farver C, Thomassen MJ, Kavuru M, Hammel J, Abu-Soud HM, Erzurum SC. NO chemical events in the human airway during the immediate and late antigen-induced asthmatic response. *Proc Natl Acad Sci USA.* 2001;98:2622–7.
10. Massaro AF, Mehta S, Lilly CM, Kobzik L, Reilly JJ, Drazen JM. Elevated nitric oxide concentrations in isolated lower airway gas of asthmatic subjects. *Am J Respir Crit Care Med.* 1996;153:1510–4.
11. Silkoff PE, Sylvester JT, Zamel N, Permutt S. Airway nitric oxide diffusion in asthma: role in pulmonary function and bronchial responsiveness. *Am J Respir Crit Care Med.* 2000;161:1218–28.
12. Khatri SB, Ozkan M, McCarthy K, Laskowski D, Hammel J, Dweik RA, Erzurum SC. Alterations in exhaled gas profile during allergen-induced asthmatic response. *Am J Respir Crit Care Med.* 2001;164:1844–8.
13. Taniguchi CM, Emanuelli B, Kahn CR. Critical nodes in signalling pathways: insights into insulin action. *Nature Rev Mol Cell Biol.* 2006;7:85–96.
14. Aguirre V, Uchida T, Yenush L, Davis R, White MF. The c-Jun NH2-terminal kinase promotes insulin resistance during association with insulin receptor substrate-1 and phosphorylation of Ser307. *J Biol Chem.* 2000;275:9047–54.
15. Paz K, et al. Elevated serine/threonine phosphorylation of IRS-1 and IRS-2 inhibits their binding to the juxtamembrane region of the insulin receptor and impairs their ability to undergo insulin-induced tyrosine phosphorylation. *J Biol Chem.* 1997;272:29911–8.
16. Emanuelli B, et al. SOCS-3 inhibits insulin signaling and is up-regulated in response to tumor necrosis factor- $\alpha$  in the adipose tissue of obese mice. *J Biol Chem.* 2001;276:47944–9.
17. Rui L, Yuan M, Frantz D, Shoelson S, White MF. SOCS-1 and SOCS-3 block insulin signaling by ubiquitin-mediated degradation of IRS1 and IRS2. *J Biol Chem.* 2002;277:42394–8.
18. Howard JK, et al. Enhanced leptin sensitivity and attenuation of diet-induced obesity in mice with haploinsufficiency of Socs3. *Nature Med.* 2004;10:734–8.
19. Gao Z, et al. Serine phosphorylation of insulin receptor substrate 1 by inhibitor kappa B kinase complex. *J Biol Chem.* 2002;277:48115–21.
20. Griffin ME, et al. Free fatty acid-induced insulin resistance is associated with activation of protein kinase C theta and alterations in the insulin signaling cascade. *Diabetes.* 1999;48:1270–4.
21. Baud V, Karin M. Signal transduction by tumor necrosis factor and its relatives. *Trends Cell Biol.* 2001;11:372–7.
22. Stuehr DJ. Mammalian nitric oxide synthases. *Biochim Biophys Acta.* 1999;1411:217–30.
23. Xie QW, Whisnant R, Nathan C. Promoter of the mouse gene encoding calcium-independent nitric oxide synthase confers inducibility by interferon gamma and bacterial lipopolysaccharide. *J Exp Med.* 1993;177:1779–84.
24. Ray Banerjee E, Jiang Y, Henderson WR Jr, Scott LM, Papayannopoulou T. Alpha4 and beta2 integrins have non-overlapping roles in asthma development, but for optimal allergen sensitization only alpha4 is critical. *Exp Hematol.* 2007;35(4):605–17.
25. Ray Banerjee E, Jiang Y, Henderson WR Jr, Latchman YL, Papayannopoulou T. Absence of  $\alpha 4$  but not  $\beta 2$  integrins restrains the development of chronic allergic asthma using mouse genetic models. *Exp Hematol.* 2009;37:715–27.
26. Laberge S, et al. Role of VLA-4 and LFA-1 in allergen-induced airway hyper responsiveness and lung inflammation in the rat. *Am J Respir Crit Care Med.* 1995;151:822–9.
27. Huang MT, Lysz T, Ferraro T, Abidi TF, Laskin JD, Conney AH. Inhibitory effects of curcumin on in vitro lipoxygenase and cyclooxygenase activities in mouse epidermis. *Cancer Res.* 1991;51:813–9.
28. Glass CK, Ogawa S. Combinatorial roles of nuclear receptors in inflammation and immunity. *Nature Rev Immunol.* 2006;6:44–55.
29. Magnan A, Frachon I, Rain B, Peuchmaur M, Monti G, Lenot B, Fattal M, Simonneau G, Galanaud P, Emilie D. Transforming growth factor beta in normal human lung: preferential location in bronchial epithelial cells. *Thorax.* 1994;49:789–92.
30. Kelley J, Kovacs EJ, Nicholson K, Fabisiak JP. Transforming growth factor—beta production by lung macrophages and fibroblasts. *Chest.* 1991;99(Suppl 3):85S–6S.
31. Coker RK, Laurent GJ, Shahzeidi S, Hernandez-Rodriguez NA, Pantelidis P, du Bois RM, Jeffery PK, McAnulty RJ. Diverse cellular TGF-beta 1 and TGF-beta 3 gene expression in

- normal human and murine lung. *Eur Respir J*. 1996;9:2501–7.
32. de Boer WI, van Schadewijk A, Sont JK, Sharma HS, Stolk J, Hiemstra PS, van Krieken JH. Transforming growth factor beta1 and recruitment of macrophages and mast cells in airways in chronic obstructive pulmonary disease. *Am J Respir Crit Care Med*. 1998;158:1951–7.
33. Lee KY, Ho SC, Lin HC, Lin SM, Liu CY, Huang CD, Wang CH, Chung KF, Kuo HP. Neutrophil-derived elastase induces TGF-beta1 secretion in human airway smooth muscle via NF-kappaB pathway. *Am J Respir Cell Mol Biol*. 2006;35:407–14.
34. Laping NJ, Grygielko E, Mathur A, Butter S, Bomberger J, Tweed C, Martin W, Fornwald J, Lehr R, Harling J, et al. Inhibition of transforming growth factor (TGF)-beta1-induced extracellular matrix with a novel inhibitor of the TGF-beta Type I receptor kinase activity: SB-431542. *Mol Pharmacol*. 2002;62:58–64.
35. Willems, et al. *Indian J Biochem Biophys*. 2011;48:262–9.

---

# Dissecting Asthma Pathogenesis Through Study of Patterns of Cellular Traffic Indicative of Molecular Switches Operative in Inflammation

6

---

## Abstract

*Background* Inflammation and degeneration are the two-edged swords that impale a pulmonary system with the maladies such as asthma and idiopathic pulmonary fibrosis. To explore critical role players that orchestrate the etiology and pathogenesis of these diseases, we used various lung disease models in mice in specific genetic knockout templates. *Materials and methods* Acute and chronic allergic asthma and idiopathic pulmonary fibrosis model in mouse was developed in various genetic knockout templates, namely  $\alpha4^{\Delta/\Delta}$  ( $\alpha41^{-/-}$ ),  $\beta2^{-/-}$ , and  $\alpha4^{-/-}$   $\beta2$  mice, and the following parameters were measured to assess the development of composite asthma phenotype—(i) airway hyper-responsiveness to methacholine by measuring lung resistance and compliance by invasive and  $P_{\text{enh}}$  by noninvasive

---

## Author's contribution

Ena Ray Banerjee is the sole author of this communication. The concept of the experiments, execution of the experiments, acquisition of data, and data analyses were all done by her only.

Dissecting Asthma Pathogenesis Through Study of Patterns of Cellular Traffic Indicative of Molecular Switches Operative in Inflammation (for identifying cellular targets spatiotemporally)

### Animal ethics

All experiments were performed under strict compliance with institutional animal ethics rules of University of Washington. All mice were bred and maintained under specific pathogen-free conditions at the UMSOM, Seattle, USA, and all experimental procedures were done in accordance with Institutional Animal Care and Use Committee guidelines on approved protocols.

This work is in press as Ray Banerjee, E. Dissect asthma pathogenesis through the study of patterns of cellular traffic indicative of molecular switches operative in inflammation (2015). *Progress in Stem Cell* (ISSN 2199-4633). 2(1):1–42 DOI: <http://dx.doi.org/10.15419/psc.v2i1.73>.



plethysmography as well as lung resistance and compliance using invasive plethysmography, (ii) in situ inflammation status in lung parenchyma and lung interstitium and also resultant airway remodeling measured by histochemical staining namely Masson's trichrome staining and hematoxylin and eosin staining, (iii) formation of metaplastic goblet cells around lung airways by alcian blue dye, (iv) measurement of Th1 and Th2 cytokines in serum and bronchoalveolar lavage fluid (BALF), and (v) serum allergen-specific IgE. Specifically, ovalbumin-induced acute allergic asthma model in mice was generated in WT (wild-type) and KO (knockout) models and readouts of the composite asthma phenotype, viz. airway hypersensitivity, serum OVA-specific IgE and IgG, Th2 cytokine in BALF and lymphocyte cell subsets, viz. T and B cells, monocytes, macrophages, basophils, mast cells and eosinophils (by Fluorescein-activated cell sorter (FACS) and morphometry in H&E-stained cell smears) were assessed in addition to lung and lymph node histology. *Results* We noticed a pattern of cellular traffic between bone marrow (BM) → peripheral blood (PB) → lung parenchyma (LP) → (BALF) in terms of cellular recruitment of key cell subtypes critical for onset and development of the diseases which is different for maintenance and exacerbations in chronic cyclically occurring asthma that leads to airway remodeling. While inflammation is the central theme of this particular disease, degeneration and shift in cellular profile, subtly modifying the clinical nature of the disease, were also noted. In addition, we recorded the pattern of cell movement between the secondary lymphoid organs (SLO), namely the cervical, axillary, inguinal, and mesenteric lymph nodes (MLN) vis-à-vis spleen and their sites of poiesis BM, PB, and lung tissue. While mechanistic role is the chief domain of the integrins ( $\alpha 4$ , i.e., VLA-4 or  $\alpha 4\beta 1$ , VCAM-1;  $\beta 2$ , i.e., CD-18 or ICAM-1). *Concluding remarks* The present paper thoroughly compares and formulates the pattern of cellular traffic among the three nodes of information throughput in allergic asthma immunobiology, namely primary lymphoid organs (PLO), SLO, and tissue spaces and cells where inflammation and degeneration occur within the purview of the disease pathophysiological onset. and ancillary signals in the above models and reports some interesting findings with respect to adult lung stem cell niches and its resident progenitors and their role in pathogenesis and disease amelioration.

#### Abbreviations

AHR	Airway hyper-reactivity/responsiveness
BALF	Bronchoalveolar lavage fluid
BM	Bone marrow
H&E	Hematoxylin and Eosin
i.p.	Intraperitoneal
i.t.	Intratracheal
i.v.	Intravenous
KO	Knockout
LNI	Inguinal lymph node
LNx	Axillary lymph node
LP	Lung parenchyma
MLN	Mesenteric lymph node

OVA	Ovalbumin
PB	Peripheral blood
P <sub>enh</sub>	Enhanced pause
PP	Peyer's patch
WBP	Whole-body plethysmography

## 6.1 Introduction

Inflammation is meant to re-establish a shift in the body's homeostatic balance. Acute inflammation is the initial response to harmful stimuli and is achieved by the increased movement of plasma and leukocytes from blood into injured tissues concomitant with a cascade of biochemical events involving the systemic role of vascular and immune system and local role of other tissue-specific cells within the injured tissue [1]. Prolonged inflammation or chronic inflammation leads to a progressive shift in the type of cells present at the site of inflammation and is characterized by simultaneous destruction and healing of the tissue from the inflammatory process. This is characterized by concurrent active inflammation and tissue destruction, attempts at repair, and may not be typically characterized by the aforementioned classic signs of acute inflammation. Instead, chronically inflamed tissue is characterized by the infiltration of mononuclear immune cells (monocytes, macrophages, lymphocytes, and plasma cells) and tissue destruction and attempts at healing, which include angiogenesis and fibrosis [2].

Asthma and COPD, however, differ significantly in their underlying etiology and involve similar inflammatory changes in the respiratory tract. While the specific nature and the reversibility of these processes largely differ in each entity and disease stage, both are characterized by lung inflammation, though patients with asthma suffer largely from reversible airflow obstruction, whereas patients with COPD experience a continuous decline in lung function as disease progresses [3]. By 2020, India alone will account for 18 % of the 8.4 million tobacco-related deaths globally [4]. In China, COPD is one of the high-frequency causes of death followed closely by ischemic heart disease and cardiovascular disease [5].

Inflammation is therefore key to etiology of most respiratory disorders, and while it is critical

for the body's defense against infections and tissue damage, it has increasingly become clear that there is a fine balance between the beneficial effects of inflammation cascades and potential for tissue destruction in the long term. If they are not controlled or resolved, inflammation cascades lead to the development of diseases such as chronic asthma, rheumatoid arthritis, psoriasis, multiple sclerosis, and inflammatory bowel disease [6].

The specific characteristics of inflammatory response in each disease and site of inflammation may differ, but recruitment and activation of inflammatory cells and changes in structural cells remain a universal feature. This is associated with the increase in the expression of components of inflammatory cascade, viz. cytokines, chemokines, growth factors, enzymes, receptors, adhesion molecules, and other biochemical mediators.

The pathogenesis of allergic asthma involves the recruitment and activation of many inflammatory and structural cells, all of which release mediators that result in typical pathological changes of asthma. The chronic airway inflammation of asthma is unique in that the airway wall is infiltrated by T lymphocytes of the T helper (Th)-type 2 phenotype, eosinophils, macrophages/monocytes, and mast cells. Accumulation of inflammatory cells in the lung and airways, epithelial desquamation, goblet cell hyperplasia, mucus hypersecretion, and thickening of submucosa resulting in bronchoconstriction and airway hyper-responsiveness are important features of asthma [7, 8]. Both cells from among the circulating leukocytes such as Th2 lymphocytes, mature plasma cells expressing IgE, eosinophils [8] and neutrophils, and local resident and structural cells constituting the "respiratory membrane" (airway epithelial cells, fibroblasts, resident macrophages, bronchial smooth muscle cells, mast cells, etc.) contribute to the pathogenesis of asthma [9]. Airway

hyper-responsiveness of asthma is clinically associated with recurrent episodes of wheezing, breathlessness, chest tightness, and coughing, particularly at night or in early morning. Furthermore, during exacerbations, the features of “acute on chronic” inflammation have been observed. Chronic inflammation may also lead to the outlined structural changes often referred to as airway remodeling which often accounts for the irreversible component of airway obstruction observed in some patients with moderate-to-severe asthma and the declining lung function.

Inflammation in COPD is associated with an inflammatory infiltrate composed of eosinophils, macrophages, neutrophils, and CD8+ T lymphocytes in all lung compartments [9] along with inflammatory mediators such as TNF- $\alpha$ , IL-8 (interleukin-8), LTB4 (leukotriene B4), ET-1 (endothelin-1), and increased expression of several adhesion molecules such as ICAM-1 [10]. The molecular mechanisms whereby inflammatory mediators are upregulated at exacerbation may be through the activation of transcription factors such as nuclear factor (NF)- $\kappa$ B and activator protein-1 that increase transcription of proinflammatory genes [11]. Acute exacerbations have a direct effect on disease progression by accelerating loss of lung function although the inflammatory response at exacerbation is variable and may depend in part on the etiologic agent [12, 13]. Current therapies for COPD exacerbations are of limited effectiveness [14].

Rational treatment depends on understanding the underlying disease process, and there have been recent advances in understanding the cellular and molecular mechanisms that may be involved [14]. Beyond the absence of curative therapy, current treatment options have inherent limitations, such as further complication by exacerbations, limitations of some orally available treatments, and even refractoriness of the most effective treatment regimens such as inhaled corticosteroids (ICSs), long-acting beta2-agonists (LABAs), methylxanthines, leukotriene modifiers, cromones, and IgE blockers. Oropharyngeal adverse events and inadequate response to ICS in a lot of patients present a threat to continued therapy [15]. Targeting oxidative damage using antioxidants such as

N-acetylcysteine has shown efficacy in chronic bronchitis [11] but is relatively ineffective in established COPD [16]. Targeting TNF $\alpha$  to ameliorate inflammation has also been disappointing [17, 18]. The use of inhaled steroids combined with long-acting  $\beta$ 2-agonists to reduce exacerbation rates in more severe diseases is now widely accepted, but their effects on mortality are still in doubt [19] and presently, there are no effective strategies beyond smoking cessation to slow disease progression in horizon [20]. These data suggest that even relatively modest immunomodulators such as ICSs might further impact on local immunity already damaged by chronic inflammation and remodeling, rendering individuals to some degree more vulnerable to significant infections [21]. Key to effective COPD therapy is the prevention of loss of alveolar smooth muscle elasticity which is irreversible by early diagnosis and more effective intervention which is currently virtually non-existent.

It is with an objective to identify targets that conventional therapy has obviously overlooked or underrated and that the pattern of cellular traffic is being studied under various pathophysiological situations. A number of genetic knockout models of mice were used, tissue-specific (lung) inflammation under asthmatic (Th1-driven) condition was explored, and immune cell traffic from their site of poiesis to their site of pathophysiological manifestation were studied [22].

In our work with various genotype knockout models of mice, the data generated and interpreted from detailed analyses of cells traveling between bone marrow (BM), peripheral blood (PB), lung parenchyma (LP), airways and the different secondary lymph organs or lymphoid tissues (cervical, axillary, inguinal, mesenteric lymph nodes (MLN) and Peyer’s patch), we have detected some specific patterns. This is a report on the pattern of cellular traffic from which certain cell subsets were discernible to play rate-limiting roles which have been presented along with comments on molecular implications of such directed movement of these key cell types. When specific molecules, critical for signaling the onset and/or development and maintenance of pathophysiology of acute allergic asthma and the associated inflammatory changes,

are absent, as in the genotype knockout models, cell trafficking is drastically altered. As apparent from the data presented in this paper, the pattern of cell traffic can actually be molecular signatures for the diagnosis of molecular causes of etiology in particular pathological manifestations of acute allergic asthma.

The clear rationale for doing the work, that is meta-analysis of data and interpretation of cellular traffic are to understand—

1. when and which cells mobilize from the site of poiesis [primary lymphoid organs (PLO)];
2. which cells are rate limiting for the sequence of steps required for onset, development, maintenance, and exacerbation of acute asthma;
3. which residual cells come back from the focal region of inflammation to secondary lymphoid organs (SLO)/tissues which may be critical for generating “central memory” cell pool;
4. key diagnostic as well as therapeutic differentiators in the etiology of several respiratory diseases with similar clinical symptoms.

Information obtained shall be key to devising therapeutic/prophylactic strategies by targeting small molecules (pharmacological intervention), cells (cell-based therapy through tissue engineering), antibody-induced neutralization or arrest of cell activation of specific cells (cell targeting) for personalized and translational medical treatment. Unless specific targets are identified in a strict spatiotemporal format, interfering of a target leads to undesirable side effects or even fatality. As outlined in the initial paragraphs, there are patient populations which are refractory to some drugs. So even for designing combination therapy, the timing and targeting are important. The same cell may behave quite differently at different times of the disease onset. The same cell may express different cellular proteins or secrete soluble proteins in its milieu, and such changes, rapid and occurring in sequence, are extremely critical information to catch the correct target and at the correct time. Work embodied in this paper attempts to elucidate just these nodes of information throughout in a cellular factory in a specific disease template, acute asthma.

## 6.2 Materials and Methods

**Animals.** C57BL6 mice were used as described previously [23–33]. *Mxcre+ $\alpha$ 4* flox/flox mice were conditionally ablated by i.p. poly(I)poly(C) injection. *cre-* mice were used as WT (wild type), and  $\alpha$ 4-ablated mice were simply called  $\alpha$ 4<sup>-/-</sup>. CD18<sup>-/-</sup> mice on a C57BL6 background were called  $\beta$ 2<sup>-/-</sup>. In total, the following number of animals was used in each group: WT = 5 per experiment, +OVA = 5 per experiment,  $\alpha$ a<sup>-/-</sup> = 5 per experiment,  $\beta$ 2<sup>-/-</sup> = 5 per experiment, Rag2 $\gamma$ C<sup>-/-</sup> (baseline) = 4 per experiment, Rag2 $\gamma$ C<sup>-/-</sup> engrafted with WT BMC = 10 per experiment, and Rag2 $\gamma$ C<sup>-/-</sup> engrafted with  $\alpha$ 4<sup>-/-</sup> BMC = 10 per experiment. A total of three independent experiments for the development and analyses of the OVA model and a total of four independent experiments for the engraftment and repopulation experiments in Rag2 $\gamma$ C<sup>-/-</sup> mouse were performed. Data presented are mean  $\pm$  SEM for all experiments, and only p value less than 0.01 have been considered.

### 6.2.1 Experimental Design for Lymphopoiesis

Five million BM cells in prewarmed HBSS were injected via tail vein in lethally irradiated (800cGY) to 6- to 8-week-old Rag2 $\gamma$ C<sup>-/-</sup> recipients, and reconstitution was followed at 5 weeks, 10 weeks, and 6 months. Tissues were collected after killing to assess the type of donor-derived versus recipient’s own reconstituted cell types. In the repopulated animals, OVA-induced asthma was induced and composite asthma phenotype noted with a detailed analysis of the cellular subtypes in the PLO, SLO, and tissues—their structural identity and their functional propensity Fig. 6.1.

**Allergen sensitization and challenge.** Mice were sensitized and later challenged with OVA (Pierce, Rockford, IL) as described previously [23]. Mice were immunized with OVA (100  $\mu$ g) complexed with aluminum sulfate in a 0.2 ml volume, administered by i.p. injection on day 0. On day 8 (250  $\mu$ g of OVA) and on days 15, 18,

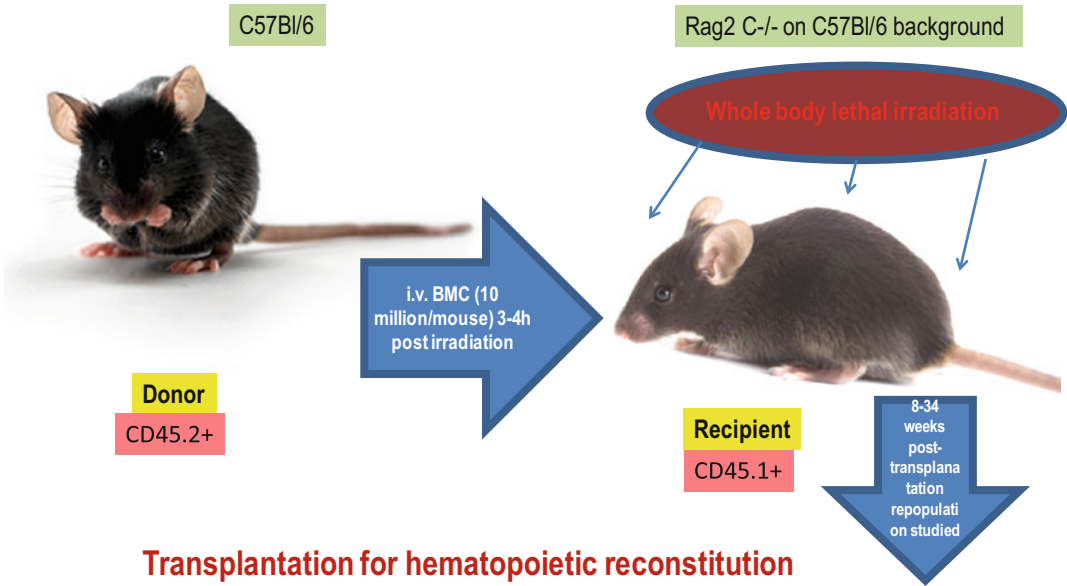


**Fig. 6.1** Study protocol for transplantation for hematopoietic reconstitution probing mobilization and homing. Five million bone marrow cells in prewarmed HBSS were injected via tail vein in lethally irradiated (800cGY) to 6- to 8-week-old Rag2 $\gamma$ C $^{-/-}$  recipients, and reconstitution was followed at 5 weeks, 10 weeks, and 6 months. Tissues were collected after killing to assess the type of donor-derived versus recipient’s own reconstituted

cell types. In the repopulated animals, OVA-induced asthma was induced and composite asthma phenotype noted with detailed analysis of the cellular subtypes in the PLO, SLO, and tissues—their structural identity and their functional propensity. Donor mice were CD45.2+, and recipients were CD45.1+ (pan-hematopoietic marker). So all CD45.2 are donor-derived, and all CD45.1+ are recipient’s own cells

and 21 (125  $\mu$ g of OVA), mice were anesthetized briefly with inhalation of isoflurane in a standard anesthesia chamber and given OVA by intratracheal (i.t.) administration. Intratracheal challenges were done as described previously [24]. Mice were anesthetized and placed in a supine position on the board. The animal’s tongue was

extended with lined forceps, and 50  $\mu$ l of OVA (in the required concentration) was placed at the back of its tongue. The control group received normal saline with aluminum sulfate by i.p. route on day 0 and 0.05 ml of 0.9 % saline by i.t. route on days 8, 15, 18, and 21 as in Fig. 6.2.

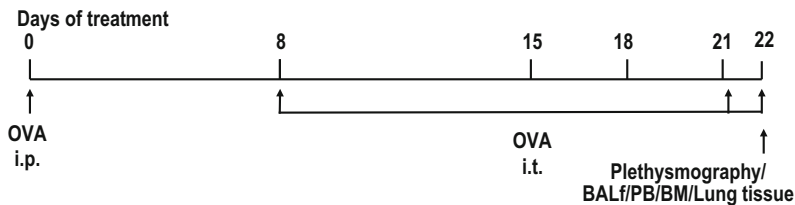


**Fig. 6.2** Study design to generate acute allergic asthma phenotype in mice. Asthma phenotype was generated as described in earlier publications [23–26]. Mice were immunized with OVA (100  $\mu$ g) complexed with aluminum sulfate in a 0.2 ml volume, administered by i.p. injection on day 0. On day 8 (250  $\mu$ g of OVA) and on days 15, 18, and 21 (125  $\mu$ g of OVA), mice were anesthetized briefly with inhalation of isoflurane in a standard anesthesia chamber and given OVA by intratracheal (i.t.) administration.

Intratracheal challenges were done as described previously [24]. Mice were anesthetized and placed in a supine position on the board. The animal’s tongue was extended with lined forceps, and 50  $\mu$ l of OVA (in the required concentration) was placed at the back of its tongue. The control group received normal saline with aluminum sulfate by i.p. route on day 0 and 0.05 ml of 0.9 % saline by i.t. route on days 8, 15, 18, and 21

**Pulmonary function testing.** In vivo airway hyper-responsiveness to methacholine was measured 24 h after the last OVA challenge in conscious, free-moving, spontaneously breathing mice using whole-body plethysmography (model PLY 3211; Buxco Electronics, Sharon, CT) as previously described [4]. Mice were challenged with aerosolized saline or increasing doses of methacholine (5, 20, and 40 mg/ml) generated by an ultrasonic nebulizer (DeVilbiss Healthcare, Somerset, PA) for 2 min. The degree of bronchoconstriction was expressed as enhanced pause ( $P_{\text{enh}}$ ), a calculated dimensionless value, which correlates with the measurement of airway resistance, impedance, and intrapleural pressure in the same mouse.  $P_{\text{enh}}$  readings were taken and averaged for 4 min after each nebulization challenge.  $P_{\text{enh}}$  was calculated as follows:  $P_{\text{enh}} = [(T_e/T_r - 1) \times (\text{PEF}/\text{PIF})]$ , where  $T_e$  is the expiration time,  $T_r$  is the relaxation time, PEF is the peak expiratory flow, and PIF is the peak inspiratory flow  $\times$  0.67 coefficient. The time for the box pressure to change from a maximum to a user-defined percentage of the maximum represents the relaxation time. The  $T_r$  measurement begins at the maximum box pressure and ends at 40 %.

**BALF.** After pulmonary function testing, the mouse underwent exsanguination by intraorbital arterial bleeding and then BAL (0.4 ml three times) of both lungs. Total BAL fluid cells were counted from a 50  $\mu$ l aliquot, the remaining fluid was centrifuged at 200 g for 10 min at 4 °C, and the supernatants stored at -70 °C for assay of BAL cytokines later. The cell pellets were resuspended in FCS, and smears were made on glass slides. The cells, after air drying, were stained with Wright-Giemsa (Biochemical Sciences Inc, Swedesboro, NJ), and their differential count was taken under a light microscope at 40X magnification. Cell number refers to that obtained from lavage of both lungs/mouse.

**Lung parenchyma.** Lung mincing and digestion were performed after lavage as described previously [8] with 100  $\mu$ l/ml collagenase for 1 h at 37 °C and filtered through a 60# sieve (Sigma). All numbers mentioned in this paper refer to cells obtained from one lung/mouse.

**Lung histology.** Lungs of other animals of same group were fixed in 4 % paraformaldehyde

overnight at 4 °C. The tissues were embedded in paraffin and cut into 5- $\mu$ m sections. A minimum of 15 fields were examined by light microscopy. The intensity of cellular infiltration around pulmonary blood vessels was assessed by hematoxylin and eosin staining. Airway mucus was identified by staining with alcian blue and periodic acid-Schiff staining as described previously [25].

**Immunohistochemical staining of the lung.** Lungs of yet other animals of the same group were processed for immunohistochemical staining following standard procedures [26]. They were stained with either anti-VCAM-1 (MK2) or anti- $\beta$ 1 (9EG7) antibody and color development done by HRP. Mouse tissues were prefixed in 4 % paraformaldehyde in 100 mM PBS (pH 7.4) for 6–12 h at 4 °C, washed with PBS 10 min 3 times and then the tissues were soaked in 10 % sucrose in PBS for 2–3 h, 15 % sucrose in PBS for 2–3 h, 20 % for 3–12 h at 4 °C and then embedded in O. C.T. compound (Tissue-Tek 4583, Sakura Finetechnical CO., Ltd, Tokyo, 103, Japan) and frozen in acetone cooled by dry ice. Frozen blocks were stored at -70 °C refrigerator until sectioned. Frozen blocks were cut on a freezing, sliding macrotome at 4  $\mu$ m (LEICA CM1850 Cryostat) and air-dried for 30 min at RT. After washing in PBS 3 times for 10 min at RT, to block endogenous peroxidase activity, 0.3 % hydrogen peroxide was applied to each section for 30 min at RT. Each slide was incubated with blocking solution (normal serum from the specific secondary antibody was derived from) to block non-specific reactions. Appropriately diluted primary antibody was applied to each slide and incubated overnight at 4 °C. After washing with PBS, slides were incubated with appropriately diluted specific biotin-conjugated secondary antibody solution for 1 h at RT. After washing with PBS, slides were incubated in AB reagent for 1 h at RT (ABComplex/HRP, Dako). After washing with PBS, slides were stained with 0.05 % DAB (3,3'-diaminobenzidine tetrahydrochloride, Sigma) in 0.05 M Tris buffer (pH 7.6) containing 0.01 %  $\text{H}_2\text{O}_2$  for 5–40 min at RT. Slides were counterstained with Mayer's hematoxylin and dehydrate in graded ethanol, xylene and mount with Mount Quik (Daido Sangyo Co. Ltd., Japan).

**CFU-c assay.** To quantitate committed progenitors, CFU-C assays were performed using methylcellulose semisolid media (Stemgenix, Amherst, NY) supplemented with an additional 50 ng of stem cell factor per ml (PeproTech, Rocky Hill, NJ) to promote the growth of hematopoietic progenitors. Next,  $0.01 \times 10^6$  cells from lung were plated on duplicate 35-mm culture dishes and incubated at 37 °C in a 5 % CO<sub>2</sub>-95 % air mixture in a humidified chamber for 7 days. Colonies generated by that time were counted using a dissecting microscope, and all colony types (i.e., BFU-E, CFU-E, CFU-G, CFU-GEMM, CFU-GM, and CFU-M) were pooled and reported as total CFU-C. Aliquots of  $1 - 10 \times 10^4$  cells were plated per 1 ml of semisolid methylcellulose (CFU-lite with Epo, Miltenyi Biotech, or complete human methylcellulose medium, Stem Cell Technologies, Vancouver, BC, Canada). CFU-C frequency was scored morphologically after 10–14 days in culture at 37 °C, 5 % CO<sub>2</sub>, in a humidified incubator.

**Fluorescein-activated cell sorter (FACS) analysis.** Cells from hemolyzed PB, BM, bronchoalveolar lavage (BAL), LP, spleen, MLN, cervical lymph nodes (CLN), axillary lymph nodes (LNx), and inguinal lymph nodes (LNI) were analyzed on a FACSCalibur (BD Immunocytometry Systems, San Jose, CA) by using the CELLQuest program. Staining was performed by using antibodies conjugated to fluorescein isothiocyanate (FITC), phycoerythrin (PE), allophycocyanin (APC), peridinin–chlorophyll–protein (Per CP-Cy5.5), and Cy-chrome (PE-Cy5 and PE-Cy7). The following BD PharMingen (San Diego, CA) antibodies were used for cell surface staining: APC-conjugated CD45 (30F-11), FITC-conjugated CD3 (145-2C11), PE-Cy5-conjugated CD4 (RM4-5), PE-conjugated CD45RC (DNL-1.9), APC-conjugated CD8 (53-6.7), PE-Cy5-conjugated B220 (RA3-6B2), FITC-conjugated IgM, PE-conjugated CD19 (ID3), PE-conjugated CD21 (7G6), FITC-conjugated CD23 (B3B4), APC-conjugated GR-1 (RB6-8C5), and PE-conjugated Mac1 (M1/70). PE-Cy5-conjugated F4/80 [Cl:A3-1 (F4/80)] was obtained from Serotec Ltd., Oxford, UK. PE-conjugated anti- $\alpha 4$  integrin (PS2) and anti-VCAM-1 (M/K-2) were

obtained from Southern Biotechnology, Birmingham, Ala. Irrelevant isotype-matched antibodies were used as controls [27].

**ELISA for cytokines.** Th2 cytokines (IL-4 and IL-5) and TNF $\alpha$  and IFN $\gamma$  in BAL and serum (previously frozen at –70 °C) were assayed with mouse Th1/Th2 cytokine CBA (BD Biosciences, San Diego, CA) following the manufacturer’s protocol. According to the manufacturer’s protocol, IL-13 and eotaxin were measured by Quantikine M kits from R&D Systems, Minneapolis, MN [23].

**OVA-specific IgE and IgG1 in serum.** Anti-mouse IgE (R35-72) and IgG1 (A85-1) from BD Biosciences, San Diego, CA, were used for measuring OVA-specific IgE and IgG1 (in serum previously frozen at –70 °C), respectively, by standard ELISA procedures as previously described [23].

## 6.3 Results

### 6.3.1 Rationale for the Study

The study was designed to develop a preclinical model of acute allergic asthma in C57Bl/6 J mouse purchased from NIN under the permission of the departmental animal ethics committee (approval dated May 12, 2010, renewed on December 30, 2013) and do a meta-analysis of unpublished earlier data generated in University of Washington, USA [23–33], together with new data generated in the University of Calcutta. Data from two main focused groups of experiments shall be shared and discussed in this work:

1. Cell traffic from PLO to & from SLO to & from pulmonary tissue to & from PLO, post complete manifestation of composite asthma phenotype [some data published in [33] which shall be further analyzed and discussed and new data presented here] and
2. Lymphopoiesis, mobilization, homing, and repopulation of PLO and SLO of lethally irradiated Rag2 $\gamma$ C $^{-/-}$  recipients from WT ( $\alpha 4$  +/+) and  $\alpha 4$ -ablated mouse BM, and then, the development (or not) of the composite asthma phenotype and inferences are made

thereof. [Here again, some published data from [31] shall be discussed in context with cellular traffic.]

$\alpha 4$ -ablated and  $\beta 2^{-/-}$  mice were developed by other laboratories [34, 35].

### 6.3.2 $\alpha 4$ + Cells in Various Tissues of $\alpha 4^{f/f}$ and $\alpha 4^{\Delta/\Delta}$ Donors Prior to Transplantation

Figure 6.3 shows the distribution of  $\alpha 4$ + cells in  $\alpha 4$ + versus  $\alpha 4$ -ablated mice. This is in donor mice itself (the mice from which BMC was prepared from femur for engraftment into

bloodstream). Understandably, PB has the lowest number of  $\alpha 4$ + cells, while surprisingly Peyer’s patch has the highest number of  $\alpha 4$ + cells in  $\alpha 4$ -ablated mice. In WT, BMC showed a greater homing and engraftment property than the KO BMC transplanted into the recipients. Cells that showed greatest (in terms of shortest time of migration and in terms of the greatest number of viable cells) homing and engraftment were the ones in PP, LNI, and MLN. Of note, these are the total number of cells including progenitors and differentiated functionally mature cells. These may be therefore labeled as the “leaky” tissues were post-ablation,  $\alpha 4$  expression still occurs, designating the transcriptome in these tissues as being non-permissive to ablation.

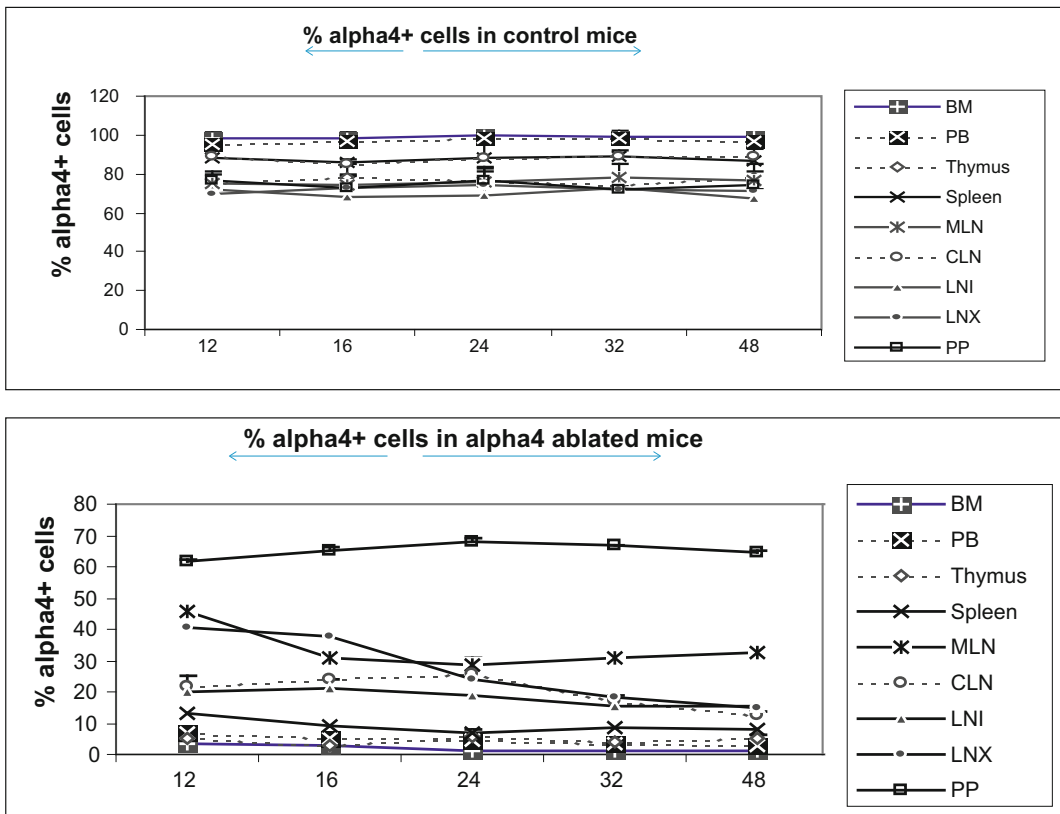


**Fig. 6.3** Distribution of  $\alpha 4$ + cells in primary and secondary lymphoid organs: donor neonatally ablated Mxcre  $\alpha 4^{-/-}$  versus WT.  $\alpha 4$ + cells were detected by flow cytometry using PS2 antibody in the donor  $\alpha 4$ -ablated mouse. Percent positive cells were converted

into total number from the total number of cells per tissue isolated and quantified after killing. Mean  $\pm$  SEM of 2 independent experiment  $n = 4/\text{group}$  is presented at  $p < 0.01$  (denoted by asterisk in figure)



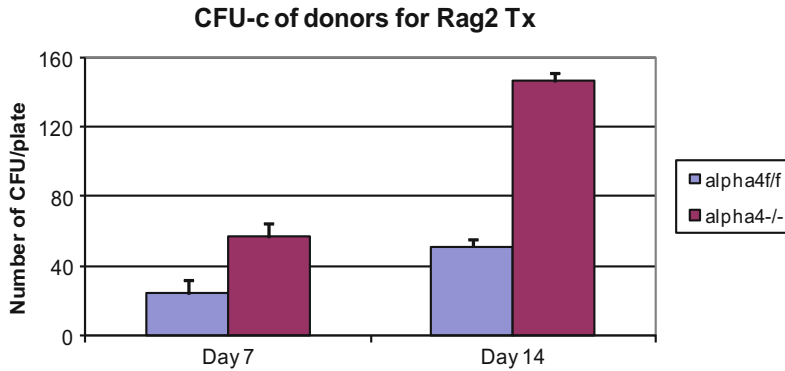


**Fig. 6.4** Donor BM CFU-C assessed before the transplant. Donor bone marrow cells were isolated from both femurs, found to be 98 % viable with trypan blue dye exclusion method and plated in 2 ml methylcellulose with IMDM and SCF 5 ng/ml and counted in a compound

microscope after 7 and 14 days. A number of colonies counted per million cells plated have been depicted as mean  $\pm$  SEM of 3 independent experiments and are presented at  $p < 0.01$  (denoted by asterisk in figure)

### 6.3.3 Clonogenic Potential of Bone Marrow Cells Used in Transplantation of Rag2 $\gamma$ C<sup>-/-</sup> Recipients

Figure 6.4 presents clonogenic potential of BM of WT versus  $\alpha 4^{-/-}$  mice.  $\alpha 4^{-/-}$  BM cells show greater colony-forming potential as found earlier [32–34].

### 6.3.4 Tissue Distribution of Hematopoietic Progenitors Post-transplantation and Engraftment at 10 Weeks

As shown from data presented in Fig. 6.5, PLO show the maximum variation among the genotype groups with or without OVA treatment in the PLO. Compared to WT, in both KO groups  $\alpha 4^{-/-}$  and  $\beta 2^{-/-}$ , there was twofold, 2.3-fold, and twofold increase in the number of progenitors in BM, respectively, post-OVA. In circulating blood, however, WT shows 1.7-fold increase in circulating progenitor number compared to 2.3-fold in both KO groups. There was a three-fold increase in hematopoietic progenitors in spleen of WT compared to 9 and 13 %,

respectively, in  $\alpha 4^{-/-}$  and  $\beta 2^{-/-}$  spleens. In the PP, WT and both KO groups show negligible change in progenitor number post-OVA. In tissue, a very curious thing is happening, compared to WT, where post-OVA increase in progenitor number in lung was tenfold, and in  $\alpha 4^{-/-}$ , it reduced half, while in  $\beta 2^{-/-}$ , the number increased by 16.5-fold. In the interstitial spaces of the lung, from the bronchoalveolar lavage fluid (BALF), the hematopoietic progenitors that were detected were 4.7-fold in WT compared to pre-OVA numbers being double in  $\alpha 4^{-/-}$  but only a 1.7-fold increase post-OVA. BALF in  $\beta 2^{-/-}$ , however, were a negligible number and obviously demonstrates a mechanistic inability to migrate across the interstitium.

### 6.3.5 Tissue Distribution of Mature and Differentiated Hematopoietic Cells

Repopulation of thymus was significantly impaired in Rag 2<sup>-/-</sup> recipients of  $\alpha 4^{\Delta/\Delta}$  cells, compared to those that received  $\alpha 4^{ff}$  donor cells (Fig. 6.6a). A decrease in total cellularity (by 43 % at 6 months) was again demonstrable at 8 months post-transplantation, indicating no restorative evidence with time post-transplantation. Double-positive (DP, CD4+/CD8+) population

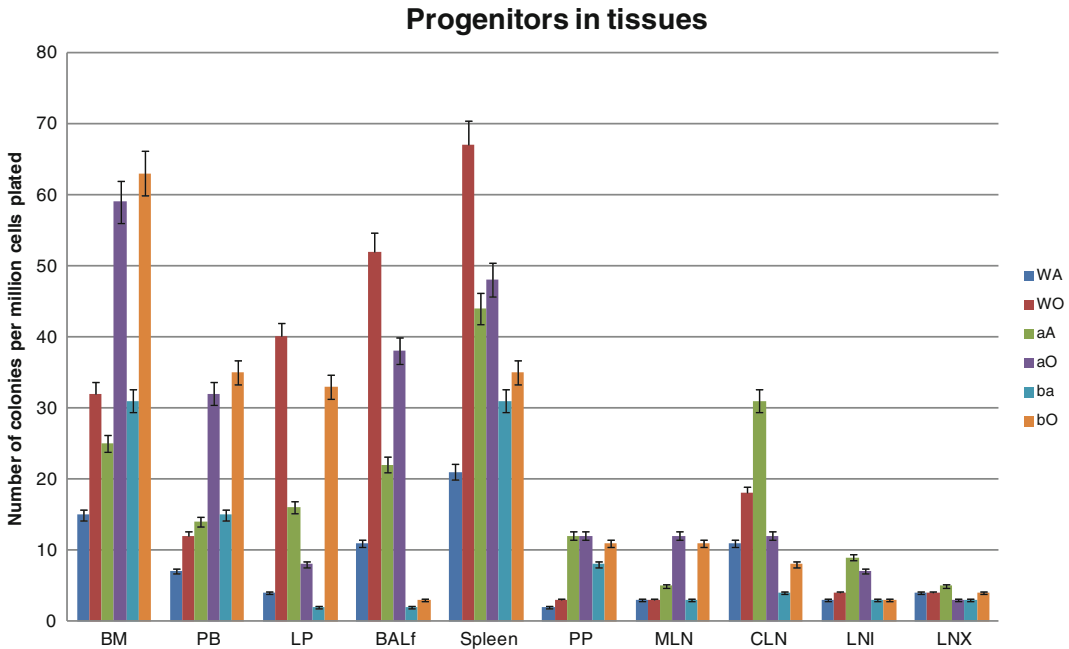


**Fig. 6.5** Progenitors in different tissues of the three genotype groups. CFU-c assays described as before were used to quantify clonogenic potential of tissues of Rag2 $\gamma$ C $^{-/-}$  recipients 10 weeks post-transplantation after they were killed. A number of colonies counted at day 10 per million cells plated have been depicted as mean  $\pm$  SEM of 4 independent experiments and are presented at  $p < 0.01$ . WA = WT + alum, WO = WT + OVA, aA =

$\alpha 4^{-/-}$ +alum, aO =  $\alpha 4^{-/-}$  +OVA, bA =  $\beta 2^{-/-}$  + alum, bO =  $\beta 2^{-/-}$  + OVA. All +alum groups have been compared with all the corresponding +OVA groups (asterisk), and all KO groups have been compared with their corresponding WR groups (hash) and are presented at  $p < 0.01$  (denoted by asterisk and hash in figure. Symbols are as explained in the preceding sentence)

(a)

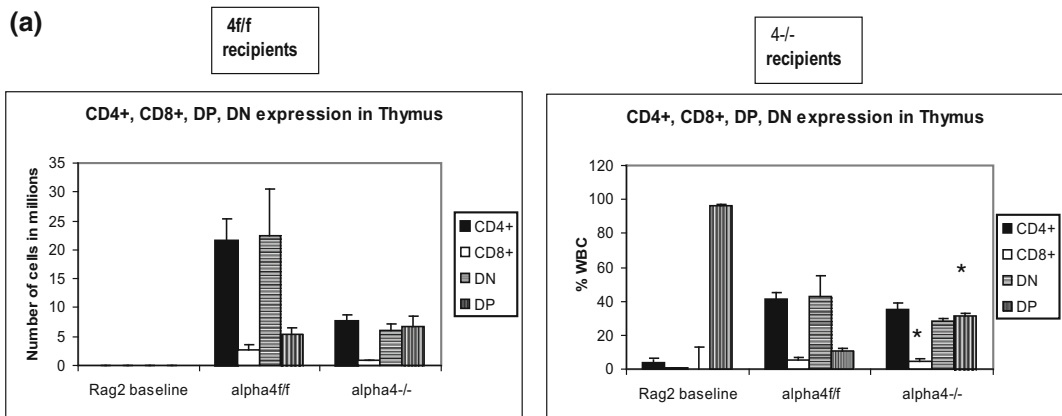


**Fig. 6.6 a-h** Cellularity in thymus and distribution of different developmental stages of T and B cells. After killing, a total number of cells were assessed by hemocytometer and type of cell subset was detected by staining and flow cytometry by the corresponding fluorochrome-tagged antibodies. A comparative number of cells positive for their phenotypic marker have been

presented as mean  $\pm$  SEM of 4 independent experiments.  $P < 0.001$  compared to baseline value in untransplanted Rag2 $\gamma$ C $^{-/-}$  was considered. Unless otherwise stated, all values are statistically significant in  $\alpha a^{+/+}$ -reconstituted and  $\alpha a^{\Delta/\Delta}$ -reconstituted animals and are presented at  $p < 0.01$  (denoted by asterisk in the figure)

(b)

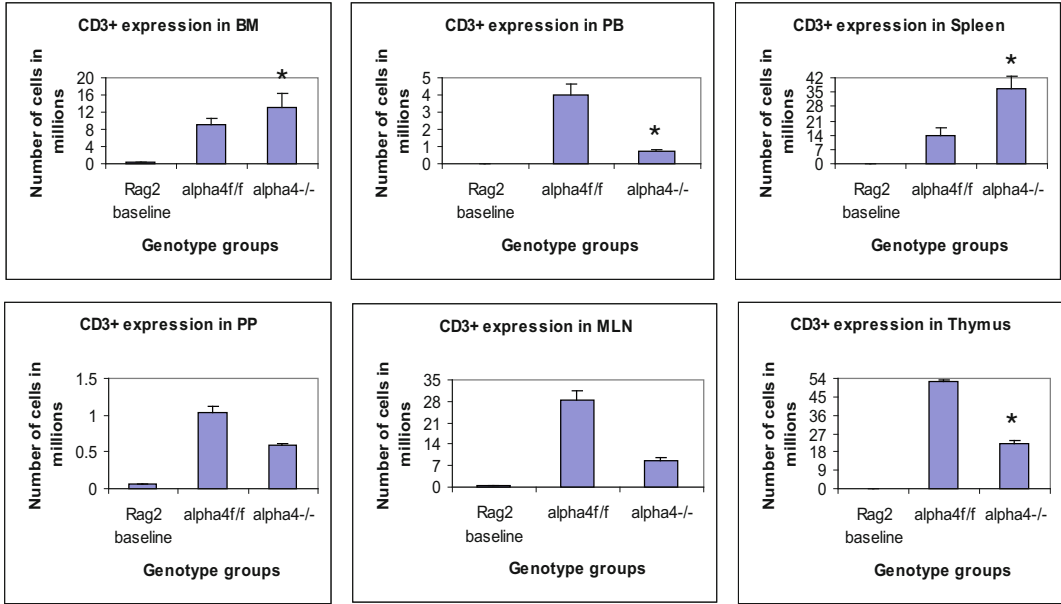


Fig. 6.6 (continued)

(c)

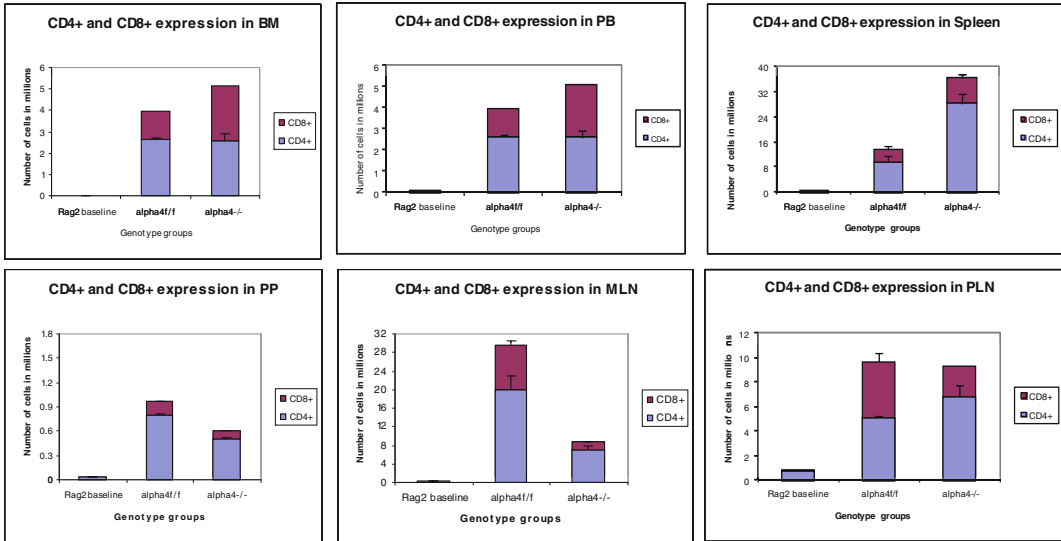


Fig. 6.6 (continued)

(d)

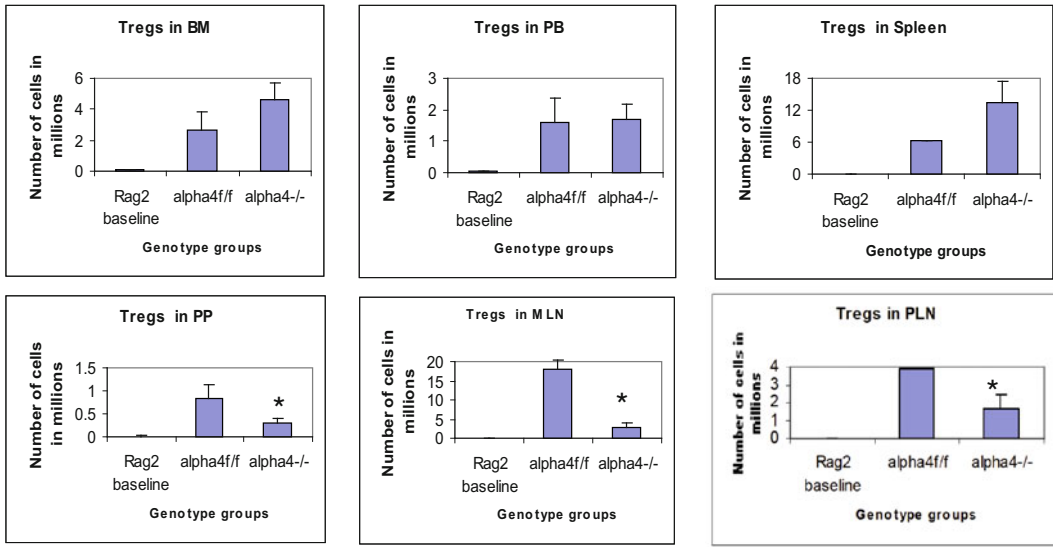


Fig. 6.6 (continued)

(e)

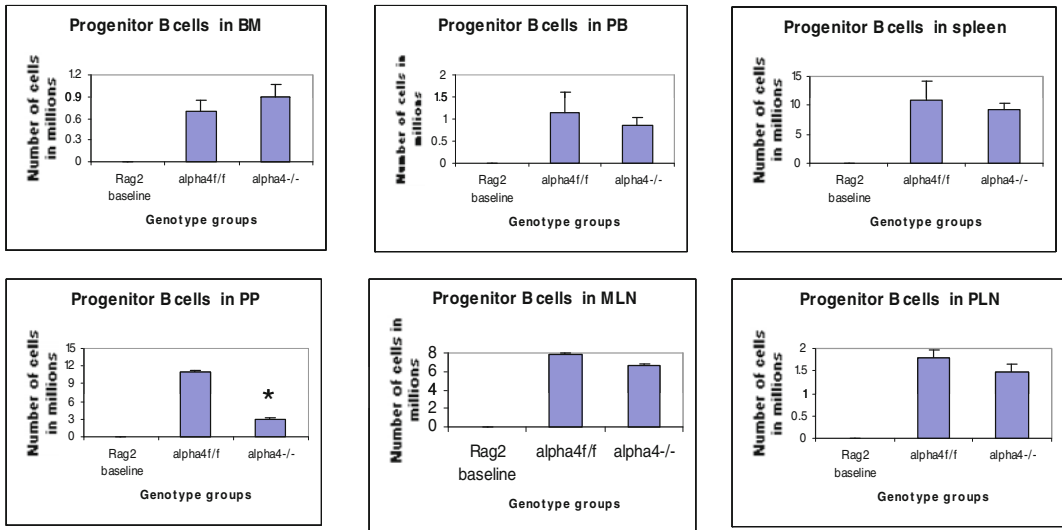


Fig. 6.6 (continued)

(f)

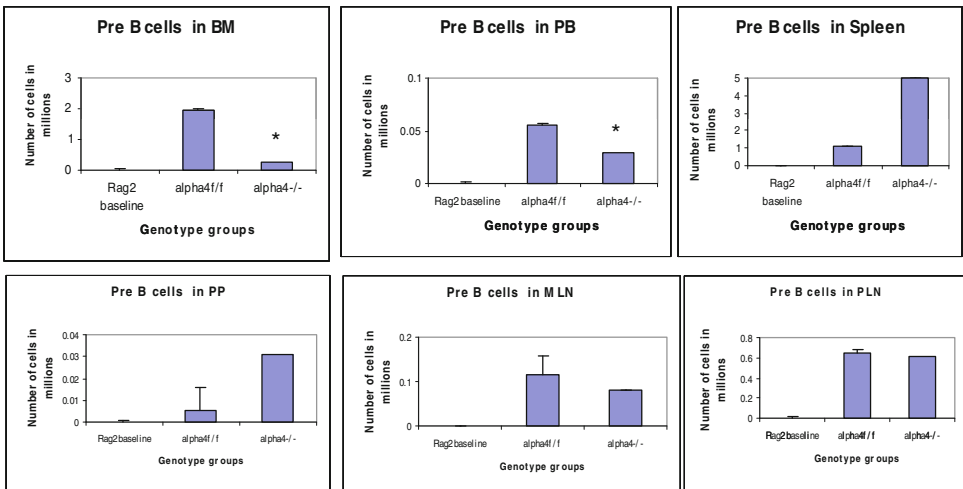


Fig. 6.6 (continued)

(g)

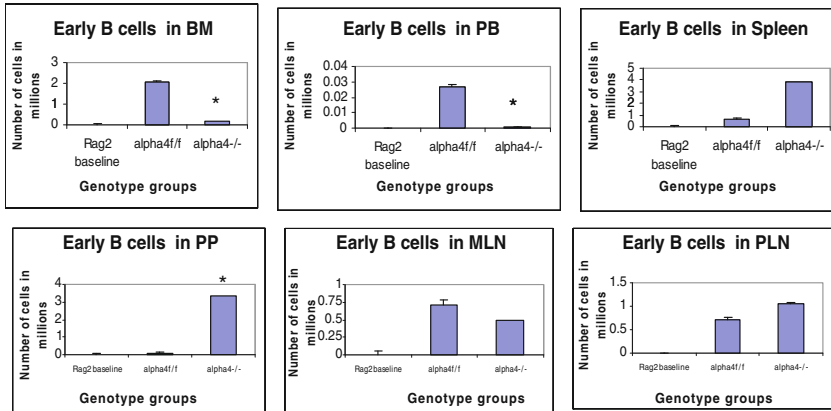


Fig. 6.6 (continued)

(h)

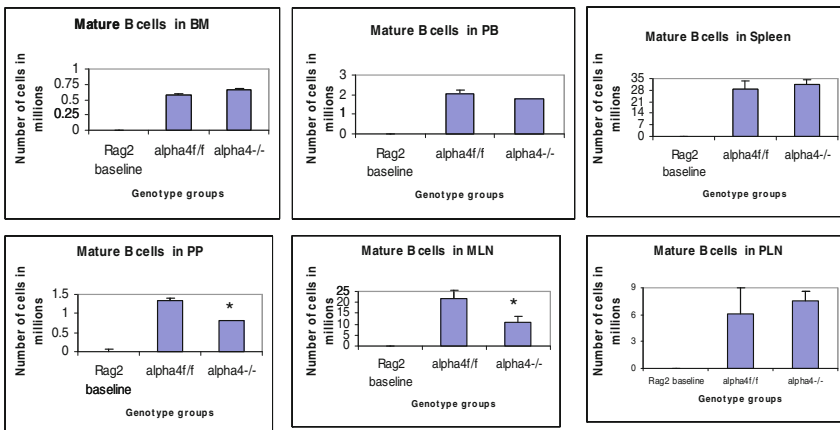


Fig. 6.6 (continued)

was the predominant one in Rag2<sup>-/-</sup> recipients of  $\alpha 4^{\Delta/\Delta}$  or  $\alpha 4^{f/f}$  donor cells. The CD4:CD8 ratio greatly favored the CD4 population (w8:1). This suggests that the total repopulation of thymus was impaired, likely because of impaired migration of BM-derived progenitors to thymus, although their subsequent maturation (to DP) was not grossly impaired in the absence of  $\alpha 4$  integrins. However, it is notable that CD8<sup>+</sup> cells were at very low levels in thymus and lower than controls, in contrast to levels in PB (w1.9:1).

### 6.3.6 Traffic Between Primary and Secondary Lymphoid Tissues (Differentiated Immune Cells Only)

#### (a) Proximal circulation

Cellularity in cervical, axillary, and LNI was similar to controls (i.e., recipients of  $\alpha 4^{f/f}$  donor cells). Detailed evaluation of subset distribution showed that there were modestly decreased proportions of mature B cells (B220+IgM<sup>+</sup>) in all LNs tested, or decreased proportions of activated T cells (CD3<sup>+</sup>/CD25<sup>+</sup>, CD3<sup>+</sup>/CD44<sup>+</sup>), but their absolute numbers were not significantly different from control groups (Fig. 6.6b–h). There was a tendency for preferential migration of CD45RC<sup>-</sup>/CD4<sup>+</sup> (memory) cells to lymph nodes, whereas CD45RC<sup>+</sup>/CD4<sup>+</sup> (naive) cells instead preferentially migrated to spleen and thymus in  $\alpha 4^{\Delta/\Delta}$  recipients. In spleen, as noted above, the cellularity, especially of red pulp, was significantly increased and concerned all developmental stages of B cells and of total T cells.

#### (b) Remote circulation

In Rag<sup>-/-</sup> recipients of  $\alpha 4^{\Delta/\Delta}$  cells both at 6 and 8 months post-transplantation, there was a significant reduction in cell numbers recovered from these tissues compared to controls (about 17-fold in PPs, 67 % less in MLNs) (Table 6.6B–D). All subsets of B and T cells were severely reduced in PPs and MLNs repopulated by  $\alpha 4^{\Delta/\Delta}$  cells. The CD4:CD8 ratio in PPs favored a CD4<sup>+</sup> profile, as seen in thymus. These data, like the ones in thymus, suggest significant homing impairment of all  $\alpha 4^{\Delta/\Delta}$  cells to these tissues.

### 6.3.7 Rate-Limiting Cells

From the above results and detailed cellular subpopulation analyses in Tables 6.1, 6.2, 6.3, 6.4, 6.5, 6.6, 6.7, and 6.8, the following data stand out: In blood, WT lymphoid cells before OVA treatment increase to 1.75-fold after OVA treatment compared to non-lymphoid cells which show insignificant increase. Whereas in  $\alpha 4^{-/-}$ , they increase by 2.3-fold, and in  $\beta 2^{-/-}$ , increase is about 1.6-fold. In both KO mice, however, there is a significant increase in number of non-lymphoid cells post-OVA compared to WT fivefold in  $\alpha 4^{-/-}$  and 1.6-fold in  $\beta 2^{-/-}$ . In lung, WT post-OVA lymphoid cells were a 106.6-fold compared to control, but in only 26.57-fold, more myeloid cells migrate to LP due to OVA-induced inflammation. In both KO, non-lymphoid cells are 16-fold and 12-fold, respectively, compared to control. In BALF, there is a 40-fold increase in number of lymphoid cells post-OVA in WT and 7.6-fold increase in myeloid cells, but other than these same cells showing a slight increase (3.5-fold) post-OVA in  $\beta 2^{-/-}$  cells, all KO cells basically failed to migrate across and show poor occurrence even compared to WT control (Table 6.1).

After the evaluation of the total and subpopulations of hematopoietic cells from PLO through blood to tissue site of inflammation (respiratory tissue), the obvious question was what fraction of the blood cells actually get recruited to SLO and thence to the inflamed tissue. Tables 6.3 onward attempts to quantitate that in detail. Percent recruited from blood to tissue as shown in Table 6.2 show a post-OVA preferential recruitment of T cells in  $\alpha 4^{+}$  cells (60-fold) to  $\alpha 4^{-}$  cells (28-fold) and none in  $\beta 2^{-}$  cells, while B cells show a complete inability to migrate to tissues in both KO (decrease by threefold) compared to 2.5-fold increase in WT cells. Macrophages (GR1-F4/80<sup>+</sup>) show no significant change in  $\beta 2^{-/-}$  compared to WT and  $\alpha 4^{-/-}$  recruitment (20-fold and 15-fold, respectively). As for a population of cells expressing both the myeloid markers, although in WT the number of cells detected was small, there was a significant increase in their recruitment from

**Table 6.1** (L = lymphoid, NL + non-lymphoid) Values represent the total number of different cells and their subsets migrated from bone marrow (BM) via circulation that is peripheral blood (PB) to lung parenchyma (LP) and interstitium (bronchoalveolar lavage fluid—BALF)

( $\times 10^6$ )			Blood	Lung	BAL	Trachea
WT	Lymphoid	Before	8.01 $\pm$ 1.3	0.015 $\pm$ 0.001	0.06 $\pm$ 0.01	0.004 $\pm$ 0.001
		After	13.9 $\pm$ 2.4	1.6 $\pm$ 0.05	2.4 $\pm$ 0.4	0.25 $\pm$ 0.15
	Non-lymphoid	Before	3.7 $\pm$ 0.7	0.07 $\pm$ 0.001	0.8 $\pm$ 0.003	0.013 $\pm$ 0.01
		After	4.3 $\pm$ 1.2	1.86 $\pm$ 0.06	6.1 $\pm$ 0.098	0.06 $\pm$ 0.03
$\alpha 4^{-/-}$	Lymphoid	Before	19 $\pm$ 3.2	0.015 $\pm$ 0.001	0.02 $\pm$ 0.009	0.012 $\pm$ 0.005
		After	44 $\pm$ 1.1	0.3 $\pm$ 0.001	0.05 $\pm$ 0.001	0.086 $\pm$ 0.07
	Non-lymphoid	Before	6.8 $\pm$ 2.1	0.05 $\pm$ 0.001	0.6 $\pm$ 0.016	0.056 $\pm$ 0.02
		After	34.8 $\pm$ 3.3	1.022 $\pm$ 0.05	0.8 $\pm$ 0.001	0.2 $\pm$ 0.1
$\beta 2^{-/-}$	Lymphoid	Before	35.9 $\pm$ 5	0.006 $\pm$ 0.0001	0.021 $\pm$ 0.01	0.014 $\pm$ 0.001
		After	57.9 $\pm$ 8.2	0.104 $\pm$ 0.05	0.08 $\pm$ 0.03	0.08 $\pm$ 0.02
	Non-lymphoid	Before	50.2 $\pm$ 8.3	0.43 $\pm$ 0.07	0.18 $\pm$ 0.001	0.16 $\pm$ 0.09
		After	79.6 $\pm$ 5.1	5.18 $\pm$ 0.03	0.64 $\pm$ 0.03	0.46 $\pm$ 0.2

Recruitment of all leukocytes and their subsets is less in  $\alpha 4^{-/-}$  lung as well as BALF compared to control. In  $\beta 2^{-/-}$  lung, except T cells and eosinophils, all other cells were increased in number (\* $P < 0.01$  compared with post-OVA control). Recruited T cells post-OVA (both CD4+ and CD8+) were CD45RC negative (memory) in control lung and BAL but mostly CD45RC positive (naïve) in  $\alpha 4^{-/-}$  and  $\beta 2^{-/-}$  mice. Note the differences between  $\alpha 4^{-/-}$  and  $\beta 2^{-/-}$  deficient mice in LP cell content. M $\phi$  denotes macrophage. (n = 12/genotype group)

blood (133-fold), but in  $\alpha 4^{-/-}$  mice, there was no difference in their recruitment post-OVA as opposed to  $\beta 2^{-/-}$  that showed feeble recruitment to the tune of thrice the number of cells recruited before OVA treatment which, however, was 166-fold higher to begin with in both KO groups.

As for the scenario in PLO (BM) other than T cells in whose number  $\alpha 4^{-/-}$  cells show 10.6-fold increase in synthesis of T cells as opposed to B cells, myeloid cells and indeed all other CD45+ cells compared to WT where an average of  $2.3 \pm 0.36$  fold increase is seen post-OVA (Table 6.3).

Tables 6.4, 6.5, 6.6, and 6.7A–D detail the count of different cell populations and is much more elaborate readout of Table 6.1. The important highlight here is that LP, BALF, and trachea being the different structural components of the respiratory tissue, the last seems to be a key node of information throughput and compared to WT and  $\beta 2^{-/-}$  mice, and  $\alpha 4^{-/-}$  mice show a much exaggerated CD4:CD8 ratio 5:1 compared to 3:1 in the former. Additionally, in all four tissues, Tables 6.5, 6.6, and 6.7C, all three species of B cells, viz. B220+IgM+ mature

plasma cells, B220+CD19+ memory cells, B220+CD23+ allergen-specific plasma cells, are severely decreased in number in  $\beta 2^{-/-}$  mice ab initio, and although there is a significant increase in these numbers after OVA treatment, the overall cell number in this KO mouse in respiratory tissue falls far short of even the numbers of these cells in the placebo-treated WT. Table 6.8B shows that both KO mice show a Th2-skewed phenotype in untreated mice which respond to OVA in terms of ration, but neither threshold number nor the composite phenotype is attained, indicating that CD4:CD8 may not be absolutely essential for the etiopathophysiology at a critical level. The interesting finding in data presented in these levels, however, is probably the most important finding of the entire work because of the memory versus naïve or immature T and B cell numbers before and after OVA treatment (Table 6.8C, D).

As regards the SLO and tissues, the first to be considered was CLN as it is anatomically proximal to the lung. Table 6.8A–C displays an increase in total number of cells. 26.5 and 31.3 % were, respectively, contributed by T and

**Table 6.2** Values represent percent cells of blood to be found in various tissues

	WT		$\alpha 4^{-/-}$		$\beta 2^{-/-}$	
	Before	After	Before	After	Before	After
<i>A % blood cells that migrated to interstitial spaces of the lung (BALF)<sup>a</sup></i>						
Total cells	7.29	46.6	2.4	1.03	0.2	0.5
T cells	0.17	14	0.014	0.05	0.02	0.14
B cells	1.68	22	0.28	0.15	0.35	0.136
GR1-F4/80+	0.7	27.6	0.07	0.09	0.4	2.3
GR1+F4/80+	13.5	21.5	0.5	2.3	0.3	0.7
GR1loF4/80hi	7.6	16.5	0.5	2.3	2.6	7.7
GR1loF4/80lo	16	13.8	0.5	1.2	0.5	0.6
GR1hiF4/80lo	9.6	73	0.04	2.16	0.03	0.35
GR1+F4/80-	15	46	0.6	0.3	0.06	0.045
<i>B % blood cells that migrated to lung parenchyma<sup>a</sup></i>						
Total cells	0.75	19.7	0.27	1.67	0.55	3.87
T cells	0.26	18.3	0.09	1.1	3	0.009
B cells	0.14	0.54	0.07	0.05	0.16	0.7
GR1-F4/80+	0.05	1.05	0.017	0.11	0.42	1.875
GR1+F4/80+	0.88	31	0.48	1.76	0.8	5.6
GR1loF4/80hi	0.04	6.15	0.12	0.2	5.4	28
GR1loF4/80lo	1.9	18.5	1.25	0.89	1.26	6.4
GR1hiF4/80lo	7	1.466	6	0.9	0.3	5.7
GR1+F4/80-	0.3	39.5	0.1	1.1	0.1	1.67
<i>C % blood cells that migrated to trachea<sup>a</sup></i>						
Total cells	1.07	1.35	0.2	0.2	0.3	0.3
T cells	0.05	3	0.013	0.37	0.02	0.08
B cells	0.07	0.176	0.18	0.06	0.15	0.3
GR1-F4/80+	0.01	0.2	0.04	0.6	0.6	0.5
GR1+F4/80+	0.0003	0.04	0.7	0.3	0.5	1.5
GR1+F4/80-	0.001	0.17	0.3	0.4	0.08	0.2

<sup>a</sup>A number of cells in PLO and SLO and tissue were calculated as tC and DC by hemocytometric analysis in a standard Neubauer hemocytometer, and DC was analyzed by double-blind counting from H&E-stained smears prepared in a cytospin (manufactured by Vision Scientific, South Korea, model Centurion Scientific C2 series) using Zeiss photograph allotment and AxioStar plus software and by flow cytometry using BD flow cytometer (BD Accuri C6 cytometer) and analyzed by BD Accuri C6 software using monoclonal fluorochrome-tagged antibody as mentioned in Materials and Methods section



**Table 6.3** Lymphoid and myeloid cells in bone marrow

Genotypes	Total ( $\times 10^6$ )	CD45+ ( $\times 10^6$ )	T cells ( $\times 10^6$ )	B cells ( $\times 10^6$ )	Myeloid cells ( $\times 10^6$ )
WT+alum	28.07 $\pm$ 8.3	25.86 $\pm$ 7.6	0.9 $\pm$ 0.05	2.485 $\pm$ 0.1	22.475 $\pm$ 10.3
WT+OVA	54.13 $\pm$ 11.6	46.5 $\pm$ 2.6	1.895 $\pm$ 0.75	6.49 $\pm$ 1.6	38.085 $\pm$ 9.2
$\alpha 4^{-/-}$ +alum	34.3 $\pm$ 6.5	28.94 $\pm$ 5.7	0.62 $\pm$ 0.2	3.675 $\pm$ 1.4	24.645 $\pm$ 1.3
$\alpha 4^{-/-}$ +OVA	104.15 $\pm$ 8.8	85.34 $\pm$ 11.9	6.57 $\pm$ 0.5	7.7 $\pm$ 0.7	71.07 $\pm$ 18.9
$\beta 2^{-/-}$ +alum	82.05 $\pm$ 11.5	67.7 $\pm$ 1.05	2.7 $\pm$ 0.9	9.7 $\pm$ 0.54	55.3 $\pm$ 1.15
$\beta 2^{-/-}$ +OVA	108.17 $\pm$ 13.2	96.7 $\pm$ 13.3	4.15 $\pm$ 1.3	10.4 $\pm$ 1.6	82.15 $\pm$ 4.6

A number of cells in PLO and SLO and tissue were calculated as tC and DC by hemocytometric analysis in a standard Neubauer hemocytometer, and DC was analyzed by double-blind counting from H&E-stained smears prepared in a cytospin (manufactured by Vision Scientific, South Korea, model Centurion Scientific C2 series) using Zeiss photograph allotment and AxioStar plus software and by flow cytometry using BD flow cytometer (BD Accuri C6 cytometer) and analyzed by BD Accuri C6 software using monoclonal fluorochrome-tagged antibody as mentioned in Materials and Methods section

B cells. Interestingly, post-OVA, this has increased by 5-fold in  $\alpha 4^{\Delta/\Delta}$  but remained the same in  $\beta 2^{-/-}$ .

## 6.4 Discussion

Figures 6.1 and 6.2 show the diagrammatic representation of the basic study protocols of transplantation for hematopoietic reconstitution and development of preclinical asthma, respectively. C57Bl/6 J mouse from NIN under permission from IAEC (University of Washington, Seattle, USA) and Departmental Animals Ethics Committee (Dept. of Zoology, University of Calcutta, India). Using this basic template of the study protocol of acute allergic asthma, migration of cells under no-disease condition (“clean” Rag2 $\gamma c^{-/-}$  where progenitors were killed off by lethal  $\gamma$ -irradiation and BM cells from donors were allowed to repopulate all PLO and SLO) and under diseased condition where two genotype knockout mice were used and acute allergic asthma induced to track and study the various nuances of cell migration in the different PLO and SLO and their subsequent recruitment to the pulmonary tissue for orchestrating inflammation.

At the outset, we must consider the significance of the donors that were chosen and the recipients’ pretreatment before transplantation. It may be conclusively deduced from Fig. 6.3 that some SLO are resistant to ablation of this

integrin. The reason may be important metabolic and transcriptomic pathways that disallow this, resulting in the immunosecretome being readjusted and repositioned such that ablation of  $\alpha 4$  is compensated. Figure 6.4, however, unambiguously excludes BMC from such non-permissiveness to ablation ensuring a 100 %  $\alpha$ -free reconstitution. As seen in previous publications, [30–34],  $\alpha 4$  has regulatory roles in mobilization, homing, and engraftment which explain their higher progenitor number in PLO (BM), circulation (PB), and spleen (SLO) in the KO groups, but not appreciable numbers post-OVA as was found in the WT (Fig. 6.5). This is key. In all other SLO assessed, namely MLN, LNI and LNX, except CLN, pattern of cellular traffic in WT versus KO groups and control versus OVA-treated groups does not follow a uniform pattern or any “trend.” The complete oppositeness of progenitor number modulation post-OVA in the two genotype groups indicates their diverse pathway action as enumerated in [30, 32, 33]. But what is interesting here is the complete separation of the cell traffic (direction and number) as evident from Tables 6.1, 6.2, 6.3, 6.4, 6.5, 6.6, 6.7, 6.8, and Fig. 6.6a–h. The picture of T cell and B cell distributions in spleen is more in line with what is present in PB and contrasts that of BM described above most likely because of longer retention and maturation of these cells in the splenic environment compared to BM. CD40+

**Table 6.4** A total count (lymphoid and myeloid cells) in blood

( $\times 10^6$ )		Total	T cells	B cells
WT	Control	11.92 $\pm$ 2.4	5.21 $\pm$ 1.3	2.8 $\pm$ 0.6
	OVA treated	18.22 $\pm$ 6.4	7.69 $\pm$ 2.4	6.25 $\pm$ 1
$\alpha 4^{-/-}$	Control	26.2 $\pm$ 8.8	13.8 $\pm$ 3.2	5.32 $\pm$ 1.7
	OVA treated	79.04 $\pm$ 22.2	18.5 $\pm$ 1.1	25.6 $\pm$ 7.5
$\beta 2^{-/-}$	Control	87.5 $\pm$ 19.8	32.2 $\pm$ 5	3.7 $\pm$ 2.3
	OVA treated	138 $\pm$ 60.1	43.3 $\pm$ 8.2	14.6 $\pm$ 1.5

## B Blood

## T cell subset

(x10 <sup>6</sup> )		CD4+	CD8+	CD4+		CD8+		CD4: CD8
				Memory	Naive	Memory	Naive	
WT	Control	4.34 $\pm$ 1.7	0.87 $\pm$ 0.02	0.06 $\pm$ 0.01	4.28 $\pm$ 2.3	0.15 $\pm$ 0.03	0.72 $\pm$ 0.1	5:1
	OVA treated	9.6 $\pm$ 1.2	0.67 $\pm$ 0.5	8.4 $\pm$ 2.4	1.2 $\pm$ 0.3	0.5 $\pm$ 0.1	0.2 $\pm$ 0.01	10:1
$\alpha 4^{-/-}$	Control	9.92 $\pm$ 2.3	0.8 $\pm$ 0.1	0.07 $\pm$ 0.001	9.85 $\pm$ 3.4	0.03 $\pm$ 0.001	0.8 $\pm$ 0.1	12:1
	OVA treated	26.3 $\pm$ 4.3	2.92 $\pm$ 0.6	21.6 $\pm$ 5.3	4.7 $\pm$ 1.4	2.45 $\pm$ 0.8	0.47 $\pm$ 0.1	9:1
$\beta 2^{-/-}$	Control	21 $\pm$ 2.5	11.2 $\pm$ 1.5	0.53 $\pm$ 0.1	20.5 $\pm$ 2.4	0.45 $\pm$ 0.02	10.75 $\pm$ 4	1.8:1
	OVA treated	36 $\pm$ 3.7	7.2 $\pm$ 2.2	29.7 $\pm$ 7	6.3 $\pm$ 0.9	6.7 $\pm$ 1.3	0.5 $\pm$ 0.01	5:1

## C Blood

(x10 <sup>6</sup> )		B220+	B220+IgM+ Mature plasma cells	B220+CD19+ Memory cells	B220+CD23+ Allergen-specific plasma cells
WT	Control	2.8 $\pm$ 0.6	1.84 $\pm$ 0.5	0.27 $\pm$ 0.12	0.79 $\pm$ 0.2
	OVA treated	6.25 $\pm$ 1	3.6 $\pm$ 1.3	8.81 $\pm$ 2.6	3.36 $\pm$ 1.08
$\alpha 4^{-/-}$	Control	5.32 $\pm$ 1.7	5.6 $\pm$ 1.9	1.23 $\pm$ 0.7	2.13 $\pm$ 0.75
	OVA treated	25.6 $\pm$ 7.5	17.4 $\pm$ 3.5	16.83 $\pm$ 3.6	17.8 $\pm$ 5.7
$\beta 2^{-/-}$	Control	3.7 $\pm$ 2.3	15.25 $\pm$ 6.7	0.56 $\pm$ 0.01	0.2 $\pm$ 0.1
	OVA treated	14.6 $\pm$ 1.5	27.5 $\pm$ 11.9	8.71 $\pm$ 3.9	14.08 $\pm$ 5.6

## D Blood

(x10 <sup>6</sup> )		GR1 -F4/80+	GR1+F4/80 +	GR1+F4/80+			GR1+F4/80-
				Gr1loF4/80hi	Gr1loF4/80lo	Gr1hiF4/80lo	
WT	Control	0.6 $\pm$ 0.5	2.6 $\pm$ 0.9	0.66 $\pm$ 0.01	0.31 $\pm$ 0.01	0.014 $\pm$ 0.001	0.72 $\pm$ 0.13
	OVA treated	0.83 $\pm$ 0.2	3.2 $\pm$ 0.6	1.3 $\pm$ 0.1	1.66 $\pm$ 1.5	0.26 $\pm$ 0.01	0.99 $\pm$ 0.02
$\alpha 4^{-/-}$	Control	0.5 $\pm$ 2.1	6.23 $\pm$ 1.4	3.3 $\pm$ 0.2	1.36 $\pm$ 0.25	0.024 $\pm$ 0.001	0.78 $\pm$ 0.03
	OVA treated	9.7 $\pm$ 3.3	18.6 $\pm$ 6.6	11.08 $\pm$ 0.5	6.7 $\pm$ 12.9	0.314 $\pm$ 0.01	10.7 $\pm$ 1.97
$\beta 2^{-/-}$	Control	0.74 $\pm$ 0.2	47.66 $\pm$ 8.3	3.05 $\pm$ 1.8	7.1 $\pm$ 4.5	14.9 $\pm$ 5	3.4 $\pm$ 11
	OVA treated	5.2 $\pm$ 0.8	54.1 $\pm$ 3.04	8.23 $\pm$ 0.9	19.9 $\pm$ 3.74	25.86 $\pm$ 2.6	19.81 $\pm$ 3.97

A number of cells in PLO and SLO and tissue were calculated as tC and DC by hemocytometric analysis in a standard Neubauer hemocytometer, and DC was analyzed by double-blind counting from H&E-stained smears prepared in a cytospin (manufactured by Vision Scientific, South Korea, model Centurion Scientific C2 series) using Zeiss photograph allotment and AxioStar plus software and by flow cytometry using BD flow cytometer (BD Accuri C6 cytometer) and analyzed by BD Accuri C6 software using monoclonal fluorochrome-tagged antibody as mentioned in Materials and Methods section

**Table 6.5** Total count (lymphoid and myeloid cells) in BALF

A BALF								
( $\times 10^6$ )		Total	T cells		B cells			
WT	Control	0.87 $\pm$ 0.01	0.009 $\pm$ 0.0001		0.047 $\pm$ 0.001			
	OVA treated	8.5 $\pm$ 0.4	1.05 $\pm$ 0.001		1.398 $\pm$ 0.15			
$\alpha 4^{-/-}$	Control	0.62 $\pm$ 0.09	0.002 $\pm$ 0.001		0.015 $\pm$ 0.001			
	OVA treated	0.82 $\pm$ 0.01	0.009 $\pm$ 0.001		0.04 $\pm$ 0.001			
$\beta 2^{-/-}$	Control	0.2 $\pm$ 0.01	0.008 $\pm$ 0.0001		0.013 $\pm$ 0.0001			
	OVA treated	0.72 $\pm$ 0.03	0.06 $\pm$ 0.0002		0.02 $\pm$ 0.001			
B BALF								
T cell subsets								
( $\times 10^3$ )		CD4+	CD8+	CD4+		CD8+		CD4: CD8
				Memory	Naive	Memory	Naive	
WT	Control	7.8 $\pm$ 2.5	0.17 $\pm$ 0.01	0	7.8 $\pm$ 2.2	0	0.17 $\pm$ 0.01	46:1
	OVA treated	1485 $\pm$ 89	15 $\pm$ 2.6	1448 $\pm$ 54	36.5 $\pm$ 7.1	14.5 $\pm$ 2.7	0.46 $\pm$ 0.01	98.6:1
$\alpha 4^{-/-}$	Control	2 $\pm$ 0.3	1 $\pm$ 0.7	0.03 $\pm$ 0.001	1.96 $\pm$ 0.1	0.05 $\pm$ 0.01	0.9 $\pm$ 0.01	2:1
	OVA treated	7.7 $\pm$ 1.2	0.26 $\pm$ 0.1	2.09 $\pm$ 0.1	5.6 $\pm$ 0.1	0.006 $\pm$ 0.001	0.25 $\pm$ 0.05	29.6:1
$\beta 2^{-/-}$	Control	5 $\pm$ 0.3	1 $\pm$ 0.4	0.125 $\pm$ 0.35	4.875 $\pm$ 1.5	0.03 $\pm$ 0.001	0.96 $\pm$ 0.15	5:1
	OVA treated	6 $\pm$ 0.2	2 $\pm$ 0.8	1.69 $\pm$ 0.8	4.3 $\pm$ 1.7	0.8 $\pm$ 0.002	1.16 $\pm$ 0.5	3:1
C BALF								
( $\times 10^3$ )		B220+	B220+IgM+ Mature plasma cells	B220+CD19+ Memory cells	B220+CD23+ Allergen-specific plasma cells			
WT	Control	47 $\pm$ 1	48.5 $\pm$ 16	5.94 $\pm$ 2.1	0.003 $\pm$ 0.001			
	OVA treated	1398 $\pm$ 150	144.5 $\pm$ 67	98.3 $\pm$ 11.5	102.7 $\pm$ 86			
$\alpha 4^{-/-}$	Control	15 $\pm$ 1	16.2 $\pm$ 6.3	13.6 $\pm$ 6.4	0.01 $\pm$ 0.001			
	OVA treated	40 $\pm$ 1	53.3 $\pm$ 12	52 $\pm$ 11	42 $\pm$ 7			
$\beta 2^{-/-}$	Control	13 $\pm$ 1	8.62 $\pm$ 1.5	4.6 $\pm$ 1.13	0.002 $\pm$ 0.001			
	OVA treated	20 $\pm$ 1	48.65 $\pm$ 8.4	31.5 $\pm$ 5.9	5.89 $\pm$ 1.8			
D BALF								
( $\times 10^3$ )		GR1-F4/80+	GR1+F4/80+	GR1+F4/80+			GR1+F4/80-	
				Gr1loF4/80hi	Gr1loF4/80lo	Gr1hiF4/80lo		
WT	Control	13 $\pm$ 3	350 $\pm$ 120	55.7 $\pm$ 11.6	52.2 $\pm$ 31	33.05 $\pm$ 11	305.7 $\pm$ 15	
	OVA treated	2100 $\pm$ 98	977 $\pm$ 98	215 $\pm$ 98	302 $\pm$ 156	760 $\pm$ 2.5	796 $\pm$ 210	
$\alpha 4^{-/-}$	Control	9.5 $\pm$ 1.6	29.8 $\pm$ 9.6	17.8 $\pm$ 1.7	7.4 $\pm$ 2.5	0.1 $\pm$ 0.01	17.2 $\pm$ 2.6	
	OVA treated	17.8 $\pm$ 1.08	426.5 $\pm$ 120	260.26 $\pm$ 34	81 $\pm$ 13.6	6.8 $\pm$ 1.2	34.2 $\pm$ 11.9	
$\beta 2^{-/-}$	Control	15 $\pm$ 1	160 $\pm$ 28	80 $\pm$ 28	37 $\pm$ 1.5	5 $\pm$ 1.4	20 $\pm$ 1.6	
	OVA treated	120 $\pm$ 31	560 $\pm$ 23	250 $\pm$ 7	70 $\pm$ 13	90 $\pm$ 3.7	25 $\pm$ 1.8	

(continued)

**Table 6.5** (continued)

F BALF								
(x10 <sup>3</sup> )		Total	Lym	Mono	Mac	Mast	PMN	Eos
F BALF								
(x10 <sup>3</sup> )		Total	Lym	Mono	Mac	Mast	PMN	Eos
WT	Control	874 ± 15	0	0	874 ± 15	0	0	0
	OVA treated	8500 ± 418	2817 ± 145	1141 ± 153	501 ± 21	40 ± 8	784 ± 19	3880 ± 45
$\alpha 4^{-/-}$	Control	623 ± 93	0	0	623 ± 93	0	0	0
	OVA treated	827 ± 17	0.6 ± 0.01	26 ± 0.4	2.6 ± 1.1	0	36.3 ± 9	0.9 ± 0.01
$\beta 2^{-/-}$	Control	204 ± 36	0	0	204 ± 36	0	0	0
	OVA treated	718 ± 15	75.9 ± 12	141.8 ± 0.5	64.9 ± 0.6	0	66.06 ± 14	0

A number of cells in PLO and SLO and tissue were calculated as tC and DC by hemocytometric analysis in a standard Neubauer hemocytometer, and DC was analyzed by double-blind counting from H&E-stained smears prepared in a cytospin (manufactured by Vision Scientific, South Korea, model Centurion Scientific C2 series) using Zeiss photograph allotment and Axiostar plus software and by flow cytometry using BD flow cytometer (BD Accuri C6 cytometer) and analyzed by BD Accuri C6 software using monoclonal fluorochrome-tagged antibody as mentioned in Materials and Methods section

(dendritic cells) were lower in all organs except the spleen, where the proportion, but not the total number, was low.

Figure 6.7 shows the pathways of induction of differentiation of various mature functionally active immune cells that are key to inflammation. Additionally, the figure also outlines the switch from progenitor (pluripotent cells) toward lineage commitment and final differentiation into competent immune cells responsible for the immune activities within tissues. Important to note are the cytokines and other factors that not only induce differentiation but also attract the cells from their sites of synthesis (PLO) to their sites of maturation (SLO) down to the tissues where they either perish in the onslaught or return to PLO or SLO (homing) with valuable information to be encoded as “central memory” cells that either become the effectors as and when they are recalled (mobilization) in the future during another exigency. Figure 6.8 represents ramifications of the network of growth factors and their receptors, adhesion and signaling molecules and transcription factors, maturation, morphogenic and their guidance molecules, and ECM proteins and proteinases. Figure 6.9 shows schematically the various functional cells populating the PLO, SLO, and migration to tissues, the known immune system lymphoid and myeloid

subpopulations, and their inducing cytokines and growth factors. Figure 6.10 depicts the major PLO and SLO in humans and that denotes their exact counterparts in mouse as they will be extrapolated to represent.

Mortality being low and repopulation of transplanted cells being 100 % by 48 weeks, we can say safely that the transplanted BMC did their job well, that is, they found the regions to home to, and then, they settled down there and all progenitors generated new clones and differentiated into the type of cells that the tissues needed. In other words, there was induction of differentiation in situ.

As for the rate-limiting steps which are key in cellular traffic resulting in the onset and development of the actual disease,  $\alpha 4$  was found to be a critical regulatory factor for myeloid cellular traffic compared to lymphoid (Table 6.1). Overall, both integrins seem to have regulatory roles in lymphoid cell migration and non-lymphoid cell migration to blood. The number of cells in BALF is the most striking and as described in [29–32] that while  $\alpha 4$  principally controls sensitization and signaling,  $\beta 2$  mainly control the migration from LP to interstitium without which onset of the asthma immunopathology cannot occur. Table 6.2 reveals a curious thing. A subpopulation of cells GR1+F4/80+ (GR1hiF4/80hi),

**Table 6.6** Total count (lymphoid and myeloid cells) in LP

A LP								
(x10 <sup>6</sup> )		Total		T cells (CD3+)		B cells (B220+)		
WT	Control	0.09 ± 0.014		0.0135 ± 0.001		0.004 ± 0.001		
	OVA treated	3.59 ± 0.1		1.41 ± 0.05		0.034 ± 0.001		
$\alpha 4^{-/-}$	Control	0.07 ± 0.03		0.0128 ± 0.001		0.0038 ± 0.0001		
	OVA treated	1.322 ± 0.04		0.209 ± 0.01		0.014 ± 0.00001		
$\beta 2^{-/-}$	Control	0.44 ± 0.12		0.0001 ± 0.00001		0.006 ± 0.00001		
	OVA treated	5.35 ± 0.97		0.004 ± 0.0001		0.1 ± 0.001		
B LP								
T cell subset								
(x10 <sup>3</sup> )		CD4+	CD8+	CD4+		CD8		CD4: CD8
				Memory	Naive	Memory	Naive	
WT	Control	13.3 ± 0.85	0.2 ± 0.01	0.95 ± 0.02	12.4 ± 0.07	0.01 ± 0.01	0.2 ± 0.01	66.5:1
	OVA treated	139 ± 12.5	10 ± 0.01	139 ± 0.7	0.001	10 ± 0.1	0.0001	14:1
$\alpha 4^{-/-}$	Control	11.8 ± 0.07	0.5 ± 0.01	0.3 ± 0.01	11.4 ± 0.03	0.064 ± 0.01	0.4 ± 0.01	24:1
	OVA treated	202.8 ± 15	6.2 ± 4.8	6.7 ± 3.5	196 ± 7.1	0.08 ± 0.03	6.2 ± 1.5	33:1
$\beta 2^{-/-}$	Control	0.16 ± 0.1	0.016 ± 0.001	0.045 ± 0.001	0.115 ± 0.01	0.02 ± 0.01	0.016 ± 0.001	10:1
	OVA treated	2.9 ± 3.3	0.9 ± 0.01	1.8 ± 0.02	1.1 ± 0.005	0.8 ± 0.01	0.1 ± 0.004	3.2:1
C LP								
(x10 <sup>3</sup> )		B220+	B220+IgM+ Mature plasma cells	B220+CD19+ Memory cells	B220+CD23+ Allergen-specific plasma cells			
WT	Control	4 ± 1	8 ± 5.5	6.7 ± 2.2	0.002 ± 0.0001			
	OVA treated	34 ± 1	28 ± 1.78	29.5 ± 1.8	31.2 ± 15.5			
$\alpha 4^{-/-}$	Control	4 ± 0.1	6 ± 3.5	5.5 ± 1.7	0.0001 ± 0.0001			
	OVA treated	14 ± 0.001	18 ± 8.5	15.7 ± 3.6	6.3 ± 3.45			
$\beta 2^{-/-}$	Control	6 ± 0.001	6 ± 3.96	3.2 ± 1.25	0.0001 ± 0.0001			
	OVA treated	100 ± 1	94 ± 12.4	76 ± 13	2.5 ± 1.2			
D LP								
(x10 <sup>3</sup> )		GR1-F4/80+	GR1+F4/80+	GR1+F4/80+			GR1+F4/80-	
				Gr1 <sup>lo</sup> F4/80 <sup>hi</sup>	Gr1 <sup>lo</sup> F4/80 <sup>lo</sup>	Gr1 <sup>hi</sup> F4/80 <sup>lo</sup>		
WT	Control	1.67 ± 0.5	23 ± 12	0.28 ± 0.1	6.9 ± 5.6	1.07 ± 0.08	6.45 ± 0.35	
	OVA treated	80 ± 13.5	1430 ± 5.7	83 ± 0.4	430 ± 12	50 ± 24	680 ± 78	
$\alpha 4^{-/-}$	Control	2.3 ± 0.85	33.7 ± 8.5	4.2 ± 1.07	17 ± 0.8	1.466 ± 0.7	3.5 ± 0.25	
	OVA treated	20 ± 0.2	328 ± 15	24 ± 0.05	60 ± 0.45	3 ± 0.35	118 ± 0.5	
$\beta 2^{-/-}$	Control	20 ± 5.8	380 ± 13.5	165 ± 34	90 ± 27	50 ± 19	37 ± 8	
	OVA treated	97.5 ± 32.5	4310 ± 40	930 ± 30	765 ± 65	1480 ± 190	920 ± 80	

A number of cells in PLO and SLO and tissue were calculated as tC and DC by hemocytometric analysis in a standard Neubauer hemocytometer, and DC was analyzed by double-blind counting from H&E-stained smears prepared in a cytospin (manufactured by Vision Scientific, South Korea, model Centurion Scientific C2 series) using Zeiss photograph allotment and AxioStar plus software and by flow cytometry using BD flow cytometer (BD Accuri C6 cytometer) and analyzed by BD Accuri C6 software using monoclonal fluorochrome-tagged antibody as mentioned in Materials and Methods section

**Table 6.7** Total count (lymphoid and myeloid cells) in trachea

A Trachea								
(x10 <sup>3</sup> )		Total		T cells (CD3+)		B cells (B220+)		
WT	Control	18.1 ± 9.8		2.8 ± 0.3		2 ± 0.7		
	OVA treated	247.5 ± 59.7		236.8 ± 82.4		11.3 ± 0.1		
α4 <sup>-/-</sup>	Control	54 ± 2.37		1.9 ± 0.2		10.6 ± 0.8		
	OVA treated	189.8 ± 5.8		69.2 ± 1		16.9 ± 0.3		
β2 <sup>-/-</sup>	Control	283 ± 18.9		8.65 ± 0.4		5.7 ± 0.7		
	OVA treated	474 ± 3.5		34.5 ± 2.35		47.4 ± 3.4		
B Trachea								
T cell subset								
(x10 <sup>3</sup> )		CD4+	CD8+	CD4+		CD8+		CD4: CD8
				Memory	Naive	Memory	Naive	
WT	Control	2.1 ± 0.3	0.7 ± 0.05	0.03 ± 0.0001	2.07 ± 0.1	0.002 ± 0.001	0.5 ± 0.01	3:1
	OVA treated	177.5 ± 0.8	60 ± 0.1	169.8 ± 1.14	0.7 ± 0.03	57.36 ± 1.1	2.5 ± 0.8	3:1
α4 <sup>-/-</sup>	Control	1.5 ± 0.03	0.4 ± 0.01	0.001 ± 0.0001	1.46 ± 0.1	0.001 ± 0.001	0.4 ± 0.01	3.75:1
	OVA treated	57.7 ± 0.16	11.5 ± 0.02	47.3 ± 1.6	10.4 ± 0.5	5.1 ± 1.6	4.8 ± 0.4	5:1
β2 <sup>-/-</sup>	Control	6.2 ± 0.01	0.2 ± 0.04	0.003 ± 0.0001	6 ± 0.05	0.001 ± 0.001	0.2 ± 0.01	31:1
	OVA treated	27 ± 0.4	7.5 ± 1.3	21.3 ± 7.5	5.7 ± 0.12	3.6 ± 2.6	3.7 ± 0.5	3.6:1
C Trachea								
(x10 <sup>3</sup> )		B220+	B220+IgM+ Mature plasma cells	B220+CD19+ Memory cells	B220+CD23+ Allergen-specific plasma cells			
WT	Control	2 ± 0.7	0.04 ± 0.001	0.03 ± 0.001	0.01 ± 0.001			
	OVA treated	11.3 ± 0.1	0.8 ± 0.01	1.5 ± 0.6	3.4 ± 0.5			
α4 <sup>-/-</sup>	Control	10.6 ± 0.8	0.01 ± 0.001	0.06 ± 0.001	0.02 ± 0.07			
	OVA treated	16.9 ± 0.3	0.6 ± 0.5	3.5 ± 1.5	4.7 ± 0.8			
β2 <sup>-/-</sup>	Control	5.7 ± 0.7	0.1 ± 0.04	0.04 ± 0.001	0.08 ± 0.001			
	OVA treated	47.4 ± 3.4	0.75 ± 0.01	4.6 ± 1.7	5.2 ± 0.65			
D Trachea								
(x10 <sup>3</sup> )		GR1-F4/80+		GR1+F4/80+		GR1+F4/80-		
WT	Control	0.2 ± 0.02		1.6 ± 0.5		12 ± 2.5		
	OVA treated	18 ± 1.7		34.5 ± 0.5		9.8 ± 2.4		
α4 <sup>-/-</sup>	Control	0.03 ± 0.001		41.5 ± 13		15 ± 0.75		
	OVA treated	7 ± 0.5		56 ± 12.5		162.6 ± 8.9		
β2 <sup>-/-</sup>	Control	0.05 ± 0.001		135.5 ± 20		27 ± 0.5		
	OVA treated	9 ± 2.8		335 ± 18.5		123 ± 7.5		

A number of cells in PLO and SLO and tissue were calculated as tC and DC by hemocytometric analysis in a standard Neubauer hemocytometer, and DC was analyzed by double-blind counting from H&E-stained smears prepared in a cytospin (manufactured by Vision Scientific, South Korea, model Centurion Scientific C2 series) using Zeiss photograph allotment and AxioStar plus software and by flow cytometry using BD flow cytometer (BD Accuri C6 cytometer) and analyzed by BD Accuri C6 software using monoclonal fluorochrome-tagged antibody as mentioned in Materials and Methods section

**Table 6.8** A total count (lymphoid and myeloid cells) in spleen

(x10 <sup>6</sup> )		Total	T cells	B cells
WT	Control	83.95 ± 25	38.87 ± 21	43.08 ± 2
	OVA treated	113 ± 21.83	58.56 ± 13.2	67.02 ± 6.03
α4-/-	Control	123.81 ± 18.97	47.73 ± 7.6	63.86 ± 12.6
	OVA treated	358.8 ± 8.5	59.31 ± 15	76.96 ± 12
β2-/-	Control	142.5 ± 42.98	52.94 ± 5.87	71.03 ± 3
	OVA treated	290.84 ± 54	69.22 ± 15.2	87.54 ± 19.24

**B Spleen**

T cell subset

(x10 <sup>6</sup> )		CD4+	CD8+	CD4+		CD8+		CD4: CD8
				Memory	Naive	Memory	Naive	
WT	Control	25.33 ± 0.323	10.53 ± 2.01	1.05 ± 0.37	20.13 ± 1.19	0.2 ± 0.07	10.33 ± 4.5	2:1
	OVA treated	52.82 ± 9.05	8.79 ± 2.2	39.63 ± 7.79	12.19 ± 2.53	6.56 ± 0.78	2.23 ± 0.76	3.7:1
α4-/-	Control	34.25 ± 6.56	5.18 ± 1.02	3.76 ± 5.04	30.49 ± 5.89	0.41 ± 0.01	4.77 ± 2.1	6.6:1
	OVA treated	30.59 ± 10.09	14.46 ± 4.3	26.3 ± 8.43	4.23 ± 1.19	12.31 ± 9.5	2.15 ± 1.08	2:1
β2-/-	Control	34.8 ± 0.06	6.93 ± 0.04	0.696 ± 0.43	34 ± 7.8	0.22 ± 0.17	6.71 ± 3.9	5:1
	OVA treated	56.39 ± 0.67	11.9 ± 2.67	28.27 ± 2.13	25.12 ± 4.8	8.05 ± 2.2	5.22 ± 1.3	4.7:1

**C Spleen**

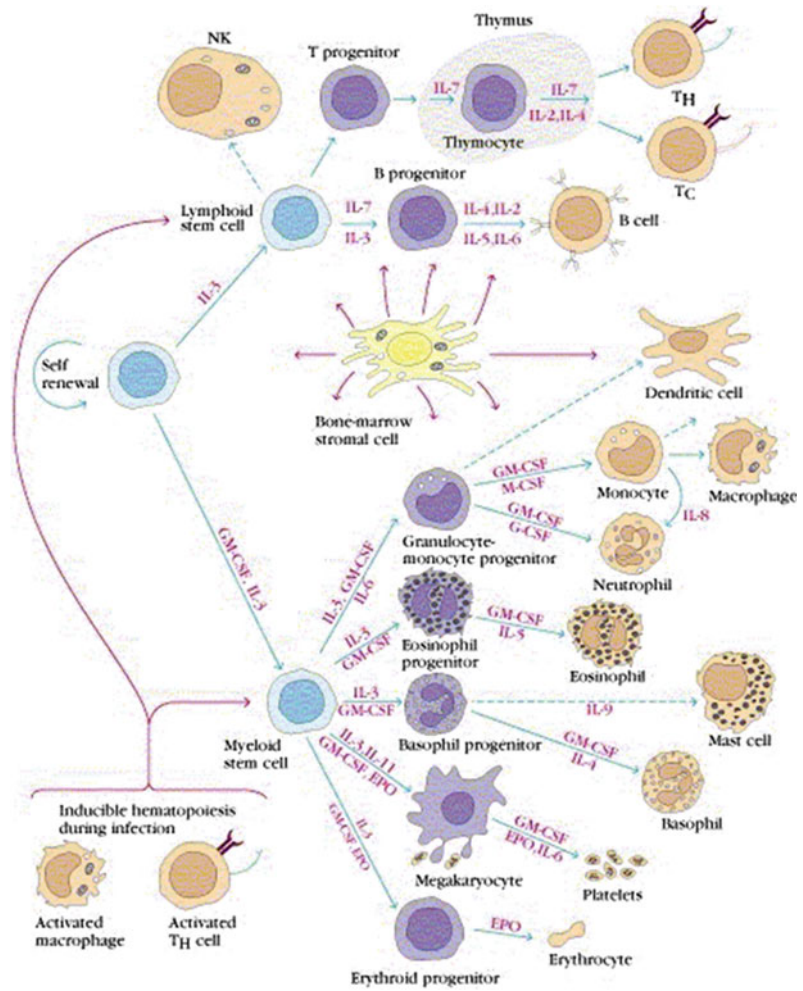
(x10 <sup>6</sup> )		B220+	B220+IgM+ Mature plasma cells	B220+CD19+ Memory cells	B220+CD23+ Allergen-specific plasma cells
WT	Control	43.08 ± 2	25.3 ± 1.8	1.018 ± 0.56	0.56 ± 0.12
	OVA treated	67.02 ± 6.03	39.4 ± 4.8	54.69 ± 32.16	21.25 ± 8.1
α4-/-	Control	63.86 ± 12.6	42.8 ± 15.3	15.4 ± 3.6	1.71 ± 0.85
	OVA treated	76.96 ± 12	161.3 ± 67.8	51.87 ± 6.95	28.76 ± 4.6
β2-/-	Control	71.03 ± 3	65.5 ± 36.7	2.2 ± 1.5	1.65 ± 0.53
	OVA treated	87.54 ± 19.24	104 ± 65.3	70.7 ± 11.7	57.69 ± 31.27

A number of cells in PLO and SLO and tissue were calculated as tC and DC by hemocytometric analysis in a standard Neubauer hemocytometer, and DC was analyzed by double-blind counting from H&E-stained smears prepared in a cytopsin (manufactured by Vision Scientific, South Korea, model Centurion Scientific C2 series) using Zeiss photograph allotment and Axiostar plus software and by flow cytometry using BD flow cytometer (BD Accuri C6 cytometer) and analyzed by BD Accuri C6 software using monoclonal fluorochrome-tagged antibody as mentioned in Materials and Methods section

probably newly formed macrophages migrated to pulmonary tissue from BM, which is a minute percent recruited from blood in normal untreated mice, shoot up in both KO groups, notwithstanding their lack of recruitment post-OVA. Either this may indicate a subclinical inflammation in the KO mice which is spontaneous in nature or it may be cells newly recruited from BM with other more extraneous and somewhat

fortuitous functions. This group needs better characterization. The GR1+F4/80- myeloid population which is definitely the new recruits from BM which have still not lost their GR1 expression may be short-lived granulocytes which show similar trend as this preceding group. The significance may be better grasped in the following tables where trends in PLO top SLO migration become clearer. The rate-limiting

**Fig. 6.7** Mediators of differentiation pathways from stem cells. The figure depicts stem cells, the lymphoid and myeloid progenitors and the various networks of cytokines, growth factors, cell-to-cell cross talk, and paracrine mediators that govern the differentiation process



cells are therefore lymphoid cells as they migrate from blood to lung tissue and thence to the interstitial spaces where the actual gas exchange occurs and this step is almost exclusively controlled by the  $\beta 2$  integrin.  $\alpha 4$  controls the lymphoid signaling, while  $\beta 2$  controls myeloid migration. So these are the rate-limiting cells from PLO to tissue. Table 6.3 reveals conclusively that although in  $\alpha 4^{-/-}$  BM, synthesis and sequestration of T cells fall quite tremendously and post-OVA their number is amplified manifold more than in WT. As mentioned in [34], this may either be due to a lack of “settling down” on the stroma of the PLO or a genuine increase in synthesis of these cells but it certainly means that

there is possibly no impairment in the upstream IL-4-IL-4R and IL-5-induced recruitment from BM in its absence. Data shown in Table 6.7D coupled with data presented in Fig. 6.6a highlight that  $\alpha 4$  is probably key to the Th1–Th2 balance. In Table 6.5, 6.6, and 6.7C, data show that although IL-4/5-induced cell recruitment is probably still operative despite the absence of  $\beta 2$  – cells from these B cells, they are unable to cross the number threshold and therefore insufficient to mount a viable pathophysiological circuit [31–37]. There may be a role for epithelial progenitors, circulating and niche-dwelling [37] which is beyond the scope of this paper and is being currently investigated.



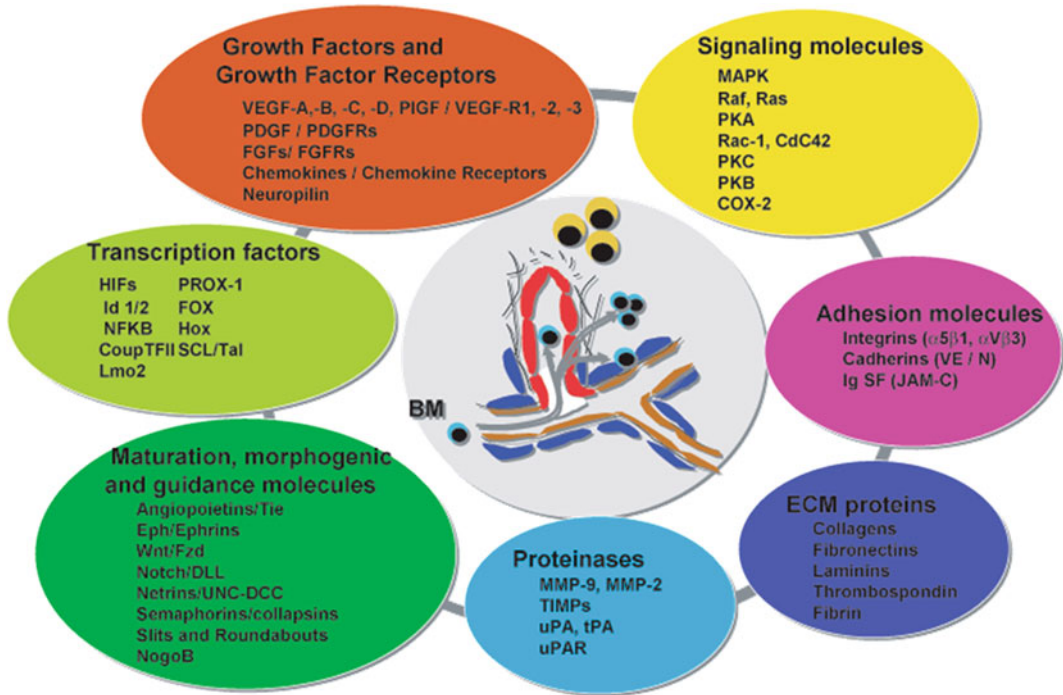


**Fig. 6.8** Ramifications of myriad factors operative in inflammation in a complex network. This figure depicts the interplay of various factors mainly non-cellular players in tandem with cells (keeping hematopoietic PLO as the focal point) orchestrating the important

functional pathways of immune response, angiogenesis, cellular activation, intracellular trafficking, protein sorting, and signaling that are critical for maintaining physiological homeostatic balance

## 6.5 Summary Findings and Conclusion—Highlights

### Observations

1.  $\alpha^{-/-}$  cells are slower to reconstitute,
2. Increased hematopoiesis in all primary and SLO in KO group,
3. Myeloid repopulation was similar in both groups,
4. B cells, pro-B cells, pre-B cells, and mature B cells significantly decreased in KO group,
5. Total T cells increased, but activated T cells decreased in KO group,
6. Repopulation of thymus was significantly impaired in KO group,
7. CD<sup>+</sup>CD8<sup>+</sup> was more in thymus, and CD<sup>+</sup> differentiation was skewed in KO group,
8. OVA-induced acute allergic asthma phenotype was impaired in all aspects,
9. All PLNs show decreased mature B cells,
10. Enhanced tendency of memory T cells (CD45RC<sup>-</sup>CD4<sup>+</sup>) to migrate to LNs in KO group,
11. Enhanced tendency of memory T cells (CD45RC<sup>+</sup>CD4<sup>+</sup>) to migrate to spleen and thymus,

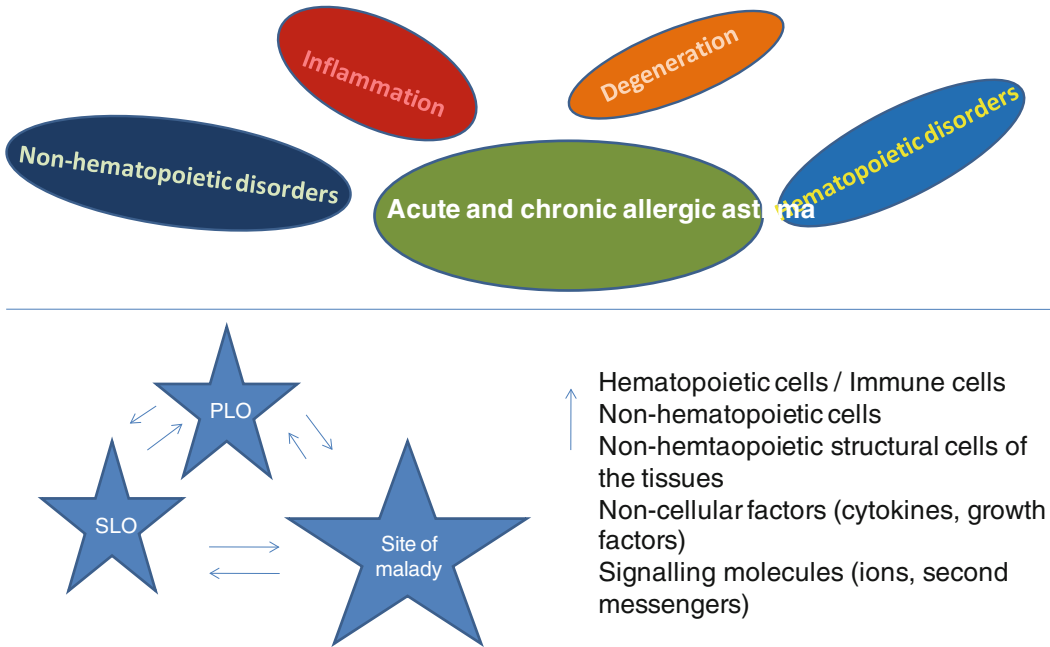


**Fig. 6.9** Schematic representation of the key inflammasomes and their pathways. The figure summarizes the overall meta-analyses template of several independent research works undertaken by this investigator and her group. Keeping the central theme as allergic acute and chronic asthma, the complex interplay of hematopoietic cells/immune cells, non-hematopoietic cells, non-hematopoietic structural cells of the tissues, non-cellular

factors (cytokines, growth factors), signaling molecules (ions, second messengers) encompassing the inside-out and outside-in signaling dictating hematopoietic and non-hematopoietic disorders and inflammation and degeneration that make a disease a complex network of pathways and the strategy to address specific targets in the pathways dictates success or failure of a diagnostic/prophylactic/therapeutic strategy

- 12. Functionality and homing impairment in KO group,
- 13.  $\alpha$ -/- probably do not have a role to play during response to OVA per se and neither to specifically T cell proliferation in response to the upstream cytokine signaling in response to OVA.

**Salient findings and clinical implications** Various small molecules inhibitors for  $\alpha$ 4 integrin such as Tysabri (Roche) and integrin Beta2/CD18 antibodies products manufactured by Biogen and Novus Biologicals and others which are specifically designed for modulation of the target molecule must take into account targeting strategies along with the timing of drug activation in a particular tissue (in pro drug formulation, through nanovehicles for timed and tissue-specific delivery). Positioning of PLO,

SLO, and inflamed tissue as nodes of cellular and information traffic and the network operative in specific temporal templates is crucial information for the success of such drugs. The role of  $\alpha$ 4 and  $\beta$ 2 is very much cell specific and tissue specific, for example, their role in BM, blood, lung, interstitial tissue spaces, trachea, and lymph nodes is not uniform. The “kicking in” is initiated possibly by  $\alpha$ 4 during initiation and “priming” of the B cells and T cells.

1. The “changing gear” is possibly orchestrated by  $\beta$ 2 during the effector phase of the disease development.

It is through the detailed mapping of such “switching on—switching off” information throughput of the cellular and non-cellular role players, and translational and personalized medicine may devise effective strategies in disease amelioration.

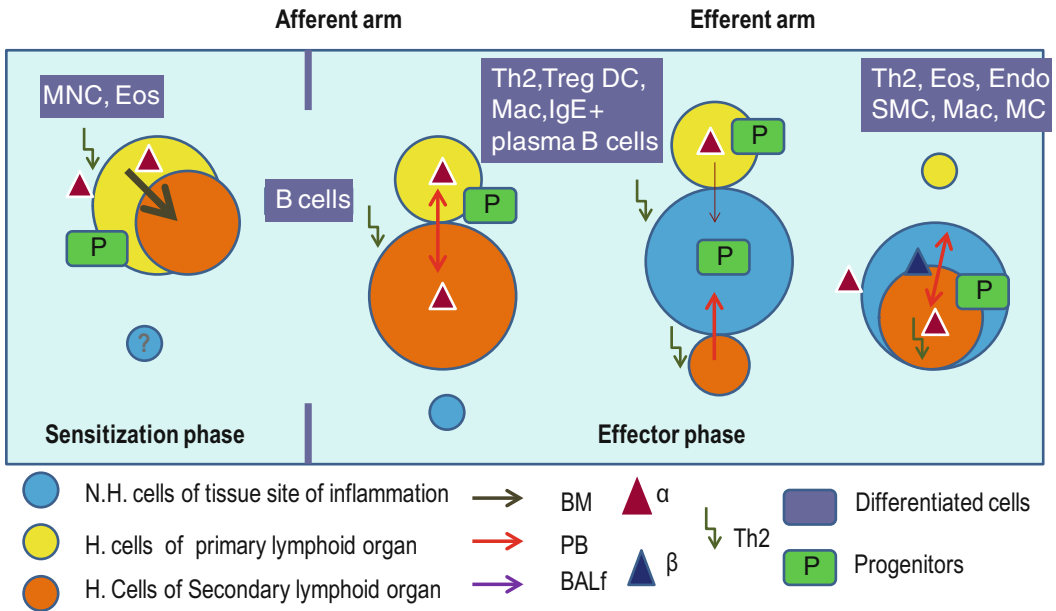


**Fig. 6.10** Summary findings and conclusion—tentative scheme of cellular traffic. This figure with appropriately designed flow diagram with symbols attempts to provide a schematic representation of its synthesized as a schematic representation of the various nodes or “cellular switches” in the given disease template which are basically existing thoroughfares of intercellular transport and communication among the three nodes of information throughput,

viz. PLO, SLO, and tissue (in this case pulmonary tissue and its ancillaries). The disease has been divided into afferent and efferent arms constituting several functional positioning of PLO, SLO, and tissue cells and their complex interactions. Their relative positioning denotes the chances of target overlap and stresses the need for more focused spatiotemporal targeting of therapeutic agents

## 6.6 Conclusion

$\alpha 4$  and  $\beta 2$  integrins control cellular migration of all lymphoid subpopulations from BM (site of poiesis) to PLO and of some subpopulations from PLO to SLO but have no effect on myeloid poiesis or homing and functionality.

**Acknowledgements** The author would like to acknowledge Professor Thalia Papayannopoulou for initiating and inducing me into the project and for providing the animals and laboratory infrastructure for carrying out the experiments. The funds for the same were provided by National Institutes of Health grants (HL58734, DK46557 to TP). Professor Arthur L. Beaudet provided the CD18<sup>-/-</sup> mice for which we gratefully acknowledge him.

**Conflict of interest** The author has declared that no conflict of interest exists.

## References

1. Udawadia ZF. *J Assoc Physicians India.* 2007;55:547–8.
2. Yang G, Rao C, Ma J, Wang L. *Int J Epidemiology.* 2006;35(3):741–8.
3. Davidson E, Liub JJ, Sheikh A. The impact of ethnicity on asthma care. *Primary Care Respir J.* 2010;19(3):202–8.
4. Sharma P, Halayko AJ. Emerging molecular targets for the treatment of asthma. *Indian J Biochem Biophys.* 2009;46(6):447–60.
5. Broide DH, Sullivan S, Gifford T, Sriramarao P. Inhibition of pulmonary eosinophilia in P-selectin- and ICAM-1-deficient mice. *Am J Respir Cell Mol Biol.* 1998;18(2):218–25.
6. Takizawa H. Novel strategies for the treatment of asthma. *Recent Pat Inflammation Allergy Drug Discovery.* 2007;1:13–9.

7. Czarnobilska E, Obtulowicz K. Eosinophil in allergic and non-allergic inflammation. *Przegl Lek.* 2005;62(12):1484–7.
8. Murphy DM, O'Byrne PM. Recent advances in the pathophysiology of asthma. *Chest.* 2010;137(6):1417–26.
9. Henderson WR Jr, et al. A role for cysteinyl leukotrienes in airway remodeling in a mouse asthma model. *Am J Respir Crit Care Med.* 2002;165:108–16.
10. Woodside DG, Vanderslice P. Cell adhesion antagonists: therapeutic potential in asthma and chronic obstructive pulmonary disease. *Biodrugs.* 2008;22(2):85–100.
11. Erlandsen SL. Detection and spatial distribution of the beta 2 integrin (Mac-1) and L-selectin (LECAM-1) adherence receptors on human neutrophils by high-resolution field emission SEM. *J Histochem Cytochem.* 1993;41:327–33.
12. Poole PJ. Oral mucolytic drugs for exacerbations of chronic obstructive pulmonary disease: systematic review. *BMJ.* 2001;322:1271–4.
13. Decramer M. Tiotropium as a first maintenance drug in COPD: secondary analysis of the UPLIFT® trial. *Lancet.* 2005;365:1552–60.
14. Rennard SI. The safety and efficacy of infliximab in moderate to severe chronic obstructive pulmonary disease. *Am J Respir Crit Care Med.* 2007;175:926–34.
15. Calverley PM. Salmeterol and fluticasone propionate and survival in chronic obstructive pulmonary disease. *N Engl J Med.* 2007;356:775–89.
16. Holgate ST. The epithelium takes centre stage in asthma and atopic dermatitis. *Trends Immunol.* 2007;28(6):248–251.
17. Cushley MJ. Inhaled adenosine and guanosine on airway resistance in normal and asthmatic subjects. *Br J Clin Pharmacol.* 1983;15:161–5.
18. Nakajima H, Sano H, Nishimura T, Yoshida S, Iwamoto I. Role of VCAM-1/VLA-4 and ICAM-1/LFA-1 interactions in antigen-induced eosinophil and T cell recruitment into the tissue. *J Exp Med.* 1994;179:1145–54.
19. Laberge S, Rabb H, Issekutz TB, Martin JG. Role of VLA-4 and LFA-1 in allergen-induced airway hyperresponsiveness and lung inflammation in the rat. *Am J Respir Crit Care Med.* 1996;151:822–829.
20. Schneider T, Issekutz TB, Issekutz AC. The role of  $\alpha 4$  and  $\beta 2$  integrins in eosinophil and neutrophil migration to allergic lung inflammation in the BN rat. *Am J Respir Cell Mol Biol.* 1999;20:448–57.
21. Chin JE, Hatfield CA, Winterrowd GE, Brashler JR, Vonderfecht SL, Fidler SF, Griffin RL, Kolbasa KP, Krzesicki RF, Sly LM, Staite ND, Richards IM. Airway recruitment of leukocytes in mice is dependent on  $\alpha 4$ -integrins and vascular cell adhesion molecule-1. *Am J Physiol.* 1997;272:L219–29.
22. Henderson WR Jr, Chi EY, Albert RK, Chu SJ, Lamm WJ, Rochon Y, Jonas M, Christie PE, Harlan JM. Blockade of CD49d ( $\alpha 4$  integrin) on intrapulmonary but not circulating leukocytes inhibits airway inflammation and hyperresponsiveness in a mouse model of asthma. *J Clin Invest.* 1997;100(12):3083–92.
23. Banerjee ER. Looking for the elusive lung stem cell niche—A perspective. *Transl Respir Med.* 2014;2:7–31.
24. Banerjee ER. Role of T cells in a gp91phox knockout murine model of acute allergic asthma. *Allergy Asthma Clin Immunol.* 2013;9(1):6–12.
25. Banerjee ER, Henderson WR Jr. Characterization of lung stem cell niches in a mouse model of bleomycin-induced fibrosis. *Stem Cell Res Ther.* 2012;3(3):21–42.
26. Banerjee ER, Laflamme MA, Papayannopoulou T, Kahn M, Murry CE, Henderson WR Jr. Human embryonic stem cells differentiated to lung lineage-specific cells ameliorate pulmonary fibrosis in a xenograft transplant mouse model. *PLoS One.* 2012;7(3):e33165:1–15.
27. Banerjee ER, Henderson WR Jr. Defining the molecular role of gp91phox in the manifestation of acute allergic asthma using a preclinical murine model. *Clin Mol Allergy.* 2012;10(1):2–16.
28. Banerjee ER. Triple selectin knockout (ELP $^{-/-}$ ) mice fail to develop OVA-induced acute asthma phenotype. *J Inflamm.* 2011;8:19. doi:10.1186/1476-9255-8-19.
29. Banerjee ER, Henderson WR Jr. NADPH oxidase has a regulatory role in acute allergic asthma. *J Adv Lab Res Biol.* 2011;2(3):103–120 (ISSN 0976-7614).
30. Banerjee ER, Jiang Y, Henderson WR Jr, Latchman YL, Papayannopoulou T. Absence of  $\alpha 4$  but not  $\beta 2$  integrins restrains the development of chronic allergic asthma using mouse genetic models. *Exp Hematol.* 2009;37:715–727.
31. Banerjee ER, Latchman YL, Jiang Y, Priestley GV, Papayannopoulou T. Distinct changes in adult lymphopoiesis in Rag2 $^{-/-}$  mice fully reconstituted by  $\alpha 4$ -deficient adult bone marrow cells. *Exp Hematol.* 2008;36(8):1004–13.
32. Ulyanova T, Banerjee ER, Priestley GV, Scott LM, Papayannopoulou T. Unique and redundant roles of  $\alpha 4$  and  $\beta 2$  integrins in kinetics of recruitment of lymphoid vs myeloid cell subsets to the inflamed peritoneum revealed by studies of genetically deficient mice. *Exp Hematol.* 2007;35(8):1256–65.
33. Banerjee ER, Jiang Y, Henderson WR Jr, Scott LM, Papayannopoulou T.  $\alpha 4$  and  $\beta 2$  integrins have non-overlapping roles in asthma development, but for optimal allergen sensitization only  $\alpha 4$  is critical. *Exp Hematol.* 2007;35(4):605–17.
34. Scott LM. *Mol Cell Biol.* 2003;23(24):9349–60.
35. Lee S-H, et al. *Nat Med.* 2003;9:1281–6.
36. Farrell RJ, Kelleher1 D. *J Endocrinol.* 2003;178:339–346.
37. Gomperts B, Belapario JA, Rao N, Randell SH, Fishbein MC, Burdick MD, Strieter RM. *J Immunol.* 2006;176:1916–1927.

---

## 7.1 Introduction

In recent years, the stem cell field has opened a new venue in regenerative and reproductive medicine. Stem cells are of the utmost importance for the biology of developing and adult organisms and have immense potential for therapeutic use in a variety of medical conditions. Stem cells provide an opportunity to dissect the cellular and molecular mechanisms controlling embryonic development, cellular differentiation, and organ maintenance and also have a great potential in developing novel cell-based therapies. Stem cells are characterized by the ability to divide asymmetrically to produce daughter cells of two types, one fated for differentiation and one to regenerate a stem cell. This cell division takes place within a cellular niche or environment where the stem cell maintains contact with the cells composing the niche, whereas the differentiating cell moves away from the niche. This niche is a subset of neighboring stromal cells and extracellular substrates. The stromal cells usually secrete growth factors to regulate stem cell function.

Although stem cells are present in many mature tissues, they are rare and difficult to locate, which makes analysis of their stem cell properties and microenvironments hard. Only a small number of cells in adult tissues (the stem cells) possess the ability to self-renew at every cell division, while producing differentiating daughter cells to maintain tissue homeostasis for an organism's lifetime. However, adult stem cells

allow patient-specific therapies to be carried out without the need for cloning to avoid immune rejection, and they provide an alternative to embryonic stem cells for use in regenerative medicine. Nonetheless, there are still fundamental questions that need to be answered before we fully understand the behavior of stem cells in living tissues. For instance, the molecular parameters that define a stem cell are not known, nor are the mechanisms that control the rate of proliferation versus differentiation of stem cells. Such questions are of major significance in stem cell research, because the characterization and study of stem cells relies on our ability to identify and culture them. Moreover, in order to understand the mechanisms controlling the establishment and maintenance of stem cell types, we need to decipher the interactions between the stem cells and the cellular microenvironments in which they are maintained—so-called stem cell niches.

---

## 7.2 The *Drosophila* Ovary

The *Drosophila* ovary provides an excellent system for studying factors required to establish and maintain stem cells and also offers several unique advantages for studying molecular and genetic networks controlling stem cell regulation. First, a small number of easily identified stem cells are located in a simple tubular structure, also known as the germarium, in which stem cells and their surrounding cells are well defined and easily distinguished from one another, facilitating qualitative

and quantitative analyses. Second, sophisticated but yet elegant genetic and molecular tools make manipulation of gene function in stem cells and their niche easy and precise. Third, more than 50 % of the *Drosophila* genes have mutations, and microarray and proteomic reagents are available due to the finished *Drosophila* genome, which dramatically enhance our ability to discover genes that encode intrinsic factors and niche signals important for controlling self-renewal, proliferation, and differentiation of stem cells. Finally, comparative studies on the stem cells in the *Drosophila* ovary and in the testis help find general stem cell regulatory mechanisms because the *Drosophila* testis also contains easily identified stem cells and niche cells. Therefore, the *Drosophila* ovary represents one of the best systems for studying basic stem cell biology.

*Drosophila* female has a pair of ovaries, which is composed of 12–16 ovarioles. Each *Drosophila* ovariole has three independent sets of stem cells: germline stem cells (GSCs) and escort stem cells (ESCs), located at the anterior tip of the germarium, and somatic stem cells (SSCs), located adjacent to the newly formed 16-cell cysts, rendering it one of the best model systems for studying stem cell biology due to reliable stem cell identification and available sophisticated genetic tools for manipulating gene functions. Decapentaplegic (Dpp) is required to maintain the anterior stem cells, whereas hedgehog is required for maintenance and cell division of the SSCs. One set, composed of two or three GSCs, is located adjacent to the cap cells at the anterior tip of each ovariole. After a stem cell division, one daughter cell retains its attachment to the cap cells whereas the other daughter (called a cystoblast) moves away from the cap cells and begins a series of differentiation steps. A second set of stem cells, adjacent to the GSCs, has recently been shown to produce sets of transitory escort cells that envelope cystocytes during the four nuclear divisions. Immediately posterior to the inner gonial sheath cells is located a third set of stem cells responsible for the somatic lineages of the ovary (SSC).

### 7.3 Identifying Stem Cells and Their Niche

The female *Drosophila* has the remarkable ability to generate a large number of eggs throughout its lifetime because of the existence of permanent stem cells. In addition to easily identified stem cells and niches in the *Drosophila* ovary, the *Drosophila* system also offers genetic and molecular tools for effectively manipulating functions of genes in both stem cells and niche cells. The FLP-mediated FRT stem cell marking system has been successfully used to generate marked mutant stem cells and determine the effect of a mutation in a given gene on the maintenance, proliferation, and differentiation of GSC, SSC, or ESC. This method has been used to demonstrate roles of different pathways and factors in the control of ovarian stem cell regulation in the *Drosophila* ovary. Recently, MARCM (mosaic analysis with a repressible cell marker) and PMML (positively marked mosaic lineage), two positive marking systems for gene overexpression, have been used to effectively study SSC regulation. In addition, the GAL4-UAS system can be used to overexpress genes, dominant-negative and RNAi constructs to manipulate gene function in a cell-specific manner. It has recently been shown that *Drosophila* GSCs can be cultured *in vitro*, together with somatically derived cells, possibly generated by SSCs. In summary, the *Drosophila* ovary will continue to provide one of the most effective systems for studying stem cell regulation.

(a) **Germline stem cells:** One of the best-characterized niches supports germline stem cells (GSCs) within the *Drosophila* ovary [1]. GSCs serve as a reservoir for the continuous production of gametes in all organisms. The GSC niches in *Drosophila* are the best studied because of well-defined structures and availability of molecular markers. Genetic and cell biological studies show that the germarial tip functions as a GSC niche. First, if the two daughters of a GSC following cell division are positioned where GSCs are normally located, both of

them adopt the GSC fate. Second, GSCs have to be directly anchored to cap cells through adherens junctions in order to continuously self-renew. Third, TFs and cap cells express several genes that are important for controlling GSC self-renewal. One recent study has implicated ESCs as a part of the GSC niche. Thus, the GSC niche is likely composed of TF/cap cells and ESCs, which are all located next to GSCs. GSCs are present in the gonads of *Drosophila* females and males. The proper maintenance and correct differentiation of GSCs are essential for fertility and fecundity. The female GSC niche contains 5–7 non-dividing somatic cap cells, which physically anchor 2–3 GSCs in each germarium. As the GSC divides to generate two daughters with the one remaining in contact with cap cells and the other one lying one cell away from the cap cells, the anterior daughter self-renews as a stem cell and the posterior one differentiates into a cystoblast due to differential signaling from their microenvironments. However, the two daughters can adopt the same cell fate, either stem cell or cystoblast, when they are put in the same environment. The two stem cell daughters become GSCs if they both stay in the niche due to available niche space following loss of one neighboring GSC (referred here as symmetric division); both of them can be turned into cystoblast, resulting in loss of the GSC, if they move away from the niche due to loss of adherens junctions. Such junctions between GSCs and cap cells are established during the niche formation. Then, cystoblast (CB), which moves away from niche, forms an interconnected 16-cell cyst by incomplete cytokinesis. The cystoblasts move away from the niche wrapped by differentiated escort cells produced from ESCs. The cyst cells are encysted by the escort cells until they reach the 16-cell stage. Only 1 out of 16 germ cells can become an oocyte and the remaining cells will then become nurse cells to support the growth of the oocyte. Furthermore, it has been shown that DE-cadherin is required for anchoring GSCs in their niche. Several

signaling pathways are responsible for niche stem cells' interaction and maintenance in the *Drosophila* ovary.

Genetic studies in the past decade have identified a number of genes with critical functions in GSC self-renewal, proliferation, and differentiation. As expected, some of these genes encode intrinsic factors, including nuclear factors and translational regulators that function inside the GSC, while the others produce proteins that function to generate signals and regulators of signal production within the niche. Several recent reviews have summarized the progress in understanding functions of these extrinsic and intrinsic factors in regulation of GSC self-renewal, proliferation, and differentiation. Two or three GSCs in the apical tip of the germarium can be reliably identified by their location (direct anchorage to posterior side of the cap cells), size (the biggest cells at the tip of the germarium), and anterior localization of a round spectrosome.

(b) **Escort stem cells:** In the *Drosophila* ovary, GSCs in the niche continuously self-renew and generate differentiated germ cells that interact physically with escort cells (ECs). ESC activities have been confirmed by lineage tracing and laser ablation experiments. It has been proposed that ESCs, which directly contact GSCs, generate differentiated ECs to maintain the EC population where ECs undergo apoptosis [2]. The germ cells released from ECs are subsequently surrounded by follicle cells, which are produced by two follicular stem cells (FSCs), to form individual egg chambers [3, 4]. Further, Pankaj Sahai-Hernandez and Todd Nystul (p. 4490) investigate the FSC niche of the *Drosophila* ovary, providing evidence that the escort cells of the germarium—which surround germline cysts and support their development—are also key for FSC maintenance. Hedgehog (Hh) and Wingless (Wg) pathways are known to promote FSC self-renewal and the distant terminal filament and cap cells were proposed to be the sources for these signals. However, the authors here show that escort cells are the essential source of Wg for FSC function,

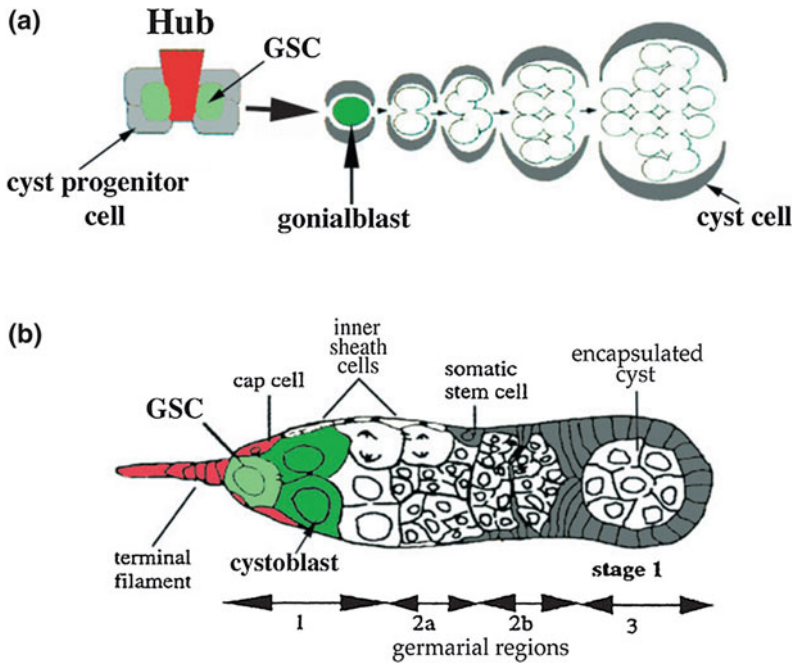


**Fig. 7.1** GSC niches in the *Drosophila* ovary and testis. **a** Schematic of the early steps in *Drosophila* spermatogenesis. **b** Schematic of a *Drosophila* germarium, which houses the GSCs

whereas Hh is produced from multiple somatic cell types—including escort cells—and acts on both FSCs and their progeny. Moreover, escort cells contact FSCs and likely provide a dynamic niche for their maintenance, revealing a new component of the niche and a new function for escort cells.

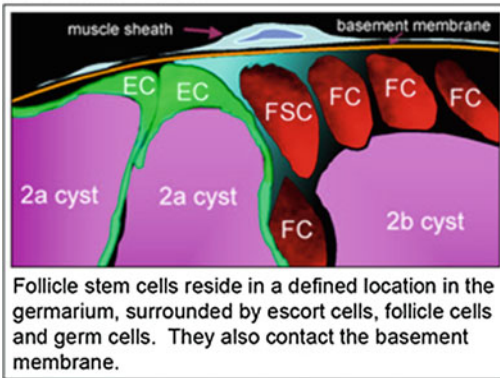
- (c) **Somatic stem cells:** Less is known about the anatomy and regulation of a second niche that controls the SSCs located midway along the germarium near the start of region 2b. SSCs divide in response to somatic Hedgehog signals to produce follicle cells that encapsulate passing cysts [3]. Inner germarium sheath (IGS) cells, which line the surface of regions 1 and 2a (Fig. 7.1), support germ cell differentiation and somatic cell production. Thin cytoplasmic processes from IGS cells envelop cystoblasts and cysts for several days prior to follicle formation. In addition, IGS cells located halfway down the germarium anchor SSCs via adherens junctions and are postulated to play a critical role

in defining the SSC niche [4]. Both anterior IGS cells and those near the SSCs have been reported to be differentiated and immobile but capable of maintaining parity with cyst number by undergoing sporadic division or death [1, 3]. Following GSC loss, IGS cells gradually disappear by apoptosis as pre-existing cysts leave the anterior germarium and acquire follicle cells [1, 5]. This destroys the SSC niches, but the released SSCs can often associate with cap cells in the vacated GSC niche and continue to divide [5].

**Follicle stem cells:** In addition, there are 2–3 FSCs located in the middle of each germarium across from each other. FSCs divide and produce a population of mitotically active follicle progenitor cells, which proliferate in the egg chambers of stage 1 to stage 6 and produce several types of differentiated cells that cover egg chambers including a follicle cell monolayer. IGS cells and cap cells act as an FSC niche and FSC behavior is regulated by several signaling pathways.



### FSC niche model



Scientists have developed a set of criteria that facilitates reliable identification of the epithelial follicle stem cells (FSCs) in the *Drosophila* ovary and mapping their interactions with neighboring cells to better understand the nature of the FSC niche. Surprisingly, they have found that the FSC niche appears much more dynamic than the few previously characterized niches. That is, it does not have a fixed position within the tissue and at least some cellular components of the niche turn over regularly during the adult life.

Using lineage analysis to follow FSC behavior, they track the patterns of FSC daughter cell migration and differentiation and investigate relevant gene function. Studies also found that the follicular epithelium surrounding each new follicle is produced by exactly two stem cells that reside in defined positions at the anterior edge of the tissue. Newly formed germ cells pass by the FSC niches one at a time and FSC divisions are coordinated with this process so that, on average, two FSC daughters contribute to each newly formed follicle. Interestingly, approximately half of the FSC daughters exhibit a directed migration between FSC niches. These migrations are a normal part of the process of enveloping incoming germ cells but also serve the important function of providing replacement stem cells when an FSC is lost from the niche. It appears that interniche migrating stem cells regularly contact the stem cell in the opposite niche and compete with the resident stem cell for niche occupancy.

This work on the characterization of the FSCs and their associated niche provides an

opportunity to use the fly ovary as a model of follicle formation (Fig. 7.2).

## 7.4 Genes and Pathways that Control the Stem Cell Niches

Genetic studies in the past decade have identified a number of genes with critical functions in stem cell self-renewal, proliferation, and differentiation. Several recent review and studies have shown the progress in understanding functions of these extrinsic and intrinsic factors in regulation of stem cell self-renewal, proliferation, and differentiation. Significant progress has been made in the past few years in gaining a better understanding of how the niche controls GSC function by identifying signaling pathways and genes that regulate these pathways.

### 7.4.1 The BMP Pathway

The BMP pathway is the best studied one for controlling GSC function and is both necessary and sufficient for GSC self-renewal and proliferation. Two BMP ligands, Dpp and Gbb, are expressed in TF/cap cells, while Gbb is also expressed in IGS cells and follicle cells. The BMP signal produced by the somatic cells directly act on GSCs to control their self-renewal and division. BMP signaling also has important roles in controlling the division of primordial germ cells (PGCs) in the developing female gonad and the recruitment of GSCs to their niche. In addition to its role in preventing GSC from differentiation, BMP signaling appears to be capable of reverting differentiated mitotic germ cell clusters into GSCs. Two other potential pathways have also been identified by studying two genes, *fs(1)Yb (Yb)* and *piwi*, that are required in somatic cells such as TFs and cap cells. Since *piwi* functions in the niche cells, it could regulate BMP production, secretion, or activation, or it could control the production of a new signal that is also essential for controlling GSC self-renewal and *bam* repression independently of the BMP

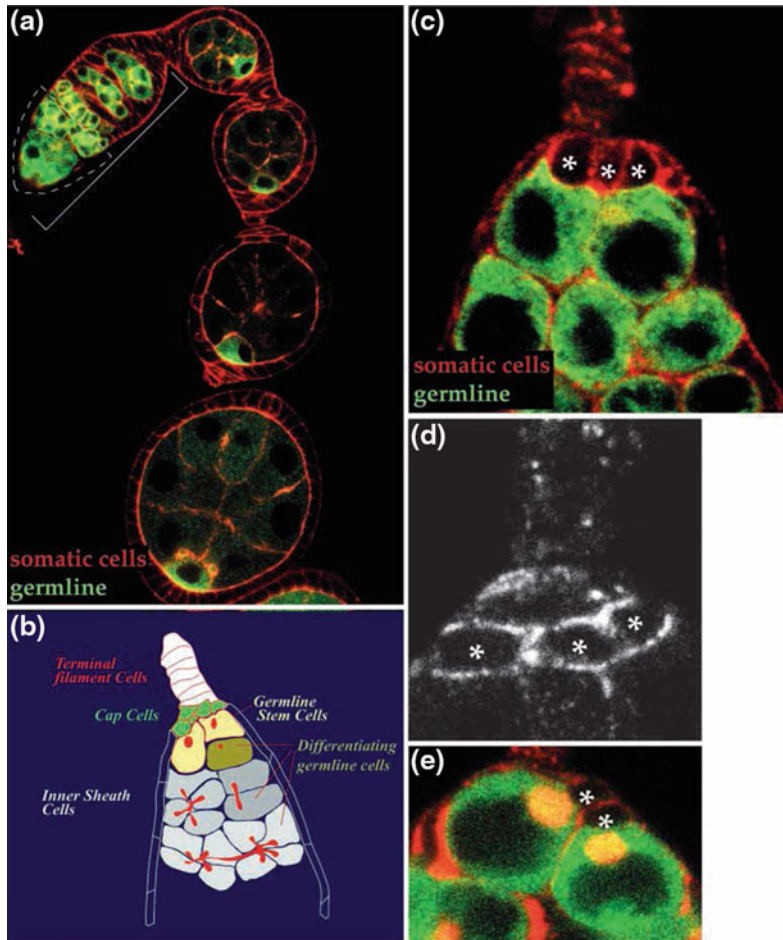


**Fig. 7.2** The germarium, a niche for germline stem cells. **a** A wild-type ovariole showing the germarium (anterior tip; bracket) and a string of developing egg chambers, all of which derive from the activity of stem cells in the germarium. The oocyte is the cell located at the posterior of the cysts that accumulate most of the green staining. The *dashed line* labels the anterior half of the germarium hosting the germline stem cells represented in **b** and pictured in **c** and **e**. *Red* F-actin staining to show the shape and arrangement of somatic and germline cells. **b** The scheme represents different cell types present in a wild-type germarium. Terminal filament cells, cap cells, and inner sheath cells are of somatic origin (the *dpp* gene is expressed in the cap cells); the differentiating germline cells are the cystoblast (daughter of a stem cell)

and the cystocytes, which form part of 2-, 4-, 8-, and 16-cell cysts. The organelle in *red* is the fusome, which acquires a spherical shape in germline stem cells and in cystoblasts in interphase, and a branched appearance in developing cysts. **c** Wild-type germarium stained with F-actin to visualize the shape of somatic cells (*red*); germline cells are stained in green. The large cells in contact with the cap cells are germline stem cells. Note the apposition of both cell types. **d** Wild-type germarium showing the localization of the armadillo protein in the junctions between the cap cells, and between the cap cells and the germline stem cells. This focal plane depicts only three cap cells. **e** Wild-type germarium showing the apical localization of the spherical fusome present in germline stem cells. Asterisks label cap cells

pathway. Two recent exciting studies in the *Drosophila* ovary have identified insulin as a systemic factor for controlling GSC proliferation.

In addition to BMP downstream components such as receptors and Smads that are required for

transducing BMP signal for maintaining self-renewal, several families of proteins have been identified to be required to maintain GSCs. Pumilio (Pum) and nanos (Nos), two translational repressors, are required for maintaining

GSCs in the adult ovary as well as for preventing precocious differentiation of PGCs in the developing female gonad likely by repressing the translation of mRNAs encoding differentiation factors. In addition, a germ cell-specific translation initiation factor encoded by *vasa* (*vas*) is required for the growth and survival of GSCs. Several differentiation-promoting factors have been identified for their essential roles in promoting cystoblast differentiation as mutations in the genes encoding these factors cause accumulation of GSC-like or cystoblast-like single germ cells. Among them, *bam* and *benign germ cell neoplasm* (*bgn*) are the best studied *bam* and *bgn* encode a novel protein and a putative RNA-binding protein, respectively, but their biochemical functions remain elusive.

SSCs and GSCs share some molecular mechanisms controlling self-renewal and proliferation. First, like the GSC, the SSC divides to generate a self-renewing SSC that remains in the niche and a differentiating daughter moving away from the niche for further proliferation and differentiation. Second, like the GSC, the SSC is also anchored to niche cells, the posterior IGS cells, through E-cadherin-mediated cell adhesion. The SSCs lacking E-cadherin are quickly lost from their niche due to the loss of the contact with the posterior IGS cells. Third, like the GSC, the SSC also requires BMP signaling for its self-renewal and proliferation. Fourth, like the GSC, the SSC also requires the insulin pathway for controlling SSC for proliferation. Finally, like the GSC that requires ISWI for its self-renewal, the SSC requires Domino (Dom), an ATP-dependent chromatin remodeling factor, for its self-renewal.

There are significant differences between these two cell types despite these similarities in mechanisms shared by GSCs and SSCs. First, the organization of the SSC niche is quite different from that of the GSC niche. The GSC niche is composed of their neighboring cells such as TF/cap cells and ESCs, while the SSC niche includes not only neighboring posterior IGS cells but also TFs/cap cells that are located over a few cells away. Second, Hh signaling is essential for self-renewal and proliferation of the SSC, while it plays a non-essential role in maintaining the

GSC. Hh, which is produced by TFs/cap cells, functions as a long-range morphogen to control SSC self-renewal and proliferation since the SSCs defective in Hh signaling are lost rapidly and hyperactive Hh signaling increases SSC number. Third, Wg signaling is essential for SSCs, but is dispensable for GSC self-renewal. Wg is also produced by TFs/cap cells and functions as a long-range signal to directly act on the SSC to control its self-renewal.

Decotto and Spradling [2] showed that the most anterior IGS cells, which directly contact cap cells and also surround GSCs with their cellular processes, are also capable of dividing and generating differentiated IGS cells. This group of IGS cells, ranging from four to six cells, is now known as ESCs, and their progeny are renamed as escort cells. Once germline cysts pass through region 2a of the germarium, they lose their connections to escort cells and become surrounded by the follicle cells. The ESC mutation for *dstat*, a transcriptional activator downstream of the JAK-STAT pathway, causes the degeneration of the germarium probably due to loss of escort cells, while overexpression of *upd*, the JAK-STAT ligand, dramatically expands the escort cell population, indicating that JAK-STAT signaling is essential for ESC maintenance and proliferation.

### 7.4.2 JAK-STAT Signaling Pathway

JAK-STAT signaling is a highly conserved regulator of stem cells and their niches. JAK-STAT activity is present in the TF, CCs, and ESCs, and signaling has a clear regulatory role for GSCs. JAK-STAT signaling specifically regulates *dpp* transcription in CCs and ESCs, thus controlling levels of BMP signaling. Interestingly, JAK-STAT signaling does not regulate *gbb*, implying that JAK-STAT activity manages the ovarian stem cell niche and limits GSC differentiation by a very precise specification of BMP levels. The importance of JAK-STAT signaling within the ovary is by no means limited to the GSC niche, as it also controls FSC maintenance, as well as specification and/or migration of the specialized FSC descendants stalk cells, polar cells, and border cells. FSCs

are not located in the stem cell niche at the anterior tip of the germarium, but reside more posterior, and provide a source of epithelial follicle cells needed to surround the germline cells and then the entire maturing egg chamber. However, some of the follicle cells differentiate into specialized cells early on, to form polar cells at either end of the developing egg chambers, or stalk cells, which act as spacers between the egg chambers. The two main pathways responsible for FSC maintenance are Hh and JAK-STAT. BMP signaling is also essential for FSC maintenance by preventing differentiation, but it is as yet unclear how it interacts with the other pathways.

Adhesion molecules, such as cadherins, are structurally important components of every stem cell niche, and the FSC niche is no exception. DE-cadherin and Armadillo/ $\beta$ -catenin anchor FSC to the neighboring inner germarial sheath cells (60) and are essential for FSC maintenance.

Surprisingly, hyperactivation of either Hh or JAK-STAT signaling can compensate for DE-cadherin-mediated FSC loss, suggesting that these pathways can strongly influence adhesive properties to support FSC maintenance. Evidence suggests that JAK-STAT signaling promotes integrin-mediated FSC: basement membrane interactions, indicating a potential mechanism. All of these data establish JAK-STAT signaling as the main control element of FSC maintenance, niche regulation, and early cell fate determination, partly in conjunction with Hh and other signaling pathways. In contrast to ESCs, FSC daughters can adopt different fates—stalk cells, polar cells, epithelial follicle cells, or, later on, border cells, depending on their positions relative to the ligand source and on their interpretation and translation of JAK-STAT activity. GSCs ultimately all have the same objective—to provide the germ cell for fertilization. It is interesting

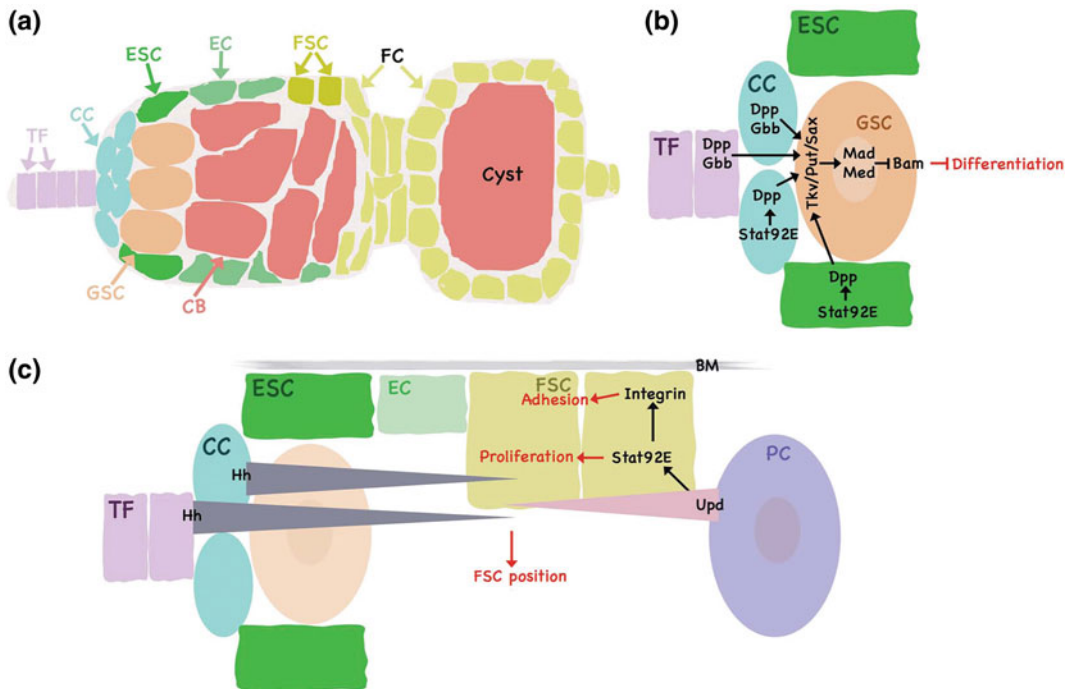


**Fig. 7.3** **a** The germarium located in the anterior tip of each ovariole contains the GSC niche, consisting of TF, CC, and ESC. The FSCs are positioned more posterior and attach to the surrounding basement membrane. **b** JAK-STAT signaling partly controls BMP signaling, which is required

for GSC self-renewal and inhibition of differentiation. **c** Antagonistic Hh and Upd gradients determine the position of FSCs within the germarium. JAK-STAT activity within FSCs regulates Integrin-mediated adhesion to the basement membrane (BM). See text for details

to note that female GSCs in *Drosophila* still give rise to two different cell types—nurse cells and the oocyte, and are thus multipotent, in contrast to their male counterparts. JAK-STAT signaling is without doubt one of the key players during oogenesis, even though it is not active within the GSCs itself. It is, however, essential for the stem cell niche and thus acts as an extrinsic factor for GSC maintenance. By controlling ESC and EC morphology and proliferation, JAK-STAT signaling organizes niche structure and thus indirectly regulates GSC maintenance (Fig. 7.3).

---

## 7.5 Conclusions

*Drosophila* stem cell systems have proven to be incredibly powerful models for studying the mechanisms by which stem cell behavior is controlled by the surrounding microenvironment and intrinsic cell fate determinants. These studies have provided a paradigm for the characterization and analysis of stem cells in other systems, including the identification of support cells that constitute the niche signals that control stem cell self-renewal and proliferation, and cell adhesion molecules that are important for holding stem cells within the niche. The three *Drosophila* adult stem cell niches discussed in this review have contributed enormously to the advancement of stem cell research, especially with regard to the important stem cell–niche relationship. In addition, they have furthered our understanding of signaling pathways, their regulations, and the networking between them. Studies on three stem cells in the *Drosophila* ovary have produced several general principles for stem cell biology. First, the stem cell niche exhibits structural asymmetry. Second, the stem cell is anchored to its niche through cadherin-mediated cell adhesion to ensure long-term self-renewal. Third, multiple signals from the niche are required for controlling stem cell self-renewal, and different stem cell types require different combination of niche signals. Fourth, self-renewing intrinsic factors and signaling cascades mediated by niche signals control stem cell self-renewal by repressing the expression of differentiation-promoting genes. And lastly, the niche can also help to

reverse differentiated cells back into stem cells. These mechanisms—attachment to, orientation toward, and signaling from a supporting niche—might also play important roles in regulating stem cell number, self-renewal, and differentiation in tissues maintained by stem cell populations in other organisms.

The identification of additional stem cell populations in *Drosophila* is hugely significant. Each new stem cell population is likely to present distinctive features and regulatory mechanisms. These may represent special adaptations, but they may also reflect conserved aspects of stem cell biology which are less easily observed in other systems. By comparing different stem cell populations within model organisms such as *Drosophila*, *C. elegans*, and vertebrates, we are much more likely to get a true understanding of how stem cell regulation has evolved and how it is conserved at the molecular level. As easily defined stem cell niches in *Drosophila* contribute to a better understanding of mammalian stem cell regulation [6], we anticipate that what we will learn from studies on the *Drosophila* GSC differentiation niche will be equally important for defining differentiation niches and studying their functions in lineage differentiation in mammalian systems.

---

## References

1. Xie T, Spradling AC. A niche maintaining germ line stem cells in the *Drosophila* ovary. *Science*. 2000;290:328–30.
2. Decotto E, Spradling AC. The *Drosophila* ovarian and testis stem cell niches: similar somatic stem cells and signals. *Dev Cell*. 2005;9:501–10.
3. Margolis J, Spradling A. Identification and behavior of epithelial stem cells in the *Drosophila* ovary. *Development*. 1995;121:3797–807.
4. Song X, Xie T. DE-cadherin-mediated cell adhesion is essential for maintaining somatic stem cells in the *Drosophila* ovary. *Proc Natl Acad Sci USA*. 2002;99:14813–8.
5. Kai T, Spradling A. Differentiating germ cells can revert into functional stem cells in *Drosophila melanogaster* ovaries. *Nature*. 2004;428:564–9.
6. Morrison SJ, Spradling AC. Stem cells and niches: mechanisms that promote stem cell maintenance throughout life. *Cell*. 2008;132:598–611; PMID: 18295578; doi:10.1016/j.cell.2008.01.038.

---

**Part II**

**Novel Antibodies as a Replacement for  
Antibiotics**

---

## 8.1 Executive Summary

Modern age has brought about the indiscriminate use of chemicals. Synthetic chemicals are used to increase food production and control diseases with the objective of improving the quality of our lives. Chemicals are not biodegradable and pollute the atmosphere, accumulate inside living bodies, and create a disturbance in the delicate balance of the ecological system governing life on planet earth. This resulted in rampant pollution that is difficult to contain and give rise to drug-resistant microorganisms that are impossible to treat. This has ultimately led to a poor ecosystem and a lowering of the quality of life of all inhabitants of earth. We humans, who are responsible for this, have woken up to the fact that we need to undo this by developing clean green sustainable technologies and eco-friendly products.

Only organic molecules that are biodegradable have the potential to accomplish this. Biosensor plans to operate in this area and develop healthcare solutions on the basis of leveraging fundamental biological processes and converting them into far more powerful and sustainable healthcare tools with distinct ecological advantages. The proprietary technology that our laboratory proposes to develop is E-compatible (eco-compatible) targeted biobodies (ETB) for healthcare applications and solutions. Biobodies are miniscule antibodies, engineered to be targeted against various pathogens and their toxins. Our laboratory will develop various applications and product lines based on

this technology for human and animal healthcare applications.

Our laboratory plans to develop a library of these antibody molecules from which antibodies suitable for a wide range of applications can be pulled out. The secreted or surface-displayed antibodies will be in an entirely novel format derived from camels that are small and stable and can easily be genetically manipulated to overcome the problems of stability, tissue penetration, and immune compatibility. These engineered antibodies will be extremely small in size and can be easily adapted for a wide range of applications. They can be fused together to increase their sensitivity, can be tagged with immunomodulatory molecules to make therapeutic products, and can easily be made more thermostable or pH tolerant and also humanized. As a strategic plan, our laboratory will operate in this area and establish research programs leading to product development around this.

For its first product, our laboratory proposes to develop value-added probiotics that when administered orally will have the ability to ameliorate the disease condition by secreting antibodies by targeting the microorganisms as well as the toxins secreted by them. The first application will be in the area of value-added feed for the poultry industry and will target infectious organisms causing chicken diarrhea. The IP thus generated will have a tremendous market value as use of antibiotics has been banned in EU necessitating the use of alternative therapies. Once the

technology is in place, it can be extended to human applications as well with a minimum investment of money and scientific inputs.

One of the technology extension possibilities will be to develop an immunotherapy molecule for the treatment of bovine mastitis along with an Israeli collaborator. The technology is in place, and the proof of concept has been established in field trials. Our laboratory will carry the development of this product forward till it is ready for the market. Application of this product will result a quick control of udder infection in cows and will result in antibiotic-free milk that will have a tremendous market. If funds are available, this project can be carried out along with the probiotic project after two years. To ensure a steady cash flow while the above projects are being developed, once the camelid library is ready, our laboratory will generate therapeutic antibodies against various microorganisms that cause cosmetic conditions such as acne, eczema, and dandruff as well as enteric conditions like diarrhea that can be licensed out.

Our laboratory is an end-to-end technology transfer and innovative technology development start-up company formed by a group of scientist entrepreneurs. Our laboratory aims to be a global player in leveraging clean and sustainable innovative technologies for various product applications in the area of human and animal health, cosmetics, nutraceuticals, and healthy food. Our laboratory will initiate the above projects keeping this objective in mind. For the probiotic project, our laboratory seeks Rs. 2.26 crores INR seed funding for a three-year period during which the product will be made ready for the market. This product will generate sales worth at least Rs. 7–8 crores per year from the fourth year onward. The IP worth of this technology that can generate other products will be in the range of USD \$100–150 million. With an additional investment of 2.42 crores, the bovine mastitis project can be carried out that will again generate revenue of 6–7 crores from the fourth year onward. Our laboratory has access to market channels and can push these products to the market. Additional revenue will be generated by out licensing the molecules to cosmetics and human healthcare companies.

## 8.2 Business Background and Philosophy

The problem of pollution due to chemicals is a direct result of compounds that are *not specific* and *non-biodegradable*. A good example of this is the rampant use of antibiotics that has given rise to the uncontrollable problem of antibiotic resistance. In the area of animal health, antibiotics are regularly used to control infections as well increase the yield of meat. As a result of this, antibiotics accumulate in the meat resulting in food products that are not suitable for human consumption. Similarly, antibiotic laced milk is no longer accepted by big milk product producers nowadays. Another example is that some personal hair care products contain compounds that kill the microorganisms involved in dandruff. Also these compounds are not specific, and in addition to the causative microorganisms of dandruff, they also kill other microorganisms on the skin which are beneficial to the consumer. Products like antiacne and creams and deodorants often result in skin rashes and allergic conditions due to their non-specific mode of action.

The above examples make it clear that consumer products and animal feed with compounds which specifically meet the demand of the consumer or society will be of great importance. The main characteristic of processes in living cells is that they are highly specific. Higher specificity and biodegradability after the desired action is achieved can be done proteins of biological origin like enzymes and antibodies. Both enzymes and antibodies are highly specific, leave no side effects, and have short half-lives as a result of which there is no problem of residual toxicity. A successful example of this development is the introduction of proteases, lipases, cellulases, and amylases in laundry products. These enzymes have a certain specificity, and because the production of these enzymes have been improved considerably by recombinant DNA techniques, these microbial enzymes can be produced by microorganisms at affordable costs. In the area of animal feed, enzymes can play an important role to reduce the environmental pollution, as has been demonstrated by the application of the enzyme phytase in animal feed by rDNA techniques.



As a result, these strict guidelines have been issued to control rampant pollution wherever necessary, antibiotics have been banned from animal use and antibiotic laced milk meat, and poultry products do not find a market in the developed markets of Europe. Strict guidelines have been issued by pollution control boards to replace chemicals of biological origin such as enzymes and antibodies.

Our laboratory has been formed in this backdrop. It has been founded with a mission to develop healthcare solutions on the basis of leveraging fundamental biological processes and converting them into far more powerful and sustainable healthcare tools with distinct ecological advantages. The proprietary technology platforms, which shall run the businesses of our laboratory, are in nature ETB for healthcare applications and solutions. Biobodies are miniscule antibodies, engineered to be targeted against various pathogens and their toxins. Through strategic collaborations, our laboratory has already ensured two proprietary biobody molecules for therapeutic applications. The mission forward is to further develop and establish its own proprietary biobody molecules for specific healthcare applications. Our laboratory will undertake research and development work in the areas of most commercial viability such as animal feed and animal and human health, as well as in areas of cosmetics and healthcare products that have been worst hit by the problems of non-specific compounds and the resulting environmental problems associated with it. Our laboratory plans to tap the huge market that is beginning to emerge as a result of the withdrawal of harmful chemicals from use and has the capability to develop suitable products on demand to address the pertinent issues as well as to be a first mover to capture the market.

---

### 8.3 The Existing Technology and Its Shortcomings

Antibodies are glycoproteins, which specifically recognize foreign molecules called antigens. When antigens invade humans or animals, an immunological response is triggered involving

the production of antibodies by B lymphocytes by which microorganisms, larger parasites, viruses, and bacterial toxins can be rendered harmless. The unique ability of antibodies to specifically recognize and bind with high affinity to virtually any type of antigen makes them useful molecules in medical and scientific research.

The development of methods of generating antibodies *in vitro* and monoclonal antibody technology (multiple copies of the same antibody molecule) has enabled the use of antibodies in many areas including immunotherapy, research, medicine, and recently in consumer applications. They have been quite successful in the market as their high selectivity and affinity to their targets reduce the chances of side effects. There are roughly 18 antibody-based products already on the market. The antibody market had sales of more than \$10 billion in 2008.

However, the use of antibodies is limited due to some technical difficulties in their large-scale production and purification and their subsequent cost factor. These antibodies have to be produced in mammalian cells and subsequently purified by a complicated process. The associated *production costs* are expensive and make their wide-scale application as immunotherapeutics prohibitive, and in order to treat a large part of the population, large amounts of conventional immunotherapy products are required. A good example is Wyeth's antibody-derived drug Enbrel which costs around \$1200 per gram to produce. One major disadvantage of these known systems is that the use of antibodies or antibody fragments *per se* (i.e., a harvested protein) in the treatment of a disease in an animal or human may result in the antibody being *degraded or digested* before they provide the desired health benefits and even before they reach the desired location. Furthermore, it is often desirable to ensure that the antibody or antibody fragments are *active in a specific region* of the body depending on the particular infection being treated. The large size and complex structures of antibody drugs exclude attractive therapeutic targets, since they cannot reach most active enzyme sites and deep receptor clefts. Additionally, mAbs must be

injected and cannot be stored well due to their inherent instability and due to their complicated structures.

Due to cost factors, antibody therapeutics are not used on a general scale (e.g., like antibiotics or vitamin and mineral supplements), and treatment of individual animals on a case-by-case basis represents an additional obstacle. As there is a widespread misconception that orally administered antibodies get digested and inactivated in the gastrointestinal tract, orally administered antibodies are not viewed as very effective drugs, at least not compared with small, simple, and stable molecules such as antibiotics.

As mentioned above, in order for per oral antibody prophylaxis and therapy to become common practice and a valid alternative to antibiotics, a system needs to be designed that allows the production of gigantic amounts of antibodies of consistent quality (specificity, affinity, and concentration). In addition, this ideal system should provide such antibodies at a cost that is comparable with that of antibiotics and in a form that allows for straightforward administration, for instance by simply mixing the therapeutic agent in the diet. Our laboratory will develop a *novel format* of highly specific antibodies and develop *novel delivery systems* to make them more targeted and effective.

---

#### **8.4 The Our Laboratory Proposal: Development of a Novel Antibody Platform and Delivery Systems**

To further develop this therapy area and to minimize the shortcomings of conventional antibodies, our laboratory proposes to develop a platform technology of a new format of extremely potent and stable antibodies, the camelid antibodies. Our laboratory will also develop novel antibody delivery systems to target the antibodies to their site of action for maximum effect. The targeting molecules will have additional therapeutic properties so that a synergistic effect is obtained that can bring the disease under control. Our laboratory will be developing two products simultaneously as

a contingency measure to reduce chances of failure and economic loss for the investor. After the first year of operations, during which time the antibody library will be ready, our laboratory will initiate work in newer application areas so that within four years three lines of products will be ready for the market. The following are the areas our laboratory will be active in:

1. Value-added probiotics for human and animal health applications.
2. An immunomodulatory technology for the treatment of infectious diseases.
3. Cosmetic and therapeutic uses of camelid antibodies for human and animal health.

Our laboratory will take up these projects one by one during the initial four-year period using the camelid antibody platform and create a stream of novel IP generating products. Our laboratory believes that innovation-driven IP generating work is the best way for the company to grow and create wealth. The present Indian market for the probiotic application only in the livestock segment alone is more than INR 150 million. There exists a further potential business value creation of an estimated INR 1000 million plus, from this technology development, within less than a decade of its development.

---

#### **8.5 A Novel Format of Antibodies: Camelid Antibodies**

Antibodies in smaller effective formats are the key to circumvent some of the critical disadvantages of conventional antibodies. Such antibody already exists in nature in the form of camelid heavy-chain antibodies, and our laboratory will use these format and tag with suitable delivery tools to develop potent therapeutic products.

Camelids (camels and llamas) have antibodies in their blood serum that consist of a single heavy chain that has three complementary determining regions. These single chain antibodies are relatively small, about 15 kilodaltons (kda) as compared to 150 kda for full length antibodies in other species. They have very good affinity for the antigens and excellent solubility and are very stable. The small size of these antibodies with

high tissue penetrability leaves the possibility of using it as a unique biological tool for various health and therapeutic applications. Unlike normal antibodies, camelid antibodies exert *complete neutralizing activity* against enzyme antigens as it has the capability of entering deep into the functional domains of the enzyme structures. Camelid antibodies have been demonstrated to exert selective inhibition against hepatitis C enzyme system as well as tetanus toxin. The single chain and the small size enable ease of manipulation by recombinant DNA technology, and the antibodies can be expressed rapidly and economically using a variety of common yeast and bacterial expression systems. The cost of specific antibody production by this technology is about less than a fifth of the cost involved in producing the same antibody on a monoclonal platform as it bypasses the use of costly hybridoma technology. Additionally, the camelid antibodies have an advantage of high temperature and low pH resistance. They have been shown to be resistant to low pH of up to 2.6. Thus, these antibodies could very well travel the low pH monogastric stomach environment and reach the gastrointestinal tract, where most of the pathogens and the toxins are present. These characteristics provide tremendous therapeutic potential to the camelid antibodies for treating GI tract-related ailments or treating GI tract-mediated pathobiological situations. Also these antibodies can withstand temperature of more than 90 °C, making them resistant to handling conditions in hot and humid conditions of India, and can very easily withstand pasteurization. Thus, camelid antibodies could be developed to neutralize many gastrointestinal pathogens and their toxins and then could be used to fortify various food products, e.g., milk and also could be used in pelleted animal feeds.

Our laboratory has the capability to develop a platform technology for generation of specific camelid antibodies to specific antigens. It will be a first such exclusive activity in India and the Asian region, leading to tremendous technology and business advantages in these markets for therapeutic and health applications. The antibodies will subsequently be expressed in probiotic bacterial or yeast systems against specific

gut-associated pathogens and their toxins, and subsequently, large-scale production of these probiotics secreting these antibodies as biobodies will be carried out.

Thus, there will be many technology and business uniqueness to such a proprietary technology.

- The intellectual property shall generate a clean technology and will be first of its kind due to its scope of application.
- The products will be ecologically sustainable with profound health benefits over the conventional therapies.
- The technology shall be a major feed antibiotic usage replacement for the livestock industry.
- The same technology could be very easily extended over a short period of time to multiple applications with significant existing preventive healthcare markets.
- Market penetration and growth shall be very fast, since it will have the potential to supplement established therapy areas.
- The technology and the product being eco-friendly shall have long sustainability with distinct advantages, and there are no chances for product obsolescence in the coming few decades.

---

## 8.6 Novel Delivery Systems

The other challenge of antibody technology is to make the molecules available in the *site of action*. Various technologies are in place but they have their shortcomings primarily due to the unstable nature of the biological products. Our laboratory plans to develop novel delivery systems to administer the antibodies in the site of action. The following are the delivery systems to be developed by our laboratory.

### 8.6.1 Probiotics

For the first type of delivery system, probiotics will be used. The gene of interest will be cloned in the probiotic and the relevant antibody will be produced at the site of action by the live cultures. These value-added probiotics will be administered

with the feed that will then colonize the gut. Probiotics are living microorganisms which upon ingestion in sufficient numbers, exert health benefits beyond basic nutrition by replacing the gut microflora. They are being increasingly used in food and feed products both for humans and livestock, and is gaining world wide prominence since naturally, they are associated with several beneficial health effects like reduction of lactose maldigestion in gut, clinical symptoms of diarrhea associated with enteropathogens or toxins, immune stimulation, antitumour activity and enhancement of mineral uptake. Once administered, they replace enteropathogenic microorganisms such as *Escherichia coli* and *Salmonella* which can produce disease in the intestinal tract. Probiotics are being used as a major preventive feed formulation to circumvent such gut-associated pathogens which relate to major economically significant diseases in livestock and human health.

Few years earlier, the data on probiotics were too limited and industry-specific for it to gain wide acceptance. Large pharmaceutical players had not focused their attention to popularize and promote it earlier. The stakes were not high, and therefore, probiotics were not heard about in the past. But now awareness, industry, and stakes on probiotics are becoming higher and higher, as big companies are getting into this field. In India, Aristo has a brand called Darolac, and Cipla and USV have their brands too. In general, the concept of probiotics is gaining momentum internationally. People have started to accept probiotics as an alternative method of treatment, which was not the case, a few years back.

Our laboratory proposes to merge the beneficial therapeutic attributes of the camel antibody molecule into the beneficial attributes of the probiotics as a health booster. In the process, our laboratory will create a value-added probiotic for animal and human health applications. Major innovativeness and the strength of the intellectual property to be generated at our laboratory shall be to merge the benefits of probiotic applications with the therapeutic benefits of the camelid antibody molecules. Specific target-based therapeutic camel antibody will be generated and

subsequent manipulations will be done to insert these antibodies into specific probiotic organisms, which will then in turn secrete these as biobodies. When fed with a consortium of probiotics comprising of these biobodies, specific mycotoxins and gut-associated pathogens will be targeted. The biobodies will be secreted in situ from the probiotic organisms in the gut and shall neutralize the disease causing etiologies and pathogens. For creating such probiotics, food grade probiotic vectors will be used, which is already approved in the EU.

### 8.6.2 Microbead Tagged Antibodies and Immunomodulators

Our laboratory has access to a proprietary technology, and the Y-complex technology has been shown to provide a non-antibiotic solution for the control of infectious diseases. The first product from this technology has already cleared clinical trials, and our laboratory will adapt this technology for Indian conditions by tagging it with camelid antibodies against specific pathogens. This consists of a microbead tagged with the antibodies and an immunomodulatory molecule in a stable formulation. These nanobodies can be applied topically, and the camelid antibodies will home in on the pathogens. This will bring the immunomodulatory molecules to the site of infection for immune clearance. Following are the salient features of this technology:

- The Y-complex technology is a biotherapeutic platform technology consisting of an immunomodulatory (something that modulates the way the living body fights attacks from pathogens) complex that specifically targets the infectious agents at the site of infection.
- The molecule brings the pathogens (disease causing microorganisms) and the macrophages (cells that gobble up pathogens and kill it) together so that the pathogens are destroyed and immune reaction is triggered simultaneously so that the inflammation is also brought under control.

- The advantage of this technology lies in the fact that a targeted immune response can be achieved in the area of inflammation bringing a rapid and irreversible amelioration of the disease condition.
- However, the biggest advantage of the Y-complex technology is its adaptability as the antibodies can be raised against any pathogen within a very short time and tagged to the complex. The immunomodulatory molecules can be engineered according to the target animal species and its immune system functioning.
- For the extension of the Y-complex technology, our laboratory in the translational research could also work toward adapting the Y-complex platform technology for different therapeutic applications in animal and human health. Our laboratory will construct a repertoire of target-specific antibodies and immunomodulator molecules that can generate multiple therapeutic products.

This technology in the present format is very suitable for topical applications and scores over the other antibiotic-based treatments as it has *no residual toxicity* and, unlike antibiotic-based treatments, is uncluttered and clean. It is also an environmentally friendly technology as *antibiotic resistance does not appear* and allows long-term use of the product and thereby *minimizes chance of product obsolescence*. If propagated judiciously, it will act as an *antibiotic replacement therapy* and will be able to capture a large chunk of the antibiotic market.

### 8.6.3 Formulation of Purified Antibodies with Cosmetics and Foodstuffs

The camelid antibodies generated by our laboratory can be purified partially or totally and be used for various therapeutic applications after proper formulation for targeted delivery. As there are antibodies extremely stable across a wide

range of temperatures and pH ranges, it can be formulated with virtually any harsh chemicals used in cosmetics and therapeutic formulations. Their small size makes it possible for it to be administered inhalation or even through a cream. A very important application will be in the area of rehydration therapy where the antibodies can be formulated with oral rehydration solution (ORS) to neutralize toxins like cholera in the gut. These antibodies also have the ability to neutralize microorganisms and toxins secreted from *E. coli*, *Staphylococcus*, and *Shigella*.

## 8.7 Our Laboratory Strategy for Creating Camelid Antibody-Based Products

As our laboratory is a start-up, it has strategically oriented its research programs so as to leave *no chance of failure*. Our laboratory will thus initiate overlapping research programs as a backup strategy in case success is not obtained, or milestones are delayed in the leading program. Our laboratory will start working with the most novel and IP generating product, value-added probiotics in the area of animal health that will be the most lucrative as well. As a backup plan, it will start working with the Y-complex technology where proof of concept has been obtained and it only needs adaptation for the Indian conditions. Though the amount of IP generated will be less, it will make up by increase in sales and its application will be in the area of bovine mastitis that has a tremendous market potential. Furthermore, as soon as the library is ready, our laboratory will initiate work to identify novel antibodies for applications in cosmetics and human and animal health so as to build up a product line for further development or out licensing. Given sufficient manpower and resources, our laboratory will have the ability to run three different program areas involving camelid antibodies that will ensure a steady supply of products and a good return on investment for the investor.

## 8.8 The First Our Laboratory Product: Value-Added Probiotics for the Poultry Industry

The present proposal from our laboratory relates in particular to introducing certain categories of antibodies into a variety of products, especially food and animal feed. BiConsort will develop value-added probiotics for use as poultry feed that will be more powerful than conventional probiotics in two ways:

1. The our laboratory probiotics will consist of a consortium of bacteria with unique properties that will be more effective than the individual bacteria that are currently being used. This consortium will be administered as a live culture and will replace the harmful bacterial in the gut and improve the microenvironment.
2. The our laboratory probiotics will be genetically engineered to secrete antitoxin secreting antibodies that will neutralize the ill effects of the toxins as well as the replace the harmful bacteria such as *E. Coli* and *Salmonella*. This will in effect have the ability to replace the currently used probiotics and antibiotics combinations.

Our laboratory will experiment with various combinations of the consortium to find out the right combination of microbes that will be easy to manufacture, synthesize, and economize.

The antibodies will be secreted from *Saccharomyces* sp. and *Lactobacillus* sp. from food grade commercially available plasmids. The product will be administered as live or inactivated cultures depending on regulatory permissiveness.

The research method and approach will devise a means of immobilizing a binding protein to the exterior of the cell wall of a microbial host cell, in particular a lower eukaryote, by producing a fusion protein which binds to the anchoring part of a cell wall anchoring protein, thereby ensuring that the binding protein is localized in or at the exterior of the cell wall of the host cell. The binding protein will bind to the specific molecule that it recognizes. The binding proteins shall include antibodies, antibody fragments, combinations of antibody fragments, and receptor proteins. Therefore, a stable functional system will be created involving transformed microorganisms, where the microorganisms are inactivated or killed while the functional activity of the system is substantially maintained. The secretory molecules will be cloned in *food grade cloning and expression vectors*, mostly confined in the species like *Lactococcus lactis*. These vectors are already approved in the EU. These secreted antibodies could be produced in situ, as well as they could be formulated into specific food products as well as feed supplements and feed additives (Fig. 8.1).

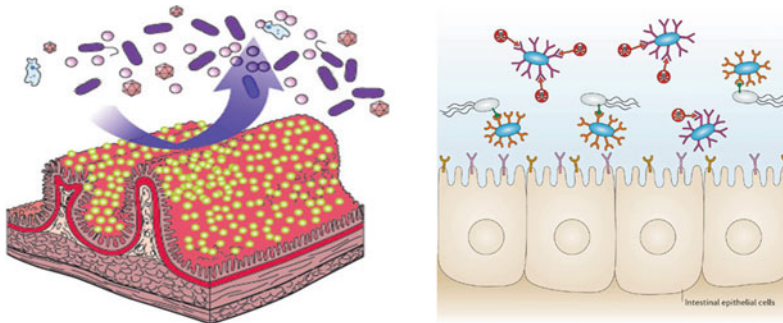


**Fig. 8.1** *Left* mode of action of probiotics. Probiotics replace harmful bacteria from the gut. *Right* mode of action of our laboratory value-added product. The

antibodies on the probiotics will also neutralize the pathogens as well as colonize the gut

### 8.8.1 The Market for Value-Added Probiotics in the Poultry Industry

The Indian poultry industry has optimized its husbandry practices to a great extent and has evolved into a highly organized industry. Optimization, in terms of genetic potential of the breeds, feed, vaccines, health medications, and equipment, has been greatly achieved, but the industry is still looking for solutions which can result in *better feed utilization for higher body weight gain and egg productivity as well as reduced disease mortality*. This will reduce the production costs and increase the profitability margins.

Although the domestic consumption has increased many folds, the price of poultry meat and egg has not increased over the years as compared to the rate of inflation in the Indian domestic consumer market. Simultaneously, the cost of feed and medication has gone up significantly, resulting in increased production cost of chicken meat and thereby reducing the profitability of the business. Thus, the poultry industry is very eager to experiment and try out innovative methods and technologies, which can lead to reduction in the production costs. The urge is for those technologies, which can add value to their product, so that they can get better price of chicken meat and eggs, especially from the elite and the educated consumers. Thus, the industry is still looking forward to solutions which can effect in better feed utilization for higher body weight gain and egg productivity and reduced disease mortality which shall lead to reduction of production costs and increase in the profitability margins.

Another reason for feed innovation is that the poultry industry is facing a ban on the use of antibiotic feed additives in many parts of the world. Consequently, there is a growing interest in finding viable alternatives for disease prevention and growth-enhancing supplements. The ban of growth promoting antibiotic usage in the EU will ultimately affect every poultry exporting country because poultry products found to have antibiotic residues of EU-banned products or to harbor bacteria such as *Salmonella typhimurium* DT104,

*Staphylococcus aureus*, *Acinetobacter*, *Listeria monocytogenes*, *Enterococcus faecalis*, pathogenic *E. coli*, or *Campylobacter jejuni* that have multiple antibiotic resistance profiles, likely will be refused. When consumers of a product develop an idea or perception about a product, no matter that there is no scientific data to support or refute the perception, that perception becomes real for that consumer. If large numbers of consumers accept those perceptions, as is happening now, then pressures are placed upon the producer to make the product conform to the standards set by the consumer. Thus, alternatives to subtherapeutic antibiotic growth promoters must be developed.

The effects of probiotics or direct-fed microbial (DFM) on gut health and performance in poultry as well as other species are widely presented. The interactions between intestinal microbiota, the gut epithelium, and the immune system are important in the competitive exclusion process. The mechanisms by which probiotics operate include spatial exclusion, microenvironmental alterations, production of antimicrobial substances, and epithelial barrier integrity. There are more microbial cells within the gastrointestinal (GI) tract than total cells within the body proper. The microorganisms most commonly observed are bacteria and yeast. Data indicate that probiotics prevent infection and colonization of the GI tract by opportunistic pathogens. Introduction of such probiotics is believed to prevent or attenuate the growth of clinical enteric pathogens in poultry, resulting in enhanced growth and performance of the host bird. This phenomenon has prompted a widespread interest in the poultry industry of probiotic usage as an alternative to the prophylactic use of antibiotics for the prevention of disease within poultry flocks. This interest has arisen as the result of growing concerns about prophylactic usage of antibiotics in poultry and other animal production systems in Europe and the USA.

India's participation in the world poultry trade to date has been negligible, despite being an internationally competitive producer of poultry meat with export potential. To exploit this export to European and Japanese markets, investment is required in a strong veterinary health care and

nutrition system as well as export-driven processing plant. Already such a scenario is emerging as could be observed from the entry of the multinational giant Tyson, in collaboration with Godrej (Real Good chicken brand) into the Indian market. Such multinational giants are not only targeting the export potentials but also intending to create brands within the huge domestic market, through value addition and consumer awareness. One of the major focuses for value addition shall be the subject of meat, food hygiene, and safety. In similarity to the trends in the developed nations' market, not only a huge investment in India shall come forth in the poultry meat processing, but hygienic meat processing has to be backward integrated into the poultry farming production systems along the international standards of HACCP (Hazard Analysis and Critical Control Point) guidelines. Stringent benchmarks in the Indian poultry production, like use of non-antibiotic feed supplements for body meat growth as well as focus on disease prevention methods, i.e., farm hygiene and biosecurity, shall be the trends in the coming decades. Thereby, technologies and business solutions rendering biosecurity and better disease control methods and non-antibiotic growth promoter products have a promising market growth potential. According to industry sources, such products shall have business growth potentials of 15–20 % in the coming decade.

The public will demand specific standards in the food production system, and if companies desire to remain in business, those companies will respond positively to consumer demands. Thus, the future for value-added probiotics appears to be very strong for the poultry industry. In response to those demands, poultry production centers such as those in the USA, Brazil, Thailand, and China will respond to the production of more products with reduced microbiological risks for humans and India needs to develop products of similar specifications to remain in the market.

The our laboratory value-added probiotic technology shall be a very good fit and the appropriate solution to the above situation. This technology will have significant effects on the feed utilization and controlling the infections and

toxicity of the gut, leading to higher body weight gain of the poultry broilers, and has significantly reduced the bird mortality due to various viral and bacterial diseases. Thus, the value-added probiotic technology stands tremendous business possibilities in the Indian and international livestock and poultry industry. This technology has got the potential to create a revolution in the Indian livestock and poultry husbandry and shall have significant beneficial impact on the environment and the livestock industry.

Based on industry sources and our own research, the market for poultry industry is estimated at around USD 3.1 billion (INR 125 billion). In addition, the layer market is estimated around USD 2.5 billion (INR 100 billion).

### **8.8.2 Poultry Farmers Cost Savings on the Usage of Value-Added Probiotics**

Value-added probiotics can be grown as liquid culture and will be applied to the poultry birds through the drinking water. The birds have very well-organized drinking water feeding systems in the poultry houses. Value-added probiotic will be added to the drinking water at a dilution level of 1:1000 or 1:2000 that will be fine-tuned during the clinical trials. This dilution will be worked out on the basis of the concentrations to which the value-added probiotic cultures will be grown and the anticipated levels of the toxin-specific antibodies could be expressed and secreted. Since it will be a consortium of cultures, the available individual species of organisms expressing the antibodies in the consortium will be important for the performance and efficacy. The platform technology will be more focused on the colonization of the probiotics in the poultry gut epithelium, secreting specific antibodies in the gut. Colonization will be enhanced in multiples, since antibodies against specific pathogenic bacteria will provide an added advantage in colonization to the probiotic microorganisms.

Every individual poultry bird (Broiler Birds) consumes 8–10 L of water during their rearing



period of 6 weeks. The probiotic cultures shall be continuously fed throughout their rearing period. So at a dilution rate of 1:1000, each bird will consume, say 8 to 10 ml of the concentrated value-added probiotic product. Simultaneously, spraying (at a dilution of 1:5000) of these probiotics in the poultry farmhouse and on the feed lots will be carried out, say at every 4-day interval. The following table shows the expected savings for the poultry farmer on the usage of value-added probiotics. Expected manufacturing cost of value-added probiotic is worked out at Rs. 100 per liter of the product. Considering the marketing and distribution costs through strategic channels, the product could be made available to the farmer at a cost of Rs. 300. Cost saving to the farmer is worked out at a dilution of 1:1000 and 1:2000 of the product usage for 1000 birds. On usage of the product, logically, there is an expectation of at least 5 % increase in the feed conversion ratio (FCR). The reason being that the product shall lead to better feed digestion and assimilation, and in the gut environment, various fungal and bacterial toxin loads will also reduce. This in turn shall lead to a better gut environment with higher metabolic activities of the associated gut epithelial cells, which in turn shall lead to higher absorption and assimilation of various nutrients, minerals, salts, and trace elements. The farmer will get a cost saving of Rs. 3 per bird, and a moderate farm produces 2–3 lakh chicken every 60 days. As he can potentially save Rs. 6–9 lakhs per batch, the farmer will have sufficient incentive to use the value-added probiotics. Furthermore, this will not only have a combination of various probiotic species in a consortium, but they shall also secrete neutralizing antibodies to specific mycotoxins and other disease causing bacterial toxins. Thus, the improvement in FCR by using the value-added probiotics is anticipated and shall be much higher than the expected level of 5 %.

### 8.8.3 Marketing Plan

As a part of its strategy, our laboratory will conduct the clinical tests of the value-added probiotics with established chicken producing

companies in India such as Venkatesh hatcheries, Suguna chicken, and Arambagh hatcheries who will act as its customers in the initial stages. Our laboratory has established professional contacts with these organizations and has received verbal assurances that the value-added probiotic products can be included as a part of the feed during the trial period.

The actual market for this product lies in the processed meat industry where clean antibiotic-free chicken meat will fetch a premium price. Our laboratory through its contacts with Godrej Tyson has the capability to push the product to the producers of such chicken.

### 8.8.4 SWOT Analysis

#### Strengths

- Research team: The best mix of complementary skills. Dr. Banerjee is a molecular biologist and Dr. Ghosh is a veterinarian with years of experience in the poultry industry. Our laboratory has experience in both the research and development and regulatory approvals. We also have in our disposal good scientific personnel who will carry out the work.
- IP Generation: The IP will have considerable commercial value as this approach can be used for multiple applications.
- Product extensions: This technology once established can easily be adapted to other application areas in human and animal health.
- Conducive business environment in India: Biotechnology is currently picking up importance in India, and the timing is right for us to start such a venture. Based on the assessment of the current business climate in India, we believe it will be possible to obtain the needed financial support from both personal contacts and angel investors should such funding be required for business growth.
- Presence of (local and export) markets: The presence of a large local market is a great advantage, and our laboratory can readily find a market for its products.

### Weaknesses

- Availability of resources: Capital is available, but since we have some work to do to establish proof of concept; the full amount may be difficult to get. We will try to overcome it by showing our long-term commitment to the project as well as the multiple projects we have so that the chances of failure are minimized.
- Lack of proof of concept: As this is a novel project, our laboratory does not have the proof of concept so it is difficult to get the funding from venture capitalists. However, this type of work is very well established in other parts of the world, and as Dr. Banerjee has first-hand experience in working in this area and has collaborations in place, this problem can be overcome.
- Bureaucratic environment in India: Time and money required to get regulatory clearances, and licenses can be frustrating. This can be overcome by getting the work done in a biotech park or an organization that has experience in this area.
- Lack of a wet laboratory facility: Since our laboratory does not have a wet laboratory facility, and it will take some time to set it up after obtaining the funds. However, work can be carried out in the laboratories of the University of Calcutta or in a biotech park.

### Opportunities

- Increasing technology opportunities: The library of recombinant molecules once generated will be the source of antibodies on demand. This will ensure a sure success of the project as our laboratory will have the ability to produce novel antibodies for multiple uses.
- Big market: Particularly with MNCs buying milk and chicken from USA, antibiotic-free milk and chicken will be mandatory.
- The delivery platforms to be delivered by our laboratory such as the probiotics and the Y-complex can be tagged with different antibodies and adapted for multiple uses in the areas of human and animal health opening up huge opportunities.

### Threats

- Competition: Camelid antibody-based applications are a big research area in the European countries with Unilever filing a number of patents in the recent years. Value-added probiotic as chicken feed as live or dead cultures or against toxins are not being worked upon and Our lab needs to hurry up to get priority.
- Resource limitation: As the proof of concept for probiotics has not been established by our laboratory, resources need to be obtained in phases and will depend on milestones. Our laboratory will be very diligent in obtaining the milestones.
- Attempts to smother the product: Big Pharma operative in the antibiotics market will attempt to smother the product by buying the product to preserve their markets. For the initial few products, our laboratory will license them out so as to ensure a cash flow.

### 8.8.5 Competitive Environment and IP Space

The company most active in the camelid antibody area is Ablynx, and they mainly work in human therapeutic area. The IP space is relatively open for the chicken probiotic markets. Unilever has file patents using similar concepts for the treatment of infections using killed yeasts expressing camelid antibodies (US 6517829). Unilever also has patents for camelid antibodies against E. coli adhesion factors (US 4971794) though not in the probiotic format. These prove that it will not be difficult to establish POC in this area. There are no reports of antibodies against mycotoxins of chickens, and it would thus be a safe area to venture into.

### 8.8.6 Financials and Milestones

The instrumentation of the laboratory will be provided by the biotech park. The list of instruments for the project with its approximate cost is

provided in the appendix. Our laboratory will require start-up funding for the working capital expenditure only. This expenditure along with the milestones expected is shown below:

Time and the milestone expected	Proposed investment (INR)
1. Year 1: Generation of a library of molecules in yeasts or phages. Screening of the library to pull out the desired antibodies against specific antigens and its neutralization. Establishment of in vitro proof of concept	<ul style="list-style-type: none"> <li>– Consumables 10 Lakhs</li> <li>– Operational expenditure: 10 Lakhs</li> <li>– Salary: 22.5 Lakhs</li> <li>– Travel: 3 Lakhs</li> <li>– Consultants fees: 1 Lakh</li> </ul> <p style="text-align: right;"><b>Total: 46.5 Lakhs</b></p>
2. Year 2: Characterization of the chosen antibodies. Measuring the affinity stability. Measurement of the ability of the antibodies to kill the live pathogens upon application in animal models. Establishment of in vivo proof of concept	<ul style="list-style-type: none"> <li>– Consumables: 10 Lakhs</li> <li>– Operational expenditure: 10 Lakhs</li> <li>– Salary: 25 lakhs</li> <li>– Travel: 2 Lakhs</li> <li>– Consultants fees: 1 Lakh</li> </ul> <p style="text-align: right;"><b>Total: 48 Lakhs</b></p>
3. Year 3: Pilot-scale manufacture, clinical trials, and regulatory approvals, IP filing, test marketing	<ul style="list-style-type: none"> <li>– Clinical trials and approvals: Rs. 75 Lakhs</li> <li>– Salary: 33.5 Lakhs</li> <li>– Consultants/tech transfer fees: 3 Lakhs</li> </ul> <p style="text-align: right;"><b>Total: 111.5 Lakhs</b></p>
Cost for the project	<b>2.06 Crores</b>
Overhead (10 % of the project cost)	<b>0.20 Crores</b>
Total project cost	2.42 Crores
4. The bovine mastitis technology extension will be taken up after the successful completion of this project within three years	

### Justification of the expenditure

Consumables will include the procurement of the following in addition to the regular molecular biology consumables.

- Vectors for yeast expression as surface display as well as secretory forms.

- Phage display system.
- Restriction enzymes.
- Purified antigens.
- Consumables for operating fermenters for generating clinical grade materials.

If vectors and phage display systems are obtained from academic labs, the expenses can be cut down considerably. The suppliers charge more for the industry as well as expect a royalty for their use.

### Clinical Trial proposal for chicken probiotics and cost

The scientific trials will be conducted across different geographical locations of India, based on the density and demographic characteristics of the poultry operations and business. The trials shall be conducted in commercial broilers and commercial layers and shall continue for 12 months. Strategically, business alliance/partnership could be built up 3 to 6 months on the completion of the trials.

*No. of birds to be included in the trial:*

1. 15,000 commercial broiler birds each × four regions × four seasons = 240,000
2. 30,000 commercial layers birds each × four regions × four seasons = 480,000

*Quantity of Product required/cost of product:*

1. Commercial broilers—4000 L/Rs. 120,000
2. Commercial layers—15,000 L/Rs. 450,000

*Trial Operative Expenses:*

To conduct the trials for a period of 12 months, technical and commercial manpower shall involve 6–8 qualified people. Expenses under different heads of operation are as follows:

1. Salaries, travel, and tour expenses: Rs. 5,500,000
2. Office and other administrative expenses: Rs. 500,000
3. National level veterinary conference expenses: Rs. 400,000
4. Regional seminars and farmers meet expenses: Rs. 600,000
5. Cost of value-added probiotic product: Rs. 570,000

Total cost of trial as budgeted is Rs. (5,500,000 + 500,000 + 400,000 + 600,000 + 570,000) = Rs. 7,570,000.

### 8.8.7 Return on Investments

The details of the tentative cash flow are attached in the appendix. By the end of the fourth year, this product will generate revenues of at least 60 Lakhs INR per month. The value-added proprietary trademark products will thus have minimum sales of 7–8 crores INR per year. Assuming a gross profit margin of 55–60 %, the gross profit will be 4 crores INR per year from the fourth year onward. After taking the cost of capital and taxation into account, the net profit will be 2.5–3.0 crores INR per year. The return on investment will be approximately 30–40 %. The sales figures will be considerably higher if better marketing strategies are adopted. A survey of the potential proprietary trademark value-added products and the value of the intellectual property will give a tentative idea for these assumptions.

#### Cash flow after the first three years of incubation

See the separate attachment.

### 8.9 Technology Extension: The Y-Complex Technology

Our laboratory has access to a proprietary immunomodulatory technology with an Israeli company where the proof of concept has been established in field trials and is ready to be commercialized after slight modifications and clinical testing in Indian conditions. Our laboratory will carry out this project as a second project using the same infrastructure but with additional expenditure in the form of milestone payments and license fees. The first area of application will be in the area of bovine mastitis that has a tremendous market in India. The salient features of the technology are as follows:

- The Y-complex technology is a biotherapeutic platform technology consisting of an immunomodulatory complex comprising of chicken antibody molecules that specifically targets the infectious agents at the site of infection.
- The molecule brings the pathogens and the macrophages together so that the pathogens are destroyed and immune reaction is

triggered simultaneously so that the inflammation is also brought under control.

- The advantage of this technology lies in the fact that a targeted immune response can be achieved in the area of inflammation bringing a rapid and irreversible amelioration of the disease condition.
- However, the biggest advantage of the Y-complex technology is its adaptability as the antibodies can be raised against any pathogen within a very short time and tagged to the complex. The immunomodulatory molecules can be engineered according to the target animal species and its immune system functioning.
- For the extension of the Y-complex technology, our laboratory in the translational research could also work toward adapting the Y-complex platform technology for different therapeutic applications in animal and human health using the camelid antibodies. Our laboratory will construct a repertoire of target-specific antibodies and immunomodulator molecules that can generate multiple therapeutic products.

This technology in the present format is very suitable for topical applications and scores over the other antibiotic-based treatments as it has no residual toxicity and, unlike antibiotic-based treatments, is uncluttered and clean. It is also an environmentally friendly technology as antibiotic resistance does not appear and allows long-term use of the product and thereby minimizes chance of product obsolescence. If propagated judiciously, it will act as an antibiotic replacement therapy and will be able to capture a large chunk of the antibiotic market.

The first therapeutic application of the platform technology by our laboratory will be for the treatment and control of bovine mastitis, an infection of the udder of the cow. The technology application has already been established in the clinical trials conducted in the IP originator's country and is ready for commercialization.

The uniqueness of this technology is as follows:

- It offers a **non-antibiotic therapeutic approach** to circumvent the issue of multiple antibiotic drug resistance in the causative

organisms aside from the substantial savings on loss due to reduced milk production and antibiotic-contaminated milk wastage consequence of antibiotic usage.

- Clinical trials have already established that the **duration of protection is higher** than antibiotics since the Y-complex technology targets a range of pathogens causing bovine mastitis. On the application of Y-complex, therapeutic-specific immune activation and modulation happen against all the selective pathogens resulting in sustained immune protection.
- Furthermore, since this technology eliminates antibiotics usage, it **ensures organic milk production**. In the present scenario of developed technologies and means, perhaps Y-complex is the only possible solution for clean milk production.

Thus, in line with the global consumer health requirements for the absence of antibiotic residues in the milk and milk products, non-antibiotic therapeutics for mastitis control shall rule the market and Y-complex technology for mastitis treatment and control could be a revolutionary environmental friendly and economically viable therapeutic approach in the established and emerging markets.

### 8.9.1 Y-Complex Technology: Business Objectives of Our Laboratory

Our laboratory objective will be to codevelop, build, and market an antibody-based antibiotic replacement therapy for bovine mastitis for the Indian and Asian markets. The Y-complex technology is a chicken antibody-based immunomodulatory technology that already exists, and our laboratory will facilitate the technology adoption for the Indian and Asian market and take it through the various stages of clinical tests, regulatory approvals, and market testing till it is ready to be commercialized.

During this time, if it gets the requisite funding, our laboratory will also set up the biological manufacturing facility for generation of sufficient

volumes of the products for clinical trials and subsequent marketing. For this technology transfer and development, it will ensure that:

- Milestones are reached in a timely manner, and continual value addition is done by innovative research to the Y-complex platform technology and intellectual property.
- Offer product development strategy that aligns with the veterinary and human health market needs business goals and regulatory requirements.
- Implement risk management and pharmacovigilance, leverage the IP, and convert it to marketable products at a higher rate through disciplined product development planning and execution, thus facilitating the development and market entry of high quality, safe, and effective products.
- As value addition and future business options, build sustainable antibody therapeutic product pipelines that can achieve critical mass within a short time, and deliver a steady and growing supply of new products. This includes various OTC and nutraceutical products.
- Our laboratory will bring forth the superiority of technology competitiveness, conduct the risk benefit analysis for the acquisition of the technology, possible technology adoption choice alternatives, technology lifecycle and its positioning, possibilities of business autonomy and the confirmation of the platform technology needs in various antibiotic replacement business segments.

### 8.9.2 The First Product of Our Laboratory Using This Technology

The first therapeutic application of the platform technology by our laboratory will be for the treatment and control of bovine mastitis, an infection of the udder of the cow caused by a host of bacteria mainly *Streptococcus* sp., *E. coli*, and *Staphylococcus* sp. The technology application has already been established in the clinical trials and is ready for commercialization. Our

laboratory will generate camelid antibodies against these bacteria and tag them to the Y-complex beads to create the final product.

The present treatments for bovine mastitis are with antibiotic results in partial success due to huge rejections of antibiotic laced milk. Furthermore, there is an increased concern of public health as it leads to the selection of resistant bacterial strains. Hence, the need for the development of a new way of treatment was always felt, and our laboratory will offer a superior Y-complex technology with non-antibiotic approach and additional immunomodulatory properties suitable for regular use.

As India is a world leader in milk production, it is strategically reorienting its animal husbandry practices for clean milk production and maintaining the international standards of quality control requirements under the pressure of global competition in the era of WTO. Multinational giants like Nestle have positioned themselves in the Indian and Chinese dairy sector. Amul, under the banner of National Dairy Development Board (NDDB), which is responsible for white revolution in India, is emerging as a multinational to the other Asian markets. This has opened up huge opportunities for clean milk that is not antibiotic laced, and the Y-complex treatment will help fulfill these objectives. This technology eliminates antibiotic usage and ensures organic milk production. In our opinion, Y-complex is the only possible solution for clean milk production.

Thus, in line with the global consumer health requirements for the absence of antibiotic residues in the milk and milk products, non-antibiotic therapeutics for mastitis control shall rule the market and Y-complex technology for mastitis treatment and control could be a revolutionary environmental friendly and economically viable therapeutic approach in the established and emerging markets.

### 8.9.3 Additional Products

As the bovine mastitis product is ready for commercialization, our laboratory will undertake R&D activities for the new product in the area of

acute infectious neonatal diarrhea, a syndrome, usually caused by bacteria or viruses, characterized by passage of unformed stool with increased frequency and often associated with vomiting. The most commonly reported causes include certain bacteria (e.g., *E. coli*, *Salmonella* sp., *Shigella* sp., *C. jejuni*) and viruses, especially rotaviruses (although rotaviruses are often also found in asymptomatic newborns). Our laboratory will develop a broad spectrum of antibodies as food additive for newborns. The raw antibodies or those tagged to the Y-complex will be added to the infant formulas and will eliminate the infectious and syndromes described in the newborns.

### 8.9.4 The Market

Bovine mastitis (an infective condition in the udder of the cow) costs the global dairy industry \$4 billion annually. In the USA alone, around \$50 million worth of bovine mastitis antibiotic products are sold annually. Bovine mastitis causes a significant economic impact for the Indian dairy industry as India is the largest milk producer in the world. As per the industry figures, the bovine mastitis treatment market is growing at 8–10 % annually and is poised to be at least a \$25–30 million (Rs. 100 crores) market by 2010. Assuming our laboratory captures a modest 5–10 % of the market in the first year, our laboratory will be able to generate revenues of Rs. 7 crores per year, with a net profit of 3.5–4 crores from the third year onward. The breakeven point will be achieved in the fourth year. The revenues can increase manifold if the international market is tapped.

### 8.9.5 Competition and IP

Since this is a proprietary technology and is patent protected, our laboratory does not anticipate any IP challenge in the area of antibody-based immunomodulatory treatment in this area. The main challenge will come from the well-established companies such as Pharmacia,

Wyeth, and Pfizer that have huge antibiotics market for this disease. Of them, Pfizer is the largest and accounts for 50 % of the sales of mastitis products internationally. In addition to that there are more than twenty domestic players manufacturing these antibiotics. Currently used antibiotics are erythromycin sulfonamide, penicillin, amoxicillin, dihydrostreptomycin, and dexamethasone along with an antihistaminic. Although the cost of individual antibiotic treatment is not prohibitive, cumulatively it adds up as they are not always effective and also due to the appearance of antibiotic-resistant strains. The Y-complex product will be a single application product, will a long-lasting effect, and will not have these problems.

It is but expected that attempts will be made by these giants to buy the rights to the use of the product or our laboratory itself with the objective of smothering the product and the technology, in that order. Our laboratory will resist the attempts as one of the founding concepts of our laboratory is the promotion of clean disruptive technology. Our laboratory may join hands with the corporates to copromote the technology as a supplement to antibiotic use. Should only this be achieved, our laboratory will forge ahead with additional applications that will have the potential to replace antibiotics eventually.

**8.9.6 Marketing and Sales Strategy**

As clean milk is a prerequisite for capturing the international markets in the era of WTO, our laboratory will approach companies having a strong presence in India such as Nestle or Amul that are into milk and milk products such as powder milk, cheese, and chocolates. Our laboratory will use these companies as a channel of communication to implement the Y-complex technology in the various dairy farms from where milk is sourced. This will ensure not only sale of our laboratory product, but also a steady supply of clean milk and milk products suitable for the international markets.

Our laboratory will also approach Pharma companies such as Zydus Cadilla and Kemin that have a good presence in the area of veterinary health to include the Y-complex product in their marketing channels for manufacturing and distributing in the market on a royalty sharing and milestone payment agreement.

**8.9.7 Financials**

The bovine mastitis program can be carried out as a backup project after the poultry project is underway. The success of this project will depend on establishing proper marketing channels for the product. The technology has been proven in clinical trials, and further clinical trials will have to be conducted in India before it is ready for manufacture or licensed out. The additional expenditure will be required as technology transfer fees, milestone payments to the coowners of the technology, as well as operational costs. The *additional costs* will be around 2.4 crores, and the chart below gives an approximate idea of the costs.

Y-complex mastitis development phase, i.e. till product registration with clinical trials

	Total	Year 1	Year 2	Year 3
(a) Technology transfer fees	5,000,000	3,000,000	2,000,000	0
(b) Clinical trials and regulatory approvals	5,000,000	1,000,000	2,000,000	2,000,000
(c) R&D costs	14,250,000	4,500,000	4,750,000	5,000,000
Total expenses	24,250,000	8,500,000	8,750,000	7,000,000

**Return on investments:** The tentative cash flow statement will be worked out. The bovine mastitis market will be at least a \$25–30 million (Rs. 100 crores) market by 2010. As the product will be innovative and will replace the use of antibiotics, our laboratory will be able capture at least 5–10 % of the market that will generate revenues of Rs. 7 crores per year, with a net

profit of 3.5–4 crores from the third year onward. The breakeven point will be achieved in the fourth year. The revenues can increase manifold if the international market is tapped.

---

### **8.10 Third Our Laboratory Product Range for Healthcare and Cosmetics Application**

As soon as the camelid library will be prepared by our laboratory and protocols standardized to isolate the antibodies, our laboratory will take up projects in the area of human health and will generate products neutralize toxins and pathogens causing human morbidity and mortality. Our laboratory will also have the ability to generate custom-designed antibodies against antigens that can be used as detection reagents. Our laboratory will take up these projects as per need (if additional cash flows can be generated using the same resources). Following are the areas our laboratory will can start work as backup projects when required.

#### **8.10.1 Antibody Fortified Pathogen and Toxin Neutralizing Oral Rehydration Therapy**

Oral rehydration therapy is given to patients with diarrhea as a way to stop the loss of and replenish body fluids. This has to be supplemented with antibiotics to control the infection. One of the main agents of diarrhea is *Vibrio cholerae* that secrete a toxin in the gut that causes the symptoms of the disease. Strains of *V. cholerae* in India have become resistant to several antibiotics, and incidences of multidrug resistance are increasing. Studies on *V. cholerae* strains show that the bacilli are resistant to several old as well as new antibiotics, including ampicillin, tetracycline, furazolidone, norfloxacin, and ciprofloxacin. About 40 pharmaceutical companies already produce ORS in India, but none

addresses the issue of rehydration as well as infection at the same time. Antibodies to the cholera toxin will address this issue and when mixed with the ORS solution will result in a better and sustainable therapy. Our laboratory may collaborate with and add value to well-established ORS brands such as Rebalanz (Dr. Reddy's Laboratory), Electral (FDC Ltd.), Prolyte (Cipla), and Redotil (Dr. Reddy's Laboratory).

#### **8.10.2 Antibody Fortified Milk and Milk Products for Cure Against Infantile Diarrhea**

As a part of its societal responsibility, our laboratory will work in the area of infantile diarrhea. Diarrheal diseases, such as cholera, shigellosis, and rotavirus, kill about 1.8 million children each year, accounting for 17 % of childhood deaths. Most of the deaths happen in children less than five years of age. These are difficult to control due to the appearance of drug-resistant strains, and currently, more than 75 % of the strains are drug resistant. Of them, Shigellosis alone is endemic throughout the world with approximately 163.2 million in developing countries. Each year, 1.1 million people are estimated to die from Shigella infection. A total of 69 % of all episodes and 61 % of all deaths attributable to shigellosis involve children of less than 5 years of age, the reason being, Shigellosis is difficult to control due to the appearance of drug-resistant strains. The median percentage of this infectious strain that has become resistance to currently used drugs is high: cotrimoxazole (99 %), nalidixic acid (97.5 %), fluoroquinolones (38.5 %), and 97 % of the strains are multidrug resistant.

Our laboratory will raise antibodies against Shigella that will be used to fortify milk drinks that will be used to cure infantile diarrhea as well as can be used as a prophylactic drink for travelers in endemic areas.



As a part of its ongoing research activity, our laboratory will also raise antibodies against other diarrhea causing pathogens such as *Campylobacter*, *Salmonella*, and *E. coli* and parasites such as *Giardia lamblia*, *Entamoeba histolytica*, and *Cryptosporidium* and create value-added milk products.

**Antibodies against infectious agents and cancer for diagnostics use:** The small size, extreme stability, and the ability to reach the target make them ideal candidate for use in diagnostics kits. Antibodies can be pulled out from the library against select antigens such as cancer, infectious diseases, and metabolic diseases markers and used in diagnostics kits.

### 8.10.3 The Corporate Philosophy to Ensure that the Undertaking Is Viable

Our laboratory recognizes that innovation thrives in an atmosphere that favors two critical factors: freedom to think and freedom to act. In a rush to generate higher R&D productivity for increased competitiveness in the biotech corporate, there is a tendency of innovation getting sacrificed in the complex myriad of technocommercial decisions. There is also a tendency to promote technologies and product that are not clean and green resulting in far greater harm than apparently visible. While on the one hand, small start-ups have the innovation but not the momentum to carry its fragile existence forward through the difficult developmental and commercialization path, on the other hand, big corporates that do not lack in terms of resources often run a high risk in losing focus on innovation. The way out is to merge innovative technologies of small smart start-ups with the mass and power of larger corporate core R&D processes. Our laboratory aims to do just that and therefore plans to select areas of clean technology for the purpose.

The evolution of the present-day biotechnology industry has been driven by a disciplined entrepreneurial spirit resulting in an accelerated discovery and technology implementation process and is responsible for the major discoveries in the drug discovery industry. Technology innovation comes from basic research and technology commercialization. This is achieved by technology transfer–technology spread concept from strategic alliances. Economic value does not increase solely with radical technology developments, but only when the developed technology is commercialized and leads to viable products.

The challenges are manifold: smart thinking and planning to attain success, tackling new and unfamiliar issues related to product commercialization, finding the right partners, negotiating the correct terms for their intellectual property, managing alliances efficiently, finding creative solutions around new sets of challenges, ensuring high R&D productivity and efficiency, and protecting intellectual property and human talent. The objective of our laboratory is to connect technologies with business feasibility through technology commercialization support in relation to corporate strategies and policies.

Established biotech companies that have a technology or a product with commercial potential are in the next phase of their evolution, viz. negotiating deals, strategic partnering, entering late stage clinical trials, and bringing products to market. Underpinning this is a culture of innovation, the promise of new cures, new technology platforms, and products. While the industry needs a supportive regulatory framework and an encouraging climate for investors, it is ultimately founded on something even more basic—strong science and research. Successful biotech companies have managed to get a handle on these twin aspects that drives technological innovation. If either of the components is missing, the results are suboptimal. This need and lacuna in the current scenario prompted the

founders of BioCosort to start this company which would aim to strike a balance between these two aspects that is key to success in the minimum possible time.

The intellectual capital of our laboratory is a knowledge of the emerging technologies as well as the hands-on technical skills in translational research. The scientists of our laboratory track the continuous process of innovation and develop the means to sustain the ever-evolving challenges of technology adoption and commercialization. Simultaneously, our laboratory also develops innovative technologies in consultation with the industry and develops marketable products in the shortest possible time. The main action area is antibiotic replacement therapy by novel antibody-based technologies.

#### 8.10.4 Mission Statement of Our Laboratory

Our laboratory will be a global player in codeveloping and leveraging clean and sustainable innovative technologies for various product applications in the area of human and animal health, cosmetics, nutraceuticals, and healthy food. Our laboratory will form an effective bridge connecting and sustaining constant technology innovation and adaptation by virtue of relentless vigilance and research to ensure appropriate application.

#### Appendix 1: Our Laboratory Activity Chart

##### Organization Setup Activities

Our laboratory has been started in Jan 2009. Tentative milestones to be attained are shown below:

No.	Item	Date	Comments
1	Preorganization planning activities	Done	Writing up business and scientific plans, Market research and pre business development activities. Determination of collaborators/partners and management and scientific teams
2	Corporate plan review and finalize open issues and negotiations with funding agencies (tie-ups with corporate houses, financial institutions, VCs, Angel Investors, Govt, e.g., DBT, DST, CSIR, and quasi-Govt, e.g., biotech parks, IIT, ILS). Collaborations/partnerships with organizations working in this area if necessary. Entering into JV/agreement with collaborators	In progress	Board of directors and scientific advisory board will be finalized after consultation with all the partners
3	Obtaining the funding and setting up of application laboratory (viz. instrumentation, infrastructure, personnel recruitment)	Oct 2009	Setting up of application laboratory and hiring of personnel with funding from investors. SOPs will be optimized simultaneously
4	Corporate setup completed and begin formal operations and standardization of instruments, testing of HVAC, first meeting to decide the course of work, timelines and deliverables	Dec 2009	Full fledged operational laboratory

(continued)

(continued)

No.	Item	Date	Comments
5	Full fledged commencement of wet laboratory work (experiments started)	Jan 2010	R&D work commences. Two different project areas, one for probiotics and the other in the area of camelid antibodies begin

## Appendix 2: Three-Year Road map

Timelines	Proposed progress chart
Oct–Dec 2009	<ul style="list-style-type: none"> <li>– Setting up of the application laboratory and making it operational</li> <li>– Hiring personnel and organizing labs to functional domains</li> <li>– Setting up of the probiotic culture facility with a small fermenter</li> <li>– Procuring antigens genes and expression of proteins for immunization of camels/llamas</li> </ul>
Jan–April 2009	<ul style="list-style-type: none"> <li>– Immunization of Llamas</li> <li>– Fine-tuning of protocols for screening of the phage library by panning. Establishing the optimized protocol for the same with a standard library</li> <li>– Organizing blood collection and RNA isolation from camels/llamas</li> <li>– Preparing the camelid library in phage, bacteria, and yeasts with the cDNA from the immunized Llama</li> </ul>
May–Aug 2010	<ul style="list-style-type: none"> <li>– Panning of the library against antigens and selection of the right clones. Transformation in <i>E. coli</i> and selection of the antibody producing clones by ELISA. Calculation of binding affinity</li> <li>– Optimization of the growth conditions for <i>Saccharomyces</i> and <i>Lactobacillus</i>. Establishing the transformation protocol with food grade secretory vectors that would give high yields</li> </ul>
Sept–Dec 2010	<ul style="list-style-type: none"> <li>– Optimization of growth conditions of the probiotic cultures in consortium</li> </ul>

(continued)

(continued)

Timelines	Proposed progress chart
	<ul style="list-style-type: none"> <li>– Introduction of the first genetically modified yeast in the consortium and accessing if the consortium secreted effective antibodies</li> <li>– Alternatively producing killed yeast and mixing with the probiotic culture to see if they are effective</li> <li>– Finalizing the composition and formulation of the consortium in the value-added probiotic format. Building up of pilot-scale live cultures in various formats and testing for the stability, resistance to contamination, maintenance of the sub populations in the consortium, etc.</li> </ul>
Jan–April 2011	<ul style="list-style-type: none"> <li>– Large-scale manufacture of the product for clinical trials</li> </ul>
May–Aug 2011	<ul style="list-style-type: none"> <li>– Clinical trials, regulatory clearances, and test marketing. Clinical trials will be conducted in various poultry farms in India. These will be the future customers for the product and in a way test marketing will also be done during clinical trials. Clinical trials will be conducted with two types of products:                         <ol style="list-style-type: none"> <li>1. Non-GMO cultures: consortium of probiotics with dead yeast cultures containing the camelid antibodies to toxins</li> <li>2. GMO cultures: consortium of probiotics containing camelid antibody secreting yeasts</li> </ol>                     Product ready for the market. It can be out licensed or manufactured by our laboratory after a fresh round of funding to set up the manufacturing facility                 </li> </ul>

Outline of the green technology development and technology extension

# Development of a Novel Format of Stable Single Chain Antibodies Against *Staphylococcus aureus* and Allergen-Specific IgE in Allergic Asthma

## 9.1 Specific Aims

### 9.1.1 Aims of the Project

Antibiotics, while having the power to control infection, neither have the capacity to counter-effects toxins produced by the microbes while in the host nor control inflammatory responses. Anti-inflammatory drugs address specific receptors, molecules, or second messengers of the inflammatory cascade but have no effect on the pathogen. Immunosuppression to control infection-induced or allergic inflammation by steroids leaves the host vulnerable to further secondary pathogen attack. This system of therapy not only creates a negative spiral of more and more drugs and therefore greater and greater drug-related toxicity or worse, multidrug resistance, but ultimately also leads to rampant abuse of the ecosystem that exists both inside and outside a living organism. We propose to develop technology that is entirely biological and most importantly eco-compatible. This study aims to develop a library of novel format stable single-chain nanobody library without the disadvantages of conventional antibodies that can have therapeutic, diagnostic, and cosmetics use as well as food supplement as nutraceuticals. This grant proposal summarizes plans to develop such a library of E-compatible (eco-compatible) targeted biobodies or nanobodies (ETB) using the novel short-chain variable fragment (scFv) technology or isolating camelid antibodies (VHH

or variable heavy-chain antibodies) and generating an antibody repertoire for further downstream screening for specific uses.

The aim of the project will be to generate antibodies in the camelid format against *Staphylococcus aureus* and its toxins as well as against IgE, using a combination of the two either as a fused dimeric antibody or a mixture of the two in appropriate formulation to curb *Staphylococcus* infections and the associated complications. It will consist of the following steps:

#### **Specific Aim 1. To generate a library of single-chain antibodies in the camelid format**

Hybridoma technology has largely been superseded by recombinant antibody technology where a large number of antibody molecules are cloned and expressed in viruses (Phages), bacteria (*Escherichia coli*), or prokaryotes (yeasts). We plan to generate two camelid antibody libraries from which suitable antibodies can be fished out as per need.

- (a) **The first library will be a naïve library** wherein the VHH genes will be cloned from unimmunized camels and will theoretically contain no bias against a particular antigen. The suitable antibody can be pulled out after a rigorous selection mechanism by panning, flow sorting, or magnetic enrichment.
- (b) **The second library will be developed from an immunized camel** where the camel will be immunized with the antigen of choice. The antiserum will contain

antibodies against that particular antigen. The genes will be cloned directly in the bacterial or yeast expression system, and suitable clones can be picked from them with ELISA.

### **Specific Aim 2 and 3: To develop these antibodies as detection reagents and therapeutic molecules**

As these molecules are extremely specific and stable, translational research will be carried out to convert these molecules into economically viable products.

- (c) These molecules will be cloned in *Saccharomyces cerevisiae* and *E. coli*, and they will be used for various applications in human and animal health
- (d) Assays will be developed to test for the ability of the molecules to detect and control infectious disease pathogens and diseases of the immune origin like asthma. The selected molecules will be further developed as detection or therapeutic molecules.

These antibody molecules will be developed against *S. aureus* a serious pathogen causing skin infection that cannot be controlled due to the appearance of multidrug-resistant strains known as methicillin-resistant *Staphylococcus aureus* (MRSA) and vancomycin-resistant *Staphylococcus aureus* (VRSA) that are resistant to all the antibiotics available in the market. The project will consist of two parts to be carried out in tandem.

- (a) The first part will consist of generation of the library and screening of the molecules against *S. aureus*, its toxins, and IgE. A basic molecular biology laboratory and a protein chemistry laboratory will be required for this.
- (b) The second part will consist of in vitro and in vivo assays to study the efficacy of these molecules in inhibiting the growth of the bacteria as well as reduction of the localized skin inflammation caused by the bacteria in a mouse model. This will be carried out in a microbiology laboratory with animal house facilities.

- (c) The third part will consist of screening of the molecules against allergen-specific IgE.
- (d) The fourth part will be to develop an acute allergic asthma and inflammation model in mouse and test the efficacy of the anti-allergen-specific IgE to ameliorate composite asthma phenotype.

---

## **9.2 Background and Significance**

### **9.2.1 Introduction**

Modern age has brought about the indiscriminate use of chemicals. Synthetic chemicals are used to increase food production and control diseases with the objective of improving the quality of our lives. Chemicals are not biodegradable and pollute the atmosphere, accumulate inside living bodies, and create a disturbance in the delicate balance of the ecological system governing life on planet earth. This resulted in rampant pollution that is difficult to contain and give rise to drug-resistant microorganisms that are impossible to treat. This has ultimately led to a poor ecosystem and a lowering of the quality of life of all inhabitants of earth. We humans, who are responsible for this, have woken up to the fact that we need to undo this by developing clean green sustainable technologies and eco-friendly products.

Only organic molecules that are biodegradable have the potential to accomplish this. Biosensor plans to operate in this area and develop healthcare solutions on the basis of leveraging fundamental biological processes and converting them into far more powerful and sustainable healthcare tools with distinct ecological advantages. The proprietary technology that my laboratory proposes to develop is E-compatible (eco-compatible) targeted biobodies or nanobodies (ETB) for healthcare applications and solutions. Biobodies or nanobodies are miniscule antibodies, engineered to be targeted against various pathogens and their toxins as well as rogue immune molecules. We propose to develop various applications and product lines based on this technology for human and animal healthcare uses.

My laboratory plans to develop a library of these antibody molecules from which antibodies suitable for a wide range of applications can be pulled out. The secreted or surface-displayed antibodies will be in an entirely novel format derived from camels (VHH or variable heavy-chain antibodies) or scFv that are small and stable and can easily be genetically manipulated to overcome the problems of stability, tissue penetration, and immune incompatibility. These engineered antibodies will be extremely small in size and can be easily adapted for a wide range of applications. They can be fused together to increase their sensitivity, can be tagged with immunomodulatory molecules to make therapeutic products, and can easily be made more thermostable or pH tolerant and also humanized.

Antibodies are powerful tools to recognize and target almost any molecule with a high degree of specificity and affinity. A bulk of the antibodies are still obtained from the antisera of animals immunized with the suitable antigen, or as monoclonal antibodies from hybridoma. Mouse hybridomas became the most reliable source of antibodies, and therapeutic products were developed for a number of in vitro applications as diagnostic and biological reagents. These antibodies, however, failed to meet the initial expectations of their use as therapeutic reagents due to their inability to be accepted by the human immune system, so their use was curtailed and a very important commercial aspect remained untapped.

In my lab, we propose to develop a library of camelid antibody molecules and develop protocols that can be used to rapidly extract antibodies of interest with minimum effort and time for various applications. We also propose to humanize these antibodies for therapeutic use as the project progresses.

### 9.2.2 Background and Significance

Camelidae express in addition to their conventional immune repertoire an equally common repertoire of heavy-chain antibodies that consist

solely of two identical heavy-chain molecules. Consequently, the antigen-binding domain of each antibody is encoded by a single gene rather than a combination of variable domain heavy-chain (VH) and light-chain genes (VL). To compensate for the lack of light chains, heavy-chain antibody variable domains have undergone several modifications, the most prevalent being the expansion of the complementary binding region 3 (CDR 3) creating an interphase between antigen and heavy-chain fragment comparable to that of conventional antibodies. To stabilize this structure, the CDR 3 loop contains an additional cysteine residue that forms a second disulfide bridge of the antibody molecule. These antibodies also lack the CH1 heavy-chain region as a consequence of which they are much smaller in size. These antibodies have a molecular weight of ~95 kDa instead of the ~160 kDa for the conventional antibodies. Finally, four of the seven highly conserved residues which in a conventional antibody forms the hydrophobic surface associated with the VL located at positions 42, 49, 50, and 52 are changed to more hydrophilic residues, making the molecule more hydrophilic.

Camelid antibodies thus have peculiar properties that make them superior to conventional antibodies for several applications.

1. *Small size and single chain:* Re-engineered antibodies are 15 kD in size, a tenth of the size of the conventional antibodies. As it is a single-chain molecule, the L and the H chains need not be brought together, and it is amenable to genetic manipulation and expression in prokaryotic and eukaryotic expression systems. It is thus easy to produce the antibodies in bulk, and they can be genetically modified by mutations to increase the affinity, binding properties, solubility, etc. These antibodies can easily be fused together end to end to create bispecific antibodies by simple molecular biology techniques.
2. *Stability:* These antibodies are extremely stable and retain activity at 90 °C. They do not need a cold chain to be transported in and can be used in products that are used in high

temperatures. They can also withstand harsh chemical and denaturant treatments and are very suitable for industrial uses

3. *Good penetrability*: These antibodies have the ability to target cryptic antigens and enzymes. The small size coupled with the long CDR 3 loop allows the antibodies to bind to cryptic antigens or antigen pockets on bacterial and viral surfaces and active sites of enzymes. So far enzymes can be inhibited *only* by camelid antibodies. Camelid antibodies will also be a method of choice to control infectious disease agents. The small size allows for good tissue penetrability making them molecules of choice to combat tumors.
4. *Functional diversity of the library*: VHH libraries generated from immunized camelids retain full functional diversity. This contrasts with the diminished diversity of conventional antibody libraries because of reshuffling of VL and VH domains during library construction. As a result, high-affinity antigen-binding VHHs can be isolated by directly screening a limited number of clones from immune libraries without prior selection using display technologies.
5. *Solubility*: The presence of the four hydrophilic residues on the CDR 3 loop confers it with good hydrophilic and solubility properties making them suitable to be used as affinity reagents in the laboratory and industry.
6. *Strict monomeric behavior*: VHH in contrast to other formats of truncated antibodies shows no signs of spontaneous dimerization so the samples are more homogeneous and effect more predictable.
7. *Less immunogenicity and good clearance*: These antibodies lack the Fc fragment and are small and do not elicit adverse immune reaction in humans and have a rapid renal clearance rate making them particularly suitable for in vivo imaging applications and treatment to snake bites. It has also been used for other therapeutic applications, such as treatment of

infectious or inflammatory diseases as it has a short serum half-life of about 2 h.

### 9.2.2.1 *Staphylococcus Aureus* Infection

*S. aureus* is an aggressive bacterial pathogen frequently part of the skin flora found in the nose and on skin. *S. aureus* can cause a range of illnesses from minor skin infections, such as pimples, impetigo, boils, cellulitis folliculitis, furuncles, carbuncles, scalded skin syndrome, and abscesses, to life-threatening diseases such as pneumonia, meningitis, osteomyelitis, endocarditis, Toxic shock syndrome (TSS), and septicemia. Its incidence is from skin, soft tissue, respiratory, bone, joint, and endovascular to wound infections. It is still one of the four most common causes of nosocomial infections, often causing postsurgical wound infections. *Staphylococcus* causes severe infections and is a leading cause of morbidity and mortality.

The most common treatment is by antibiotics like penicillin, but resistance to this class of drugs mediated by penicillinase has already appeared. The problem is accentuated methicillin resistance mediated by the *mec* operon. This led to the use of glycopeptide antibiotics like vancomycin and that led to the appearance of vancomycin-resistant strains mediated by Van a gene. Today, *S. aureus* has become resistant to many commonly used antibiotics. A majority of all *S. aureus* isolates are sensitive to penicillin with a similar picture in the rest of the world. As a result of this, the multidrug-resistant forms of the bacteria are incurable and this is being called a superbug in recent years and has resulted in a large number of deaths due to hospital-borne infections in recent years.

Resistance to these antibiotics has also led to the use of new, broad-spectrum anti-Gram-positive antibiotics such as linezolid because of its availability as an oral drug. First-line treatment for serious invasive infections due to MRSA is currently glycopeptide antibiotics (vancomycin and teicoplanin). There are number of problems

with these antibiotics, mainly centered around the need for intravenous administration (there is no oral preparation available), toxicity, and the need to monitor drug levels regularly by means of blood tests. The glycopeptide antibiotics do not penetrate very well into infected tissues particularly in the brain and meninges and in cardiac tissues.

This is compounded by the fact that *S. aureus* is capable of secreting several toxins that are associated with specific diseases. They are pyrogenic toxin superantigens (PTSAgs) that have superantigen activities that induce TSS and food poisoning. This group includes the toxin TSST-1, which causes TSS associated with tampon use. The other toxins are exfoliative toxins (proteases) that cause Staphylococcal scalded skin syndrome (SSSS), which occurs most commonly in infants and young children. It also may occur as epidemics in hospital nurseries. Depending on the strains, the other toxins are alpha-toxin, beta-toxin, delta-toxin, and several bicomponent toxins. The bicomponent toxin Pantan-Valentine leukocidin (PVL) is associated with severe necrotizing pneumonia in children.

Thus, no drugs currently exist that can successfully control *Staphylococcus* infection as well as ameliorate the effects of the toxins and the inflammation caused by it. Multifunctional camelid antibodies can target the pathogen as well as the toxin.

Administered with anti-IgE antibodies, they will have the ability to drastically and rapidly reduce the local and systemic inflammation. It can be administered locally or parenterally and will not be limited by its inability to penetrate tissues. As these antibodies are extremely stable, they can be used as disinfecting solutions and will have the ability to drastically bring down the incidences of nosocomial infections.

### 9.2.2.2 Allergic Asthma

Asthma is a chronic allergic airway disease characterized by persistent inflammation and airway hyper-responsiveness (AHR). T cells, especially Th2 cells secreting IL-4, IL-5, and IL-13, are pivotal in orchestrating the disease process, and adoptive transfer of Ag-primed T

cells in naïve animals can induce eosinophilia, AHR, and late airway responses. Apart from Th2, other effector cells for AHR and asthma are the eosinophils and mast cells. Under the influence of chemoattractants and IL-5, eosinophils proliferate, migrate into the lung, and are activated to secrete histamine, leukotrienes, and other mediators. Mature mast cells are sources of histamine, proteases, heparin, and lipid mediators, released upon allergen-induced IgE cross-linking as the initial step in the inflammation process.

IgE plays a major role in allergic disease by causing the release of histamine and other inflammatory mediators from mast cells. A mainstay of treatment of allergic disease, including asthma, is allergen avoidance and treatment of symptoms. Presently, the most effective treatments of allergic diseases are directed toward a regulation of the inflammatory process with corticosteroids. A more direct approach without the negative effects of corticosteroids consists in regulating the allergic process at the level of the initiator of the allergic inflammation, IgE, via an anti-IgE.

Various receptors and molecules and cell types have been studied in the cascade of events whereby the composite asthma phenotype develops and subsequently exacerbations lead to the development of the fibrosis characteristic of chronic asthma or *status asthmaticus*. These cells, receptors, and even whole cells have been evaluated as potential drug targets. Allergen-specific IgE developed as a result of unregulated proliferation of the particular antibody subtype that memory B cells encode following the first few exposure to the allergen, is one of the principal factors touted to contribute to the pathogenesis of asthma and its exacerbations.

The concept of using anti-IgE antibodies as a treatment for allergy has been widely disclosed in the scientific literature. A few representative examples are as follows. Demonstrated that an anti-IgE monoclonal antibody could specifically block passive cutaneous anaphylaxis reaction when injected intradermally before challenging



with the antigen; U.S. Pat. No. 4,714,759 discloses a product and process for treating allergy, using an antibody specific for IgE; and discuss the prevention of the development of allergic responses with monoclonal antibodies which block mast cell IgE sensitization.

Antagonists of IgE in the form of receptors, anti-IgE antibodies, binding factors, or fragments thereof have been disclosed in the art. For example, U.S. Pat. No. 4,962,035 discloses DNA encoding the alpha-subunit of the mast cell IgE receptor or an IgE-binding fragment thereof. (Hook et al. Federation Proceedings Vol. 40, No. 3, Abstract #4177) disclose monoclonal antibodies, of which one type is anti-idiotypic, a second type binds to common IgE determinants, and a third type is directed toward determinants hidden when IgE is on the basophil surface. U.S. Pat. No. 4,940,782 discloses monoclonal antibodies which react with free IgE and thereby inhibit IgE binding to mast cells and react with IgE when it is bound to the B cell FcE receptor, but do not bind with IgE when it is bound to the mast cell FcE receptor, nor block the binding of IgE to the B cell receptor. U.S. Pat. No. 4,946,788 discloses a purified IgE-binding factor and fragments thereof, and monoclonal antibodies, which react with IgE-binding factor and lymphocyte cellular receptors for IgE, and derivatives thereof.

Omalizumab (commercial name Xolair) from Genentech/Novartis is an anti-IgE humanized monoclonal antibody that is prescribed for patients with severe cases of allergic asthmatic exacerbations. Other anti-inflammatory humanized monoclonal antibodies such as anti-TNF $\alpha$  ligand antagonist (Infliximab) from Centocor and IL-1 $\beta$  antagonist (Canakinumab) from Novartis are in early phases (II and I respectively) of clinical trial. The limitation of the existing antiallergen-specific IgE is that it has to be given subcutaneously for 2–4 weeks and discontinued after 16 weeks of maximum use to avoid development of systemic reactions. The large size of the antibody and its formulation also necessitates

administration by injection rather than through inhalation route. In addition, patients with previous history of hypersensitivity and even in some cases without any history have been known to go into severe anaphylactic shock because of cross-immune reaction.

In contrast, camelids have the ability of extreme tissue penetration and allows formulation as nanoparticles to be inhaled in case of allergic attacks.

---

### 9.3 Conclusions of Published Studies of Relevance to the Project

#### (a) conducted in India

To our knowledge, a few laboratories in India in IISc, Bangalore, and University of Delhi South Campus undertake studies on the selection of scFv by phage display technology in lieu of monoclonal antibody technology, but no study has been done with camelid antibodies that let alone develop the technology for downstream translational purposes.

#### (b) conducted elsewhere

At the beginning of the 1990s, recombinant DNA technology like chimerization and humanization has allowed the cloning and expression of antibody genes resulting in products with better clinical efficiency which could then be expressed as recombinant antibodies in eukaryotic cells. This has resulted in a wave of approvals for therapeutic immunoglobulins. These antibodies have been quite successful in the market as their high selectivity and affinity to their targets reduce the chances of side effects. There are roughly 18 antibody-based products already on the market and a number of them under various stages of approvals (<http://www.fda.gov/cber/efoi/approve.htm>), and some of them like the anti-CD20 molecule Rituximab (Rituxan) used for cancer therapy are blockbuster drugs whose revenue from sales is second only to Lipitor, the cholesterol lowering drug. The antibody market had sales of more than \$10 billion

in 2008. But the large size and complex structures of antibody drugs exclude some attractive therapeutic targets, such as most enzyme active sites and deep receptor clefts, cryptic antigens in viral envelopes and tumors, and prions. Furthermore, they are also costly to produce in mammalian cells. For example, Wyeth's antibody-derived drug Enbrel costs around \$1200 per gram to produce. mAbs must be injected and cannot be stored well and their large size results in slow clearance rates as a result of which several promising antibodies could not be commercialized due to toxicity issues.

These difficulties prompted the search for other formats of antibodies. The first target was the removal of the Fc part whose effects were not required for most applications, which was initially achieved by limited proteolysis with enzymes such as papain and pepsin and later by genetic engineering. The resulting products were considerably smaller consisting of the single variable VH and VL domains and were in various formats such as scFv or antibody-binding (Fab) formats or bivalent antibodies generated by fusing the two together. They have improved tissue penetrability and improved pharmacokinetics and are tolerated better by the immune system. Many of these products have shown a lot of promise and are now in clinical trials.

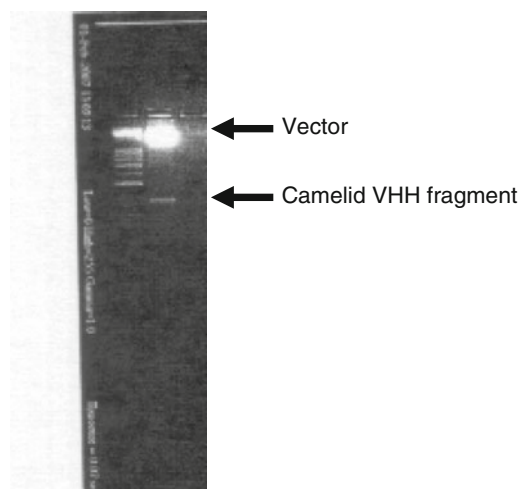
However, these antibodies generally had lower affinity than the parent antibody, which were poorly soluble and prone to aggregation. This is a result of the complexity of the antibody structure where the light and the heavy chains need to come together to form a functional antibody. Their production in microbial cells is often cumbersome, especially when producing multivalent formats, because of the requirement for domain association. To overcome these difficulties, attempts were made to create even smaller antibodies with adequate antigen-binding ability. To reduce the size of the antibodies and to overcome the difficulties posed by bringing the

light and the heavy chains together, attempts were made to do away with the light chain or the heavy chain altogether. These results were further corroborated by the use of molecular biology techniques where single heavy chains from mouse were expressed in bacterial expression systems. Although they retained their antigen-binding ability, their affinity and solubility were reduced.

The serendipitous discovery of naturally occurring single-chain antibodies in animals revived interest in these molecules. These fully functional antibodies are found in camelids (camel, alpaca, and llama) and sharks and consist of a truncated single heavy chain with modified complementary determining regions. These antibodies have unique properties that make them ideal candidates for research and development activities in the areas of therapeutics, diagnostics, and cosmetics.

### 9.3.1 Preliminary Data

#### (1) Isolation of VHH fragment (Fig. 9.1)



PCR and cloning of VHH fragments: Figure shows the isolation of the VHH fragment from the vector by restriction enzyme digestion.

- (2) Generation of model of inflammation for validation of anti-inflammatory parameters in a in vivo model of pulmonary inflammation (Figs. 9.2, 9.3, 9.4, and 9.5

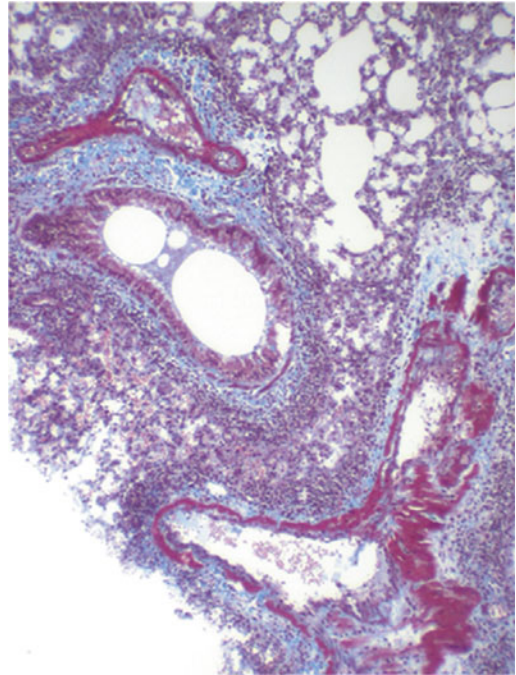
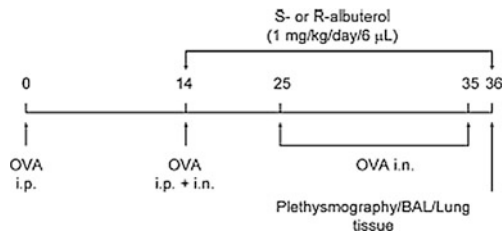


**Fig. 9.1** Acute asthma model: study design

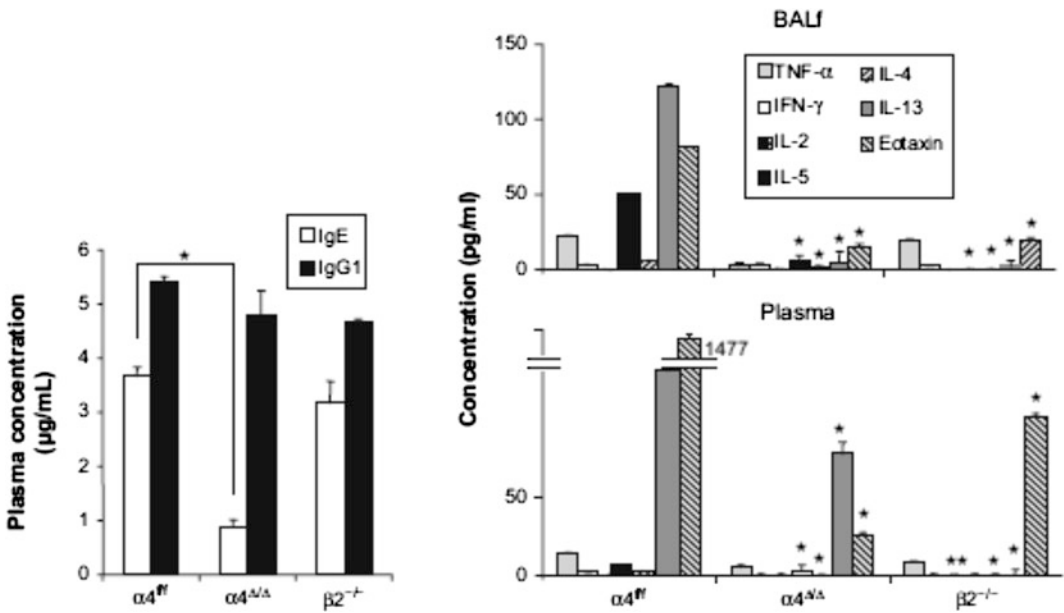
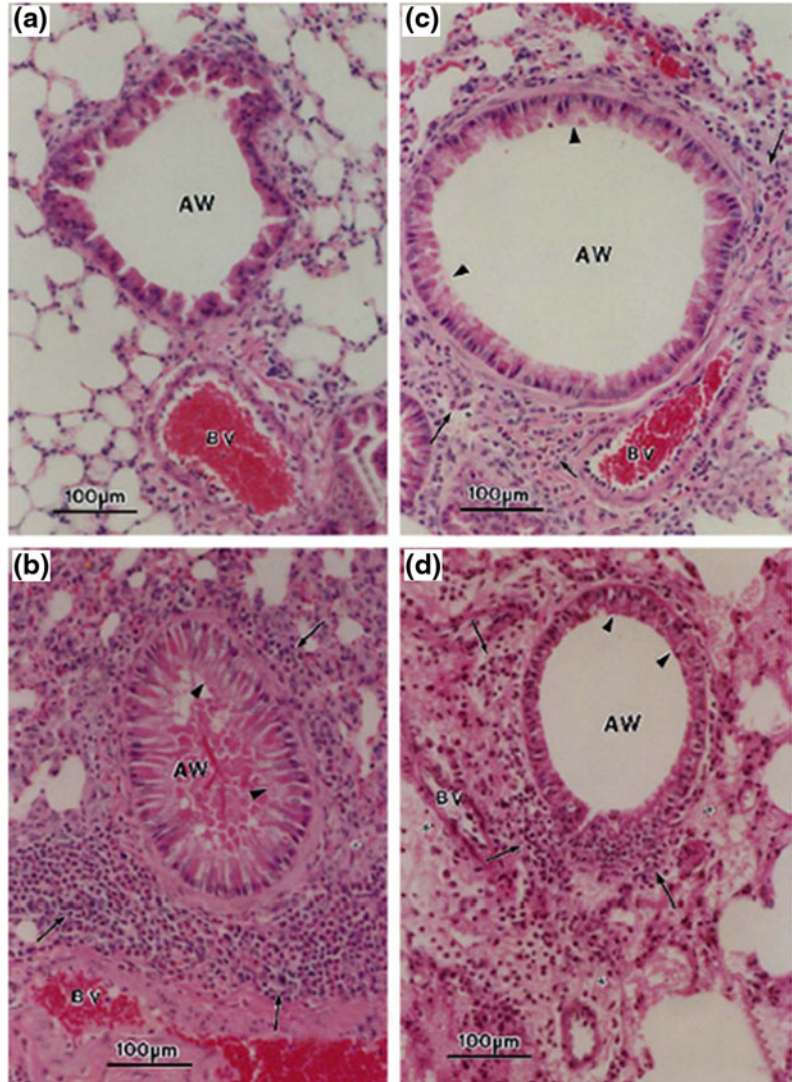


**Fig. 9.2** Effect of (R)- and (S) albuterol enantiomers on airway histopathology in a mouse asthma model. Lung tissue was obtained on day 36 from saline-treated control animals (a), OVA-treated control animals (b), OVA-treated mice administered (R)-albuterol (c), and OVA-treated mice administered (S)-albuterol (d), and sections were stained with hematoxylin and eosin. *Arrows* indicate eosinophils and other inflammatory cells, *arrowheads* indicate mucus, and *asterisks* indicate edema. *AW* airway; *BV* blood vessel. *Bars* = 100  $\mu$ m



## 9.4 Research Design/Methods

The project will involve the following steps:

(A) Development of naïve and biased ETB library

1. Immunization of the camel and monitoring the immune response  
A 1- to 1.5-year-old male llama will be given five doses of crude cell extract of *S. aureus* membrane preparation containing 500  $\mu$ g of emulsified INTA oil

adjuvant (42.5 % Marcol 52, 6.5 % Arlacel C, 1 % Tween 80), at days 0, 21, 28, and 40. Serum and blood samples will be taken at days 0, 4, and 7 after each inoculation. The antibody response will be monitored by ELISA and blood will be drawn after adequate immune response is detected.

2. Isolating the B lymphocytes  
900 ml of blood will be collected 4 days after the last injection, and mononuclear cells will be extracted by Ficoll-Paque gradient centrifugation,

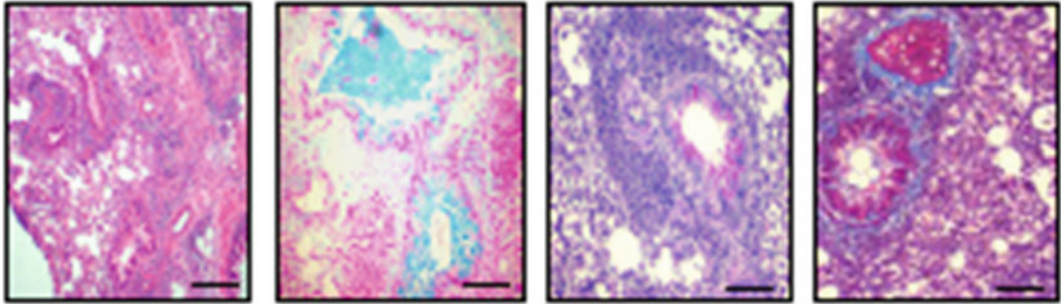


**Fig. 9.3** Assessment of inflammation in lung parenchyma of OVA-treated mice. The four panels represent stains. **a** hematoxylin–eosin for inflammatory recruitment. **b** Alcian blue-stained metaplastic goblet cells. **c** PAS stain of luminal mucin and **d** Masson’s trichrome stain

**Fig. 9.4** Effect of (R)- and (S)-albuterol enantiomers on allergen-induced airway mucus hypersecretion. The number of goblet cells (**a**) and mucus occlusion of airway diameter (**b**) was determined. \**P* < 0.05 versus OVA

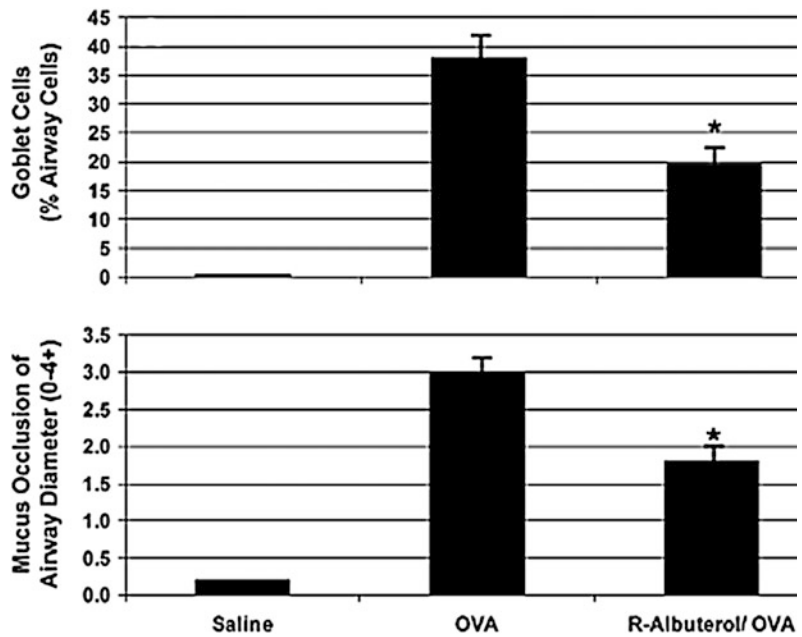
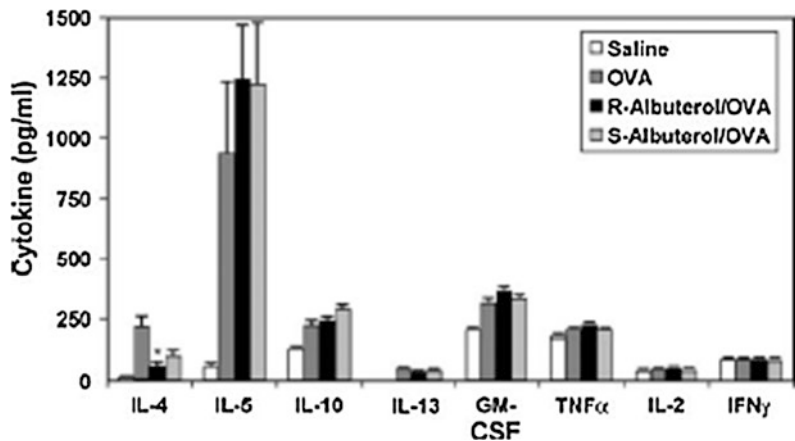


**Fig. 9.5** Effect of (R)- and (S)-albuterol enantiomers on BAL fluid cytokine levels in OVA-treated mice. BAL fluid was assayed for  $T_H1$  and  $T_H2$  cytokines. \**P* < 0.05 versus OVA



pelleted, frozen in liquid nitrogen, and then kept at  $-80^{\circ}\text{C}$  till further use.

3. Purifying the B lymphocytes by flow sorting/chromatography with labeled antigen

Staphylococcus antigen (or purified membrane preparation) will be magnetically and fluorescently (FITC or PE) labeled, incubated with the B cells, and magnetically enriched (X 2) and flow sorted (X 2) to get an enriched population of the B cells expressing the appropriate antibodies. This step can be omitted, and enrichments can be introduced at later stages.

4. Isolating the genetic material and the VHH part of the antibody by RT-PCR  
Total RNA will be extracted by using a commercially available RNA extraction kit. RT will be carried out and first-strand cDNA will be synthesized from RNA by using Superscript III reverse transcriptase, with oligo(dT) 12–18 primers or random primers. In a 20  $\mu\text{l}$  reaction mixture, 0.2, 1, or 5  $\mu\text{g}$  of total RNA will be used. The VHH fragment will be isolated by nested PCR. The cDNA encoding VHH and VH was specifically amplified by PCR using the primers F (GTCC TGGCTGCTCTTCTACAAGG) and (R GGTACGTGCTGTTGAACTGT TCC), annealing at the leader and at the CH2 sequences. The 600-bp fragment (VHH-CH2 without the CH1 exon) will be eluted from an 1.6 % agarose gel after separation from the 900-bp fragment (VH-CH1-CH2 exons). VHH fragments will then be amplified with one additional nested PCR with primers annealing at the framework 1 and framework 4 regions (AACATGCCATGACTCGCGGCTC AACCGGCCATGGCTGAKGTBCAG CTGCAGGCGTCTGGRRGAGG and

ATTATTATTCAGATTATTAGTGC GG CCGCGTGAGGAGACGGTGA CCWGGGTCC, respectively), followed by the use of primers containing the restriction sites for further cloning steps:

5. Enrichment of the clone by biopanning  
Final PCR fragments will be ligated by using the recommended restriction sites into a suitable phagemid vector. Ligated material will be transformed into *E. coli* TG1 cells. The colonies from the plated cells will be collected, washed, and stored at  $-80^{\circ}\text{C}$  in LB medium supplemented with glycerol (50 % final concentration). Specific VHH will be selected from the library using the phage display technology. The VHH library will be infected with M13 helper phages (Invitrogen), and phage particles expressing the VHH repertoire will be rescued and precipitated with polyethylene glycol. Enrichment in specific binders will be performed by three rounds of in vitro selection, i.e., by the so-called biopanning. Immunotubes will be coated overnight at  $4^{\circ}\text{C}$  with an anti-RV antiserum from guinea pig (1/5000 dilution in carbonate buffer [pH 9.6]), and  $2 \times 10^5$  focus-forming units (FFU) will be captured after a blocking step. The bound phage particles will be eluted with 100 mM triethylamine (pH10.0) and immediately neutralized with Tris (pH 7.4). The eluted phages will be used to infect exponentially growing TG1 cells. After the second or third round of biopanning, individual colonies were grown, and the corresponding VHH clones will be analyzed by phage ELISA.
6. Expression of the antibodies by *E. coli* and yeast systems  
For large-scale production (400 ml) in *E. coli*, the VHH-encoding gene frag-

ments were recloned in suitable expression vectors having a peptide tag like c-myc or 6 X His. After induction of VHH gene expression, a soluble protein fraction will be prepared by disruption of cells with a French press. This process will be followed by the removal of the insoluble proteins via high-speed centrifugation (30 min at 13,000 X *g* at 4 °C). The antibody fragments were purified from the lysate via their hexahistidine tail using Talon column material (Clontech).

For secretion by *S. cerevisiae*, the fragments were recloned in episomal vector. Production will be on a 0.5-L (shake flasks) or a 10-L scale. The VHH fragments will be purified by ion-exchange chromatography with Mono-S-Sepharose (Pharmacia) after concentrating the culture supernatant by ultrafiltration. The purification yield will be determined by measuring the optical density at 280 nm OD<sub>280</sub>. The purity will be analyzed on Coomassie-stained 15 % sodium dodecyl sulfate-polyacrylamide gel electrophoresis gels.

#### 7. Characterization of the antibodies

Characterization of the antibody will include affinity determination ( $K_D$ ), determination of the  $K_{off}$  and the  $K_{on}$  rate constants, and stability analysis. The affinity will be determined by using equilibrium-based kinetic analysis by measuring the degree of binding over a wide range of antigen concentrations. The  $K_{off}$  rate will be determined by measuring the degree of antigen binding remaining after saturation at various time points in the presence of excess volume of unlabeled antigens. With these two values, the  $K_{on}$  rate can be calculated. The stability will be calculated after

exposing the antibody to multiple temperatures as well as pH values for various time points and measuring the ability to bind antigens by ELISA.

#### B. Establishment of proof of concept:

##### 1. Assay for the functional activity of the antibody and characterization against *S. aureus* infection:

As a model system, we intend to use *S. aureus* to study the following parameters—(i) inhibition of bacterial colonization by the use of nanobodies through topical and systemic applications, (ii) the ability of the nanobodies to neutralize the toxins secreted by *S. aureus*, and (iii) reduce *S. aureus*-inflicted inflammation.

##### (a) Neutralization assays for bacteria and MIC determination:

*S. aureus* will be grown in tryptic soy broth or agar (TSB or TSA; Becton Dickinson) or in brain heart infusion (BHI) medium (Becton Dickinson).

All strains were tested for (i) growth on BHI (BD) containing different doses of the camelid antibodies and incubating the plate for 48 h at 35 °C. 99 % inhibition of growth as compared to the control plate with no antibiotics will be considered as the MIC concentration. For a preliminary screen with different antibodies, the tests will be done in the liquid medium and monitoring the OD at various time points. The tests will be done with both drug-susceptible and drug-resistant strains with and without the drugs in the presence of antibiotics to see the effect of the supplemental effect of the addition of the antibodies.

- (b) In vivo studies to see the effect of the antibodies in an animal model: *S. aureus* strain SH1000 will be grown to mid-log phase (OD<sub>600</sub> of 0.6) in BHI medium and subsequently washed three times with BHI medium.  $1 \times 10^7$  bacteria will be injected subdermally into the peritoneal cavity of Swiss white Hla(ICR)CVF female mice (16–20 g) with a 26-gauge needle fitted to a 1-ml syringe. The inflammatory reaction will be allowed to develop, and the VHH antibodies will be applied one by one and in various combinations to see the effect on the site of inflammation. They will be antibodies against *S. aureus*, the toxins, as well as the anti-IgE antibodies. The antibodies can also be injected, and the effect on the inflammation as well as the reduction in the amount of the circulating pathogens in the blood can be quantified.
2. Development of acute allergic asthma model to test efficacy of anti-IgE camelid antibody:  
Composite asthma phenotype will be developed as described in, and evaluations of inflammation and allergic responses in the respiratory tract will be evaluated as described in detail there. Preclinical asthma phenotype will be developed by ovalbumin allergen sensitization and challenge as standardized in the PI's laboratory (Ray Banerjee 2005, 2007, 2008, 2009) and the composite phenotype assessed by immunological, histological, and biochemical techniques. Lung parenchyma and airway remodeling will be assessed through specific staining techniques standardized in the lab. Systemic inflammation will be evaluated by thorough qualitative and quantitative evaluation of bone marrow, blood, and spleen in addition to local lung tissue. Status of progenitor populations in bone marrow as well as local lung tissue will be assessed by specialized techniques like CFU-c (colony-forming units-count) assay to further check the status of cellular mobilization under these inflammatory conditions and how the antibodies may help ameliorate disease status.
- C. Preparation of anti-VHH antibody as secondary antibody applications:  
Anti-VHH antibodies will be prepared as secondary antibodies to detect VHH molecules. To prepare a polyclonal antibody against VHH, 2.0 ml of a mixed emulsion of equal volumes of purified VHH solution ( $1 \text{ mg ml}^{-1}$ , inactivated by 3 % [vol/vol] formalin for 24 h at 28 °C) and Freund's complete adjuvant (Sigma) will be injected subcutaneously at two to four sites on each of two White female rabbits (body weight about 2 kg). At 2 and 4 weeks after the first injection, 1.0 ml of a mixed emulsion of equal volumes of purified VHH solution and Freund's incomplete adjuvant (Sigma) will be injected subcutaneously. On the 7th day after the last injection, antibody titers will be determined by Western blotting. If the titers were >1:1000, blood will be withdrawn by venipuncture and an antiserum will be prepared. The specificity of the antibody against VHH will be confirmed by immunoblotting with purified and crude VHH preparations from the recombinant *E. coli*, in which the antibody reacted with a single protein.



### 9.4.1 Significance and Technology Extensions

As camelid antibodies are extremely stable in high temperatures and low pH, antibodies will be developed against toxic proteins and microorganisms. As short serum half-life because of a rapid renal clearance limits the efficacy of VHHs in many parenteral applications, they are ideal molecules to be administered orally. Following applications can be developed. As the antibodies will be panned from a library, multiple projects will be taken up in the first year.

- (a) **Antibodies against Cholera toxins:** Antibodies will be developed against cholera toxin in the camelid format. For this purpose, collaborations will be developed with National institute of Cholera and Enteric diseases and other academic labs. This antibody can be added to the oral rehydration solution for immediate relief. The anti-diarrheal market is worth about \$20 billion annually with \$ 5 billion in the OTC segment.
- (b) **Antibodies against diarrhea causing microorganisms for use as nutraceutical supplement.** This will be based on the above principles. Antibodies will be raised against *Campylobacter*, *Salmonella*, *Shigella*, and *E. coli* (*E. coli*, *Giardia lamblia*, *Entamoeba histolytica*, and *Cryptosporidium*). The antibodies can be directly secreted from probiotics, and value-added probiotics can be made for use in human and animal health industry.
- (c) **The diagnostics industry alone is worth 1000 crores, and camelid antibodies can be used to design diagnostic kits with superior properties:** This technology once developed will rapidly generate the required antibodies as per the demands of the diagnostics industry.
- (d) These antibodies can be **humanized** and can be used for chronic therapeutic applications such as targeting tumors and cancer therapy.

### 9.4.2 Anticipated Pitfalls and Ways to Overcome Them

Since these antibodies will be produced from bacterial and yeast expression systems, their glycosylation patterns will not be the same as produced by hybridoma technology. The way around it is to introduce recombinant yeast expression systems with additional glycosylation abilities and of course to humanize them. This might limit their therapeutic potential.

In fermenters, yield may vary from batch to batch which will need some standardization and continuous monitoring.

Clonal stability may be a potential problem. Selection pressure may be enforced in that case to reinstate stability.

Compared to conventional antibodies, the simple structure and extreme stability and specificity make them an ideal candidate to overcome the difficulties of conventional antibodies. The technology is full proof and cost-effective compared to raising monoclonal antibodies and non-specificity of polyclonal antibodies.

These antibodies may be administered orally, sublingually, topically, intravenously, subcutaneously, nasally, vaginally, rectally, or by inhalation, therein lies the advantage of these antibodies, and various formulations may be envisaged to overcome problems of administration.

### 9.4.3 Expected Outcome

Multiple antibodies against a single antigen may be obtained. The properties of these antibodies can easily be improved upon by genetic engineering techniques. The library size will be of the order of  $10^9$  molecules that can be potentially enriched and screened for any number of antigens. Antibodies enriched and screened against a certain antigen may have used in diagnostics

---

(sandwich ELISA, as imaging agent because of their high tissue penetrating ability) or as research tools. Since these are single-chain antibodies, they can easily be humanized by fusing a 300-400 bp Fc fragment from humans to the antigen-binding domain. This may be used in prolonged therapy in chronic treatment regimens like cancer or for short time treatments such as anti-venom therapy or wound healing or cosmetic use etc. In food supplements or as prophylactic use, antiallergic or antidiarrheal antibodies may be used.

# Development of a Novel Format of Stable Single-Chain Antibodies Against Alkaline Phosphatase as Therapeutic Molecules

## 10.1 Introduction

Antibodies or immunoglobulins are sequestered in all vertebrates. Of them, camelids, nurse sharks, and spotted ratfish have been found to possess structurally different kinds of antibodies. These antibodies are composed of two heavy chains similar to conventional antibodies referred to as heavy-chain antibodies (HCAs) [1], but contrary to the structure found in conventional antibodies, they possess lack the CH1 domain [2]. Nanobodies are antibody-derived engineered therapeutic proteins that contain the unique structural and functional properties of naturally occurring heavy-chain antibodies. The nanobody technology was originally developed following the discovery that camelidae (camels and llamas) possess fully functional antibodies that lack light chains. These heavy-chain antibodies contain a single variable domain (VHH) and two constant domains (CH<sub>2</sub> and CH<sub>3</sub>) [3].

One of the reasons behind the interest shown by the industry in VHH is that the single domain allows production in microorganisms. The high levels of production and the subsequent purification is very efficient, which enables cheap production of large quantities of VHHs. To select the VHH with the desired properties from a large collection of VHH, phage display is performed [4]. Phage display uses bacteria and bacterial viruses, known as bacteriophage, to select antigen-specific antibody fragments (in our case

VHH). This technology combines the VHH displayed on bacteriophage particles to the DNA encoding this VHH, which is present in the phage. One of the strengths of this method is this coupling of phenotype to genotype.

One of the most prominent advantages of VHHs over conventional antibodies is their performance at high temperatures which is evident from the fact that they can withstand incubation of even two hours at high temperatures up to 90 °C [5].

In the industry, the applications using antibody technology are increasing rapidly as well. In medicine, antibodies are used as fusion proteins, to function as a carrier to target-specific effector substances to a specific location, the so-called magic bullet approach [6]. Previously, sdAbs able to bind small molecules (caffeine and methotrexate) or toxins (botulinum, ricin, cholera, and scorpion), and viruses (rotavirus, HIV, vaccinia and Marburg) have been isolated [7, 8].

The remarkable proof-of-principle studies published since then point to a tremendous diagnostic and therapeutic potential of single-domain antibody reagents derived from these heavy-chain antibodies. Numerous sdAbs have already proven useful for basic research and improved diagnostic tools. In vivo studies have underscored the favorable biodistribution of sdAbs, including deep penetration into dense tissues and rapid elimination via kidney. sdAbs should also prove useful for neutralizing soluble extracellular proteins including toxin components.

This study aims to develop a library of novel format stable single-chain nanobody library against alkaline phosphatase without the disadvantages of conventional antibodies that can have therapeutic, diagnostic, and cosmetic use as well as food supplement as nutraceuticals. We described here the methods of isolating camelid antibodies (VHH or variable heavy-chain antibodies) and generating an antibody repertoire for further downstream screening for specific uses. We believe that camelid antibodies will be a method of choice to control infectious disease agents.

## 10.2 Materials and Methods

### 10.2.1 Immunized Protocol

Immunized male animal was Kachchi and Jaisalmeri breed. Immunized animal was at age of three years. Every seven days after higher dose applied and total 105 days immunized. At first, 100 µg of alkaline phosphate enzyme (SRL, Cat. No. 0148190) was mixed with 1 ml PBS and 1 ml Freund adjuvant (Sigma). Total volume was 2 ml. The enzyme mixed around 25–30 min by vigorous shaking. When the mixture was in gel formation, we stop mixing. On the first day, 100 µg of enzyme was injected to the camel. After seven days, higher dose of 150 µg of enzyme adjuvant mixture subcutaneously was injected. Total 105 days, animal was killed and then blood was collected from immunized animal and control animal. Control animal was injected only PBS.

### 10.2.2 Isolation of Antigen-Specific Nanobodies

(a) **Separation of peripheral blood lymphocytes:** 5 ml of anticoagulant fresh blood was taken and mixed with 0.9 % NaCl solution (SRL, cat. No. 1949134) (nuclease-free water) in a 15-ml Falcon centrifuge tubes. Before Hisep 1077 (Sigma-Aldrich) used, it was kept outside at room temperature. Added slowly 2.5 ml Hisep 1077

(Sigma-Aldrich) in a 15-ml Falcon centrifuge tubes. Blood mixture was added overlap to the Hisep 1077. Care was taken so that blood mixture and Hisep were in separate layer. Carefully centrifuged (REMI, cat. No. R 23-2/10/) the mixture of blood at 2800 rpm for 20 min at room temperature. Three distinguished layers were observed, in which top layer was plasma, interphase appeared white ring which was peripheral blood lymphocyte, and the bottom layer was Hisep. Interphase was carefully collected to a new 1.5-ml Eppendorf tube; equal volume of freshly prepared PBS (1 × with nuclease-free water) was added for washing and then centrifuged (REMI, cat. No. R 23-2/10/) at 2200 rpm for 10 min at 4 °C [9–11]. Decanted supernatant. Cell counted with the help of hemocytometer (Neubauer-improved, REF 06 100 10). Cell can be stored at –20 °C in RNAlater (RNAlater Solution, Ambion, Life technologies, Lot. No. 1211035) for a long time without freezing and thawing [9–11].

(b) **RNA isolation from Peripheral Blood Lymphocyte:** Sample was taken from –20 °C and kept at room temperature for 10 min. 250 µl of sample was taken and 750 µl Trizol (Ambion, Life technologies, Cat. No. 15596-026) was added. The sample was resuspended by several times by pipetting. Sample was incubated for 5 min at room temperature. 200 µl of chloroform (MERCK, Batch No. IF11610206) was added in 1-ml TRIZOL (Ambion, Life technologies) cap tube and shaken vigorously or vortexed (REMI, Model No. CM 101) for 20–30 s and then incubated at room temperature for 5 min. Finally, the sample was centrifuged (VISION-Model No. VS-15000CFNII) at 12,000 rpm for 15 min at 4 °C. Only 300 µl of sample (upper aqueous phase) was taken carefully and kept it in a new tube and added with 100 % chilled alcohol (MERCK, Lot. No. K44583383), made up to 1.5 ml volume. The sample was kept at –20 °C for next day use. Next day, sample was centrifuged (VISION-Model No. VS-15000CFNII) at

13,000 rpm for 10 min at 4 °C. The supernatant was removed and only the pellet was taken to perform further procedure. 400 µl of 75 % chilled alcohol (MERCCK, Lot. No. K44583383) (prepared by nuclease-free water, Himedia, ML064-10X 500ML) as added and the sample was inverted 4–5 times and then centrifuged (VISION-Model No. VS-15000CFNII) at 9000 rpm, at 4 °C for 5 min. The supernatant was discarded very carefully by pipetting. All the tubes were kept inside the Laminar Air Flow ( ) for air-drying. 20 µl of nuclease-free water (Himedia, ML064-10X500ML) [12] was added. Eluted sample was treated with DNase I enzyme (Invitrogen, Cat. No. 18068-015, 1 U/µl). 1 µg of RNA sample was taken (10 µl) with 2 µl of Dnase reaction buffer (10×) and 1 µl of Dnase I enzyme. 7 µl of nuclease-free water (Himedia, ML064-10X500ML) was added. Now, the total volume was 20 µl. The total sample was incubated at room temperature, for 15 min and 1 µl of 25 mM EDTA (Invitrogen, Cat. No. 18068-015) solution was added. Heat inactivated the enzyme activity at 65 °C for exactly 10 min [12].

- (c) **First-strand cDNA synthesis:** Total RNA sample was taken and 8 µl of Random Hexamer (Bioline, 100 µg/ml) was added and mixed well properly, then incubated at 70 °C for 10 min, 25 °C for 15 min, and, finally, stored at 4 °C. In this mixture, 6 µl of strand buffer (Invitrogen, 5×), 3 µl of DTT (Invitrogen, 0.1 M), 6 µl of dNTPs (Taqara, 2.5 mM) mixture were added also with 1 µl of nuclease-free water (Himedia, ML064-10X500ML) and 1 µl of reverse transcriptase (Invitrogen, 200 U/µl). The PCR (Applied biosystems Veriti™ 96-Well Fast Thermal Cycler, 0.1 ml, Invitrogen,) was set at 25 °C for 10 min, 37 °C for 60 min, 42 °C for 60 min, 80 °C for 15 min, and then stored at 4 °C. Sample was stored at -20 °C for long-time storage without freezing and thawing [13].
- (d) **First PCR:** 2 µl of buffer was taken (10×). 2 µl of dNTPs (2.5 mM), 1 µl of forward

primer (Call 001), 1 µl of reverse primer (Call 002), 0.5 µl of Taq polymerase (Invitrogen, 5 U/µl), 11.5 µl of nuclease-free water (Himedia, ML064-10X500ML) were added with the buffer. Total reaction volume was 20 µl. The temperature was set at 95 °C for 5 min, 95 °C for 45 s, 57 °C for 45 s, 72 °C for 45 s, 72 °C for 10 min, and 4 °C for store. PCR was run for 35 cycles. Each reaction product was checked by 1 % agarose gel (Invitrogen, UltraPure™ Agarose, Cat. No. 16500-100) using gel casting tray (HinTech, India, 5 in. × 2.6 in., 8 comb). 5 µl of sample was loaded in each well depends on the DNA concentration. Ran around 1 h (100 V, Tarson, Electrophoresis power supply, model No. MC 01) in TAE buffer 1 × used Electrode, code No. 7145, PCR product was 700 bp [13]. Gel Doc (BioRad, model No. Universal Hood, Serial No. 76S/08119) and Quantity One software version 4.6.3 were used for imaging analysis.

- (e) **Gel elute first PCR product: (Himedia Hipurification kit, Cat. No. MB539)**

**Prepared Washing Buffer**—250 µl of gel wash buffer was mixed with 1000 µl ethanol (Made in China, XK-13-011-00009). Two reagents were mixed properly. 700-bp product was cut with the help of sharp knife and kept it in an Eppendorf tube (Tarson, cat. No. 500020). 100 µl of gel-binding buffer was added in the same tube and kept it in the water bath, to maintain the temperature at 55 °C for 10 min and the gel solution was mixed continuously to dissolve. All solutions were taken and poured it in a fresh column and then centrifuged (VISION-Model No. VS-15000CFNII) at 12,000 rpm for 2 min 30 s. at 27 °C. 300 µl of gel-binding buffer was added and the sample was centrifuged (VISION-Model No. VS-15000CFNII) at 12,000 rpm, for 2 min 30 s at 27 °C. Mixed buffer was discarded and then 600 µl of washing buffer was added. Again the sample was centrifuged (VISION-Model No. VS-15000CFNII) at

12,000 rpm for 2 min 30 s at 27 °C. The empty column was centrifuged at 12,000 rpm, for 2 min at 27 °C. A new column was taken with 20 µl of elution buffer. The sample was centrifuged (VISION-Model No. VS-15000CFNII) at 12,000 rpm, at 4 °C, for 2 min 30 s. Column was opened, and only the supernatant was taken into another microcentrifuge tube (Tarson, cat. No. 500020). Sample was stored at -20 °C.

- (f) **Second PCR:** 1.5 µl of sample was taken with 1.5 µl of forward primer pstI (283.77 pmol/µl in 200 µl H<sub>2</sub>O, T<sub>m</sub> 67 °C) 1.5 µl of Not I (454.45 pmol/µl in 200 µl H<sub>2</sub>O, T<sub>m</sub> 74 °C), 3 µl of 10× reaction buffer, 3 µl of dNTPs, 1 µl of Taq polymerase enzyme (Invitrogen, cat. No. 11615-010, 5 U/µl), and 18.5 µl of nuclease-free water (Himedia, ML064-10X500ML). The temperature was set at 95 °C for 5 min, 95 °C for 45 s, 61 °C for 45 s, 72 °C for 45 s, 72 °C for 10 min, and 4 °C store [13]. Reaction product was checked in 1 % agarose gel (Invitrogen, UltraPure™ Agarose, Cat. No. 16500-100) and 400-bp product was obtained by using gel casting tray (5 in. × 2.6 in.) and electrode (Tarson, 100 V, 1 h). Total sample was loaded and 400-bp product was eluted by using Himedia Purification kit (Cat. No. MB512-20 PR). Gel Doc (BioRad, model No. Universal Hood, Serial No. 76S/08119) and Quantity One software version 4.6.3 were used for imaging analysis.
- (g) **Purified product digest by PstI and NotI:** Preparation of master mix for NotI enzymatic digestion. 16.25 µl of NEB buffer was added with 1 µl of NotI enzyme (NEB, cat. No. R3189S, 20 U/µl), 1.5 µl of BSA, and 85.25 µl of nuclease-free water (Himedia, ML064-10X500ML). The sample was mixed up properly with pipette and 16 µl of master mix was taken in each tube. 9 µl of sample was added. All reactions were carried out in Eppendoff tube. The sample was incubated for exactly 1 h, at

37 °C, in BOD. Master mix for PstI (NEB, cat. No. R3140S, 20 U/µl) was prepared for enzymatic digestion. 3.5 µl of NEB buffer was added with 1 µl of PstI enzyme (NEB, cat. No. R3140S, 20 U/µl), 1 µl of BSA, 29.5 µl of nuclease-free water (Himedia, ML064-10X500ML). 5 µl of master mix was taken into 22 µl previously digested sample, mixed up by pipetting, and incubated exactly for 45 min, at 37 °C, in BOD. Digested product was kept in 4 °C. Sample was stored at -20 °C for long-time storage [13, 14]. Reaction product was checked in 1 % agarose gel (Invitrogen, UltraPure™ Agarose, Cat. No. 16500-100) and 400-bp product was obtained by using gel casting tray (5 in. × 2.6 in.) and electrode (Tarson, 100 V, 1 h). Gel Doc (BioRad, model No. Universal Hood, Serial No. 76S/08119) and Quantity One software version 4.6.3 were used for imaging analysis.

- (h) **Plasmid isolation (PHEN4 vector)—maxi preparation:** (i) Alkaline solution-I: 50 mM glucose (HIMEDIA, MB025-500G), 25 mM Tris-Cl (SRL, Extrapure, cat. No. 204991) (pH 8.0), 10 mM EDTA (Chromous Biotech, Cat. No. Bio 13, conc. 0.5 M) (pH 8.0). Solution-I was prepared from standard stocks in batches of ~100 ml autoclave for 15 min, at 15 psi (1.05 kg/cm<sup>2</sup>) on liquid cycle, and stored at 4 °C. (ii) Alkaline solution-II: 0.4 N NaOH (BDH, AnalaR, Product No. 89021) (freshly diluted from 10 N stock), 2 % (W/V) SDS (MERCK, Batch No. MF9M591363). (iii) Alkaline solution-III: 60 ml of 5 M potassium acetate (MERCK, Batch No. QL4Q643063), 11.5 ml of glacial acetic acid (MERCK, 99–100 %, Batch No. CF4C640570), and 28.5 ml of nuclease-free water (Himedia, ML064-10X 500ML). The resulting solution was 3 M with respect to potassium and 5 M with respect to acetate. The solution was stored at 4 °C and transferred to an ice bucket just before use. (iv) STE buffer: sodium chloride-Tris-EDTA buffer, 10×- pH 8.0. 10× solution containing 100 mM Tris-HCl (SRL, Extrapure, cat.

No. 204991), 10 mM EDTA (Chromous Biotech, Cat. No. Bio 13, conc. 0.5 M) (pH 8.0), and 1 M NaCl (SRL, extrapure AR, Batch No. T.826207). Autoclaved.

**Cell harvested:** Early morning, 5 ml primary culture was inoculated at 37 °C, in BOD shaker at 160 rpm. The mouth of the shaker was closed. Care was taken for decontamination. On same day evening, turbidity for bacterial growth was checked. 0.5 % inoculum was inoculated to 50 ml LB (HIMEDIA, M1245-500G) ampicillin (Bio-line, Cat. No. Bio-87025) medium and kept in BOD shaker, at 160 rpm for overnight culture. Next day, 50 ml culture media was taken in a sterilized centrifuge tube (Tarson, Cat. No. 542040) inside the Laminar Air Flow and the mouth was closed tightly and then culture media was centrifuged (HERMLE, Model No. Z323K, Made in Germany) at 4000 rpm, for 6 min, at 4 °C temperature. Supernatant was discarded and only the hard pellet was taken. 10 ml of STE buffer was added. The tube was vortexed for 1 min so that precipitate will be dissolved. Do not vortex long time, so that genomic DNA came out. Genomic DNA was taken in one tube and centrifuged at 9000 rpm for 6 min at 4 °C. Only the pellet was taken and 10 ml 1 ml alkaline solution-I, freshly prepared Lysozyme (stock 10 mg/ml, Amresco) were added and vortexed for 1 min, and then incubated for 10 min in an ice bucket. After incubation, 20 ml freshly prepared alkaline solution-II was added and inverted mixing several times. Tubes were kept in ice exactly for 5 min. 15 ml of chilled solution-III was added. The reagent was mixed three times and incubated for 30 min (maximum) in ice, and then centrifuged (HERMLE, Model No. Z323K, Made in Germany) at 13,000 rpm for 15 min, at 4 °C. Supernatant was taken by filter paper. Around 40 ml supernatant was taken. 0.7–0.8 volume of supernatant was added with 32 ml of isopropanol. Mixing was carried out by inverted position by 2–3 times, incubated at room temperature for 20 min, and then

centrifuged (HERMLE, Model No. Z323K, Made in Germany) at 13,000 rpm for 15 min at room temperature. Supernatant was discarded by using paper towel. Only the pellet was taken and 5 ml 70 % alcohol (used Merck 100 % alcohol, added nuclease-free water) was added. The sample was vortexed so that the pellet was partially dissolved and centrifuged (HERMLE, Model No. Z323 K, made in Germany) at 13,000 rpm for 15 min, at 4 °C. Alcohol was decanted and pellet was completely dried. Pellet was stored in –20 °C for overnight. Next day, 500 µl nuclease-free water (Himedia, ML064-10X500ML) was added and thoroughly mixed up. 30 µl Rnase A (Invitrogen, Cat. No. 12091-021) was added and kept in BOD incubator (APS Enterprise, Kolkata) for 3 h at 37 °C [15].

- (i) **Plasmid purification by phenol–chloroform–isoamyl alcohol:** 500 µl sample was taken in a Eppendoff tube and equal amount of saturated phenol (HIMEDIA, Cat. No. MB082-100ML): isoamyl alcohol: chloroform (HIMEDIA, Cat. No. MB115-500ML) in 25:24:1 ratio was added and vortexed (REMI, Model No. CM 101) vigorously at least 3 min. Then, the sample was centrifuged (VISION-Model No. VS-15000 CFNII) 13,000 rpm, 15 min, at 4 °C. There were three distinguished layers. Only the aqueous phase was taken. The experiment was repeated twice. 3 M 0.1 volume of sodium acetate (MERCK, Cat. No. 6227), pH 5.2 was added and incubated the sample for 10 min at room temperature. 0.8 volume of isopropanol (SRL, Cat. No. 094773) was added and incubated for 20 min. The sample was kept at –20 °C for overnight. Next day, the sample was centrifuged (VISION-Model No. VS-15000CFNII) at 13,000 rpm, for 15 min at 4 °C. The supernatant was decanted and 500 µl of 70 % alcohol (MERCK, Made in Germany, Lot. No. K44583383) was added into the pellet. And the sample was vortexed and centrifuged (VISION-Model No. VS-15000CFNII) at 13,000 rpm for 15 min. Alcohol was decanted, and the pellet

was kept in Laminar Air flow for drying. Pellet should not be dried completely. 500  $\mu$ l of nuclease-free water (ML064-10X500ML) was added, and the pellet was dissolved and reaction product was checked in 1 % agarose gel (Invitrogen, UltraPure™ Agarose, Cat. No. 16500-100) [15]. Gel Doc (BioRad, model No. Universal Hood, Serial No. 76S/08119) and Quantity One software version 4.6.3) were used for imaging analysis.

(j) **PHEN4 vector digested by PstI and NotI:**

DNA sample was taken 2  $\mu$ l (2  $\mu$ g/ $\mu$ l) and PstI NEB enzyme (cat. No. R3140S, 20 u/ $\mu$ l), 2.5  $\mu$ l of NEB cut smart buffer (10 $\times$ ), 1  $\mu$ l of BSA were added, and finally 18.5  $\mu$ l of nuclease-free water. Total volume 25  $\mu$ l was kept in 37 °C inside BOD incubator (APS ENTERPRISE, Kolkata, India) for exactly 15 min. Immediately after digestion, mixture was kept in 4 °C. Master mix for NotI enzymatic digestion was prepared. 2  $\mu$ l of NotI enzyme (NEB, Cat. No. R3189S, 20 u/ $\mu$ l), 1  $\mu$ l of BSA, and 3  $\mu$ l of NEB buffer (10 $\times$ ) were taken. 24  $\mu$ l of nuclease-free water (ML064-10X500ML) was added. Total reaction volume 30  $\mu$ l was distributed in 6 1.5-ml Eppendorf tubes, and each tube contained 5  $\mu$ l of master mix. 5  $\mu$ l of digested product (PstI) was added previously in each tube and kept in 37 °C in BOD incubator for 30 min and then immediately kept in 4 °C refrigerator. 1  $\mu$ l of XhoI (NEB, 10 U/ $\mu$ l) sequence was added in each tube and kept it in BOD incubator (APS ENTERPRISE, Kolkata, India) for another 30 min. Sample was stored at -20 °C [13, 16]. Gel Doc (BioRad, model No. Universal Hood, Serial No. 76S/08119) and Quantity One software version 4.6.3 were used for imaging analysis.

(k) **Gel elute digested phen4 product: (Himedia Hipurification kit, Cat. No. MB 539)**

**Prepared Washing Buffer**—250  $\mu$ l gel wash buffer was mixed with 1000  $\mu$ l of ethanol. Two reagents were mixed properly. PHEN4 digested product was checked in 1 % freshly prepared agarose gel (Invitrogen, UltraPure™ Agarose, Cat. No. 16500-100). Around 4500 bp product was cut with the

help of sharp knife and kept it in an Eppendorf tube. 100  $\mu$ l of gel-binding buffer was added in the same tube and kept it in the water bath at the temperature 55 °C for 10 min. The gel solution was mixed continuously for dilution. All solution were taken and poured it in a fresh column and then centrifuged (VISION-Model No. VS-15000CFNII) at 12,000 rpm for 2 min 30 s at 27 °C. 300  $\mu$ l gel-binding buffer was added and centrifuged (VISION-Model No. VS-15000CFNII) at 12,000 rpm, for 2 min 30 s at 27 °C. The mix buffer was discarded. 600  $\mu$ l of washing buffer was added and again centrifuged (VISION-Model No. VS-15000CFNII) at 12,000 rpm, 2 min 30 s at 27 °C. And the empty column was centrifuged (VISION-Model No. VS-15000CFNII) at 12,000 rpm, for 2 min at 27 °C. A new column was taken. 20  $\mu$ l of elution buffer. was added and centrifuged (VISION-Model No. VS-15000CFNII) at 12,000 rpm, at 4 °C, for 2 min 30 s. Column was opened and only the liquid was taken into the microcentrifuge tube. Sample was stored at -20 °C. Gel Doc (BioRad, model No. Universal Hood, Serial No. 76S/08119) and Quantity One software version 4.6.3 were used for imaging analysis.

(l) **Ligation reaction:** 1  $\mu$ l of eluted digested Phen4 vector (50 ng/ $\mu$ l), 3  $\mu$ l of 2nd PCR double-digested product (around 12 ng/ $\mu$ l), 5  $\mu$ l of ligation buffer 5  $\mu$ l, and 1  $\mu$ l of T4 ligation enzyme were added. Now, total reaction volume was 10  $\mu$ l. Reaction mixture was kept at 17 °C, overnight in BOD (care was taken so that temp. distributed equally). Next morning, reaction mixture was taken out and kept in -20 °C [13, 17].

(m) **Competent cell preparation of TG1:**

200  $\mu$ l of TG1 bacteria culture was inoculated in 5 ml LB broth (HIMEDIA, M1245-500G). No antibiotic was added. The mouth of the tube was closed; before closing the mouth, the mouth of the tube was hated to reduce contamination. The tube was kept in BOD shaker (AMALGAMATE, India), overnight for 37 °C, at 150 rpm.



Next day, turbidity of the bacterial culture was observed to confirm growth. 0.1 % bacterial culture was inoculated into 50 ml LB broth in a 250-ml conical flask and kept in BOD shaker incubator (AMALGAMATE, India), at 150 rpm for 50–60 min. O.D was checked every 30 min at 600 nm. When O.D was 0.3, immediately the culture was kept in ice to stop further growth. 50 ml of culture was measured in a centrifuge tube and centrifuged (HERMLE, Model No. Z323 K, Madein Germany) at 2700 rpm, for 10 min, at 4 °C. Supernatant was discarded and the precipitate was dried with the help of standing position and paper towel was used to drain out the media. chilled 0.1 M CaCl<sub>2</sub> (HIMEDIA, Cat. No. MB034-500G) was added and kept it in ice for 20 min and then centrifuged (HERMLE, Model No. Z323K, Made in Germany) at 2700 rpm, for 10 min at 4 °C. The precipitate was observed and dissolved it as much as required in 1.5 ml nuclease-free water (Himedia, ML064-10X 500ML). One Eppendoff tube rack was taken and filled with little amount of water and all competent cells. The tube was kept in the rack, so that temperature equally distributed and kept it in 4 °C for overnight. Next day, transformation was carried out [13, 15, 18].

- (n) **Transformation:** Three-competent cell tube was taken: labeled ligated product, positive control, and negative control. Inside the hood, DNA was added. Ligated product was Phen4 vector and desired gene product, positive control was Phen4 vector only, and negative control was nothing. It is gently tapped for mixing and kept in ice-chilled bucket for 30 min. Heat shock was maintained at the exact temperature of 42 °C. All Eppendoff tubes were closed with parafilm. All the tubes were kept at 42 °C for exact 90 s. Then, the tubes were kept in ice for 15 min exactly. 900 µl of LB (HIMEDIA, M1245-500G) broth was added in each tube for recovery of the cell and kept it 37 °C for

1 h in a BOD shaker, at 150 rpm. From this, 200 µl of transformed cells were taken and put on LB agar plate containing ampicillin (Bioline, Cat. No. Bio 87025) The sample was spread thoroughly with the help of the sterilized spreader and kept it for some time for drying inside the Laminar Air Flow. All the tubes were kept inverted in position for overnight growing, at 37 °C, in BOD. Next day, colony was observed and compared with positive and negative controls [15].

- (o) **Colony screening:** Before colony screening, wooden toothpick was sterilized by autoclave. Ten colonies were picked up from the ligated plate as it is mentioned before on top of the agar plate. Individual colony with toothpick was selected into 6 ml LB broth (HIMEDIA, M1245-500G) and ampicillin (Bioline, Cat. No. Bio-87025) mixture. Care was taken, so that contamination was less. Spirit lamp was used inside the Laminar Air Flow. The edge of the test tube was heated and immediately closed with cotton plug, it was kept at 37 °C, for overnight growth, at 150 rpm in BOD shaker [13, 19].
- (p) **Colony PCR using GIII primer:** PCR on 10 independent colonies was performed in order to determine the vector with the right insert size. dNTPs (2.5 mM), universal reverse primer (Bioserve Accelerating Discovery, 20 µM) and GIII primer (Bioserve Accelerating Discovery, 20 µM), Taq DNA polymerase (Invitrogen 2.5 u/µl), PCR buffer were combined and the total volume was made up to 20 µl. A single colony was touched with sterile toothpick. Cells were taken into the PCR by stirring the toothpick in the reaction mix centrifuged for 35 cycles and the temperature was 95 °C for 5 min, 95 °C for 45 s, 57 °C for 45 s, 72 °C for 45 s, 72 °C for 10 min, and 4 °C for storage. By using 5 µl of each reaction for analytical gel electrophoresis on a 1 % agarose gel (Invitrogen, UltraPure™ Agarose, Cat. No. 16500-100) in 1 × TAE buffer, the sample was checked. DNA smart ladder (PUREGENE, Cat. No. PG300-500DI) was

preferably used as DNA molecular weight marker (100–3000 bp). The PCR product from the vector with a full VHH sequence was 700 base pairs [13, 20, 21]. Gel Doc (BioRad, model No. Universal Hood, Serial No. 76S/08119) and Quantity One software version 4.6.3 were used for imaging analysis.

- (q) **Preparation of phagemids:** 100  $\mu$ l of library stock was inoculated into 100 ml TY containing ampicillin (Bioline, Cat. No. Bio-87025, 100  $\mu$ g/ml) and glucose (2 %). Growth at 37 °C for 2–3 h with shaking at 150 rpm.  $10^{12}$  pfu M13KO7 helper phage (NEB, Cat. No. N0315S, Conc.  $1.0 \times 10^{11}$  pfu/ml) was added and incubated for 30 min without shaking at room temp. and then centrifuged (VISION-Model No. VS-15000CFNII) at 4000 rpm for 10 min. Cells were resuspended in 300 ml  $2 \times$  TY containing ampicillin (Bioline, 100  $\mu$ g/ml) and kanamycin (Bioline, 70  $\mu$ g/ml), incubated overnight at 37 °C, with shaking at 150 rpm, and then centrifuged (VISION-Model No. VS-15000CFNII) at 8000 rpm, for

30 min at 4 °C. Supernatant containing phages was transferred to a fresh tube. 1/6th volume, that is, 50 ml, of PEG (HIMEDIA, MB149-500G)/NaCl (SRL, cat. No. 194-9134) solution was added and mixed well by inverting several times and then placed in ice for 30 min. The solution was centrifuged (VISION-Model No. VS-15000CFNII) at 4000 rpm, for 30 min, at 4 °C. Supernatant was removed. The tubes were allowed to drain by using paper tissue. phage pellet was resuspended in PBS to final volume 1 ml and then centrifuged (VISION-Model No. VS-15000CFNII) at 13,000 rpm, for 5 min to remove bacterial cells, debris. The supernatant was transferred to a fresh micro-centrifuge tube [22–24].

### 10.3 Results

See Figs. 10.1, 10.2, 10.3, 10.4, 10.5, 10.6, 10.7, and 10.8



**Fig. 10.1** 2nd PCR from alkaline phosphatase from 1st PCR sample. Using 1 % agarose gel. For image analysis, Gel Doc (Bio Rad, Serial no. 76S/08119, software Quantity One, version 4.6.3)

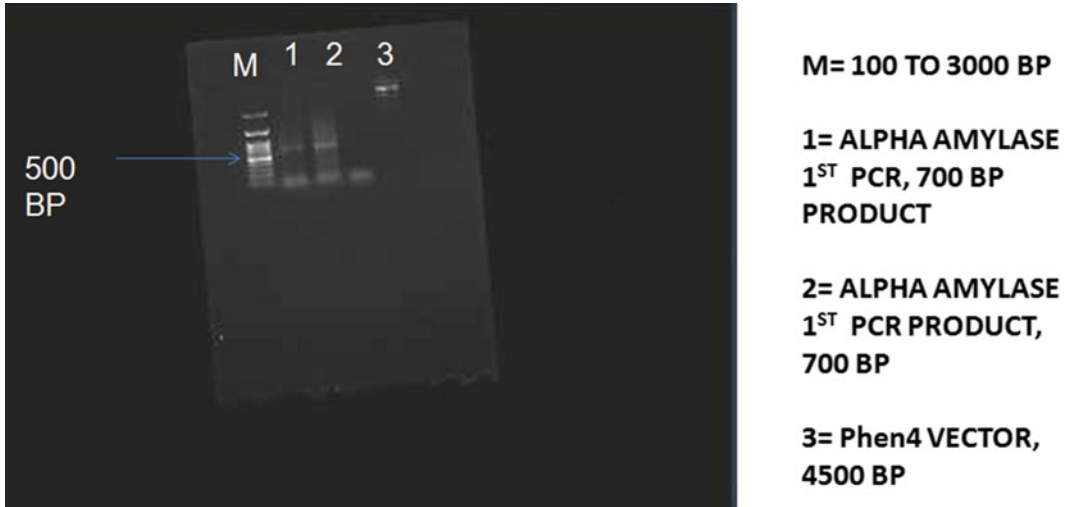


**Fig. 10.2** 1st PCR product of alpha amylase from c-DNA. Using 1 % agarose gel. For image analysis used Gel Doc (Bio Rad, Serial no. 76S/08119 software Quantity One, version 4.6.3)

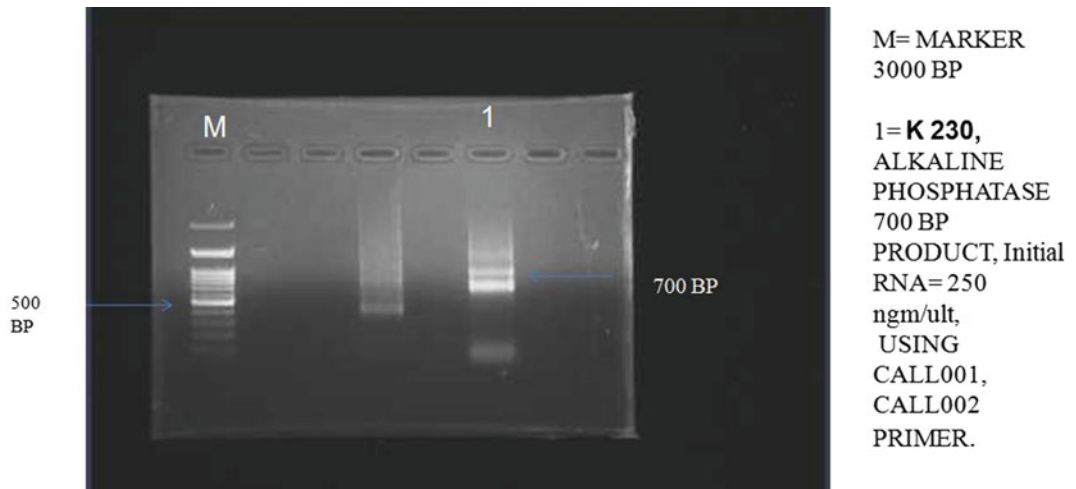


**Fig. 10.3** 1st PCR product of immunized alkaline phosphatase camelid blood. Using 1 % agarose gel. For image analysis used Gel Doc (Bio Rad, Serial no. 76S/08119, Software Quantity One, version 4.6.3)

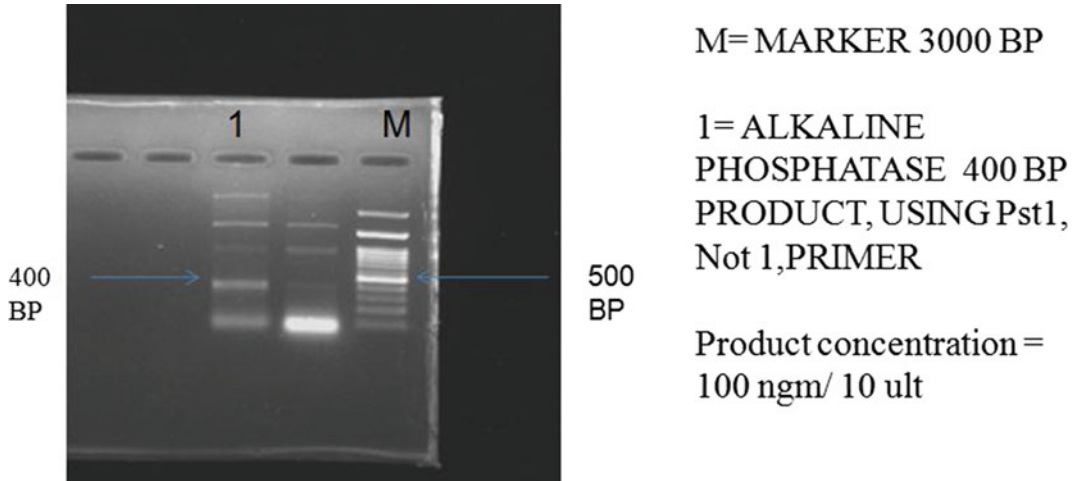


**Fig. 10.4** 2nd PCR product of immunized alkaline phosphatase camelid blood. Using 1 % agarose gel. For image analysis used Gel Doc (Bio Rad, Serial no. 76S/08119, software Quantity One, version 4.6.3)

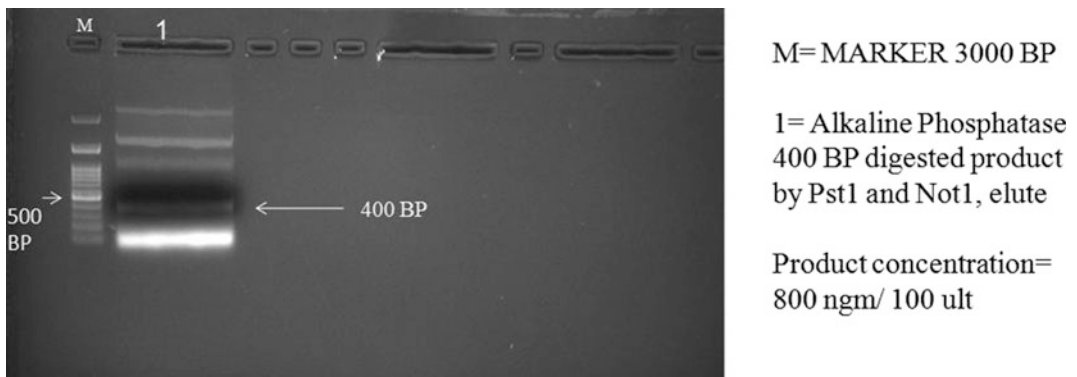


**Fig. 10.5** Alkaline phosphatase digested by Pst1 and Not1 and elute. Using 1 % agarose gel. For image analysis used Gel Doc (Bio Rad, Serial no. 76S/08119, software Quantity One, version 4.6.3)

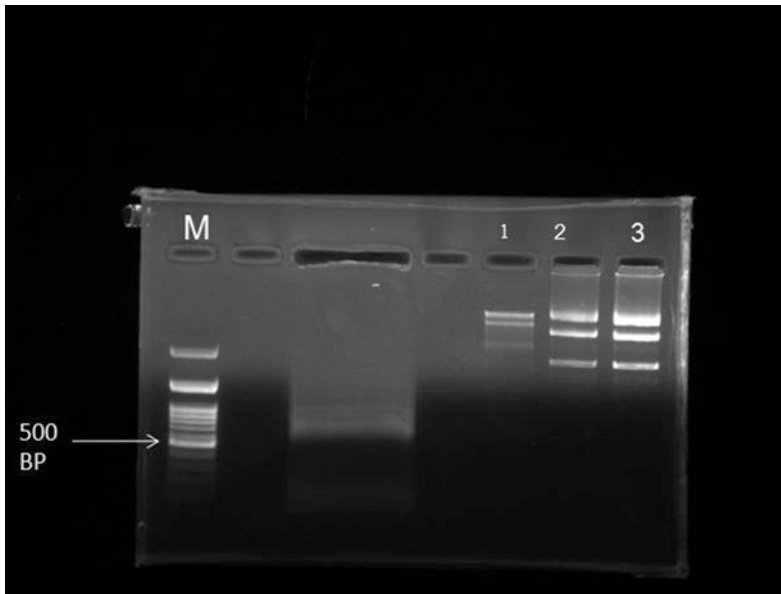


**Fig. 10.6** Phen4 plasmid isolation by alkaline solution-I, II, III. Using 1 % agarose gel. For image analysis used Gel Doc (Bio Rad, Serial no. 76S/08119, software Quantity One, version 4.6.3)

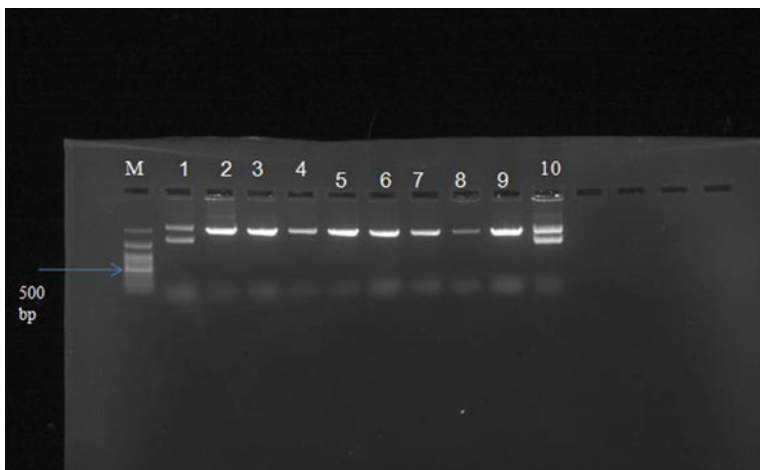


**Fig. 10.7** Phen4 digested by Pst1, not1 product and XhoI sequence added. Using 1 % agarose gel. For image analysis used Gel Doc (Bio Rad, Serial no. 76S/08119, software Quantity One, version 4.6.3)

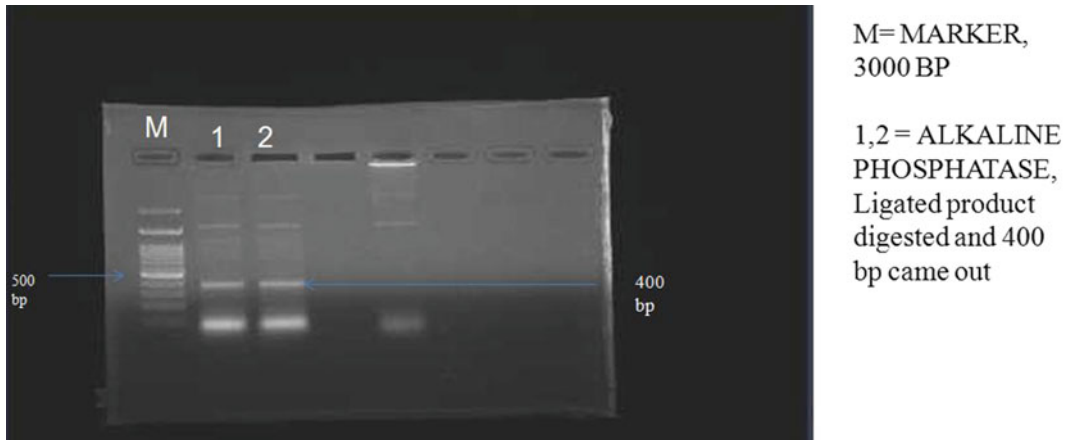


**Fig. 10.8** After digestion of ligated product by Pst1 and Not 1, 400 bp was come out. Using 1 % agarose gel. For image analysis used Gel Doc (Bio Rad, Serial no. 76S/08119, software Quantity One, version 4.6.3)

## References

- Saerens D, Muyldermans S, Ghassabeh GH, Isolation of antigen—specific nanobodies. *Antibody Eng.* 2010;2.
- Graef RR, et al. Isolation of a highly thermal stable llama single domain antibody specific for *Staphylococcus aureus* enterotoxin B. *BMC Biotechnol.* 2011;11:86.
- Jacqueline M, et al. Camelid single domain antibody (VHH) as neuronal cell intrabody binding agents and inhibitors of *Clostridium botulinum* neurotoxin proteases. *Toxicon* 2010;1–9.
- Monegal A, et al. Immunological application of single-domain llama recombinant antibodies isolated from a naive library. *Protein Eng. Des. Sel.* 2009;1–8.
- De Genst E, et al. Chemical basis for the affinity maturation of a camel single domain antibody. *Biol. Chem.* 2004;53593–53601.
- Dolk Edward, et al. Isolation of llama antibody fragments for prevention of dandruff by phage display in shampoo. *Appl. Environ. Microbiol.* 2005;71(1):442.
- Wesolowski Janusz, et al. Single domain antibodies: promising experimental and therapeutic tools in infection and immunity. *Med. Microb. Immunol.* 2009;198:157–74.
- Davies Julian, Riechmann Lutz. Single antibody domains as small recognition units: design and in vitro antigen selection of Camelized, human VH domains with improved protein stability. *Protein Eng.* 1996;9(6):531–7.
- Amos DB, Pool P. HLA typing. In: Rose NR, Friedman H, editors. *Manual of clinical immunology.* Washington, DC: American Society for Microbiology; 1976. p. 797–804.
- Winchester RJ, Ross G. Methods for enumerating lymphocyte populations. In: Rose NR, Friedman H, editors. *Manual of clinical immunology.* Washington, DC: American Society for Microbiology; 1976. p. 64–76.
- Thorsby E, Bratlie A. A rapid method for preparation of pure lymphocyte suspensions. In: Terasaki PI, editors. *Histocompatibility testing;* 1970. p. 665–666.
- Sambrook J, Fritsch EF, Maniatis T. *Molecular cloning: a laboratory manual.* 2nd ed, vol. 3. NY: Cold Spring Harbor Laboratory Press, Cold Spring Harbor; 1989.
- Ghahroudi MA, Desmyter A, Wyns L, Hamers R, Muyldermans S. Selection and identification of single domain antibody fragments from camel heavy—chain antibodies. *FEBS Lett.* 1997;414:521–6.
- Alvarez-Reuda N, Behar G, Ferre V, Pugniere M, Roquet F, Gastinel L, Jacquot C, Aubry J, Baty D, Barbet J, Birkle S. Generation of llama single-domain antibodies against methotrexate, a prototypical hapten. *Mol Immunol.* 2007;44:1680–90.
- Sambrook J, Fritsch EF, Maniatis T. *Molecular cloning: a laboratory manual,* 2nd edn, vol. 1. NY: Cold Spring Harbor Laboratory Press, Cold Spring Harbor; 1989.
- Koch-Nolte F, Reyelt J, Schöbow B, Schwarz N, Scheuplein F, Rothenburg S, Haag F, Alzogaray V, Cauerhff A, Goldbaum FA. Single domain antibodies from llama effectively and specifically block T cell ecto-ADP-ribosyltransferase ART2.2 in vivo. *FASEB J.* 2007;21:3490–8.
- Ladenson RC, Crimmins DL, Landt Y, Ladenson JH. Isolation and characterization of a thermally stable recombinant anti-caffeine heavy-chain antibody fragment. *Anal. Chem.* 2006;78:4501–8.
- Lauwereys M, Ghahroudi MA, Desmyter A, Kinne J, Hölzer W, De Genst E, Wyns L, Muyldermans S.

- Potent enzyme inhibitors derived from dromedary heavy-chain antibodies. *EMBO J.* 1998;17:3512–3520.
19. Maass DR, Sepulveda J, Pernthaner A, Shoemaker CB. Alpaca (*Lama pacos*) as a convenient source of recombinant camelid heavy chain antibodies (VHHs). *J. Immunol. Methods.* 2007;324:13–25.
  20. Nguyen VK, Muyldermans S, Hamers R. The specific variable domain of camel heavy chain antibodies is encoded in the germline. *J. Mol. Biol.* 1998;257:413–8.
  21. Nguyen VK, Hamers R, Wyns L, Muyldermans S. Camel heavy-chain antibodies: diverse germline VHH and specific mechanisms enlarge the antigen-binding repertoire. *EMBO J.* 2000;19:921–31.
  22. Nguyen VK, Desmyter A, Muyldermans S. Functional heavy-chain antibodies in camelidae. *Adv. Immunol.* 2001;79:261–96.
  23. Van der Linden R, de Geus B, Stok W, Bos W, van Wassenaer D, Verrips T, Frenken L. Induction of immune responses and molecular cloning of the heavy chain antibody repertoire of *Lama glama*. *J. Immunol. Meth.* 2000;240:185–95.
  24. Vu KB, Ghahroudi MA, Wyns L, Muyldermans S. Comparison of llama VH sequences from conventional and heavy chain antibodies. *Mol. Immunol.* 1997;34:1121–31.

# Development of a Novel Format of Stable Single-Chain Antibodies Against Alpha Amylase as Therapeutic Molecules

## 11.1 Introduction

Antibodies or immunoglobulins are sequestered in all vertebrates. Of them, camelids, nurse sharks, and spotted ratfish have been found to possess structurally different kinds of antibodies. These antibodies are composed of two heavy chains similar to conventional antibodies referred to as heavy-chain antibodies (HCAs) [1], but contrary to the structure found in conventional antibodies, they possess the lack of CH<sub>1</sub> domain [2]. Nanobodies are antibody-derived engineered therapeutic proteins that contain the unique structural and functional properties of naturally occurring heavy-chain antibodies. The nanobody technology was originally developed following the discovery that Camelidae (camels and llamas) possess fully functional antibodies that lack light chains. These heavy-chain antibodies contain a single variable domain (VHH) and two constant domains (CH<sub>2</sub> and CH<sub>3</sub>) [3].

One of the reasons behind the interest shown by the industry in VHH is that the single domain allows production in microorganisms. The high levels of production and the subsequent purification are very efficient, which enables cheap production of large quantities of VHHs. To select the VHH with the desired properties from a large collection of VHH, phage display is performed [4]. Phage display uses bacteria and bacterial viruses, known as bacteriophage, to select antigen-specific antibody fragments (in our case

VHH). This technology combines the VHH displayed on bacteriophage particles to the DNA encoding this VHH, which is present in the phage. One of the strengths of this method is this coupling of phenotype to genotype.

One of the most prominent advantages of VHHs over conventional antibodies is their performance at high temperatures which is evident from the fact that they can withstand incubation of even 2 h at high temperatures up to 90 °C [5].

In the industry, the applications using antibody technology are increasing rapidly as well. In medicine, antibodies are used as fusion proteins, to function as a carrier to target specific effector substances to a specific location, the so-called magic bullet approach [6]. Previously, sdAbs able to bind small molecules (caffeine and methotrexate), or toxins (botulinum, ricin, cholera, and scorpion), and viruses (rotavirus, HIV, vaccinia, and Marburg) have been isolated [7, 8].

The remarkable proof-of-principle studies published since then point to a tremendous diagnostic and therapeutic potential of single-domain antibody reagents derived from these heavy-chain antibodies. Numerous sdAbs have already proven useful for basic research and improved diagnostic tools. In vivo studies have underscored the favorable biodistribution of sdAbs, including deep penetration into dense tissues and rapid elimination via kidney. sdAbs should also prove useful for neutralizing soluble extracellular proteins including toxin components.



This study aims to develop a library of novel format of stable single-chain nanobody library against alkaline phosphatase without the disadvantages of conventional antibodies that can have therapeutic, diagnostic, and cosmetics use as well as food supplement as nutraceuticals. We described here the methods of isolating camelid antibodies (VHH or variable heavy chain antibodies) and generating an antibody repertoire for further downstream screening for specific uses. We believe that camelid antibodies will be a method of choice to control infectious disease agents.

## 11.2 Materials and Methods

### 11.2.1 Immunized Protocol

Immunized male animal was Kachchi and Jaisalmeri breed. Immunized animal was at the age of three years. Every seven days after higher dose applied and total 105 days immunized. At first, alpha amylase enzyme (SRL, Cat. No. 0148190) of 100 µgm was mixed with 1 ml PBS and 1 ml Freund adjuvant (Sigma). Total volume was 2 ml. Enzyme was mixed around 25–30 min by vigorous shaking. When the mixture was in gel formation, we stop mixing. On the first day injected 100 µgm enzyme into the camel. After seven days, higher dose of 150 µgm enzyme adjuvant mixture was subcutaneously injected. Total 105 days animal was killed, and then blood was collected from immunized animal and control animal. Control animal was injected with only PBS.

#### 11.2.1.1 Isolation of Antigen-Specific Nanobodies

(a) **Separation of peripheral blood lymphocytes:** 5 ml of anticoagulant fresh blood was taken and mixed with 0.9 % NaCl solution (SRL, Cat. No. 1949134) (nuclease-free water) in a 15-ml Falcon tube. Before Hisep 1077 (Sigma-Aldrich) was used, it was kept outside at room temperature. 2.5 ml Hisep 1077 (Sigma-Aldrich) was added slowly in a 1-ml Falcon tube. Added blood

mixture overlaps with the Hisep 1077. Care was taken so that blood mixture and Hisep were found in a separate layer. The mixture of blood (REMI, Cat. No. R 23-2/10/) was carefully centrifuged at 2800 rpm for 20 min at room temperature. We observed three distinguished layer in which top layer was plasma, interphase layer appeared white ring which was peripheral blood lymphocyte, and the bottom layer was Hisep. Interphase to a new 1.5-ml Eppendorf tube was carefully collected. Equal volume of freshly prepared PBS (1 × with nuclease-free water) was added for wash. Then, it was centrifuged (REMI, Cat. No. R 23-2/10/) at 2200 rpm for 10 min at 4 °C [9–11]. Decanted supernatant cell was counted with the help of hemocytometer (Neubauer-improved, REF 06 100 10). Cell can be stored at –20 °C in RNA-later (RNAlater Solution, Ambion, Life technologies, Lot. No. 1211035) for long time without freezing and thawing [9–11].

(b) **RNA isolation from peripheral blood lymphocyte:** Sample was taken from –20 °C and kept at room temperature for 10 min. 250 µl sample was taken and added 750 µl Trizol (Ambion, Life technologies, Cat. No. 15596-026). The sample was resuspended several times by pipetting. The sample was incubated for 5 min at room temperature. 200 µl chloroform (MERCK, Batch No. IF11610206) was added in 1-ml Trizol (Ambion, Life technologies) cap tube. It was shaken vigorously or vortexed (REMI, Model No. CM 101) for 20–30 s, incubated at room temperature for 5 min, and centrifuged (VISION-Model No. VS-15000CFNII) at 12,000 rpm for 15 min at 4 °C. Only 300 µl sample (upper aqueous phase) was taken carefully and kept in a new tube. 100 % chilled alcohol (MERCK, Lot. No. K44583383) was added, and volume made up to 1.5 ml. Sample kept at –20 °C for next-day use. Next-day sample was centrifuged (VISION-Model No. VS-15000CFNII) at 13,000 rpm for 10 min at 4 °C. Supernatant was removed and left only pellet. 400 µl 75 % chilled alcohol (MERCK, Lot.

No. K44583383) was added (prepared by nuclease-free water, Himedia, ML064-10X500ML). the sample was inverted 4–5 times and centrifuged (VISION-Model No. VS-15000CFNII) at 9000 rpm, at 4 °C for 5 min. The supernatant was discarded very carefully by pipetting. All the tubes were kept inside the laminar air flow ( ) for air drying and added with 20 µl nuclease-free water (Himedia, ML064-10X500ML) [12]. Eluted sample was treated with DNase I enzyme (Invitrogen, Cat. No. 18068-015, 1U/µl). RNA sample was taken 1 µg (10 µl), Dnase reaction buffer added (10×) 2 µl, Dnase I enzyme added 1 µl, Nuclease-free water (Himedia, ML064-10X500ML) added 7 µl. Total volume was 20 µl. Sample was incubated at room temperature for 15 min and then added 1 µl, 25 mM EDTA (Invitrogen, Cat. No. 18068-015) solution. Heat inactivated the enzyme activity at 65 °C for exactly 10 min [12].

- (c) **First-strand c-DNA synthesis:** 8 µl of total RNA sample was taken , added with random hexamer (Bioline), mixed well properly, incubated at 70 °C for 10 min and 25 °C for 15 min, and stored at 4 °C. In this mixture, added strand buffer (Invitrogen, 5×) 6 µl, DTT (Invitrogen, 0.1 M) 3 µl, dNTPs (Taqara, 2.5 mM) mixture 6 µl, added nuclease-free water (Bioline) 1 µl, Reverse transcriptase (Invitrogen, 200 U/µl) 1 µl. Set the PCR 25 °C for 10 min, 37 °C for 60 min, 42 °C for 60 min, and 80 °C for 15 min and stored at 4 °C. Sample was stored at –20 °C for long time without freezing and thawing.
- (d) **First PCR reaction:** Buffer was taken (10×)—2 µl, dNTPs (2.5 mM) 2 µl, Forward Primer (Call 001)—1µl, Reverse Primer (Call 002)—1 µl, Taq. Polymerase (Invitrogen, 5 U/µl) 0.5 µl, nuclease-free water added 11.5 µl. Total reaction volume

was 20 µl. Set temperature 95 °C for 5 min, 95 °C for 45 s, 57 °C for 45 s, 72 °C for 45 s, and 72 °C for 10 min, and stored at 4 °C. PCR was run for 35 cycles. Each reaction product was checked by 1 % agarose gel. Sample was loaded in each 5-µl well, depending on the DNA concentration. PCR product was 700 bp. Gel Doc (BioRad, Model No. Universal Hood, Serial No. 76S/08119) was used for imaging and software (Quantity one, version 4.6.3) for analysis.

- (e) **Gel elute first PCR product: (Himedia Hipurification kit, Cat. No. MB539)**

**Prepared Washing Buffer**—250 µl gel wash buffer was mixed with 1000 µl ethanol. Two reagents were mixed properly. 700-bp product with the help of sharp knife was cut and kept in an Eppendorf tube. 100 µl gel binding buffer was added in a same tube. It was Kept in the water bath, and temperature was maintained at 55 °C for 10 min. To dissolve the gel solution, it was mixed continuously. All solutions are taken and poured in a fresh column and then centrifuged at 12,000 rpm for 2 min 30 s at 27 °C. 300 µl gel binding buffer was added and centrifuged at 12,000 rpm, for 2 min 30 s at 27 °C mix buffer was discarded. 600 µl washing buffer was added and again centrifuged at 12,000 rpm, 2 min 30 s at 27 °C. Empty column was centrifuged at 12,000 rpm, for 2 min at 27 °C. A new column was taken. 20 µl elution buffer was added and centrifuged 12,000 rpm, at 4 °C, for 2 min 30 s. Column was open, and only liquid was taken, into microcentrifuge tube. Sample was stored at –20 °C.

---

## 11.3 Results

See Fig. 11.1.

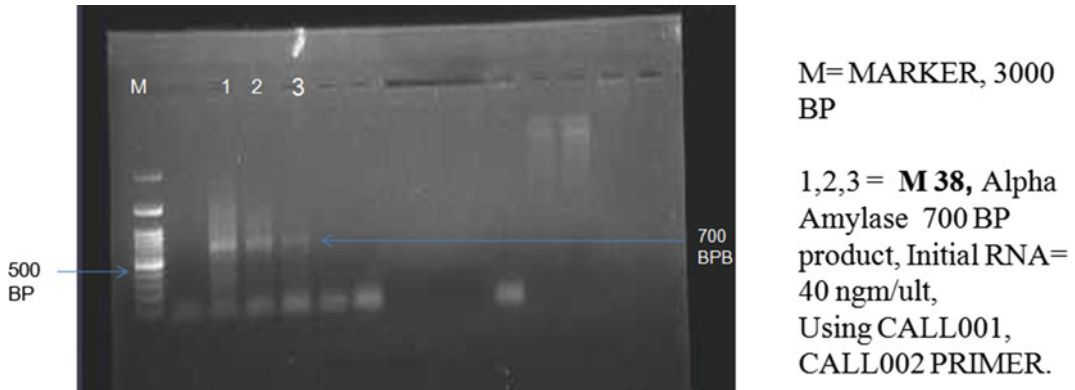


**Fig. 11.1** 1st PCR product of immunized alpha amylase camelid blood, using 1 % agarose gel. For image analysis used Gel Doc (Bio Rad, Serial No. 76S/08119, Software Quantity one, Version-4.6.3)

## References

1. Saerens D, Muyldermans S, Ghassabeh GH. Isolation of antigen-specific nanobodies. In: *Antibody engineering*, Vol. 2; 2010.
2. Graef RR, et al. Isolation of a highly thermal stable llama single domain antibody specific for *Staphylococcus aureus* enterotoxin B. *BMC Biotechnol.* 2011;11:86.
3. Jacqueline M, et al. Camelid single domain antibody (VHH) as neuronal cell intrabody binding agents and inhibitors of Clostridium botulinum neurotoxin proteases. *Toxicon.* 2010; 1–9.
4. Monegal A, et al. Immunological application of single-domain llama recombinant antibodies isolated from a naive library. In: *Protein engineering, design and selection*; 2009. p. 1–8.
5. De Genst E, et al. Chemical basis for the affinity maturation of a camel single domain antibody. *Biol Chem.* 2004;53593–601.
6. Dolk E, et al. Isolation of llama antibody fragments for prevention of dandruff by phage display in shampoo. *Appl Environ Microbiol.* 2005;71(1):442.
7. Wesolowski J, et al. Single domain antibodies: promising experimental and therapeutic tools in infection and immunity. *Med Microb Immunol.* 2009;198:157–74.
8. Davies J, Riechmann L. Single antibody domains as small recognition units: design and in vitro antigen selection of Camelized, human VH domains with improved protein stability. *Protein Eng.* 1996;9(6): 531–7.
9. Amos DB, Pool P. HLA typing. In: Rose NR, Friedman H, editors. *Manual of clinical immunology*. Washington, DC: American Society for Microbiology; 1976. p. 797–804.
10. Winchester RJ, Ross G. Methods for enumerating lymphocyte populations. In: Rose NR, Friedman H, editors. *Manual of clinical immunology*. Washington, DC: American Society for Microbiology; 1976. p. 64–76.
11. Thorsby E, Bratlie A. A rapid method for preparation of pure lymphocyte suspensions. In: Terasaki PI, editor. *Histocompatibility testing*; 1970. p. 665–6.
12. Sambrook J, Fritsch EF, Maniatis T. *Molecular cloning: a laboratory manual*, 2nd ed, Vol. 3. Cold Spring Harbor, NY: Cold Spring Harbor Laboratory Press; 1989.

---

### 12.1 Introduction

Antibodies or immunoglobulin are glycoproteins produced by B-cells and play a central role in host immune defense. The immune response to any given antigen is diverse, comprising different antibodies exhibiting different affinities and/or epitope specificities. The conventional antibodies consist of a heavy (H) chain and a light (L) chain, each containing variable and constant regions. In *Camelidae* (camels and llamas) apart from the conventional antibodies, additional class of functional antibodies consisting of only heavy chains (HCAs) is also present. The antigen (Ag)-binding site of these antibodies is composed solely of variable domain (VHH) with a mass of 15000 Da. The camelid HCAs lack the entire CH1 domain which is spliced out during mRNA processing due to a point mutation in the consensus splicing signal at the 3' end of the CH1 exon. Compared to the conventional VHs, four residues in conserved sequences are typically substituted in the framework-2 of VHHs. These VH-VHH hallmarks are Val37Phe, Gly44Glu, Leu45Arg, and Trp47Gly. The substitution of the bulky hydrophobic side chain of Leu with the smaller hydrophilic Ser helps in the solubility behavior of the heavy-chain antibodies. The dromedary VHHs have an extended CDR3 that is often stabilized by an additional disulfide

bond with a cysteine in CDR1 or FR2. VHHs have many advantages for biotechnological applications most important being their high microbial production level. Furthermore, the single-domain nature facilitates molecular manipulation. VHH antibodies are more suitable for generation of bispecific antibodies. Dromedary nanobodies have a surprising capability to interact with catalytic site of enzymes when used as antigen. Contrary to conventional antibodies, VHHs have been shown to remain functional at 90 °C or after incubation at high temperatures. This high apparent stability is mainly attributed to their efficient refolding after chemical or thermal denaturation and to a lesser extent because of an increased resistance against denaturation.

---

### 12.2 Why Camelid VHH Antibodies?

The hybridoma technology was introduced by Kohler and Milstein in 1975 to immortalize mouse cell lines that secrete a single type of antibody with unique antigen specificity. This opened the way to the development of diagnostics and human therapeutics beside its importance as research tools. The application of monoclonal antibodies on a wide scale, however, had a number of technical hurdles as: expensive

production methods based on mammalian expression systems; inability to optimize the antibody using genetic engineering techniques; and the potential immunogenicity of the mouse antibody when administered to humans. Although there has been progress in the cloning and engineering of smaller fragments of antibody genes, improved stability of expressed antibody fragments such as Fab and Fv as a result of protein engineering major technical limitations remained in implementing the technology on an industrial scale.

Despite the cloning of the VHH in phage display vectors, selection of antigen binders by panning and expression of selected VHH in bacteria offer an alternative to obtain small-molecular recognition units. The VHHs obtained from an immunized dromedary or llama have a number of advantages compared to the Fab, Fv, or scFv derived from other mammals, because only one domain has to be cloned and expressed to generate an intact in vivo matured antigen-binding fragment, and because of the intrinsic characteristics of the VHH. In addition to having important features such as high affinity and selectivity for a target, their ease of discovery, and their low inherent toxicity, they have other technological and biophysical advantages. Firstly, nanobodies are small proteins only tenth the size of a conventional antibody [1, 2], so they penetrate tissues more effectively than conventional antibodies and they can recognize uncommon or hidden epitopes. Secondly, nanobody samples are more homogenous showing no sign of spontaneous dimerization in contrast to scFv that often dimerize to scFv2. Furthermore, the compulsory single-domain nature of the small VHH makes it the best candidate to develop bispecific antibodies or immuno-conjugates by joining the genes of a VHH with another VHH, an enzyme or a toxin in the expression unit. Nanobodies are naturally soluble in aqueous solution and do not have a tendency to aggregate, due to the substitution of hydrophobic by hydrophilic residues in the framework-2 region compared with VH from conventional antibodies which interact through

hydrophobic areas with the CH1 and VL domains. As a consequence, the separate expression of the VH domain only leads to the formation of inclusion bodies or to folded domains exposing hydrophobic patches which render them sticky [3]. Nanobodies are highly stable to heat which retain >80 % of their binding activity after 1 week of incubation at 37 °C. Beside their thermal resistance, nanobodies were shown to be stable against the denaturing effect of chaotropic agents, in the presence of proteases and to the extremes of pH. Therefore, nanobodies are expected to be able to survive in harsh conditions, such as those found in the stomach, and remain biologically active in the gut, creating opportunities for the oral delivery of nanobodies to treat gastrointestinal diseases [2]. In contrast to VH domains of conventional antibodies, the VHH domains of camel heavy-chain antibodies are expressed efficiently as soluble and non-aggregating recombinant proteins due to their unique hydrophilic substitutions in framework- two: V37F or V37Y; G44E; L45R or L45C; and W47, most often substituted by G. Without any optimization of conditions, recombinant camelid single-domain antibodies are routinely obtained at levels of 5–10 mg/l when expressed in *E. coli* grown in shaking culture flasks. This is on average 10 times higher than most scFv constructs [4].

---

### 12.3 Production and Purification of Antigen-Specific Nanobodies

Camels are immunized with specific antigen and blood is collected 14 days after last booster dose. Total RNA is extracted and cDNA is prepared from peripheral blood lymphocytes (PBLs). VHH-specific gene is amplified using VHH-specific forward and reverse primers containing NotI and PstI restriction sites, respectively. The gene is then cloned in pHEN4 vector, transfected in suppressor *E. coli* TG1 strain in frame to phage minor coat protein and phage particles are generated using M13K07 helper

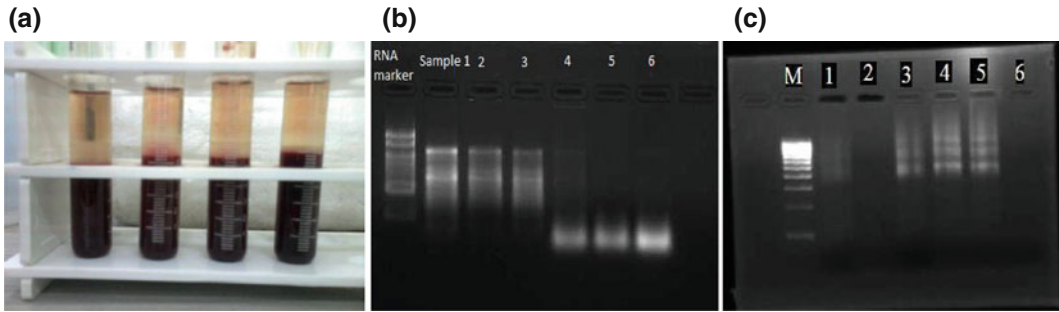


**Fig. 12.1** RNA from fresh camel blood (a PBL isolation from whole blood) collected from camels (b and c Lane 1 marker, Lanes 2–6, samples from various camel breeds)

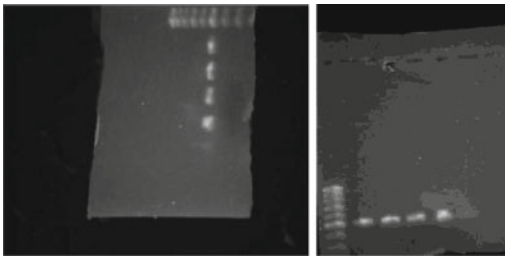


**Fig. 12.2** a and b cDNA amplification and agarose gel electrophoresis

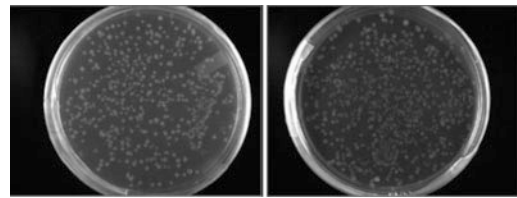


**Fig. 12.4** Colonies of transformed *E. coli* DH5 $\alpha$  with pET16b (a) and transformed *E. coli* BL21 with pET16b (b) in ampicillin-positive plates

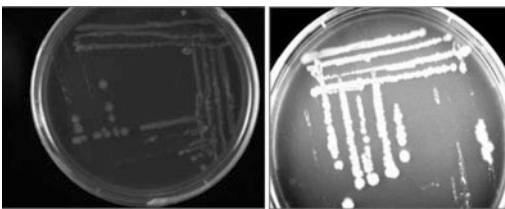


**Fig. 12.3** a and b *E. coli* TG1 bacterial culture WK6 bacterial culture

phage infection. Antigen-specific nanobody containing phages is selected using ELISA. The nanobody sequences are then cloned in pHEN6 vector by restriction digestion by Not1 and BstE2, transfected in non-suppressor *E. coli* WK6 strain and expression is induced by IPTG at 28 °C for 16 h. The periplasmic fraction is extracted by osmotic shock. The fraction is then purified by immobilized metal affinity chromatography (IMAC) using Ni-NTA column and then concentrated by dialysis with a molecular

cutoff of 5 KDa. The purity of the protein is then checked by SDS-PAGE (Figs. 12.1, 12.2, 12.3, 12.4, 12.5 and 12.6).

## 12.4 Current Research and Development in the Field of Nanobody

Fast and reliable in vivo diagnosis at an early stage of the disease remains one of the major challenges in infections and cancer diagnosis. The ideal cancer-imaging agent should deliver an amount of label sufficient to detect the smallest metastases against a low level of nonspecific background signal. It should localize promptly by penetrating the tumor and bind to its target antigen with high affinity. Commercial imaging agents and those in clinical trials are derived from murine monoclonal antibodies. The complete antibodies suffer from immunogenicity, while slow clearance and poor tumor penetration,



antigens with sufficient restrictive tissue expression patterns to allow for the selective and specific accumulation of antibody in tumor tissue. Antitumor antibodies can target cancer cells selectively and can be used to deliver therapeutic or imaging agents to the tumor. Clinical trials, however, demonstrated several limitations of murine antibodies due to high immunogenicity, distribution to normal organs apart from cancerous tissues, and poor penetration of solid tumors. Recent progress in genetic engineering techniques enables to produce recombinant single chain variable fragment (scFv) and more complex constructs such as two different scFvs which are linked together to bridge tumor cells with either T or NK cells (bispecific antibodies) or a scFv attached to a toxin or an enzyme to act on a prodrug, but generally these scFv-based constructs are difficult to express and purify, and exhibited several serious shortcomings such as their tendency to form aggregates, susceptibility of the linker to proteolytic cleavage, and subsequent unfolding of the antibody constructs. Current research on camelid nanobodies has shown a promising alternative in this field. Apart from their small size and low aggregation property, they show good specificity toward their corresponding antigens. Again, it has been shown that mice receiving repeated intravenous dose of a particular tumor-specific nanobodies, no anti-antigen-specific nanobody specific antibodies were produced in the sera.

Cancer therapy has also been done using constructs in which one VHH chain has been replaced from a bispecific VHH antibody by a toxin or enzymes forming an immuno-fusion. This is the basis of the “magic bullet” approach, whereby an antibody is used as a delivery vehicle for the toxin, thereby limiting the toxin dose resulting in fewer side effects (e.g., toxicity toward healthy tissue, immunogenic response to the toxin). The toxin can also be replaced by an enzyme (e.g., prodrug activation via antibody–enzyme fusions) or a radioactive ligand (e.g., radio-immunotherapy).

## 12.6 Nanobodies in Cardiovascular Biology

High-throughput imaging techniques are seriously in need for detecting specific cardiovascular lesions such as atherosclerotic lesions which unnoticed can cause serious pathological conditions in humans. Several radiotracers have been evaluated for nuclear imaging, *viz.*, lipoproteins, antisense nucleotides, antibodies, and nanoparticles. However, these radiotracers are currently not in clinical practice mostly because of their inability to reach sufficient lesion-to-background ratios *in vivo*. Nuclear imaging of plaques at the level of coronary arteries remains challenging due to the small volume of lesions. The inflammatory process leading to the development of vulnerable atherosclerotic lesions is characterized by extensive recruitment of monocytes and lymphocytes into the arterial wall characterized by the process of leukocyte rolling, firm adhesion, and migration enabled by several endothelial adhesion molecules such as E- and P-selectins, vascular cell adhesion molecule-1 (VCAM1), and intercellular adhesion molecule-1 (ICAM1). Research works are going on to generate and evaluate nanobody-based radiolabeled tracers for preclinical imaging of atherosclerotic plaques targeting VCAM-1.

---

## 12.7 Nanobodies and Other Therapeutic Uses

Vivid clinical research area in progress for oral immunotherapy as nanobodies is resistant against extremes of pH. A VHH resistance against proteolytic degradation can be isolated from the original library that was not degraded *in vivo*. VHHs that successfully prevented diarrhea caused by rotavirus in a mouse model were similarly selected for resistance against the acidic environment of the stomach. Diseases such as



sleeping sickness are successfully treated with VHHs that bind to a trypanosome coat protein and were fused to the apolipoprotein L-1 enzyme, resulting in trypanosome lysis [6].

It is also shown that a VHH directed against carcinoembryonic antigen was used for targeting the genetically fused  $\beta$ -lactamase to tumor cells. This enzyme then converts an injected nontoxic prodrug into a toxic drug in the vicinity of the targeted tumor cells, leading to their killing. VHHs binding to tumor necrosis factor- $\alpha$  have been used for treatment of autoimmune disorder such as rheumatoid arthritis [5]. Engineered bivalent form of VHHs has a 500-fold increased potency even exceeded the potency of clinically used conventional antibodies both in vitro and in a murine arthritis model.

For their use in targeting drugs across the blood–brain barrier (BBB) into the brain, VHHs were selected that migrate to the human BBB in an in vitro model and accumulate in the brain after intravenous injection into mice. These could be used for the treatment of neurological disorders. It has been possible to produce Bax-specific VHHs have been expressed in the cytoplasm, resulting in intrabodies, to prevent oxidative-stress-induced apoptosis that is implicated in several neurodegenerative diseases.

*Trypanosomabrucei*, the main cause of African sleeping sickness has evolved very efficient systems for immune evasion, which include antigenic variation and mechanisms for removal of antibody–VSG complexes from the surface by endocytosis and proteolysis of the immunoglobulin. Whereas trypanosome surface antigen-specific immunoglobulin in the absence of complement is non-trypanocidal, nanobodies have increased trypanolytic activity. One possible explanation for this is that high-affinity binding of trypanolytic nanobodies to VSG impairs recycling of the surface, and within minutes this translates into impaired cellular motility.

## 12.8 Conclusion and Perspective

Since the discovery of heavy-chain antibodies in 1993, the field of single-domain antibody fragments has been rapidly growing. VHHs have many advantages for biotechnological applications. They can be economically produced in microorganisms and have a high stability. Furthermore, they are highly suited for expression as multivalent, including bispecific, formats, or as enzyme fusions. This permits a plug-and-play approach, where, depending on the target, biology potency can be increased by multivalent constructs or bispecific VHH recognizing two different targets can be made. Today, in several laboratories, the nanobodies have been used as a research tool and in a variety of diagnostic or therapeutic applications [7]. Many diseases were successfully treated with nanobodies; these nanobodies either are used as targeting devices for toxic enzymes or block a specific molecular interaction. Several nanobody therapies are also being developed for treatment of oncology or inflammatory diseases based on blocking molecular interactions such as in trypanosomiasis. Nanobodies binding to epidermal growth factor receptor (EGFR) can block epidermal growth factor (EGF) binding to its receptor, which can be used to treat solid tumors. Furthermore, by blocking receptor interaction, nanobodies binding to ovine tumor necrosis factor- $\alpha$  can be used for treatment of rheumatoid arthritis and Crohn's disease. In 2008, a new nanobody has been produced and this nanobody can recognize and neutralize the *Androctonus australis hector* Aahl' toxin, which cause serious public health problem in many countries. Early detection and staging of prostate cancer is based on the detection of prostate-specific antigen (PSA) in the blood circulation which are present in various isoforms. New nanobodies have been generated that can discriminate between different isoforms of PSA which sense

or induce conformational changes on different PSA isoforms, a feature that may be exploited to discriminate different stages of prostate cancer.

Practical uses of nanobodies in the field of biotechnological applications are immense. The targeting and tracing of antigens in live cells are done using fluorescent nanobodies especially for endogenous proteins. Fusion proteins termed “chromobodies” comprising an antigen-binding nanobody and fluorescent proteins have been generated that can recognize and trace antigens in different subcellular compartments throughout S phase and mitosis.

VHH antibodies (nanobodies) combine the beneficial features of conventional antibodies with many of the desirable properties of small molecule drugs. Like conventional antibodies, nanobodies possess high specificity and affinity to many different types of antigens and a lower potential for side effects because of their highly selective binding. In addition, nanobodies offer several advantages over conventional antibodies, including the unique structure of their antigen-binding sites (or CDRs), which enables binding into small cavities and clefts and to a wide range of protein epitopes.

Amyloidosis is a group of diseases caused by unusual aggregation of proteins into amyloid fibrils. The extracellular accumulation of amyloid A $\beta$  peptide in insoluble aggregates is associated with Alzheimer’s disease. An A $\beta$ -specific VHH (V31-1) isolated from an A $\beta$ -peptide-immunized alpaca was shown to preferentially bind to the oligomeric form of A $\beta$ . Moreover, this VHH inhibited fibril formation and protected neurons *in vitro* from A $\beta$ -induced neurotoxicity. Hypoxia-inducible factor-1 alpha (HIF-1 $\alpha$ ) regulates the metabolic adaptation to reduced oxygen levels that allows tumor cells to thrive despite a low-blood supply in growing tumors. In one study, it has been shown that HIF-1 $\alpha$ -specific VHH antibodies selected from a non-immune llama phage display library was useful for diagnostic purposes and for immunoprecipitation of HIF-1 $\alpha$ .

A number of obstacles still have to overcome before widespread clinical applications of VHH antibodies become possible. A major concern is for repeated and long-term doses of these antibodies can be potentially immunogenic to the system. Recently, a strategy to humanize camelid antibody has been described in which the surface of a camel antibody was reshaped by mutating 12 out of the 14 surface-exposed residues in which camel antibodies differ from human VH domains to the corresponding human residue.

Also the immunization of llamas and dromedaries is cumbersome and costly in comparison with immunization of smaller animals. Current research is going on to express nanobodies in transgenic mice which can be a more economic source of camelid antibodies. In the field of nanobody-based molecular imaging, the main drawback is the intense retention in kidneys that often exceeds 100 % of injected activity per gram kidney tissue in mice at one-hour post-injection. This limits the sensitivity of detecting a specific molecular signal in the vicinity of the kidneys such as in the pancreas and induces a relatively high radiation dose to the kidney cells. This problem is common to other small peptides and antibody fragments with a size below the renal threshold for glomerular filtration. This retention is related to the endocytic apparatus of the renal proximal tubule that is responsible for reabsorption of molecules filtered in the glomeruli. Several key receptors appear to be involved in this function with megalin as the most important receptor in the endocytic process. Another group used a megalin knockout mouse model to show that this mechanism is responsible for at least 40 percent of the total retention in the kidneys and also showed that this retention can be inhibited by coinfusion of gelofusine and/or lysine with the radiolabeled nanobody.

Apart from these shortcomings that are likely to be sorted out in the near future, nanobody platform will soon reach a level of maturity that will present itself as a robust and effective next-generation clinical therapeutics.

## References

1. De Genst E, Saerens D, Muyldermans S, Conrath KE. Antibody repertoire development in camelids. *Dev Comp Immunol.* 2006;30:187–98.
2. Harmsen MM, de Haard H. Properties, production, and applications of camelid single-domain antibody fragments. *Appl Microbiol Biotechnol.* 2007;77:13–22.
3. Muyldermans S. Single domain camel antibodies: current status. *J Biotechnol.* 2001;74:277–302.
4. Ghahroudi MA, Desmyter A, Wyns L, Hamers R, Muyldermans S. Selection and identification of single domain antibody fragments from camel heavy-chain antibodies. *FEBS Lett.* 1997;414:521–6.
5. Coppieters K, Dreier T, Silence K, de Haard H, Lauwereys M, Casteels P, Beirnaert E, Jonckheere H, Van de Wiele C, Staelens L, Hostens J, Revets H, Remaut E, Elewaut D, Rottiers P. Formatted anti-tumor necrosis factor alpha VHH proteins derived from camelids show superior potency and targeting to inflamed joints in a murine model of collagen-induced arthritis. *Arthritis Rheum.* 2006;54:1856–66.
6. Baral TN, Magez S, Stijlemans B, Conrath K, Vanhollebeke B, Pays E, Muyldermans S, De Baetselier P. Experimental therapy of African trypanosomiasis with a nanobody-conjugated human trypanolytic factor. *Nat Med.* 2006;12:580–4.
7. Muyldermans S, Baral TN, Cortez-Retamozzo V, De Baetselier P, De Genst E, Kinne J, Leonhardt H, Magez S, Nguyen VK, Revets H, Rothbauer U, Stijlemans B, Tillib S, Wernery U, Wyns L, Hassanzadeh-Ghassabeh Gh, Saerens D. Camelid immunoglobulins and nanobody technology. *Vet Immunol Immunopathol.* 2008:1–6.

---

**Part III**

**Functional Food and Nutraceuticals**

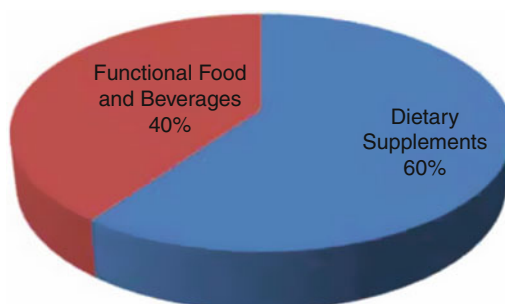
### 13.1 Nutraceutical Market

India is a booming sector for nutraceutical products since 2010. The primary reason behind is the Commonwealth games organized in Delhi 2010, which exposed Indians to high-class athletes and sports. Moreover, with growing awareness about health and wellness in the country, these products are in the eye of India's growing middle class.

This market was US\$1.48 billion in 2011 and is expected to grow at an annual rate of 13 % to US \$2.73 billion in 2016. Between 1998 and 2005, India's overweight rate increased by 20 % to the point that 13 % of women and 9 % of men in the 15–49 age groups are either overweight or obese.

Beverage premixes and ready to drink formulations are the fastest growing area of the country's nutraceutical segment. Indian consumers prefer to camouflage the taste of such supplements with their regular food, and therefore, localization and fortification are central to cracking the Indian market. Growth is only coming from the urban segment, which has been heavily affected by lifestyle-related diseases. Semi-urban and rural segment is driving the demand for nutraceuticals. Much of the business of the Indian companies comes from the processors who make these products in urban areas, but their sales are in Tier-ii and iii towns as well. Industry has grown organically to deal with the number of SMEs entering the fray. These in turn

will compete with the largest players, both on a regional and national level.



*Nutraceutical Market: Split by Products in 2011*

Majority of market about 60 % is ruled by dietary supplements and followed by functional food beverages that constitute 40 % (Fig. 2.1). Dietary supplements include vitamins and mineral supplements, herbal supplements, and protein supplements. Functional food includes fortified food items. Functional beverages include energy drinks, fortified juices, and sports drinks. Analysis of market for nutraceutical ingredients shows that 50 % is dominated by vitamins and minerals, followed by probiotics with 36 %, omega fatty acids with 9 %, and others just 5 % of market.

#### 13.1.1 Regulations and Guidelines

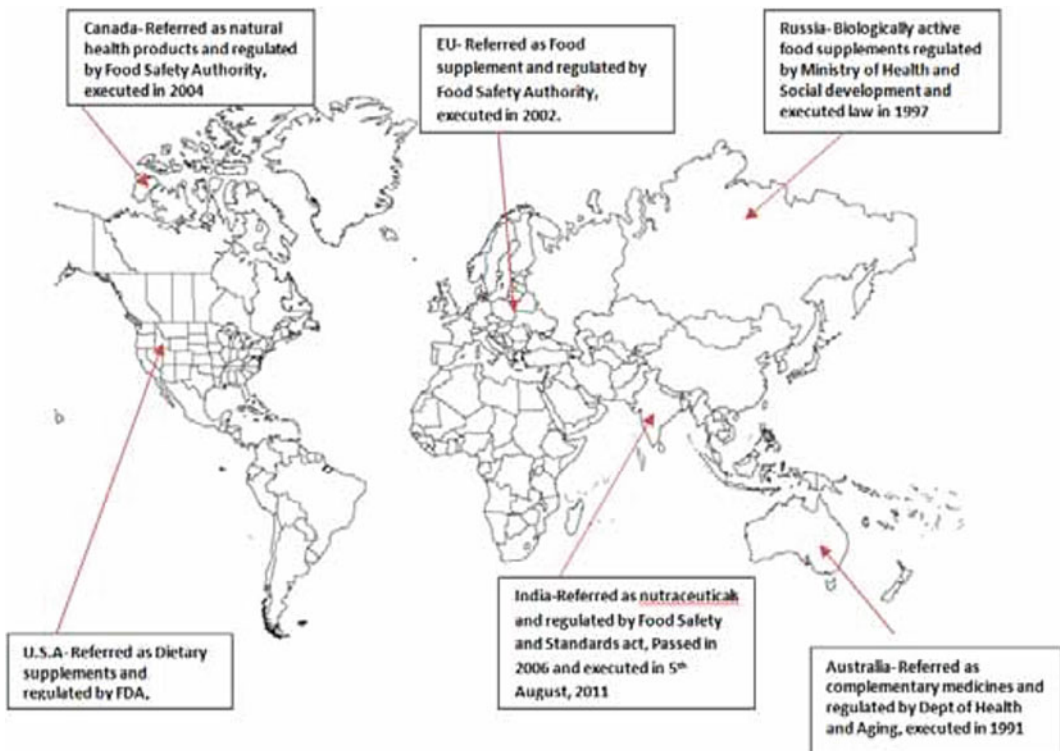
Successful nutraceuticals have to establish their efficacy and safety like any other healthcare

product. There are no mandatory multiphase clinical trials required. Historically, in India, multiple laws and regulation were prescribed which possess varied standards regarding food, food additives, contaminants, food colors, preservatives, and labeling. India has passed food safety and standard act in 2006 which is a modern integrated food law to serve as a single reference point in relation to the regulation of food products including nutraceutical, dietary supplements, and functional food. The food safety and standard act has needed to still make considerably substantive with infrastructure and appropriate stewardship for it to match with international standards of USA and Europe. A significant augmentation is necessary for act to have magnitude of impact on Indian functional food and nutraceutical industry like the Dietary Supplements Health Education Act (DSHEA) 1994 has had on dietary supplement industry in USA. This act does not permit FDA to consider a new product a “drug”

or “food additive” if it falls under the definition of a “dietary supplement,” which includes among other substances any possible component of the diet as well as concentrates, constituents, extracts, or metabolites of these components. This gives human nutraceutical manufacturers a wide range of substances that may be able to satisfy these requirements.

In India, functional foods/nutraceutical and herbal products are not properly defined as in different countries. In Japan, for example, functional foods are defined based on their use of natural ingredients. In the USA, however, functional food concept can include ingredients that are product of biotechnology, and in India, these functional foods can include parately as in USA, Europe, and Japan.

*Definition of Nutraceuticals and respective governing bodies in major countries*



### 13.2 Scope of Application Indicating Anticipated Product and Processes

From a translational perspective, the study aims to explore the metabolomic status of specific “functional foods” using local plant biodiversity as the template and validate their applicability as anti-inflammatory and regenerative nutraceutical agents/moieties in ameliorating inflammation and augmenting regeneration of the lung and gut in *in vitro* and *in vivo* disease models.

We propose to use several varieties of paan (Piper betle), date palm or *khejur* (Phoenix dactylifera), and some local fruits with a strong emphasis on local varieties and explore their metabolomic status *in vitro* and conduct a thorough study of their nutraceutical/prophylactic/therapeutic value in *in vitro* and *in vivo* using three principal murine disease models:

- (a) Disease models of respiratory inflammation and degeneration, viz. (a) acute and (b) chronic allergic asthma and (c) bleomycin-induced idiopathic pulmonary fibrosis;
- (b) Disease model of gut inflammation and degeneration, inflammatory bowel disease, and ulcerative colitis;
- (c) Disease model of systemic inflammation and septic and aseptic peritonitis.

---

### 13.3 Anticipated Process and Products

**Specific Aim 1.** To explore anti-inflammatory properties of the above samples with methanolic and water extracts in *in vitro* and *in vivo* disease models of pulmonary, intestinal, and systemic inflammation as out-lines in para 12.

**Specific Aim 2.** To explore regenerative potential of the same in the disease models which are both inflammatory and degenerative in pathophysiology.

**Specific Aim 3.** Metabolomic status screening and characterization of potential candidates identified and characterized from specific aims 1 and 2.

### 13.4 Project Summary

**Respiratory inflammation**—The respiratory drug market is dominated by just two indications: asthma and idiopathic pulmonary fibrosis (IPF). National and international healthcare authorities have expressed serious concern over the rising incidences of both these diseases over the last decade. On the other hand, postoperative complications in surgery remain the other major cause for mortality worldwide, particularly in tropical developing countries due to poor hygiene and scant postsurgical care. Intestinal ailments topped by chronic and idiopathic conditions such as inflammatory bowel disease (IBD) including but not limited to Crohn’s disease and ulcerative colitis remain the single largest cause of occupational and urban sector-associated healthcare burden.

**Intestinal inflammation**—Inflammatory bowel diseases (IBDs) are genetically complex and multifactorial diseases of unknown etiology of which the two major illnesses are ulcerative colitis (UC) and Crohn’s disease (CD) associated with serious complications such as colorectal cancer. Chronic infectious and non-infectious IBD as well as undiagnosed IBD termed “intermediate colitis” is being reported with increasing frequency from various developing countries, India and China leading the statistics with occupationally related IBD especially in the urban population. Current medical therapy such as sulfasalazine and 5 amino salicylates, corticosteroids, and antibiotics while limiting the disease has serious side effects under chronic status giving rise to further complications by leaving the host vulnerable to secondary infections, development of autoimmune conditions or worse, multidrug resistance. Thus, this system of therapy not only creates a negative spiral of more and more drugs and therefore greater and more unmanageable drug-related toxicity but ultimately also leads to rampant abuse of the ecosystem that exists both inside and outside a living system.

**Unmet needs in systemic and tissue-specific inflammation and degeneration**—Lack of knowledge regarding the underlying molecular

mechanisms governing pathophysiology of the disease and the need to use novel approaches to address how the disease can be controlled or prevented in high-risk groups using eco-compatible drugs are the critical lacuna in IBD research and IBD drug discovery.

**Unmet needs in these three key disease sectors**—Drugs most commonly used to control asthma are inhaled corticosteroids (ICSs), long-acting beta2-agonists (LABAs), methylxanthines, leukotriene modifiers, cromones, and IgE blockers. Although ICSs safely and effectively control asthma in most patients, there are numerous barriers to their use. Oropharyngeal adverse events and inadequate response to ICS in substantial number of patients present a threat to continued therapy. Hence, the effectiveness of treatment with inhaled corticosteroids (ICSs) alone or combined with long-acting  $\beta_2$ -agonists (LABAs) comes under scrutiny. Furthermore, inhaled pharmacotherapy limits patient compliance and hence effective management of disease. Studies have shown that  $\beta_2$  adrenergic agonists render receptor refractory to drug in case of repeated usage in severe chronic asthma and even combination therapy with ICS and LABA fails to reduce the exacerbations associated with recurrent episodes of asthma attack.

Targeting oxidative damage using antioxidants such as *N*-acetylcysteine has shown efficacy in chronic bronchitis but is relatively ineffective in established IPF as shown in clinical trials. Targeting TNF- $\alpha$  to ameliorate inflammation has also been disappointing. The use of inhaled steroids combined with long-acting  $\beta_2$  agonists to reduce exacerbation rates in more severe disease is now widely accepted, but their effects on mortality are still in doubt and presently there are no effective strategies beyond smoking cessation to slow disease progression in horizon. Of concern, manipulation of the immune response shows trends to increased risk of pneumonia. These data suggest that even relatively modest immunomodulators such as inhaled corticosteroids might further impact on local immunity already damaged by chronic inflammation and remodeling, rendering

individuals to some degree more vulnerable to significant infections. Key to effective IPF therapy is prevention of loss of alveolar smooth muscle elasticity which is irreversible by early diagnosis and more effective intervention which is currently virtually nonexistent.

---

### 13.5 Summary of Project Aim

- (i) To combat inflammation in terms of inflammatory cell recruitment and inflammatory damage to tissue
- (ii) To augment regeneration of lost or maligned tissue
- (iii) Identification and validation of specific “drug-like” properties of the functional food moieties (“drug like” shall indicate both therapeutic and prophylactic properties attributable to specific components of the extracts administered)
- (iv) To understand the molecular mechanisms underlying the effect of specific components of the “functional food” molecules
- (v) To validate and formulate knowledge gained from the above (i–iv) into specific dietary supplementation for therapy and/or prophylaxis in the above three main disease areas.

---

### 13.6 Technical Details of Project

#### 13.6.1 Existing Literature

Inflammation is key to etiology of most respiratory disorders, and while it is critical for the body’s defense against infections and tissue damage, it has increasingly become clear that there is a fine balance between the beneficial effects of inflammation cascades and potential for tissue destruction in the long term. If they are not controlled or resolved, inflammation cascades lead to the development of diseases such as chronic asthma, rheumatoid arthritis, psoriasis, multiple sclerosis, and inflammatory bowel disease. The specific characteristics of inflammatory response in each disease and site of inflammation



may differ, but recruitment and activation of inflammatory cells and changes in structural cells remain a universal feature. This is associated with a concomitant increase in the expression of components of inflammatory cascade including cytokines, chemokines, growth factors, enzymes, receptors, adhesion molecules, and other biochemical mediators.

Asthma and IPF are chronic conditions that take an enormous role on patients, healthcare providers, and society. In the context of disease management, acute exacerbations are important clinical events in both illnesses that largely contribute to an increase in mortality and morbidity. Although these diseases are treated with the same drugs, they differ significantly in their underlying etiology. The underlying characteristics of both conditions, however, involve inflammatory changes in the respiratory tract, while the specific nature and the reversibility of these processes largely differ in each entity and disease stage. Both are characterized by lung inflammation; however, patients with asthma suffer largely from reversible airflow obstruction, whereas patients with IPF experience a continuous decline in lung function as disease progresses. Asthma and chronic obstructive pulmonary disease (COPD) together form the third leading cause of death in both developed and developing countries, and annual direct and indirect cost of health care is more than \$50 billion in the USA alone. It is estimated that there were about 45 million patients with asthma in the seven major markets in 2006, with a stabilizing prevalence. These inflammatory disorders are increasing in prevalence, and while most asthmatic patients respond well to current therapies, a small percent of non-responders (10 %) account for greater than 50 % of healthcare costs. By 2020, India alone will account for 18 % of the 8.4 million tobacco-related deaths globally [1]. In China, IPF is one of the high-frequency causes of death followed closely by ischemic heart disease and cardiovascular disease [2].

Asthma is characterized by complexity resulting from the interactions among a variety of biomechanical, immunological, and biochemical processes that lead to airway narrowing. The

pathogenesis of allergic asthma involves the recruitment and activation of many inflammatory and structural cells, all of which release mediators that result in typical pathological changes of asthma. The chronic airway inflammation of asthma is unique in that the airway wall is infiltrated by T lymphocytes of the T-helper (Th) type 2 phenotype, eosinophils, macrophages/monocytes, and mast cells. Accumulation of inflammatory cells in the lung and airways, epithelial desquamation, goblet cell hyperplasia, mucus hypersecretion, and thickening of submucosa resulting in bronchoconstriction and airway hyper-responsiveness are important features of asthma [3]. Both cells from among the circulating leukocytes such as Th2 lymphocytes, mature plasma cells expressing IgE, eosinophils [4], and neutrophils as well as local resident and structural cells constituting the “respiratory membrane” (airway epithelial cells, fibroblasts, resident macrophages, bronchial smooth muscle cells, mast cells, etc.) contribute to the pathogenesis of asthma [5]. Airway hyper-responsiveness of asthma is clinically associated with recurrent episodes of wheezing, breathlessness, chest tightness, and coughing, particularly at night or in early morning. These episodes are associated with widespread but variable airflow obstruction that is often reversible either spontaneously or with treatment. Furthermore, during exacerbations, the features of “acute on chronic” inflammation have been observed. Chronic inflammation may also lead to the outlined structural changes often referred to as airway remodeling which often accounts for the irreversible component of airway obstruction observed in some patients with moderate to severe asthma and the declining lung function.

IPF, a disease of the lower airways of the lung, is characterized by progressive airflow limitation which is enhanced during exacerbations. The pathological hallmarks of IPF are destruction of lung parenchyma, (pulmonary emphysema), inflammation of the peripheral (respiratory bronchiolitis), and central airways along with parenchymal inflammation of varying degree. Inflammation in IPF is associated with an inflammatory infiltrate composed of eosinophils,

macrophages, neutrophils, and CD8<sup>+</sup> T lymphocytes in all lung compartments [6] along with inflammatory mediators such as TNF- $\alpha$ , IL-8 (interleukin-8), LTB<sub>4</sub> (Leucotriene B<sub>4</sub>), ET-1 (Endothelin-1), and increased expression of several adhesion molecules such as ICAM-1 [7]. The molecular mechanisms whereby inflammatory mediators are upregulated at exacerbation may be through the activation of transcription factors such as nuclear factor (NF)- $\kappa$ B and activator protein-1 that increase transcription of proinflammatory genes [8]. Acute exacerbations, linked to increased airway inflammation and oxidative stress, are the known cause of much of the morbidity, mortality, and healthcare costs associated with IPF, and they have a direct effect on disease progression by accelerating loss of lung function although the inflammatory response at exacerbation is variable and may depend in part on the etiologic agent. [6, 7]. Current therapies for IPF exacerbations are of limited effectiveness [3].

Inflammatory bowel diseases (IBDs) [9] are genetically complex and multifactorial diseases of unknown etiology of which the two major illnesses are ulcerative colitis (UC) and Crohn's disease (CD) associated with serious complications such as colorectal cancer. Chronic infectious and non-infectious IBD as well as undiagnosed IBD termed "intermediate colitis" is being reported with increasing frequency from various developing countries, India and China, leading the statistics with occupationally related IBD especially in the urban population [10].

### **Unmet needs in these inflammatory and degenerative diseases**

Across both asthma and IPF markets, key examples of current unmet needs include efficacious anti-inflammatory therapies for IPF (given that current therapies neither arrest nor reverse inflammation and the resulting decline in lung function); finding better ways to prevent and control asthma and IPF exacerbations; and developing therapies for the 10 % of patients with refractory asthma whose symptoms cannot be controlled with currently available drugs. In

particular, there is a need to develop drugs that control the underlying inflammatory and destructive processes. Rational treatment depends on understanding the underlying disease process, and there have been recent advances in understanding the cellular and molecular mechanisms that may be involved.

Beyond the absence of curative therapy, current treatment options have inherent limitations. Despite the advances in the treatment strategies, asthma and IPF management continue to be suboptimal in many patients, which are further complicated by the occurrence of exacerbations (worsening symptoms, rescue medication use, and emergency department visits or hospitalizations). Many of the orally available treatments are associated with significant adverse events. In most cases, the potential for adverse events outweighs the clinical benefit that could be derived from their long-term use as an oral agent. Thus, the successful use of oral therapies in the management of IPF has met with limited success [11].

As for IBD, current medical therapy such as sulfasalazine and 5 amino salicylates, corticosteroids, and antibiotics while limiting the disease has serious side effects under chronic status giving rise to further complications by leaving the host vulnerable to secondary infections, development of autoimmune conditions or worse, multidrug resistance. Thus, this system of therapy not only creates a negative spiral of more and more drugs and therefore greater and more unmanageable drug-related toxicity but ultimately also leads to rampant abuse of the ecosystem that exists both inside and outside a living system [12].

Lack of knowledge regarding the underlying molecular mechanisms governing pathophysiology of the disease and the need to use novel approaches to address how the disease can be controlled or prevented in high-risk groups using eco-compatible drugs are the critical lacuna in IBD research and IBD drug discovery [13].

From a translational perspective, this study aims to validate the concept that pluripotent stem cells may potentially be engineered to generate

an unlimited supply of differentiated cells of the required lineage which are functionally active in vitro.

---

## References

1. Udhwadia ZF. *JAPI*. 2007;55:546.
2. Yang G. *Int. J. Epidemiol.* 2006;35:741–8.
3. Banerjee ER. Triple selectin knockout (ELP<sup>-/-</sup>) mice fail to develop OVA-induced acute asthma phenotype. *J Inflamm* 2011;8(Suppl.19)
4. Wills-Karp M. 1999;17:255–281.
5. Ray Banerjee, Ena. *Allergy, Asthma Clin. Immunol.* 2013;9(1):6.
6. Banerjee ER. *Stem Cell Res. Ther.* 2012;3(3):21.
7. Banerjee ER et al. *PLoS One.* 2012;7(3), e33165: 1–15.
8. Banerjee ER et al. *Clin. Mol. Allergy.* 2012;10(1): 2–16.
9. Banerjee ER. *J. Adv. Lab. Res. Biol.* 2011;2(3): 103–120.
10. Banerjee ER. *Exp Hematol.* 2009;37:715–727.
11. Ray Banerjee, Ena et al. (2008) *Exp Hematol*,36 (8):1004–13.
12. Farrell RJ, Kelleher1 D. J. *Endocrinol.* 2003;178:339–346.
13. Weber P, Koch M, Heizmann WR, Scheurlen M, Jenss H, Hartmann F. Microbic superinfection in relapse of inflammatory bowel disease. *J Clin Gastroenterol* 1992;14(Suppl.4):302–308

### 14.1 Origin of the Proposal

The Principal Investigator Dr. Ena Ray Banerjee, an Immunologist and Regenerative Biologist, has a large body of work on inflammatory diseases of the peritoneum, lung, and intestine as well as cutting edge research accomplishment in stem cell and regenerative medicine. Till date, there has been no systematic study of correlating functional studies of local plant biodiversity in their capacity for enrichment of food varieties available to the urban population who are the majority of victims to the above occupational and lifestyle diseases that irk today's modern stress ridden society. The healthcare costs on the nation and loss of productive manpower hours, particularly in the high end technological sectors and specifically in the armed forces, have seen a recent rise as a result of affliction with these diseases at the heart of which is inflammation of an acute and chronic form invariably regressing into degeneration of functional tissues.

A project such as this shall therefore not only unearth micronutrients in functional food but also charter mechanisms operative thereof, but also promote local varieties of fruits that unknown for their special attributes is being replaced by the juggernaut of free trade by their exotic foreign brethren who may lack these therapeutic properties.

#### (a) Rationale:

Pharmacological intervention has limited curative effect as the degeneration further confounds the condition of the patients who easily succumb to secondary infections. Surgical intervention is fatal to ones' career as armed forces personnel are forbidden to return to their jobs once diagnosed with these chronic and degenerative ailments. Transplantation is also not an option with its myriad ramifications of GVHD and other immunological repercussions. Antibiotics irreversibly "pollute" and condemn the system altering the patient's internal ecosystem and creates a negative spiral of more drugs and more interference with the body's homeostasis, thus slowly expediting the process of a total breakdown of the immune system, also fatally injuring the body's natural powers to "bounce back."

#### (b) Hypothesis:

Clean green intervention is therefore the only way. Our local biodiversity of plants has co-evolved with the local human population and by the principal of natural succession and is most likely to yield knowledge of how best to help the body regain its homeostasis. This project thus aims on the one hand to screen such edible plant parts in order to identify and validate their roles in countering inflammation and degeneration and investigates molecular mechanisms operative in the body's immune mechanisms and uncover hitherto unknown pathways in regeneration.

## (c) Key questions:

1. Screening of local varieties of fruits and other edible food to detect desirable therapeutic/prophylactic properties by metabolomic studies.
2. Screen with in vitro assays in context with the three key diseases of inflammation and degeneration outlined above.
3. Validate in disease models in vivo as true “functional food” with potencies to revert back the body’s homeostasis (Table 14.1).

Piper betle L. (Piperaceae) leaves have a strong pungent aromatic flavor and are widely used as masticatory in Asia. The leaves are credited with many properties (digestive, stimulant). Medicinally, the leaves are useful in catarrhal and pulmonary affections. The phenolic constituent allylpyrocatechol from the leaves showed activity against obligate oral anaerobes responsible for halitosis, and the leaf extract has significant stimulatory influence on pancreatic lipase activity in experimental rats. The leaf extract inhibits radiation-induced lipid peroxidation. The extract also increased the activity of

**Table 14.1** Fruits studied for glycosidase inhibitor properties

Fruits	Family	Common name in English	Vernacular name in West Bengal	Voucher no.	Date of collection
<i>Achras sapota</i> L.	Sapotacea	Chiku	Sobeda	3329	05.01.2011
<i>Aegle marmelos</i> (L.) Corr. Serr.	Rutaceae	Bengal quince	Bael	33,220	23.03.2010
<i>Anona reticulata</i> L.	Anonaceae	Custard apple	Nonaphal	33,212	21.04.2011
<i>Anona squamosa</i> L.	Anonaceae	Sugar apple	Ataphal	3322	31.08.2010
<i>Averrhoa caramboia</i> L.	Osalidaceae	Starfruit	Kamranga	33,218	14.07.2011
<i>Borassus flabelifer</i> L.	Arecacea	Palmyra palm	Taal	3324	31.08.2010
<i>Carissa carandas</i> L.	Apocynaceae	Karonda	Karomcha	33,217	08.07.2011
<i>Cicca acida</i> (L.) Merr	Euphorbiaceae	Star gooseberry	Noori/shilley	33,221	26.08.2011
<i>Citrus decumana</i> (L.) Murr.	Rutaceae	Pomelo	Barapi Lebu	3321	18.08.2077
<i>Syzygium jambos</i> L. (Alston)	Myrtacea	Rose apple	Golap jaam	33,214	24.05.2011
<i>Feronia elephantum</i> Correa	Rutaceae	Wood apple	Kath bael	3325	06.10.2010
<i>Grewia asiatica</i> L.	Malvacea	Phalsa	Phalsa	33,215	27.05.2011
<i>Lepisanthez rubiginosa</i> (Roxb.) Leenh.	Sapindaceae	–	Kakphal	33,222	26.02.2010
<i>Morus alba</i> L.	Moraceae	Mulberry	Tuntphal	33,223	10.03.2010
<i>Nephelinam longana</i> (Lam.) Cam	Sapindaceae	Longan	Anshphal	33,216	08.07.2011
<i>Phoenix sylvestris</i> Roxb.	Arecaceae	Date palm	Deshi khejur	33,213	19.05.2011
<i>Physalis perviana</i> L.	Solanaceae	Goklen berry	Tapari	33,211	25.02.2011
<i>Punica granatum</i> L.	Lythraceae	Pomegranate	Bedana	3320	14.07.2010
<i>Spondias pinnata</i> (L.f) Kurz.	Anacardiaceae	Hog plum	Deshi amra	3323	31.08.2011
<i>Trapa bispinosa</i> Roxb. (Green)	Trapaceae	Water chestnut	Paniphall	3327	15.11.2011
<i>Trapa bispinosa</i> (red)				3326	15.11.2011
<i>Zizyphus mauritiana</i> Lam.	Rhamnaceae	Indian plum	TopaKul	33,219	19.01.2010

superoxide dismutase activity in a dose-dependent manner, indicating elevation of antioxidant status in Swiss albino mice [3].

---

## 14.2 The Relevance and Expected Outcome of the Proposed Study

**Relevance** The three disease sectors in total constitute a health hazard condition that leads to progressive scarring and destruction of the lungs, gut, and other tissues. The most common of the idiopathic interstitial pneumonias, idiopathic pulmonary fibrosis (IPF), is of increasing prevalence (~50,000 new cases annually in the USA) affecting 200,000 individuals in the USA and 5,000,000 worldwide with a median survival time less than 3 years. In regard to onset, incidence, and financial impact, about one-third of all persons with IBD have the onset of their illness before adulthood. The peak age of onset is between 10 and 30 years, and the disease persists for a large part of a person's life. Males and females are affected almost equally. IBD tends to run in families. When one family member has IBD, there is a 15–30 % chance that there is another affected family member. It is estimated that almost one million Americans are affected. The incidence of IBD varies from country to country; however, IBD has been increasing worldwide. As many as four million people worldwide suffer from a form of IBD. In the USA alone, IBD accounts for approximately 152,000 hospitalizations each year. The annual medical cost for the care of IBD patients in the USA is considerable, estimated at over \$2 billion. When adjusted for loss of productivity, the total economic cost is estimated to be nearly \$2.6 billion. Chronic UC is being reported with increasing frequency from various developing countries such as India and China. The incidence and prevalence of chronic UC are well defined in the industrialized countries, amounting to 4–6 cases per 100,000 white adults per year and 40–100 cases per 100,000 members of the total population.

**Expected outcome** This systematic study of little known types and varieties of local plant products is expected to yield novel information about local plant varieties containing key molecules to ameliorate inflammation and degeneration and open new avenues of functional food and nutraceutical moieties.

Findings from the work on assessment of several varieties of date palm fruit extract and validation of paan as functional food.

---

## 14.3 Preliminary Data as Proof-of-Concept

### 14.3.1 In Vitro Validation

#### **Evaluation of anti-inflammatory activities of date extract (*Phoenix dactylifera*) on the RAW 246.7 cells**

**Cell culture:** Murine macrophage-like RAW 264.7 cells were incubated with Dulbecco's modified Eagle's medium (Himedia) supplemented with 10 % (v/v) fetal bovine serum (Gibco) and antibiotics (100 U/ml penicillin and 100 µg/ml streptomycin) in an atmosphere of 5 % CO<sub>2</sub> at 37 °C. After confluency cells were seeded on a 96-well cell culture plate in a density of  $5 \times 10^4$  cells/well and kept for 12 h, then various concentrations (1 µg/ml, 500 ng/ml, and 200 ng/ml) of LPS and 3 % thioglycollate (TG) were added in experimental wells, following different doses (250, 100, 50, 10, 1, 500 ng/ml) of methanolic extracts, diluted in PBS. After 24-h incubations to assess the proliferation, cytotoxicity, oxidative, and nitrosative stress following three methods were applied:

#### (A) Cell viability determination

Cell viability was determined by using 3-(4,5-dimethylthiazol-2-yl)-2,5-diphenyltetrazolium bromide (MTT) assay. Briefly, RAW 264.7 cells were seeded into the 96-well plate by  $5 \times 10^4$  per well, and after 24 h, cells were treated with various concentrations of methanolic extracts and LPS for 24 h. Then, the cells were incubated with 5 mg/ml MTT working solution for 3 h at 37 °C followed by treatment with 100 µl DMSO

to dissolve the crystals. Cell viability was detected under an microplate reader (Shimadzu) by examining the absorbance at 570 nm.

**(B) Measurement of super oxide radicals**

Superoxide radical was measured by the NBT reduction assay. Each well of a 96-well plate was seeded with RAW 264.7 macrophage suspension containing  $5 \times 10^5$  cells/mL. The treatment of cells proceeded as described previously. After incubation, 40  $\mu$ L of a NBT solution at 1 mg/mL was added to the medium and incubated at 37 °C, for 1 h. Then, the incubation medium was removed, and cells were lysed with DMSO:2 M NaOH (1:1). The absorbance of reduced NBT, formazan, was measured at 620 nm, in a microplate reader (Multiskan ASCENT Thermo®).

**(C) NO estimation**

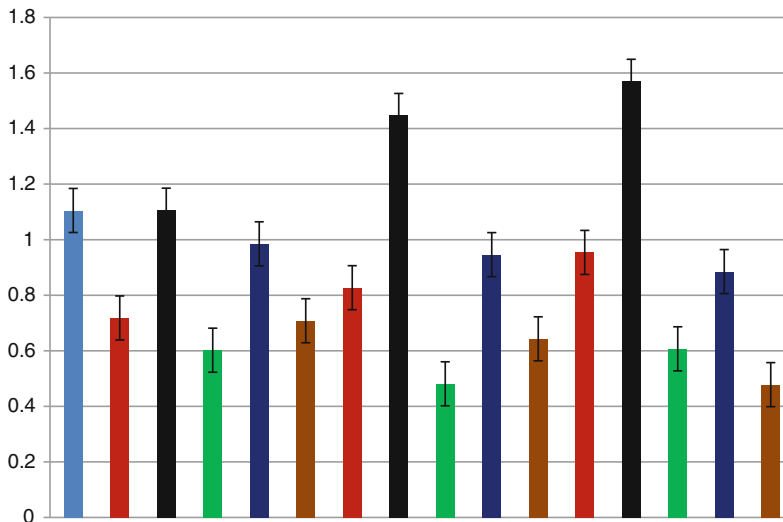
In culture, the NO released by the macrophages into the medium is converted to several nitrogen derivatives, from which only nitrite is stable, being easily measured by Griess reagent (1.0 % sulphanilamide and 0.1 % *N*-(1)-naphthylethylenediamine in 5 % phosphoric acid). After incubation, 100  $\mu$ L of culture medium supernatant was mixed with the same volume of Griess reagent, during 10 min, at room temperature. The nitrite produced was determined by measuring the optical density at 540 nm, in a microplate reader (Shimadzu).

**14.3.1.1 Results**

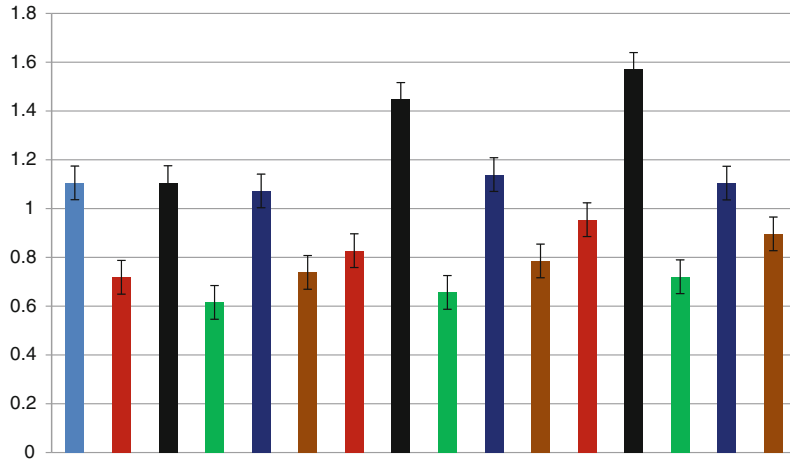
**(A) Cell viability:**

1. LPS-induced inflammation:

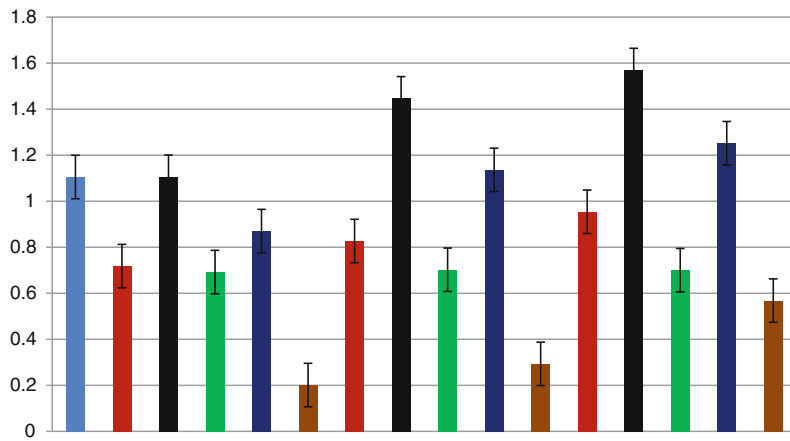
**LPS1 : 1  $\mu$ g/ml LPS2 : 500 ng/ml LPS3 : 200 ng/ml**  
**Drug A: 250  $\mu$ g/ml Drug B: 250  $\mu$ g/ml Drug C: 250  $\mu$ g/ml**  
**Dexamethasone : 9 nM ( positive control )**  
**Control (without treatment)**



**LPS1 : 1 µg/ml LPS2 : 500 ng/ml LPS3 : 200 ng/ml**  
**Drug A: 100 µg/ml Drug B: 100 µg/ml Drug C: 100 µg/ml**  
**Dexamethasone : 9 nM ( positive control )**  
**Control (without treatment)**

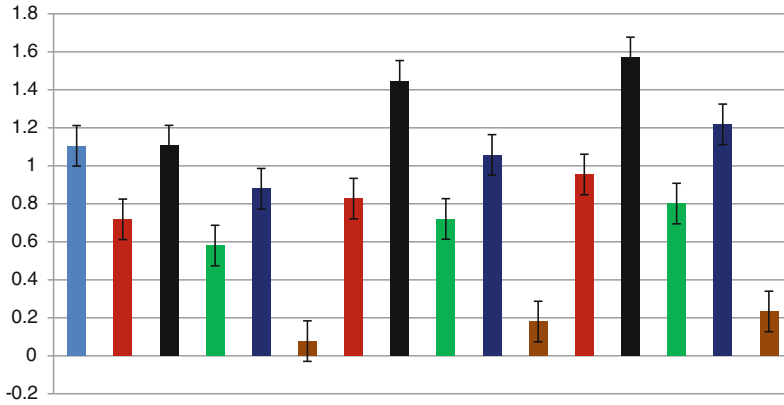


**LPS1 : 1 µg/ml LPS2 : 500 ng/ml LPS3 : 200 ng/ml**  
**Drug A: 50 µg/ml Drug B: 50 µg/ml Drug C: 50 µg/ml**  
**Dexamethasone : 9 nM ( positive control )**  
**Control (without treatment)**

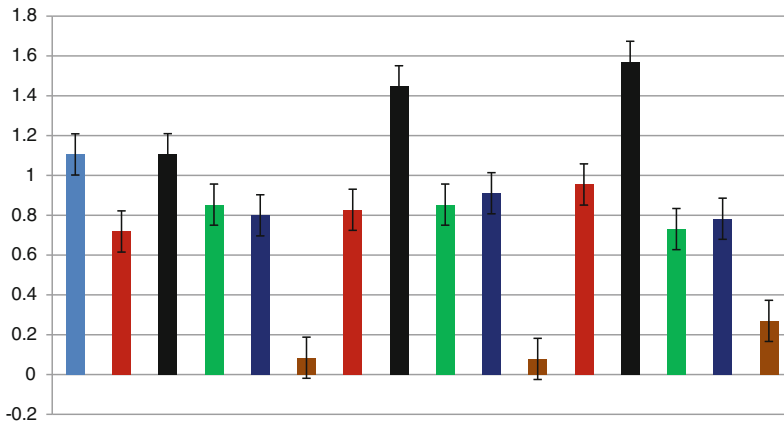




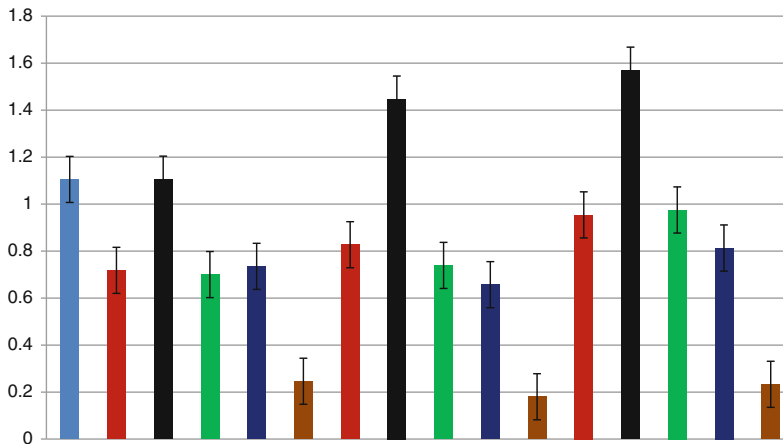
**LPS1 : 1 µg/ml LPS2 : 500 ng/ml LPS3 : 200 ng/ml**  
**Drug A: 10 µg/ml Drug B: 10 µg/ml Drug C: 10 µg/ml**  
**Dexamethasone : 9 nM ( positive control )**  
**Control (without treatment)**



**LPS1 : 1 µg/ml LPS2 : 500 ng/ml LPS3 : 200 ng/ml**  
**Drug A: 1 µg/ml Drug B: 1 µg/ml Drug C: 1 µg/ml**  
**Dexamethasone : 9 nM ( positive control )**  
**Control (without treatment)**



**LPS1 : 1 µg/ml LPS2 : 500 ng/ml LPS3 : 200 ng/ml**  
**Drug A: 500 ng/ml Drug B: 500 ng/ml Drug C: 500 ng/ml**  
**Dexamethasone : 9 nM ( positive control )**  
**Control (without treatment)**



Different herbal extracts exert their effects on cell line in a dose-dependent manner; for example, some doses acts as anti-inflammatory, whereas there are some doses performing as proinflammatory. In the entire scenario, dexamethasone has been taken as positive control to evaluate the anti-inflammatory activities on the LPS-induced inflammation on RAW cell line.

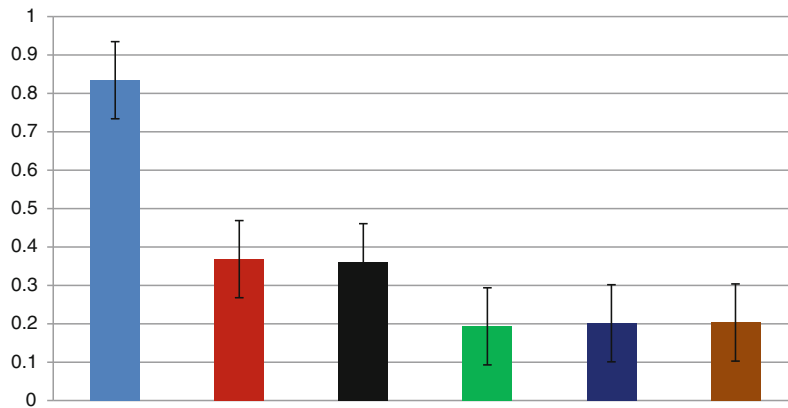
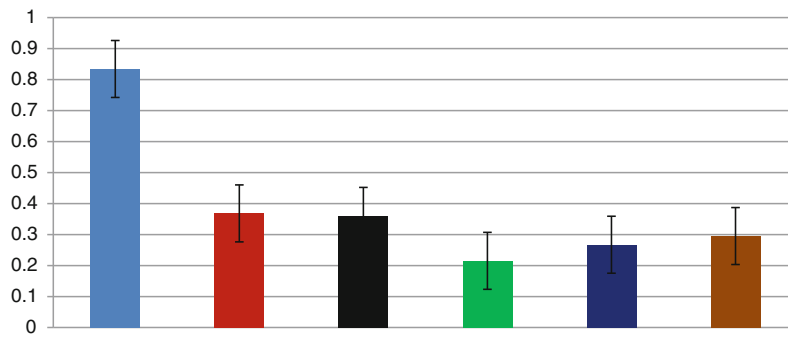
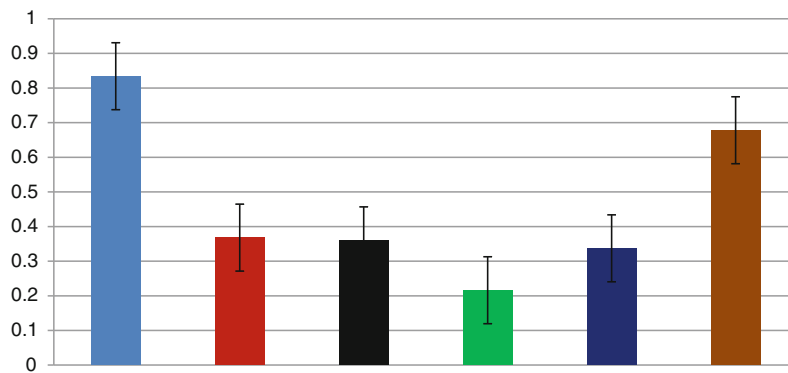
For the extract named as A, 250, 100, 50, and 10 µg/ml doses act as proinflammatory reducing the cell viability in all three LPS-treated samples, whereas the 500 ng/ml dose shows very little anti-inflammatory activities in 200 ng/ml LPS-treated cells though in other two LPS doses, it retains its proinflammatory activities as well.

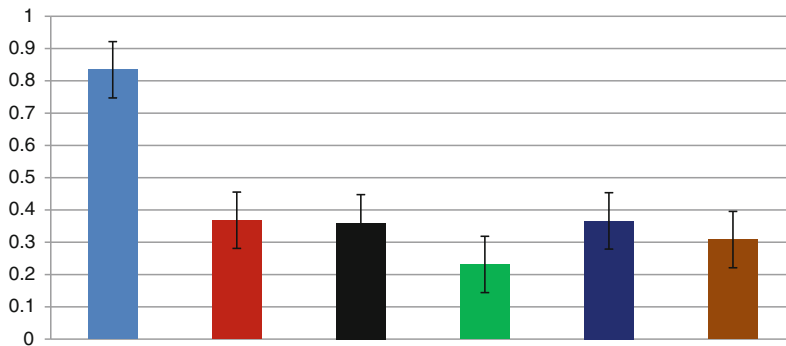
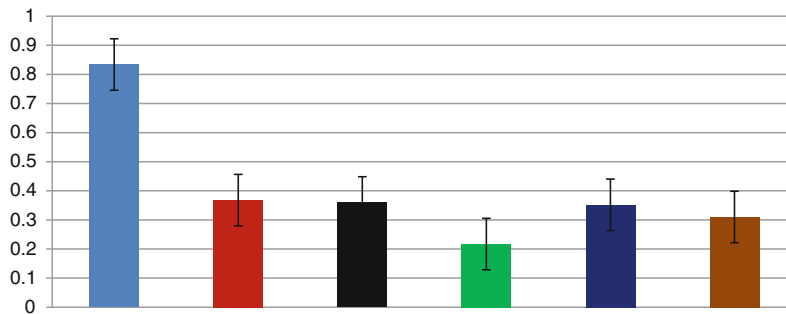
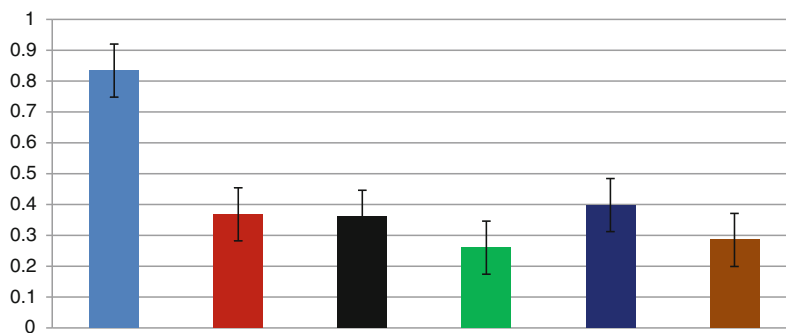
The sample B in 250 µg/ml dose increases the cellular vitality near about 1.5-folds in comparison with the 1 µg/ml LPS-treated cell, just reaching its normal, i.e., untreated proliferative rate though this concentration of extract is not sufficient for 500 and 200 ng/ml LPS-treated cells. But the 100 µg/ml dose of the extract is sufficient to increase cell vitality in all three

LPS-treated cells, where it significantly increases cell vitality in 200 ng/ml LPS dose. Same result has been obtained in 100 and 10 µg/ml doses of the extract where it significantly increases the cell vitality in both 500 and 200 ng/ml LPS-treated cells. In both 1 and 500 ng/ml doses of the extract, there is no such significant alterations in cell vitality in any of the LPS-treated cell sample. This result clearly points out that this extract shows its anti-inflammatory activities on LPS-treated RAW cells by increasing cell viability.

In all doses of the extract C, there is no such alternations in increasing the LPS-treated cell viability; moreover, in 10, 1, and 500 ng/ml doses, it exerts a strong pro-inflammatory activities where it reduces four to fivefold cell viability in comparison with the LPS-treated cells, i.e., most of the cells die under this particular type of treatment. Though this result fails to explain any detail idea about the anti-inflammatory activities of this particular type of extract but it is clear that in low concentration, this methanolic extract can reduce the cell viability, even it can kill the cell in a very high number.

## 2. 3 % TG-induced inflammation:

**3% TG 9 nM dexamethasone 250 µg/ml methanolic extract (A,B,C)****3% TG 9 nM dexamethasone 100 µg/ml methanolic extract (A,B,C)****3% TG 9 nM dexamethasone 50 µg/ml methanolic extract (A,B,C)**

**3% TG 9 nM dexamethasone 10 µg/ml methanolic extract (A,B,C)****3% TG 9 nM dexamethasone 1 µg/ml methanolic extract (A,B,C)****3% TG 9 nM dexamethasone 500 µg/ml methanolic extract (A,B,C)**

After 3 % TG treatment, cellular viability decreases near about 50 % which is a clear demonstration of inflammatory response, but it is very interesting to note that any of the methanolic extract fail to show any anti-inflammatory action in a significant manner.

The methanolic extract of the sample A exhibits a strong pro-inflammatory action by reducing cell viability in all six doses, whereas the sample B shows very little anti-inflammatory action in 500 ng/ml dose, but in higher doses, it significantly reduces the cell viability pronouncing its

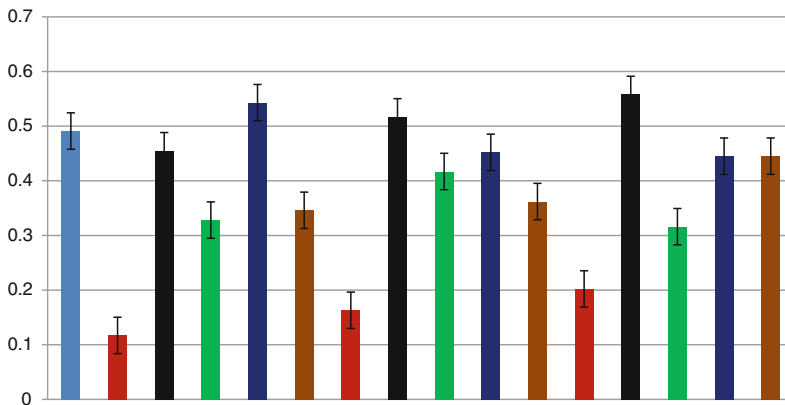
pro-inflammatory response, but at the same time, in 50, 10, and 1 µg/ml dose, it shows neither proinflammatory or anti-inflammatory response as the cell viability remains same as 3 % TG-treated sample which is actually just 50 % lower than the control group.

A very interesting result has been obtained in case of methanolic extract of sample C where it shows a strong proinflammatory response in 250 and 100 µg/ml dose, reducing cell viability near about 25–30 %, respectively. 50 µg/ml dose exhibits a very good example of

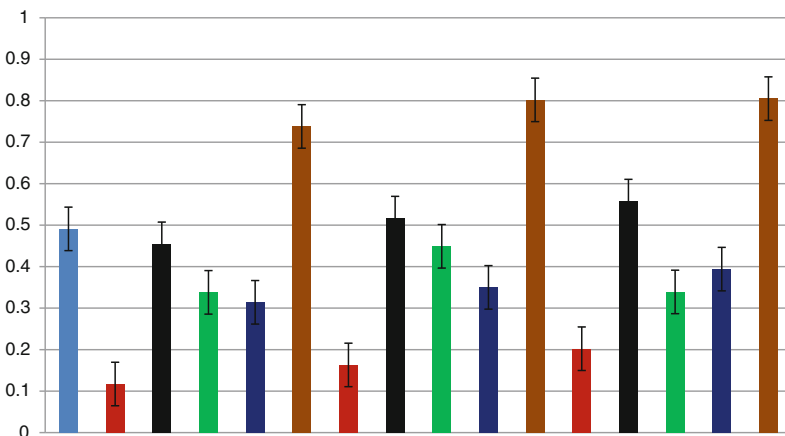
anti-inflammatory action in 3 % TG-treated cells increasing the cell viability near about twofold than the 3 % TG-treated cells, just reaching the control group. Again this, same extract shows proinflammatory actions in lower dose; that is, this particular methanolic extract can perform both proinflammatory and anti-inflammatory manner depending on the concentration, which can be said properly as “in a dose-dependent manner.”

- (B) Measurement of super oxide radicals:  
 1. On LPS-induced inflammation:

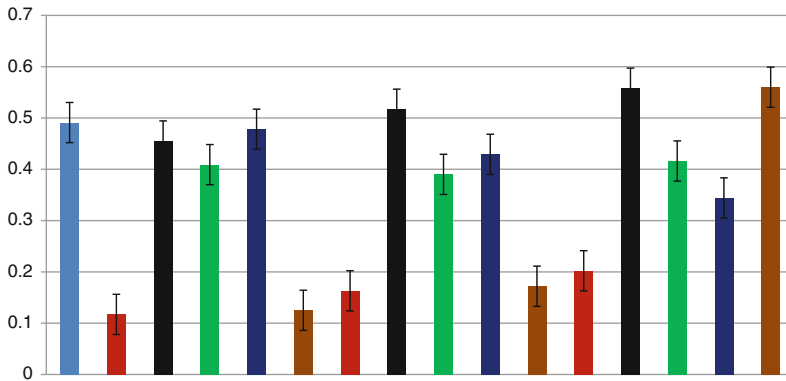
**LPS1 : 1 µg/ml LPS2 : 500 ng/ml LPS3 : 200 ng/ml**  
**Drug A: 250 µg/ml Drug B: 250 µg/ml Drug C: 250 µg/ml**  
**Dexamethasone : 9 nM ( positive control )**  
**Control (without treatment)**



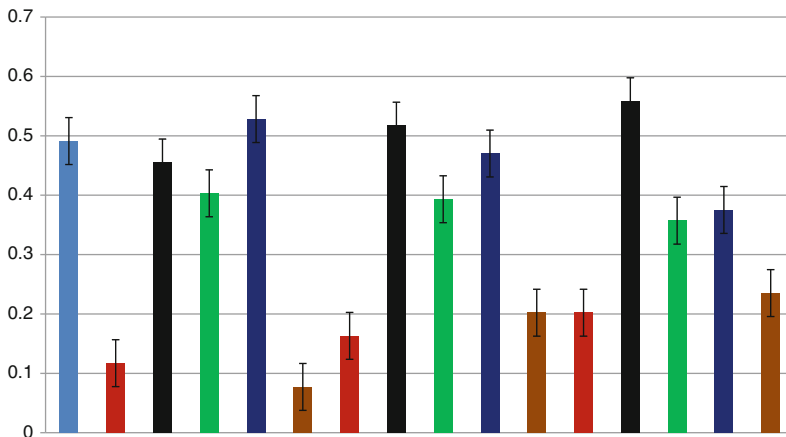
**LPS1 : 1 µg/ml LPS2 : 500 ng/ml LPS3 : 200 ng/ml**  
**Drug A: 100 µg/ml Drug B: 100 µg/ml Drug C: 100 µg/ml**  
**Dexamethasone : 9 nM ( positive control )**



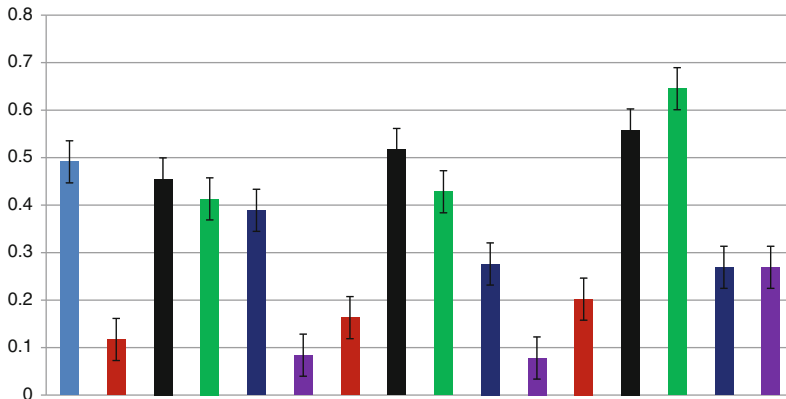
**LPS1 : 1 µg/ml LPS2 : 500 ng/ml LPS3 : 200 ng/ml**  
**Drug A: 50 µg/ml Drug B: 50 µg/ml Drug C: 50 µg/ml**  
**Dexamethasone : 9 nM ( positive control )**



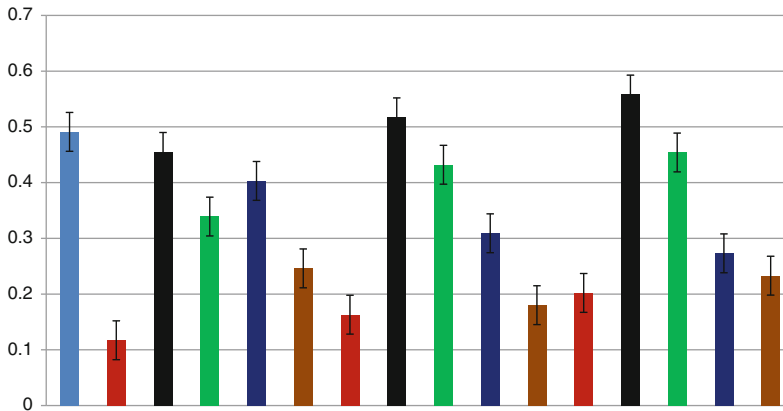
**LPS1 : 1 µg/ml LPS2 : 500 ng/ml LPS3 : 200 ng/ml**  
**Drug A: 10 µg/ml Drug B: 10 µg/ml Drug C: 10 µg/ml**  
**Dexamethasone : 9 nM ( positive control )**



**LPS1 : 1 µg/ml LPS2 : 500 ng/ml LPS3 : 200 ng/ml**  
**Drug A: 1 µg/ml Drug B: 1 µg/ml Drug C: 1 µg/ml**  
**Dexamethasone : 9 nM ( positive control )**



**LPS1 : 1 µg/ml LPS2 : 500 ng/ml LPS3 : 200 ng/ml**  
**Drug A: 500 µg/ml Drug B: 500 µg/ml Drug C: 500 µg/ml**  
**Dexamethasone : 9 nM ( positive control )**



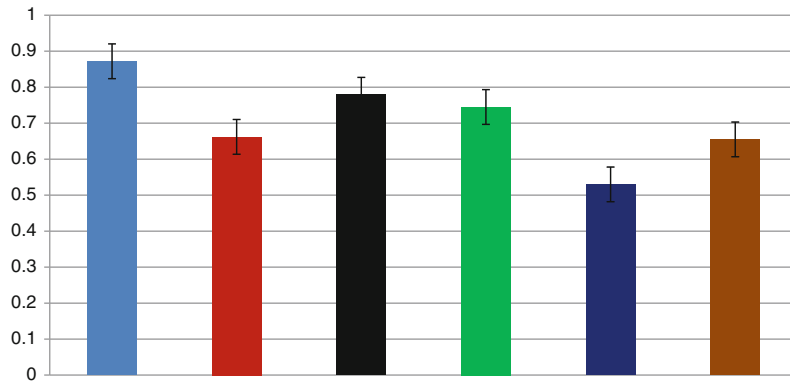
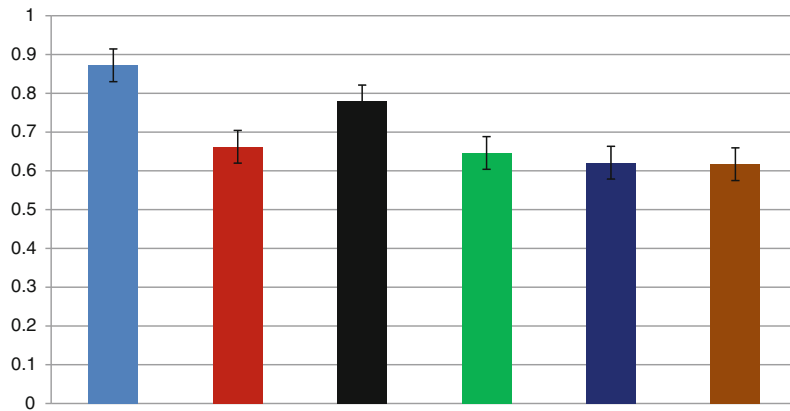
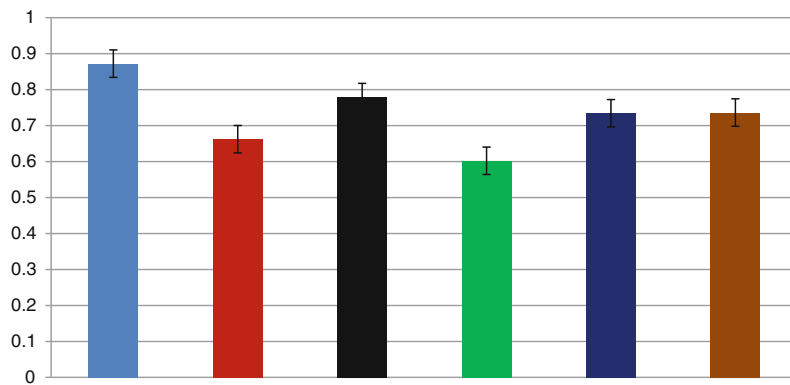
To measure the inhibition of superoxide ion generation, NBT methods were applied where a very interesting result has been obtained.

The methanolic extract of A significantly inhibits the superoxide ion production in LPS-treated cells in all groups where this inhibition value is near about threefold (in case of 250 µg/ml dose) to fourfold, but it reaches to the control value in case of 1 and 500 ng/ml dose of the extract where LPS dose was 500 and 200 ng/ml. This mean that particular methanolic extract is useful to inhibit the superoxide ion production in LPS-treated RAW cells, but at the same time in concentration cell loses its viability, shown in the previous result, so there should be some other signaling pathway by which this extract inhibits the superoxide ion generation which ultimately reduces the cell viability.

Same result has been obtained in case of the methanolic extract named as B, where it shows a potent anti-inflammatory action by reducing the superoxide ion production in LPS-treated RAW cells at the particular concentrations of 250, 50, and 10 µg/ml dose, but the result is not significant in other doses. So this can be concluded that this extract can show an useful anti-inflammatory property in a range between 10 and 250 µg/ml as the cell show a high rate of viability in this range so this can be taken as optimum dose having anti-inflammatory activities on LPS-induced inflamed RAW cells.

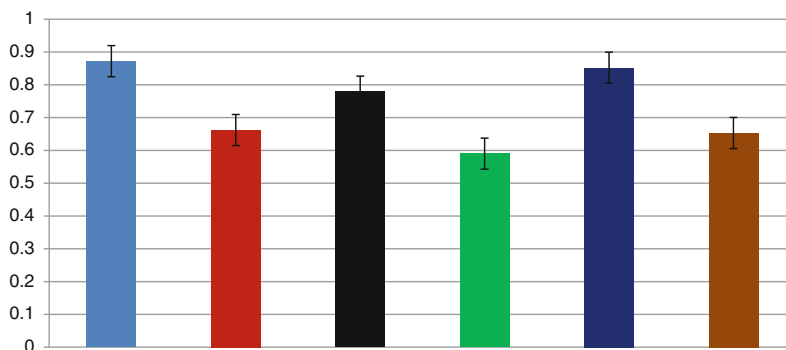
Just like other two extracts, another extract C also shows a potent anti-inflammatory action at a particular concentration which is 100 µg/ml. In lower doses, it does not exhibit inhibitory activities of superoxide ion in a significant level.

## 2. TG-induced inflammation:

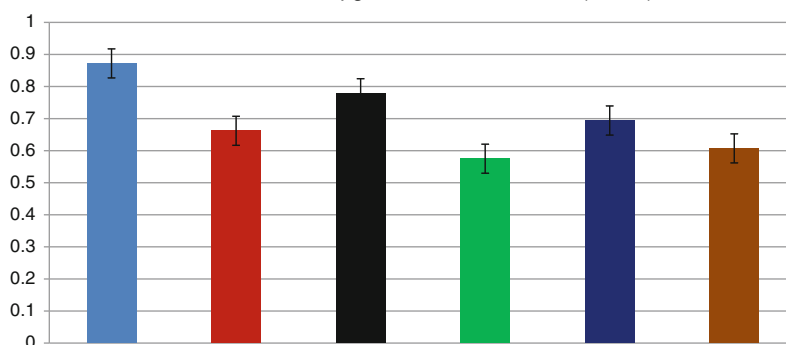
**3% TG 9 nM dexamethasone 250 µg/ml methanolic extract (A,B,C)****3% TG 9 nM dexamethasone 100 µg/ml methanolic extract (A,B,C)****3% TG 9 nM dexamethasone 50 µg/ml methanolic extract (A,B,C)**



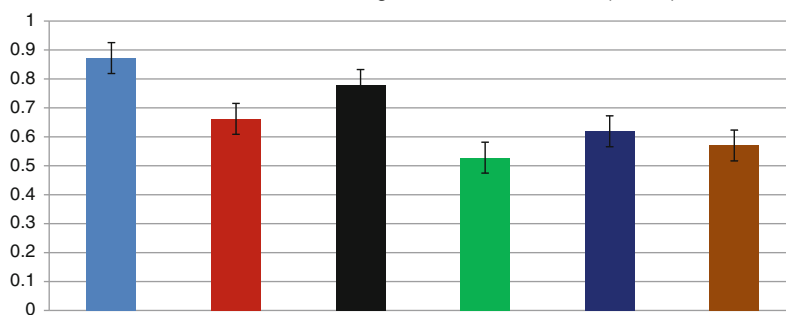
**3% TG 9 nM dexamethasone 10 µg/ml methanolic extract (A,B,C)**



**3% TG 9 nM dexamethasone 1 µg/ml methanolic extract (A,B,C)**



**3% TG 9 nM dexamethasone 500 ng/ml methanolic extract (A,B,C)**



The capability to inhibit the superoxide ions in 3 % TG-treated RAW cells, various doses of the extract have been used, in which 250 µg/ml dose of the methanolic extract A has been shown any significant result, whereas in lower doses, it has a potent proinflammatory

activity also which can be correlated with the MTT assay result, and in lower doses, this drug also has been reported to reduce the cell viability.

The extract B has been shown to inhibit the ROS production in 10 µg/ml dose in a significant level. But in other doses, there is no such significant alternation in

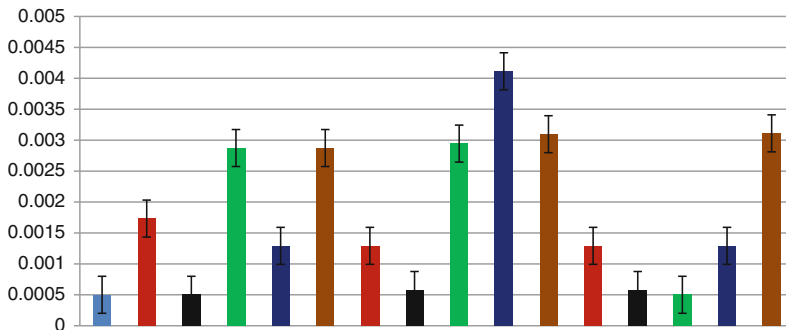
ROS production in comparison with the only TG-treated cells.

The extract C does not alter the ROS production in any significant level; that is, after the C extract treatment at various concentrations in 3 % TG-treated RAW cells, the superoxide ion production remains as much as same in comparison with only 3 % TG-treated cells. But as our previous result regarding cell viability

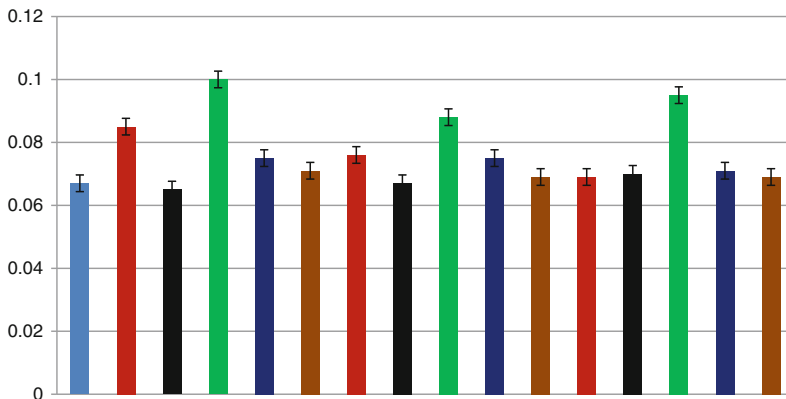
study has been advocated that at certain concentrations, this extract can retain the cell viability of TG-treated cell as like as the control group, there should be definite any pathway to this which most probably not via the ROS scavenging mechanism, may be any other one.

**14.3.2 NO Estimation**

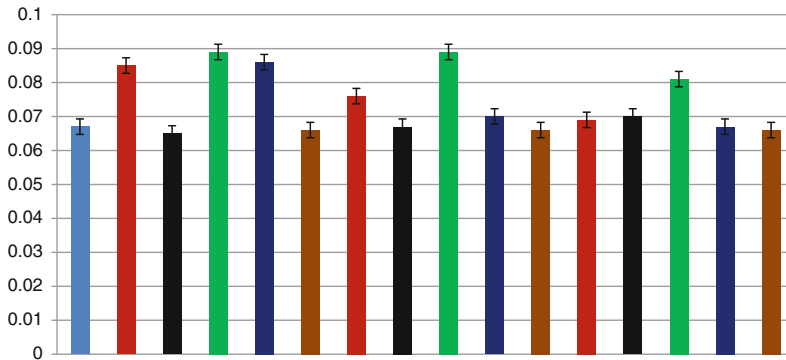
**LPS1 : 1 µg/ml LPS2 : 500 ng/ml LPS3 : 200 ng/ml**  
**Drug A: 250 µg/ml Drug B: 250 µg/ml Drug C: 250 µg/ml**  
**Dexamethasone : 9 nM ( positive control )**



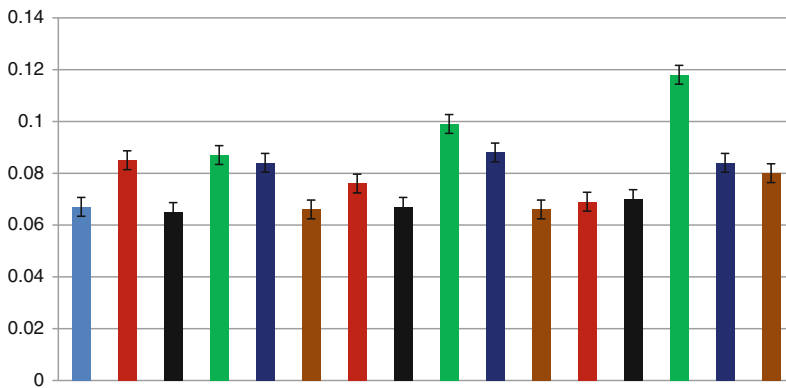
**LPS1 : 1 µg/ml LPS2 : 500 ng/ml LPS3 : 200 ng/ml**  
**Drug A: 100 µg/ml Drug B: 100 µg/ml Drug C: 100 µg/ml**  
**Dexamethasone : 9 nM ( positive control )**



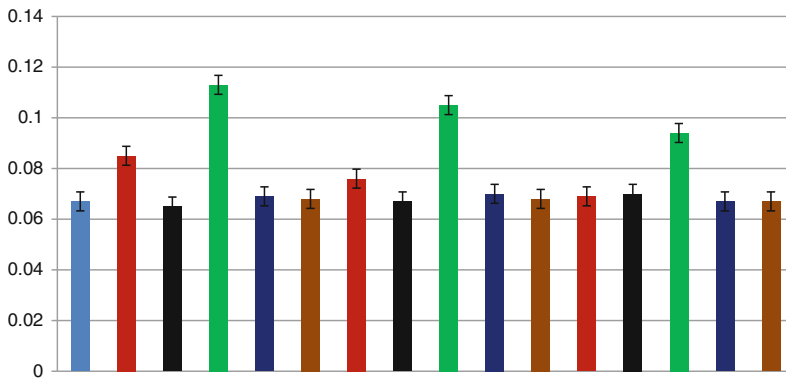
LPS1 : 1 µg/ml LPS2 : 500 ng/ml LPS3 : 200 ng/ml  
Drug A: 50 µg/ml Drug B: 50 µg/ml Drug C: 50 µg/ml  
Dexamethasone : 9 nM ( positive control )



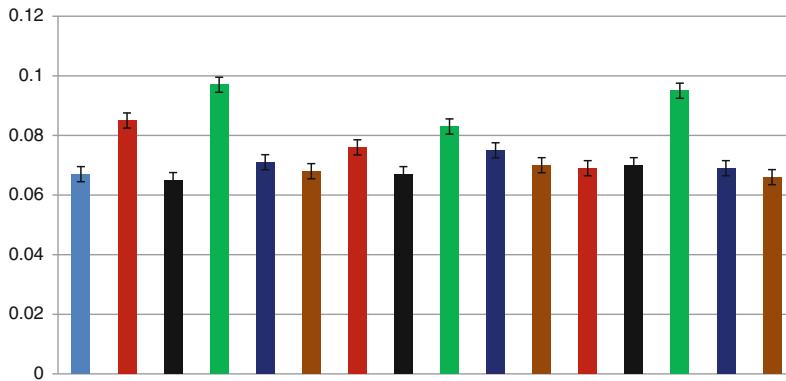
LPS1 : 1 µg/ml LPS2 : 500 ng/ml LPS3 : 200 ng/ml  
Drug A: 10 µg/ml Drug B: 10 µg/ml Drug C: 10 µg/ml  
Dexamethasone : 9 nM ( positive control )



LPS1 : 1 µg/ml LPS2 : 500 ng/ml LPS3 : 200 ng/ml  
Drug A: 1 µg/ml Drug B: 1 µg/ml Drug C: 1 µg/ml  
Dexamethasone : 9 nM ( positive control )



**LPS1 : 1 µg/ml LPS2 : 500 ng/ml LPS3 : 200 ng/ml**  
**Drug A: 1 µg/ml Drug B: 1 µg/ml Drug C: 1 µg/ml**  
**Dexamethasone : 9 nM ( positive control )**

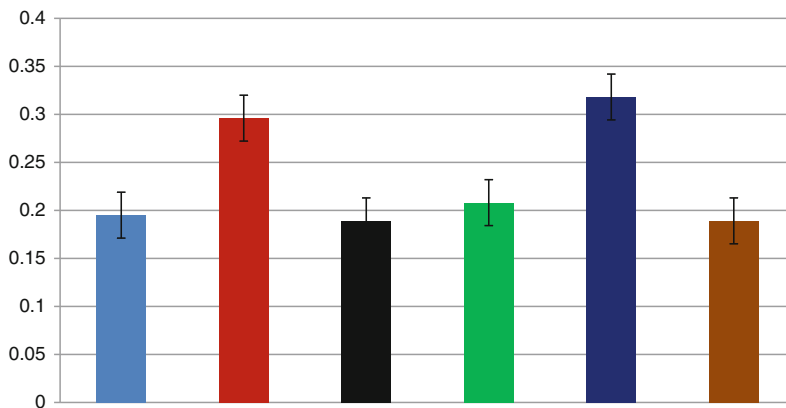


The methanolic extract A has been shown a strong proinflammatory activities regarding the nitrosative burst as in all doses, it increases the NO level in TG-treated cells in comparison with the only 3 % TG-treated group. At the same time, the extracts B and C have been shown to scavenge RNS molecule by reducing the NO level at higher doses, but not in the lower doses. So these two extracts, viz B and C, are a potent anti-inflammatory molecule only at the higher doses.

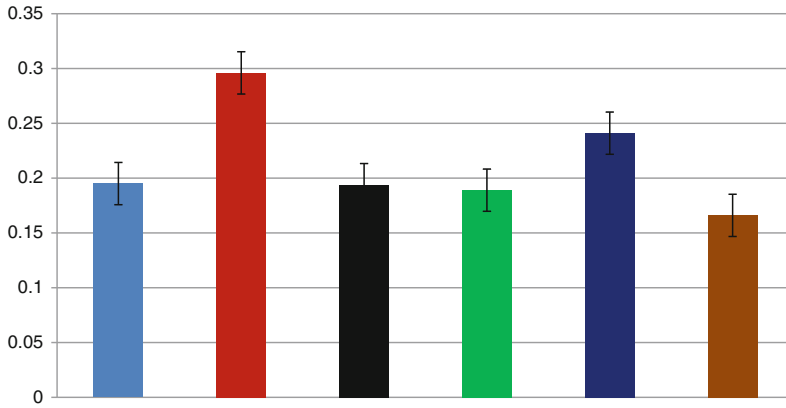
The methanolic extracts of A and C both can reduce the NO level in a significant manner, i.e., near about 2- to 3-fold reduction, in all the doses, whereas the extract B is not so much potent to scavenge the ROI by inhibiting the NO production in its higher doses, but this is active in lower dose treated groups. So these extracts work in a dose-dependent manner and also depend on what type of antigen has been applied on the concerned cell type.

TG-induced inflammation

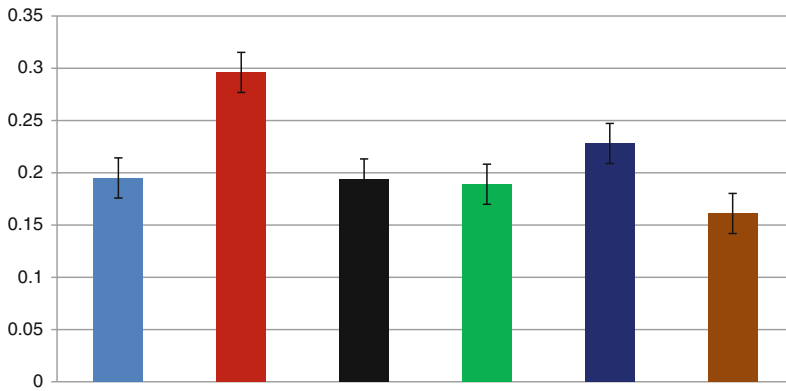
**3% TG 9 nM dexamethasone 250 µg/ml methanolic extract (A,B,C)**



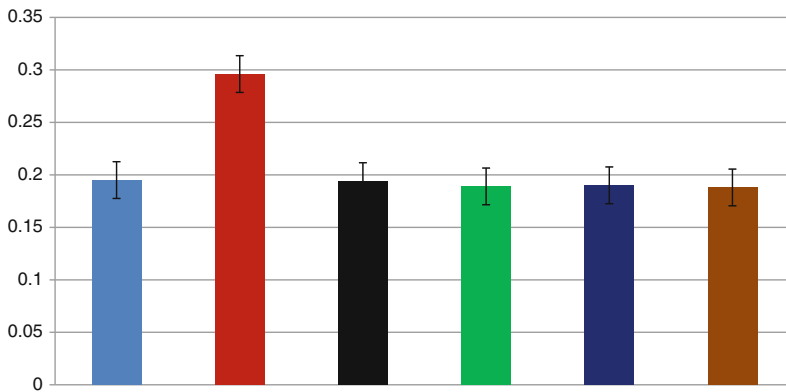
**3% TG 9 nM dexamethasone 100 µg/ml methanolic extract (A,B,C)**

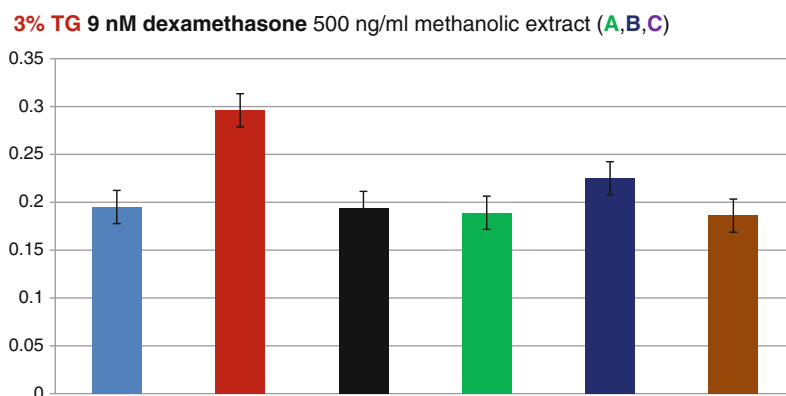
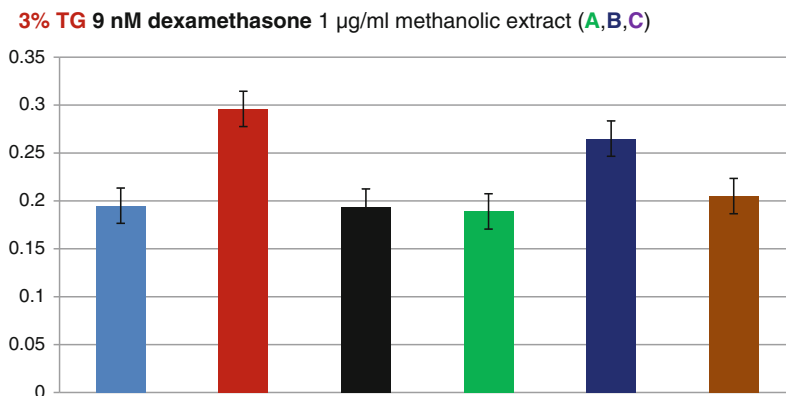


**3% TG 9 nM dexamethasone 50 µg/ml methanolic extract (A,B,C)**



**3% TG 9 nM dexamethasone 10 µg/ml methanolic extract (A,B,C)**





#### 14.4 Specific Objectives Revisited at the Initiation of Project

Specific Aim 1. To explore anti-inflammatory properties of the above samples with methanolic and water extracts in in vitro and in vivo disease models of pulmonary, intestinal, and systemic inflammation as outlined in para 12.

Specific Aim 2. To explore regenerative potential of the same in the disease models which are both inflammatory and degenerative in pathophysiology.

Specific Aim 3. Metabolomic status screening and characterization of potential candidates

identified and characterized from specific aims 1 and 2.

#### 14.5 Research Design

- Extracts of edible plant parts:
- In vitro assays of inflammation:
  - Expressional profiling of iNOS and NFKB activities.
  - To evaluate the proinflammatory and anti-inflammatory activities of these extracts, a direct correlation between the TNF- $\alpha$  and TGF- $\beta$ 1 expression.
  - To evaluate the exact level of ROI and RONI scavenging activity, DAF-FM (for ROS) and Dihydro rhodamine (for RNS).

- Evaluation of total cell viability flow cytometric analysis by using Propidium iodide.
  - Evaluation of antiapoptotic activities (whether present or not) of these extracts flow cytometric analysis by using Annexin V.
- In vivo preclinical disease models

### 14.5.1 Animals to Be Used in These Experiments

From the data of various experiments, we know that mice do not spontaneously develop asthma; for this reason to investigate the processes underlying the asthma, an artificial asthmatic-like reaction has to be induced in the airways of the experimental animals. The most commonly used strain of mouse for antigen challenge models is BALB/c as they develop a good T-helper cell 2 (Th2)-biased immunological response (Boyce and Austen 2005). However, C57BL/6 strain has been used successfully in allergen challenge studies (Kumar et al. 2008). So in this experimental purpose inbred BALB/c, C57BL/6 and swiss albino strain of mice, collected from the available animal facility of us, will be selected as wild type from which different knockout model, both single and double knockout model, will be generated.

### 14.5.2 Allergen Sensitization and Challenge

For **acute asthma model**, mice will be sensitized and later challenged with OVA [12]. Mice will be immunized with OVA (100 µg) complexed with aluminum sulfate in a 0.2 ml volume, administered by i.p. injection on day 0. On days 8 (250 µg of OVA) and on days 15, 18, and 21 (125 µg of OVA), mice will be anesthetized briefly with inhalation of isoflurane in a standard anesthesia chamber and given OVA by intratracheal (i.t.) administration (Iwata A, Ji, 2001). Mice will be anesthetised and placed in a supine position on the board and extending the animal's tongue with lined forceps 50 µg/l of OVA (in the required concentration) will be placed at the back

of its tongue. The control group will receive normal saline with aluminum sulfate by i.p. route on day 0 and 0.05 ml of 0.9 % saline by i.t. route on days 8, 15, 18, and 21.

For **chronic asthma model**, mice (8- to 12-week-old) will be sensitized with 50 µg OVA (grade V; Sigma-Aldrich, St. Louis, MO) in 0.5 mg aluminum hydroxide by s.c. injections on days 0, 7, 14, and 21 and then challenged with OVA (20 µg per mouse) intranasally on days 23, 25, and 28 (Song et al. 2009) followed by additional intranasal challenges with OVA twice a week for 8 week. Control mice will be administered PBS instead of OVA for sensitization and challenges.

For **IPF model**, treatment was performed with adult Balb-C mice. Sixteen mice were anaesthetized using propofol received a single dose of bleomycin(naproleo, miracalus) both intratracheally and intranasally, bleomycin 0.075 U/ml bleomycin dissolved in 1 ml of 0.09 % sterile saline water, from here 16 mice received a single dose of bleomycin at day 0, 20 µl was administered intranasally and 40 µl from intra tracheally. Mice were administered with 40 µl of fisetin, 40 µl of curcumin, and 40 µl mesoporous carbon nano(MCN) particle conjugated fisetin intratracheally at day 7,14, and 21; and at the day 28, they were killed and organ such as lung, bone marrow, liver, bronchoalveolar lavage, and peripheral blood were collected. Weight and other parameter of mice were taken on a regular basis according to rodent health monitoring program (RHMP).

Mice developed marked interstitial and alveolar fibrosis, detected by Masson's trichrome staining, lung morphology was detected by hematoxylin eosine staining, collagen content was detected by hydroxyproline estimation, blood smear preparation and cytospin sample staining with hematoxylin was used to quantify the differential cell count of blood, and clonogenic potential was detected by colony-forming unit (CFU) assay. Weight of mice was taken in a regular basis to observe the development of fibrosis.

For **septic and aseptic peritonitis model**, BALB/c mice were used in this study. All experiments were performed according to rules

laid down by the institutional and departmental animal ethics committee and the animals housed under specific pathogen-free conditions at the animal housing vivarium of the Department of Zoology, University of Calcutta. All data are presented as mean  $\pm$  SEM, and only p values of less than 0.05 have been considered.

**Induction of Peritonitis:** Thirty-nine BALB/c mice (6–8 week old, weighing 25 g) were divided into 13 groups ( $n = 3$ ): Control, TG24, TG24F, TG24MF, TG48, TG48F, TG48MF, TG72, TG72F, TG72MF, TG96, TG96F, and TG96MF. 400  $\mu$ l of 3 % TG was injected intraperitoneally (200  $\mu$ l near each hind leg).

For **IBD model**, the following assays were done. Treatment was performed with adult Balb/c mice. Control group was devoid of any experimental treatment, and Group 2 was administered with 40  $\mu$ l of 3 % DSS Sicco Pvt. Ltd., India (3 g DSS in 100 ml autoclaved water), by oral gavage on day 0 and day 5 to induce colitis. Group 3 was treated with 3 % DSS similar to Group 2 for induction of colitis, and in addition, 200  $\mu$ l of whey water containing  $1 \times 10^8$  CFU (approx.) of probiotics (ABT) was administered on day 5, day 7, and day 10 of treatment to ameliorate the inflammation caused by DSS treatment. Control group was administered equal volume of autoclaved water by gavage at the same point in time when experimental groups received intervention. Group 2 was also administered buffer at the same points in time when Group 3 was administered probiotics. All 3 groups of mice were killed on day 14. Organs such as bone marrow, intestine, colon, spleen, Peyer's patch, lung, kidney, and peripheral blood were collected for further assays.

### 14.5.3 Bronchoalveolar Lavage Fluid and Lung Tissue Collection

Mice will be killed 24 h after the last allergen challenge, and bronchoalveolar lavage fluid (BALF) will be pooled after three washes with saline (0.5 ml each). Total and differential cell counts will be done, and BALF supernatants will

be stored at  $-70$  °C for further evaluation. Right lungs will be snap-frozen, and left lungs will be perfused with 4 % paraformaldehyde to preserve pulmonary structure, fixed in 4 % paraformaldehyde, and paraffin-embedded sections for histological analysis.

### 14.5.4 Assessments of Cell Viability, Cell Number and Cell Shape and Size

Specific cell counter come image analyzer will be used to count and assess the cell number, viability, and their shape, collected from the BALF, bone marrow, and spleen.

### 14.5.5 Flow Chamber Studies

Rolling of bone marrow cells collected from the femurs of control and treated mice on endothelial adhesion molecules under conditions of flow will be evaluated in an in vitro parallel plate flow chamber (Rao et al. 2007; Han et al. 2008). Interaction of bone marrow cells ( $2 \times 10^5$ ) with recombinant mouse (rm) VCAM-1–, rmGal-3–, ICAM-1–, Selectin (10 mg/ml in PBS, 200 ml per cover slip), or PBS (control)-coated glass cover slips at a flow rate of 1 ml/min (wall shear stress, 1.0–2.0 dynes/cm<sup>2</sup>) will be evaluated and recorded to manually determine the number of interacting cells. Results will be expressed as the number of rolling cells per minute.

### 14.5.6 Determination of ROS and RNS Level

To detect the ROS and RNS, following methods will be applied

1. Assessment of myeloperoxidase (MPO): myeloperoxidase, found in circulating neutrophils, monocytes, and lung tissue macrophages, is a member of heme peroxidase superfamily stored within the azurophilic granules of leukocytes [18]. This has ability



- to use chloride as a cosubstrate with hydrogen peroxide to generate chlorinating oxidants such as hypochlorous acid which causes tissue damage and initiation of propagation of acute and chronic inflammatory diseases (Podrez et al. 2000; Zhang et al. 2001), so MPO-derived chlorinated compounds are specific biomarkers for disease progression (Malle et al. 2007).
2. Thiol detection method: Thiols are extremely efficient antioxidants which are able to protect cellular lipids, proteins, and nucleic acids against peroxidative damage due to their strong reductive capacity and their ability to react with free radicals (Wlodek 2002), so the detection and measurement of free thiols (i.e., free cysteine, glutathione, and cysteine residues on proteins) are important to study ROS and RNS production.
  3. Glucose Assay: Glucose ( $C_6H_{12}O_6$ ) is a ubiquitous fuel molecule in biological system. It is oxidized through a series of enzyme-catalyzed reactions to form carbon dioxide and water, yielding the universal energy molecule ATP. Due to its importance in metabolism, glucose level is a key diagnostic parameter for many metabolic disorders.
  4. Nitrate and nitrite estimation: In response to inflammatory stimuli, endothelial cells and macrophages produce nitric oxide (NO), which leads to the peroxynitrite, destruction of iron sulfur clusters, thiol nitosation, and nitration of protein tyrosine residues at its elevated level. So, the amount of NO produced in different biological systems can vary over several orders of magnitude, and its subsequent chemical reactivity is diverse. In the system, the produced NO is converted into nitrate and nitrite, and the relative proportion of these two molecules is variable.
  5. Flow cytometric study to detect ROS production:  
The fluorescent intensity of the compounds oxidized by ROS can be measured by dihydrorhodamine 123 and 2,7 dichlorofluorescein diacetate compounds that can diffuse into the cells, then deacetylated, and lose their fluorescence [21]. When oxidized by ROS, they become highly fluorescent. It can be quantified which reflect the rate and quantity of the ROS produced in the concerned sample tissue or cell.
  6. Electron spin resonance spectroscopy:  
Hydroxyl radical formation after allergen treatment in both in vivo and in vitro model will be assessed by electron spin resonance (ESR) spectroscopy (Shi et al. 2003).
  7. Immunocytochemical methods to detect nitrotyrosine:  
The immunohistochemical method to detect the nitrotyrosine is a good method to detect peroxynitrite and other RNSs (Liliaua et al. 1999) as the peroxynitrite is the reaction product of superoxide and nitric oxide and it plays crucial role in the inflammatory responses in asthma [24].

#### **14.5.7 Cytochrome c Reduction or Nitro Blue Tetrazolium (NBT) Reduction Method (Used for Leukocyte NADPH Oxidase Activity)**

Cytochrome c reduction and NBT reduction both can accurately predict whether ROS have been produced by leukocytes or by other. The two most commonly used reagents to detect superoxide anion radicals are NBT and ferricytochrome c (Cyt). Superoxide formed by electron transfer from a donor to molecular oxygen can be quenched by NBT and Cyt, and these reagents get reduced to diformazan and ferricytochrome c, respectively. Detection of superoxide is confirmed when addition of the enzyme superoxide dismutase (SOD) causes a decrease in production of diformazan from NBT or no production of ferricytochrome c from cytochrome c. Hence, it is concluded that cytochrome c reduction only measures extracellularly released superoxide, whereas NBT may be reduced by, extracellular superoxide, or other molecules as well [26].

### 14.5.8 Biochemical Assessments of ROS and RNS Regulating Enzymes

Different enzymes, such as superoxide dismutase and catalase regulating the reactive oxygen and nitrogen species, will be biochemically evaluated along with the quantitative measurements of ascorbic acid as a potent antioxidant by following conventional methodologies. SOD, an essential antioxidant that catalyzes superoxide radicals to hydrogen peroxide, presents in three forms in the mammalian system as (i) the copper-zinc superoxide dismutase (Cu, ZnSOD) located in the cytosol, (ii) the manganese superoxide dismutase (MnSOD) primarily a mitochondrial enzyme, and (iii) extracellular superoxide dismutase (EC-SOD) usually found on the outside of the plasma membrane. Both intracellular and extracellular SOD activities are decreased in asthmatic lungs, which may be related to oxidant inactivation and/or nitration of various SOD isoforms loss of SOD activity undoubtedly potentiates extracellular matrix damage and tissue injury through increased formation of reactive oxygen and nitrogen species.

### 14.5.9 NO Estimation

Nitric oxide (NO), a relatively stable free radical, is increased in exhaled air of asthmatic individuals, threefold higher than normal NO concentrations in the lower airway and in the exhaled breath, as compared to healthy individuals, and this excessive NO production is increasingly implicated in the pathogenesis of inflammation in asthma [4, 5]; due to this reason, exhaled NO levels are inversely correlated with airflow parameters in asthmatic patients[5–8].

### 14.5.10 Immunoblots

After extraction and quantification of proteins from the lung, spleen, and lymph nodes, 10 % (w/v) homogenate will be prepared for Western blot. Equal amounts of proteins (50 µg)

determined by Folin's method will be loaded on SDS PAGE (10 %) for electrophoresis. Thereafter, proteins will be transferred electrophoretically to nitrocellulose membrane (NC) (Sigma-Aldrich, St. Louis, USA) overnight at 4 °C. NC will then be blocked for 60 min with Tris-buffered saline (TBS) (Tris 50 mM, pH 7.6) and then incubated with primary antiserum for one hour. Then, membranes will be washed for 10 min each (3 washes) in TBS-Tween 20. Then, NC membrane will be incubated with secondary conjugated with serum immunoglobulin (antirabbit IgG HRP, Santacruz, USA) (1:500) for 30 min and then again washing in TBS for 10 min (3 times). Signals will be detected using an ECL kit (Bio-Rad, Hercules, CA, USA). Blot for each protein will be repeated for three times. The densitometric analysis of the blots will be performed by scanning and quantifying the bands for density value by using computer assisted image analysis (Image J 1.38×, NIH, USA), and then, only the densitometric data will be presented as the mean of the integrated density value  $\pm$  S.E.M. A prestained multicolor broad range marker will be also run along with sample proteins to clarify the position of band obtained.

### 14.5.11 Assessment of GLUTs

To correlate the inflammatory pathways with the metabolic alternations, targeting the glucose transporters (GLUTs) helps in the transportation of main energy fuel glucose inside a cell and is very essential. As reported that GLUT 1 plays crucial role in mouse lung, after allergen treatment this has been aimed to find out any kind of alternations in GLUT1 protein expression. On the other hand from the work of several researchers, this has been established that expression of GLUT4 and 8 is insulin-dependent, so these two also have been targeted after allergen treatment.

### 14.5.12 Assessment of IRS1

It has now been established that IRS-1 is phosphorylated at serine residues by various kinases

that interfere with the ability of this protein to engage in insulin receptor signaling and result in alterations in insulin action [27–29]. In addition, suppressor of cytokine signaling (SOCS) proteins seems to inhibit insulin action at the level of insulin receptor substrates, although through a different mechanism 55–57 [30–32]; through the IRS-modifying enzymes, mounting evidence indicates that activation of JNK, IKK, and conventional protein kinase C (PKC) is central to mediating insulin resistance in response to various stresses leads to insulin resistance. They have all been reported to be able to inhibit insulin action by serine phosphorylation of IRS-1 (Gao et al. 2002; Aguirre et al. 2001; Griffin et al. 1999), although the activity of IKK in this regard has not yet been well established under physiological conditions. IRS-1 serine phosphorylation disrupts insulin receptor signaling through several distinct mechanisms and blocks insulin action 60, 61. These kinases also exert powerful effects on gene expression, including promoting further inflammatory gene expression through activation of activator protein-1 (AP-1) complexes and NF- $\kappa$ B (Baud et al. 2001). However, this aspect has not yet been thoroughly explored in metabolic homeostasis.

#### **14.5.13 Expressional Profiling of MUC5AC**

Hyperproduction of goblet cells and mucin in the airway epithelium is an important feature of airway inflammatory diseases such as asthma. MUC5AC expression involves the notch signaling pathways depending on epidermal growth factor (EGF)-stimulated generation of the notch intracellular domain (NICD) in a RBP-J $\kappa$ -dependent manner (). It is now established that ERK activation is necessary for the regulation of EGF receptor (EGFR)-mediated MUC5AC expression by notch signaling. So expressional profiling of this protein molecule is important biomarker to investigate the both acute and chronic form of asthma pathophysiology in an experimental model system.

#### **14.5.14 Expressional Profiling of NOS2 Protein**

Nitric oxide synthases (NOS) are enzymes responsible for synthesis of endogenous NO. These enzymes, present in three isoforms as NOS1 (neuronal), NOS2 (inducible), and NOS3 (endothelial) convert L-arginine to NO and L-citrulline in a reaction that requires oxygen and NADPH (Stuehr et al. 1999). Airway epithelia are a major cellular source of NOS2 in the healthy lung [4] as they produce high levels of NO in asthma due to increased NOS2 protein and activity. At the transcriptional level, murine NOS2 protein is regulated by a combination of the interferon  $\gamma$  (IFN $\gamma$ ) activation of Janus kinase (JAK)/signal transducer and activator of transcription1 (STAT1) pathway with the interleukin-1 $\beta$ (IL-1 $\beta$ ) and/or tumor necrosis factor- $\alpha$ (TNF- $\alpha$ ) and/or endotoxin-mediated activation of nuclear factor  $\kappa$ B (NF- $\kappa$ B) [9, 10].

#### **14.5.15 Expressional Profiling of Cell Adhesion Molecules**

Our previous studies [11–14] have shown the involvement of various families of adhesion molecules, viz. a4b1, b2, VCAM-1, and selectin facilitate leukocyte transmigration, adherence to parenchymal cells, and Th2 response, in the pathophysiology of various inflammatory disease models such as allergic asthma. Assessment of these key cell adhesion molecules in response to high ROS and RNS level in allergen-treated animal model in relation to metabolic alterations is a key goal to investigate in this project.

#### **14.5.16 Expressional Profiling of Cyclooxygenase 2 (COX-2) as Well as Lipoxygenase (LOX)**

As the experimental data suggest that two enzymes cyclooxygenase-2 (COX-2) as well as

lipoxygenase (LOX) involved in inflammation [16], so the expressional profiling of these two molecules is a key feature in this pathway.

#### 14.5.17 Expressional Profiling of Proinflammatory Molecules

TNF- $\alpha$  is a proinflammatory cytokine that activates various signal transduction cascades improving the insulin sensitivity and glucose homeostasis, advocating the fact that metabolic, inflammatory, and innate immune processes are coordinately regulated, and it is also proved that ligands to all three PPAR family members suppress production of proinflammatory cytokines, mostly through suppression of NF- $\kappa$ B [33]. So our aim is to correlate the expression of TNF- $\alpha$  along with the metabolic alternations in case of inflammatory responses in asthma as this field has still remained untouched for researchers.

TGF- $\beta$  is another important mediator involved in tissue remodeling in the asthmatic lung where TGF- $\beta$  is believed to play an important role in most of the cellular biological processes leading to airway remodeling involving itself in epithelial changes, subepithelial fibrosis, airway smooth muscle remodeling, and microvascular changes (Halwani et al. 2011) as in the lungs, almost all structural immune cells, as well as inflammatory cells recruited to the airways during an exacerbation of asthma, are able to express and secrete TGF- $\beta$ 1. In individuals without asthma, airway epithelium seems to be the major site of TGF- $\beta$ 1 expression (Magnan et al. 1994). However, other structural cells in the airways, such as fibroblasts (Kelley et al. 1991), endothelial cells (Coker et al. 1996), vascular smooth muscle cells (de Boer et al. 1998), and ASM cells (Lee et al. 2006), are also potential sources of this cytokine. Here, we have aimed to find out the molecular switch which correlate the expression of these cytokines with the metabolic alternations at the genomic levels. By using specific inhibitors or monoclonal

antibodies (GC1008) against the TGF $\beta$  [<http://clinicaltrials.gov/ct/show/NCT00125385>, at ClinicalTrials.gov; accessed February 20, 2010] or its signaling molecules in recent years, different groups have opened a veritable window to study its specific role in the said signalling pathway.

#### 14.5.18 Use of Two-Dimensional Electrophoresis System to Assess the Novel Proteins

Two-dimensional electrophoresis is a useful tool to analyze the protein pattern of various and complex biological materials to connect the genome to the proteome and to provide valuable information on various protein expressions by which we can get a picture of some novel protein molecule involved in this pathway, except the traditional ones.

#### 14.5.19 Fluorescin-Activated Cell Sorter (FACS) Analysis

Cells from hemolysed peripheral blood (PB), bone marrow (BM), bronchoalveolar lavage (BAL), lung parenchyma (LP), spleen, mesenteric lymph nodes (MLN), cervical lymph nodes (CLN), axillary lymph nodes (LNx), and inguinal lymph nodes (LNI) will be analyzed on a FACS Calibur (BD Immunocytometry Systems, San Jose, CA) by using the CELLQuest program. Staining will be performed by using antibodies conjugated to fluorescein isothiocyanate (FITC), phycoerythrin (PE), allophycocyanin (APC), peridinin chlorophyll protein (Per CP-Cy5.5), and Cy-chrome (PE-Cy5 and PE-Cy7). The following antibodies will be used for cell surface staining: CD45, CD3, CD4, CD45RC, CD8, B220, IgM, CD19, CD21, CD23, GR-1, Mac1 (M1/70), F4/80 (Cl: A3-1 (F4/80)), anti- $\alpha$ 4 integrin, antiselectin, and anti-VCAM-1(M/K-2). Irrelevant isotype-matched antibodies will be used as controls.

### 14.5.20 Measurement of Lung Cytokines by Cytometric Bead Array

Lung tissue of control and OVA-exposed mice will be homogenized in lysis buffer (PBS containing 1 % Triton X-100, 1 mM PMSF, and protease inhibitor mixture). After measuring the protein concentration of the lysates, Th1 (IL-2 and IFN- $\gamma$ ) and Th2 (IL-4 and IL-5) cytokine levels as well as that of IL-13 in the lung lysate supernatants will be analyzed using mouse Th1/Th2 cytokine and IL-13 cytometric bead array (CBA) kits (catalog nos. 551287 and 558349; BD Biosciences, San Jose, CA), expressing the level of each cytokine as picograms of cytokine per milligram of protein.

### 14.5.21 Quantitative Assessments of Specific Protein Molecules

ELISA for TNF- $\alpha$ , MIP-2, and IFN- $\gamma$  in BAL and serum (previously frozen at  $-80^{\circ}\text{C}$ ) will be measured along with the quantitative assessments of OVA-specific IgE and IgG1 (in serum previously frozen at  $-70^{\circ}\text{C}$ ).

### 14.5.22 Histological Assessments

1. Hematoxylin and eosin staining for lung tissues:  
Paraffin-embedded lung tissue sections will be stained by hematoxylin and eosin to detect detail cellular architectures.
2. Masson's trichrome staining for collagen fibers:  
This will be used to detect the deposition of collagen fibers in airways which is the important biomarker for airway remodellings.
3. Alcian blue/PAS for acid and neutral mucopolysaccharides.
4. Toluidine blue stain for mast cells.
5. Wright's stain for differential blood cell counting.

### 14.5.23 Immune Histochemical Techniques

Immunohistochemical methods will be applied for the localization of GLUT1, GLUT4, GLUT8, MMP9, MMP12, TNF- $\alpha$ , TGF- $\beta$ 1, NOS2, nitrotyrosine, MUC5AC, VCAM1, selectin, and MIP-2.

### 14.5.24 Collection of Airway Smooth Muscle Cells and Its Culture

Collection and treatment of airway smooth muscle cells will be done by method proposed by using standard protocol.

Here, after collecting ASM, those will be treated by TNF- $\alpha$ , TGF- $\beta$ 1, and allergen to detect the different ROS and RNS biomarkers along with the measurement of GLUT1, GLUT4, GLUT8, and NOS2 as well as the screening of different cytokines to correlate them in an in vitro system.

### 14.5.25 Collection of Alveolar Macrophages and Their Treatment

Collection and treatment of macrophage cells from the lung will be done by method proposed by using standard protocol. Such cells will be similarly treated and assessed mentioned above.

### 14.5.26 Use of Specific Inhibitors

Specific inhibitor molecules will be used in this purpose to investigate our goal of which few inhibitors are enlisted below:

1. NEM: NADPH oxidase inhibitor,
2. S1: MMP12 inhibitor,
3. TIMP1: endogenous inhibitor of MMP9,
4. Dideoxy glucose: specific inhibitor for glucose metabolism,
5. Mercaptoethylguanidine (MEG): inhibitor of iNOS.

### 14.5.27 Use of RNAi Techniques

Specific siRNAs will be used this purpose to correlate the metabolic alternations with the inflammatory responses in asthma. Here, some siRNAs are enlisted which will be extensively used in this purpose: GLUT1, GLUT4, GLUT8, MMP9, MMP12, and NOS2.

### References

1. Das S, Das S, De B. In Vitro Inhibition of Key Enzymes Related to Diabetes by the Aqueous Extracts of Some Fruits of West Bengal, India. *Current Nutrition & Food Science*. 2012; 8: 19–24
2. Dasgupta N, De B. Antioxidant activity of Piper betle L. leaf extract in vitro. *Food Chemistry*. 2004; 88: 219–24
3. Pollock JD, Williams DA, Gifford MAC, Ling LL, Du X, Fisherman J, et al. Mouse model of X-linked chronic granulomatous disease, an inherited defect in phagocyte superoxide production. *Nature Genetics*. 1995; 9 (2): 202–09
4. Dweik RA, Comhair SA, Gaston B, Thunnissen FB, Farver C, Thomassen MJ, et al. NO chemical events in the human airway during the immediate and late antigen-induced asthmatic response. *Proc Natl Acad Sci USA*. 2001; 98: 2622–7
5. Guo FH, Comhair SAA, Zheng S, Dweik RA, Eissa NT, Thomassen MJ, et al. Molecular mechanisms of increased nitric oxide (NO) in asthma: evidence for transcriptional and post-translational regulation of NO synthesis. *J Immunol*. 2000; 164 (11): 5970–80
6. Khatri SB, Ozkan M, McCarthy K, Laskowski D, Hammel J, Dweik RA, et al. Alterations in exhaled gas profile during allergen induced asthmatic response. *Am J Respir Crit Care Med*. 2001; 164: 1844–8
7. Silkoff PE, Sylvester JT, Zamel N, Permutt S. Airway nitric oxide diffusion in asthma. *Am. J. Respir. Crit. Care Med*. 2000; 161: 1218–28
8. Massaro AF, Mehta S, Lilly CM, Kobzik L, Reilly JJ, Drazen JM. Elevated nitric oxide concentrations in isolated lower airway gas of asthmatic subjects. *Am J Respir Crit Care Med*. 1996; 153: 1510–4
9. Stuehr DJ. Mammalian nitric oxide synthases. *Biochim Biophys Acta*. 1999; 1411 (2-3): 217–30
10. Xie QW, Whisnant R, Nathan C. Promoter of the mouse gene encoding calcium-independent nitric oxide synthase confers inducibility by interferon gamma and bacterial lipopolysaccharide. *J Exp Med*. 1993; 177 (6): 1779–84
11. Banerjee ER, Jiang Y, Henderson WR Jr, Scott LM, Papayannopoulou T. Alpha4 and beta2 integrins have nonredundant roles for asthma development, but for optimal allergen sensitization only alpha4 is critical. *Exp Hematol*. 2007; 35 (4): 605–17
12. Banerjee ER, Latchman YE, Jiang Y, Priestley GV, Papayannopoulou T. Distinct changes in adult lymphopoiesis in Rag2-/- mice fully reconstituted by alpha4-deficient adult bone marrow cells. *Exp Hematol*. 2008; 36 (8): 1004–13
13. Banerjee ER, Jiang Y, Henderson WR Jr, Latchman Y, Papayannopoulou T. Absence of alpha 4 but not beta 2 integrins restrains development of chronic allergic asthma using mouse genetic models. *Exp Hematol*. 2009; 37 (6): 715–27
14. Laberge S, Rabb H, Issekutz TB, Martin JG. Role of VLA-4 and LFA-1 in allergen-induced airway hyper-responsiveness and lung inflammation in the rat. *Am J Respir Crit Care Med*. 1995; 151 (3 Pt 1): 822–9
15. Laberge S, Cruikshank WW, Kornfeld H, Center DM. Histamine-induced secretion of lymphocyte chemoattractant factor from CD8+ T cells is independent of transcription and translation. Evidence for constitutive protein synthesis and storage. *J Immunol*. 1995; 155 (6): 2902–10
16. Huang SS, Brod RD, Flynn HW, Jr. Management of endophthalmitis while preserving the uninvolved crystalline lens. *Am J Ophthalmol*. 1991; 112(6): 695–701
17. Yamada M. Differentiation of human myeloid leukemia HL-60 cells and myeloperoxidase synthesis. *Seikagaku*. 1984; 56 (9): 1138–41
18. Yamada M, Kurahashi K. Regulation of myeloperoxidase gene expression during differentiation of human myeloid leukemia HL-60 cells. *J Biol Chem*. 1984; 10. 259 (5): 3021–5
19. Podrez EA, Abu-Soud HM, Hazen SL. Myeloperoxidase-generated oxidants and atherosclerosis. *Free Radic Biol Med*. 2000; 28 (12): 1717–25
20. Włodek L. Beneficial and harmful effects of thiols. *Pol J Pharmacol*. 2002; 54 (3): 215–23
21. Imrich A, Kobzik L. Flow cytometric analysis of macrophage oxidative metabolism using DCFH. *Methods Mol Biol*. 1998; 91: 97–108
22. Shi T, Schins RP, Knaapen AM, Kuhlbusch T, Pitz M, Heinrich J, et al. Hydroxyl radical generation by electron paramagnetic resonance as a new method to monitor ambient particulate matter composition. *J Environ Monit*. 2003; 5: 550–6
23. Viera L, Ye YZ, Estévez AG, Beckman JS. Immunohistochemical methods to detect nitrotyrosine. *Methods Enzymol*. 1999; 301: 373–81
24. Ischiropoulos H, Zhu L, Chen J, Tsai M, Martin JC, Smith CD, Beckman JS. Peroxynitrite-mediated tyrosine nitration catalyzed by superoxide dismutase. *Arch Biochem Biophys*. 1992; 298 (2): 431–7
25. Ischiropoulos H, Zhu L, Beckman JS. Peroxynitrite formation from macrophage-derived nitric oxide. *Arch Biochem Biophys*. 1992; 298 (2): 446–51
26. Pollock JS, Forstermann U, Tracey WR, Nakane M. Nitric oxide synthase isozymes antibodies. *Histochem J*. 1995; (10): 738–44

27. Taniguchi CM, Emanuelli B, Kahn CR. Critical nodes in signaling pathways: insights into insulin action. *Nat Rev Mol Cell Biol.* 2006; 7: 85–96
28. Aguirre V, Uchida T, Yenush L, Davis R, White MF. The c-Jun NH (2)-terminal kinase promotes insulin resistance during association with insulin receptor substrate-1 and phosphorylation of Ser (307). *J Biol Chem.* 2000; 275: 9047–54
29. Paz K, Hemi R, LeRoith D, Karasik A, Elhanany E, Kanety H, Zick Y. A molecular basis for insulin resistance. Elevated serine/threonine phosphorylation of IRS-1 and IRS-2 inhibits their binding to the juxtamembrane region of the insulin receptor and impairs their ability to undergo insulin-induced tyrosine phosphorylation. *J Biol Chem.* 1997; 272: 29911–8
30. Howard JK, Cave BJ, Oksanen LJ, Tzamei I, Bjorbaek C, Flier JS. Enhanced leptin sensitivity and attenuation of diet-induced obesity in mice with haploinsufficiency of Socs3. *Nature Medicine.* 2004; 10: 734–8
31. Emanuelli B, Peraldi P, Filloux C, Chavey C, Freidinger K, Hilton DJ, Hotamisligil GS, Van Obberghen E. SOCS-3 inhibits insulin signaling and is up-regulated in response to tumor necrosis factor-alpha in the adipose tissue of obese mice. *J Biol Chem.* 2001; 276 (51): 47944–9
32. Rui L, Aguirre V, Kim JK, Shulman GI, Lee A, Corbould A, et al. Insulin/IGF-1 and TNF-alpha stimulate phosphorylation of IRS-1 at inhibitory Ser307 via distinct pathways. *J Clin Invest.* 2001; 107 (2): 181–9
33. Glass WG, Rosenberg HF, Murphy PM. Chemokine regulation of inflammation during acute viral infection. *Curr Opin Allergy Clin Immunol.* 2003; 6: 467–73

## Subchapter-C: Translational Outcome Research with Date Extracts as Functional Food in Diseases Involving Oxi-Flammatory Pathways.

# 15



The work have been published as:

(1) Mukherjee, K., Paul, P., and Ray Banerjee, E. Free radical scavenging activities of date palm (*Phoenix sylvestris*) fruit extracts. (2014) *Natural Products Chemistry & Research*. 2:151. Doi:10.4172/2329-6836.1000151.

(2) Mukherjee, K., Paul, P., and Ray Banerjee, E. Evaluation of date palm (*Phoenix sylvestris*) fruit extracts as functional food. (2014) *International Journal of Science, Engineering and Technology*. 3 (11): 1-8. ISSN: 2277-1581.

(3) Das, R., Paul, P., Mukherjee, K., Mitra, S., Singh, U. P., and Ray Banerjee, E. Anti-Oxiflammatory profile of date extracts (*Phoenix sylvestris*). (2015) *Biomedical Research and Therapy*. 2(5): 15-38. DOI: <http://dx.doi.org/10.15419/bmrat.v2i5.79>, (ISSN: 2198-4093).

© Springer Science+Business Media Singapore 2016

E.Ray Banerjee, *Perspectives in Translational Research in Life Sciences and Biomedicine*, DOI 10.1007/978-981-10-0989-1\_15

233



**Abstract**

Fruit of date palm (*Phoenix sylvestris* L.) is edible and used as an anti-geriatric, antioxidant ethnomedicine. In this study, three different types of date extracts, namely methanolic, acidic ethanolic and basic ethanolic, were evaluated for their putative in vitro scavenging effects on reactive oxygen species (ROS) where scavenging of hydroxyl radicals (basic ethanolic > acidic ethanolic > methanolic), superoxide radicals (acidic ethanolic > basic ethanolic > methanolic), and DPPH radical (acidic ethanolic > methanolic > basic ethanolic), [nitric oxide (NO)] (methanolic > acidic ethanolic > basic ethanolic) and inhibition of lipid peroxidation (basic ethanolic > acidic ethanolic > methanolic) were found to occur in a dose-dependent manner. Their flavonoid and phenolic contents proved to be the source of this potent free radical scavenging activity and indicated a direct correlation with their total antioxidant capacity. On human embryonic kidney cell line (HEK) and murine RAW macrophages, bacterial lipopolysaccharide (LPS)-induced inflammation, the date extracts applied therapeutically inhibit intracellular oxidative stress significantly. This reinstatement of cellular homeostasis presumably occurs via mitochondrial pathways.

**Keywords**

Inflammation • Antioxidant • Phenolic compounds • Scavenger activities • Reactive oxygen nitrogen intermediates

**15.1 Introduction**

One of the most primitive and yet effective mechanisms, the mammalian physiology adopts in an exigent situation which although predominantly nonspecific is remarkably fast and conclusive for the next phases of immune response or structural tissue remodeling to kick in, is inflammation. Inflammatory response occurs in a phase-wise manner [1]. Inflammation is the principal and sometimes critical initiator of most disorders. A cross talk between the structural and the immune cells causes destruction on the one hand and healing or reconstruction on the other. In diseases such as asthma, rheumatoid arthritis, psoriasis, multiple sclerosis, obesity and inflammatory bowel disease [2], the first phase of disease onset followed by establishment, development,

maintenance and exacerbations leads to a completion of various steps that are characteristic of the particular inflammatory disease. Although specific characteristics of inflammatory response in each disease and their site of occurrence may vary, a universal feature governing this stepwise phenomenon is the complex interplay among the various cell subsets of the inflammatory cascade and tissue-resident cells and the network of signaling governing the two [2, 3], affecting various target tissues [4].

Unmet needs in medicine and unknown phenomena prevailing in the mechanism of disease onset remain [5]. In traditional medicine that has provided solution to prevailing health issues at a global level, medicinal plants continue to provide valuable therapeutic agents. To avoid and mitigate various side effects and complications of modern medicine and to address the unmet needs

of diseases, especially in the context of emerging complex etio-pathophysiological pathways, traditional medicine is gaining importance and is now being studied systematically using biotechnological tools, to find the scientific basis of their therapeutic actions.

Phytochemicals from fruits and other edible plant parts have been shown to possess significant antioxidant properties that may be associated with lower incidence and lower mortality rates of degenerative diseases in human. Different biological properties, antioxidant capacities, and radical scavenging activities of various herbal extracts have been widely demonstrated, using in vitro techniques and in vivo models by different groups of researchers [6–8]. The antiproliferative and anti-inflammatory activities of these herbal extracts have been documented in human oral, breast, colon, cervical, and prostate cancer cell lines as well as preclinical animal models by attenuating certain inflammatory intermediates, including nitric oxide, NF- $\kappa$ B, and TNF $\alpha$  [9, 10].

This study was designed to identify anti-inflammatory potential in extracts from date which is a well-known ethnomedicine with high nutritive value. Among its contents, large amounts of several phenolic and non-phenolic compounds and other uncharacterized moieties may contribute to its use as a food supplement, a functional food, or a nutraceutical substance with prophylactic and therapeutic functions in oxidative inflammatory diseases. Comparison of antioxidant and anti-inflammatory activities of date extracted by three distinct methods, namely methanolic extracts, basic ethanolic extracts, and acidic ethanolic extracts, has been assessed along with the evaluation of their antioxidative/anti-inflammatory capabilities and validation of these results using both murine and human cell lines where inflammation was induced using *E. coli* LPS, which is the most potent and well-characterized proinflammatory agent. In addition, intracellular cell organelle-specific targeting of this extract has also been assessed in order to seek information regarding its mode of action in modulating the inflammatory cascade in

a biological system, which is the most critical part for any drug discovery program addressing inflammatory disorders.

---

## 15.2 Materials and Methodologies

### 15.2.1 Extraction of Date

Figure 15.1 shows the detailed extraction procedure for three different date extracts. Mesocarp tissue of date fruit was macerated and treated with 50 % water–methanol solution at 4 °C. This was then divided into two parts: Part A was evaporated to dryness, and the remaining part was rinsed with water, dried at 50 °C, and alkaline hydrolyzed with sodium hydroxide (0.1 M) and filtered. The filtrate which was to become part B was acidified at pH 2.0, extracted with ethyl acetate, and rinsed with 1 % sodium bicarbonate and water. The organic layer was evaporated into dryness and then dissolved in water. The residue of processed part A was alkaline hydrolyzed with 2 M sodium hydroxide and filtered. The filtrate was further acidified at pH 2.0 and extracted with ethyl acetate and rinsed with 1 % sodium bicarbonate and the organic layer evaporated into dryness.

### 15.2.2 Reagents

Chemicals, such as ethylenediamine tetra acetic acid (EDTA), trichloroacetic acid (TCA), butanol, ammonium molybdate and sodium dodecyl sulfate, benzoic acid, sodium phosphate, and DMSO were purchased from E. Merck (India) Limited. 1,1 Diphenyl-2-picrylhydrazyl and malondialdehyde, potassium ferricyanide, and thiobarbituric acid (TBA) were procured from Sigma, USA. N-butanol, ferrous sulfate, ferric chloride, Folin's reagent, riboflavin, naphthylethylenediamine dihydrochloride, and sulfanilamide in phosphoric acid, sodium bicarbonate, sodium hydroxide, potassium hydroxide were purchased from Sisco Research Laboratories PVT. Ltd., India. Nitroblue tetrazolium, MTT reagent [(4,5-dimethylthia-

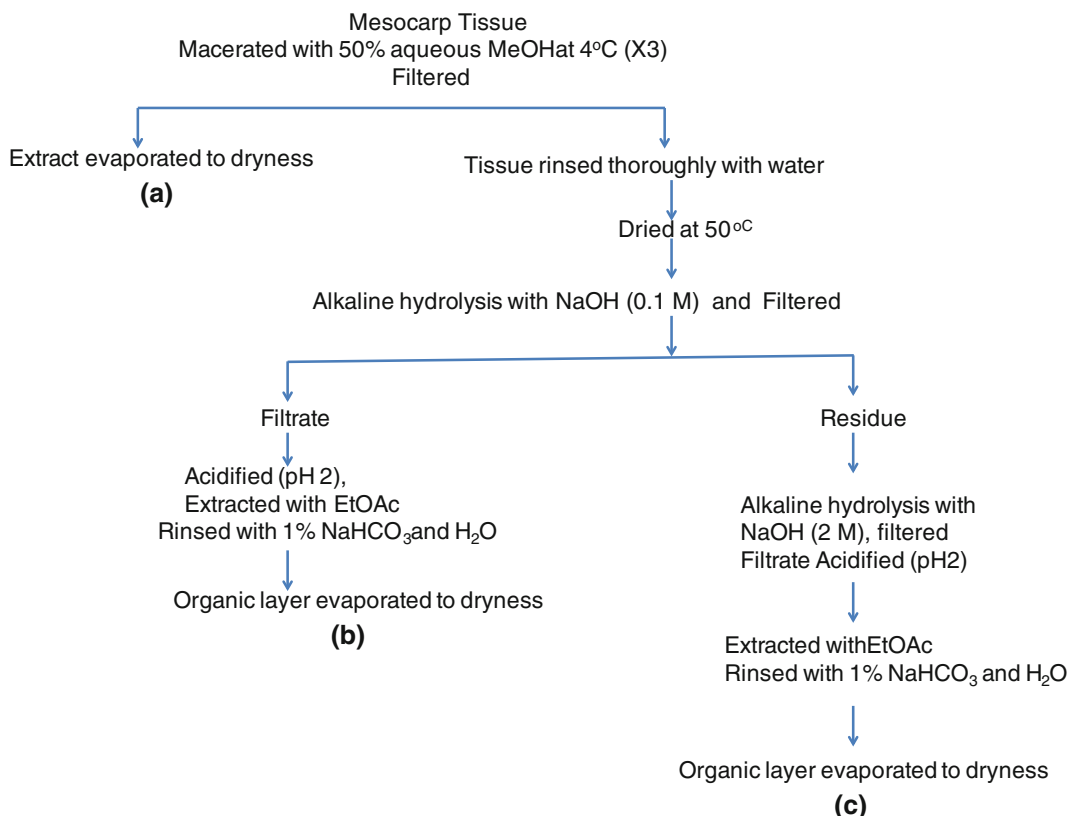


**Fig. 15.1** Schematic flowchart for the extraction of bioactive compounds from mesocarp tissue of *Phoenix sylvestris* L. using various solvent system and methanolic

extract represented as A, acidic ethanolic as B, and basic ethanolic extract as C

zol-2-yl)-2,5-diphenyltetrazolium bromide], and DMEM media were purchased from Himedia, India. Fetal bovine serum (FBS) was purchased from Gibbco. DCFH-DA and DHR 123 were purchased from Invitrogen. All other reagents were of analytical grade.

### 15.2.3 DPPH Radical Scavenging Activity

The antioxidant activity of the extracts was measured on the basis of the scavenging activity of the stable 1,1-diphenyl-2-picrylhydrazyl (DPPH) free radical [11]. Aqueous extract was added to a 0.004 % methanol solution of DPPH on a 96-well ELISA plate. Absorbance at

517 nm was determined after 30 min, and the percent inhibition activity was calculated.

### 15.2.4 Assay of Superoxide Radical $O_2^-$ Scavenging Activity

The method used by Martinez et al. [12] for determination of the superoxide dismutase was studied in the riboflavin-light-nitrobluetetrazolium (NBT) system [13]. Each 0.1 ml of reaction mixture contained 50 mM phosphate buffer (pH 7.8), 13 mM methionine, 2l M riboflavin, 100  $\mu$ M EDTA, NBT (75  $\mu$ M), and various doses of sample solution. The production of blue formazan was followed by monitoring the

increase in absorbance at 560 nm after 15 min of illumination from a fluorescent lamp.

### 15.2.5 Assay of Hydroxyl Radical (–OH) Scavenging Activity

The assay was based on the benzoic acid hydroxylation method [14]. Hydroxyl radicals were generated by direct addition of iron(II) salts to a reaction mixture containing phosphate buffer. In a 24-well plate, 0.15 ml of sodium benzoate (10 mM) and 0.15 ml of  $\text{FeSO}_4 \cdot 7\text{H}_2\text{O}$  (10 mM), and EDTA (10 mM) were added. Then the sample solution and a phosphate buffer (pH 7.4, 0.1 M) were added to give a total volume of 1.6 ml. Finally, 0.15 ml of an  $\text{H}_2\text{O}_2$  solution (10 mM) was added. The reaction mixture was then incubated at 37 °C for 2 h. After that, the fluorescence was measured at 407 nm emission (Em) and excitation (Ex) at 305 nm. Measurement of spectrofluorometric changes has been used to detect the damage by the hydroxyl radical.

### 15.2.6 Lipid Peroxidation Assay

A modified thiobarbituric acid reactive species (TBARS) assay [15] was used to measure the lipid peroxide formed using egg yolk homogenates as lipid-rich media [16] where lipid peroxidation was induced by  $\text{FeSO}_4$  and malondialdehyde (MDA), produced by the oxidation of polyunsaturated fatty acids, and reacts with two molecules of thiobarbituric acid (TBA) yielding a pinkish red chromogen with an absorbance maximum at 532 nm which was measured using a 96-well ELISA plate. Percentage inhibition of lipid peroxidation by different concentrations of the extract was calculated.

### 15.2.7 Nitric Oxide (NO) Scavenging Activity

Nitric oxide was generated by spontaneous decomposition of the sodium nitroprusside

(20 mM) in phosphate buffer (pH 7.4) which interacts with oxygen molecule to produce nitrite ions, which can be measured by the Griess reactions. 1 ml of each solution was taken and diluted with 1 ml of Griess reagent [1 % sulfanilamide, 2 %  $\text{H}_3\text{PO}_4$  and 0.1 % *N*-(1-anphthyl)ethylene-diamine]. Similarly, a blank was prepared containing the equivalent amount of reagents (only the sodium nitroprusside and PBS), but without the extract. The absorbance of these solutions was measured at 540 nm wavelength against the corresponding blank solution. Ascorbic acid (100 µg/ml) was used as the positive control. The percentage inhibition of nitric oxide was calculated as follows.

### 15.2.8 Determination of Total Antioxidant Capacity

The assay is based on the reduction of Mo(VI) to Mo(V) by the extract and subsequent formation of a green phosphate/Mo(V) complex at acid pH [17]. Each well of a 96-well ELISA plate containing extract and reagent solution (0.6 M sulfuric acid, 28 mM sodium phosphate, and 4 mM ammonium molybdate) was incubated at 95 °C for 90 min. After the mixture had cooled to room temperature, the absorbance of each solution was measured at 695 nm against a blank. The antioxidant capacity was expressed as ascorbic acid equivalent (AAE).

### 15.2.9 Determination of Reducing Power

The reducing power of date extracts was determined according to the method [18] where different concentrations of extracts were mixed with phosphate buffer and potassium ferricyanide. The mixture was incubated at 50 °C for 20 min. A portion (2.5 ml) of trichloroacetic acid was added to the mixture. The upper layer of solution (2.5 ml) was mixed with distilled water (2.5 ml) and  $\text{FeCl}_3$ , and the absorbance was measured at 700 nm. Increased absorbance of the reaction

mixture indicated increased reducing power. Ascorbic acid was used as positive control.

### 15.2.10 Determination of Total Flavonoid Content

Total flavonoid content was determined using aluminum chloride ( $\text{AlCl}_3$ ) according to a known method, 15 using Fisetin as a standard. The date extract (0.1 ml) was added to 0.3 ml distilled water followed by 5 %  $\text{NaNO}_2$  (0.03 ml). After 5 min at 25 °C,  $\text{AlCl}_3$  (0.03 ml, 10 %) was added. After further 5 min, the reaction mixture was treated with 0.2 ml of 1 mM NaOH. Finally, the reaction mixture was diluted to 1 ml with water and the absorbance was measured at 510 nm. The results were expressed as mg Fisetin/g date extract.

### 15.2.11 Determination of Total Phenolic Content

The total phenolic content of the date extracts was determined using the Folin–Ciocalteu reagent. The reaction mixture contained: 200  $\mu\text{l}$  of diluted extract, 800  $\mu\text{l}$  of freshly prepared diluted Folin–Ciocalteu reagent, and 2 ml of 7.5 % sodium carbonate. The final mixture was diluted to 7 ml with deionized water. Mixtures were kept in dark at ambient conditions for 2 h to complete the reaction. The absorbance at 765 nm was measured. Gallic acid was used as standard and the results were expressed as mg gallic acid (GAE)/g of the date extract.

### 15.2.12 UV-based Spectrophotometric Analysis

The samples of various extracts were analyzed using UV–Vis spectrophotometer. About 40 mg of the air-dried samples was dissolved in 1 ml methanol and then diluted to 1 mg/ml solution in different volumetric flasks and then applied on

the spectrophotometer and scanned through the UV and visible region. The herbal functional groups were determined by analyzing the peaks.

### 15.2.13 Cell Culture

RAW 267.4 murine macrophage cell line and HEK 293 cell line were obtained from NCCS, Pune, India. The cells were grown in DMEM medium containing 5 % inactivated fetal bovine serum, penicillin (100 U/mL), and streptomycin (20  $\mu\text{g}/\text{mL}$ ) and kept at 37 °C in a T-25 tissue culture flasks. Cells were grown to confluence in a humidified atmosphere containing 5 %  $\text{CO}_2$ .

### 15.2.14 Cell Viability Using MTT Assay

To test the cytotoxicity,  $5 \times 10^4$  cells/well were seeded in a 96-well plate and incubated for 24 h with different concentrations of the date extract. The cells were washed, and each well was filled with 100  $\mu\text{L}$  of medium and 10  $\mu\text{L}$  of a tetrazolium salt, MTT. The plate was incubated for various time periods, and the absorbance was measured at 540 nm wavelength. The percentage of viable cells was calculated using the absorbance of the control cells without extract as 100 %. The assay was performed in triplicate twice.

### 15.2.15 Proteomic Analyses of Extracts

#### 15.2.15.1 HPLC Analyses

Crude methanolic A, basic ethanolic B, and acidic ethanolic C were filtered by 0.22- $\mu\text{m}$  syringe filter (Millipore) and, first, then crude methanolic A, basic ethanolic B, and acidic ethanolic C extracts were analyzed with RP-HPLC by using Waters 515 System with C-18 column as stationary phase. The mobile phases were water (HPLC grade) and 90 % acetonitrile. Sample volume was 100  $\mu\text{l}$ . Flow rate was 0.5 ml/min.

### 15.2.15.2 TLC Analyses

Methanolic extract (A), acidic ethanolic extract (B), and basic ethanolic extract (C) were applied on silica gel-coated TLC plates (Millipore, Germany) by using capillary tubes and developed in a TLC chamber using mobile phase methanol: water:chloroform (2.5:0.2:7.3 v/v). The developed TLC plates were air dried and observed under ultraviolet light UV at both 254 and 366 nm. TLC plates were sprayed with Liebermann's solution, heated at 100–105 °C, and visualized under daylight. The movement of the analyze was expressed by its retention factor (Rf).

## 15.3 Methods

Taking 0 % inhibition in the mixture without plant extract, regression equations were prepared from the concentrations of the three date extracts which were collected by three different methods, and percentage inhibition of free radical formation/prevention in different systems of assay was calculated, viz., DPPH assay, superoxide radical scavenging assay, hydroxyl radical scavenging assay and lipid peroxidation assay, and nitric oxide radical scavenging assay. IC<sub>50</sub> values (concentration of sample required to scavenge 50 % of available free radicals or to prevent lipid peroxidation by 50 %) were calculated from these regression equations. IC<sub>50</sub> value is inversely related to the activity of the extracts.

### 15.3.1 Assay of Hydroxyl Radical (OH) Scavenging Activity

Superoxide radical was measured by the NBT reduction assay. Each well of a 96-well plate was seeded with RAW 264.7 macrophages suspension containing  $0.5 \times 10^4$  cells/mL. The treatment of cells proceeded as described previously. After incubation, 40 µL of a NBT solution at 1 mg/mL was added to the medium and incubated at 37 °C, for 1 h. Then, the incubation medium was removed and cells were lysed with

DMSO:2 M NaOH (1:1). The absorbance of reduced NBT, formazan, was measured at 620 nm, in a microplate reader (Multiskan ASCENT Thermo®).

### 15.3.2 NO Estimation

In culture, the NO released by the macrophages into the medium is converted to several nitrogen derivatives, from which only nitrite is stable, being easily measured by Griess reagent (1.0 % sulfanilamide and 0.1 % *N*-(1)-naphthylethylenediamine in 5 % phosphoric acid). After incubation, 100 µL of culture medium supernatant was mixed with the same volume of Griess reagent, during 10 min, at room temperature. The nitrite produced was determined by measuring the optical density at 540 nm, in a microplate reader (Shimadzu).

### 15.3.3 ROS Measurement

Intracellular formation of ROS was assessed by using oxidation sensitive dye DCFH-DA as a substrate. RAW macrophage cells were seeded in a 24-well black plate at a concentration of  $5 \times 10^4$  cells/mL. Cells were treated with 1 µg/ml of *E. coli* LPS and then therapeutically various concentrations of date extracts were added onto it and incubated for 6 h. Negative control cells, i.e., only LPS treated as well as cells without any treatment, were incubated for the same time period and then washed in PBS and after the addition of DCF-DA (5 µg/mL) incubate for 30 min at 37 °C in dark. Non-fluorescent DCFH-DA dye that freely penetrates into cells gets hydrolyzed by intracellular esterase to 207-dichlorofluorescein (DCFH) and is trapped inside the cells. The formation of 207-dichlorofluorescein (DCF) due to oxidation of DCFH in the presence of ROS was read after 30 min at an excitation wavelength of 485 nm and emission wavelength of 525 nm using a spectrofluorometer. Percent scavenging power of hydroxyl, superoxide, and peroxide radicals was computed taking that by ascorbic acid as 100 %.

### 15.3.4 Measurement of Mitochondrial Membrane Potential (MMP)

Mitochondrial membrane potential was monitored by the fluorescent dye, Rhodamine 123. It is a cell permeable cationic dye that preferentially enters into mitochondria based on highly negative mitochondrial membrane potential ( $W_m$ ). Depolarization of MMP results in the loss of Rhodamine 123 from the mitochondria and a decrease in intracellular fluorescence intensity. After the addition of 1  $\mu\text{g/ml}$  *E. coli* LPS, various concentrations of date extracts were added to RAW macrophages cell line and incubated for 6 h in 37 °C. After incubation, the cells were washed twice in cold PBS, and then Rhodamine 123 (10  $\mu\text{M}$ ) was added and incubated for 30 min at 37 °C in dark. Fluorescence was measured by spectrofluorometer with an excitation wavelength of 485 nm and emission wavelength of 525 nm.

### 15.3.5 TLC of Khejur Extracts

Methanolic extract (A), acidic ethanolic extract (B), and basic ethanolic extract (C) were applied on silica gel-coated TLC plates (Millipore, Germany) by using capillary tubes and developed in a TLC chamber using mobile phase methanol:water:chloroform (2.5:0.2:7.3 v/v). The developed TLC plates were air dried and observed under ultraviolet light UV at both 254 and 366 nm. TLC plates were sprayed with Liebermann's solution, heated at 100–105 °C, and visualized under daylight. The movement of the analyze was expressed by its retention factor ( $R_f$ ).

### 15.3.6 HPLC Analysis

Crude methanolic A, basic ethanolic B, and acidic ethanolic C were filtered by 0.22- $\mu\text{m}$  syringe filter (Millipore) and, first, then crude methanolic A, basic ethanolic B, and acidic ethanolic C extract were analyzed with RP-HPLC by using Waters

515 System with C-18 column as stationary phase. The mobile phase was water (HPLC grade) and 90 % acetonitrile. Sample volume was 100  $\mu\text{l}$ . Flow rate was 0.5 ml/min.

### 15.3.7 Statistical Analysis

Statistical differences among samples were tested by Student's  $t$  test. A  $p$  value less than 0.05 or 0.01 (as applicable vis-à-vis the assay performed) was considered statistically significant.

---

## 15.4 Results

Taking 0 % inhibition in the mixture without plant extract, regression equations were prepared from the concentrations of the three date extracts which were collected by three different methods, and percentage inhibition of free radical formation/prevention in different systems of assay was calculated, viz., DPPH assay, superoxide radical scavenging assay, hydroxyl radicals scavenging assay and lipid peroxidation assay, and nitric oxide radical scavenging assay.  $IC_{50}$  values (concentration of sample required to scavenge 50 % of available free radicals or to prevent lipid peroxidation by 50 %) were calculated from these regression equations.  $IC_{50}$  value is inversely related to the activity of the extracts (Table 15.1; Fig. 15.2).

Various concentrations of date extracts, collected by three distinct methods, required to scavenge 50 % free radical or to prevent lipid peroxidation by 50 %.  $IC_{50}$  value is inversely related to the activity of the extracts where both acidic and ethanolic date extracts are more active to scavenge the superoxide ions in an in vitro assay system than the methanolic date extracts, whereas there is no significant variation in all these three extracts to scavenge the hydroxyl radical but for the DPPH radical scavenging activity and nitric oxide scavenging activity is greater in acidic ethanolic extracts in comparison with the methanolic extracts and basic ethanolic extracts, respectively. Interestingly, prevention of lipid peroxidation activity is highest in basic

**Table 15.1** DPPH radical scavenging activity: DPPH radical scavenging activity (DPPH assay shows that in this system, the radical scavenging activities of the three date palm extracts are in this order: acidic ethanolic extracts > methanolic extract > basic ethanolic extract)

Concentrations	Methanolic extract (IC <sub>50</sub> 22.91 µg/ml) $Y = 9.919x + 22.74$ , $r^2 = 0.909$ % inhibition ± SD (n = 5)	Acidic ethanolic extract (IC <sub>50</sub> 14.61 µg/ml) $Y = 16.65X + 6.718$ , $r^2 = 0.933$ % inhibition ± SD (n = 5)	Basic ethanolic extract (IC <sub>50</sub> 36.44 µg/ml) $Y = 6.783X + 2.773$ , $r^2 = 0.930$ % inhibition ± SD (n = 5)	Ascorbic acid (IC <sub>50</sub> 4.82 µg/ml) $Y = 15.06X + 16.62$ , $r^2 = 0.963$ % inhibition ± SD (n = 5)
1 mg/ml	74.68 ± 1.66	86.28 ± 1.82	38.88 ± 1.20	89.24 ± 1.25
250 µg/ml	56.69 ± 1.58	72.26 ± 1.40	30.15 ± 1.32	75.46 ± 1.20
100 µg/ml	53.11 ± 1.42	61.11 ± 1.26	19.40 ± 1.36	70.00 ± 1.30
50 µg/ml	49.22 ± 1.39	49.22 ± 1.02	14.28 ± 1.28	45.56 ± 1.30
10 µg/ml	28.82 ± 1.87	14.53 ± 0.96	12.90 ± 2.00	28.86 ± 1.28

Various concentrations of date palm extracts, collected by three distinct methods, scavenge hydroxyl radical in a dose-dependent manner [ $r^2 = 0.832$  ( $p < 0.01$ ) for methanolic extract;  $r^2 = 0.852$  ( $p < 0.01$ ) for acidic ethanolic extract; and  $r^2 = 0.882$  ( $p < 0.01$ ) for basic ethanolic extract]. As per IC<sub>50</sub> values, basic ethanolic extract is more potent to scavenge the hydroxyl radicals (IC<sub>50</sub> 17.00 µg/ml) than the acidic ethanolic extracts (IC<sub>50</sub> 17.30 µg/ml) and methanolic extracts (IC<sub>50</sub> 18.20 µg/ml)

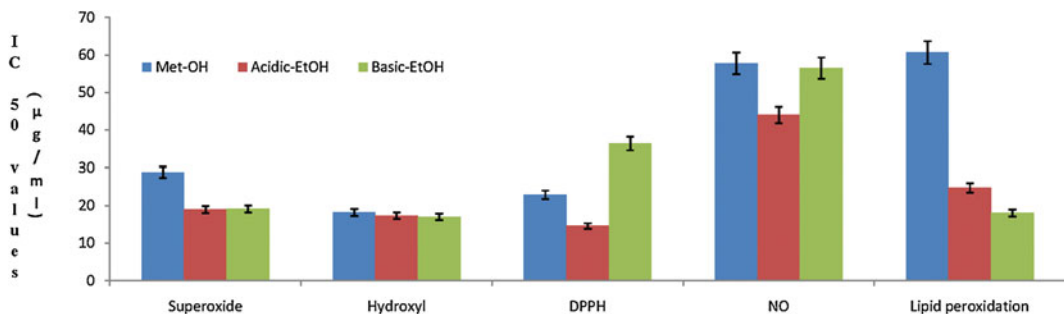


**Fig. 15.2** Comparison of IC<sub>50</sub> values of three different extracts of date palm

ethanolic extracts than the acidic ethanolic extracts and methanolic extracts, respectively. So, the scavenging power of various free radicals or to prevent the lipid peroxidation activities is different in all these three extracts, and it exerts the activity in a dose-dependent manner.

### 15.4.1 DPPH Radical Scavenging Activity

Antioxidants, on interaction with DPPH transfer an electron (hydrogen atom) to DPPH, neutralizing its free radical character [19]. The color changes from purple to yellow and its absorbance

at wavelength 517 decreases. Various concentrations of date extracts, collected by three distinct methods, quenched DPPH free radical in a dose-dependent manner [ $r^2 = 0.909$  ( $p < 0.01$ ) for methanolic extract;  $r^2 = 0.933$  ( $p < 0.001$ ) for acidic ethanolic extract;  $r^2 = 0.930$  ( $p < 0.001$ ) for basic ethanolic extract]. IC<sub>50</sub> values were 22.91 µg/ml for methanolic extract, 14.61 µg/ml for acidic ethanolic extract, and 36.44 µg/ml for basic ethanolic extract. DPPH assay shows that in this system, the radical scavenging activities of the three varieties of date extracts are in the order acidic ethanolic extract > methanolic extract > basic ethanolic extract (Table 15.2; Fig. 15.3).



**Table 15.2** Hydroxyl radical (OH) scavenging activity: hydroxyl radical (OH) scavenging activity (hydroxyl radical scavenging assay shows that in this system, the hydroxyl radical scavenging activities of the three date palm extracts are in this order: basic ethanolic extracts > acidic ethanolic extract > methanolic extract)

Concentrations	Methanolic extract (IC <sub>50</sub> 18.20 µg/ml) $Y = 13.73X + 0.098$ , $r^2 = 0.832$ % inhibition ± SD (n = 5)	Acidic ethanolic extract (IC <sub>50</sub> 17.30 µg/ml) $Y = 11.95X + 43.19$ , $r^2 = 0.852$ % inhibition ± SD (n = 5)	Basic ethanolic extract (IC <sub>50</sub> 17.00 µg/ml) $Y = 12.93X + 30.19$ , $r^2 = 0.882$ % inhibition ± SD (n = 5)
1 mg/ml	81.01 ± 0.066	96.84 ± 0.048	87.49 ± 0.038
250 µg/ml	41.50 ± 0.034	90.57 ± 0.053	84.67 ± 0.046
100 µg/ml	36.90 ± 0.058	89.75 ± 0.054	77.38 ± 0.076
50 µg/ml	28.08 ± 0.068	71.70 ± 0.064	60.64 ± 0.066
10 µg/ml	19.04 ± 0.098	46.49 ± 0.071	34.83 ± 0.042

Various concentrations of date palm extracts, collected by three distinct methods, scavenge superoxide radical in a dose-dependent manner [ $r^2 = 0.809$  ( $p < 0.01$ ) for methanolic extract;  $r^2 = 0.908$  ( $p < 0.01$ ) for acidic ethanolic extract; and  $r^2 = 0.928$  ( $p < 0.01$ ) for basic ethanolic extract]. As per IC<sub>50</sub> values, acidic ethanolic extract is more potent to superoxide radicals (IC<sub>50</sub> 19.00 µg/ml) than the basic ethanolic extracts (IC<sub>50</sub> 19.15 µg/ml) and methanolic extracts (IC<sub>50</sub> 28.88 µg/ml)

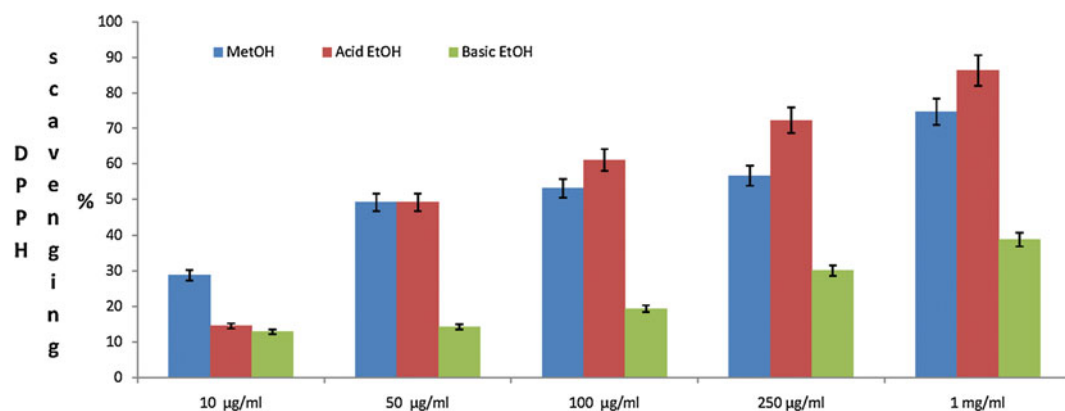


**Fig. 15.3** DPPH radical scavenging activities (DPPH assay shows that in this system, the radical scavenging activities of the three date palm extracts are in this order: acidic ethanolic extracts > methanolic extract > basic ethanolic extract). Various concentrations of date palm extracts, collected by three distinct methods, quenched DPPH free radical in a dose-dependent manner [ $r^2 = 0.909$  ( $p < 0.01$ ) for methanolic extract;  $r^2 = 0.933$

( $p < 0.01$ ) for acidic ethanolic extract;  $r^2 = 0.930$  ( $p < 0.01$ ) for basic ethanolic extract]. As per IC<sub>50</sub> values, acidic ethanolic extract is more potent to scavenge the DPPH radicals (IC<sub>50</sub> 14.61 µg/ml) than the methanolic extracts (IC<sub>50</sub> 22.91 µg/ml) and basic ethanolic extracts (IC<sub>50</sub> 36.44 µg/ml). Ascorbic acid has been shown as positive control

#### 15.4.2 Assay of Hydroxyl Radical (OH) Scavenging Activity

By the addition of iron(II) salts to a phosphate buffer containing reaction mixture, hydroxyl radicals can be generated [20]. Benzoate, weakly fluorescent, after monohydroxylation forms highly fluorescent

hydroxybenzoates [21]. Measurement of this spectrofluorometric changes has been used to detect damage by hydroxyl radical. Date extracts collected by three distinctly separate methods were found to be a powerful scavenger of hydroxyl radicals. There is a linear correlation between concentration of extract and <sup>0</sup>OH scavenging activity [ $r^2 = 0.832$  ( $p < 0.01$ ) for methanolic extracts of date;

**Table 15.3** Superoxide radical scavenging assay: superoxide radical  $O_2^{\cdot -}$  scavenging activity (superoxide radical scavenging assay shows that in this system, the superoxide radical scavenging activities of the three date palm extracts are in this order: acidic ethanolic extracts > basic ethanolic extract > methanolic extract)

Concentrations	Methanolic extract (IC <sub>50</sub> 28.88 µg/ml) $Y = 8.66X - 0.16$ , $r^2 = 0.809$ % inhibition ± SD (n = 5)	Acidic ethanolic extract (IC <sub>50</sub> 19.00 µg/ml) $Y = 13.36X - 3.936$ , $r^2 = 0.908$ % inhibition ± SD (n = 5)	Basic ethanolic extract (IC <sub>50</sub> 19.15 µg/ml) $Y = 13.40X - 6.724$ , $r^2 = 0.928$ % inhibition ± SD (n = 5)
1 mg/ml	51.5 ± 0.011	65.60 ± 0.114	58.90 ± 0.025
250 µg/ml	25.60 ± 0.015	53.80 ± 0.017	54.60 ± 0.028
100 µg/ml	22.80 ± 0.004	25.58 ± 0.011	26.12 ± 0.0053
50 µg/ml	16.40 ± 0.003	20.40 ± 0.005	17.28 ± 0.0009
10 µg/ml	12.80 ± 0.004	15.46 ± 0.007	10.54 ± 0.0017

Various concentrations of date palm extracts, collected by three distinct methods, scavenge superoxide radical in a dose-dependent manner [ $r^2 = 0.809$  ( $p < 0.01$ ) for methanolic extract;  $r^2 = 0.908$  ( $p < 0.01$ ) for acidic ethanolic extract; and  $r^2 = 0.928$  ( $p < 0.01$ ) for basic ethanolic extract]. As per IC<sub>50</sub> values, acidic ethanolic extract is more potent to superoxide radicals (IC<sub>50</sub> 19.00 µg/ml) than the basic ethanolic extracts (IC<sub>50</sub> 19.15 µg/ml) and methanolic extracts (IC<sub>50</sub> 28.88 µg/ml)

$r^2 = 0.835$  ( $p < 0.01$ ) for acidic ethanolic extracts of date;  $r^2 = 0.882$  ( $p < 0.01$ ) for basic ethanolic extracts of date]. IC<sub>50</sub> values are 18.20 µg/ml for methanolic date extracts, 17.30 µg/ml for acidic ethanolic date extracts, and 17.00 µg/ml for basic ethanolic extracts. Highest hydroxyl radical scav-

enging activity was found in the date extract collected by using basic ethanolic methods. The hydroxyl radical scavenging properties of date extracts are basic ethanolic extracts > acidic ethanolic extracts > methanolic extracts (Table 15.3; Fig. 15.4).

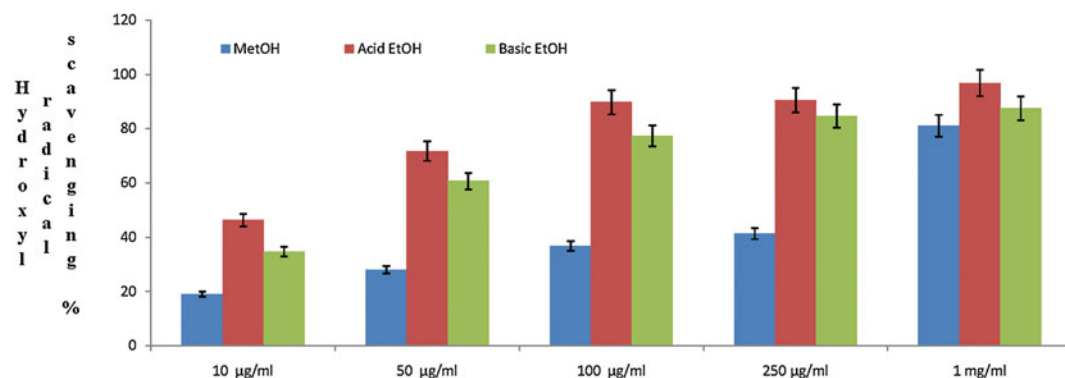


**Fig. 15.4** Hydroxyl radical (OH) scavenging activity (hydroxyl radical scavenging assay shows that in this system, the hydroxyl radical scavenging activities of the three date palm extracts are in this order: basic ethanolic extracts > acidic ethanolic extract > methanolic extract). Various concentrations of date palm extracts, collected by three distinct methods, scavenge hydroxyl radical in a dose-dependent manner [ $r^2 = 0.832$  ( $p < 0.01$ ) for

methanolic extract;  $r^2 = 0.852$  ( $p < 0.01$ ) for acidic ethanolic extract;  $r^2 = 0.882$  ( $p < 0.01$ ) for basic ethanolic extract]. As per IC<sub>50</sub> values, basic ethanolic extract is more potent to scavenge the hydroxyl radicals (IC<sub>50</sub> 17.00 µg/ml) than the acidic ethanolic extracts (IC<sub>50</sub> 17.30 µg/ml) and methanolic extracts (IC<sub>50</sub> 18.20 µg/ml). Ascorbic acid has been shown as positive control

### 15.4.3 Superoxide Radical O<sub>2</sub><sup>-</sup> Scavenging Activity

Photochemical reduction of flavins generates O<sub>2</sub> which reduces NBT, resulting in the formation of blue formazan [13]. Three types of date extracts inhibited the formation of the blue formazan and % inhibition is proportional to the concentration [ $r^2 = 0.809$  ( $p < 0.01$ ) for methanolic extract;

$r^2 = 0.908$  ( $p < 0.01$ ) for acidic ethanolic extract;  $r^2 = 0.928$  ( $p < 0.01$ ) for basic ethanolic extract]. IC<sub>50</sub> values were 28.88 µg/ml for methanolic extract, 19.00 µg/ml for acidic ethanolic extract, and 19.15 for acidic ethanolic extract. The superoxide ion scavenging activities of all these three extracts are acidic ethanolic extract > basic ethanolic extract > methanolic extracts (Table 15.4; Fig. 15.5).

**Table 15.4** Lipid peroxidation inhibition assay: lipid peroxidation inhibition assay (lipid peroxidation assay shows that in this system, to prevent the lipid peroxidation, the three date palm extracts are in this order: basic ethanolic extract > acidic ethanolic extract > methanolic extracts)

Concentrations	Methanolic extract (IC <sub>50</sub> 60.69) $Y = 4.02X + 5.618$ , $r^2 = 0.870$ % of inhibition ± SD ( $n = 5$ )	Acidic ethanolic extract (IC <sub>50</sub> 24.75) $Y = 10.22X - 3.023$ , $r^2 = 0.635$ % of inhibition ± SD ( $n = 5$ )	Basic ethanolic extract (IC <sub>50</sub> 18.03) $Y = 13.28X + 10.56$ , $r^2 = 0.978$ % of inhibition ± SD ( $n = 5$ )
1 mg/ml	28.68 ± 1.62	63.60 ± 2.68	80.28 ± 2.99
250 µg/ml	19.50 ± 1.53	22.9 ± 1.28	61.50 ± 2.90
100 µg/ml	14.9 ± 1.42	19.5 ± 1.02	48.44 ± 1.20
50 µg/ml	14.2 ± 0.68	16.75 ± 2.10	34.56 ± 1.08
10 µg/ml	11.2 ± 0.89	15.54 ± 1.04	27.32 ± 0.92

Various concentrations of date palm extracts, collected by three distinct methods, inhibit lipid peroxidation, using egg yolk homogenate as a substrate, in a dose-dependent manner [ $r^2 = 0.870$  ( $p < 0.01$ ) for methanolic extract;  $r^2 = 0.635$  ( $p < 0.01$ ) for acidic ethanolic extract; and  $r^2 = 0.978$  ( $p < 0.01$ ) for basic ethanolic extract]. As per IC<sub>50</sub> values, basic ethanolic date palm extract is more potent to inhibit the lipid peroxidation (IC<sub>50</sub> 18.03 µg/ml) than the acidic ethanolic extracts (IC<sub>50</sub> 24.75 µg/ml) and methanolic date palm extracts (IC<sub>50</sub> 60.69 µg/ml)

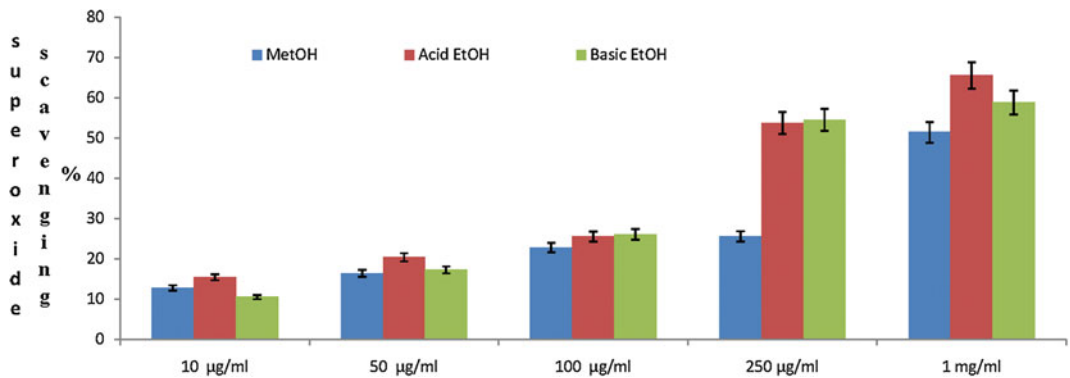


**Fig. 15.5** Assay of superoxide radical O<sub>2</sub><sup>-</sup> scavenging activity (superoxide radical scavenging assay shows that, in this system, the superoxide radical scavenging activities of the three date palm extracts are in this order: acidic ethanolic extracts > basic ethanolic extract > methanolic extract). Various concentrations of date palm extracts, collected by three distinct methods, scavenge superoxide

radical in a dose-dependent manner [ $r^2 = 0.809$  ( $p < 0.01$ ) for methanolic extract;  $r^2 = 0.908$  ( $p < 0.01$ ) for acidic ethanolic extract;  $r^2 = 0.928$  ( $p < 0.01$ ) for basic ethanolic extract]. As per IC<sub>50</sub> values acidic ethanolic extract is more potent to the superoxide radicals (IC<sub>50</sub> 19.00 µg/ml) than the basic ethanolic extracts (IC<sub>50</sub> 19.15 µg/ml) and methanolic extracts (IC<sub>50</sub> 28.88 µg/ml)

### 15.4.4 Nitric Oxide (NO) Scavenging Activity

The calculated  $IC_{50}$  values of all three different date extracts suggested that methanolic extract is most potent extract to scavenge the NO molecules followed by acidic ethanolic extracts and basic ethanolic extracts. But surprisingly, there is little or no significant variation of NO radical scavenging properties of all three date extracts (Table 15.5; Fig. 15.6).

### 15.4.5 Lipid Peroxidation Inhibition Assay

Egg yolk lipids undergo rapid non-enzymatic peroxidation when incubated in the presence of ferrous sulfate. Lipid peroxides are likely involved in numerous pathological events, including inflammation, metabolic disorders, and cellular aging [22, 23]. Date extracts inhibited lipid peroxidation in a concentration-dependent manner [ $r^2 = 0.870$  ( $p < 0.01$ ) for methanolic extract;

**Table 15.5** Total antioxidant capacity: total antioxidant capacity (equivalent to ASA/mg of plant material) (the phosphomolybdenum method is quantitative method to detect the antioxidant activity, expressed as the number of equivalents of ascorbic acid where acidic ethanolic date palm extract had a higher capacity than the basic ethanolic date palm extracts, followed by methanolic date palm extracts)

Concentrations	Methanolic extract (equivalent to ASA/mg of plant material) ( $n = 5$ )	Acidic ethanolic extract (equivalent to ASA/mg of plant material) ( $n = 5$ )	Basic ethanolic extract (equivalent to ASA/mg of plant material) ( $n = 5$ )
1 mg/ml	104.67 $\pm$ 1.224	382.154 $\pm$ 2.20	282.18 $\pm$ 2.62
250 $\mu$ g/ml	96.54 $\pm$ 3.587	231.77 $\pm$ 1.92	195.84 $\pm$ 2.18
100 $\mu$ g/ml	93.72 $\pm$ 4.662	124.32 $\pm$ 1.86	115.55 $\pm$ 2.14
50 $\mu$ g/ml	88.58 $\pm$ 4.424	101.922 $\pm$ 2.17	106.89 $\pm$ 2.66
10 $\mu$ g/ml	83.64 $\pm$ 2.553	87.54 $\pm$ 3.24	98.19 $\pm$ 2.26

Determination of the total antioxidant capacity of three different date palm extracts, based on the basis of the reduction of Mo(VI) to Mo(V). Results were expressed as equivalent to ascorbic acid (ASA)/mg of plant material ( $n = 5$ ). Acidic ethanolic date palm extract had a higher capacity than the basic ethanolic date palm extracts, followed by methanolic date palm extracts

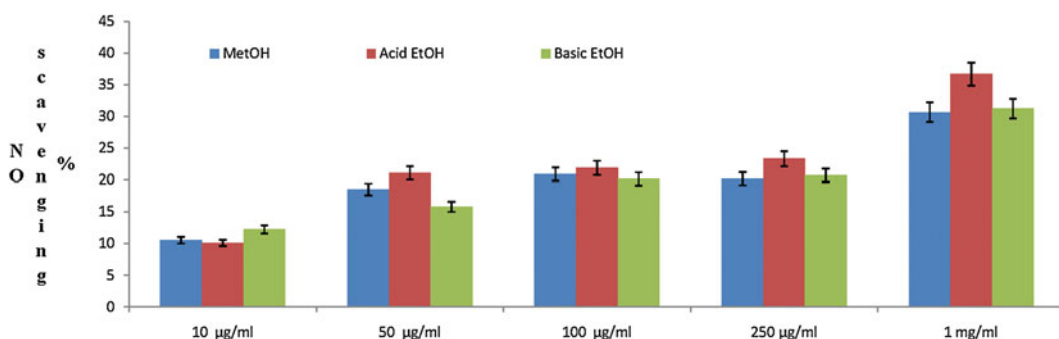


**Fig. 15.6** Nitric oxide (NO) scavenging activity (nitric oxide scavenging assay shows that in this system, the NO radical scavenging activities of the three date palm extracts are in this order: methanolic extract > acidic ethanolic extract > basic ethanolic extract). Various concentrations of date palm extracts, collected by three distinct methods, scavenge NO radicals, sodium nitroprusside used as substrate, in a dose-dependent manner [ $r^2 = 0.852$  ( $p < 0.01$ ) for methanolic extract;  $r^2 = 0.857$

( $p < 0.01$ ) for acidic ethanolic extract;  $r^2 = 0.900$  ( $p < 0.01$ ) for basic ethanolic extract]. As per  $IC_{50}$  values, methanolic date palm extract is more potent to the NO radicals ( $IC_{50}$  5.505  $\mu$ g/ml) than the acidic ethanolic extracts ( $IC_{50}$  5.60  $\mu$ g/ml) and basic ethanolic extracts ( $IC_{50}$  5.505  $\mu$ g/ml). But there is no significant difference in all these three different extracts of date palm to scavenge the nitric oxide in a vitro system

**Table 15.6** Total flavonoid and phenol content: total flavonoid and phenol content (though the basic ethanolic extract contains maximum phenolic contents than other two tested extracts, but the bioactive flavonoid content is highest in acidic ethanolic extracts. Methanolic date palm extract is very poor in containing phenol and flavonoids)

Type of samples	Flavonoid (mg Fisetin/g of extract)	Phenol (mg gallic acid/10 g of extract)
Methanolic extract	15.44 ± 0.872	411.09 ± 2.69
Acidic ethanolic extract	60.96 ± 0.996	1127.34 ± 4.68
Basic ethanolic extract	26.07 ± 1.26	1158.50 ± 6.728

Total flavonoid content of the date palm extracts was determined using aluminum chloride (AlCl<sub>3</sub>), whereas the total phenolic content was determined using the Folin–Ciocalteu reagent ( $n = 5$ ). Results were expressed as mg of flavonoid contents in Fisetin/g of extracts and mg of gallic acid/10 mg of the extract, taking ± SD. Total flavonoid and phenol contents show a direct correlation with the total antioxidant capacity of the tested compounds. Acidic ethanolic extract is rich in both phenolic and flavonoid contents, and it can be correlated with its radical scavenging activities and total antioxidant properties, as the data have shown, than the other two tested extracts of date palm

$r^2 = 0.635$  ( $p < 0.01$ ) for acidic ethanolic extract;  $r^2 = 0.9596$  ( $p < 0.01$ ) for basic ethanolic extract]. IC<sub>50</sub> values for the inhibition of lipid peroxidation were 60.69 µg/ml for methanolic extract, 24.75 µg/ml for acidic ethanolic extract, and 18.03 µg/ml for basic ethanolic extract. The results suggest that consumption of date may afford a cytoprotective effect by lowering the lipid peroxidation level (Table 15.6; Fig. 15.7).

#### 15.4.6 Determination of Reducing Power

The reducing power of different date extract samples using the potassium ferricyanide reduction method was evaluated. It has been investigated from the Fe<sup>3+</sup>–Fe<sup>2+</sup> transformation in the presence of three different extract samples. Highest activity was found in basic ethanolic extracts, followed by acidic ethanolic extracts of date, and the lowest activity was found in methanolic extract of date (Figure 15.8).

#### 15.4.7 Total Antioxidant Capacity (Equivalent to ASA/mg of Plant Material)

Total antioxidant capacity of date extract is expressed as the number of equivalents of ascorbic acid. The assay is based on the reduction of Mo(VI) to Mo(V) by the extract and subsequent formation of a green phosphate/Mo(V) complex at acid pH. The phosphomolybdenum method is quantitative

since the antioxidant activity is expressed as the number of equivalents of ascorbic acid [17]. Acidic ethanolic extract had a higher capacity than the other two varieties. The results from various free radical scavenging system revealed that the three date extract samples collected by three different methods had significant antioxidant activity. The extracts were found to have different levels of antioxidant activity in the systems tested. The antioxidant activities of the three varieties were in the order acidic ethanolic extract > basic ethanolic extract > methanolic extract (Fig. 15.9).

#### 15.4.8 Total Flavonoid and Phenol Content

Total flavonoid content expressed as Fisetin equivalents was 15.44 ± 0.872 mg/g plant material in methanolic extract, 60.96 ± 0.996 mg/g plant material in acidic ethanolic extract, and 26.07 ± 1.26 mg/g plant material in basic ethanolic extract, respectively. Total phenolic concentration showed close correlation with the antioxidant activity, being highest in basic ethanolic extract and lowest in methanolic extract of date. Plant phenolics present in fruit and vegetables have received considerable attention because of their potential antioxidant activity [24]. Natural polyphenols have chain-breaking antioxidant activities and are believed to prevent many degenerative diseases, including cancer and atherosclerosis [25] (Fig. 15.10a, b).

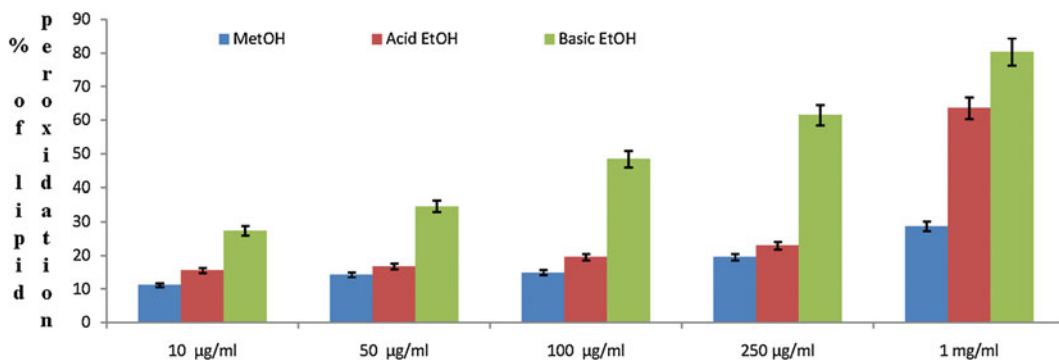


**Fig. 15.7** Lipid peroxidation inhibition assay (lipid peroxidation assay shows that in this system, to prevent the lipid peroxidation, the three date palm extracts are in this order: basic ethanolic extract > acidic ethanolic extract > methanolic extracts). Various concentrations of date palm extracts, collected by three distinct methods, inhibit lipid peroxidation, using egg yolk homogenate as a substrate, in a dose-dependent manner [ $r^2 = 0.870$

( $p < 0.01$ ) for methanolic extract;  $r^2 = 0.635$  ( $p < 0.01$ ) for acidic ethanolic extract;  $r^2 = 0.978$  ( $p < 0.01$ ) for basic ethanolic extract]. As per  $IC_{50}$  values, basic ethanolic date palm extract is more potent to inhibit the lipid peroxidation ( $IC_{50}$  18.03 µg/ml) than the acidic ethanolic extracts ( $IC_{50}$  24.75 µg/ml) and methanolic date palm extracts ( $IC_{50}$  60.69 µg/ml)

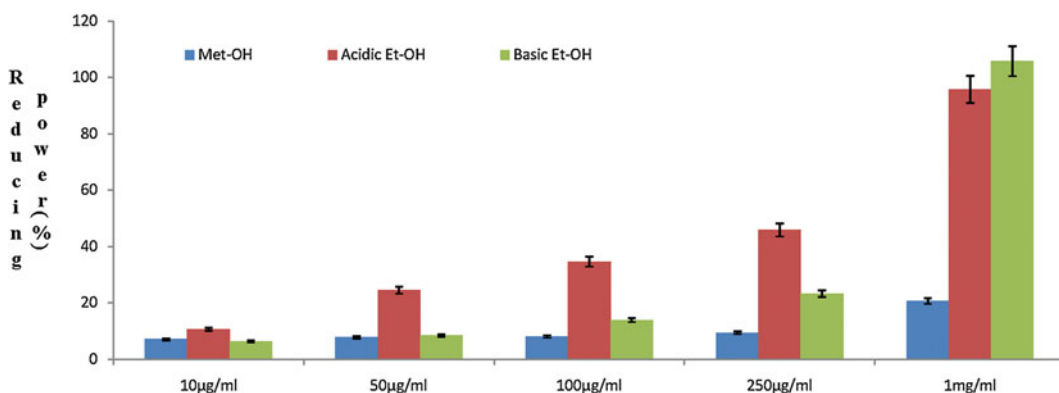


**Fig. 15.8** Determination of reducing power (the reducing power activities are highest in acidic ethanolic extract followed by basic ethanolic and methanolic extracts of date palm). Various concentrations of date palm extracts, collected by three distinct methods, reduce ferric ions in a dose-dependent manner [ $r^2 = 0.640$  ( $p < 0.01$ ) for

methanolic extract;  $r^2 = 0.864$  ( $p < 0.01$ ) for acidic ethanolic extract;  $r^2 = 0.646$  ( $p < 0.01$ ) for basic ethanolic extract]. The reducing power activities are highest in acidic ethanolic extract followed by basic ethanolic and methanolic extracts of date palm

### 15.4.9 UV-Based Spectrophotometric Analysis

When different extracts of date were analyzed in a UV-Vis spectrophotometer to assess their solubility in different solvents to determine actual active compounds remain in that solution, we got a striking result where date extracts in basic

ethanolic solvents yielded best solubility in comparison with their acidic ethanolic solvent, whereas the methanolic extracts failed to show any such significant peak, indicating very low or no solubility of the date extract into it which states that ethanolic solvent is the best to exhibit the potent anti-inflammatory biological activities of the date which correlates with the cellular analysis further (Fig. 15.11).

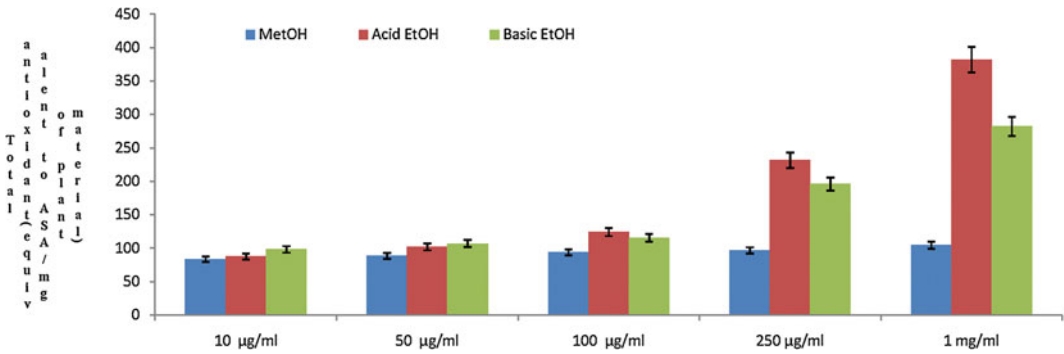


**Fig. 15.9** Total antioxidant capacity (equivalent to ASA/mg of plant material) (the phosphomolybdenum method is quantitative method to detect the antioxidant activity, expressed as the number of equivalents of ascorbic acid where acidic ethanolic date palm extract had a higher capacity than the basic ethanolic date palm extracts, followed by methanolic date palm extracts).

Determination of the total antioxidant capacity of three different date palm extracts, based on the basis of the reduction of Mo(VI) to Mo(V). Results were expressed as equivalent to ascorbic acid (ASA)/mg of plant material ( $n = 5$ ). Acidic ethanolic date palm extract had a higher capacity than the basic ethanolic date palm extracts, followed by methanolic date palm extracts

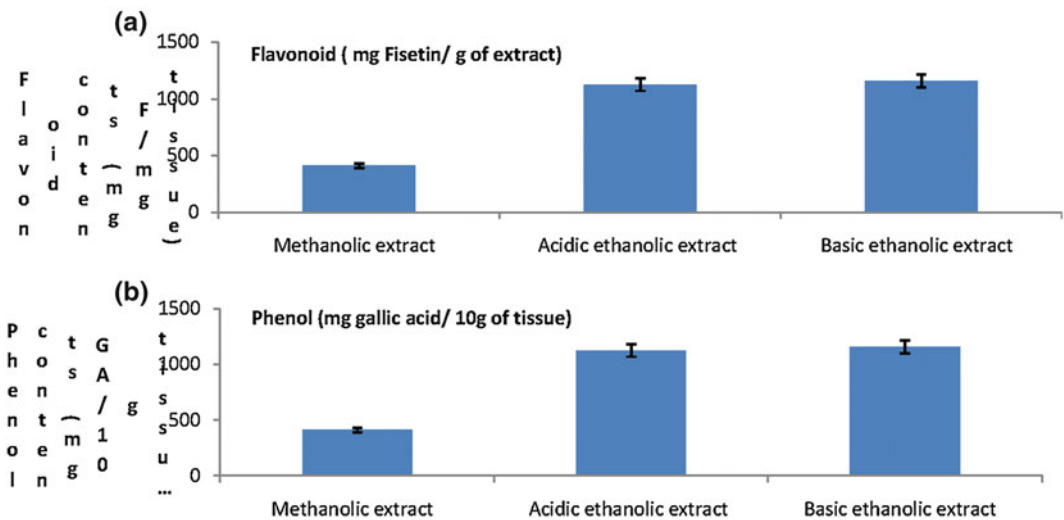


**Fig. 15.10** Flavonoid and phenol contents in three date palm extracts (though the basic ethanolic extract contains maximum phenolic contents than other two tested extracts, but the bioactive flavonoid content is highest in acidic ethanolic extracts. Methanolic date palm extract is very poor in containing phenol and flavonoids). Total flavonoid content of the date palm extracts was determined using aluminum chloride ( $AlCl_3$ ) whereas the total phenolic content was determined using the Folin–Ciocalteu reagent ( $n = 5$ ). Results were expressed as mg of Flavonoid contents in Fisetin/g of extracts and mg of

gallic acid/10 mg of the extract, taking  $\pm$  SD. Total flavonoid and phenol contents show a direct correlation with the total antioxidant capacity of the tested compounds. Acidic ethanolic extract is rich in both phenolic and flavonoid contents, and it can be correlated with its radical scavenging activities and total antioxidant properties, as the data have shown, than the other two tested extracts of date palm. **a** Total flavonoid contents in three different date palm extracts, **b** total phenol contents in three different date palm extracts

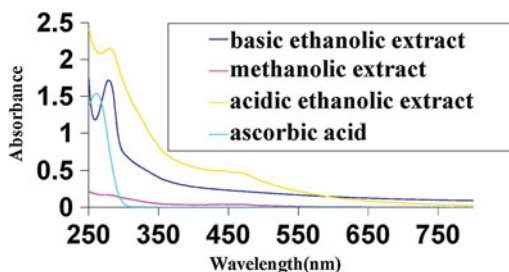


**Fig. 15.11** UV-based spectrophotometric analysis. UV-Vis-based spectrophotometric analysis reveals that acidic and basic ethanolic extracts contain maximum amounts of phenolic compounds which come under the UV zone where the methanolic extracts show very poor quantities of these compounds in this area under study. Significantly, the acidic ethanolic extracts indicate that it contains more phenolic and flavonoid contents than the standard control ascorbic acid solution which has been correlated with the radical scavenging activities, lipid peroxidation inhibitory potential, total phenolic and flavonoid contents, and the total antioxidant properties also

#### 15.4.10 Cell Viability of RAW Macrophages

In order to ascertain the anti-inflammatory activities of the date extracts, collected by three distinct methodologies, LPS-induced preclinical in vitro models, using both RAW macrophage such as murine cell lines and HEK, human embryonic kidney cell lines were used. Cells were seeded into the 96-well plate and incubated for 12 h, and then 1  $\mu\text{g/ml}$  LPS was added into it following the various doses of the extracts and incubated for both 1 and 24 h time periods, respectively. In both the models using RAW macrophages, three extracts possess their anti-inflammatory activities by regulating the cell viability in a dose-dependent manner where methanolic extracts are not potent to maintain cell viability in 24-h inflammatory models in comparison with other two extracts where acidic ethanolic extracts retain the cell viability significantly in its lower doses, i.e., 100, 50, 10, and 1  $\mu\text{g/ml}$ , respectively, in both 1 and 24 h models

(Fig. 15.12a, b), but the basic ethanolic extracts maintain the cell viability only in higher doses, i.e., 250, 100, and 50  $\mu\text{g/ml}$ , where in lower doses (1  $\mu\text{g/ml}$ ) it acts as proinflammatory causing the cell death (Fig. 15.12c). So all these extracts may act as either anti-inflammatory or a proinflammatory depending on their doses and nature of extraction.

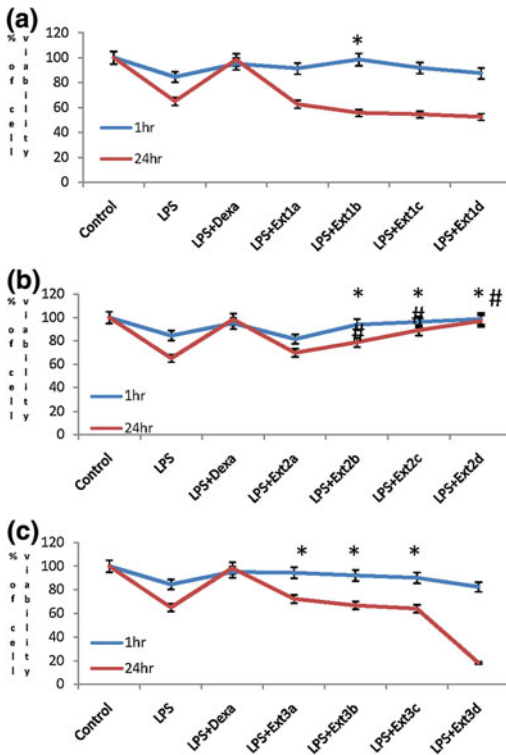
#### 15.4.11 Assay of Hydroxyl Radical (OH) Scavenging Activity

As the in vitro study suggested that all three date crude extracts have potent hydroxyl radical and superoxide ion scavenging activities, the ex vivo result, using RAW macrophages, also advocated the same where acidic ethanolic extract has been shown to have strongest hydroxyl radical scavenging power, >50 % inhibition (Fig. 15.13b), followed by basic ethanolic (Fig. 15.13c) and methanolic extracts (Fig. 15.13a). This may have been accomplished by modulating the mitochondria-associated NADPH oxidase activity.

#### 15.4.12 NO Estimation

None of the tested compounds induced changes in NO basal levels, when incubated without LPS (data not shown). To evaluate the nitrosative stress, Griess reagents were used. After 24 h LPS treatment cellular NO production increases near about twofold (Fig. 15.14a) in comparison with the untreated control samples, whereas the three date extracts ameliorate the LPS-induced NO production to the basal level such as untreated group in a dose-dependent manner which strongly showing their NO scavenging capabilities which is already been established by the in vitro assays. Here, dexamethasone has been taken as positive control (Fig. 15.14a-c).





◀ **Fig. 15.12 a** Cell viability determination using MTT assay. RAW 264.7 cells were treated with 1  $\mu\text{g}/\text{ml}$  of *E. coli* LPS and then methanolic date palm extracts were added into it therapeutically and incubated for two different time periods, 1 and 24 h. Taking control as 100 % viability, data were calculated ( $p < 0.01$ ). Dexamethasone (9 nM) was used as positive control ( $a = 250$ ,  $b = 100$ ,  $c = 50$ ,  $d = 10$  ng/ml) (asterisk for 1 h group, hash for 24 h group in comparison with the untreated control group). **b** Cell viability determination using MTT assay. RAW 264.7 cells were treated with 1  $\mu\text{g}/\text{ml}$  of *E. coli* LPS and then acidic ethanolic date palm extracts were added into it therapeutically and incubated for two different time periods, 1 and 24 h. Taking control as 100 % viability, data were calculated ( $p < 0.01$ ). Dexamethasone (9 nM) was used as positive control. ( $a = 250$ ,  $b = 100$ ,  $c = 50$ ,  $d = 10$  ng/ml) (asterisk for 1 h group, hash for 24 h group in comparison with the untreated control group). **c** Cell viability determination using MTT assay. RAW 264.7 cells were treated with 1  $\mu\text{g}/\text{ml}$  of *E. coli* LPS and then basic ethanolic date palm extracts were added into it therapeutically and incubated for two different time periods, 1 and 24 h. Taking control as 100 % viability, data were calculated ( $p < 0.01$ ). Dexamethasone (9 nM) was used as positive control. ( $a = 250$ ,  $b = 100$ ,  $c = 50$ ,  $d = 10$  ng/ml) (asterisk for 1 h group, hash for 24 h group in comparison with the untreated control group). Cell viability assay using three different date palm extracts shows that for 1 h LPS-induced model there is no significant variation to maintain cell viability of all three extracts, whereas in 24 h model, acidic ethanolic extract is more capable to inhibit LPS-induced inflammation than other two tested extracts in a dose-dependent manner. In lower doses, basic ethanolic extract shows proinflammatory activities on murine RAW macrophages

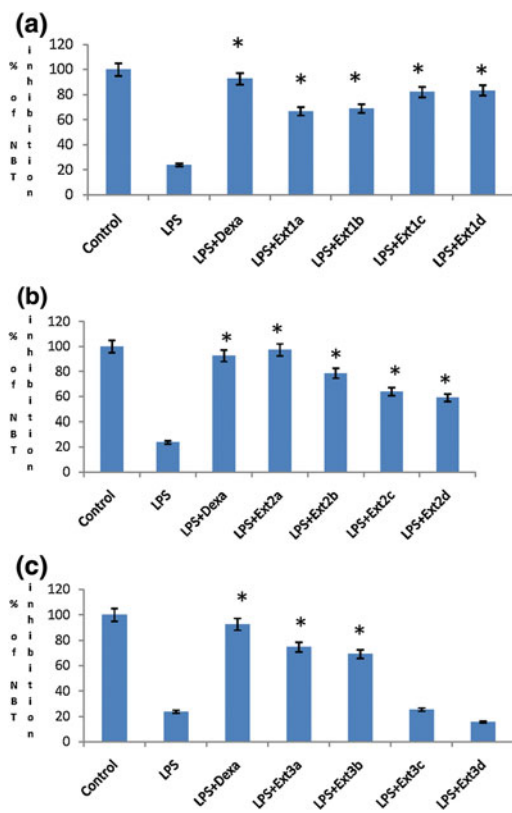
### 15.4.13 Cell Viability of HEK 293 Cells

To investigate the cytotoxicity of the three date extracts, MTT assay was performed as MTT is reduced by mitochondrial dehydrogenase to form formazan, an insoluble purple compound and one can measure the cytotoxicity in terms of the intensity of the purple compound, whereas, dead cells do not form any purple formation because the enzyme was degraded and lack of regular function. Among the three extracts of date, acidic ethanolic extracts ameliorated the LPS-induced cell death to retain the cell viability in both 1 and 24 h inflammatory models (Fig. 15.15b) followed by basic ethanolic (Fig. 15.15c) and methanolic extracts (Fig. 15.15a) in a dose-dependent manner. In lower doses, all these three extracts fail to inhibit LPS-induced cell death, whereas they are active only in the higher concentrations, i.e., in 250 and 100  $\mu\text{g}/\text{ml}$  doses which is similar to the LPS-induced inflammatory models applied on murine macrophage cell line. These data suggest

that acidic ethanolic extracts contain potent anti-inflammatory compound(s) which is/are able to inhibit the LPS-induced cytotoxicity in a dose-dependent manner. Dexamethasone was used as positive control in the entire study.

### 15.4.14 ROS Measurement

The evidence presented above suggests that date extracts mediate its effects through the antioxidant pathway. We used a DCF-DA probe to examine whether this mechanism can scavenge ROS inside the RAW macrophage cells. Cells were treated with *E. coli* LPS and then various concentrations of date extracts were added into it therapeutically and incubated for 6 h and analyzed by fluorescent spectrophotometer. Date



◀ **Fig. 51.13** **a** Superoxide ion scavenging activities of methanolic date palm extracts on LPS (1  $\mu\text{g/ml}$ )-induced RAW macrophages, after 24 h incubation, were determined by using NBT inhibition methods, taking control group as 100 % inhibition ( $p < 0.05$  in comparison with the untreated control group). Dexamethasone (9 nM) was used as positive control ( $a = 250$ ,  $b = 100$ ,  $c = 50$ ,  $d = 10$   $\mu\text{g/ml}$ ). **b** Superoxide ion scavenging activities of acidic ethanolic date palm extracts on LPS (1  $\mu\text{g/ml}$ )-induced RAW macrophages, after 24 h incubation, were determined by using NBT inhibition methods, taking control group as 100 % inhibition ( $p < 0.05$  in comparison with the untreated control group) Dexamethasone (9 nM) was used as positive control ( $a = 250$ ,  $b = 100$ ,  $c = 50$ ,  $d = 10$   $\mu\text{g/ml}$ ). **c** Superoxide ion scavenging activities of basic ethanolic date palm extracts on LPS (1  $\mu\text{g/ml}$ )-induced RAW macrophages, after 24 h incubation, were determined by using NBT inhibition methods, taking control group as 100 % inhibition ( $p < 0.05$  in comparison with the untreated control group). Dexamethasone (9 nM) was used as positive control ( $a = 250$ ,  $b = 100$ ,  $c = 50$ ,  $d = 10$   $\mu\text{g/ml}$ ). Superoxide scavenging assay, following NBT inhibition method, using three different date palm extracts, shows that for 24 h LPS-induced model, both acidic ethanolic extract and methanolic extract are more capable to inhibit LPS-induced inflammatory oxidative burst than the basic ethanolic tested extracts in a dose-dependent manner. In lower doses, basic ethanolic extract shows proinflammatory activities by induced oxidative stress on murine RAW macrophages

extracts ameliorate in LPS-induced ROS levels in a significant manner over the control in a dose-dependent manner. This effect was observed best in acidic ethanolic extracts where it inhibits the ROS generation in higher doses, i.e., in 250 and 100  $\mu\text{g/ml}$ , and increases ROS levels slightly thereafter. ROS levels decreased significantly in methanolic and basic ethanolic extracts also but increases significantly in its lower doses compared to control cells (Fig. 15.16).

#### 15.4.15 Measurement of Mitochondrial Membrane Potential (MMP)

After the assessment of total cellular antioxidant property, in the next phase we targeted Mitochondria, the most important site inside the cell

for ROS generation. Here, we have found that all three extracts of date are capable to reduce LPS-induced oxidative stress in murine macrophage-like cells significantly in comparison with the control group in a dose-dependent manner which advocates that the date extracts ameliorate the LPS-induced oxidative stress by targeting the mitochondria in a dose-dependent manner and thus maintain the cell viability (Fig. 15.17).

#### 15.4.16 TLC Analyses

Sample A:

Extract A showed several peaks as shown in Fig. 15.18; however, only two peaks show appreciably high absorbance when observed with 254 nm wavelength. The peak at 23.5 min is the major peak while that at 34.0 min is a minor peak. The peak at 23.5 min appears about 20-fold attenuated when observed with 370 nm

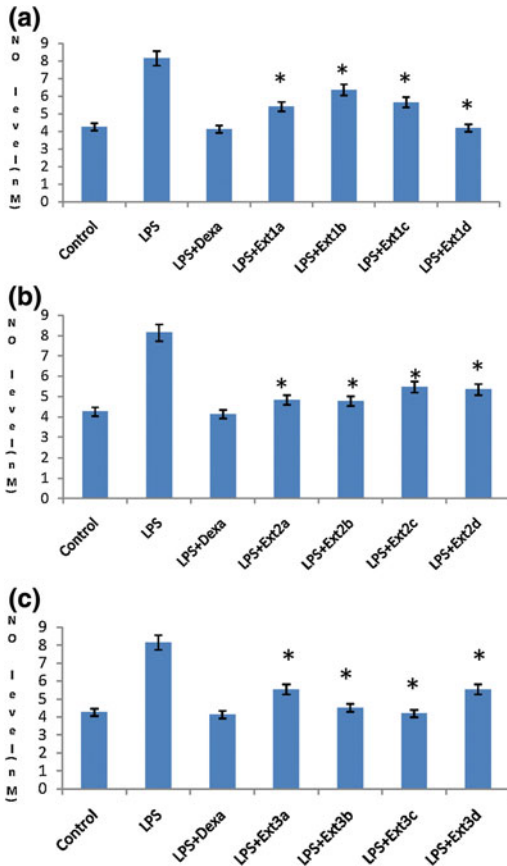


**Fig. 15.14** **a** NO levels (nM) were determined using Griess reagent from LPS (1 µg/ml)-stimulated RAW macrophages supernatant, where methanolic date palm extracts at various concentrations were added therapeutically and incubation time was 24 h ( $p < 0.05$ ). Dexamethasone (9 nM) was used as positive control ( $a = 250, b = 100, c = 50, d = 10$  µg/ml). **b** NO levels (nM) were determined using Griess reagent from LPS (1 µg/ml)-stimulated RAW macrophages supernatant, where acidic ethanolic date palm extracts at various concentrations were added therapeutically and incubation time was 24 h ( $p < 0.05$ ). Dexamethasone (9 nM) was used as positive control ( $a = 250, b = 100, c = 50, d = 10$  µg/ml). **c** NO levels (nM) were determined using Griess reagent from LPS (1 µg/ml)-stimulated RAW macrophages supernatant, where basic ethanolic date palm extracts at various concentrations were added therapeutically and incubation time was 24 h ( $p < 0.05$ , in comparison with the untreated control group). Dexamethasone (9 nM) was used as positive control ( $a = 250, b = 100, c = 50, d = 10$  µg/ml). Nitric oxide (NO) scavenging assay, following Griess reagent method, using three different date palm extracts show that for 24 h LPS-induced model, all three date palm extracts, viz., methanolic, acidic ethanolic, and basic ethanolic are capable to inhibit LPS-induced NO production in a dose-dependent manner on murine RAW macrophages

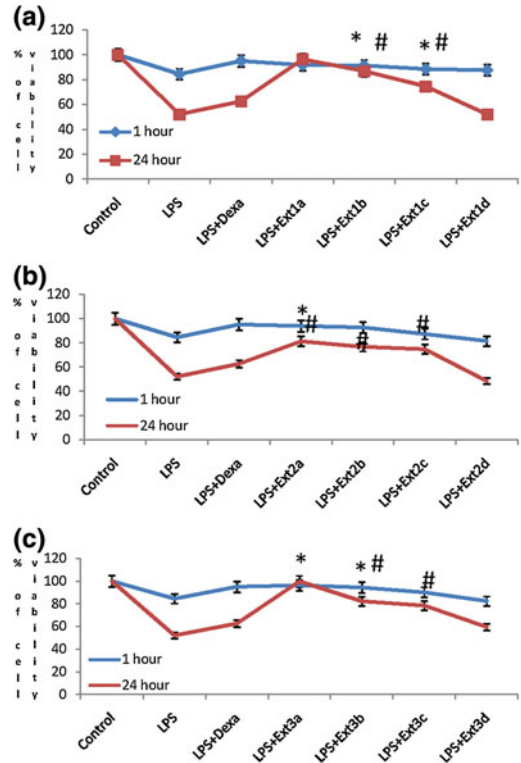


**Fig. 15.15** **a** Cell viability determination using MTT assay. HEK 293 cells were treated with 1 µg/ml of *E. coli* LPS and then methanolic date palm extracts were added into it therapeutically and incubated for two different time periods, 1 and 24 h. Taking control as 100 % viability, data were calculated ( $p < 0.01$ ). Dexamethasone (9 nM) was used as positive control ( $a = 250, b = 100, c = 50, d = 10$  g/ml) (asterisk for 1 h group, hash for 24 h group in comparison with the untreated control group). **b** Cell viability determination using MTT assay. HEK 293 cells were treated with 1 µg/ml of *E. coli* LPS and then acidic ethanolic date palm extracts were added into it therapeutically and incubated for two different time periods, 1 and 24 h. Taking control as 100 % viability, data were calculated ( $p < 0.01$ ). Dexamethasone (9 nM) was used as positive control ( $a = 250, b = 100, c = 50, d = 10$  µg/ml) (asterisk for 1 h group, hash for 24 h group). **c** Cell viability determination using MTT assay. HEK 293 cells were treated with 1 µg/ml of *E. coli* LPS and then basic ethanolic date palm extracts were added into it therapeutically and incubated for two different time periods, 1 hour and 24 h. Taking control as 100 % viability, data were calculated ( $p < 0.01$ ). Dexamethasone (9 nM) was used as positive control ( $a = 250, b = 100, c = 50, d = 10$  µg/ml) (asterisk for 1 h group and hash for 24 h group). Cell viability assay using three different date palm extracts shows that for 1 h LPS-induced model, there is no significant variation to maintain cell viability of all three extracts, whereas in 24 h model, both acidic and basic ethanolic extracts are more capable to inhibit LPS-induced inflammation than the methanolic extract in a dose-dependent manner on human embryonic kidney cell lines

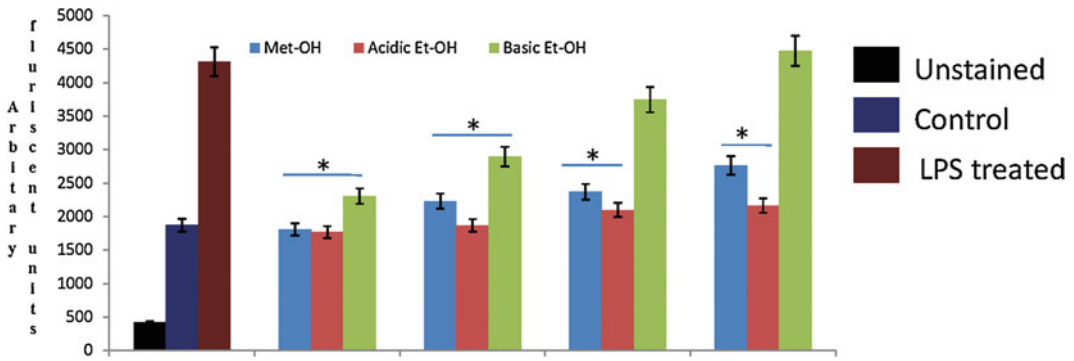


**Fig. 15.16** Intracellular ROS measurement in RAW macrophages (all three date palm extracts are capable to inhibit LPS-induced oxidative stress in RAW macrophages in a dose-dependent manner). Intracellular formation of ROS was assessed by using oxidation sensitive dye DCFH-DA as a substrate where non-fluorescent DCFH-DA dye, that is freely penetrate into cells, gets hydrolyzed by intracellular esterase to 207-dichlorofluorescin (DCFH) and traps inside the cells. The formation of 207-dichlorofluorescin (DCF) due to oxidation of DCFH in the presence of ROS was read after 30 min at an excitation wavelength of 485 nm and emission

wavelength of 525 nm using a spectrofluorometer. Intracellular ROS scavenging activities of three date palm extracts followed a dose-dependent manner where at 250, 100, and 50 µg/ml doses all three extracts are capable to inhibit LPS-induced oxidative stress in RAW macrophages significantly, but at lower dose, i.e., 10 µg/ml only methanolic and acidic ethanolic extracts are capable to reduce oxidative burst significantly (\**p* < 0.05 in comparison with the untreated control group). From these data, it can be concluded that all three date palm extracts are capable to inhibit LPS-induced oxidative stress in RAW macrophages in a dose-dependent manner

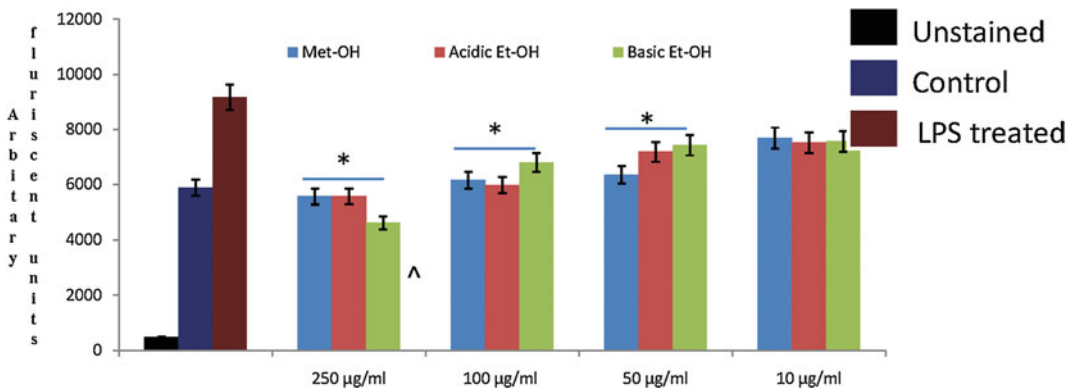
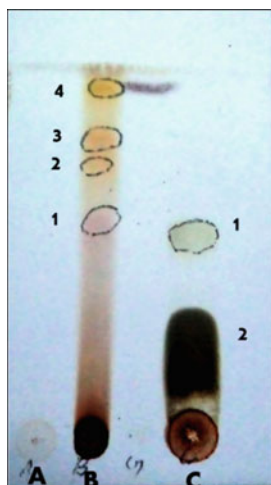


**Fig. 15.17** Mitochondrial ROS measurement in RAW macrophages (all three date palm extracts are capable to inhibit LPS-induced mitochondrial oxidative stress in RAW macrophages in a dose-dependent manner). Mitochondrial ROS production was monitored by the fluorescent dye, Rhodamine 123, where due to oxidative stress depolarization of mitochondrial membrane potential results in the loss of Rhodamine 123 from the mitochondria and a produce the fluorescence intensity. Mitochondrial ROS scavenging activities of three date palm extracts followed a dose-dependent manner where at

250, 100, and 50 µg/l doses all three extracts are capable to inhibit LPS-induced mitochondrial oxidative stress in RAW macrophages significantly, but at lower dose, i.e., 10 µg/ml though they reduce mitochondria oxidative burst in comparison with the LPS-treated group, but as the values are so much higher than the control group, so the values are not counted (\**p* < 0.05 in comparison with the untreated control group). From these data, it can be concluded that all three date palm extracts are capable to inhibit LPS-induced mitochondrial oxidative stress in RAW macrophages in a dose-dependent manner



Sample Name	Number of Bands	Rf value
B	4	1. 0.58
		2. 0.73
		3. 0.81
		4. 0.95
C	2	1. 0.32
		2. 0.56

**Fig. 15.18** TLC profile of A, B, and C extracts. No band was observed in extract A. In extracts B and C, 4 and 2 bands were observed, respectively. *R<sub>f</sub>* values of samples B and C are given

wavelength while the peak at 34.0 min is not observed at this wavelength.

#### Sample B:

Extract B shows four closely spaced peaks between 6.0 and 9.0 min appearing at 6.7, 7.3, 7.8, and 8.4 min with major peak being at 7.3 min when observed with 254 nm wavelength. These peaks were also observed with 370 nm wavelength but with about fourfold attenuation in peak absorbance values.

#### Sample C:

Extract C showed roughly three distinct peaks. They were at 5.1–5.2, 6.3, and 7.9 min using 254 nm wavelength. The first two peaks are major peaks but are not well separated. The third peak at 7.9 min is a minor peak in this sample. There is another minor peak at about 6.8 min observed

with 254 nm wavelength which may be a spurious peak as it lies on the shoulder of the 6.3 min peak and did not appear in repeat scan. The absorbance maxima of these peak positions remained similar when seen in 370 nm wavelength although their intensities were attenuated by about 10-fold. Comparing the absolute absorbance values of peak maxima of sample C with others samples (A and B), it indicates that sample C contains much higher concentration of compound(s) as similar values of samples (100–200 ml) were injected for HPLC analysis in each case.

### 15.4.17 HPLC Analyses

See Fig. 15.19a–f.

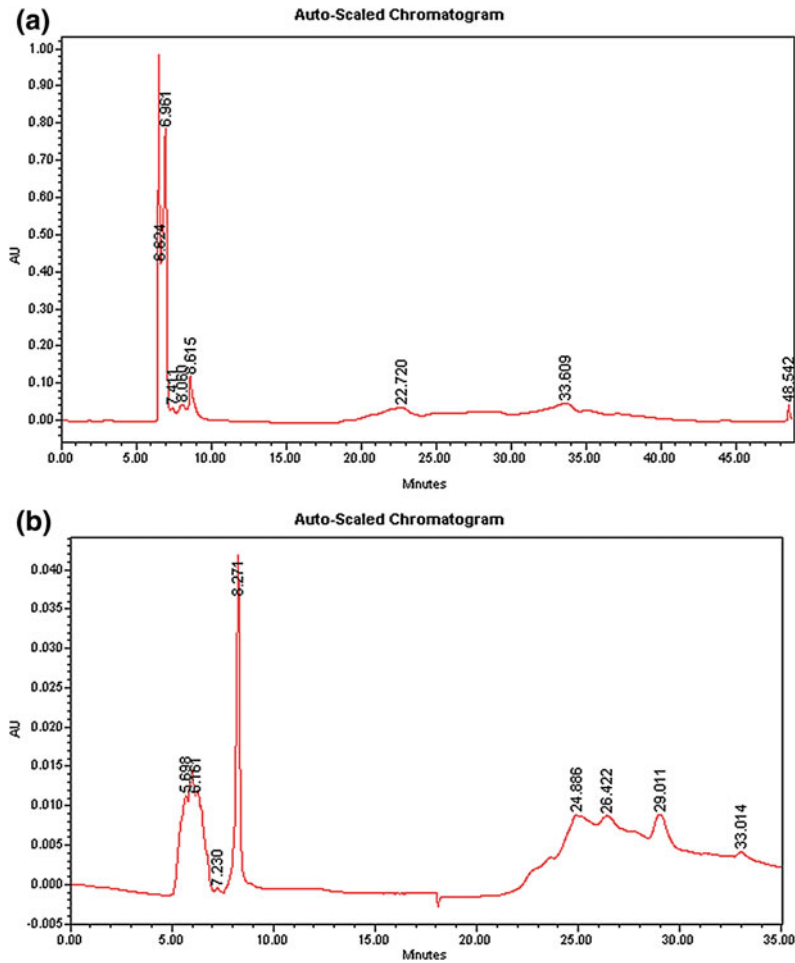


**Fig. 15.19 a** HPLC profile of methanolic extract (A) of *Phoenix sylvestris* L. crude methanolic extract was analyzed by HPLC, detecting several peaks at 254 nm and their HPLC retention times are 6.62, 6.96, 7.41, 8.06, and 8.61 min, respectively. **b** HPLC profile of methanolic extract (A) of *Phoenix sylvestris* L. crude methanolic extract was analyzed by HPLC detecting several peaks at 370 nm and their HPLC retention times are 5.69, 6.16, 7.23, 8.27, 24.88, 26.42, 29.01, and 33.01 min, respectively. **c** HPLC profile of basic ethanolic extract (B) of *Phoenix sylvestris* L. crude acidic ethanolic extract was analyzed by HPLC, detecting several peaks at 254 nm. And their HPLC retention times are 5.72, 6.67, 7.31, 7.84, and 8.41 min, respectively. **d** HPLC profile of basic ethanolic

extract (B) of *Phoenix sylvestris* L. crude acidic ethanolic extract was analyzed by HPLC, detecting several peaks at 370 nm. And their HPLC retention times are 6.82, 7.31, 7.89, 8.57 min, respectively. **e** HPLC profile of acidic ethanolic extract (C) of *Phoenix sylvestris* L. crude acidic ethanolic extract was analyzed by HPLC, detecting several peaks at 254 nm, and their HPLC retention times were 5.14, 6.30, 6.77, 7.94, 23.61, and 33.89 min, respectively. **f** HPLC profile of acidic ethanol extract (C) of *Phoenix sylvestris* L. Crude acidic ethanolic extract was analyzed by HPLC, detecting several peaks at 370 nm. And their HPLC retention times were 5.31, 7.44, 7.97, 16.79, 19.39, 22.88, 23.59, and 24.51 min, respectively

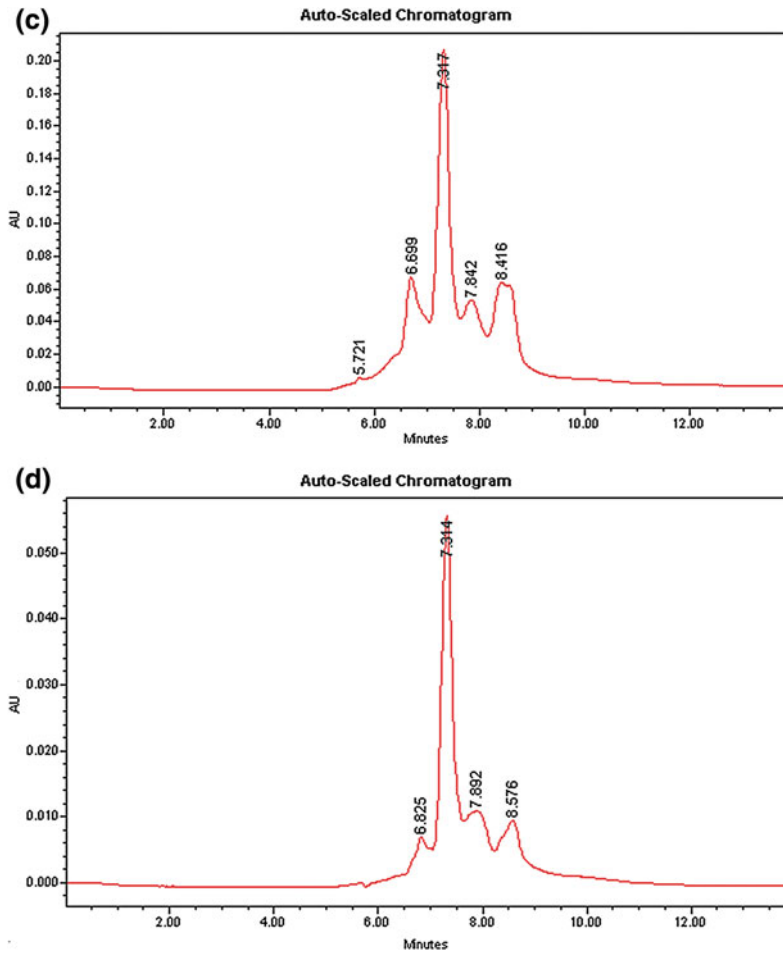


Fig. 15.19 (continued)

## 15.5 Discussion

In the present study to evaluate anti-inflammatory potential of the extracts of date collected by three different extraction procedures (Fig. 15.1) where one or more fractions of the mesocarp tissue are likely to be included and the rest excluded, various inflammatory markers were used against a powerful and well-characterized proinflammatory stimulus—LPS, a major component of the outer membrane of Gram-negative bacteria. This molecule shows potent proinflammatory action on various cell types, including macrophages, endothelial cells, and fibroblasts [26]. LPS-induced inflammation in RAW 264.7 and HEK 291 cell lines by interacting

with TLR4, a transmembrane receptor on macrophages, which recognizes molecules derived from Gram-negative bacteria activating the downstream NF- $\kappa$ B (nuclear factor kappa) signaling pathway leading to increased production of cytokines, and/or ROS/RNS generation following the activation of mitogen-activated protein kinases (MAPK) and NF $\kappa$ B-mediated signaling pathway which ultimately drive the tissue degeneration.

Fruit constitutes an important part of a balanced diet as they are natural sources of food nutrient needed by human and animals due to having protein, carbohydrate, minerals, and dietary fibers. *Phoenix dactylifera*, belongs to tree palm family Arecaceae, consumed throughout the world and are important part of the diet in

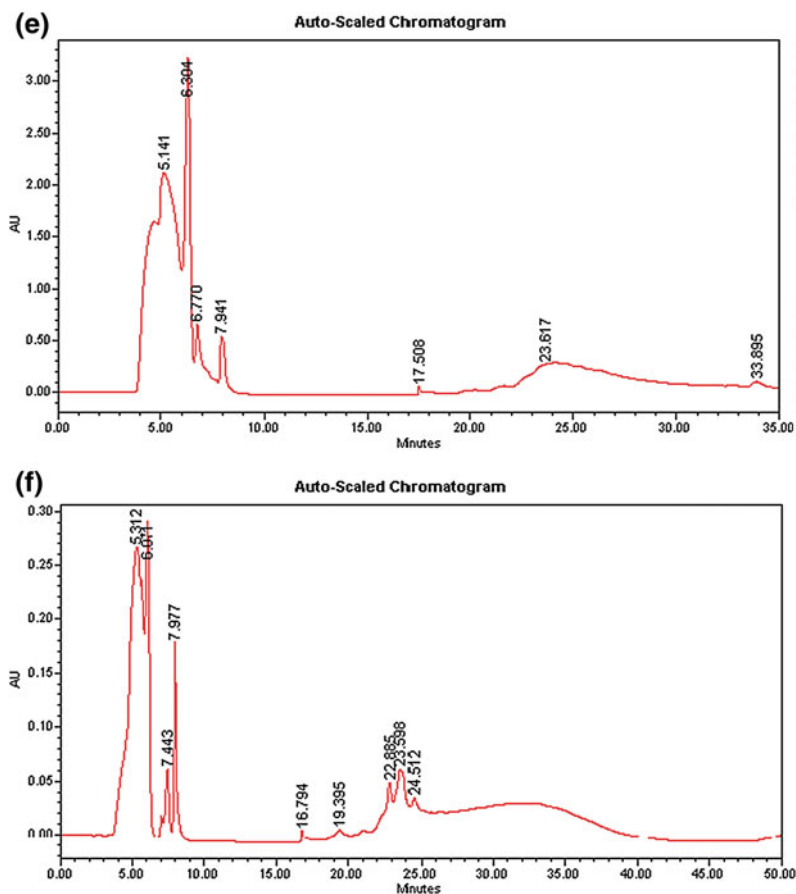


**Fig. 15.19** (continued)

the Middle East [27]. Phytochemical screening has revealed dried date pollens to contain sterols and other supplements such as vitamins and cofactors [28] and lack volatile substances [29]. Phytochemical analyses of fruit flesh and seed of date revealed the presence of flavonoids (luteolin, methyl luteolin, quercetin, and methyl quercetin), flavanols (catechin, epicatechin) [30–32], free phenolic acids (protocatechuic acid, vanillic acid, syringic acid, and ferulic acid) [33, 34] tannins, glycosides, cardiac glycosides and steroids (cholesterol, stigmasterol, campesterol, and  $\alpha$ -sitosterol) essential amino acids [35–37], and nine bound phenolic acids (gallic acid, protocatechuic acid, p-hydroxybenzoic acid, vanillic acid, caffeic acid, syringic acid, p-coumaric acid, ferulic acid, and o-coumaric acid) [29, 37],

respectively. In the past few years, many pharmacological studies have been conducted on *P. dactylifera* [38–40]. Various in vitro and in vivo antioxidant activities have been carried out on various extracts of different parts of *P. dactylifera* [41]. Oral administration of the methanolic and aqueous extracts of edible portion of *P. dactylifera* fruits suppressed the swelling in the foot while the methanolic extract of date seeds showed significant reduction in adjuvant arthritis in rats [42] and on gentamicin-induced nephrotoxicity in rats [43].

In the present study, date fruit was extracted using various organic solvents and their antioxidative and anti-inflammatory activities were evaluated. Phenolic compounds as well as flavonoids are a group of poly-phenolic compounds



possessing free radical scavenging properties, potential inhibitory actions of hydrolytic and oxidative enzymes as well as anti-inflammatory action. Obtained data have clearly demonstrated that date extracts, depending on their mode of collection, possess potent antioxidative properties indicated by significant inhibition of lipid peroxidation (Fig. 15.7), superoxide radical scavenging, hydroxyl radical scavenging, DPPH radical scavenging, and nitric oxide (NO) scavenging activities. The calculated  $IC_{50}$  values of date indicate strong antioxidative properties of these crude extracts.

Data obtained from studies using these date extracts, collected by three different methods, indicate potent antioxidative properties by showing significant inhibition of lipid peroxidation, superoxide radical scavenging, hydroxyl radical scavenging, DPPH radical scavenging, and nitric oxide (NO) scavenging activities. The calculated  $IC_{50}$  values of these three extracts of date have revealed strong antioxidative properties (Fig. 15.9), their anti-inflammatory potencies warranted confirmation through additional studies on cells. Both human and murine cell lines were assessed. Oxidative stress being the main driving force in any inflammatory cascade, studies designed to evaluate their ameliorative effect during and post-oxidative stress induced inflammation.

As we have identified the antioxidative capacity (Fig. 15.9) of dietary date extracts, collected by three different extraction procedures, i.e., methanolic, basic ethanolic, and acidic ethanolic methods, (Fig. 15.1) as an interesting lead that can stabilize the intracellular reactive oxygen and nitrogen intermediates in both murine and human cell lines *in vitro* at non-cytotoxic concentrations, we were therefore interested to evaluate the *in vivo* anti-inflammatory activities of these compounds in preclinical models, but before this cytotoxic and anti-inflammatory properties of these three extracts have been evaluated thoroughly, targeting the mitochondrial reactive oxygen and nitrogen intermediates (Fig. 15.17).

The acidic ethanolic extracts of date extract ameliorate the LPS-induced oxidative stress by

inhibiting the NO production (Fig. 15.6) and subsequently protecting the mitochondrial respiratory chain complex function, thus maintaining the cellular homeostasis or cell viability *per se*. As we have mentioned earlier that oxidative stress and mitochondrial dysfunction are key features for any inflammatory cascade and here the date extracts are capable of inhibiting this, these crude extracts must have potent anti-inflammatory power. Another important point to be noted here is that the acidic ethanolic extract of the date has shown potent anti-inflammatory properties in murine RAW macrophages (Fig. 15.12b) in comparison with the other two extracts (Fig. 15.12a, c), whereas in the case of LPS-induced human HEK cells, the methanolic extract (Fig. 15.15a) is better to inhibit the LPS-induced oxidative stress and to maintain the cellular homeostasis, than both acidic and basic ethanolic extracts. From studies done by various researchers as stated and referred in the preceding paragraphs, we now know that in plants various phenolic compounds and flavonoids, which are basically secondary metabolites of the pentose phosphate, shikimate, and phenylpropanoid pathways, exhibit strong antioxidative redox properties allowing them to act as reducing agents, hydrogen donors, and singlet oxygen quenchers and also many of them have been shown to exhibit the antagonist for the classical NF $\kappa$ B signaling pathways and for this reason in past few years there has been an upsurge of interest in the therapeutic potentials of medicinal plants as antioxidants in reducing such free radical-induced tissue injury. Although several phytochemicals have been shown to possess pharmacological properties of potential interest anti-inflammatory properties and/or therapy, their activity in the *in vitro* and *in vivo* preclinical model organisms is still not well understood due to the variations of their extraction and collection procedures, heterogeneous solubility in different solvents, and most importantly route of administration of these compounds in a dose-dependent manner different disease models. The mechanism by which various date extracts mediate its antioxidant effects remains unclear.

Mitochondria are the major source for ROS generation in the cell. Evidence from our studies suggests the role of mitochondria in date-induced ROS scavenging pathways (Fig. 15.17). It is possible that date extracts inhibit the mitochondrial enzymes that lead to production of ROS and thus maintain the oxidative stress-induced cell damage (Fig. 15.16). The inhibition of ROS by date extracts could occur through its interaction with thioredoxin reductase, thus changing its activity to NADPH oxidase, which could then lead to the scavenging of ROS. It is not clear yet which structural group or compound of date extracts is responsible for inhibiting the ROS production. Present extracts of date also have shown a high level of phenol (Fig. 15.10b) and flavonoid (Fig. 15.10a) content and this may be the reason behind their anti-inflammatory activities.

We can conclude that the inhibitory effect of date extracts on LPS-induced inflammation in RAW macrophages is via the downstreaming of the classical TLR4-mediated signaling cascades scavenging the mitochondrial ROS production (Fig. 15.17). Until phytochemical screening of these extracts is carried out, this will be very early to conclude. However, it is true that the compounds present in these extracts can inhibit the endotoxin-induced oxidative stress (Fig. 15.16) in both murine and human cell lines in a dose-dependent manner. The phytochemical screening and the structure activity relationship of these extracts are under investigation now along with the detailed anti-inflammatory signaling pathways. But the question what compound(s) is/are exactly present in these extracts that are truly exhibiting the anti-inflammatory properties and the signaling pathways that they follow, is still not clear yet. For this HPLC and mass spectrometry of the samples themselves are being carried out and from database analysis individual eluants shall be used in anti-inflammatory and antioxidative assays to assess their anti-inflammatory potential. This is the ongoing work in the laboratory.

Acting as second messengers, transient free radicals, synthesized during regular metabolism, often trigger further downstream sequence of activation networks. But produced in unregulated catabolic cycles, they demonstrate deleterious compounds such as toxins and wastes which further contribute to the disease etiology. Studies on intermediate free radicals specially reactive oxygen species (ROS) and their action on cellular physiology have shown that they play a pivotal role in causing secondary tissue degeneration in various inflammatory diseases, such as rheumatoid arthritis [44], multiple sclerosis [45], thyroiditis, and type 1 diabetes [46] is.

ROS are known to perform essential role in immune response to pathogens, including bacterial killing via induction of superoxide anion during respiratory burst in activated macrophages and neutrophils [47, 48]. Further studies on patients with chronic granulomatous disease (CGD) or genetically engineered mice lacking components of the NADPH oxidase enzyme (NOX) [49, 50] provide corroborative data.

Reactive oxygen species (ROS) oxidatively modify DNA, proteins, lipids, and small intracellular molecules. Lipids, for example, pulmonary surfactants, react with ROS to produce lipid peroxides that perpetrate increased membrane permeability and inactivation of surfactants [51]. Further, ROS react with cellular proteins and inhibit protein synthesis by disabling proteins involved in translation and translocation. This effectively impairs cellular metabolism. ROS also damage nucleic acids by modifying purine and pyrimidine bases and by causing DNA-strand breakage. Overproduction of ROS and oxidative stress has been found to be critical in pathophysiology of other complex syndromes such as cancer, asthma, cystic fibrosis, ischemia-reperfusion injury, drug-induced toxicity, and aging.

Natural products have yielded as many as 70 % of the drugs used today for inflammation and degeneration. Consumption of large portions of fruits and vegetables has been recommended

for the reduction of risk of cardiovascular diseases, autoimmune diseases, cancer, and various other chronic illnesses although little is known about the actual active compounds or moieties which are beneficial. It is an important project to identify and validate direct action and participation of such active ingredients in modulating disease pathophysiology.

Figures 15.18 and 15.19, show data on proteomic analyses by TLC, HPLC, and MS data. On preliminary investigation, TLC data reveal that extract A may not contain important compounds although anti-inflammatory activity was seen in the other two extracts. Clear peaks were not obtained in scan data of the other two which necessitates further purification steps and MS analyses of the individual peaks and NMR. This work is ongoing and is beyond the scope of this work.

## 15.6 Conclusion

In this study, three different types of date extracts, namely methanolic, acidic ethanolic, and basic ethanolic, produce effects on reactive oxygen species where scavenging of hydroxyl radicals, superoxide radicals, nitric oxide scavenging activity, and inhibition of lipid peroxidation were found to occur in a dose-dependent manner. Moreover, they have a significant inhibition of anti-inflammatory activities. In vitro experiments prove that the effects of the extracts are likely mediated through inhibition of mitochondria-derived (ROS) scavenging pathways. This is an important finding as it shows not only the extracts' pathway of action but also proves the direct involvement of a subcellular signaling network that can be interfered with, using a natural products without the possibility of drastic side effects. Ongoing proteomic analysis has already revealed scan data using various sensitive chromatographic techniques of certain specific peaks. Further analyses are needed to conclusively identify the peaks to reveal identity of one or more compounds for detailed characterization and development into novel drug entities.

## References

1. Crunkhon P, Meacock S. Mediators of the inflammation induced in the rat paw by carrageenan. *Br J Pharmacol.* 1971;42:392–402.
2. Winter CA, Risley E, Nuss G. Carrageenan-induced edema in hind paw of the rat as an assay for anti-inflammatory drugs. *Proc Soc Exp Biol Med.* 1962;111:544–7.
3. Vinegar R, Schreiber W, Hugo R. Biphasic development of carrageenan oedema in rats. *J Pharmacol Exp Ther.* 1969;66:96–103.
4. Robbins SL, Cortran RS. Acute and chronic inflammation. In: *Pathologic basis of disease.* vol 7, pp 47–87. Elsevier Publication; 2004.
5. Mohan H. Inflammation and healing. In: *Textbook of pathology.* pp 114–121. New Delhi: Jaypee Publication; 2002.
6. Chatpaliwar VA, Johrapurkar AA, Wanjari MM, Chakraborty RR, Kharkar VT. Anti-inflammatory activity of *martynia diandra glox.* *Indian Drugs.* 2002;39:543–5.
7. Amann R, Schuligoi R, Lanz I, Donnerer J. Histamine induced edema in the rat paw-effect of capsaicin denervation and a cgrp receptor antagonist. *Eur J Pharmacol.* 1995;279:227–31.
8. Dray A. Inflammatory mediators of pain. *Br J Anesth.* 1995;75:25–131.
9. Whittle BA. The use of changes in capillary permeability in mice to distinguish between narcotic and non-narcotic analgesic. *Br J Pharmacol Chemother.* 1964;22:24–253.
10. Miles AA, Miles E. Vascular reactions to histamine, histamine-liberator and leukotaxine in the skin of guinea-pigs. *J Physiol.* 1992;118:228–57.
11. Braca A, De Tommasi N, Di Bari L, Pizza C, Politi M, Morelli I. Antioxidant principles from *Bauhinia tarapotensis.* *J Nat Prod.* 2001;64:892–5.
12. Martinez AC, Marcelo EL, Marco AO, Moacyr M. Differential responses of superoxide dismutase in freezing resistant *Solanum curtibolum* and freezing sensitive *Solanum tuberosum* subjected to oxidative and water stress. *Plant Sci.* 2001;160:505–15.
13. Beauchamp C, Fridovich I. Superoxide dismutase: improved assays and an assay applicable to acrylamide gels. *Anal Biochem.* 1971;44:276–87.
14. Chung SK, Osawa T, Kawakishi S. Hydroxyl radical scavenging effects of spices and scavengers from brown mustard (*Brassica nigra*). *Biosci Biotechnol Biochem.* 1997;61:118–23.
15. Ohkawa M, Ohisi N, Yagi K. Assay for lipid peroxides in animal tissue by thiobarbituric acid reaction. *Anal Biochem.* 1979;95:351–8.
16. Ruberto G, Baratta MT, Deans SG, Dorman HJD. Antioxidant and antimicrobial activity of *Foeniculum vulgare* and *Crithmum maritimum* essential oils. *Planta Med.* 2000;66:687–93.
17. Prieto P, Pineda M, Aguilar M. Spectrophotometric quantitation of antioxidant capacity through the

- formation of a phosphomolybdenum complex: specific application to the determination of vitamin E. *Anal Biochem.* 1999;269:337–41.
18. Salah N, Miller NJ, Paganga G, Tijburg L, Bolwell GP, Rice-Evans C. Polyphenolic flavanols as scavengers of aqueous phase radicals and as chain-breaking antioxidants. *Arch Biochem Biophys.* 1995;322(2):339–46.
  19. Naik GH, Priyadarsini KI, Satav JG, Banavalikar MM, Sohoni PP, Biyani MK, Mohan H. Comparative antioxidant activity of individual herbal components used in Ayurvedic medicine. *Phytochemistry.* 2003;63:97–104.
  20. Gutteridge MC. Reactivity of hydroxyl and hydroxyl radicals discriminated by release of thiobarbituric acid-reactive material from deoxy sugars, nucleosides and benzoate. *Biochem J.* 1984;224:761–7.
  21. Gutteridge MC. Ferrous salt promoted damage to deoxyribose and benzoate. *Biochem J.* 1987;243:709–14.
  22. Ames BN. Dietary carcinogens and anticarcinogens—oxygen radicals and degenerative diseases. *Science.* 1983;221:1256–64.
  23. Wiseman H, Halliwell B. Damage to DNA by reactive oxygen and nitrogen species: role of inflammatory disease and progression to cancer. *Biochem J.* 1996;313:17–29.
  24. Lopez-Velez M, Martinez-Martinez F, Del Valle-Ribes C. The study of phenolic compounds as natural antioxidants in wine. *Crit Rev Food Sci Nutr.* 2003;43:233–44.
  25. Roginsky V. Chain breaking antioxidant activity of natural polyphenols as determined during the chain oxidation of methyl linoleate in Triton X-100 micelles. *Arch Biochem Biophys.* 2003;414:261–70.
  26. Mohamed DA, Al-Okbi SY. In vitro evaluation of antioxidant activity of different extracts of *Phoenix dactylifera* L. fruits as functional foods. *Deutsche Lebensmittel Rundschau.* 2005;101:305–8.
  27. Barh D, Mazumdar BC. Comparative nutritive values of palm saps before and after their partial fermentation and effective use of wild date (*Phoenix sylvestris* Roxb.) sap in treatment of anemia. *Res J Med Med Sci.* 2008;3:173–6.
  28. Ishurd O, Ali Y, Wei W, Bashir F, Ali A, Ashour A, Pana Y. An alkali-soluble heteroxylan from seeds of *Phoenix dactylifera* L. *Carbohydr Res.* 2003;338:1609–12.
  29. Hussein MM, Wafaa A, Helmy, Salem HM. Biological activities of some galactomannans and their sulfated derivatives. *Phytochemistry.* 1998;48:479–84.
  30. Al-Shahib W, Marshall RJ. The fruit of the date: its possible use as the best food for the future? *Int J Food Sci Nut.* 1993;54:247–59.
  31. Heftmann E, Bennett RD. Identification of estrone in date seeds by thin layer chromatography. *Naturwissenschaften.* 1965;52:431–8.
  32. Bennett RD, Heftmann E. Isolation of Estrone and cholesterol from the date *Phoenix dactylifera*. *Phytochemistry.* 1966;5:231–5.
  33. Mahran GH, Abdul-Wahab SM, Attia AM. A phytochemical study of date pollen. *Planta Med.* 1976;29:171–5.
  34. Tabeta S, Uehare IO, Zahid M, Zhou H, Yoshioka P, Yuanjiang.  $\alpha$ -D-glucan structure. *Carbohydr Res.* 2002;337:1325–8.
  35. Biglari F, Abbas FM, AlKarkhi AME. Antioxidant activity and phenolic content of various date (*Phoenix dactylifera*) fruits from Iran. *Food Chem.* 2008;107:1636–41.
  36. Ziouti AC, Modafar EL, Fleuret AS, Boustani EL, Macheix JJ. Phenolic compounds in date cultivars sensitive and resistant to *Fusarium oxysporum*. *Biologia Plant.* 1996;38:451–7.
  37. Hong YJ, Tomas-Barberan FA, Adel A, Kader S, Alyson E. The flavonoid glycosides and procyanidin composition of Deglet Noor dates (*Phoenix dactylifera*). *J Agric Food Chem.* 2006;54:2405–411.
  38. Ishurda O, John FK. The anti-cancer activity of polysaccharide prepared from Libyan dates (*Phoenix dactylifera* L.). *Carbohydr Polym.* 2005;59:531–5.
  39. Abdulla Y, Al-Taher. Possible anti-diarrhoeal effect of the date (*Phoenix Dactylifera* L.) spathe aqueous extract in rats. *Sci J King Faisal Univ (Basic and Appl Sci).* 2008;9:1429–35.
  40. Al-Qarawi AA, Ali BH, Al-Mougry SA, Mousa HM. Gastrointestinal transit in mice treated with various extracts of date (*Phoenix dactylifera* L.). *Food Chem Toxicol.* 2003;41:37–9.
  41. Vayalil PK. Antioxidant and antimutagenic properties of aqueous extract of date fruit (*Phoenix dactylifera* L. Arecaceae). *J Agric Food Chem.* 2002;50:610–17.
  42. Mohamed BA, Nabil AH, Hanan AS. Protective effects of extract from dates (*Phoenix Dactylifera* L.) and ascorbic acid on thioacetamide-induced hepatotoxicity in rats. *Iran J Pharm Res.* 2008;7:193–201.
  43. Javanmardi J, Stushno C, Locke E, Vivanco JM. Antioxidant activity and total phenolic content of Iranian *Ocimum* accessions. *Food Chem.* 2003;83:547–50.
  44. Filippin LI, Verdelino R, Marroni NP, Xavier RM. Redoxsignalling and the inflammatory response in rheumatoid arthritis. *Clin. Exp Immunol.* 2008;152(3):415–22.
  45. Gilgun-Sherki Y, Melamed E, Offen D. The role of oxidative stress in the pathogenesis of multiple sclerosis: the need for effective antioxidant therapy. *J Neurol.* 2004;251:261–8. doi:10.1111/j.1365-2249.2008.03634.x.

46. Chen J, Gusdon AM, Thayer TC, Mathews CE. Role of increased ROS dissipation in prevention of T1D. *Ann N Y Acad Sci.* 2008;150:157–66.
47. Lambeth JD. NOX enzymes and the biology of reactive oxygen. *Nat Rev Immunol.* 2004;4:181–9.
48. Kanayama A, Miyamoto Y. Apoptosis triggered by phagocytosis related oxidative stress through FLIPS down-regulation and JNK activation. *J Leukoc Biol.* 2007;82:1344–52.
49. Morgenstern DE, Gifford MA, Li LL, Doerschuk CM, Dinauer MC. Absence of respiratory burst in X-linked chronic granulomatous disease mice leads to abnormalities in both host defense and inflammatory response to *Aspergillus fumigatus*. *J Exp Med.* 1997;185:207–18.
50. Shiloh MU, MacMicking JD, Nicholson S, Brause JE, Potter S, Marino M, Fang F, Dinauer M, Nathan C. Phenotype of mice and macrophages deficient in both phagocyte oxidase and inducible nitric oxide synthase. *Immunity.* 1999;10:29–38.
51. Yang Q, Kim YS, Lin Y, Lewis J, Neckers L, Liu ZG. Tumour necrosis factor receptor 1 mediates endoplasmic reticulum stress induced activation of the MAP kinase JNK. *EMBO Rep.* 2006;7:622–7.

---

**Part IV**

**Bio-Green-Technology as a  
Multi-disciplinary Interface Amongst  
the Life Sciences**

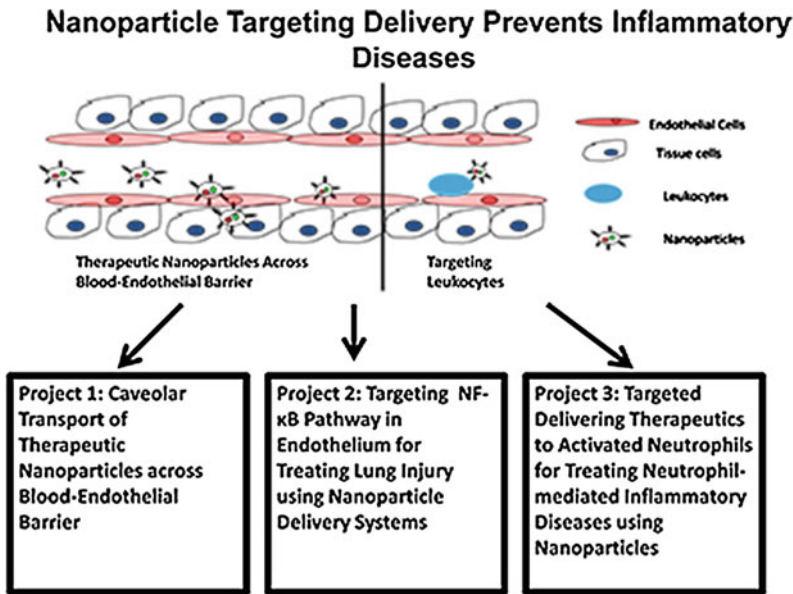
---

## 16.1 Introduction

Inflammation is a complex response to local injury or other trauma which is characterized by redness, heat, swelling, and pain. Inflammation involves various immune system cells and numerous mediators. Inflammatory process is the net result of a cascade of highly regulated events propagated upon stimulation and is the major process through which the body repairs tissue damage and defends itself against foreign materials. Acute inflammation is typically caused by an external chemical, mechanical, or pathogenic influence; has a relatively short duration; and is a necessary protection tool that removes foreign bodies and damaged tissue, preventing further damage. Aberrant or chronic inflammation requires no external stimulus and can cause a range of painful and debilitating symptoms. Such uncontrolled inflammation is often indicative of a more serious, underlying cause whose analysis may be used as a diagnostic marker for a number of conditions, including autoimmune, infectious, neurological, cardiovascular, and metastatic diseases [1].

Although therapeutic drugs are available, their benefits are limited by the adverse side effects observed from long-term use at high doses. A better, yet less practical, approach is to administer the drugs directly to the site of inflammation using interarticular injections that require skillful applications at a number of sites, making it an expensive therapy with regard to both time and cost. The most desirable approach would be the development of vectors, such as nanoparticles, capable of targeting and delivering their payload directly to the site of inflammation [1].

The term nanoparticles refers to materials with at least one dimension between approximately 1 and 100 nm and usually contain from several hundreds to  $10^5$  atoms [2]. Nanoparticles are an attractive choice because they can carry chemotherapeutic warheads, serve as imaging agents, and act as the active therapeutic agent themselves. The ideal nanoparticle-based therapeutics should have specific targeting to pathologic tissues, which minimizes or avoids off-target effects of the active therapeutic agents on healthy tissues [3].



Nanoparticles such as liposome-encapsulated drugs have been shown to be potential candidates and have been used to encapsulate and deliver clodronate and glucocorticoid drugs to target arthritis in an animal model [4]. In another arthritis model, studies showed that i.v. administered clodronate liposomes could suppress the onset of disease by targeting macrophages [5]. An alternative approach encapsulated the glucocorticoid prednisolone in PEG-coated liposomes and administered the nanoparticles to adjuvant-induced arthritic rats. Thus, coating liposomes with PEG polymers enhances stability in vivo and has led to a range of long-circulating drug carriers known as sterically stabilized liposomes [6].

### 16.1.1 Nanoparticle as a Drug Carrier

Polymeric nanoparticles made from natural and synthetic polymers have received the majority of attention due to their stability and ease of surface modification [7]. They can be tailor-made to achieve both controlled drug release and disease-specific localization by tuning the polymer characteristics and surface chemistry [7, 8]. It has been established that nanocarriers can

become concentrated preferentially to tumors, inflammatory sites, and at antigen sampling sites by virtue of the enhanced permeability and retention (EPR) effect of the vasculature. Once accumulated at the target site, hydrophobic biodegradable polymeric nanoparticles can act as a local drug depot depending on the makeup of the carrier, providing a source for a continuous supply of encapsulated therapeutic compound at the disease site, e.g., inflammation and solid tumors. These systems in general can be used to provide targeted (cellular or tissue) delivery of drugs, improve bioavailability, sustain release of drugs, or solubilize drugs for systemic delivery. This process can be adapted to protect therapeutic agents against enzymatic degradation (i.e., nucleases and proteases) [7]. Thus, the advantages of using nanoparticles for drug delivery are a result of two main basic properties: small size and use of biodegradable materials.

### 16.1.2 Drug Delivery by Nanoparticles

Nanoparticles, because of their small size, can extravasate through the endothelium in inflammatory sites, epithelium (e.g., intestinal tract and



liver), and tumors, or penetrate through microcapillaries. In general, the nanosize of these particles allows for efficient uptake by a variety of cell types and selective drug accumulation at target sites [7]. Many studies have demonstrated that nanoparticles have a number of advantages over microparticles ( $>1\ \mu\text{m}$ ) as a drug delivery system. Nanoparticles have another advantage over larger microparticles because they are better suited for intravenous delivery. The smallest capillaries in the body are 5–6  $\mu\text{m}$  in diameter. The size of particles being distributed into the bloodstream must be significantly smaller than 5  $\mu\text{m}$ , without forming aggregates, to ensure that the particles do not cause an embolism [7].

The use of biodegradable materials for nanoparticle preparation allows for sustained drug release within the target site over a period of days or even weeks. Biodegradable nanoparticles formulated from poly(lactide-co-glycolide) (PLGA) and poly(lactic acid) (PLA) have been developed for sustained drug delivery and are especially effective for drugs with an intracellular target [9]. Greater and sustained antiproliferative activity was observed in vascular smooth muscle cells that were treated with dexamethasone-loaded nanoparticles and then compared to cells given drug in solution [10]. Hence, nanoparticles can be effective in delivering their contents to intracellular targets.

Nanoparticles have high cellular uptake when compared to microparticles and are available to wider range of cellular and intracellular targets due to their small size and mobility. Nanoparticles can cross the blood–brain barrier following the opening of endothelium tight junctions by hyperosmotic mannitol, which may provide sustained delivery of therapeutic agents for difficult-to-treat diseases such as brain tumors [7]. Drug release is also affected by the size of the particle, and small particles have larger surface-area-to-volume ratio; therefore, most of the drug associated with small particles would be

at or near the surface of the particle, leading to faster drug release [10].

### 16.1.3 Nanoparticle-Mediated Drug Targeting

Targeted delivery of nanoparticles can be achieved actively or passively. Active targeting requires the therapeutic agent to be achieved by conjugating the therapeutic agent or carrier system to a tissue or cell-specific ligand [11]. Passive targeting is achieved by incorporating the therapeutic agent into a macromolecule or nanoparticle that passively reaches the target organ. Drugs encapsulated in nanoparticles or drugs coupled to macromolecules can passively target tumors through the EPR (enhanced permeability and retention) effect. Alternatively, catheters can be used to infuse nanoparticles to the target organ or tissues.

Liposomes have been demonstrated to be useful for delivering pharmaceutical agents. These systems use “contact-facilitated drug delivery,” which involves binding or interaction with the targeted cell membrane. This permits enhanced lipid–lipid exchange with the lipid monolayer of the nanoparticle, which accelerates the convective flux of lipophilic drugs (e.g., paclitaxel) to dissolve through the outer lipid membrane of the nanoparticles to targeted cells [7]. Such nanosystems can serve as drug depots exhibiting prolonged release kinetics and long persistence at the target site. Nanoparticles also can be formulated to deliver drugs across several biological barriers. Antineoplastics, antiviral drugs, and several other types of drugs are markedly hindered because of inability of these molecules to cross the blood–brain barrier (BBB) [12]. The application of nanoparticles to deliver across this barrier is extremely promising. It has been reported that nanoparticles can cross the BBB following the opening of tight junctions

by hyperosmotic mannitol, which also may provide sustained delivery of therapeutic agents for difficult-to-treat diseases such as brain tumors [7].

### 16.1.4 Receptor-Mediated Targeting of Nanoparticle

In order to target a nanoparticle to particular cell, the knowledge of receptors on the target plays an important role. Hence, the functionalization of nanoparticle is a widely used technique that allows for conjugation with targeting ligands which possess inherent ability to direct selective binding to cell types or states and therefore confer smartness to nanoparticles. These targeting ligands fall into several general classes: small molecules, polypeptide-based peptides, protein domains, antibodies, and nucleic acid-based aptamers [3].

Carbohydrates, which interact weakly with some cell surface receptors, can also serve as nanoparticle small molecule-targeting ligands. Carbohydrates permit nanoparticle glycotargeting, which is based on endogenous lectin interactions with carbohydrates. A disadvantage of this targeting method is that glycotargeting often requires multiple interacting carbohydrates to achieve strong enough binding strength. One known example uses galactose or galactose mimics as ligands to asialoglycoprotein receptor, an endocytotic cell surface lectin receptor highly expressed on hepatocyte surfaces. DC-SIGN is a C-type lectin receptor preferentially expressed by dendritic cells. Lex and ManLAM carbohydrates, for example, can be used to enhance the binding and uptake of the nanoparticles by dendritic cells, although their targeting features are not as effective as DC-SIGN-specific antibodies that are presumably more specific and potent [3].

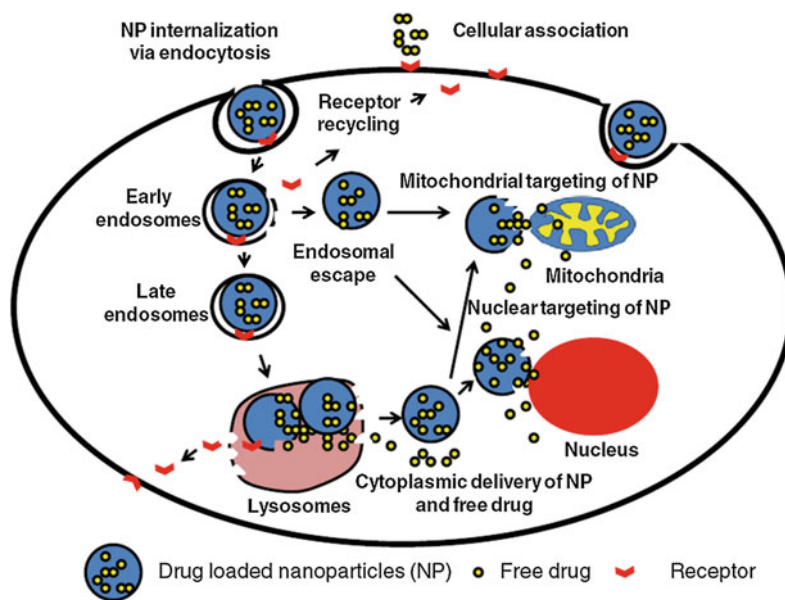
Only specialized cells such as macrophages are capable of phagocytosis, a form of endocytosis in which the cell engulfs larger particles. Almost all cells, however, can internalize NPs by pinocytosis. Four different basic pinocytotic mechanisms are currently known, macropinocytosis, clathrin-mediated endocytosis, caveolae-mediated endocytosis, and mechanisms independent of clathrin and caveolin. Upon incorporation

by an organism, NPs interact with extracellular biomolecules dissolved in body fluids, including proteins, sugars, and lipids prior to their encounter with the plasma membranes of cells. A layer of proteins forms on the NP surfaces, called protein corona. Consequently, cell surface receptors, which activate the endocytosis machinery, actually encounter NPs enshrouded in biomolecules rather than bare particles [13].

### 16.1.5 Cellular Uptake of Nanoparticles by Macrophages

Histological analysis of chronic inflammation often indicates localized populations of macrophages and lymphocytes, as well as compromised blood vessels, fibrosis, and tissue necrosis. Macrophage cells are key members of the mononuclear phagocyte system (MPS) and play a number of crucial roles in inflammation, including phagocytosis, antigen presentation, and the production of various cytokines and immune regulators [14]. The MPS contains monocytes, which circulate the blood and upon maturation often become macrophages, and resident tissue macrophages that can take many forms. Resident macrophages are found in all organs and connective tissues, and they have a major function in the primary immune response of tissues. Their activation secretes chemokines that adhere to circulating monocytes, trafficking MPS cells to the inflammation site, and generating an immune response.

The ability to visualize the migration of MPS cells would be advantageous both therapeutically and diagnostically, as alterations in macrophage clearance contribute to many common disorders, including atherosclerosis, autoimmunity, and major infections [15]. Since macrophages are phagocytotic, their labeling is a relatively straightforward task, requiring no transfection agents, and, as discussed at length later, this has been exploited in a number of nanoparticle strategies [3]. It has been suggested that permeable vascular walls can aid nanoparticle localization at the site of inflammation and this has



Endocytic pathway of drug-loaded nanoparticles targeting different cellular organelles

been exploited by the use of untargeted nanoparticles whose recruitment by macrophages has allowed the activated cells to deliver their probe payload to the site of inflammation. Alternatively, it is possible to accumulate nanoparticles at the inflammation locale by the use of surface-modified probes that have been functionalized to target specific analytes present at the active site. Both targeted and untargeted approaches have been applied to a range of techniques, including MRI, fluorescence, and Raman spectroscopy, for the detection of inflammation [3].

## 16.2 Conclusion

Inflammation plays a pivotal role in the development of many diseases, including heart disease, Alzheimer's disease, arthritis, and some forms of cancer. Hence, use of nanoparticle technologies can be utilized to detect and image areas of inflammation by acting as diagnostic probes. The ability to specifically target sites of inflammation may facilitate the detection of diseases in the preclinical stage, in turn, allowing

earlier intervention and better-targeted treatment. Furthermore, nanoparticles can be used to target and image selected biological structures and cells, such as macrophages, generating information with regard to the roles such cells play in the initiation and pathogenesis of inflammatory disease. Nanoparticles have also been used as molecular vehicles for the delivery of pharmaceuticals, and conjugation to a nanoparticle directly increases the efficacy of the payload. Exploitation of using nanoparticles facilitates the treatment of targeted areas without damaging to nontarget areas.

One of the most challenging problems in the targeted delivery of nanoparticles is to develop high-quality targeting ligands that can give rise to more specific accumulation of nanoparticles in affected targeted areas than in other tissues. Such smart molecules can be developed through affinity selection from combinatorial libraries displaying small molecules, short peptides, antibodies and antibody fragments, engineered protein domains, and nucleic acid aptamers. The availability of these types of targeting ligands and their successful conjugation with nanoparticles will have significant applications in targeted

imaging, diagnosis, and treatment of tumors and other inflammatory diseases that are based on nanotechnology. A variety of coating materials (magnetic or non-magnetic with different thicknesses, composition, etc.) are currently being studied with direct effect on the functionalization and toxicity of nanoparticles and therefore their applications in biomedicine.

---

## References

1. Stevenson R, Hueber AJ, Hutton A, Graham D. Nanoparticles and inflammation. *Sci. World J.* 2011; 11:1300–12.
2. Issa B, Obiat IM, Albiss BA, Haik Y. Magnetic nanoparticle. *Int. J. Mol. Sci.* 2013;14:21266–305.
3. Friedman AD, Claypool SE. Smart targeting of nanoparticles. *Curr. Pharm. Des.* 2013;19 (35):6315–29.
4. Metselaar JM, Wauben MHM, Wagenaar-Hilbers JPA, Boerman OC, Storm G. Complete remission of experimental arthritis by joint targeting of glucocorticoids with long circulating liposomes. *Arthritis Rheum.* 2003;48:2059–66.
5. Richards PJ, Williams AS, Goodfellow RM, Williams BD. Liposomal clodronate eliminates synovial macrophages, reduces inflammation and ameliorates joint destruction in antigen induced arthritis. *Rheumatology.* 1999;38:818–25.
6. Allen TM, Brandeis E, Hansen CB, Kao GY, Zalipsky S. A new strategy for attachment of antibodies to sterically stabilized liposomes resulting in efficient targeting to cancer cells. *Biochim. Biophys. Acta.* 1995;1237:99–108.
7. Singh R, Lillard Jr JW. Nanoparticles based drug delivery. *Exp. Mol. Pathol.* 2009;86(3):215–23.
8. Moghimi SM, Hunter AC, Murray JC. Long-circulating and target-specific nanoparticles: theory to practice. *Pharmacol. Rev.* 2001;53:283–318.
9. Panyam J, Labhasetwar V. Biodegradable nanoparticles for drug and gene delivery to cells and tissue. *Adv. Drug. Del. Rev.* 2003;55:329–47.
10. Redhead HM, Davis SS, Illum L. Drug delivery in poly(lactide-co-glycolide) nanoparticles surface modified with poloxamer 407 and poloxamine 908: in vitro characterisation and in vivo evaluation. *J. Control. Release.* 2001;70:353–63.
11. Lamprecht A, Ubrich N, Yamamoto H, Schäfer U, Takeuchi H, Maincent P, Kawashima Y, Lehr CM. Biodegradable nanoparticles for targeted drug delivery in treatment of inflammatory bowel disease. *J. Pharmacol. Exp. Ther.* 2001;299:775–81.
12. Fornaguera C, Dols-Perez A, Caldero G, Garcia-Celma M, Camarasa J, Solans C. PLGA nanoparticles prepared by nano-emulsion templating using low-energy methods as efficient nanocarriers for drug delivery across the blood-brain barrier. *J. Control. Release.* 2015;211:134–43.
13. Treuel L, Jiang X, Nienhaus GU. New views on cellular uptake. *J. Roy. Soc. Interface* 2014;10: 20120939.
14. Fujiwara N, Kobayashi K. Macrophages in inflammation. *Curr. Drug Targets Inflamm. Allergy.* 2005;4 (3):281–6.
15. Moghimi SM, Hunter AC, Murray JC. Nanomedicine: current status and future prospects. *FASEB J.* 2005;19(3):311–30.